

Mithun Chakraborty · Raman Kr. Jha ·
Valentina Emilia Balas ·
Samarendra Nath Sur ·
Debdatta Kandar *Editors*

Trends in Wireless Communication and Information Security

Proceedings of EWCIS 2020

Lecture Notes in Electrical Engineering

Volume 740

Series Editors

Leopoldo Angrisani, Department of Electrical and Information Technologies Engineering, University of Napoli Federico II, Naples, Italy
Marco Arteaga, Departament de Control y Robótica, Universidad Nacional Autónoma de México, Coyoacán, México
Bijaya Ketan Panigrahi, Electrical Engineering, Indian Institute of Technology Delhi, New Delhi, Delhi, India
Samarjit Chakraborty, Fakultät für Elektrotechnik und Informationstechnik, TU München, Munich, Germany
Jiming Chen, Zhejiang University, Hangzhou, Zhejiang, China
Shanben Chen, Materials Science and Engineering, Shanghai Jiao Tong University, Shanghai, China
Tan Kay Chen, Department of Electrical and Computer Engineering, National University of Singapore, Singapore, Singapore
Rüdiger Dillmann, Humanoids and Intelligent Systems Laboratory, Karlsruhe Institute for Technology, Karlsruhe, Germany
Haibin Duan, Beijing University of Aeronautics and Astronautics, Beijing, China
Gianluigi Ferrari, Università di Parma, Parma, Italy
Manuel Ferre, Centre for Automation and Robotics CAR (UPM-CSIC), Universidad Politécnica de Madrid, Madrid, Spain
Sandra Hirche, Department of Electrical Engineering and Information Science, Technische Universität München, Munich, Germany
Faryar Jabbari, Department of Mechanical and Aerospace Engineering, University of California, Irvine, CA, USA
Limin Jia, State Key Laboratory of Rail Traffic Control and Safety, Beijing Jiaotong University, Beijing, China
Janusz Kacprzyk, Systems Research Institute, Polish Academy of Sciences, Warsaw, Poland
Alaa Khamis, German University in Egypt El Tagamoa El Khames, New Cairo City, Egypt
Torsten Kroeger, Stanford University, Stanford, CA, USA
Yong Li, Hunan University, Changsha, Hunan, China
Qilian Liang, Department of Electrical Engineering, University of Texas at Arlington, Arlington, TX, USA
Ferran Martín, Departament d'Enginyeria Electrònica, Universitat Autònoma de Barcelona, Bellaterra, Barcelona, Spain
Tan Cher Ming, College of Engineering, Nanyang Technological University, Singapore, Singapore
Wolfgang Minker, Institute of Information Technology, University of Ulm, Ulm, Germany
Pradeep Misra, Department of Electrical Engineering, Wright State University, Dayton, OH, USA
Sebastian Möller, Quality and Usability Laboratory, TU Berlin, Berlin, Germany
Subhas Mukhopadhyay, School of Engineering & Advanced Technology, Massey University, Palmerston North, Manawatu-Wanganui, New Zealand
Cun-Zheng Ning, Electrical Engineering, Arizona State University, Tempe, AZ, USA
Toyooki Nishida, Graduate School of Informatics, Kyoto University, Kyoto, Japan
Federica Pascucci, Dipartimento di Ingegneria, Università degli Studi "Roma Tre", Rome, Italy
Yong Qin, State Key Laboratory of Rail Traffic Control and Safety, Beijing Jiaotong University, Beijing, China
Gan Woon Seng, School of Electrical & Electronic Engineering, Nanyang Technological University, Singapore, Singapore
Joachim Speidel, Institut of Telecommunications, Universität Stuttgart, Stuttgart, Germany
Germano Veiga, Campus da FEUP, INESC Porto, Porto, Portugal
Haitao Wu, Academy of Opto-electronics, Chinese Academy of Sciences, Beijing, China
Junjie James Zhang, Charlotte, NC, USA

The book series *Lecture Notes in Electrical Engineering* (LNEE) publishes the latest developments in Electrical Engineering - quickly, informally and in high quality. While original research reported in proceedings and monographs has traditionally formed the core of LNEE, we also encourage authors to submit books devoted to supporting student education and professional training in the various fields and applications areas of electrical engineering. The series cover classical and emerging topics concerning:

- Communication Engineering, Information Theory and Networks
- Electronics Engineering and Microelectronics
- Signal, Image and Speech Processing
- Wireless and Mobile Communication
- Circuits and Systems
- Energy Systems, Power Electronics and Electrical Machines
- Electro-optical Engineering
- Instrumentation Engineering
- Avionics Engineering
- Control Systems
- Internet-of-Things and Cybersecurity
- Biomedical Devices, MEMS and NEMS

For general information about this book series, comments or suggestions, please contact leontina.dicecco@springer.com.

To submit a proposal or request further information, please contact the Publishing Editor in your country:

China

Jasmine Dou, Editor (jasmine.dou@springer.com)

India, Japan, Rest of Asia

Swati Meherishi, Editorial Director (Swati.Meherishi@springer.com)

Southeast Asia, Australia, New Zealand

Ramesh Nath Premnath, Editor (ramesh.premnath@springernature.com)

USA, Canada:

Michael Luby, Senior Editor (michael.luby@springer.com)

All other Countries:

Leontina Di Cecco, Senior Editor (leontina.dicecco@springer.com)

**** This series is indexed by EI Compendex and Scopus databases. ****

More information about this series at <http://www.springer.com/series/7818>

Mithun Chakraborty · Raman Kr. Jha ·
Valentina Emilia Balas · Samarendra Nath Sur ·
Debdatta Kandar
Editors

Trends in Wireless Communication and Information Security

Proceedings of EWCIS 2020

 Springer

Editors

Mithun Chakraborty
Department of Electronics
and Communication Engineering
Amity University
Ranchi, Jharkhand, India

Valentina Emilia Balas
Aurel Vlaicu University of Arad
Arad, Romania

Debdatta Kandar
North Eastern Hill University
Shillong, Meghalaya, India

Raman Kr. Jha
Amity University
Ranchi, Jharkhand, India

Samarendra Nath Sur
Sikkim Manipal Institute of Technology
Majitar, Sikkim, India

ISSN 1876-1100

ISSN 1876-1119 (electronic)

Lecture Notes in Electrical Engineering

ISBN 978-981-33-6392-2

ISBN 978-981-33-6393-9 (eBook)

<https://doi.org/10.1007/978-981-33-6393-9>

© The Editor(s) (if applicable) and The Author(s), under exclusive license to Springer Nature Singapore Pte Ltd. 2021

This work is subject to copyright. All rights are solely and exclusively licensed by the Publisher, whether the whole or part of the material is concerned, specifically the rights of translation, reprinting, reuse of illustrations, recitation, broadcasting, reproduction on microfilms or in any other physical way, and transmission or information storage and retrieval, electronic adaptation, computer software, or by similar or dissimilar methodology now known or hereafter developed.

The use of general descriptive names, registered names, trademarks, service marks, etc. in this publication does not imply, even in the absence of a specific statement, that such names are exempt from the relevant protective laws and regulations and therefore free for general use.

The publisher, the authors and the editors are safe to assume that the advice and information in this book are believed to be true and accurate at the date of publication. Neither the publisher nor the authors or the editors give a warranty, expressed or implied, with respect to the material contained herein or for any errors or omissions that may have been made. The publisher remains neutral with regard to jurisdictional claims in published maps and institutional affiliations.

This Springer imprint is published by the registered company Springer Nature Singapore Pte Ltd. The registered company address is: 152 Beach Road, #21-01/04 Gateway East, Singapore 189721, Singapore

To the founder President of Amity Education group Dr. Ashok K. Chauhan, the first person to have faith in me as an Editor.

To my father, mother, wife and my children whose constant motivation and enthusiasm helped me to work rigorously towards completion.

And to YOU, our readers for inspiring us to come up with this topic deemed fit with the current technological advancement.

Preface

Wireless communication and information security are the two most essential terms in the context of the Internet of Things, cloud computing, data mining, Industry 4.0, implementation of smart cities, etc. These are also the minimum requirement to understand the design and working of the recent technological advancement from the Internet of Things to smart cities, from intelligent radar radio to smart transportation, from connected interoperable devices to smart healthcare systems. As the devices, technologies to be used in these said applications would be intelligent, cooperative, connected and interoperable; therefore, it is essential for the scientists, engineers, industrialist and academicians to fully understand both the fundamentals and also the implementation and application principles of the emerging trends on wireless communication technologies and information security. This is so that they can use most of the appropriate and effective techniques to suit their design application needs.

Trends in wireless communication and information security is a precise yet complete book covering the wireless communications and intelligent systems, signal and image processing in engineering applications, data communication and information security, IoT and cloud computing, and intelligent electronic devices. This book marks its signature differently from the similar books available in more than one way. Each chapter in the book in regard to the fundamentals of technological aspects or implementation is amply illustrated with design, diagrams and validated with results. Each chapter comprehensively demonstrates its vision. Unlike most of the books of similar topics that are either superficially covering the topic in brief or is too voluminous having redundant information, this book is edited keeping in mind the research challenges faced by the scientists, research scholars and professors to be allowing them to propose some solution to the challenges faced working with the frontier electronics and computer technologies.

The book is divided into five parts covering the major subtopics of enabling wireless communication technologies and intelligent systems, Internet of Things and

cloud computing, signal and image processing in industrial and real-life applications, secured data communication and smart devices.

Jharkhand, India
Jharkhand, India
Arad, Romania
Majitar, India
Shillong, India

Mithun Chakraborty
Raman Kr. Jha
Valentina Emilia Balas
Samarendra Nath Sur
Debdatta Kandar

Acknowledgements

The frontier theme chosen for congregating the ideas of researchers, academicians and industrialist has attracted the attention of budding researchers across the globe with very high impact.

We extend our gratitude and thanks to all the contributors towards making the book on the topic of emerging trends on wireless communication and information security a comprehensive one.

We acknowledge the honest effort of all the stake holders in maintaining the actual benchmark towards reviewing of articles providing feedback for improvement and finally bringing out a strong scrutinized bunch of quality articles in this volume.

We would also like to take this opportunity to express our heartfelt thanks and appreciation to all the reviewers for sparing their valuable time in setting the benchmark of all the articles included in the volume.

Contents

Wireless Communications and Intelligent Systems

Free Space Optical Communications to <i>Connect the Unconnected</i> Globally in Remote Places: Technology Issues Relevant to Implementing Systems	3
Arun K. Majumdar	
A Study of Black Hole Attacks in Delay Tolerant Network	9
Puneet and Anamika Chauhan	
A Survey on Open-Source SCADA for Industrial Automation Using Raspberry Pi	19
Khaidem Bidyanath, Athon Abonmei, and Simon Tongbram	
Extended Microstrip Line-Fed Circularly Polarized Dielectric Resonator Antenna for WiMAX and 5G Applications	27
Ayan Pal, Arunabho Panja, Amibrata Samadder, Saswata Banerjee, Juin Acharjee, and Kaushik Mandal	
PPM-SIM Based FSO System Under Various Environmental Conditions	37
Pritam Keshari Sahoo	
Single Layered Mantle Cover for Cloaking at Dual Frequencies in Antenna Application	43
N. Kumutha and N. Amutha	
Optical Noise Cancellation Using Artificial Neural Network	53
Sarita Kumari	
Digital Chaos Encryption-Based Sub-Block Partition by a Hybrid PTS Approach and PAPR Reduction Using HSOSS Algorithm	61
Mrinmoy Sarkar, Asok Kumar, and Bansibadan Maji	

Millimeter Wave: A Novel Approach for Integrating Radar and Communication for Autonomous Driving	69
M. Chakraborty, A. Banerjee, D. Kandar, and B. Maji	
Throughput Analysis of MIMO HetNet System with Lattice Reduction Aided Precoding	81
Samarendra Nath Sur, Rabindranath Bera, Biswajit Dara, and Mithun Chakraborty	
Modern Radar Topology for Bio-medical Applications	89
Subhankar Shome, Mithun Chakraborty, Biswajit Dara, Rabindranath Bera, and Bansibadan Maji	
Ensuring Reliability in Vehicular Collision Avoidance Using Joint RFID and Radar-Based Vehicle Detection	99
Pallabi Biswas, Mithun Chakraborty, Rabindranath Bera, and Shubhankar Shome	
Signal and Image Processing in Engineering Applications	
Dimensional Analysis and Gradation of Rice Grain Using Image Processing	109
Suman Kumar Bhattacharyya and Sagarika Pal	
Feature Dimension Reduction for Efficient Classification of Dermoscopic Images with Feature Fusion	121
Rik Das, Anish Anurag, Govind Kumar Jha, and Mahua Banerjee	
Feature Edge-Detail Preservation of Random-Valued Impulse Noise in Images	129
Patitapaban Rath, Rajesh Siddavatam, and Pradeep Kumar Mallick	
Sparse Auto-encoder Improved Texture-Based Statistical Feature Estimation for the Detection of Defects in Woven Fabric	143
Sourav Tola, Sugata Sarkar, Jayanta K. Chandra, and Gautam Sarkar	
Evaluation of ML-Based Sentiment Analysis Techniques with Stochastic Gradient Descent and Logistic Regression	153
Mausumi Goswami and Pratik Sabata	
A Comparative Analysis of Sentiment Analysis Using RNN-LSTM and Logistic Regression	165
Mausumi Goswami and Prachi Sajwan	
Android-Based Assistance System for Visually Impaired Person Using Deep Learning and Augmented Reality	175
Abhigyan Baruah, Aryan Dev, Jasowanta Das, and Santanu Kumar Misra	

Data Communication and Information Security

Towards Data Storage, Availability and Scalability with the Aid of Blockchain 189
 Meenakshi Kandpal, Rabindra Kumar Barik, Chinmaya Misra, and Saneev Kumar Das

Countermeasures of Different Jamming Attacks in Wireless Sensor Networks 197
 Vikash Kumar Agarwal, Amit Kumar Rai, and Nitish Kumar

Detecting Acute Lymphoblastic Leukemia Through Microscopic Blood Images Using CNN 207
 Afrin Alam and Shamama Anwar

Blockchain Marketplace—A Novel Overview for Real-Time Implementation 215
 Anindita Jena

Applying Machine Learning Algorithms in Network-Based Intrusion Detection Systems 229
 Nilesh Kumar Sahu and Itu Snigdha

Principal Component Analysis in Body Sensor Networks for Secure Data Transmission 237
 Manorama and Itu Snigdha

Quantum Inspired Multiobjective Optimization in Clustered Homogeneous Wireless Sensor Networks for Improving Network Lifetime and Coverage 247
 Pradeep Kanchan, D. Shetty Pushparaj, and Baraá A. Attea

A Review of Wireless Charging in WSN 261
 Supriya Gupta and Md. Amir Khusru Akhtar

Vibration Measurement Using Accelerometer Sensor and Fast Fourier Transform 273
 Sarita Kumari

Intelligent Fire Outbreak Detection in Wireless Sensor Networks 281
 Dhiraj Chaurasia, Saikat Kumar Shome, and Partha Bhattacharjee

IoT and Cloud Computing

Lightweight Authenticated Encryption for Cloud-assisted IoT Applications 295
 Zainab S. AlJabri, Jemal H. Abawajy, and Shamsul Huda

Botnet Dynamics and Measures for India 301
 Md. Amir Khusru Akhtar, Mohit Kumar, and Ashwani Kumar

Google Controlled Car	311
Sagnik Ghosh and Prasun Chowdhury	
Security of IoT with Blockchain: Basic Study	319
Anindita Jena	
IoT-Based Smart Irrigation and Related Environment Parameters Monitoring: An Empirical Review	333
Parijata Majumdar, Sanjoy Mitra, and Munesh Chandra Trivedi	
Smart Water Management in Irrigation System Using IoT	341
Aparajita Das, Yasharth Gupta, Neeraj Vijay Wedhane, and Md. Ruhul Islam	
A Study on Cloud Employment Tracking System	353
Manisha Gupta, Poulami Paul, and Abhishek Roy	
A Study on Mediclaim Processing in Connected Healthcare System	363
Subhasish Mohapatra and Abhishek Roy	
Designing and Implementing Cloud Security Using Multi-layer DNA Cryptography in Python	375
Md. Irfan Alam and Satya Narayan Singh	
Intelligent Electronic Devices	
Nanometer-Scale Photodetectors for High Performance and Unique Functionality	389
Hiroshi Inokawa, Hiroaki Satoh, Amit Banerjee, Anitharaj Nagarajan, Revathi Manivannan, Alka Singh, Tomoki Nishimura, and Koki Isogai	
Design and Development of Terahertz Medical Screening Devices	395
M. P. Karthikeyan, Debabrata Samanta, Amit Banerjee, Arjya Roy, and Hiroshi Inokawa	
Design and Characterization of a Multilayer Reversible “Carry Look-Ahead Adder” by Using QCA Spin Technique	405
Rupsa Roy, Swarup Sarkar, and Sourav Dhar	
Author Index	415

About the Editors

Mithun Chakraborty is working as Professor, Department of ECE in Amity University Jharkhand, India. He has an earlier involvement of Professor in ECE in K L University, Andhra Pradesh, India. Dr. Chakraborty has 14 years of professional experience. He also has served as Associate Professor of ADAMAS University Kolkata, India. His research area is joint operation of radar and communication to facilitate next generation transportation systems. He has many national and international journal and conference publications. He has served as the reviewer of Circuits, Systems and Signal Processing Springer. Dr. Chakraborty has also organized many national level workshops and seminars and also played the role of convenor of national conferences.

Raman Kr. Jha is presently operating as Vice Chancellor of Amity University Jharkhand. He is responsible for providing strategic direction to the institution's employees and for fostering the University's high-level contacts. As an earlier involvement of VC of Indus International University, he has built on Indus's strong links with business and industry, both nationally and internationally. He established partnerships and research collaborations with leading universities in the USA, Malaysia, India, UK and Sri Lanka. Dr. Jha has been the recipient of a number of scholarships and awards including Merit Scholarship from Central Government, Scholarship from Centre of Advanced Studies in M.Sc. from the University of Delhi, UGC-CSIR NET fellowship during Ph.D. and Active Member of the Indian Academy of Science. Professor Jha's current research spans a broad range of interests, including quantum computing; image processing; group theory; neutrino physics; quarkonium physics and particlization of matter. He has also served as Principal, Dean, Student Affairs, Head of the Physics department and Head of the Department of Information Technology. He has also several national and international journal publications of high impact factor.

Valentina Emilia Balas is currently Full Professor in the Department of Automatics and Applied Software at the Faculty of Engineering, "Aurel Vlaicu" University of Arad, Romania. She holds a Ph.D. in Applied Electronics and Telecommunications from Polytechnic University of Timisoara. Dr. Balas is the author of more than

300 research papers in refereed journals and international conferences. Her research interests are in intelligent systems, fuzzy control, soft computing, smart sensors, information fusion, modeling and simulation. She is Editor-in-Chief to *International Journal of Advanced Intelligence Paradigms* (IJAIP) and to *International Journal of Computational Systems Engineering* (IJCSysE), Editorial Board Member of several national and international journals and is Evaluator Expert for national, international projects and Ph.D. thesis. Dr. Balas is Director of Intelligent Systems Research Centre in Aurel Vlaicu University of Arad and Director of the Department of International Relations, Programs and Projects in the same university.

Samarendra Nath Sur was born in Hooghly, West Bengal, India, in 1984. He received B.Sc. degree in Physics (Hons.) from the University of Burdwan in 2007. He received M.Sc. degree in Electronics Science from Jadavpur University in 2007 and M.Tech. degree in Digital Electronics and Advanced Communication from Sikkim Manipal University in 2012. He received his Ph.D. degree from NIT, Durgapur. Since 2008, he has been associated with the Sikkim Manipal Institute of Technology, India, where he is currently Assistant Professor in the Department of Electronics and Communication Engineering. His current research interests include broadband wireless communication (MIMO and spread spectrum technology), advanced digital signal processing and remote sensing. He is Member of the Institute of Electrical and Electronics Engineers (IEEE), (IEEE-IoT) Institution of Engineers (India) (IEI) and International Association of Engineers (IAENG). He has published more than 34 SCI/Scopus indexed international journal and conference papers. He was the recipient of the University Medal and Dr. S.C. Mukherjee Memorial Gold Centered Silver Medal from Jadavpur University in 2007. He also serves as the reviewer of *International Journal of Electronics*, Taylor and Francis, *IET Communication*, *Ad Hoc Networks*, Elsevier, and *IEEE transactions on Signal Processing*.

Debdatta Kandar has 16 years of professional experience. Currently holding the post of Associate Professor in the Department of Information Technology, NEHU, India. He also has served earlier S.K.P. Engineering College, Tiruvannamalai, Tamil Nadu, and Sikkim Manipal Institute of Technology, Sikkim. He has several years of industry experience too. He has authored more than 50 national and international journals and conferences and 5 book chapters and has supervised 7 Ph.D. research scholars. He received “Young Scientist” award from Union Radio Science International (URSI GA-2005) at Vigyan Bhawan, Delhi, for his research work. President of India, Dr. A. P. J. Abdul Kalam invited him to his residence on that occasion. The administrative responsibilities he has undertaken are Head, Department of Information Technology, NEHU, Chairman, Board of Undergraduate Studies in Information Technology, NEHU, Shillong, Member, Academic Council, NEHU, Shillong, Member, School Board, School of Technology, NEHU, Shillong, Member, Board of Professional Studies in Information Technology, NEHU, Member, Board of Professional Studies in Computer Applications Department, Member, Board of Professional Studies in Biomedical Engineering, and served as Members of various College Inspection Teams nominated by Vice Chancellor time to time.

Wireless Communications and Intelligent Systems

Free Space Optical Communications to Connect the Unconnected Globally in Remote Places: Technology Issues Relevant to Implementing Systems



Arun K. Majumdar

Abstract In this research work, I discussed the potential of free space optical communication (FSOC)/optical wireless communication [1–4] as the most viable technology solution for providing connectivity to almost half of the world population living in rural areas without any Internet access. This population is obviously missing out on the life-changing benefits of connectivity from financial services to health and education, job creation and civic/social engagement, just to name a few. Some of the reasons behind this “digital divide” include (according to World Economic Forum’s Internet for All report) • infrastructure (a good, fast connection is not available, no regular electricity to many people), • affordability (a large percentage of population living below the poverty line), • education, skills and cultural issues as barriers and local adoption and use (80% of online content is only available in ten languages).

Keywords FSOC · Wi-Fi hotspots · OWC · AO · SWD-WDM

1 Introduction

How to bridge The Digital divide?

I will focus on the potential technology based on optical wireless communication (OWC) to provide global Internet connectivity including remote places *anytime anywhere*. Connectivity can mean and fall in any of the categories like not connected (without any Internet connectivity), under connected (limited/intermittent connectivity), connected (access the Internet with medium download/upload speed) and state-of-the-art connectivity (very good and uninterrupted connectivity). The concept technology discussed in this paper also addresses how to provide basic connectivity to the unconnected population.

A. K. Majumdar (✉)
San Diego, CA 92111, USA
e-mail: a.majumdar@ieee.org

Colorado State University, Pueblo, CO 81001, USA

Some Background and Recent Statistics

Demand for High-Speed Communication and Tremendous Growth of Data traffic.

- Over 80% of the world will be connected to the Internet by 2020 via mobile phones, smart devices, social web, gaming and video-centric applications.
- There will be 5.3 billion total Internet users (66% of global population) by 2023.
- Globally, there will be nearly **628 million public Wi-Fi hotspots**
- **Mobile** plus everyday application services (talking, **Facebook, YouTube, Video entertainment, video gaming**, etc.) need high-speed Internet: Global Internet users will continuously increase and most will be mobile.
- Future data speed of 10 gigabit speeds in the coming years.
- Billions of people in developing world are still without Internet access, new UN report finds.

1.1 Digital Divide

Global connectivity with high-capacity communications can bridge the digital divide—critical to economic opportunity, job creation, education and civic engagement.

Potential Technology Solution:

Free Space Optical Communication by Developing Global Internet Connectivity.

Why optical wireless communications (OWC)?

- RF: 300 kHz–300 GHz
- Optical: 300 THz (1 THz = 10^{12} Hz)
- Aperture size (antenna size/telescope size) and range.

Huge Modulation Bandwidth.

RF and microwaves: bandwidth up to 20% of the carrier frequency.

Optical ~1% of carrier frequency ($\sim 10^{16}$ Hz), allowable bandwidth 100 THz ($\sim 10^5$ times that of a typical RF carrier).

Shorter wavelength of optical beam helps to stay more focused.

“Global Internet Connectivity” or “Connecting the Unconnected”.

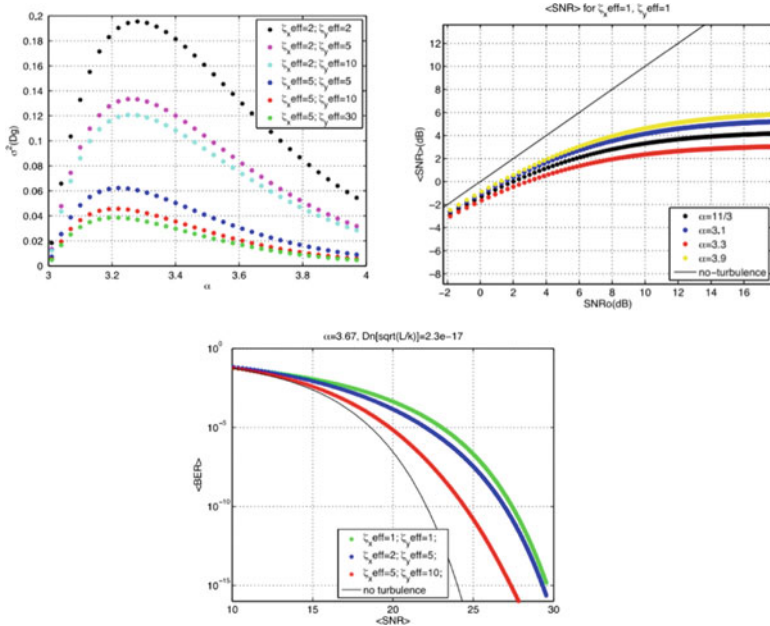
Potential Solution:

- Need to bring reliable and affordable Internet to those without it
- Requires rural backhaul connectivity (FSO links, HAP, Satellite, Underwater): High-speed backhaul in rural areas
- All optical-based free space optics (FSO) technology for creating a three-dimensional global communication grid: A powerful tool to address connectivity bottlenecks and can allow worldwide access to the Internet independent of terrestrial limitations (wireless links through air and satellite communications providing access to fixed and mobile services)

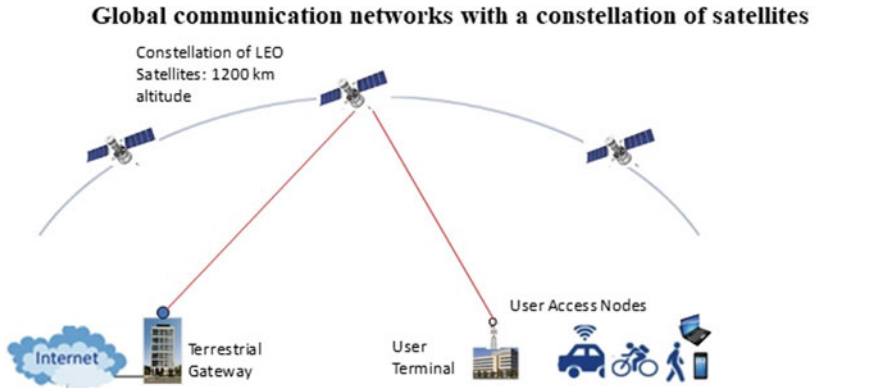
- Can handle indoor, outdoor, terrestrial, space and underwater links
- Visible Light Communication (VLC) can provide state-of-the-art practical solutions by creating Li-Fi for both fixed and mobile platforms toward all optical networks for Internet connectivity.

Critical issues to implement FSOC/OWC technology to accomplish global connectivity.

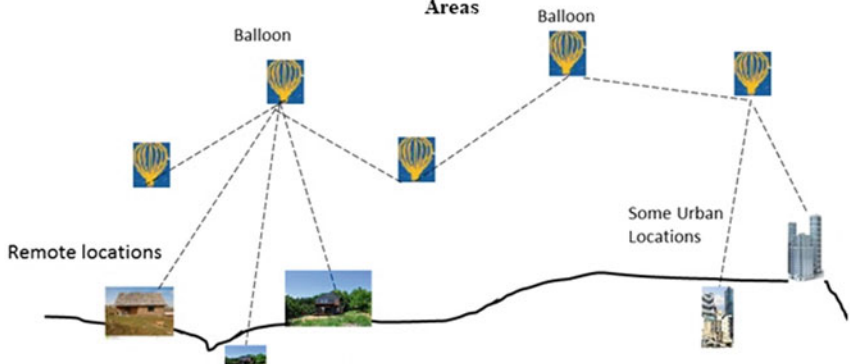
- Atmospheric optical propagation effects due to anisotropic turbulence (non-Kolmogorov models) (asymmetric slant paths / uplink and downlink) between fixed or moving platforms for full-duplex communication data transfer direct effects on FSO link performance (scintillation index, probability of fade, SNR and BER) for OWC systems beam spread and wander, and influence of wind speed through anisotropic non-Kolmogorov turbulence: significant effects on OWC performance
- When a constellation of satellites or a number of balloons are used to establish remote connectivity, optical propagation path/communication links characteristics change: need to use seamless switching methods to handover in the presence of slightly different propagation paths (for hybrid satellite/terrestrial networks): angular diversity and temporal variations
- Establish efficient and reliable optical networks for terrestrial, air, space and underwater terminals.



Reference: Italo Toselli and Olga Korotkova, "General scale-dependent anisotropic turbulence and its impact on free space optical communication system performance," JOSA A, Vol 32, No. 6/June 2015



A schematic of a basic concept similar to Project Loon to build ring of connectivity in Remote Areas



Source: Arun K. Majumdar, "Optical Wireless Communications for Broadband Global Internet Connectivity: Fundamental and Potential Applications," Elsevier, Amsterdam, Netherlands 2019

1.2 Some Final Comments

For very rural and remote areas to establish connectivity, important concerns will be

- Very low cost: Smart phones should be available and extremely affordable
- Reliability: Engineers and technicians are not available to fix the problems

Some specific potential technology solutions:

Optical satellite and (a constellation of optical satellites) providing Internet together with free space optical communications are wireless telecommunications networks to beam data over Earth's surface at nearly the speed of light, and to provide cheap, fast Internet to remote areas, airplanes, ships and cars.

The solution to the problem of our world of increasingly digitally interconnected is light. Visible light communication (VLC) technology has tremendous indoor and outdoor applications for secure network access (Li-Fi) and extensively adopting in

retail, hospitals, residential, commercial, smart cities, aviation and many more even in remote areas. VLC LED-based channels promise to deliver high-speed data in many environments with high SNR and minimum infrastructure expenses.

- Adaptive optics (AO) can offer potential solutions.
- Some recent research and development areas which will help in achieving connecting to remote areas include:
Photonics switching hardware for fast optical networks, for example high-capacity SDM-WDM optical networks, low-latency Li-Fi mobile networks, vehicular optical camera communication (OCC) and mobile backhaul, integrated photonic switch (with the lowest signal loss in high-speed data transmission) development toward the goal of “fully optical” high-capacity switching
Broadband over power lines and VLC using street lights
- Nanofabrication technology will hopefully be a key enabler to such integration, reducing cost and power consumption, size and weight. Adaptive optics (AO) can offer potential solutions for optical satellites or balloons solutions for accomplishing high data rate in various turbulence propagation paths.

One special example just appropriate for the current COVID-19 situation.

Assuming the all optical wireless communication connectivity is established, this special example describes a proposed architecture of establishing communication link for delivering medical consultation services in remote and isolated locations in both developed and developing countries. The technique is based on multi-hop relay-based free space optical communication link for delivering medical services in remote areas [5].

References

1. Majumdar AK, Ricklin JC (eds) (2008) Free-space laser communications: principles and advances. Springer
2. Majumdar AK (2015) Advanced free space optics (FSO): a systems approach. Springer
3. Majumdar AK (2019) Optical wireless communications for broadband global internet connectivity: fundamental and potential applications. Elsevier, Amsterdam, Netherlands
4. Majumdar AK, Ghassemlooy Z, Arockia Brazil Raj A (eds) (2019) Principles and applications of free space optical communications, IET (The Institution of Engineering and Technology, UK)
5. Miglani R, Malhotra JS, Majumdar AK, Tubbal F, Raad R (2020) Multi-hop relay based free space optical communication link for delivering medical services in remote areas. IEEE Photon J 12(4)

A Study of Black Hole Attacks in Delay Tolerant Network



Puneet and Anamika Chauhan

Abstract DTN is the latest growing technology having unique characteristics such as longer delays, intermittent connectivity and limited resources or constrained resources. Delay tolerant networks is a store and forward method which delivered the messages to the nearest potential forwarder by replicating copies of the original messages. DTN is created to handle long delays in wireless networks and handle the intermittent connectivity. An information at particular node is delivered only if it has higher particular than the current node. DTN is studied and implemented in opportunistic network environment (ONE) simulator. DTN is having characteristics like disconnected paths, long delays, higher mobility, uplinks, and downlinks, which leads to network vulnerabilities. These vulnerabilities lead to the compromisation of nodes and can cause security threats as these compromised nodes can disrupt the routing protocols in the network. DTN is exposed to different network layer attacks. Attacks on network layer like gray hole and black hole attack can destroy the topology of the network resulting in loss of data and damage to the network. This paper discusses about the black hole, type of black hole attacks, and different detection techniques in delay tolerant networks.

Keywords Delay tolerant network (DTN) · Wireless networks · Network connectivity · Opportunistic network environment (ONE) · ONE simulator

1 Introduction

A DTN is an ad-hoc network which tries to resolve various issues of heterogeneous networks such as facing failures in point to point and continuous connectivity. DTN is extremely useful in various applications areas such as: providing connectivity in remote areas where providing an infrastructure connection is costly, wireless sensor

Puneet (✉) · A. Chauhan
Department of Information Technology, Delhi Technological University, New Delhi, India
e-mail: puneetbisarwal@gmail.com

A. Chauhan
e-mail: anamika@dce.ac.in

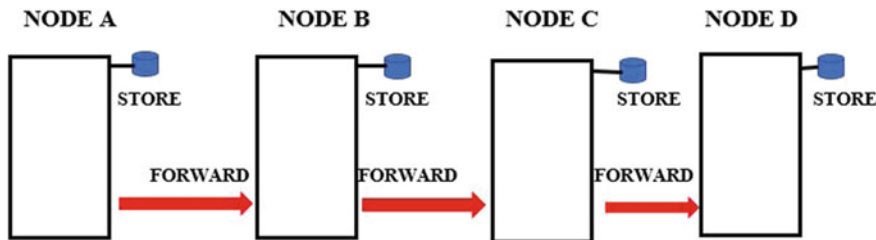


Fig. 1 Store and forward message

network for tracking wildlife animals and birds, military communications and control sensors, and equipment. DTN networks are highly desirable for use in war-prone areas, remote places in relief efforts, and in disaster scenarios. DTN which is also known as delay and disruption-tolerant network is used where there is a lack of connectivity in the network which results in spontaneous end-to-end paths being insufficient for communication. In such cases where there are no network infrastructures, a critical mode of communication can be given by DTNs network. DTN is a complete wireless network as there is no base station as compared to an existing wireless network.

DTN is a type of architecture in which it can forward, store, or carry the messages. It stores information in the node buffer until a possible forwarder is found and forward it to the next node's buffer which is available in the network [1].

In DTN protocol stack, there is a bundle layer, and in this layer, the messages are stored as "bundles." These bundles are sent as soon as they come across with a receiver node. The requirement for DTN network is due to node disconnection by equipment failure (Fig. 1).

In DTN, message transmission through intermediate nodes is difficult because the intermediate nodes can act as a malicious node, a malicious node either drop the message or not forward the message to the destination.

In DTN, in scenarios where nodes have intermittent and opportunistic communication connectivity, networks are established. DTN does not have a very large storage space, very limited power supply, and battery-operated devices may be used. One of the challenges of DTNs is the intermittent connectivity while another challenge may be handling misbehaving nodes. Misbehave means acting badly or improperly. Misbehave node in a network does not perform its task properly. It is possible to classify misbehaving nodes into two types: malicious and selfish. A selfish node is one which drops all messages to save its own energy and prefers not to contribute to the network while forwarding only its own packets or messages. Malicious nodes acts as a forwarder and sends copies of the original message to as many nodes as possible. These nodes attempt to hamper various parameters of the network. Malicious nodes attack routine network operations and are not concerned about their gains in the process. To handle these types of nodes, DTN security protocols must be more invulnerable and powerful. The existence of such nodes in vehicle DTNs

results in the loss of crucial data or messages that may trigger more road accidents or may cause resource wastage in resource constraints DTNs.

The structure of the paper is defined below. Architecture of DTN is discussed in Sect. 2. While challenges in DTN are discussed in Sect. 3. In Sect. 4, we had discussed AODV protocols, black hole attacks, and different detection techniques. In Sect. 5, conclusion and future work is discussed.

2 DTN Architecture

In extreme and challenging environmental conditions, continuous connectivity is not feasible. DTN research group [2] developed the architectural and protocol design principles required to address this problem and provide interoperable communications in such environments. Example-space network (SN), deep space network (DSN), military equipment, underwater submarines, forms of disaster response, and ad-hoc sensors/actuator networks.

Initially, Kevin Fall proposed the challenged network in delay tolerant networks in 2003, but it was properly documented and standardized by the DTN research group as RFC 4838 in 2007 [3, 4]. Message switching abstraction is a key component in the DTN network and is developed to work as an overlay network. It works on top of protocol stack for the various types of networks to make provision for the gateway feature between them, also called 'bundle layer' [5].

The DTN architecture requires a small re-vamp of the design of the Internet protocol layer that had already been developed. Depending on their appropriateness for each region in the network, the transport layer below the bundle layers is chosen. Figure 2 gives us an idea or an overlay of how the bundle layer looks like compared to the Internet protocol layers.

3 Challenges in DTN

We discussed various challenges during data transmission in DTN in this section. These are the following areas:

- i. **Capacity to Store:** The capacity to store message of every node is limited or confined. Due to this, at whatever point an experience happens to the node, the node attempts to swap each and every information they have in their storage or buffer. If the nodes have an unlimited storage capacity, the node will flood it with similar kind of information or messages, and adversity will arise [6].
- ii. **Battery or Power Constraints:** The battery or power constraint is limited to the node. So, the node have to perform their operations in that limited battery.
- iii. **Network Capacity:** Limiting the basic system is also a crucial element in determining the measure of information that can be transmitted. On the off chance

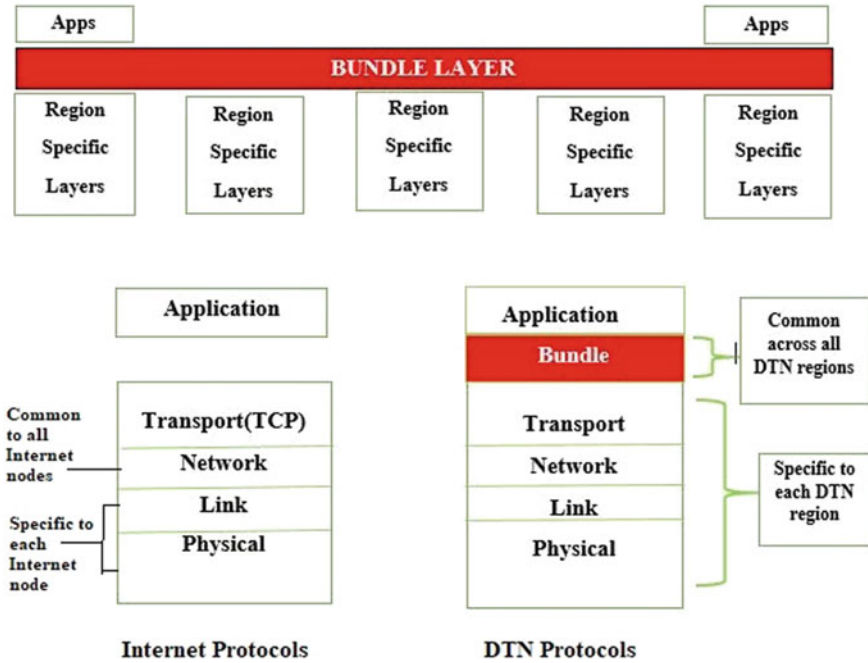


Fig. 2 DTN bundle layer architecture

that, in the mid of experience, different nodes are trying to forward information, and the system may be congested. Therefore, this component decides whether or not to divide a message or data packets with a specific end goal of transmitting it from source to target node.

- iv. Encounter Schedule: Every node has a specific end goal of sending the data from the transmitter to the destination node, the node will not transmit if the receiver’s node is unreachable and immediately transmit the message to the receiver’s node if it becomes reachable.

4 AODV Protocol

4.1 Ad-hoc on Demand Distance Vector Protocol (AODV)

Route Discovery

It uses route request (RREQ) packet which is broadcasted by the sender’s node for the discovery of the route in the network. After that, the participating nodes continuously look over the routing table to get the path for the receiver’s node [7]. In the end, the route reply packet (RREP) is transmitted to the sender’s node, if it discovers a better and updated route in the network. When multiple route requests are received, then the

node chooses the shortest route for data transmission. Figure 3 indicates the details in RREQ and RREP.

Maintenance of Route

The nodes in mobile ad-hoc network (MANET), as the name suggests have mobility. The routes are being divided into sender and receivers if there is any change in the topology [8]. At this point, the route error (RERR) packet will be produced if there is any breakage in the route.

4.2 Black Hole Attack

The malicious node can provide a manipulated metrics to other nodes that comes into contact with the malicious nodes and attracts packets from the attacks which is done by black hole. In this attack, most of the data packets of the participating nodes are attracted by the malicious nodes. The node forcefully tries to create a path by its own. When the path is created, then instead of forwarding packets the malicious node drops them, thus creating a black hole.

The effect of black hole is that it exploits routing protocols like AODV, and its functionality in the network is degraded.

Black hole types [9].

Single node black hole

There is only one malicious node present between the transmitter and the destination (Fig. 4).

Source IP	Source Sequence Number	Destination IP	Destination Sequence Number	Lifetime
-----------	------------------------	----------------	-----------------------------	----------

(a)

Source IP	Source Sequence Number	Destination Sequence Number	Timestamp	Lifetime
-----------	------------------------	-----------------------------	-----------	----------

(b)

Fig. 3 Packet in AODV **a** RREQ, **b** RREP

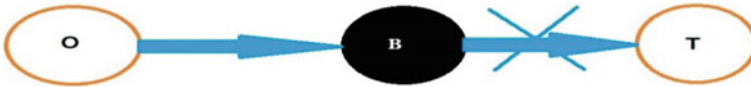


Fig. 4 Single node black hole

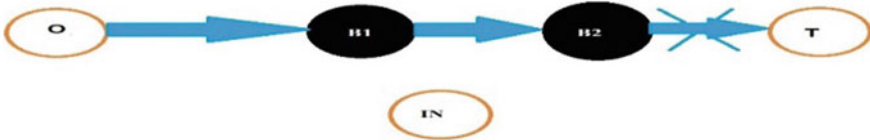


Fig. 5 Multiple black hole node

Multiple Black Hole

There are many malicious node present between the sender and the receiver (Fig. 5).

Origin node 'O' tries to find a path for data transmission to the target node 'T' as shown in Fig. 6. It begins the process of route discovery by transmitting the packet of RREQ across the entire network. From Fig. 6, we can see that nodes 'B' and '1' accept the RREQ data packet from origin 'O'. Black node is a hostile node, and hence, it immediately produces RREP data packets without examining its routing tables.

Origin node 'O' immediately receives RREP from the black node, so it initiates data transfer to the black node, presuming it generates the shortest route to target node 'T'. Malicious black node discards the data packets, instead of sending those to the target node 'T', thus the decrease of overall throughput in the network can be seen (Table 1).

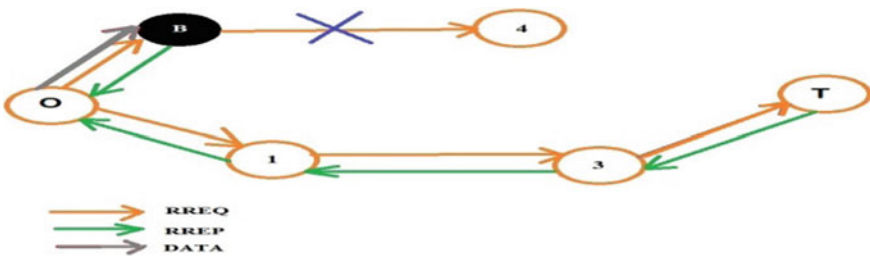


Fig. 6 Black hole attack in AODV

Table 1 Comparative analysis of black hole attack

Sr. no.	Techniques	Routing protocol	Simulator	Results and remark
1	Reply based on destination and next hop information scheme [10]	AODV	NS-2	Throughput is increased in ADOV, and the overhead is minimized. Malicious node is not found which act in group
2	Scheme based on shared hop and sequence number [11]	AODV	NS-2	Verify routes from 80 to 99% due to long delays, the last sequence number can be put in the table by the attacker
3	2-ACK scheme [12]	Dynamic source routing (DSR)	NS-2	Packet delivery ratio (PDR) is achieved up to 91% even if the node is malicious at 40% challenging to derive triplet information
4	Ignorance scheme [13]	ADOV	NS-2	Minimize additional overhead, PDR increased by 19% node packet loss in the network increased by 4%
5	Sequence number and voting scheme based on neighbors [14]	AODV	–	False detection rate is reduced, and malicious node was not found in the group
6	Neighbors opinion scheme [15]	AODV	–	With minimal delay and overhead, better security is achieved, and PDR is high with few additional delay
7	Packet delivery information scheme [16]	PROPHET	NS-2	100% is the detection rate, false positive rate is less, More independent examination method
8	Sequence number scheme [17]	AODV	NS-2	More packets delivered, data packet drops are dependent on the number of nodes and speed
9	Ranks given to nodes [18]	Modified AODV	–	Can judge new nodes as a black hole, energy efficient

(continued)

Table 1 (continued)

Sr. no.	Techniques	Routing protocol	Simulator	Results and remark
10	Using ‘NTT’ & ‘PB’ for Neighbor trust values [19]	AODV, TSDRP	NS-2	Present in large network, robustly built, overhead increased additional node calculations
11	NHBADI [20]	AODV	NS-2	Delay decreased, packet delivery fraction (PDF) increased
12	Using threshold levels for secure route discovery (SRD) [21]	AODV, SRDAODV	NS-2	Increase in packet delivery fraction (PDF) and overhead
13	Using ‘fm’ and ‘rm’ for Neighbor trust values [22]	Modified AODV	NS-2	Increase in PDF and overhead. Nodes must perform additional calculations
14	Base node sends bogus RREQ packets [23]	AODV	NS2-2.34	Increase in throughput, packet delivery ratio and slight increase in delay. Cannot protect against black hole node without base node

5 Conclusion and Future Work

The paper describes, various attack in DTN, its architecture, and its challenges that are presented. This review paper also describes about malicious and selfish nodes which is a major security challenges. This paper also compare black hole attack detection schemes with results, and limitations have been provided. In future, it is intended to propose a new methodology that detects black hole nodes and prevent network from black hole node attack.

References

1. Goncharov V (2010) Delay-tolerant networks. Institut fur Informatik, Albert Ludwigs Universitat Freiburg, Lehrstuhl fur Rechnernetze und Telematik
2. IRTF (2009) Delay tolerant networking research group, <https://www.dtnrg.org>
3. Kevin F (2003) A delay-tolerant network architecture for challenged internets. In: Proceedings of the 2003 conference on applications, technologies, architectures, and protocols for computer communications. ACM, pp 27–34
4. IRTF (2007) RFC 4838—DTN Architecture, <https://www.ietf.org/rfc/rfc4838.txt>
5. Warthman F (2012) Delay-and disruption-tolerant networks (DTNs). A Tutorial. V.0. Inter-planetary Internet Special Interest Group

6. Khabbaz MJ, Assi CM, Fawaz WF (2011) Disruption-tolerant networking: a comprehensive survey on recent developments and persisting challenges. *IEEE Commun Surveys Tutor* 14(2):607–640
7. Tamilselvan L, Sankaranarayanan V (2007) Prevention of blackhole attack in MANET. In: *The 2nd international conference on wireless broadband and ultra wideband communications (AusWireless 2007)*. IEEE, pp 21–21
8. Mandala S, Abdul HA, Abdul SI, Habibollah H, Md AN, Yahaya C (2013) A review of blackhole attack in mobile adhoc network. In: *2013 3rd international conference on instrumentation, communications, information technology and biomedical engineering (ICICI-BME)*. IEEE, pp 339–344
9. Su M-Y, Kun-Lin C, Wei-Cheng L (2010) Mitigation of black-hole nodes in mobile ad hoc networks. In: *International symposium on parallel and distributed processing with applications*. IEEE, pp 162–167
10. Deng H, Li W, Agrawal DP (2002) Routing security in wireless ad hoc networks. *IEEE Commun Mag* 40(10):70–75
11. Al-Shurman M, Seong-Moo Y, Seungjin P (2004) Black hole attack in mobile ad hoc networks. In: *Proceedings of the 42nd annual Southeast regional conference*. ACM, pp 96–97
12. Liu K, Deng J, Varshney PK, Balakrishnan K (2007) An acknowledgment-based approach for the detection of routing misbehavior in MANETs. *IEEE Trans Mob Comput* 5:536–550
13. Dokurer S, Erten YM, Can EA (2007) Performance analysis of ad-hoc networks under black hole attacks In: *Proceedings 2007 IEEE SoutheastCon*. IEEE, pp 148–153
14. Deb, M (2008) A cooperative black hole node detection mechanism for ADHOC networks. In: *Proceedings of the world congress on engineering and computer science*, pp 343–347
15. Medadian M, Mohammad HY, Amir MR (2009) Combat with black hole attack in AODV routing protocol in MANET. In: *2009 First Asian himalayas international conference on internet*. IEEE, pp. 1–5
16. Ren Y, Mooi CC, Jie Y, Yingying C (2010) Detecting blackhole attacks in disruption-tolerant networks through packet exchange recording. In: *2010 IEEE international symposium on a world of wireless, mobile and multimedia networks (WoWMoM)*. IEEE, pp 1–6
17. Tseng F-H, Chou L-D, Chao H-C (2011) A survey of black hole attacks in wireless mobile ad hoc networks. *Hum-Cent Comput Inf Sci* 1(1):4
18. Biswas S, Tanumoy N, Sarmistha N (2014) Trust based energy efficient detection and avoidance of black hole attack to ensure secure routing in MANET. In: *2014 applications and innovations in mobile computing (AIMoC)*. IEEE, pp 157–164
19. Chaubey, N, Akshai A, Savita G, and Keyurbhai AJ (2015) Performance analysis of TSDRP and AODV routing protocol under black hole attacks in manets by varying network size. In: *2015 fifth international conference on advanced computing & communication technologies*. IEEE, pp 320–324
20. Babu MR, Usha G (2016) A novel honeypot based detection and isolation approach (NHBADI) to detect and isolate black hole attacks in MANET. *Wireless Personal Commun* 90(2):831–845
21. Tan, S, Keecheon K (2013) Secure Route Discovery for preventing black hole attacks on AODV-based MANETs. In: *2013 IEEE 10th international conference on high performance computing and communications & 2013 IEEE international conference on embedded and ubiquitous computing*. IEEE, pp 1159–1164
22. Siddiqua A, Kotari S, Arshad AKM (2015) Preventing black hole attacks in MANETs using secure knowledge algorithm. In: *2015 international conference on signal processing and communication engineering systems*. IEEE, pp 421–425
23. Jain S, Ajay K (2015) Detecting and overcoming blackhole attack in mobile Adhoc Network. In: *2015 international conference on green computing and internet of things (ICGCIoT)*. IEEE, pp 225–229

A Survey on Open-Source SCADA for Industrial Automation Using Raspberry Pi



Khaidem Bidyanath, Athon Abonmei, and Simon Tongbram

Abstract Modern industries require advance monitoring, controlling, and reliable supervision of the various industrial processes. In today's world, industries use computer-integrated manufacturing (CIM) to create an automation process of production systems with the use of computers. Besides the use of CIM, industries also use programmable logic controller (PLC) for industrial automation in supervisory control and data acquisition (SCADA) system. These systems, i.e., CIM, PLCs are expensive and use specialized advance software which becomes a barrier for most of the medium and small size industries for their automation process. In this survey paper, different authors replaced programmable logic controller (PLC) by Raspberry Pi which is a small computer. Replacing PLC by Raspberry Pi reduces the cost of constructing an automation system and also has its own built-in Wi-Fi, USB, Ethernet, Bluetooth, HDMI, etc. This paper surveys different methods for creating an automation system for the industrial process using various specialized software using SCADA along with Raspberry pi (a low-cost computer which can act as a soft PLC).

Keywords CIM · SCADA · PLC · Python · Raspberry Pi

1 Introduction

Industrial automation is the phenomenon of using control systems such as computers, robots, etc., in industries for handling different processes without the use of manual labor. Operators, automation systems, monitoring systems, etc., and many other systems are involved in a production line which produces lots of data. To handle these enormous amounts of data, the methods of CIM systems are being used and

K. Bidyanath (✉) · A. Abonmei · S. Tongbram

Department of Electrical Engineering, National Institute of Technology, Manipur, India
e-mail: khaidembidyanath@gmail.com

A. Abonmei

e-mail: athonjob@gmail.com

S. Tongbram

e-mail: simontongbram@gmail.com

are explained in [1]. In SCADA systems, the hardware components of industries and factories are being controlled in real time with the transfer of data. Supervisory control and data acquisition (SCADA) are a control system architecture that uses computers, data communication systems and graphical user interface (GUI) for supervisory monitoring and controlling of several processes and activities and also uses other devices such as PLC and PID controllers to interface with the industrial processes. Today's industrial automation system came into existence through different stages, and these different stages of automation system are discussed in [2]. With the advancement of microprocessors and microcontrollers, several new tools such as PLCs come into existence.

Different methods for automation systems for industries are available such as [3] presents the development of a SCADA system using relays in smart transmission system laboratory. Paper [4] discusses the method for constructing a SCADA system for controlling a boiling system. In the SCADA system, all the workstations are connected to a centralized control unit or system such as PLC, and this is explained in [5]. Paper [6] introduces a SCADA device that behaves as a remote terminal unit (RTU) and also collects the required information from the PLC.

In [7], an open-source SCADA system is constructed which is associated with OPC-UC middleware solution. The paper [7] gives details information about the various structures for programmable control systems such as structured text (ST), ladder diagram (LD), sequential function chart (SFC), instruction list (IL), function block diagram (FBD). In [8], the concept of industrial automation in small-scale industries like paper cutting using a programmable logic controller (PLC) is introduced. The paper [9] introduces a method for controlling the flow of water for a specific amount of time using solenoid which is being controlled by PLC. Similarly, [10] gives the idea of controlling water flow using PLC and SCADA. The idea of human-machine interface (HMI) is used in [11].

This survey paper is divided into six sections: Sect. 1, introduction, Sect. 2, important terms and definitions discussing some terms used in SCADA system and industrial automation, Sect. 3, analysis of the systems discussing some methods for the industrial automation using SCADA system, Sect. 4, discussing the implementation methods of the proposed systems, Sect. 5 consequence: discussing the results obtained from these proposed systems, and Sect. 6, conclusion.

2 Important Terms and Definitions

2.1 Supervisory Control and Data Acquisition (SCADA)

It is a computer system for collecting and evaluating actual-time information. SCADA systems are mainly used for observing and manipulating electrical appliances or devices mainly in industries like machinery, energy, oil refining, and conveying, etc. The basic SCADA system consists of a programmable logic controller

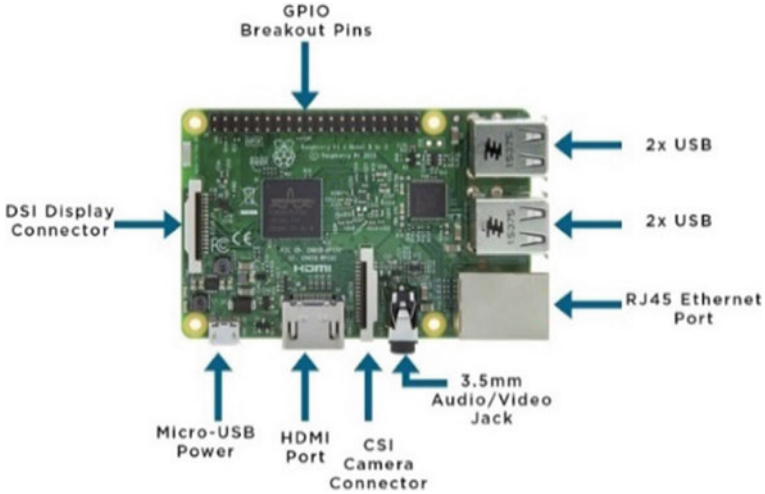


Fig. 1 Raspberry Pi

(PLC) or remote terminal unit (RTU). PLCs and RTUs gather the information from the industrial appliances or devices, sensors, and transfers these collected messages to the computer with SCADA software.

2.2 Raspberry Pi

The Raspberry Pi is one of the cheapest computers which helps students in learning computer programming and even professionals in their projects. Raspberry Pi runs on open-based software and allows mixing and matching software according to our work (Fig. 1).

2.3 Programmable Logic Controller (PLC)

A PLC is a computer mainly construct to perform accurately even in rigid external environments which mainly include high temperatures extremely dry seasons, rainy seasons, etc. PLC’s main function consists of automation of the factory activities such as the conveying systems. It can also be set up and modify according to the function and requirement of the activity or function of the plant. The main advantage of using PLC is that it can be re-programmed for other tasks.

2.4 Computer-Integrated Manufacturing (CIM)

Computer-integrated manufacturing indicates the utilization of computers for machinery and computerization of various industrial activities. CIM consists of different systems like computer-aided design (CAD) and computer-aided manufacturing (CAM) which gives less amount of error and decreases the use of human involvement in the industrial processes. It is mostly used in automation, rockets, space constructing factories, etc.

2.5 Python

Python is a simple and an object-oriented programming language. Python is easy to learn and simple programming language compared to other programming languages.

2.6 Remote Terminal Unit (RTU)

A remote terminal unit is an electronic device that consists of a microprocessor. The device is connected or interfaced with different objects such as sensors. The whole RTU acts as a part of a SCADA system and controls the electrical devices from the incoming information of the sensors.

2.7 Master Terminal Unit (MTU)

In the SCADA system, the master terminal unit commands the RTUs which are installed at remote places to gather the messages or information, stores them and processes the information to human interfaces, and helps to take control decisions.

2.8 Opc-Ua

OPC unified architecture is a machine-to-machine transmission manner for industrial automation construct by the OPC Foundation.

3 Analysis of the Systems

In this survey section, different industrial automation systems proposed by different authors are being discussed.

In industrial automation, there are compatibility issues while combining different systems, so, paper [12] uses the free OPC-UA project in the SCADA system to avoid compatibility issues that is communicating between different systems. The OPC server of this proposed system is being developed in Raspberry Pi, and they use Linux as their operating system for the Raspberry Pi. For this proposed system, the OPC-UA server has the ability to controlling databases using MySQL, real-time monitoring of the systems. The main aim of developing this SCADA system is for controlling a DC motor with the help of a motor driver.

The diagram of the system for the suggested system of [12] is given below (Fig. 2).

Industrial automation can also be done with the help of the Internet such as [13] uses the World Wide Web for collecting real-time data from the devices (Fig. 3).

Fig. 2 System overview for controlling the speed of DC motor

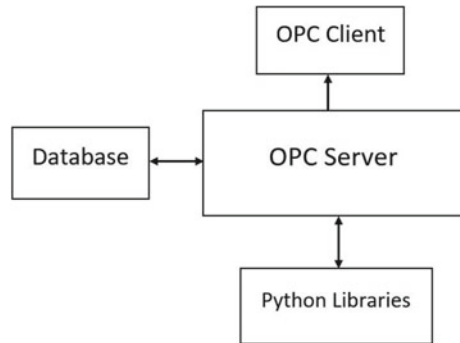


Fig. 3 SCADA system using internet

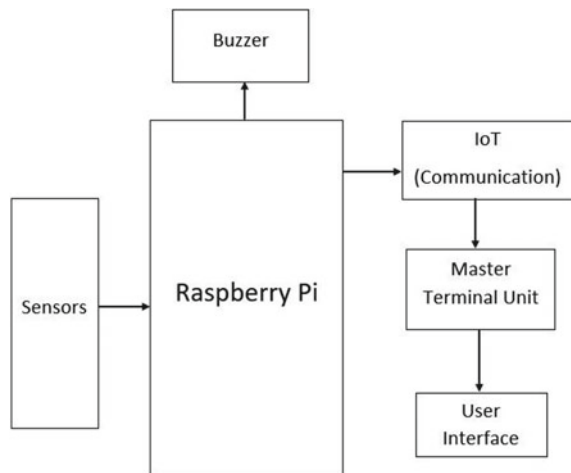
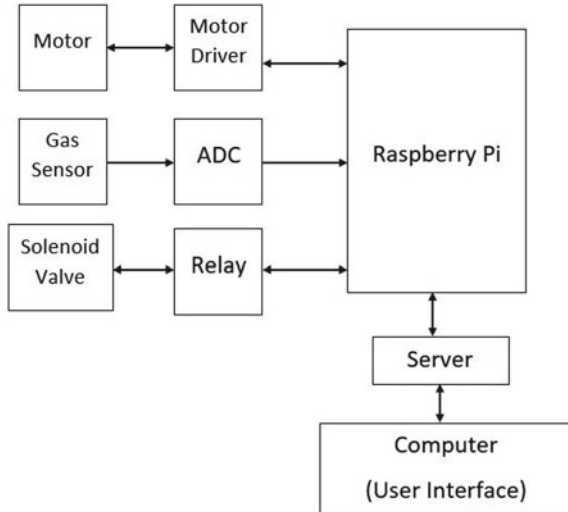


Fig. 4 SCADA system using Raspberry Pi



The above diagram uses Raspberry Pi as a controller for controlling various sensors, i.e., temperature sensor, vibration sensor, etc. The data collected by the sensors is being transferred to the controller, i.e., Raspberry Pi and is received by the computer of the user with the help of IoT. The user can control the actions of the sensors through the computer’s user interface.

The paper [14] created a SCADA system for industrial automation without the use of OPC server and OPC client, which makes it very easy to monitor and control the whole system. The main aim and objective of [14] is to observe and manipulate the devices remotely without the use of manual labor. In this system, the Raspberry Pi acts as a programmable logic controller (PLC). Their proposed system consists of controlling a DC motor, a gas sensor, and a solenoid valve. The data from these devices are transferred directly to the Raspberry Pi acting as a PLC. The data received by the Raspberry Pi is then transferred to the server. From the computer, the devices are being monitored and controlled remotely. The server of [14] is being created with the use of Microsoft Surface Studio (Fig. 4).

4 Implementation of the SCADA Systems

In this survey section, the implementation process of different systems is being explained in detail. The architecture of the system implementation of [12] is performed with the interactions of the three levels, i.e., field control, which consists of different types of sensors, control level, which helps in controlling the various devices used in their proposed system, and supervisory level which helps in collecting data from various devices and monitoring the whole systems. This system develops the

SCADA or human-machine interface (HMI) in Python and is being developed as an OPC client which is going to connect to the OPC server for collecting the actual-time information of the various devices. This specific system has its fault sensing technique (i.e., AFTC system).

Paper [13] uses Python language for the user interface of the SCADA system. All the sensors of the system of [13] are connected to the Raspberry Pi, which acts as a controller. The information collected from the sensors is transferred to the microcontroller, i.e., Raspberry Pi, and the data can be seen on a screen.

[14] creates its server using Microsoft Azure. For the proper working of the virtual machine, the authors installed UBUNTU on the virtual machine. To monitor the data about the devices, a graphical user interface is created using Microsoft Visual Studio. For the Raspberry Pi which is going to act as a PLC, the authors installed Raspbian Stretch on the Raspberry Pi. For receiving data from the gas sensor, an analog-to-digital converter is used (ADC). The authors use the pulse width modulation method for controlling and monitoring the DC motor.

5 Consequences

In this survey section, the results and consequences of the SCADA system proposed by different authors are being discussed with details. Paper [12] develops their system perfectly by controlling the DC motor. One of the most important advantages of [12] is the detection of faults, and the type of faults will be displayed on the human-machine interface (HMI) of the SCADA system.

The SCADA system of [13] for the industrial automation system controls the sensors which are connected to the Raspberry Pi. Sensors such as temperature sensors and proximity sensors are being controlled in real time. The system of [13] supports the monitoring and controlling different devices from a computer with the use of the Internet for transferring of data. This proposed system is low cost and gave an idea about adding different kinds of sensors to an industrial system for the monitoring and controlling purposed.

Paper [14] controls their devices, i.e., DC motor, gas sensor, and solenoid valve, with the help of GUI that they developed. For their system, when they set the motor to a specific rpm, the DC motor starts rotating at that specific rpm, for the gas sensor, the alarm turns on when the sensor detects any faults and finally for controlling the water level, the solenoid valve is set at a specific range. When the water level falls below the minimum set point, the valve automatically turns on, on the other hand, when the water level is higher than the maximum setpoint, the valve turns off automatically.

6 Conclusion

In this survey paper, we came to know that the use of Raspberry Pi as a controller for SCADA is the best option because of its multiple features and low cost. The use of Internet or IoT communications using Raspberry Pi for creating a SCADA system is easy in construction for controlling some sensors for small systems. IoT for data transfer is very secure. With the above mention features that we observed from the use of Raspberry Pi, it is much efficient and less complex.

References

1. Abdelhafid Rachidi AT, Abdellah, K (2014) Toward an automation increasingly interconnecting. *Int J Sci Eng Res*
2. Amit G, Mahadev P (2014) PLC based industrial automation system. In: International conference of recent trends in engineering and management science-RTM
3. Almas MS, Vanfretti L, Gjerde JO, Stig L (2014) Open source SCADA implementation and pmu integration for power system monitoring and control applications. *IEEE*, pp 1–5
4. Endi M, Elhalwagy Y, Hashad A (2010) Three-layer PLC/SCADA system architecture in process automation and data monitoring. *IEEE*. 2:774–779
5. Deepak KA (2015) Application of SCADA System in Steel Industries. *Int J Sci Res Publicat* 05(06)
6. Shashank GH, Santosh RD, Deshpande RG, Sandeep BK, Sachin RC (2015) Implementation of SCADA in industries using wireless technologies. In: International conference on industrial instrumentation and control (IICIC). College of Engineering Pune, India
7. Minchala LI, Ochoa S, Velecela E, Astudillo DF, Gonzalez J (2015) An open-source SCADA system to implement advanced computer integrated manufacturing. *IEEE Latin America Trans* 14(12):4657–4662
8. Swapnil C, Sukhdev R, Suryakant P, Anupama P (2016) Automation in Newspaper Cutting Using PLC. *Int J Indust Electron Electri Eng* 04(05)
9. Namrata R, Rohan W, Dinesh G, Amol T (2017) Automatic water distribution and leakage detection using PLC and SCADA. *Int Res J Eng Technol (IRJET)* 04(02) (2017)
10. Swarupa ST, Divya AP, Ajinkya RS, Mule KC (2017) Design and implementation of water level management Using PLC and SCADA visualization. In: International journal of advanced research in electrical, electronics, and instrument engineering (IJAREEIE), vol. 6, issue 4
11. Rohmer E, Singh SPN, Freese, M (2016) Development of PLC based Industrial Automation with System Monitoring. In: 4th international conference on science, technology and management
12. Daniel FM, Jonnathan AP, Andres V, Luis IM, Darwin A (2017) Open source SCADA system for advanced monitoring of industrial processes. *Int Conf Inform Syst Comput Sci*
13. Neha C, Samiksha S, Nayan R, Twinkal D, Priyanka K (2017) Review paper on industrial datalogging system using raspberry Pi. *Int J Res Emerging Sci Technol Special issue*
14. Bettstetter C, Vogel H-J, Eberspacher J (1999) GSM phase 2+ general packet radio service GPRS: architecture, protocols, and air interface. *IEEE Commun Surveys Tuts* 2(4):2–14. Third Quarter

Extended Microstrip Line-Fed Circularly Polarized Dielectric Resonator Antenna for WiMAX and 5G Applications



Ayan Pal, Arunabho Panja, Amibrata Samadder, Saswata Banerjee, Juin Acharjee, and Kaushik Mandal

Abstract In this paper, a unique, simple, and concise structure of a circularly polarized (CP) cylindrical dielectric resonator antenna (CDRA) usable for wireless band applications is proposed. The CDRA is excited by a meandered-shaped microstrip feedline ending with a circular extension. The combined effect of this feeding mechanism along with a partial ground plane satisfies the criteria for generating circular polarization. The proposed design is operating in the frequency range of 2.80–3.41 GHz centered at 3.39 GHz with an axial ratio (AR) bandwidth of 9.14% and peak gain of 3.9 dBi. The designed structure exhibits 3-dB axial ratio beamwidth (ARBW) of 42° and 102° with AR_{\min} of 0.54 dB and cross-polarization discrimination (XPD) of 30 dB and 31 dB in two principal planes at $\phi = 0^\circ$ and $\phi = 90^\circ$, respectively. The reconfigurability between left-hand CP (LHCP) and right-hand CP (RHCP) field can be obtained by taking the mirror image of the extended meandered-shaped microstrip feedline. The antenna can be preferred for different wireless applications such as WiMAX and 5G.

Keywords Circular polarization · Dielectric resonator antenna · Cylindrical DRA · Axial ratio · Axial ratio beamwidth · Cross-polarization discrimination

1 Introduction

In the last few decades, dielectric resonator antenna (DRA) has been extensively researched by scientists due to its beneficial features such as higher impedance bandwidth, small space requirement, negligible conductor loss, significant gain improvement, and ease of applying various excitation techniques [1, 2]. A circularly polarized (CP) wave radiates power in the horizontal and vertical planes as well as every plane in

A. Pal (✉) · A. Panja · A. Samadder · S. Banerjee · J. Acharjee
Department of Electronics and Communication Engineering, St. Thomas' College of Engineering and Technology, Kolkata, West Bengal, India
e-mail: gst.ayanpal@gmail.com

K. Mandal
Institute of Radio Physics and Electronics, University of Calcutta, Kolkata, West Bengal, India

between it, and the plane of polarization rotates in a pattern by making one complete revolution during each wavelength. For CP, an antenna must support two orthogonal modes (perpendicular field of equal amplitude) with a 90° phase difference between them [3]. The antenna is insensitive to transmitter and receiver orientation, offers less sensitivity to propagation effects, and is suitable for satellite communications [4]. As a result of the mentioned reasons and considering its operating range, it can be concluded that CP is necessary for smooth and hassle-free wireless communication for WIMAX and 5G applications. CPDRA has gained immense popularity in the field of wireless and satellite communication over linearly polarized DRA as it is not affected due to polarization mismatch and nullifies the effect of multipath interference [5, 6]. CPDRA can be achieved in various ways. Researchers have found that one of the ways by which CP can be achieved in DRA is by varying the coupling slots [7–9]. Another technique that has been found is by varying the feed structure used to excite the DRA and by changing the dimensions of the ground plane to achieve CP [10–12]. For instance, a question-mark shaped feed has been used which provides a quadrature-phase difference between two orthogonal modes, thus generating CP [13]. Similarly, a rectangular feed has been modified by removing parts of it to obtain the required conditions to generate CP [12]. CP has also been achieved by restructuring the shape of the DRA [14–16]. Very recently insertion of slots for CP generation is one of the reported techniques [17, 18]. A single feed CP rectangular DRA using the new coupling method of dual-mode slot-line ring resonator (SSRR) has also been investigated [19]. Conformal rectangular open half-loops can also be used for excitation [20].

In this article, the design of a cylindrical DRA (CDRA) with a modified feeding structure for realizing CP is presented. A meandered-shaped microstrip feedline is used to enhance the electrical length. The feedline is ended with a circular extension that produces mutual coupling with the partial ground plane to realize CP. All the simulations are conducted in full-wave-based ANSYS HFSS. Large separation between the LHCP and RHCP justifies the performance of CP in the operating frequency band.

2 Circularly Polarized Dielectric Resonator Antenna Design and Analysis

2.1 Antenna Design

Figure 1 shows the geometrical structure of the proposed CDRA. Easily available low-cost FR4 substrate with dielectric constant $\epsilon_r = 4.4$, height $h = 1.6$ mm is used as the base of DRA, and the feedline is printed on it. A cylindrical-shaped dielectric resonator is designed using the substrate Arlon AD410 with relative permittivity of $\epsilon_r = 4.1$, height $H = 20.8$ mm, and loss tangent $\tan \delta = 0.003$. A meandered-shaped microstrip feedline of length 67.5 mm with a circular extension of radius $r = 5.2$ mm

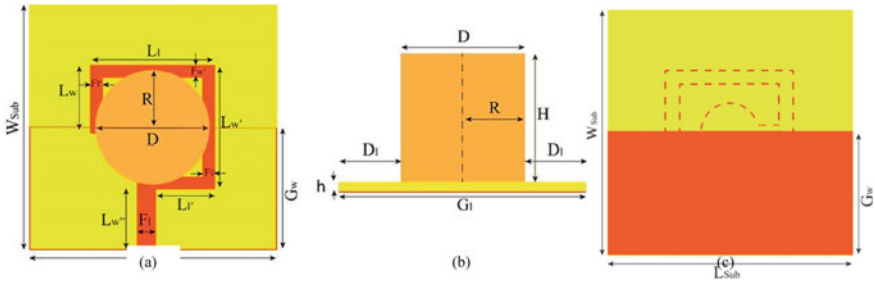


Fig. 1 Antenna configuration **a** Top view, **b** Side view, **c** Bottom view [The optimum dimensions of antenna elements are listed as follows: $L_{Sub} = 40$ mm, $W_{Sub} = 40$ mm, $h = 1.6$ mm, $L_{w''} = 11$ mm, $L_{l'} = 11.5$ mm, $L_{w'} = 16$ mm, $L_l = 16$ mm, $L_w = 7$ mm, $L_{l''} = 6$ mm, $L = 67.5$ mm, $F_l = 3$ mm, $F_{l'} = F_{l''} = F_{w'} = F_{w''} = 2$ mm, $G_w = 20$ mm, $H = 20.8$ mm, $R = 9.2$ mm, $D = 18.4$ mm, $D_l = 10.8$ mm, $d = 10.4$ mm, $r = 5.2$ mm]

is placed on one side of the substrate to excite the CDRA. A partial ground plane of dimensions $20\text{ mm} \times 40\text{ mm}$ is placed on another side of the FR4 substrate to generate orthogonal components of electric fields by the mutual coupling effect with the modified microstrip feedline.

The stepwise improvement of the proposed CP CDRA from the reference antenna is depicted in Fig. 2. Initially, in Fig. 2a, a meandered-shaped microstrip feed is applied to the CDRA which is taken as reference 1. In Fig. 2b, the CDRA is excited

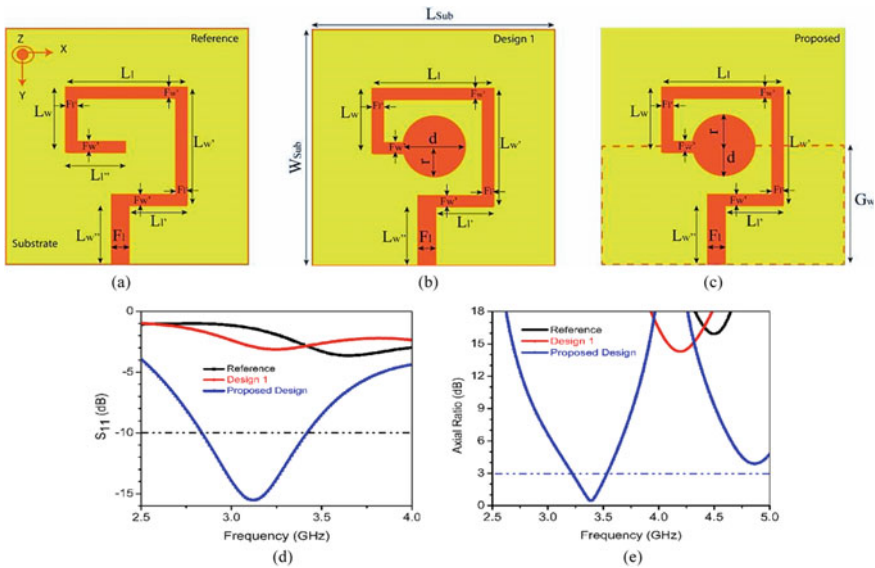


Fig. 2 Stepwise improvement of CP CDRA feeding mechanism: **a** Reference **b** Design 1 **c** Proposed design and response characteristics **d** Reflection coefficient **e** AR bandwidth

through a meandered-shaped microstrip feedline ending with a circular extension identified as design 1. For the reference antenna and design 1, a full metallic ground plane is used. In the final design in Fig. 2c, a partial ground plane has been taken for proper mutual coupling with the placed CDRA. With the improvement of the structure, stepwise improvement of their response in terms of reflection coefficient and AR bandwidth is depicted in Fig. 2d and e.

2.1.1 Antenna Parametric Analysis

Some of the parameters of the proposed structure play an important role in the performance improvement of the designed CP CDRA. The effects of these parameters are discussed below.

Effect of Change in Radius of Circular Extension

In Fig. 3, the effect of changing the radius of the circular extension of the feedline is shown. In Fig. 3a, reflection coefficient is shown for the different values of the radius of the circular extension. For a radius of 4.7 mm, the -10 dB bandwidth obtained is 640 MHz. On increasing the radius to 5.2 mm, a slight reduction in impedance bandwidth (IBW) is observed. However, on increasing the radius to 5.7 mm, the IBW is diminished by 210 MHz resulting in a bandwidth of 400 MHz. Figure 3b depicts the AR bandwidth for varying radii. For radii of 4.7 mm and 5.7 mm, the AR bandwidth is 284 MHz and 293 MHz, respectively. However, for radius of 5.2 mm, the secured AR bandwidth increases to 310 MHz. In Fig. 3c, the value of 3-dB ARBW is illustrated for $\phi = 0^\circ$ and $\phi = 90^\circ$ after changing the radius of circular extension. It is observed that for only $r = 5.2$ mm, the 3-dB ARBW is greater than 100° and 42° for $\phi = 90^\circ$ and $\phi = 0^\circ$, respectively.

Effect of Change in Height of DRA

The effect of change in the height of CDRA on various parameters is depicted in Fig. 4. It is observed in Fig. 4a that the IBW is maximum when $H = 20.8$ mm. For $H = 19.2$ mm and 22.4 mm, the bandwidth is 546 MHz and 560 MHz, respectively. The AR Bandwidths for $H = 20.8$ mm and 22.4 mm are approximately the same, but it is a bit wider for $H = 19.2$ mm as shown in Fig. 4b. However, when compared to $H = 19.2$ mm and 22.4 mm, the convergence of IBW and AR bandwidth is more for $H = 20.8$ mm. From Fig. 4c, it can be observed that the 3-dB ARBW for $H = 19.2$ mm at $\phi = 0^\circ$ is less than that of $H = 20.8$ mm while that of $H = 22.4$ mm is same as that of $H = 20.8$ mm. The 3-dB ARBW for $\phi = 90^\circ$ is maximum for $H = 19.2$ mm and 20.8 mm. Hence, optimum results are obtained for when $H = 20.8$ mm.

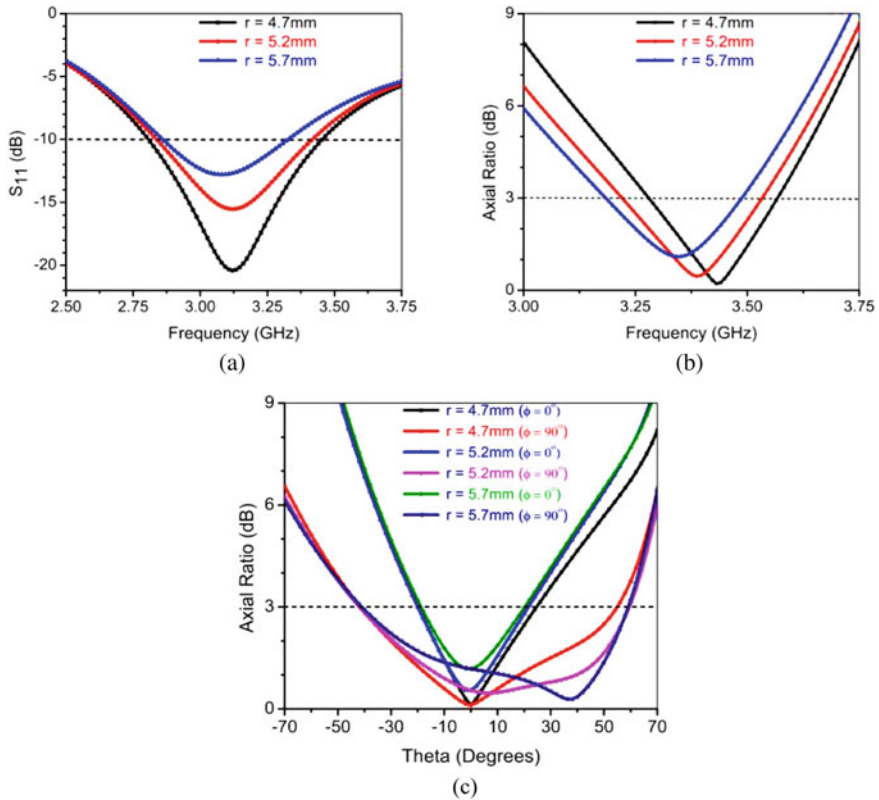


Fig. 3 Effect of change in radius of circular extension in **a** Reflection coefficient **b** AR bandwidth and **c** 3-dB ARBW in different planes

3 Result and Discussion

The proposed designed structure provides IBW of 19.55% (2.80–3.41 GHz) and AR bandwidth of 9.14% (3.22–3.53 GHz) as observed in Fig. 5a. The resonating frequency is achieved at 3.39 GHz with an ARmin of 0.54 dB. Justification of the generation of CP at the operating frequency is reflected in Fig. 5b. It shows that for different planes, a large variation of the elevation angle AR achieved is below 3 dB. The CP radiation patterns for the primary planes $\phi = 0^\circ$ and 90° are displayed in Fig. 6. In the boresight direction, the difference between LHCP and RHCP, i.e., XPD, is 30 dB and 31 dB, respectively.

Less variation of gain throughout the operating frequency band is observed which also justifies the stable performance of the proposed antenna as shown in Fig. 7. The maximum realized gain at the operating band is 3.9dBi. Radiation efficiency variation from 85.5% to 94%, which is acceptable for practical applications, has also been portrayed in Fig. 7.

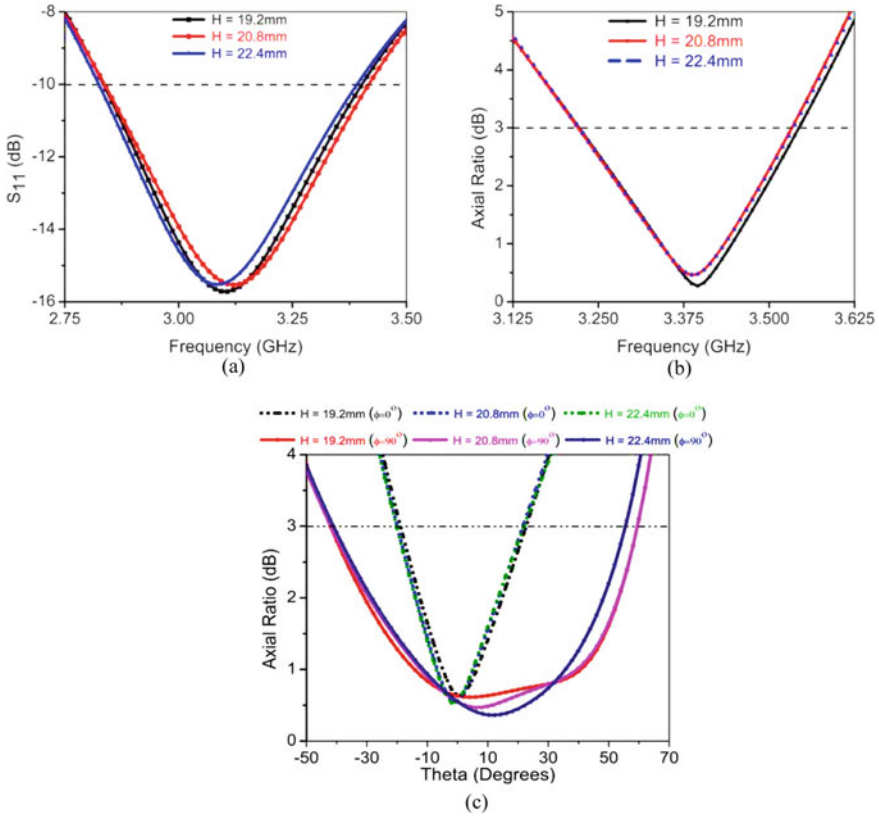


Fig. 4 Effect of change in height of CDRA on **a** Reflection coefficient **b** AR bandwidth and **c** 3-dB ARBW in different planes

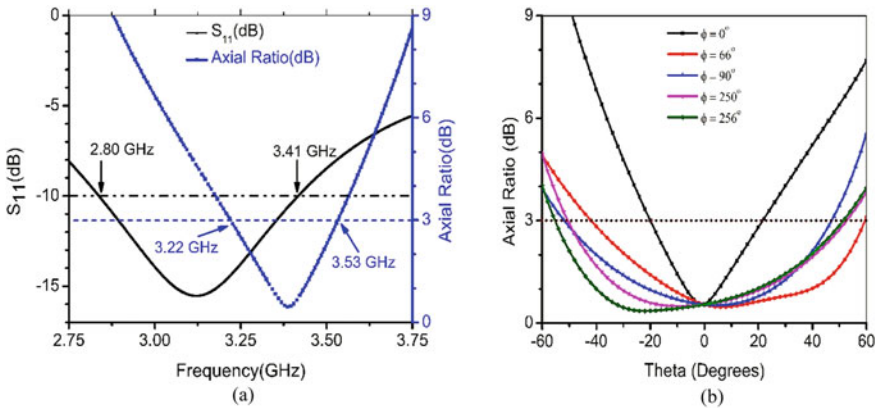


Fig. 5 Simulated S_{11} , AR bandwidth and 3-dB ARBW of proposed CP antenna

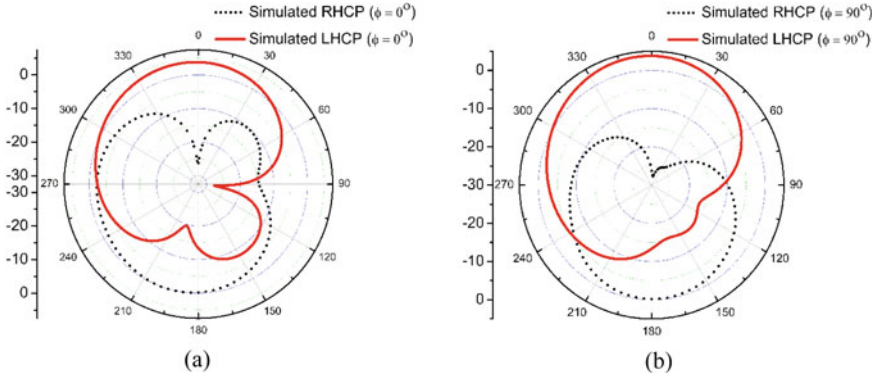
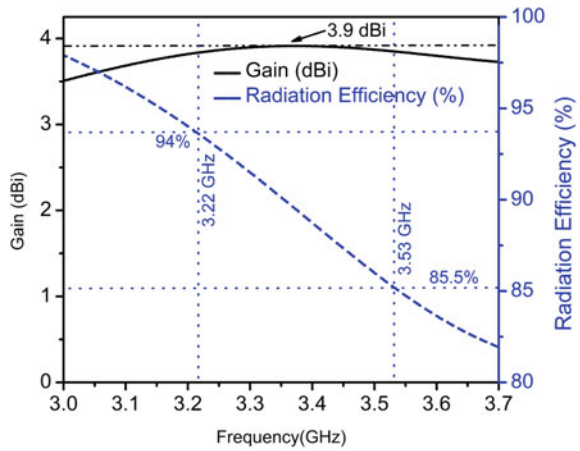


Fig. 6 Simulated CP radiation patterns of proposed design at 3.39 GHz for the plane of **a** $\phi = 0^\circ$ and **b** $\phi = 90^\circ$

Fig. 7 Effect on gain and radiation efficiency with frequency variation



The recognition of CP nature can be easily understood by observing the electric field distribution with changing phase angle as shown in Fig. 8. Clockwise movement of field distribution is observed which ensures LHCP radiation. The alteration of CP nature (LHCP to RHCP) can be adjusted by considering the mirror image of the extended microstrip feedline.

Table 1 shows the performance analysis of the proposed antenna in comparison with the other similar reported structures.

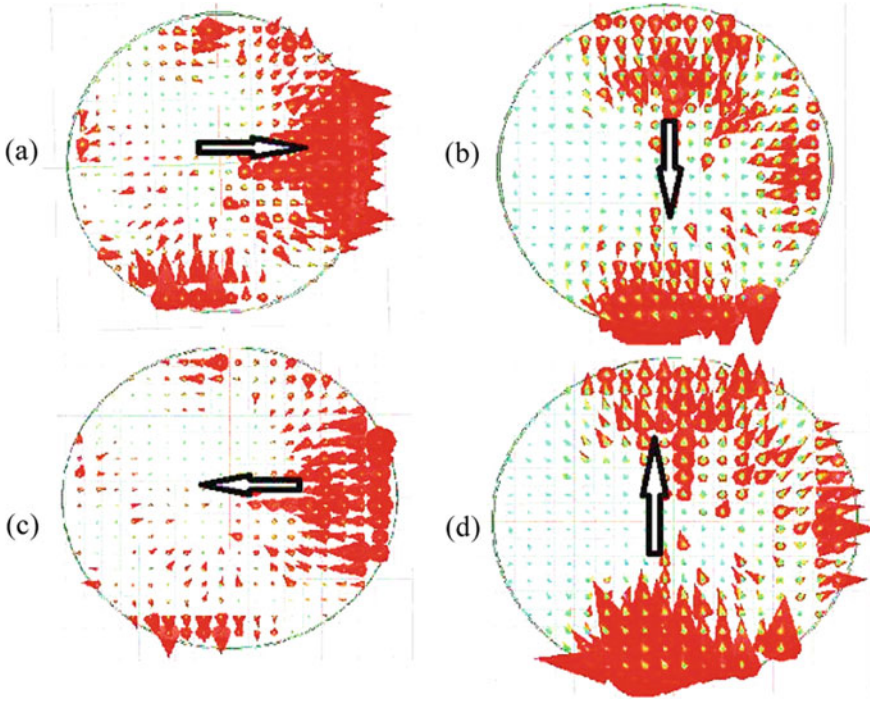


Fig. 8 Electric field distribution at the CP frequency of 3.39 GHz for $\theta =$ a 0° b 90° c 180° d 270°

4 Conclusion

In this article, the design of a CDRA with CP characteristics of higher XPD performance is presented and analyzed. Due to the mutual coupling effect between the partial ground plane and meandered-shaped microstrip feedline, orthogonal fields with equal magnitude and opposite phase are being generated. The obtained IBW and AR bandwidth are 19.55 and 9.1%, respectively. A gain of 3.9dBi is procured at the operating frequency 3.39 GHz with a substantial amount of ARBW (42° at $\phi = 0^\circ$ and 102° at $\phi = 90^\circ$). LHCP is observed at the upper CP band, whereas RHCP can be obtained by the mirror image of the extended microstrip line. Owing to its operating range, the proposed design is expected to be purposive as an economical alternative in WiMAX and 5G applications.

Table 1 Performance of the proposed antenna with other reported articles

References	DRA structure	Size of antenna	S ₁₁ (GHz)	Axial ratio bandwidth (%)	Gain (dBi)	Radiation efficiency (%)	Cross-polarization discrimination (dB)	
							$\phi = 0^\circ$	$\phi = 90^\circ$
[8]	Cylindrical	$\pi \times 0.25 \lambda \times 0.25 \lambda$	2.33–2.54	8.3	1.3	80 (approx.)	25 (approx.)	20 (approx.)
[11]	Cylindrical	$0.40\lambda \times 0.40\lambda$	2.57–3.78	19.26	1.97	88 (approx.)	20.37	NM
[12]	Rectangular	$0.468 \lambda \times 0.468 \lambda$	2.0–4.0	58.36	2.31	NM	19	30
[18]	Hemisphere	$1.19 \lambda \times 1.19 \lambda$	2.15–2.66	2.36	6.7	NM	33	17
[19]	Rectangular	$0.7 \lambda \times 0.7 \lambda$	3.16–3.66	2.85	3.84	NM	NM	NM
[20]	Cylindrical	$7.8 \lambda \times 7.8 \lambda$	5.61–6.8	3.63	4	NM	18	20
Proposed	Cylindrical	$0.45 \lambda \times 0.45 \lambda$	2.80–3.41	9.1	3.9	94	30	31

NM Not mentioned

References

1. Kumari R, Gangwar RK (2016) Circularly polarized dielectric resonator antennas: design and developments. *Wireless Pers. Commun* 86:851–886
2. Fakhte S, Oraizi H, Karimian R (2014) A novel low-cost circularly polarized rotated stacked dielectric resonator antenna. *IEEE Antenn Wirel Pr* 13:722–725
3. Sharma S, Tripathi CC (2016) A comprehensive study on a circularly polarized antenna. In: 2016 second international innovative applications of computational intelligence on power, energy and controls with their impact on humanity (CIPECH)
4. Qian ZH, Leung KW, Chen RS (2004) Analysis of circularly polarized dielectric resonator antenna excited by a spiral slot. *Progress in Electromagnetics Research (PIER 47)*, pp 111–121
5. Altaf A, Yang Y, Lee KY, Hwang KC (2015) Circularly polarized Spidron fractal dielectric resonator antenna. *IEEE Antenn Wirel Pr* 14:1806–1809
6. Bao XL, Ammann MJ (2011) Monofilar spiral slot antenna for dual-frequency dual-sense circular polarization. *IEEE Trans Antennas Propag* 59:3061–3065
7. Perron A, Denidni TA, Sebak AR (2010) Circularly polarized microstrip/elliptical dielectric ring resonator antenna for millimeter-wave applications. *IEEE Antenn Wirel Pr* 9:783–786
8. Yang N, Leung KW, Lu K, Wu N (2016) Omnidirectional circularly polarized dielectric resonator antenna with logarithmic spiral slots in the ground. *IEEE Trans Antennas Propag* 65:839–844
9. Yang SLS, Kishk AA, Lee KF (2008) Wideband circularly polarized antenna with L-shaped slot. *IEEE Trans Antennas Propag* 56(6):1780–1783
10. Iqbal J, Illahi U, Sulaiman MI, Alam M, Mazliham MS (2018) A circularly polarized rectangular dielectric resonator antenna excited by E-shaped feed. *Int J Eng Technol* 7:1448–1450
11. Kumar R, Park, CW, Chaudhary RK (2017) A wideband circularly polarized cylindrical DRA loaded with SRR and excited with a question shaped microstrip feed line. In: 32nd general assembly and scientific symposium of the international union of radio science (URSI GASS). *IEEE*, pp 1–4
12. Kumari R, Gangwar RK (2018) Circularly polarized rectangular dielectric resonator antenna fed by a flag shape microstrip line for wideband applications. *Microw Opt Techn Let.* 60:2577–2584
13. Kumar R, Chaudhary RK (2015) A wideband circularly polarized cubic dielectric resonator antenna excited with modified microstrip feed. *IEEE Antenn Wirel Pr* 15:1285–1288
14. Chair R, Yang SLS, Kishk AA, Lee KF, Luk KM (2006) Aperture fed wideband circularly polarized rectangular stair shaped dielectric resonator antenna. *IEEE Trans Antennas Propag* 54:1350–1352
15. Pan Y, Leung KW (2010) Wideband circularly polarized trapezoidal dielectric resonator antenna. *IEEE Antenn Wirel Pr* 9:588–591
16. Zhou YD, Jiao YC, Weng ZB, Ni T (2015) A novel single-fed wide dual-band circularly polarized dielectric resonator antenna. *IEEE Antenn Wirel Pr* 15:930–933
17. Ray M, Mandal K, Nasimuddin (2019) Low profile circularly polarized patch antenna with wide 3-dB Beamwidth. *IEEE Trans Antennas Propag* 18(12):2473–2477
18. Bhagat SK, Karra AK, Babu SS (2019) A compact size dielectric resonator antenna for multiband application: design and analysis. *Int J Recent Technol Eng* 7:390–392
19. Wang C, Chen G, Liu H, Ma Z, Zhang X (2019) Single-feed circularly polarized rectangular dielectric resonator antenna coupled with a dual-mode slot-line square ring resonator. *IEICE Electron Expr* 16:83–88
20. Sulaiman MI, Khamas SK, Basarudin H (2014) A singly-fed wideband circularly polarized cylindrical dielectric resonator antenna using conformal half-loop excitation. In: 2014 4th international conference on engineering technology and technopreneuship (ICE2T), *IEEE*, pp 209–212

PPM-SIM Based FSO System Under Various Environmental Conditions



Pritam Keshari Sahoo

Abstract This manuscript investigates various performances of pulse position modulation–subcarrier intensity modulation (PPM-SIM) model under various environmental conditions. The considered PPM is pulse shaped by half-cosine pulse and modulated over an orthogonal subcarrier signal. This system is analyzed under various atmospheric turbulences like log-normal (weak) and gamma-gamma (strong) for various environmental conditions like rain and dense fog of minimal visibility. The impact of environmental conditions on the performance parameters like bit error rate (BER) and information capacity is numerically analyzed for a comparative analysis. This manuscript aims to study the feasibility of a spectral efficient PPM based free-space optics (FSO) system for various adverse weather conditions.

Keywords FSO · PPM · Log-normal · Gamma-gamma · Spectral efficiency · BER

1 Introduction

FSO is the communication system where free-space (i.e., air/vacuum) is used as the communication medium. FSO is an optical communication system where data are transmitted through free-space medium using light as the propagating wave. Its function is analogous to fiber optics communication apart from the transmission medium. High information capacity, immune to electro-magnetic interference, unregulated frequency spectrum, low installation cost, etc., are the attributes through which the FSO system has gained popularity since some decades past. Atmospheric turbulences due to temperature and pressure variation and presence of foreign elements like rain, fog, and haze limit the propagation distance of optical signal up to few hundred meters [1]. The FSO channel is a random time-varying channel model represented by log-normal and gamma-gamma mathematical models, respectively, for weak and strong atmospheric turbulences [2, 3].

P. K. Sahoo (✉)
Amity University Jharkhand, Ranchi 834001, India
e-mail: sahoo.pritamkeshari@gmail.com

Going through performance study of various modulation techniques since 2010 [4–11], pulse position modulation (PPM) has obtained maximum preference due to its superior error performance results. Because of the above cause, authors [2] have proposed a hybrid modulation technique based on PPM for cellular back-haul application. Further, the authors [12] have proposed a new kind of system design by which the poor spectral efficiency of PPM can be overcome and to make it eligible as a spectral efficient modulation for cellular back-haul application. Though, PPM has been studied under various atmospheric turbulences such as weak and strong, its performances for various weather conditions are left untouched. Hence, this manuscript analyzed the error performance study and maximum capacity study under the influence of atmospheric turbulences and various weather conditions like dense fog and rain. At the end, a conclusive statement on performance degradation in dB for rain and dense fog is drawn for the PPM based back-haul FSO system model.

2 System and Channel Model

The considered system is a PPM based system [12], where every PPM symbol is pulse shaped by a half-cosine signal. This method is to reduce the inter channel interference (ICI) caused by frequency deviation due to fading. The system model in [12] has multiplied a subcarrier orthogonal frequency to each parallel output line of the PPM encoder. This novel model of PPM encoder has shown significant spectral advantages over traditional PPM encoder [13]. During the propagation of laser beam, optical signal undergoes fading. For weak atmospheric turbulence, this fading channel model can be represented by log-normal distribution, and for strong atmospheric turbulence, gamma-gamma model is widely accepted. Though, the authors have analyzed the system performances under diverse atmospheric turbulence conditions, the weather conditions like dense fog and rain are not considered as a part of deteriorating factor for the light wave. This manuscript incorporates the effects of fog and rain on the exposed light signal.

The attenuation due to fog and rain is given by (1) [14, 15]

$$\gamma(\lambda) = \frac{3.91}{V} \left(\frac{\lambda}{550} \right)^{-\delta} \quad (1)$$

V is the visibility in km, λ is the operating wavelength in nm, and δ is the parameter related to the particle size distribution and V . Kim model is suitable for low visibility due to dense fog and heavy rain. δ by the Kim model is given by.

$\delta =$	1.6	$V > 50$ km
	1.3	$6 \text{ km} < V < 50 \text{ km}$
	$0.16 V + 0.34$	$1 \text{ km} < V < 6 \text{ km}$

(continued)

(continued)

	V-0.5	0.5 km < V < 1 km
	0	V < 0.5 km

In this manuscript, we have chosen the value of $\delta = 0.16 V + 0.34$ for rain attenuation at a visibility between 1 and 2 km. However, for dense fog attenuation, $\delta = 0$ at a visibility within 0.2 km. Hence, for dense fog situation, the atmospheric channel attenuation becomes independent of wavelength.

The overall error probability under the weak and strong atmospheric turbulence is given by (2) and (3)

$$P_e = \frac{1}{(M-1)\sqrt{\pi}} \sum_{i=1}^N w_i \left[1 - \left(1 - \frac{1}{2} \operatorname{erfc} \left(\frac{RG\gamma I_0 e^{(\sqrt{2}x_i \sigma_z + \mu_z)}}{\sqrt{4\sigma_{ICI}^2 + \frac{2\sigma_{n,i}^2}{v}}} \right) \right)^{(M-1)} \right] \quad (2)$$

$$P_e = \frac{2^{(\alpha+\beta-3)}}{\pi\sqrt{\pi}\Gamma(\alpha)\Gamma(\beta)} G_{5,2}^{2,4} \left(\frac{8(RG\gamma I)^2}{(\alpha\beta)^2 [2\sigma_{ICI}^2 + \sigma_n^2]} \middle| \begin{matrix} \frac{1-\beta}{2} & 1 - \frac{\beta}{2} \\ 0 & \frac{1-\alpha}{2} \end{matrix} \begin{matrix} 1 - \frac{\alpha}{2} & 1 \\ 1 & 1 \end{matrix} \right) \quad (3)$$

where

$$\sigma_{n,i}^2 = 2qG^2 F_A R\gamma I_0 \exp(\sqrt{2}\sigma_z x_i + u_z) \Delta f + \frac{4k_B T F_n}{R_l} \Delta f \quad (4)$$

3 Result and Discussion

Figure 1 represents the BER plot as a function of received average irradiance for weak and strong atmospheric turbulence. The numerical results prove their ideality under the rainy atmospheric condition of visibility within 2 km. For weak atmospheric turbulence, i.e., scintillation, half-cosined PPM is about 8 dBm power efficient over PPM at a fixed BER level of 10^{-15} . For higher atmospheric turbulence, i.e., when we consider gamma-gamma channel model, the improvement in half-cosined PPM persists, but at 5 dBm more power efficiency.

The BER plot as a function of received average irradiance for weak and strong atmospheric turbulence is shown in Fig. 2. The numerical results prove their nature likewise in Fig. 1. Under the dense fog atmospheric condition of visibility within 0.2 km, the obtained results show a significant degradation in error performances. For weak as well as strong atmospheric turbulences, half-cosined PPM and PPM are about 20 dBm less power efficient over rainy atmospheric condition.

This result in Fig. 3 compares the error performances under rainy and dense fog environmental condition. For weak atmospheric turbulence, the system BER

Fig. 1 BER against received average irradiance for rainy atmosphere

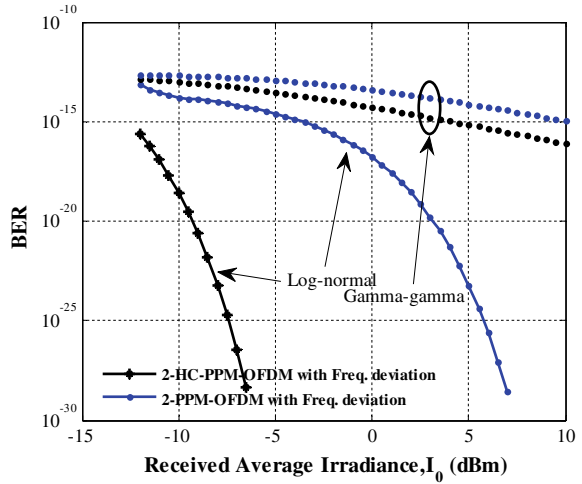
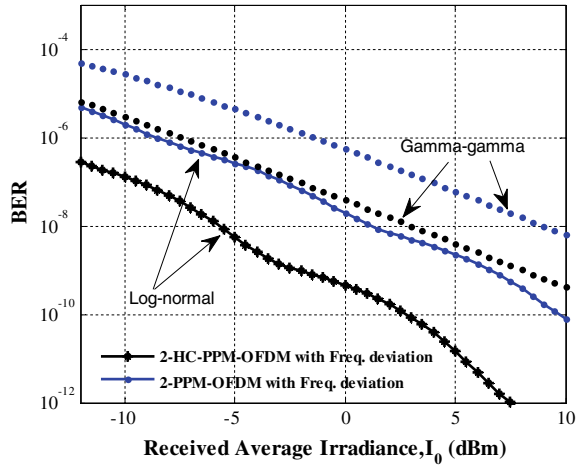


Fig. 2 BER against received average irradiance for dense fog atmosphere



performance decays at a rate of 10^5 times for dense fog environment over rainy environment at a distance of 2 km. In other way, we roughly can conclude that at a reference bit error rate of 10^{-10} , the light can travel 500 m more in rainy condition than in dense fog condition.

This result of Fig. 4 is the evaluation of average link capacity comparison for dense fog and rainy environment under weak atmospheric turbulence. Because of the high signal-to-noise ratio (SNR) value of half-cosine PPM, it maintains highest capacity of about 1 and 2.5 Gbps more data rate over PPM-MSK and PPM, respectively, at 10 dBm received optical power. Though, the improvement in data rate is observed with increase in received optical power, the system rate is approximately 15 Gbps higher in case of rainy atmospheric condition over dense fog condition.

Fig. 3 BER against link distance for dense fog and rainy atmosphere

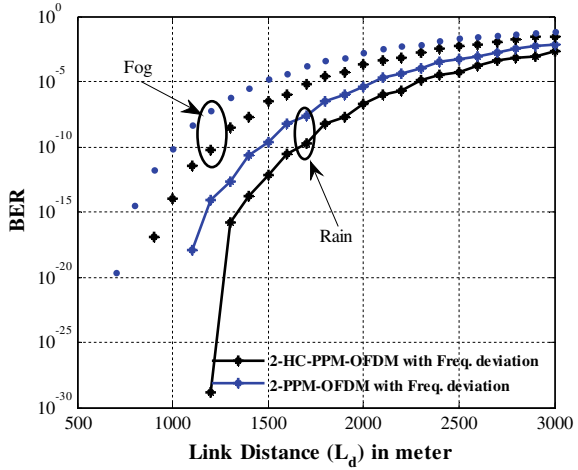
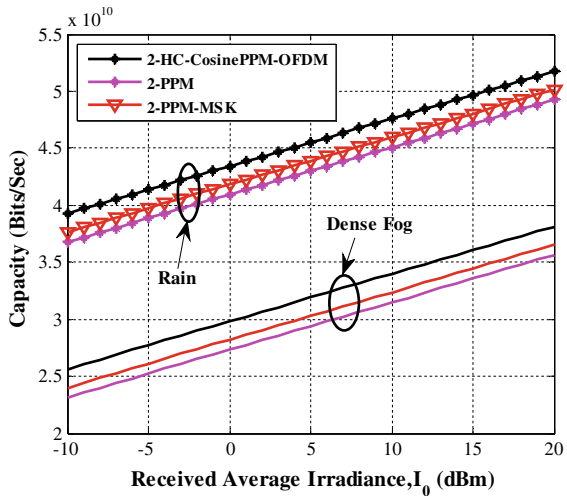


Fig. 4 BER against link capacity for dense fog and rainy atmosphere



4 Conclusion

In this manuscript, authors have explored the environmental attenuation on a new model of HC-PPM-OFDM without serial conversion of PPM. Authors have numerically studied and compared some vital parameters like BER and capacity under both rainy and dense fog weather conditions. Finally, we conclude that the fog attenuation is more deteriorating than the attenuation by rain. Fog attenuation can limit our transmission distance up to 1.6 km which is around 600 m less than the rain attenuation.

References

1. Sahoo PK, Prajapati YK, Tripathi R (2018) PPM- and GMSK-based hybrid modulation technique for optical wireless communication cellular backhaul channel. *IET Commun* 12(17):2158–2163
2. Sahoo PK, Yadav AK, Prajapati YK, Tripathi R (2019) Phase-sampled detection of hybrid modulation impaired by gamma-gamma turbulence. *Microw Opt Technol Lett* 1–8
3. Esmail MA, Fathallah H, Alouini MS (2016) Outdoor FSO communications under fog: attenuation modeling and performance evaluation. *IEEE Photonics J* 8(4):1–22
4. Ma J, Jiang Y, Yu S et al (2010) Packet error rate analysis of OOK, DPIM and PPM modulation schemes for ground-to-satellite optical communications. *Opt Commun* 283(2):237–242
5. Dabiri MT, Sadough SMS, Khalighi MA (2017) FSO channel estimation for OOK modulation with APD receiver over atmospheric turbulence and pointing errors. *Opt Commun* 402:577–584
6. Popoola WO, Ghassemlooy Z (2009) BPSK subcarrier intensity modulated free-space optical communications in atmospheric turbulence. *J Lightw Technol* 27(8):967–973
7. Sahoo PK, Prajapati YK, Tripathi R (2020) Hybrid mapped optical-OFDM using nonlinear companding technique for indoor visible light communication application. *IET Commun* 14(17):3073–3079
8. Dubey D, Prajapati YK, Tripathi R (2020) Performance enhancement of hybrid-SIM for optical wireless downlink communication with aperture averaging and receiver diversity. *IET Commun* 14(18):3194–3202
9. Sahoo PK, Yadav A (2020) A comprehensive road map of modern communication through free-space optics. *J Opt Commun* <https://doi.org/10.1515/joc-2020-0238>
10. Chen Y, Li Z, Liu P et al (2017) The BER performance comparison of MSK and GMSK schemes for short-range visible light communication. In: *IEEE 9th international conference on communication software and networks (ICCSN)*. Guangzhou, pp 611–614
11. Ghassemlooy Z, Popoola W, Rajbhandari S (2012) *Optical wireless communications: system and channel modeling with MATLAB*. CRC, New York, NY, USA
12. Sahoo PK, Prajapati YK, Tripathi R (2019) Performance analysis of pulse position modulation-based hybrid technique for cellular backhaul free-space optical link. *Opt Eng* 58(1):016119
13. Liu H, Liao R, Wei Z, Hou Z, Qiao Y (2015) BER analysis of a hybrid modulation scheme based on PPM and MSK subcarrier intensity modulation. *IEEE Photonics J* 7(4):7201510–7201520
14. Ghoname S, Fayed HA, El Aziz AA, Aly MH (2016) Performance analysis of FSO communication system: effects of fog, rain and humidity. In: *Sixth international conference on digital information processing and communications (ICDIPC)*. Beirut, pp 151–155
15. Sahoo PK, Yadav AK, Prajapati YK, Tripathi R (2020) Optimum APD gain evaluation of FSO system for inter-building laser communication application. In: *L Advances in VLSI, communication, and signal processing. Lecture notes in electrical engineering*, vol. 587. Springer

Single Layered Mantle Cover for Cloaking at Dual Frequencies in Antenna Application



N. Kumutha and N. Amutha

Abstract A single layer of modulated meta-surface is proposed for cloaking the conducting object (satisfying the quasi static condition) at two frequencies. In order to study the cloaking behavior in practical scenario, the cloaking effect of modulated meta-surface is verified using dipole antenna. The modulated meta-surface structure designed using CST microwave studio suite can cloak the conducting object from two different frequencies of 4 and 5 GHz. The simulated result of the S parameter and radiation patterns verifies the cloaking effect at these dual frequencies. Though S parameter verifies the cloaking effect at dual frequencies, results of radiation pattern of dipole antenna clearly differentiate the cloaking phenomenon with that of the resonating behavior of cloaked structures.

Keywords Mantle cloak · Microwave cloak · Modulated meta-surface · Frequency selective surfaces · Dipole antennas

1 Introduction

Many work toward microwave electromagnetic cloaking in antenna application using transformation optics [1], transmission line networks [2], microwave network cloaking [3, 4], mantle cloaking [5, 6], had been reported in past decade. However, recently these methods are applied for hiding a passive object from an electromagnetic source, thereby reducing the radar cross section [7–11] as well as the interference between two neighboring antennas [12–16].

N. Kumutha (✉)

MAAS Research Solutions LLP, Madurai, Tamil Nadu, India

e-mail: kumutha.nas@gmail.com

N. Amutha

Department of EEE, Nalanda College of Engineering, Chandi, Bihar, India

e-mail: amuthaeence@gmail.com

Later, the concept was extended to multi-frequency cloaking of transformation theory [17]. Also, meta-material-based LC circuits of ten layers were made to cover an object for cloaking at dual frequencies [18]. The multi-frequency cloaking concept was also reported for optical frequencies using multiple layers [19]. In microwave network cloaking method, the multi-layer covers were reduced to a single layer for the plane wave and electric line source excitation by varying the width of microstrip lines that interconnects the metallic patches [20] and also by introducing a U shaped slot over metallic patch [21]. However, due to the bulky nature of meta-material, Alu et al. in 2015 introduced the mantle cloaking technique for multiband applications through two layers each with different FSS of meta-surface cover [22]. In 2016, two different configurations each with three different meta-surface covers were wrapped around the radiator for cloaking at dual frequencies [23].

In early literature, dual frequency in case of mantle cloaking is achieved through two or more layer. By considering the advantages of mantle cloaking such as a thin cloaking material and efficient cloaking for radiating elements, an attempt of dual frequency cloaking using a single layer meta-surface mantle cloaking was proposed and verified with the electric field distribution and radar cross section for a plane wave illumination source [24]. However, the practicality of plane wave source is seldom apparent [25]. Hence in this paper, the single layer meta-surface for dual frequency cloaking is verified by applying the electromagnetic field source, say for example dipole antennas. The dipole antenna operating at 4 and 5 GHz frequencies was considered for study.

2 Design of Dual Band Single Layered Meta-Surface Cloak

For an object to be made invisible, scattering of intended waves by the object has to be reduced. The intended waves can be an optical wave, microwave, etc. The principle of reducing the total scattering in mantle cloaking is that the scattered field of the covered object is compensated using the scattered field of the patterned cloak surface.

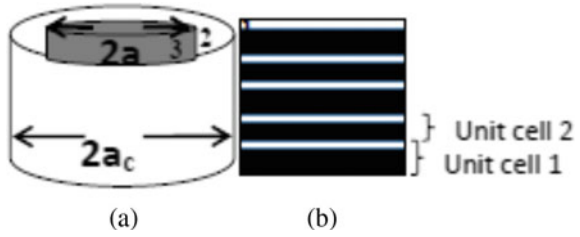
Consider that the TM wave from an electric source is illuminating the conducting cylindrical object. In order to satisfy the quasi static condition (object size \ll operating wavelength) of mantle cloaking, the smaller sized cylindrical object of radius ' a ' is covered by a dielectric cylinder of radius ' a_c ' as shown in Fig. 1a.

The incident electric field in the form of the superposition of the cylindrical waves can be written as [26],

$$E_Z^{\text{inc}} = E_0 \sin \theta \sum_{n=-\infty}^{\infty} j^n J_n(k_1 \rho \sin \theta) e^{-jk_1 z \cos \theta} e^{-jn\varphi} e^{j\omega t}$$

The scattered Z components in the form of electric and magnetic fields for the regions 1, 2 and 3 can be written as [26],

Fig. 1 **a** Cylindrical object with dielectric cover,
b Modulated FSS structure



Region I,

$$E_Z^{sca} = \sum_{n=-\infty}^{\infty} a_n^I H_n^2(\lambda_1 \rho) e^{-jk_1 z \cos \theta} e^{-jn\varphi} e^{j\omega t}$$

$$H_Z^{sca} = \sum_{n=-\infty}^{\infty} b_n^I H_n^2(\lambda_1 \rho) e^{-jk_1 z \cos \theta} e^{-jn\varphi} e^{j\omega t}$$

Region II,

$$E_{Z2} = \sum_{n=-\infty}^{\infty} [a_n^{II} H_n^2(\lambda_2 \rho) e^{-jk_1 z \cos \theta} e^{-jn\varphi} e^{j\omega t} + A_n^{II} H_n^1(\lambda_2 \rho) e^{-jk_1 z \cos \theta} e^{-jn\varphi} e^{j\omega t}]$$

Region III,

$$E_{Z3} = \sum_{n=-\infty}^{\infty} a_n^{III} J_n(\lambda_3 \rho) e^{-jk_1 z \cos \theta} e^{-jn\varphi} e^{j\omega t}$$

$$H_{Z3} = \sum_{n=-\infty}^{\infty} b_n^{III} J_n(\lambda_3 \rho) e^{-jk_1 z \cos \theta} e^{-jn\varphi} e^{j\omega t}$$

where $\lambda_1 = k_1 \sin \theta$

$$\lambda_2 = \sqrt{k_2^2 - k_1^2 \cos^2 \theta}$$

$$k_2^2 = -j\mu_2\omega(\sigma_2 + j\epsilon_2\omega)$$

$$\lambda_3 = \sqrt{k_3^2 - k_1^2 \cos^2 \theta}$$

$$k_3^2 = -j\mu_3\omega(\sigma_3 + j\epsilon_3\omega)$$

Similarly, the ϕ components of electric and magnetic field for the incident and scattered fields in all the three regions are calculated. The eight unknowns $a_n^I, b_n^I, a_n^{II}, b_n^{II}, A_n^{III}, B_n^{III}, a_n^{III}, b_n^{III}$ are found out with the help of boundary conditions like the tangential electric and magnetic fields are continuous at the material interfaces.

$$\begin{aligned}
 & (a_n^I, a_n^{II}, A_n^{III}, b_n^I, b_n^{II}, B_n^{III}, a_n^{III}, b_n^{III}) \times \sum_{n=-\infty}^{\infty} [e^{-jk_1 z \cos \theta} e^{-j\omega t} e^{j\omega t}] \\
 & \times \begin{bmatrix} H_n^2(\lambda_1 \rho) \frac{mb}{\rho} H_n^2(\lambda_1 \rho) \left(\frac{1}{\lambda_2^2} - \frac{1}{\lambda_1^2}\right) \frac{-jk_1^2}{\mu_1 \epsilon \omega \lambda_1} H_n^2(\lambda_1 \rho) & 0 & 0 & 0 & 0 & 0 & 0 \\ H_n^2(\lambda_2 \rho) & 0 & \frac{jk_2^2}{\mu_2 \epsilon \omega \lambda_2} H_n^2(\lambda_2 \rho) & 0 & H_n^2(\lambda_2 \rho) & 0 & \frac{-jb}{\rho \lambda_2^2} H_n^1(\lambda_2 \rho) & \frac{-jk_2^2}{\mu_2 \epsilon \omega \lambda_2} H_n^1(\lambda_2 \rho) \\ H_n^2(\lambda_2 \rho) & 0 & \frac{jk_2^2}{\mu_2 \epsilon \omega \lambda_2} H_n^2(\lambda_2 \rho) & 0 & 0 & H_n^2(\lambda_2 \rho) & \frac{-jb}{\rho \lambda_2^2} H_n^1(\lambda_2 \rho) & \frac{-jk_2^2}{\mu_2 \epsilon \omega \lambda_2} H_n^1(\lambda_2 \rho) \\ 0 & \frac{jb_1 \omega}{\lambda_1} H_n^2(\lambda_1 \rho) & \frac{mb}{\rho} H_n^2(\lambda_1 \rho) \left(\frac{1}{\lambda_2^2} - \frac{1}{\lambda_1^2}\right) & 0 & H_n^1(\lambda_2 \bar{\rho}) & 0 & 0 & 0 \\ 0 & \frac{-jb_1 \omega}{\lambda_2} H_n^1(\lambda_2 \rho) & 0 & H_n^2(\lambda_2 \rho) & 0 & H_n^2(\lambda_2 \rho) & \frac{jb_1 \omega}{\rho \lambda_2^2} H_n^2(\lambda_2 \rho) & \frac{-jb}{\rho \lambda_2^2} H_n^2(\lambda_2 \rho) \\ 0 & \frac{-jb_1 \omega}{\lambda_2} H_n^1(\lambda_2 \rho) & 0 & H_n^1(\lambda_2 \rho) & 0 & H_n^1(\lambda_2 \rho) & \frac{jb_1 \omega}{\rho \lambda_2^2} H_n^1(\lambda_2 \rho) & \frac{-jb}{\rho \lambda_2^2} H_n^1(\lambda_2 \rho) \\ 0 & 0 & 0 & 0 & -J_n(\lambda_3 \rho) & 0 & \frac{jb}{\rho \lambda_3^2} J_n(\lambda_3 \rho) & \frac{jk_3^2}{\mu_3 \epsilon \omega \lambda_3} J_n(\lambda_3 \rho) \\ 0 & 0 & 0 & 0 & 0 & 0 & -J_n(\lambda_3 \rho) & \frac{jb}{\rho \lambda_3^2} J_n(\lambda_3 \rho) \end{bmatrix} \\
 & = \sum_{n=-\infty}^{\infty} [e^{-jk_1 z \cos \theta} e^{-j\omega t} e^{j\omega t}] \begin{bmatrix} E_0 \sin \theta^n J_n(\lambda_1 \rho) \\ \frac{mb}{\rho} E_0 \sin \theta^n J_n(\lambda_1 \rho) \left(\frac{1}{\lambda_1^2} - \frac{1}{\lambda_2^2}\right) \\ \frac{-jk_1^2}{\mu_1 \epsilon \omega \lambda_1} E_0 \sin \theta^n J_n(\lambda_1 \rho) \\ 0 \\ 0 \\ 0 \\ 0 \\ 0 \end{bmatrix}
 \end{aligned}$$

The scattered wave impedance can be obtained by taking the ratio of Z component of scattered electric field and magnetic field. Among the eight unknowns, the parameters a_n^I, b_n^I determine the wave impedance. Assuming the zero reflection, reactance rather than impedance is considered. From the above matrix, the scattering reactance of the dielectric cover along with a conducting cylinder is obtained as in Table 1.

This reactance should be compensated by the surface reactance of the patterned dielectric cover for scattering cancellation. The frequency selective surface (FSS)

Table 1 Parameters for the modulated meta-surface cloak

Parameter	Value (in mm approx.)	$f = 5$ GHz ($\lambda = 60$ mm)	$f = 4$ GHz ($\lambda = 75$ mm)
Length of an object (L)	65	–	–
Radius of an object (a)	3.23	$\lambda/18$	$\lambda/23$
Radius of a cloak (a_c)	3.86	$\lambda/15$	$\lambda/19$
Scattered reactance (Ω)	–	310	390
Gap (G)	2	$\lambda/30$	$\lambda/37$
D_1	10	$\lambda/6$	$\lambda/7$
D_2	8	$\lambda/7$	$\lambda/9$

was then introduced in the dielectric cover for creating the compensating surface reactance. In this paper, 1D conformal metallic strip of FSS structures is considered. The corresponding surface reactance is given as [27],

$$X_s = \frac{-j\eta_0 c\pi}{\omega(f_r + 1)D} \left(\frac{1}{\log \csc\left(\frac{\pi g}{2D}\right)} \right)$$

The cloaking at dual frequency was performed by modulating the metallic strip. It is done by varying the geometry of unit cell as shown in Fig. 1b. This geometry variation creates impedance difference that leads to changes in phase velocity and finally the propagation path of the surface wave varies.

Consider an electric field source of dipole antenna operating at a frequency of 5 GHz. Assume, the excitation source is hidden by a finite length of the conducting cylindrical object, and so the object is covered by a patterned FSS dielectric cover as shown in Fig. 2.

The calculated scattered reactance of the covered object for the dimensions provided in Table 1. In order to compensate this reactance, the proposed FSS structure was designed.

The corresponding equivalent circuit of the modulated structure as designed in ADS software is as shown in Fig. 3. Similarly, an antenna of 4 GHz operating frequency is considered.

Fig. 2 Scenario of modulated meta-surface cloak with 5 GHz dipole antenna

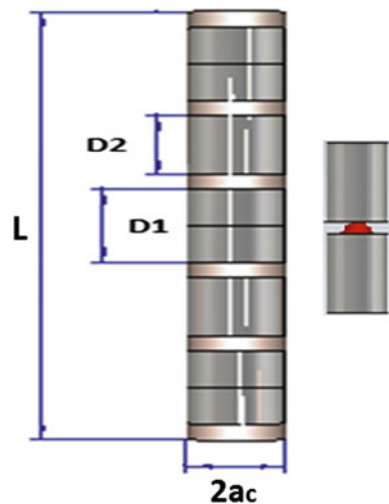
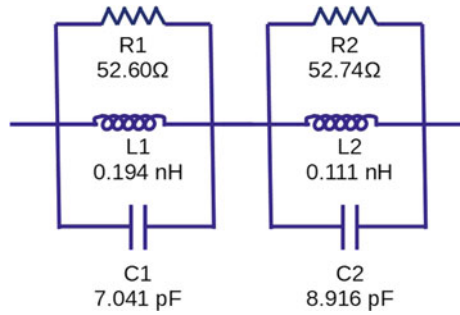


Fig. 3 Equivalent circuit of surface reactance calculation



3 Numerical Results and Discussion

This section numerically verifies the cloaking at dual frequencies using CST Microwave Studio Suite. An electric field excitation from a dipole source of 5 GHz is excited toward the bare finite conducting cylindrical object and the cloaked object of the modulated 1 D patterned FSS structure, and simulated results were recorded. The similar simulation was performed with 4 GHz dipole antenna.

Figure 4 shows the simulated results of both 4 and 5 GHz for the proposed FSS structures. The degradation performance in the scattering parameter of ‘without cloak’ identifies the hindrance of a conducting object. But with the proposed FSS covered object, restoration of the antenna parameters at 4 and 5 GHz can be obtained as similar to the isolated source. This verifies the cloaking effect of the patterned structure. From Fig. 4, the resonating behavior of 4 GHz antenna is also identified at 6 and 6.8 GHz.

Due to the resonating behavior of FSS structures, the S parameter result alone does not verify the cloaking effect. It can be further validated by the radiating property of the dipole antennas. Though the simulated S parameter of Fig. 4 shows the resonating

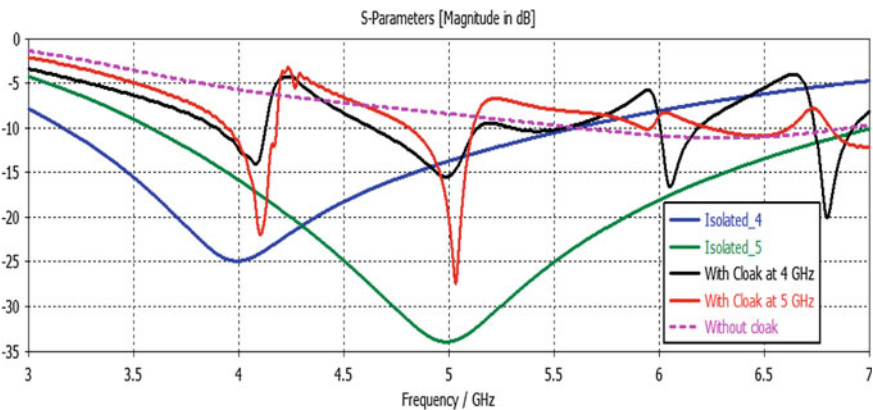
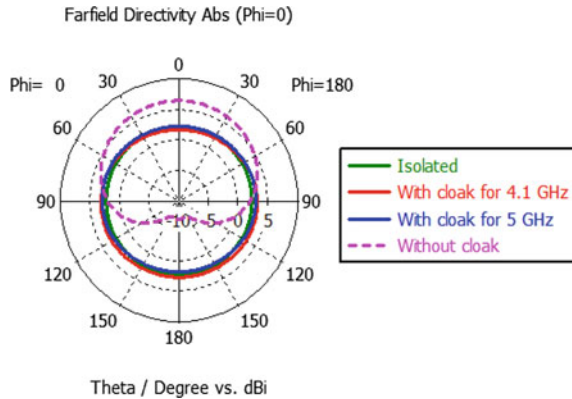


Fig. 4 Simulated S parameter for the dipole antenna of 4 and 5 GHz frequencies

Fig. 5 Radiation pattern for without object, with bare object and with cloak at 4 and 5 GHz



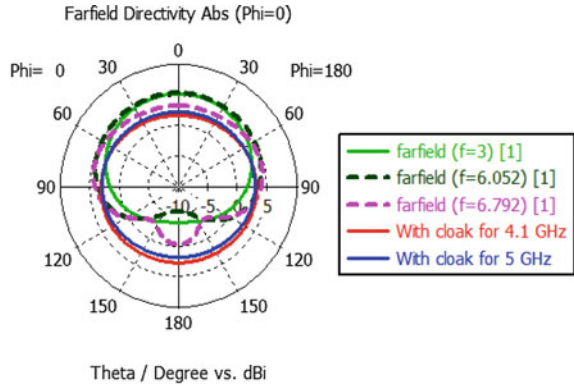
effect at 4, 5, 6 and 6.8 for 4 GHz dipole antenna, the cloaking effect can only have been identified at 4 and 5 GHz as in Fig. 4. Due to the different geometrical variation of a unit cell, both the resonating and cloaking effect can be identified at 4 and 5 GHz frequencies as in Fig. 5.

Figure 6a and b shows the radiation pattern at $\phi = 0^\circ$ and $\phi = 90^\circ$ for various frequencies. The theoretical radiation patterns of dipole were preserved for $\phi = 0^\circ$ and $\phi = 90^\circ$ only at 4 and 5 GHz frequencies compared to the other frequencies. The cloaking effect at dual frequencies was thus verified.

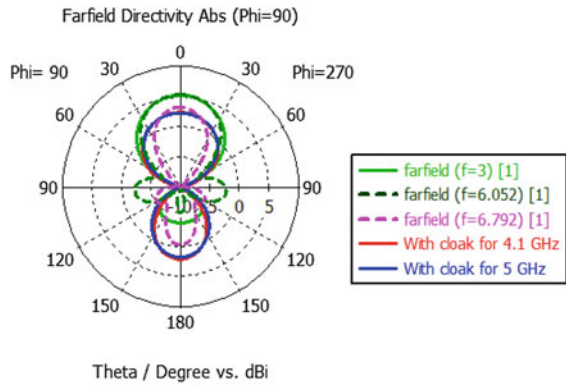
4 Conclusion

In this paper, the cloaking phenomenon for the proposed cloaking cover design at dual frequencies of 4 and 5 GHz was verified by exciting using a practicably accepted electric field excitation of dipole antenna. The simulated results of S parameter and radiation patterns differentiate the resonating and cloaking effects by the proposed mantle cover. Thus, the properly patterned modulated FSS structures in a single layer using mantle cloaking technique can cloak at dual frequencies. This can be further extended to multiband with more modulated patterned meta-surface structure in a single layer.

Fig. 6 Radiation patterns for various frequencies with modulated FSS structured cloak **a** $\phi = 0^\circ$ and **b** $\phi = 90^\circ$



(a)



(b)

References

1. Pendry JB, Schurig D, Smith DR (2006) Controlling electromagnetic fields. *Science* 312:1780–1782
2. Alitalo P, Luukkonen O, Jylha L, Venermo J, Tretyakov SA (2008) Transmission line networks cloaking objects from electromagnetic fields. *IEEE Trans Antennas Propag* 56(2):416–424
3. Wang J, Qu S, Ma H, Zhang J, Wang X, Xu Z (2013) Super thin cloaks based on microwave networks. *IEEE Trans Antennas Propag* 61(2):748–754
4. Wang J, Qu S, Ma H, Zhang J, Wang X, Xu Z (2015) Design of super thin cloaks with arbitrary shapes using interconnected patches. *IEEE Trans Antennas Propag* 63(1):384–389
5. Alu A, Cloak M (2009) Invisibility induced by a surface. *Phys Rev B* 80:245115
6. Chen PY, Alu A (2010) Patterned metallic surfaces to realize 1-D, 2-D and 3-D ultrathin invisibility cloaks. In: *IEEE international symposium on antennas and propagation society (APSURSI) 2010*. Canada
7. Kwon D-H, Werner DH (2008) Restoration of antenna parameters in scattering environments using electromagnetic cloaking. *Appl Phys Lett* 92(11):113507
8. Vehmas J, Alitalo P, Tretyakov SA (2011) Transmission-line cloak as an antenna. *IEEE Antennas Wireless Propag Lett* 10:1594–1597

9. Vehmas J, Alitalo P, Tretyakov SA (2012) Experimental demonstration of antenna blockage reduction with a transmission-line cloak. *IET Microwave Antennas Propag* 6(7):830–834
10. Monti A, Toscano A, Bilotti F (2012) Metasurface mantle cloak for antenna applications, IEEE international symposium on antennas and propagation. APSURSI, USA
11. Jiang ZH, Sieber PE, Kang L, Werner DH (2015) Restoring intrinsic properties of electromagnetic radiators using ultra light weight integrated metasurface cloaks. *Adv Funct Matter* 25:4708
12. Teperik T, de Lustrac A (2015) Electromagnetic cloak to restore the antenna radiation patterns affected by nearby scatter. *AIP Adv* 5:127225
13. Monti A, Soric J, Alu A, Bilotti F, Toscano A, Vegni L (2012) Overcoming mutual blockage between neighboring dipole antennas using a low-profile patterned metasurface. *IEEE Antennas Wirel Propag Lett* 11:1414
14. Bernety HM, Yakovlev AB (2015) Reduction of mutual coupling between neighbouring strip dipole antennas using confocal elliptical metasurface cloaks. *IEEE Trans Antennas Propag* 63(4):1554–1563
15. Kumutha N, Hariharan K, Manimegalai B (2015) Reduction of interference between two neighbouring antennas by a modulated metasurface. In: IEEE international WIE conference on electrical and computer engineering (WIECON-ECE). Bangladesh, pp 247–250
16. Monti A, Soric J, Barbuto M, Ramaccia D, Vellucci S, Trotta F, Alu A, Toscano A, Bilotti F (2016) Mantle cloaking for co-site radio-frequency antennas. *Appl Phys Lett* 108:113502
17. Gao Y, Huang JP, Yu KW (2009) Multifrequency cloak with multishell by using transformation medium. *J Appl Phys* 105(12):124505
18. Shao J, Zhang H, Lin Y, Hao X (2011) Dual-frequency electromagnetic cloaks enabled by LC-based metamaterial circuits. *Progress Electromag Res (PIERS)* 119:225–237
19. Alu A, Engheta N (2008) Multifrequency optical invisibility cloak with layered plasmonic shells. *Phys Rev Lett* 100:113901
20. Wang J, Qu s, Xu Z, Zhang A, Ma H, Chen H (2013) Multifrequency super-thin cloaks. *Photon Nanostruct Fundament Appl.* 12:130–137
21. Archana R, Srivastava KV (2017) Dual-band cloak using microstrip patch with embedded u-shaped Slot. *IEEE Antennas Wireless Propag Lett* 16:2848–2851
22. Soric JC, Monti A, Toscano A, Bilotti F, Alu A (2015) Multiband and wideband bilayer mantle cloaks. *IEEE Trans Antennas Propag* 63(7)
23. Jiang ZH, Werner DH (2016) Dispersion engineering of metasurfaces for dual frequency quasi-three-dimensional cloaking of microwave radiators. *Optics Express* 24(9)
24. Kumutha N, Hariharan K, Amutha N, Manimegalai B (2017) Dual band single layered metasurface cloak. In: Presented at IEEE international microwave and RF conference (IMaRC). Ahmedabad, India
25. Wait JR (1958) Transmission and reflection of electromagnetic waves in the presence of stratified media. *J Res Nat Bureau Stand* 61(3)
26. Balanis CA (1989) *Advanced engineering electromagnetics*. Wiley, New York, USA
27. Padooru YR, Yakovlev AB, Chen PY, Alu A (2012) Analytical modeling of conformal mantle cloaks for cylindrical objects using subwavelength printed and slotted arrays. *J Appl Phys* 112:0349075

Optical Noise Cancellation Using Artificial Neural Network



Sarita Kumari

Abstract This paper represents the study of magneto-optic sensor behavior using terbium-doped glass (TDG) rod as Faraday rotator. The performance of photo-detector is affected by different types of noises present in the optical path/medium. An artificial neural network has trained for cancelation of noise present in optical signal. The trained network has been able to perform de-noising of optical signal with mean of error in network to 0.44%.

Keywords Magneto-optic sensor · TDG · ANN · Noise cancelation · Faraday rotation

1 Introduction

The magneto-optic (MO) sensor is based on Faraday effect [1–3], which says that the plane of polarization of any linearly polarized light beam passing through Faraday rotator is altered under the presence of strong magnetic field. It can be used for many non-contact-type applications in the field of sensing, industry, astronomy, biomedical, etc. The sensor can be used for measurement of various parameters like displacement, current, pressure, temperature, vibration etc., in real time. It has many advantages over any other traditional sensor such as no effect from external electromagnetic and stray capacitance, electrical isolation, and large bandwidth. The integration with digital control system is easier for any monitoring and remote sensing and control purpose. It uses both magnetic and optical phenomena for the measurement.

ANN is a prototype of human brain which can process almost all kinds of input–output relationship. It has become very popular for problem-solving tool in almost all the fields. It can solve very complex problem and can work on nonlinear behavior of the system. ANN is widely applicable for forecasting, identification and control, classification, and optimization [4].

S. Kumari (✉)

Electronics and Communication Engineering Department, Amity University Jharkhand, Ranchi, India

e-mail: gs.sarita@gmail.com

Mathematically, a neuron k can be described by Eq. (1) and (2), where X_1-X_m are input signals, $W_{k1}-W_{km}$ are synaptic weights of neuron, b_k is bias, $\varphi(\bullet)$ is activation function, and Y_k is the output.

$$U_k = \sum_{j=1}^m W_{kj} X_j \quad (1)$$

$$Y_k = \varphi(U_k + b_k) \quad (2)$$

Noise is unwanted signal which interferes with original signal in measurement or communication process. Noise cancelation technique aims at removing or minimizing the unwanted parameters or noises present in the signal. There are different types of noises like white noise, colored noise, thermal noise, shot noise, electromagnetic noise, etc. [5].

Various works in the field of ANN and noise reduction have been done by the researchers worldwide. M. basu and team have developed an analytical neural network for ALU of microprocessor [6]. Fatemeh Bagheri et al. have implemented Hopfield neural network for modeling of ECG signal and to remove noisy signal for the same [7]. Lubna Badri analyzed and compared recurrent and multi-layer back propagation ANN for noise removal [8]. Many researchers have applied functional link artificial neural network (FLANN) for channel equalization for digital applications [9], nonlinear noise removal [10], prediction of machinery noise for opencast mines [11], etc.

In this article, the noise cancelation of optical signal using artificial neural network is proposed. The neural network has been trained in an application specific manner, using a data preprocessing that is implemented before the training takes place; hence, dimensionally increasing the data that is to be input into the ANN. The construction of the ANN is made of standard artificial neurons utilizing tan-sigmoid and linear transfer functions in the hidden and output layers, respectively. This also enables simpler circuitry, using a reduced number of components. Once the network is trained, the weights and the biases can be used to construct the electronic circuits for the individual neurons. Simulations have been performed to test several deep learning ANN architectures with two hidden layers employing a maximum of 20 neurons per layer.

2 Theory

The linearly polarized beam having intensity I_0 , incidents on the magneto-optic element with α_p azimuth. The Stokes vector S_{out} of the output beam is given in Eq. (3).

$$S_{out} = I_0 M_{ana} M_{rot} S_{in} \quad (3)$$

where M_{rot} , M_{ana} are Mueller matrices of Faraday rotator and analyzer, respectively. S_{in} is the normalized Stokes vector of linearly polarized input beam which is given by Eq. (2)–(4).

$$M_{\text{rot}} = \begin{bmatrix} 1 & 0 & 0 & 0 \\ 0 & \cos 2\theta & -\sin 2\theta & 0 \\ 0 & \sin 2\theta & \cos 2\theta & 0 \\ 0 & 0 & 0 & 1 \end{bmatrix} \quad (4)$$

$$m_{\text{ana}} = \frac{1}{2} \begin{bmatrix} 1 & \cos 2\alpha_a & \sin 2\alpha_a & 0 \\ \cos 2\alpha_a & \cos^2 2\alpha_a & \cos 2\alpha_a \sin 2\alpha_a & 0 \\ \sin 2\alpha_a & \cos 2\alpha_a \sin 2\alpha_a & \sin^2 2\alpha_a & 0 \\ 0 & 0 & 0 & 0 \end{bmatrix} \quad (5)$$

$$S_{\text{in}} = \begin{bmatrix} 1 \\ \cos 2\alpha_p \\ \sin 2\alpha_p \\ 0 \end{bmatrix} \quad (6)$$

where α_a is the transmission angle of the analyzer and θ is the Faraday rotation angle.

A linear horizontally polarized monochromatic beam is applied as input and the expression for detected intensity can be calculated by combining Eqs. (3)...(5), and (6).

$$I = \frac{I_0}{2} [1 + \cos 2(\theta - \alpha_a)] \quad (7)$$

Keeping $\alpha_a = 0$ in Eq. (7), we get,

$$I = I_0 \cos^2 \theta \quad (8)$$

Equation (8) follows the Malus's law which states that the intensity I of the light transmitted by the analyzer is directly proportional to the square of the cosine of angle analyzer and the polarizer [3].

The plane of polarization of incident polarized light is rotated by an angle θ in the presence of uniform magnetic field. The rotation depends on magnetic field B and path length of light passing through the sensor L . V_{verdet} is proportionality constant known as Verdet constant. Due to temperature dependency of Verdet constant, the Faraday rotation can be applicable for temperature measurement also.

$$\theta = V_{\text{verdet}} BL \quad (9)$$

3 Experimental Setup

The schematic diagram of the experimental setup is shown in Fig. 1.

The setup consists of a source to generate the highly coherent and monochromatic beam of light, a sheet polarizer to convert un-polarized light beam to linearly polarized light beam, and TDG rod as a Faraday rotator sensor is placed inside the externally powered solenoid coil to generate magnetic field. Another polarizer, i.e., crystal polarizer is placed after sensor called as analyzer. The optical signal from analyzer is sensed by PIN photodetector and converted into electrical signal for measurement and computation purpose.

A 5 mW diode-pumped solid-state laser having 635 nm wavelength is used for analysis. The laser light becomes polarized after passing through the sheet polarizer. TDG rod (Magneto-optic sensor) is placed inside the solenoid coil within the region of uniform magnetic field (1.2 cm), i.e., 4.6–5.8 cm starting from one end of solenoid. The optical signal is received on crystal polarizer and HP PIN photodiode is used to sense the optical signal. The output of PIN photo diode detector is used as the input of neural network.

The specification of solenoid coil used in experimental set-up is given in Table 1.

It is observed that photodiode output depends on the state of polarization of the optical signal. Number of experiments was performed and the experimental data was plotted using MATLAB software. The signal from photodetector is fed as the input to the neural network system. The output of photo diode detector was recorded for different analyzer angles keeping polarizer at horizontal position ($\alpha_p = 0$).

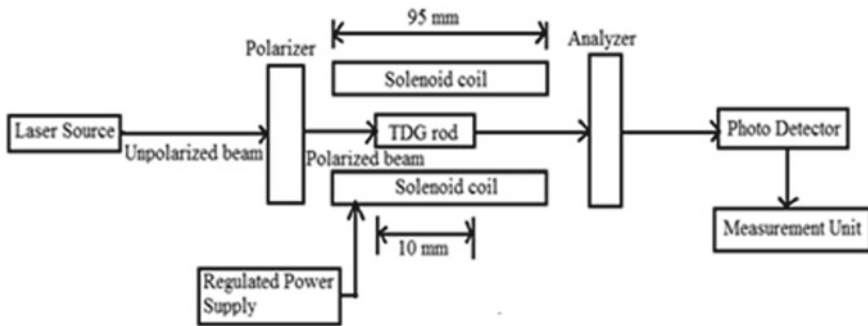


Fig. 1 Experimental setup

Table 1 Solenoid details

Length	Diameter	Number of turns	Material
95 mm	12 mm	2600	Copper

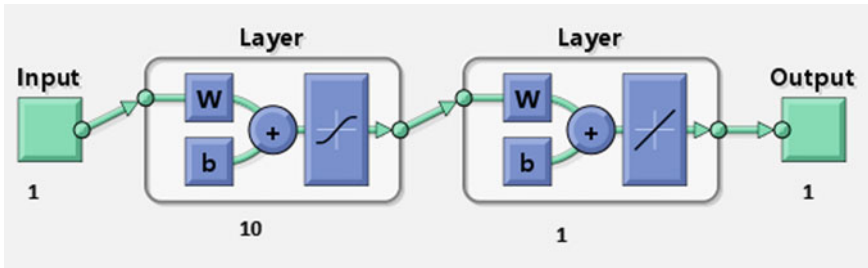


Fig. 2 ANN architecture using two hidden layers

4 Simulation

MATLAB neural network toolbox was used to perform the simulation. Neural network is trained in an application-specific manner, using a data preprocessing that is implemented before the training takes place, hence dimensionally increasing the data that is to be input into the ANN. The construction of the ANN is made of standard artificial neurons utilizing tan-sigmoid and linear transfer functions in the hidden and output layers, respectively. This also enables simpler circuitry, using a reduced number of components. Once the network is trained, the weights and the biases can be used to construct the electronic circuits for the individual neurons. Several simulations were performed to achieve the best possible network architecture shown in Fig. 2. The two-layer ANN is designed. First network has TANSIG neuron and the second layer has PURELIN neuron. Multiple layers of neurons which have nonlinear transfer function train the ANN for linear and nonlinear relation of input–output functions. Feed-forward back propagation method is applied for this ANN where the signals are sent in reverse direction for learning.

5 Result and Discussion

The relationship between changes in analyzer angle with respect to per unit change in photodetector output is shown in Fig. 3. It represents theoretical result in comparison with the experimental result which follows the Malus's law as mentioned in Eq. (6). It states that the intensity of plane-polarized light that passes through an analyzer varies as the square of the cosine of the angle between the plane of the polarizer and the transmission axes of the analyzer. It also represents the predicted plot from artificial neural network which shows very high accuracy with theoretical result. This means that the network has been trained quite well.

Figure 4 represents the regression plot for training, validation, and testing purpose. It also represents overall regression factor which is 99.9% after applying the ANN. The trained network was a deep learning neural network with two hidden layers having 20 neurons in each layer.

Fig. 3 Normalized output intensity versus analyzer position curve

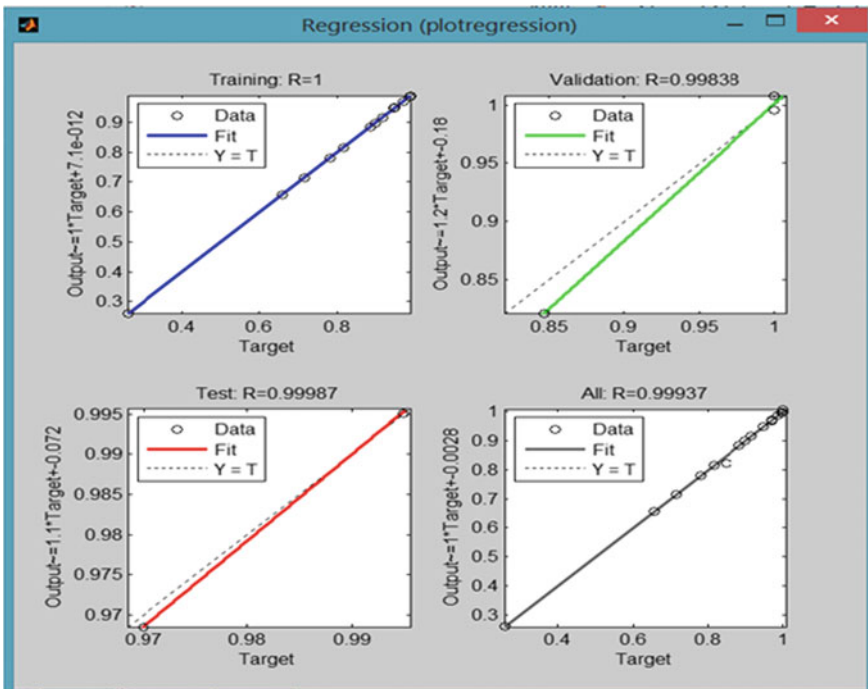
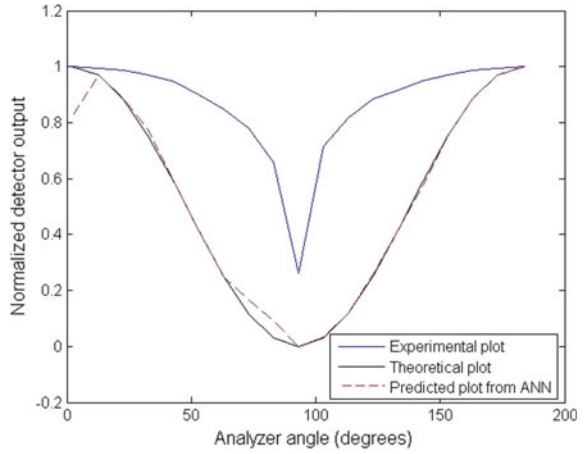


Fig. 4 Regression plots

6 Conclusion

ANN can find pattern or input–output relationship among many non-linear and dynamic systems. The neural network was trained well and successfully canceled the optical noise involved in the detector output signal. The mean value of network error was calculated as 0.44%.

References

1. Hecht E (1987) Optics. Addison-Wesley. Low price edition, Reading
2. Jenkins FA, White HE (1976) Fundamentals of Optics, 4th edn. McGraw- Hill, New York
3. William A (1962) Shurcliff. Harvard University Press, Cambridge, Massachusetts, Polarized Light Production And Use
4. Haykin S Neural networks: a comprehensive foundation, second Edition. Published by Prentice Hall.
5. Saeed VV (2000) Advanced digital signal processing and noise reduction, Second Edition. Wiley
6. Mainak B, Abhishek P, Abhijit M (2015) An analytical neural network for arithmetic logic unit of microprocessors. IISRR-Int J Res 1(2)
7. Bagheri F, Ghafarnia N, Bahrami F (2013) Electrocardiogram (ECG) signal modeling and noise reduction using hopfield neural networks. ETASR Eng Technol Appl Sci Res 3(1):345–348
8. Lubna B (2010) Development of neural networks for noise reduction. Int Arab J Inform Technol 7(3)
9. Patra JC, Pal RN (1995) A functional link artificial neural network for adaptive channel equalization. Signal Process Elsevier Sci 43:181–195
10. Ganapati P, Debi PD (2003) Functional link artificial neural network for active control of nonlinear noise processes. In: International workshop on acoustic echo and noise control (IWAENC2003). Kyoto, Japan
11. Santosh KN, Debi PT (2011) Application of functional link artificial neural network for prediction of machinery noise in opencast mines. In: Advances in fuzzy systems. Hindawi Publishing Corporation

Digital Chaos Encryption-Based Sub-Block Partition by a Hybrid PTS Approach and PAPR Reduction Using HSOSS Algorithm



Mrinmoy Sarkar, Asok Kumar, and Bansibadan Maji

Abstract Decreasing the peak-to-average power ratio (PAPR) is a great challenge for data communication using OFDM. Here is introduced a new hybrid optimized partial transmit sequence (PTS) for minimizing the PAPR, where data encryption is done with 4D DFT-based hyper-chaotic sequence. An innovative hybrid seagull optimization and salp swarm (HSOSS) optimization are proposed here to produce a phase weight factor for the PTS. Several sizes of the subcarrier are investigating the new approaches performance. The proposed model is implemented in MATLAB platform and performances are calculated with factors like bit error rate (BER) with respect to signal-to-noise ratio(SNR), PAPR complementary cumulative distribution function (CCDF) in regard to SNR, and the finally, based on the computation time, final results are compared.

Keywords OFDM · PAPR · PTS · HSOSS · CCDF · SNR

1 Introduction

In wireless communication system, OFDM is considered as an effective technology for the high-speed data rate. Worldwide interoperability for microwave access IEEE.802.16 [1], wireless local area network (WLAN) IEEE.802.11 [2], and digital video broadcasting (DVB) are the several communication frameworks based on the OFDM systems known as transmission data technology. The elevated PAPR is the key

M. Sarkar (✉)

Department of Electronics and Communication Engineering, Bankura Unnayani Institute of Engineering, Bankura, West Bengal 722146, India
e-mail: mrinmoysarkar.phd@gmail.com

A. Kumar

Dean of Students Welfare, Vidyasagar University Midnapur, West Bengal, Midnapur 721102, India
e-mail: asok_km650@rediffmail.com

B. Maji

Department of Electronics and Communication Engineering, NIT, Durgapur 713209, India
e-mail: bmajjecenit@yahoo.com

difficulty of the OFDM systems, and the high power amplifiers (HPAs) are occurred by high PAPR multicarrier signal [3].

PAPR is calculated per OFDM symbol, which is used for enumerating envelope fluctuations. The amount of CCDF minimization measured the capability of PAPR reduction [4]. One of the well-known PAPR minimization approaches is named PTS approach. The time-domain (T.D), modulation (IFFT), and frequency-domain (F.D) are the three aspects used to review the various ordinary and modified-PTS schemes. In distinct sub-blocks, the addition of power of time domain is also known as cost function, which is generated to reduce the complexity in PTS [5].

The improved DFT-based and chaotic chirp matrix approaches [6] are proposed to simultaneously achieve security performance and PAPR reduction. Moreover, orthogonal-phase (Q) and chaotic self-phase (I) encryption approach are also proposed to realize scheme encryption using linking symbols in the time and frequency domain [7]. PTS, trellis-assisted constellation subset selection (TACSS) and non-linear commanding transforming, active constellation extension (ACE) [8], selected mapping, peak windowing, tone injection, coding, filtering and clipping, and clipping are the various solutions introduced to eliminate the high PAPR issue in OFDM. PTS is the most efficient and attractive scheme among these schemes, because, which has high PAPR reduction without signal distortion. With several evolutionary algorithms for optimization named genetic algorithm (GA), particle swarm optimization (PSO), and artificial bee colony (ABC) [9].

2 Related Works

Arun Kumar and Manisha Gupta [10] have suggested a PTS and SLM PAPR minimization for FBMC. An elementary successive optimization approach was introduced for implementing the proposed model, which enhance the performance and the difficulty of design was less.

The combination of PTS and Gaussian pulse-based TR approaches was introduced by M. Vijayalakshmi and K. Ramalinga Reddy for reducing the PAPR [11].

A new PTS scheme based on multi-population cultural algorithm adopting knowledge migration (MCAKM) has been introduced by Tarik Hadj Ali and Abdelkrim Hamza for best phase rotation factors search [12].

A proficient PTS scheme based on particle swarm optimization (PSO) was introduced by Mehdi HosseinzadehAghdama and Abbas Ali Sharifi for minimizing the PAPR [13]. The modulated signals in OFDM were transmitted by a huge amount of subcarriers, which have maximum PAPR.

Minimum-complexity side data-free new PTS approach was proposed by Samriti Kalia and Alok Joshi to diminish PAPR in OFDM Systems [14]. A new PTS approach without side information and with reduced complexity was proposed here.

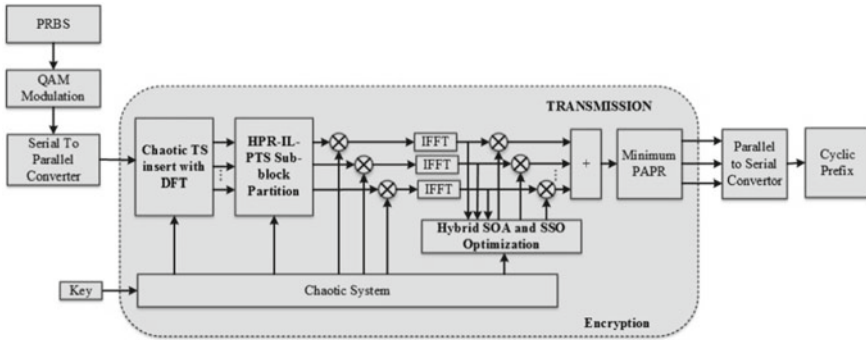


Fig. 1 Schematic block diagram

3 Proposed Methodology: A 4D Hyper-Chaotic-Based Hybrid Optimized PTS for PAPR Reduction

In this research, data encryption is taken by the 4D digital hyper-chaos, and then a new hybrid sub-block partition is taken by the PR-IL-PTS approach and finally, the phase weighting factors are optimized by HSOSS algorithm for PAPR minimization. Hence, the data transmission in OFDM system is securely transmitted and the minimization of PAPR is also achieved.

The overall schematic model of proposed PTS approach is demonstrated in Fig. 1, A pseudo-random binary sequence (PRBS) is given to the serial to parallel (S/P) converter after the QAM modulation. The converted sequences are given to the chaotic TS with DFT for the security purpose, which is given to the sub-block partition by HPR-IL-PTS. Inverse Fast Fourier Transformation is performed on the partitioned signals, and then each signal is multiplied with weight factors generated with HSOSS algorithm. Now the minimum PAPR signal is proceeded. Then the signals are converted parallel to serial stream and guard bands are provided with cyclic prefix.

4 Implementation: Results and Discussion

The correlation parameters are used to produce better performance in PAPR minimization. The performances are demonstrated in terms of CCDF, BER, CCDF in terms of number of subcarriers, CCDF as regards sub-blocks, PAPR reduction with respect to number of iterations, CCDF in terms of sub-block partition methods, and total generation cost and time complexity. The proposed model is compared with existing PAPR reduction methods such as original OFDM, PTS, GWO-PTS, HWOMFO and it shows the proposed scheme outcomes are maximum compared to others. Data encryption is done by the 4D chaotic hyper TS and the sub-blocks are

partitioned effectively by HPR-IL-PTS approach and it compared with original PR-PTS and IL-PTS and the phase weighting factors are obtained by HSOSS algorithm. The BER performance in OFDM with respect to SNR in dB is shown in Fig. 2; it shows that the proposed model achieved less error rate. The main goal of this research is to obtain very less BER and PAPR reduction. This figure shows that the proposed model achieves best performance than the other existing approaches. At SNR = 4.3 dB, then, the BER value of the proposed model is 10^{-8} , but the actual OFDM has 10^{-1} .

Figure 3 demonstrates the CCDF in terms of SNR in dB; it shows the comparison of CCDF of proposed approach with existing approaches. The proposed scheme HSOSS is compared with existing models such as original OFDM, PTS, GWO-PTS, and HWOMFO. The proposed model achieves low CCDF at SNR = 4 dB, this performance is better compared to that of actual OFDM. For the proposed model, the SNR = 4 dB, then the CCDF value is 10^{-17} .

Figure 4, here the proposed model compared with existing HWOMFO and PS-GWO. It is the convergence diagram; it gives convergence rate of PAPR with respect to the number of iterations. Compared to PS-GWO, the proposed model achieves

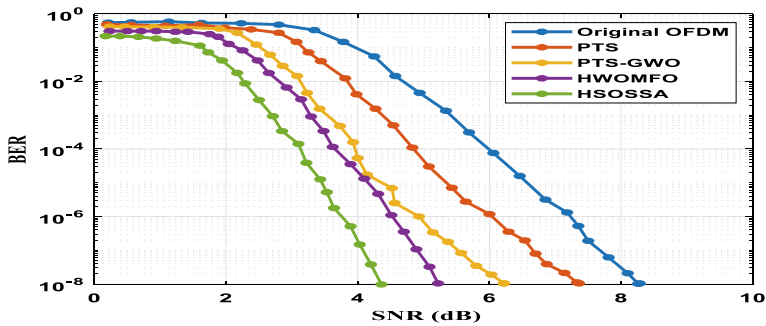


Fig. 2 BER with respect to SNR in dB

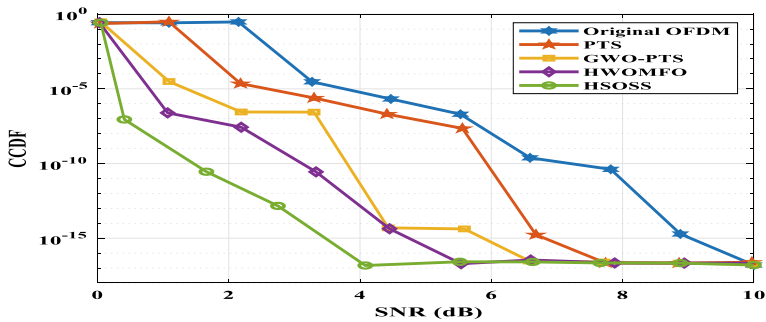
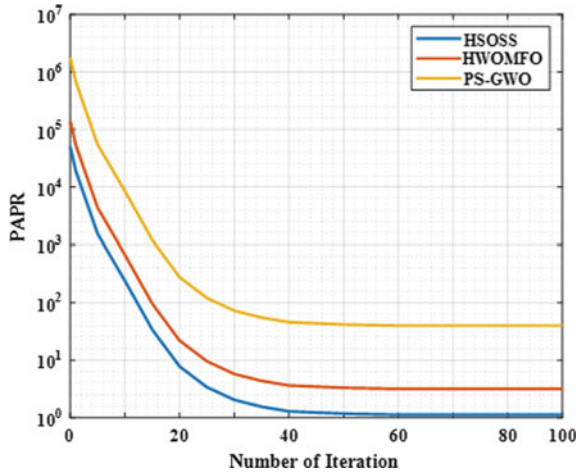


Fig. 3 CCDF versus SNR Performance in dB

Fig. 4 PAPR reduction with respect to number of iterations



easily convergence rate. The proposed (HSOSS) model gets converge rate at the twentieth iteration, but PS-GWO gets converge at thirtieth iteration.

CCDF versus SNR performance for different subcarriers is shown in Fig. 5. The subcarriers taken from 16 to 256 and the proposed scheme's CCDF value are shown by every subcarriers.

Figure 6 shows the CCDF performance in terms of PAPR for different sub-blocks at initial condition. The sub-block partitions are done by the hybrid PR-IL-PTS partition approach. Blocks are divided by 2, 4, 6, and 8 sub-blocks; compared with original OFDM, the sub-block partition approach has better CCDF performance. The PAPR value is 3.8 dB, and then the CCDF is 10^{-6} .

Comparison of CCDF performance of proposed algorithm with respect to SNR is demonstrated in Fig. 7. Here, the proposed sub-block partition approach is compared with existing partition approach PR-PTS and IL-PTS. The proposed sub-block partition method archives very less CCDF compared to other two approaches.

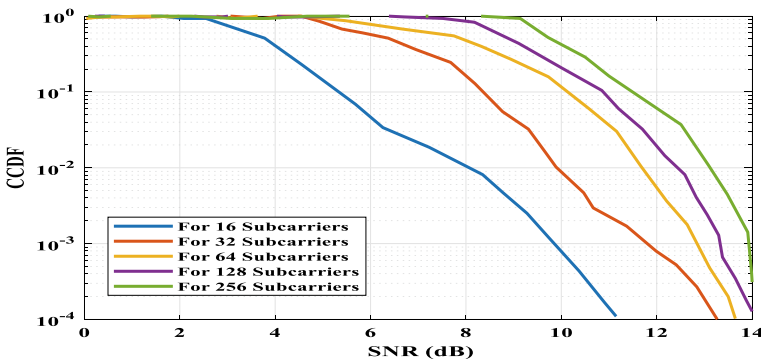


Fig. 5 CCDF of PAPR performance with respect to SNR for different subcarriers

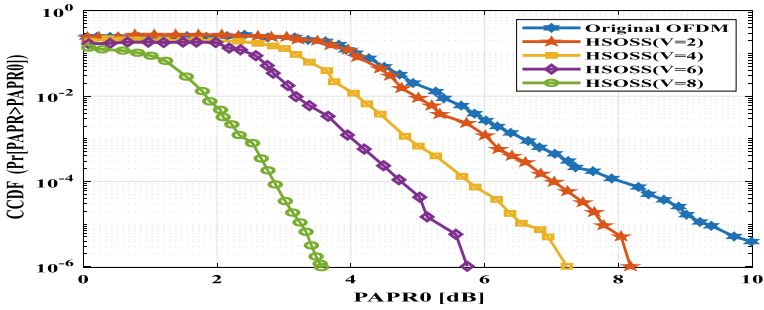


Fig. 6 CCDF performance in terms of PAPR for different sub-blocks at initial condition

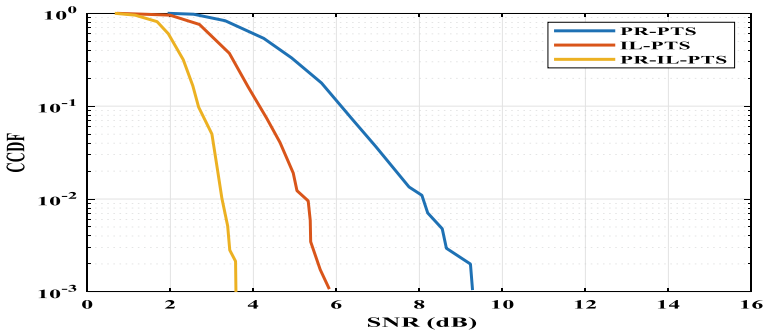


Fig. 7 CCDF with respect to SNR for sub-block partition approaches

5 Conclusion

The new hybrid optimized PTS approach is introduced in this research for decreasing BER and PAPR in OFDM. The sub-blocks are partitioned efficiently by HPR-IL-PTS approach, which achieves the maximum performance. The optimal phase weighting factors are obtained by a new hybrid SOSS algorithm, which proceed the scheme with low PAPR. The encoded signals are modulated using QAM modulation. Next, the signals are encrypted by 4D hyper-chaotic sequences. The chaotic TS is inserted with DFT for the encryption. Then, the encrypted signals are efficiently partitioned. The new hybrid optimized PTS approach is introduced in this research to diminish the PAPR and BER in OFDM. The sub-blocks are partitioned efficiently by HPR-IL-PTS approach, which achieves the maximum performance. After the partitions, the IFFT is used over the modulated signal, and the cyclic prefix is inserted here. In the receiver side, the reverse process of transmission takes place.

References

1. Rahmatallah Y, Mohan S (2013) Peak-to-average power ratio reduction in OFDM systems: a survey and taxonomy. *IEEE Commun Surveys Tutori* 15(4):1567–1592
2. Chen Z, Kang SG (2014) A three-dimensional OFDM system with PAPR reduction method for wireless sensor networks. *Int J Distrib Sens Netw* 10(3):312308
3. Praveenkumar P, Amirtharajan R, Thenmozhi K, Rayappa JBB (2013) OFDM with low PAPR: A novel role of partial transmits sequence. *Res J Inform Technol* 5:35–44
4. Jayashri R, Sujatha S, Dananjayan P (2015) DCT based partial transmit sequence technique for PAPR reduction in OFDM transmission. *ARNP J Eng Appl Sci* 10(5):2182–2186
5. Sarkar M, Kumar A, Bansibadan M (2019) PAPR reduction and encryption based on hybrid optimized PTS and chaotic DFT sequences in OFDM systems. *Int J Eng Adv Technol*
6. Ramli K, Taher M, Audah L, Shah NS, Ahmed M, Hammoodi A (2018) An enhanced partial transmit sequence based on combining Hadamard matrix and partitioning schemes in OFDM systems. *Int J Integrat Eng* 10(3):1567–1592
7. Sarkar M, Kumar A, Bansibadan M (2020) Security aware hybrid precoding based peak to average power ratio reduction approaches for telecommunication system. *Int J Commun Syst*
8. Prasad S, Jayabalan R (2020) PAPR reduction in OFDM systems using modified SLM with different phase sequences. *Wireless Pers Commun* 110(2):913–929
9. Lahcen A, Mustapha H, Ali E, Saida A, Adel A (2019) peak-to-average power ratio reduction using new swarm intelligence algorithm in OFDM systems. *Procedia Manuf* 32:831–839
10. Kumar A, Gupta. M (2020) Peak-to-average power ratio reduction in FBMC using SLM and PTS techniques. In: *Multimedia big data computing for IoT applications*. Springer, Singapore, pp 163–183
11. Vijayalakshmi M, Reddy KR (2020) An effective hybrid approach for PAPR reduction in MIMO-OFDM. *Analog Integr Circ Sig Process* 102(1):145–153
12. Ali TH, Hamza A (2019) PTS scheme based on MCAKM for peak-to-average power ratio reduction in OFDM systems. *IET Commun* 14(1):89–94
13. Aghdam MH, Sharifi AA (2019) PAPR reduction in OFDM systems: an efficient PTS approach based on particle swarm optimization. *ICT Express* 5(3):178–181
14. Kalia S, Joshi A (2019). low-complexity side information-free novel PTS technique for PAPR reduction in OFDM systems. In: *Advances in signal processing and communication*. Springer, Singapore, pp 65–71

Millimeter Wave: A Novel Approach for Integrating Radar and Communication for Autonomous Driving



M. Chakraborty, A. Banerjee, D. Kandar, and B. Maji

Abstract Joint operation of radar and communication is one of the most essential arena of research for the past two decades in the field of intelligent transportation systems. For commercial viability, the joint system must be cost effective with lesser complexity, minimized intercarrier interference between the systems so that the same can be used autonomous driving of smart transportation system. Here, we have proposed a joint radar communication platform using 77 GHz millimeter wave vehicular radar. The reason behind choosing this radar to provide a common platform is that this radar has become very popular as vehicular radar nowadays. We have used the chirp signal as a common carrier frequency for radar and communication; but, unlike the radar, the chirp frame used to modulate the communication data is made orthogonal. The two chirp signals of identical frequency are added together and transmitted. Because of the orthogonal relationship between the radar and the communication signal, intercarrier interference is reduced. As well as the FMCW chirp radar is inherently Doppler tolerant, therefore, precision velocity estimation is also possible. Subsequently, in this work, we have assessed the behavior of 77 GHz automotive FMCW radar with single antenna as well as with multiple antennas. These high-frequency radars can combat the harsh environmental conditions such as low-light quality and poor weather. Hence, 77 GHz FMCW radar sensors are chosen in the automotive applications. Results proved that FMCW automotive STAP radar gives enhanced performance in respect of target car appearance in Doppler processing and the range-Doppler coupling compensation with low bit error rate.

M. Chakraborty (✉)

Amity University Jhrakhand, Ranchi 834001, India
e-mail: mchakraborty@mc.amity.edu

A. Banerjee

National University of Singapore, Singapore, Singapore
e-mail: amitbanerjeeiacseru@gmail.com

D. Kandar

Department. of IT, NEHU, Shillong, India
e-mail: kdebdatta@gmail.com

B. Maji

NIT Durgpur, Durgpur, West Bengal, India
e-mail: bmajiecenit@yahoo.com

Keywords FMCW · ICI · RADAR RADIO · mmW

1 Introduction

Specific vehicular safety applications including revenue collection at toll plaza at 5.9 GHz spectrum are enabled with existing sensing and communication technology in intelligent transportation systems [1] but they suffer from a very low data rate. Although on the positive side, they are having low latency. The advanced intelligent transportation system requiring the vehicles to deal with heavy data traffic from cloud, live data stream from the radar sensors of itself, and other vehicles, cameras, LIDAR, data with the road side unit, data from satellite, etc. [2, 3]. Management of this information flood for real-time decision making requires a vehicular technology having large bandwidth support with very low noise performance. Intelligent transportation system featured with this vehicle to anything (V2X) real-time sensing and communication can be deemed fit by simultaneous millimeter wave (mmW) sensing and communication [4, 5]. The accurate range estimation by almost few centimeters [6] due to the highly directional beam of mmW radar sensor at 77 GHz make it a viable candidate for the vehicular safety applications. Wireless communication at mmW suffers due to high attenuation loss [7, 8]. To combat this loss increasing signal to noise ratio, directional adaptive beam forming with signal combining [9] is implemented at the receiver. Again the receiver improved performance is obtained by the application of channel estimation [10]. Although it is affected by the scattering due to the large attenuation loss and high absorption loss at the operating wavelength [11, 12]. The beam formation[13, 14] and combination are constrained by few RF blocks at the front end in millimeter wave transmitter and receiver containing high speed A/D converters which consumes measurable power as well as incur high costs. The authors have proposed here an intelligent transportation system in road scenario, whereby a vehicle containing radar with motion detects two moving cars as targets, using 77 GHz mmW radar sensor [15, 16], estimates their velocity and distance information and communicates with the fixed road side unit by forming directional beams, assuming the mmW road side units or base stations are enabled with beam forming capability.

The rest of this paper is organized as follows. Section 2 presents contribution in the field of joint radar communication applications with problem identification, Sect. 3 describes the system model for joint radar radio, Sect. 4 presents the proposed model with its advantages, and finally, Sect. 5 gives the conclusion with the novelty of the proposed work.

2 Related Contribution

Joint operation of radar and communication was the topic of concern since last decade for many applications like autonomous driving, cooperative driving, anti-terrorism, human lives protection in earthquake affected areas, etc. Many researchers have put their effort in finding the solution possible for the relevant problems. In the literature of Sturm and Zwick [17] using OFDM radar, the authors have detected static or dynamic objects with the radar. In [18] published work by M. Braun, C. Sturm has designed radar subsystem but limited with channel design, bandwidth, design of radar frame, etc. In the literature [19] of Y. L. Sit, L. Reichardt, C. Sturm multiobject detection in a multipath scenario is established using OFDM radar. But these articles did not address the issue of joint simultaneous radar sensing and wireless communication considering the intercarrier interference. The researchers have shown radar sensing but did not present reception of communication information. In the literature of Y. Nijsure, Y. Chen, S. Boussakta [20], the authors have demonstrated the design of joint radar communication using UWB PPM, but the system was limited by different pulse delay for binary communication data and communication data rate, radar target detection probability, and proof of detected targets in range–Doppler map. Literature [21] of F. Hu and G. Cui have used the concept of joining the radar and communication by using stepped frequency continuous waveform as a carrier to modulate the communication data. The limitations of the designed system were AWGN channel which is considered; only single static target was detected. In [5], P. Kumari and J. Choi have proposed an IEEE 802.11ad-based radar sensing long-range using 60 GHz radio. But they did not present how the radar and communication waveforms are separated in transmitter.

2.1 Problem Definition

Going through the relevant literatures, the problem areas identified as joint operation of radar sensing and wireless communication without intercarrier interferences between the systems managing the issue of scarcity of spectrum for operation in a user populated environment.

2.2 Proposed Solution

Joining the radar sensing and wireless communication is proposed to be implemented using the millimeter waveform (mmW). The major problem of spectrum scarcity can be eliminated using the millimeter wave spectrum band. Because the mmW spectrum is not populated with users, hence in the idle spectrum, it would be easy to achieve 550 MHz bandwidth at a time. Along with that the proposed system mixes radar and

communication with phase angle separation making the system adequately protected from intercarrier interference (ICI).

3 System Modeling

As part of the system design, we model radar model with target, its transmitter receiver, and communication system model. This section will discuss these system modeling.

3.1 Radar System Model

We have chosen to operate with the frequency modulated continuous wave [FMCW] radar [22, 23] because of its low power requirement and smaller size and it can easily be installed in the vehicle. The FMCW radar transmitter transmits a continuous wave. A sinusoidal signal is used to modulate the baseband. The received echo is same as transmitted wave delayed in time by Δt which is related to the range. Because the signal is always sweeping through a frequency band, the frequency difference at any moment during the sweep remains constant and is usually called the beat frequency which can be translated to range.

3.2 Target Modeling

The target vehicles are modeled as car 1 and car 2 having their area in square meter. The distance of target car 1 is 150 m from the vehicle containing the radar with a speed of 90 km per hour, whereas the distance of target car 2 is 100 m with a speed of 150 km per hour. The channel for the radar imaging is taken as free space.

3.3 Radar Transmitter

Uniform linear array of 12 elements, each of the elements are isotropic radiator, and spacing between any two is $\lambda/2$. Radar is installed on a vehicle having platform velocity. We have assumed that the radar is a mono-static frequency modulated continuous wave radar, operating at 77 GHz. The radar can distinguish two targets at distances of 300, 500 m, and estimates the relative velocity and Doppler.

3.4 Radar Receiver

Receiver collects the reflected target car signatures. De-chirp operation is performed on the echo signal and buffered for each sweep of the transmit signal. This de-chirped signal helps to find the beat frequency and Doppler shift resulting in an estimation of range and speed of each target.

3.5 Communication System Model

As the communication with the road side unit is done using mmW, therefore, it is assumed that the fixed road side units which are forming a part of the vehicular cloud are also enabled with mmW transceiver. Also, there should be a mechanism for frequency down conversion to exist in these fixed RSUs, so that they can further communicate with the base transceiver stations (BTS). For implementation, we have assumed here that the front end of the communication system of the mobile vehicle is configured to have multiple input single output (MISO) transmit beam formation and a (Fixed) road side unit (RSU) enabled with single antenna and working as a receiver. The transmitter transmits OFDM data frame at the base band level. The mobile unit transmitter contains multiple antenna (12 element) with a transmit power of 9 W and gain -8 dB. The communication unit of the mobile vehicle will continuously form the beams while approaching or leaving a RSU for maintaining high signal to noise ratio.

4 Proposed Model

The integration of radar sensing and wireless communication is proposed here by using the common waveform, i.e., FMCW chirp. The FMCW chirp signal is used for vehicular target detection, and the same waveform is utilized with its 90° phase shifted version for transmission of OFDM communication data. As shown in the following block diagram of Fig. 1 in the transmitting section of the proposed joint RADAR RADIO system, the chirp generator output is fed simultaneously to the first input of the summer block and the 90° phase shifter circuit. The phase shifter output is fed to the modulator whose other input is the base band communication OFDM data frame. The output of the modulator is fed to the second input of the summer. Hence, the base band communication data is used to modulate the 90° phase shifted version of FMCW chirp signal. The output of the summer which is the joint RADAR RADIO signal is passed through a microwave circulator and is transmitted through the antenna to the multipath channel. This makes the radar and the communication signals orthogonal to each other which eliminate the probability of intercarrier interference (ICI) between the radar and wireless communication.

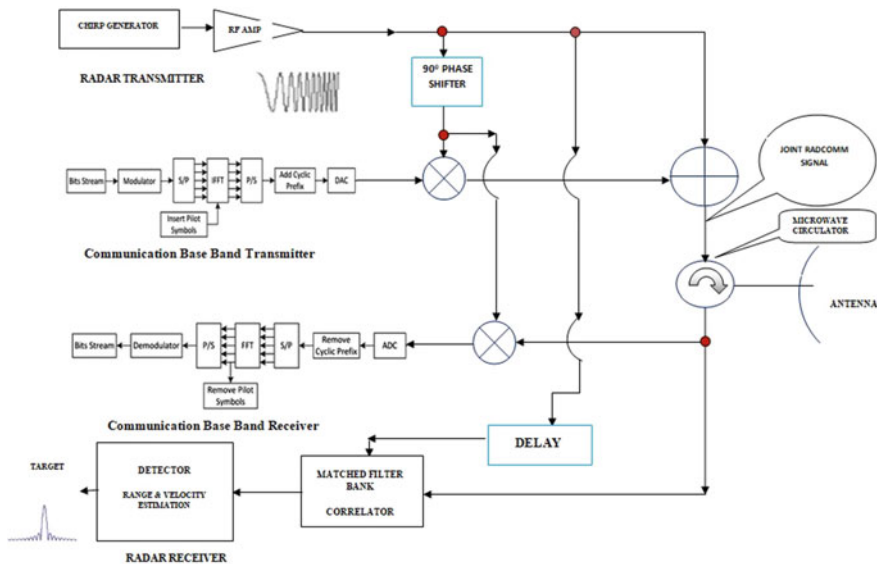


Fig. 1 Proposed FMCW RADAR RADIO block diagram

This meets the proposed objective of using a common waveform and removal of ICI dictating the novelty of the proposed system.

4.1 Signal Modeling at the Transmitter

The baseband OFDM data frame for N contiguous subcarriers at z th time instant is represented as,

$$S_z(t) = \left(\frac{1}{N}\right) \sum_{k=0}^{N-1} X_{z,k} e^{j2\pi k_n T} \quad (1)$$

where $X_{z,k}$ is the symbol of the k th subcarrier, $j = \sqrt{-1}$. And its spectrum is given by

$$S(f) = \sum_{k=0}^{N-1} X_{z,k} \sqrt{T} \frac{\text{Sin}(\pi(f - f_n)T)}{(\pi(f - f_n)T)} \quad (2)$$

FMCW radar signal generated is shown in Fig. 2

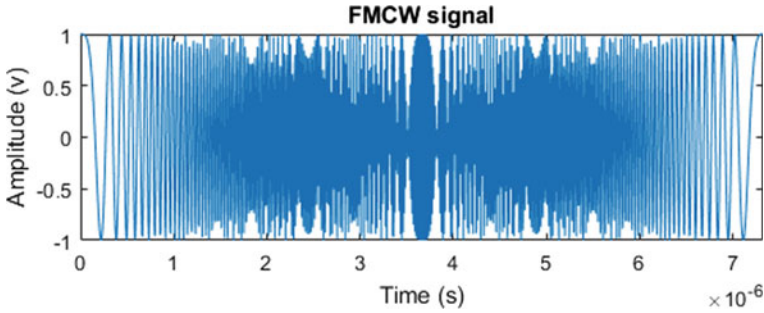


Fig. 2 Generated FMCW waveform for transmission

$$S_{\text{FMCW-radar}}(t) = V_C \text{Cos} \left\{ 2\pi f_C t + k \frac{t^2}{2} \right\} \quad (3)$$

90° phase shifted FMCW signal used for modulating communication data is

$$S_{\text{FMCW-phased}}(t) = V_C \text{Cos} \left\{ 2\pi f_C t + k \frac{t^2}{2} + \frac{\pi}{2} \right\} \quad (4)$$

Assuming the serial data sequence required to be transmitted is $\{d_0, d_1, d_2, \dots, d_{N-1}\}$, where each of the d_k is a complex number such that $d_k = (a_k + j \cdot b_k)$.

Hence

$$\begin{aligned} D_k &= \sum_{n=0}^{N-1} \sum d_n e^{-j2\pi nk/N} \\ &= \sum_{n=0}^{N-1} d_n e^{-j2\pi f_n t_k} \text{ for } k = 0, 1, 2, \dots, (N-1) \end{aligned} \quad (5)$$

where $f_n = \frac{n}{\text{NTD}}$ and $t_k = k\text{DT}$, DT is symbol duration. Considering the real part of the data, D_k is $Y_k = \text{Re}$

$$\{D_k\} = \sum_{n=0}^{N-1} [a_n \text{Cos} 2\pi f_n t_k + b_n \text{Sin} 2\pi f_n t_k] \quad (6)$$

The modulated communication data is of the form

$$\begin{aligned} S_{\text{FMCW-comm}}(t) &= \left\{ \sum_{n=0}^{N-1} [a_n \text{Cos} 2\pi f_n t_k + b_n \text{Sin} 2\pi f_n t_k] \right\} \\ &V_C \text{Cos} \left\{ 2\pi f_C t + k \frac{t^2}{2} + \frac{\pi}{2} \right\} \end{aligned} \quad (7)$$

Hence, the transmitted single carrier RADAR RADIO signal is

$$S_{\text{RADAR RADIO}}(t) = V_C \text{Cos} \left\{ 2\pi f_C t + k \frac{t^2}{2} \right\} + \left\{ \sum_{n=0}^{N-1} [a_n \text{Cos} 2\pi f_n t_k + b_n \text{Sin} 2\pi f_n t_k] \right\} \cdot V_C \text{Cos} \left\{ 2\pi f_C t + k \frac{t^2}{2} + \frac{\pi}{2} \right\} \quad (8)$$

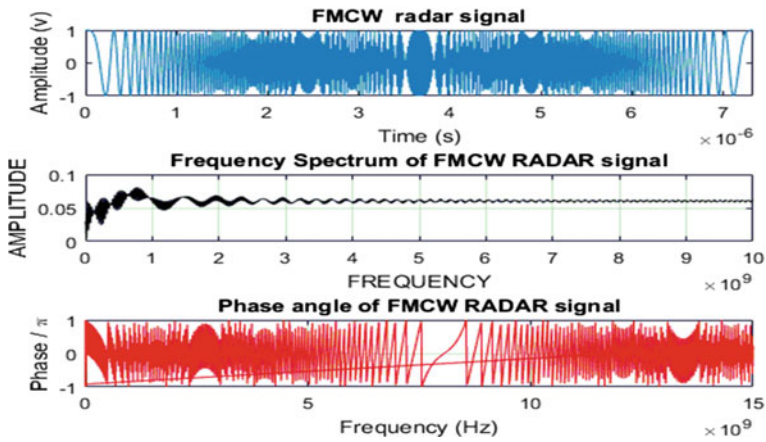


Fig. 3 FMCW radar signal in time, its spectrum, and angle plot

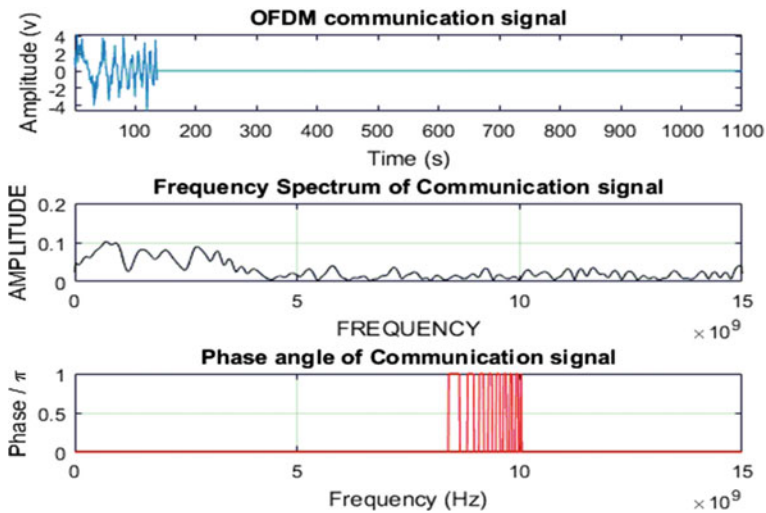


Fig. 4 OFDM communication signal in time, its spectrum, and angle plot

Figures 3 and 4 show the complex FMCW radar signal waveform and OFDM communication signal modulated on the same frequency modulated continuous wave carrier, respectively. Each of these figures shows the signal in time domain, its spectrum, and the phase angle versus frequency plot. From these two figures, it is obvious that the radar and the communication signals are differentiated in their phase angle. Hence, when these two signal waveforms are added to generate a complex integrated radar radio signal, intercarrier interference between these two systems is reduced.

4.2 Receiver Processing for Radar and Communication

The proposed RADAR RADIO system assumes that enough isolation is provided between the transmit and receive antennas with a low or no side lobes present in the antenna pattern, so that the leakage power from the transmitter to receiver is almost zero avoiding receiver saturation, and receiver internal circuitry is adequately protected from damage as well. The mono-static radar receiver receives the target or object intercepted echo signal. For simplicity of the system, we assumed that the target signature is received only at the direct path, neglecting the reflected path contribution. The received signal is first passed through the circulator and reaches to the radar receiver, where it is matched filtered and correlated with a delayed version of the transmitted FMCW chirp signal used for radar. The output of the matched filter is

$$y(t) = \int_{-\infty}^{\infty} h(\tau).h^*(t - \tau)d\tau \quad (9)$$

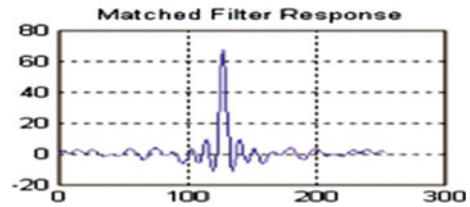
where $h(\tau)$ is the signal and $h^*(t - \tau)$ is the complex conjugate impulse response of the matched filter.

The signal is passed through a bank of matched filter for multiple target detection and subsequently passed through a detector circuit where the target range and velocity are estimated.

For the communication receiver, coherent demodulation specifically quadrature demodulation is utilized; i.e., the incoming complex signal is multiplied with 90 degree phase shifted version of the FMCW radar chirp signal, and the result is passed through a band pass filter tuned to the carrier frequency of the OFDM data frame. The output of the filter is demodulated by an OFDM demodulator to retrieve the communication data (Fig. 5).

This will not deteriorate the performance of the radar target detection as we are not interested in small object location change in millimeter (which may be reflected by the phase difference between the tx chirp and rx chirp frame) in the on-road scenario (Where the minimum range of the vehicles/objects are to be several meters or more).

Fig. 5 Matched filter response



5 Conclusion with Novelty

We proposed the joint radar communication operation by millimeter wave. This is the best possible way of integrating the two systems together because nowadays vehicular radars are millimeter wave radars. Now, if the same millimeter wave carrier is used to carry the OFDM communication data, then a wide communication bandwidth can be achieved with a very low BER by using multiple input multiple output antenna. MIMO inherently reduces interference, noise, clutter by the application of transmit, and receive beam formation technique. Also the spectrum scarcity issue will not exist in millimeter wave system operating at 77 GHz. In this system, the RSU are to be enabled with millimeter wave communication. The only hurdles to remove are the possible conversion of the ultra-high-frequency communication to high frequency for communication between RSU in vehicular cloud and the BTS of the current cell.

References

1. Kenney JB (2011) Dedicated short range communication standards in United States. Proc IEEE, 00(7), <https://doi.org/10.1109/JPROC.2011.2132790>
2. Stephen E (2010) Intelligent transportation systems, explaining international IT application leadership. In: The information technology and innovation foundation
3. Technical Report, M2M Enablement.: Intelligent transportation systems. Telecommunication Engineering Centre, Department of Telecommunications, Ministry of Communication and Information Technology, Release
4. Robert WH Vehicular mm Wave Communication: Opportunities and Challenges, Wireless Networking and Communications Group Department of Electrical and Computer Engineering The University of Texas at Austin.
5. Kumari P, Choi J, Gonz'alez-Prelcic N (2017) IEEE 802.11ad-based radar: an approach to joint vehicular communication-radar system. arXiv:1702.05833v1[cs.IT]
6. Shahmansoori A, Garcia GE, Destino G Position and Orientation estimation through millimeter wave MIMO in 5G system, arXiv:1702.01605v2[cs.IT], Available: Error! Hyperlink reference not valid.
7. Yu Y, Peter GMB (2011) Chapter 2 Millimeter wave wireless communication, Available: <https://www.springer.com/in>
8. Adhikari P (2008) Understanding millimeter wave wireless communication. Loea Corporation, San Diego

9. Kutty S, Sen D (2016) Beamforming for millimeter wave communication: an inclusive survey. Published in IEEE communication surveys & tutorials vol. 18(2), second quarter 2016, pp 949–973
10. Guo Z, Wang X, Heng W (2017) Millimeter wave channel estimation based on 2-D beam space MUSIC method, Published in: IEEE transactions on wireless communications, vol. 16(08), pp 5384–5394
11. Xiao M, Mumtaz S (2017) Millimeter wave communication for future mobile networks, arXiv:1705.06072v1 [cs.IT], <https://arxiv.org/pdf>
12. Akdeniz MR, Liu Y, Samimi MK, Sun S, Rangan S, Rappaport TS, Erkip S (2014) Millimeter wave channel modeling and cellular capacity evaluation. IEEE J Sel Areas Commun 32(6):1164–1179
13. Sohrabi F, Yu W (2017) Hybrid analog and digital beamforming for millimeter wave OFDM large scale antenna arrays, arXiv:1711.08408v1 [cs.IT], <https://arxiv.org/pdf>
14. Molisch AF, Ratnam VV (2017) Hybrid beamforming for massive MIMO: a survey, arXiv:1609.05078v2 [cs.IT]
15. Hasch J, Topak E, Zwick T, Waldschmidt C (2012) Millimeter-wave technology for automotive radar sensors in the 77 GHz frequency band. IEEE Trans Microwave Theory Tech 60(3):845–860
16. Folster F, Rohling H, Lubbert (2005) An automotive radar network based on 77 GHz FMCW sensors. Published in: 2005 IEEE international radar conference
17. Sturm, C, Zwick, T (2010) Joint radar sensing and communications based on OFDM signals for intelligent transportation networks, LS Telecom Summit 2010. Lichtenau, Germany
18. Braun M, Sturm C, Jondra FK) On the frame design for joint OFDM radar and communications. Jondra
19. Sit Y, Reichardt L, Sturm C, Zwick T (2011) Extension of the OFDM joint radar-communication system for a multipath, multiuser scenario. IEEE. 978–1–4244–8900–8/11
20. Yogesh N, Chen Y, Said B, Chau Y, Yong HC, Zhiguo D. (2012) Novel system architecture and waveform design for cognitive radar radio networks. IEEE Trans Vehic Technol 61(8)
21. Hu F, Cui G, Yuan L (2015) Integrated radar and communication system based on stepped frequency continuous waveform. In: 2015 IEEE radar conference (RadarCon), [https://doi.org/10.1109/RADAR.2015.7131155\(2015\)](https://doi.org/10.1109/RADAR.2015.7131155(2015))
22. Automotive Radar High-resolution 77 GHz radar, www.nxp.com/files/microcontrollers/doc/fact_sheet/AUTORADARFS.pdf.
23. Hyun E, Lee JH (2009) Method to improve range and velocity error using de-interleaving and frequency interpolation for automotive FMCW radars. Int J Signal Process Image Process Pattern Recognition 2(2)

Throughput Analysis of MIMO HetNet System with Lattice Reduction Aided Precoding



Samarendra Nath Sur, Rabindranath Bera, Biswajit Dara,
and Mithun Chakraborty

Abstract Massive multiple-input and multiple-output (mMIMO) and heterogeneous networks (HetNets) are the most promising solutions for achieving high spectral efficiency and are the main ingredient for the 5th generation (5G) communication system. In this paper, the sum-rate of the mMIMO-HetNet system has been investigated. Considering the existence of small cell networks in future generation cellular systems, interference suppression is a point of concern. In the paper, we have considered lattice reduction aided precoder (LRP) for the system performance improvement.

Keywords Massive multiple-input multiple-output (mMIMO) · Heterogeneous network (HetNet) · Millimeter wave (mmWave) · Lattice reduction · Precoder

1 Introduction

The recent surge in the data intensive applications, the 5G cellular networks have gained tremendous attention. In order to satisfy the users demand in terms of coverage and capacity, massive MIMO (mMIMO) and HetNets have gained significant attention [1–5]. And this combination is considered to be one of the promising solutions for the 5G networks to achieve the desired spectral efficiency [1, 6–10].

In a mMIMO system, the base station (BS) exploits the advantages of large numbers of antennas for the improvement of spectral efficiency. Whereas, in the case of HetNet, where small cells provide local capacity enhancement. Therefore, by

S. N. Sur (✉) · R. Bera

Department of Electronics and Communication Engineering, Sikkim Manial Institute of Technology, Sikkim Manial University, East Sikkim 737136, India
e-mail: samar.sur@gmail.com

B. Dara · M. Chakraborty

Department of Electronics and Communication Engineering, Amity School of Engineering and Technology, Amity University Jharkhand, Ranchi 834001, India

© The Author(s), under exclusive license to Springer Nature Singapore Pte Ltd. 2021
M. Chakraborty et al. (eds.), *Trends in Wireless Communication and Information Security*,
Lecture Notes in Electrical Engineering 740,
https://doi.org/10.1007/978-981-33-6393-9_10

exploiting the superiority of both the systems, a combined mMIMO-HetNet system [11] has been considered as a key ingredient for future generation communication systems.

Now in the case of a small cell, inter-tier, and intra-tier interferences can cause significant degradation in spectral efficiency [12]. In this architecture, the interference associated with the mMIMO base station (MBS) and small cell base stations (SBSs) is the main issue to overcome [13]. Therefore, efficient interference mitigation techniques to be explored.

Over past decades lots of precoding algorithms have been reported in the literature. The simplest type is matched filtering (MF) precoding and it relies upon the CSIT [14]. Similar to MF, ZF precoder is also a popular method to eliminate interference based upon the availability of CSIT. This precoder is ineffective for inter-user interference (IUI). But its effectiveness depends on the perfect knowledge of channel state information. As per the studies in [2, 15], in the case of a HetNet system, ZF precoder is not suitable for the removal of IUI and inter-cell-interference (ICI). Signal-to-leakage-plus-noise-ratio (SLNR) maximization precoding [16, 17] is an effective method to mitigate IUI using CSIT. Further, MMSE based precoder is used to mitigate ICI. Similar to the single cell, SLNR precoding scheme is further extended to multi cell precoder, known as multi-cell minimum mean square error (M-MMSE) precoding [18, 19]. But all these schemes do not always maximize the sum spectral efficiency. In order to enhance the spectral efficiency, weighted MMSE precoding [16, 20] has been proposed. And also some extensive researches have been proposed and reported in [20, 21] to maximize the spectral efficiency of the system.

In this context, mMIMO is an effective and efficient technology to address the issue of interference. But having a large number of antennas is only possible in the case of macro-cell BSs. In the case of a HetNet, implementation cost and the complexity put limits in the number of antennas in BSs corresponding to the small cell. Under such condition conventional precoder like zero forcing (ZF), minimum mean square error (MMSE) will not be effective [17]. In this paper, authors have evaluated the performance of the mMIMO-HetNet system with lattice reduction aided (LRA) precoder [22–24]. Here authors have analyzed the gain in spectral efficiency of the system with LRA aided ZF and MMSE receivers. Lattice reduction (LR) [25] is an efficient tools to improve the system performance with low complexity [26–28]. Over decades different variants of LR algorithms have been proposed but in this paper, authors have considered Lenstra-Lenstra-Lovhave been proposed but in this paper, authors have considered Lenstrasz algorithm (LLL) algorithm [29] for the design of the precoder. We assume that each BSs, within the small cell and macro cell, have the full knowledge of the channel state information (CSIT). Details Description of the system has been discussed in the system model section.

This paper is organized as follows. Section 2 explains the mMIMO-HetNet system model. Section 3 describes the transmission model related to macro-cell and small cells. Section 4 shows the simulation results. Finally, Sect. 5 concludes this paper.

2 System Model

Figure 1 shows a typical model for mMIMO-HetNet network. As in the figure, it consists of a macro-cell base station (MSB) with a massive MIMO antenna system and some full duplex small cell base stations (SBSs). Here, MSB consisting of N antennas to extend support for K number of single antenna macro-cell users (M-UE) and S number of single antenna small-cell users (S-UE). Here SBSs support its corresponding S-UE in full duplex mode. As in [30], we have considered that SBSs are capable of operating in out-of-band full duplex mode (OBFD), where access link and backhaul link are conducted in orthogonal channels and also in in-band full-duplex mode (IBFD), in which the access link and the backhaul link is established over the same frequency band. For the analysis purpose, here in this paper, OBFD SBS is represented as S_{OBFD} and for IBFD it is S_{IBFD} . To have a more practical environment, here, we have considered the co-tier and cross tier interferences. And also, path loss, shadowing effect and small scale fading effects are considered to configure the wireless channel. Here we have compared the performance of the LR aided ZF precoder with the linear counterparts. And also we have considered that CSI is fully available at MSB and transmission across the tiers is perfectly synchronized. Along with the LRP, here in this paper, to maximize the overall system throughput, a greedy algorithm based centralized coordination scheme has been utilized.

3 Transmission Model

In this section, we will discuss the transmission model for the mMIMO-HetNet network [30].

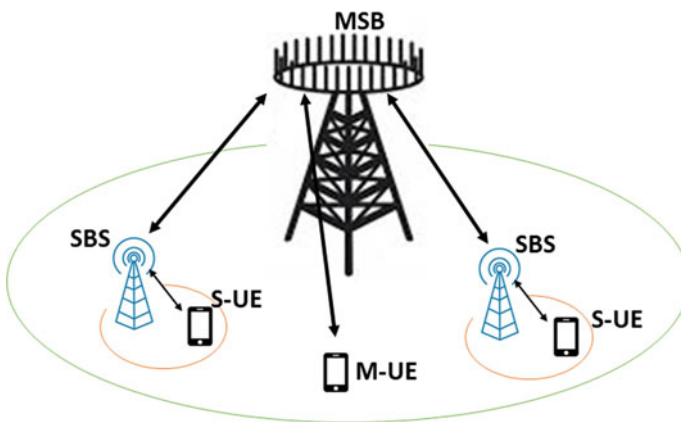


Fig. 1 mMIMO-HetNet system model

3.1 For Macro-Cell

In the case of the macro cell transmission model, MSB is responsible to support M-UE and all the M-UE will experience interference originated from surrounding SBSs. Therefore the receives signal at the k th M-UE can be represented as

$$y_{M-UE,k}(t) = H_{B-MU,k}Wx_{B-MU}(t) + \sum_{j \in S_{\text{OBFD}}} H_{S-MU,jk}x_{S-MU,j}(t) + n(t) \quad (1)$$

where, $H_{B-MU,k}$ represents the channel matrix corresponding to MBS and the k th M-UE. W represents downlink precoder having dimension $[N \times K]$ and x_{B-MU} represents the $[K \times 1]$ symbol vector. Similarly, $H_{S-MU,jk}$ denotes the channel matrix between j th SBSs and k th M-UE and x_{B-MU} represents the transmitted symbols from the small cell base station j th SBSs. The term $n(t)$ corresponding to the noise vector.

3.2 For Small-Cell

As, in [30], the received signals for OBFD and IBFD configurations are represented here. In the case of the OBFD mode of operation, SBSs suffer from co-tier interference originated from SBSs, which are operating in IBFD mode. Therefore, the received signal at the SBSs can be represented as

$$y_{\text{SBS},j}^{\text{OBFD}}(t) = H_{B-S,j}Gx_{B-S}(t) + \sum_{n \in S_{\text{IBFD}}} H_{S-S,jn}x_{S-SU,n}(t) + n(t) \quad (2)$$

Here, $H_{B-S,j}$ is for channel matrix between MBS and the j th SBS and precoding matrix is presented by G . x_{B-S} is the symbol vector from MBS to SBSs. And $H_{S-S,jn}$ denotes the channel matrix related to paths between j th SBS and n th SBS and it results in co-tier interference.

Now, the S-UEs are suffering from both co-tier interference and cross-tier interference. under the OBFD mode of SBS operation. Therefore the received signal corresponding to S-UE can be represented as

$$y_{S-UE,j}^{\text{OBFD}}(t) = H_{S-SU,jj}x_{S-SU,j}(t) + \sum_{p \in S_{\text{OBFD}} \setminus j} H_{S-SU,jp}x_{S-SU,p}(t) + H_{B-SU,j}Wx_{B-MU,j}(t) + n(t) \quad (3)$$

where, $H_{S-SU,jj}$ represents the channel vector related to the paths between j th SBS and corresponding S-UE. This channel matrix is related to the SBS operating under

OBFD mode. And $H_{S-SU,jp}$ depicts the channel matrix between the p th SBS and j th S-UE. Similarly, $H_{B-SU,j}$ relates to the channel matrix between the MBS and the j th S-UE.

And to mitigate the interference, proper design of precoder (W) is required. And in this paper we have explored LRP.

In case of IBFD, the received signal at i th SBS is given by

$$y_{SBS,i}^{\text{IFBD}}(t) = H_{B-S,i}Gx_{B-S}(t) + \sum_{q \in \mathcal{S}_{\text{IBFD}} \setminus i} H_{S-S,iq}x_{S-SU,q}(t) + \sqrt{I_{si}}w(t) + n(t) \quad (4)$$

As in [30], $\sqrt{I_{si}}w(t)$ represent the self interference vector. The received signal suffers from both co-tier interference and self-interference. Similarly, under IBFD mode of operation, the S-UE suffers from both co-tier and cross-tier interference and under such condition the received signal can be represented as

$$y_{S-UE,i}^{\text{IFBD}}(t) = H_{S-SU,ii}x_{S-SU,i}(t) + \sum_{q \in \mathcal{S}_{\text{IBFD}} \setminus i} H_{S-SU,iq}x_{S-SU,q}(t) + H_{B-SU,i}Gx_{B-S}(t) + n(t) \quad (5)$$

4 Performance Evaluation

Table 1 represents the parameter used for simulation and analysis. As presented in the table, here, we have used a circular cell structure. And from the channel perspective, we have considered Rayleigh distribution as small fading characteristics and also we have taken into account LOS/NLOS path loss and shadowing factors.

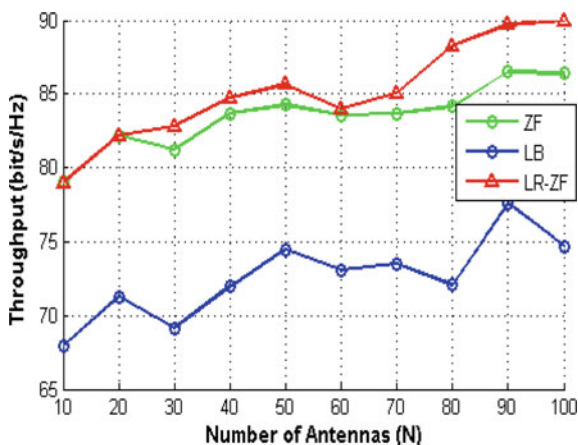
Figure 2 shows the variation in downlink throughput with the variation in the number of antennas in MSB. During the simulation, we have considered 10 M-UEs and 20 single antenna S-UEs. The effectiveness of the LR aided ZF precoder (LR-ZF) is clearly visible from the Fig. 2. One important point to observe here is that, with the increase in the number of MBS antennas, the change in the throughput is very slow. And also if you compare the throughput corresponding to ZF and LR-ZF with respect to lower bound (LB), the achievable gain due to precoders is clearly visible.

To have results as in Fig. 3, we have taken 10 M-UEs and 20 antennas at the MBS. As in Fig. 3, the growth in the downlink throughput is almost linearly with the change in the number of single antennas SBSs. Out of these results, one can easily conclude that LR-ZF provides the best precoder in comparison to other precoder systems.

From the above results, it is clear that lattice aided precoders have more interference rejection capabilities than the convention linear precoder. This is because of the fact that the lattice reduction method produces more orthogonal basis vectors and it helps to mitigate the effect of the interferences.

Table 1 Simulation parameters

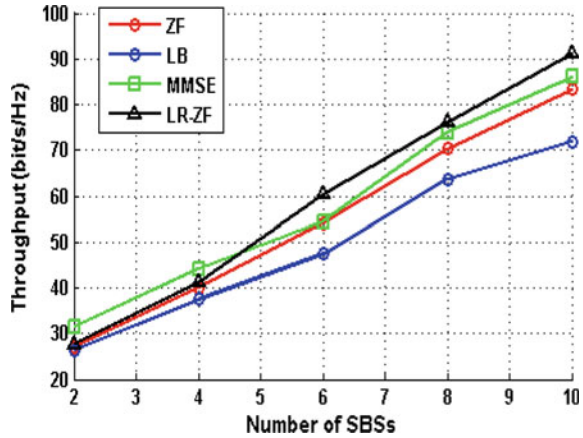
<i>System parameters</i>	
Transmitted power	MBS: 46 dBm
	SBS: 24 dBm
Bandwidth	20 MHz
Carrier frequency	2 GHz
Noise power spectral density	-174 dBm/Hz
Network topology	Macro-cell radius = 1000 m
	Small-cell radius = 40 m
<i>Propagation parameters</i>	
Channel	Rayleigh fading, Path loss, Shadowing
MBS-M-UE/S-UE	$PL_{\{Los\}}(d) = 30.8 + 24.2\log\{10\}(d)[dB]$
	$PL_{\{NLos\}}(d) = 2.7 + 42.8\log\{10\}(d)[dB]$
	Shadowing Factor = 6 dB
SBS-M-UE/S-UE	$PL_{\{Los\}}(d) = 41.1 + 20.9\log\{10\}(d)[dB]$
	$PL_{\{NLos\}}(d) = 32.9 + 37.5\log\{10\}(d)[dB]$
	Shadowing factor = 3 dB/6 dB

Fig. 2 Downlink throughput variation with number of antennas at MBS

5 Conclusion

In this paper, we have analyzed the performance of the mMIMO-HetNet system. The main focus of this paper is to show the improvement in the throughput due to the utilization LR aided precoder. Effectiveness on the LR aided precoder has been established by comparing its performance with its linear counterparts (ZF/MMSE). From the simulated results it is clearly proven that LR-ZF performs much better than conventional ZF/MMSE precoder.

Fig. 3 Downlink throughput variation with number of antennas at SBS



References

- Li H, Wang Z, Wang H (2020) Joint user association and power allocation for massive MIMO HetNets with imperfect CSI. *Sign Process* 107588
- Ghosh A, Mangalvedhe N, Ratasuk R, Mondal B, Cudak M, Visotsky E, Thomas TA, Andrews JG, Xia P, Jo HS, Dhillon HS, Novlan TD (2012) Heterogeneous cellular networks: from theory to practice. *IEEE Commun Mag* 50(6):54–64
- Dhillon HS, Kountouris M, Andrews JG (2013) Downlink MIMO HetNets: modeling, ordering results and performance analysis. *IEEE Trans Wireless Commun* 12(10):5208–5222
- Hosseini K, Hoydis J, Ten Brink S, Debbah M (2013) Massive MIMO and small cells: how to densify heterogeneous networks. In: *Proceedings of the IEEE international conference on communication (ICC)*, June 2013, pp 5442–5447
- Chen N, Rong B, Zhang X, Kadoch M (2017) Scalable and flexible massive MIMO precoding for 5G H-CRAN. *IEEE Wireless Commun Mag* 24(1):46–52
- Alamu O, Gbenga-Ilori A, Adedun M, Imoize A, Ladipo O (2020) Energy efficiency techniques in ultra-dense wireless heterogeneous networks: an overview and outlook. *Int J Eng Sci Technol*
- Ni S, Zhao J, Yang HH, Quek TQS, Gong Y (2018) Small cell range expansion with interference mitigation for downlink massive MIMO HetNets. In: *Proceedings of the Globecom*, Dec. 2018, pp 1–6
- Yang HH, Geraci G, Quek TQS (2016) Energy-efficient design of MIMO heterogeneous networks with wireless backhaul. *IEEE Trans Wireless Commun* 15(7):4914–4927
- Zhao J, Quek TQS, Lei Z (2015) Heterogeneous cellular networks using wireless backhaul: fast admission control and large system analysis. *IEEE J Sel Areas Commun* 33(10):2128–2143
- Zhou Y, Tian L, Liu L, Qi Y (2019) Fog computing enabled future mobile communication networks: a convergence of communication and computing. *IEEE Commun Mag* 57(5):20–27
- Ni S, Zhao J, Yang HH, Gong Y (2019) Enhancing downlink transmission in MIMO HetNet with wireless backhaul. *IEEE Trans Veh Technol* 68(7):6817–6832
- Lv W, Zhang Z, Jiao C, Zhong C (2017) Interference coordination in full-duplex HetNet with large-scale antenna arrays. In: *2017 IEEE international conference on communications (ICC)*. IEEE, New York, pp 1–6
- Gupta AK, Dhillon HS, Vishwanath S, Andrews JG (2014) Downlink multi-antenna heterogeneous cellular network with load balancing. *IEEE Trans Commun* 62(11):4052–4067
- Lo TK (1999) Maximum ratio transmission. In: *Proceedings of the IEEE international conference on communication (ICC)*, vol 2, June 1999, pp 1310–1314

15. Bogale TE, Le LB (2016) Massive MIMO and mmWave for 5G wireless HetNet: potential benefits and challenges. *IEEE Veh Technol Mag* 11(1):64–75
16. Sadek M, Tarighat A, Sayed AH (2007) A leakage-based precoding scheme for downlink multi-user MIMO channels. *IEEE Trans Wireless Commun* 6(5):1711–1721
17. Han D, Lee N (2020) Noncooperative precoding for massive MIMO HetNets: SILNR maximization precoding. arXiv preprint [arXiv:2001.04073](https://arxiv.org/abs/2001.04073) (2020)
18. Patcharamaneepakorn P, Armour S, Doufexi A (2012) On the equivalence between SLNR and MMSE precoding schemes with single antenna receivers. *IEEE Commun Lett* 16(7):1034–1037
19. Bjornson E, Hoydis J, Sanguinetti L (2017) Massive MIMO has unlimited capacity. *IEEE Trans Wireless Commun* 17(1):574–590
20. Christensen SS, Agarwal R, De Carvalho E, Cioffi JM (2008) Weighted sum-rate maximization using weighted MMSE for MIMOBC beamforming design. *IEEE Trans Wireless Commun* 7(12):4792–4799
21. Choi J, Lee N, Hong S-N, Caire G (2019) Joint user selection, power allocation, and precoding design with imperfect CSIT for multi-cell MU-MIMO downlink systems. *IEEE Trans Wireless Commun* 19(1):162–176
22. Stern S, Fischer RF (2016) Advanced factorization strategies for latticereduction-aided pre-equalization. In: *Proceedings of the IEEE international symposium on information theory (ISIT)*, Jul 2016, pp 1471–1475
23. Windpassinger C, Fischer R (2004) Low-complexity near-maximum likelihood detection and precoding for MIMO systems using lattice reduction. In: *Proceedings of the IEEE information theory workshop*, Mar 2004, pp 345–348
24. Lanneer W, Nuzman C, Lefevre Y, Tsiaflakis P, Coomans W, Moonen M (2020) Lattice reduction aided precoding design in downstream G.fast DSL networks. *IEEE Access* 8:19208–19220
25. Halak B, El-Hajjar M, Hassanein A (2018) Hardware efficient architecture for element-based lattice reduction aided K-best detector for MIMO systems. *J Sens Actuator Netw* 7:22
26. Kim H, Park J, Lee H, Kim J (2014) Near-ML MIMO detection algorithm with LR-aided fixed-complexity tree searching. *IEEE Commun Lett* 18(12):2221–2224
27. Sur SN, Bera R, Bhoi AK, Shaik M, Marques G (2020) Capacity analysis of lattice reduction aided equalizers for massive MIMO systems. *Information* 11(6):301
28. Sur SN, Bera S, Bera R, Maji B (2019) Capacity analysis of lattice reduction aided detection in massive-MIMO systems. In: *Proceedings of the URSI Asia-Pacific radio science conference (AP-RASC)*, New Delhi, India, 9–15 March 2019; pp 1–4
29. Lenstra AK, Lenstra HW, Lovász L (1982) Factoring polynomials with rational coefficients. *Mathematische annalen* 261, no. ARTICLE, pp 515–534
30. Zhang Z, Lyu W (2017) Interference coordination in full-duplex HetNet with large-scale antenna arrays. *Front Inform Technol Electron Eng* 18(6):830–840

Modern Radar Topology for Bio-medical Applications



**Subhankar Shome, Mithun Chakraborty, Biswajit Dara,
Rabindranath Bera, and Bansibadan Maji**

Abstract Radar was associated with military industries in earlier centuries. This day's several industries, like automobile, mining, medical, etc., are also using radars. It is becoming very popular for contact less bio-medical investigation on human body, because of its less microwave energy radiation over short distance. Continuous monitoring of cardio respiratory activity, breast tumor diagnostics, imaging of blood circulation are few emerging areas of research in bio-medical applications. Continuous wave, frequency modulated, ultra-wideband, these are few popular radars which researcher start implementing in bio-medical application. Now recent radar topologies, mainly advance antenna technologies, like MIMO, array and Phased MIMO radar are also becoming very popular in medical applications because of effective performance ability in low signal-to-noise ratio environment. On the other hand, advance computational techniques like soft computing is also becoming part of the modern radar which can improve noise performance Doppler tolerance in bio-medical application.

Keywords RADAR · MIMO · Array · Phased MIMO · Soft computing · AI

S. Shome (✉)

St. Mary's Technical Campus Kolkata, Barasat, West Bengal, India
e-mail: subho.ddj@gmail.com

M. Chakraborty · B. Dara

Amity University Jharkhand, Nivaranpur Main Road, Ranchi, Jharkhand, India

R. Bera

ECE Department, Sikkim Manipal Institute of Technology, Sikkim Manipal University, Sikkim 737136, India

B. Maji

National Institute of Technology Durgapur, A-Zone, Mahatma Gandhi Rd, Durgapur, West Bengal 713209, India

1 Introduction

The idea of remotely monitoring human body functions was generated in nineteenth century [1, 2]. In twenty-first century, radars are penetrated into civilized society from war field. In several ways, radars are helping society in regular activity. Bio-medical is one of the areas in which radar researcher puts a significant effort to make a difference. Non-contact continuous less harmful human body monitoring the idea of nineteenth century now became a key target using radar imaging. In a short distance scenario, a radar signal illuminating a human body for imaging is a very low-power microwave signal and less harmful than a X-ray imaging, but at the same time a very challenging job also. Continuous heartbeat monitoring, breast tumor and other tumor diagnostics, imaging of blood circulation are few challenging areas for active researchers. Low-intensity bio-medical signal detection and processing using modern radar are the main area of work. Initially, researchers start working with popular radars like CW [3], FMCW [4], UWB [5], Doppler [6], etc. In case of heartbeat monitoring or pulse rate monitoring, Doppler processing is one of the common practices. The main objective of the work is divided into three parts: (1) clear target identification: In an active zone, several living and non-living targets are present, so it is essential. (2) Mutual interference rejection: It is very important in case of adjacent subject elimination and (3) Vital signs or symptoms identification with minimal noise and less errors. But always these objectives become challenging due to low SNR bio-medical signals. So, researcher starts thinking about multi-antenna techniques which can improve low noise signal detection and also thinking about soft computing toll which can efficiently process bio-medical radar data to provide error less monitoring of physiological functions. Multi-antenna techniques are already well established for low SNR signal in communication, even in radar also. The same multi-antenna radar can be very useful for bio-medical radar also. From here, use of MIMO, array and phased MIMO radar are in research for bio-medical applications. This radar uses multiple number of antennas in the transmitter and receiver side. The number of antenna elements creates simultaneous transmission and reception paths to improve the SNR and robustness of the signal [7]. The challenges under this part, to reduce the numbers of antenna in MIMO array configuration [8], reduce the interferences between collocated transmit received antenna elements [9] and calculations of coupling behaviors which effects on array performance [10]. By overcoming these challenges, modern radars are capable to handle with bio-medical signals like heartbeat. Heartbeat and respiration, both information can be trace from chest displacement which is a non-contact measurement. Heartbeat variation is ranged between 0.2 and 0.5 mm [11], but respiration displacement is higher than heartbeat; now, to filter out this type of different signal, radar system needs strong computational tools in which soft computing is helping a lot now a days. Soft computing tools like neuron network can help to classify bio-medical radar signals in a very efficient way.

2 Bio-medical Applications

2.1 Pathological Applications

In every medical emergency, doctors mostly depend on pathological test, which need body contact activity with patient, time consuming and expensive. Microwave imaging is getting popular for last few years for pathological applications. This type of pathological test is done with the help of radar by illuminating human body using closely spaced antennas and acquisition of the signal echo. Wisconsin-Madison University, Bristol University and Calgary University developed the best cancer detection system following confocal microwave imaging (CMI) technique. Similar pathological test is done on human bladder, hemorrhagic stroke in the head [12] and various others.

2.2 Remote Monitoring on Health Condition

Remote monitoring of health condition known as vital sign monitoring is basically contactless and continuous monitoring of our body parameters like heartbeat, breath and respiration activity. Not only that, bio-medical radar also experimented to measure blood vessel movements and to sense speech. This information is generally extracted by processing the radar echo in time domain. This continuous monitoring is very much effective to prevent infant death syndrome (SIDS) or sleep apnea; even this can be used in automobile industry which can monitor and alert drowsy driver to avoid critical situations.

3 Radar Topologies of Different Times for Bio-medical Uses

3.1 Continuous Wave Radar

Continuous wave frequency modulated (FMCW) radar is one of the popular radars under this category in which S_x is considered as radio frequency wave which is transmitted over space and the reflected signal from object is denote by S_r .

$$S_x = \pi r^2 \cos \vartheta(t), \quad \text{where } \vartheta(t) = 2\pi \int_0^t F(t') dt' \quad (1)$$

$S_r(t)$ is the received signal by radar which consist of:

$$s_r(t) = \sum_m c_m \cos \vartheta(t - \tau_m) \quad (2)$$

Here, c_m reflects strength independent to each target and τ signal transmission from the radar toward the target and back. In a micro-power, FM radar is designed and developed to measure human heart rate and monitor respiration. Respiratory and cardiac rates are measured using radar as well as using conventional method. Multiple objects are tested from a single measurement under same research article using FM radar. A good range resolution capability is noted in this experiment.

3.2 Doppler Radar

Doppler radar is a type of continuous wave radar; it uses the Doppler effect signal for motion detection. Doppler radar can extract distance and phase information which helps to measure the vital signs of human body. Researchers are targeted to solve several problem areas listed below using Doppler radar: (1) clear target identification; (2) elimination of mutual interference, especially in the case of two adjacent subjects within range resolution limit; and (3) vital sign retrieval with minimal ambient noise. Doppler radar generally follows a three-step process in medical signal analysis. In the first step, the data acquisition takes place using radar hardware for which the human object needs to place very nearby to the transmitting antenna. Next, feature extraction takes place in which signal parameters are analyzed using different algorithms. Frequency estimation is generally done by MUSIC algorithm, and FFT algorithm is generally used for phase history profiling. These signal information are required in range integration for vital signs extraction. Respiration and heart rate retrieval can be done using auto-regressive (AR) method, which comes under the final step.

Commonly, the chest displacement due to respiration and heartbeat variation is ranged between 4 to 12 mm and 0.2 to 0.5 mm consequently. On the other hand, variation of respiration rate in rest position is between 0.1 and 0.3 Hz, while the interval of heartbeat rate varies between 1 and 3 Hz. Therefore, the signal contains both respiration and heartbeat where the respiration displacement is large than heartbeat because of that a filtering technique is needed to filter noise and unwanted signal from raw detected signal.

3.3 UWB Radar

An extremely short pulse is the key to generate an extremely high bandwidth. The radar system is categorized in terms of functional bandwidth (B_F) as given below:

Narrowband (NB) if $0 \leq B_F \leq 0.01$.

Wideband (WB) if $0.01 \leq B_F \leq 0.25$.
 Ultra-wideband (UWB) if $0.25 \leq B_F \leq 2.00$.

The UWB radar is developed using strobed sampling method for detection of heart rate through wall. A human object is placed opposite side of a clay brick wall, and the reflected pulses from the object return into the received antennas through the wall. Now, the radar receiver will receive two types of signal due to two different types of reflection object. The signal reflected back from the wall can be treated as stationary signal which has a time variant characteristic, and the part of the transmitted signal reflected back from human object can be treated as nonstationary signal in which phase variation will occur due to human heartbeat and respiration.

These radars are exposed to a human body for perimeter monitoring; here health hazard issue taken under consideration, this happen due to microwave radiation towards human body, by the radar. In [13], safety aspect of people is taken under consideration for UWB radar. In this article, the compliance of electromagnetic fields radiated by a UWB radar as per International Commission on Non-Ionizing Radiation Protection (ICNIRP) is evaluated. UWB radar SAR limit averaged over whole body (SAR_{WB}), SAR as averaged over 10 g in the head and trunk (SAR_{10g}) and in the limbs (SAR_{10gL}) are reported under these article. The radiation limit of UWB radar used for medical signal processing and perimeter monitoring of human body between 3.1 and 10.6 GHz shall not exceed the EIRP value of -41.3 dBm,

3.4 Modern Radar in Critical Medical Applications

Modern radars are enabled with multiple antennas and more advanced signal processing. This type of radar is used for two-dimensional or three-dimensional imaging of the human body which can be used for medical diagnosis. Mainly, two types of microwave imaging techniques are used in breast cancer detection; first is tomography and another confocal imaging. A complete electrical profile of breast is attempted to map in tomography imaging which needs an antenna array to receive a passive electromagnetic field of the body [14]. In the confocal imaging, location of the significant scatters is mapped, which also explore the antenna array.

The multi-antenna system will increase the cost, size and complexity. So our aim is to design an array system with a minimum number of elements. The number of the antenna element can be determined by sidelobe level (ISL) idea, which can be calculated from Eq. 1:

$$ISL = -20 \log_{10} N_E \quad (3)$$

where minimum number of element is represented by N_E .

Transmit and received antenna number can be derived from Eq. 4:

$$N_E = N_{Tx} \cdot N_{Rx} \quad (4)$$

N_{Tx} is the number of transmit antenna element, and N_{Rx} is number of received antenna element.

The total number of antenna in antenna array is:

$$N = N_{Tx} + N_{Rx} \quad (5)$$

Here, the main challenge comes to choose the number of antenna elements and to deal with coupling between them to construct the antenna array. Phased array creates a problem due to network feeding loss, and also, there is some problem of far field as the object is closely placed to the antenna in medical diagnosis. Near field-focused antennas are in research for a long time for this type of application. Array configurations of NF-focused microstrip antenna are very useful to concentrate the signal power in a specific small geographical area using the beam forming method. This can heat a convicted tissue without affecting the adjacent one by concentrating the microwave energy into a specific spot, here are the advantages of modern technologies in radar.

3.5 *Intelligent Radar*

The strong computation techniques are used to process complex data matrix, received from multiple antenna in modern radars. Another complex computation is used these days to introduce intelligence in radar system. The modern radars are becoming intelligent day by day in which artificial intelligence (AI), deep learning and machine learning are becoming important parts of the system. In two ways, intelligence can be incorporate in radars, (i) by improving the pulse compression technique, which is unique target detection ability, used in most of the radar system, (ii) by reducing the repetitive task and increasing the diagnostic precision in medical radar.

In article [15], the improvement in pulse compression technique using artificial neural network (ANN) is shown. Adaptive filter algorithms are very useful to find optimum matched filter coefficients for pulse compression technique. This can be efficiently designed using multi-layer perceptron networks with adequate weight and bias parameters under ANN. Back-propagation algorithm (BPA) is used to implement multi-layer perceptron networks. It is an intelligent pulsed compression process which can be used for intelligent radar which researchers are targeting near future. How ANN can improve the performance and how to optimize the filter coefficient that is analyzed using convergence rate analysis. This is done by varying neurons and hidden layers and by applying different adaptive filter. Noise performance and Doppler tolerance test is also done to determine the performance enhancement (Fig. 1).

AI or ML algorithms can analyze a pattern similarly to the way a doctor analyze it; this is another vital area in which intelligence is contributing a lot. In article, convolutional neural network (CNN) is discussed which can help for radiology. Convolutional neural network (CNN) is the widely used deep neural network in the

Number of neurons in the HIDDEN LAYER	SNR = 1 dB	SNR = 5 dB	SNR = 10 dB	SNR = 15 dB	SNR = 20 dB	SNR = 25 dB
1	0.2697	13.965	37.8197	41.6916	43.2368	43.5327
3	1.1668	19.8091	37.8114	40.8114	42.1449	42.8214
5	4.1712	20.1232	38.7173	41.4815	42.6685	43.2707
7	2.041	21.6259	39.8674	42.653	43.7414	44.2466
9	5.3084	27.8965	41.0523	44.582	45.9905	46.7106
11	3.5948	14.7718	32.9811	44.0575	46.1658	46.4402
13	9.0224	21.303	37.0488	43.7983	46.2642	46.7362
15	3.7224	15.8543	35.0372	44.1597	46.3064	46.5465
17	3.8924	16.8811	37.886	44.3849	45.8557	46.1104
19	5.6383	20.9294	36.2993	43.0907	45.8804	47.3765
20	4.0719	16.1363	33.6252	43.4301	46.2728	46.8659

Fig. 1 Signal-to-sidelobe ratio (SSR) improvement for pulse compression technique using MLP

area of image classification, object detection, text recognition, action recognition and many more CNN was initially inspired by visual cortex of animals, For large volume images like RGB images, ANNs lead to an explosion in the number of weights which requires more memory and computation data. This problem can be solved using CNNs by using the sparse connections and parameter sharing. Like ANNs, CNNs also have neurons, weights and objective. The major properties of CNNs are the presence of sparse connection between the layers and the weights which are shared between output neurons in hidden layer (Fig. 2).

Convolution is basic component of CNN which performs feature extraction; it is basically combination of nonlinear and linear operation. The input is an image that will hold pixel values. It has three dimensions such as width, height and depth (RGB

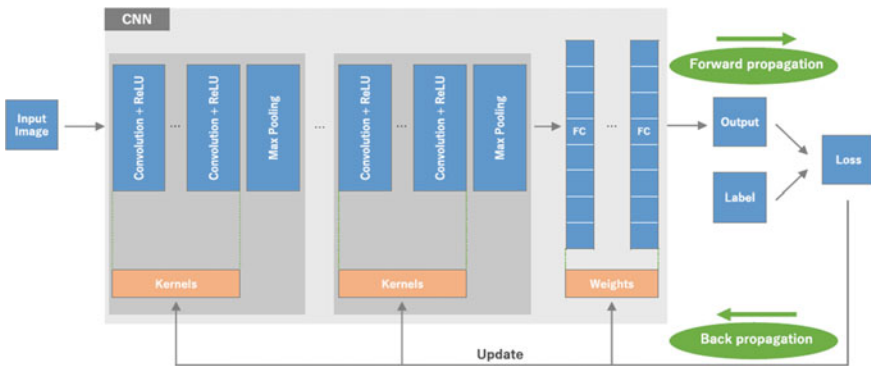


Fig. 2 Overview of a convolution neural network (CNN) architecture and the training process

channels); example is $[50 \times 50 \times 3]$ [16]. The convolutional layer will compute the output of neurons that are connected to local regions in the input. The layer's parameters are composed of a set of learnable filters (or kernels), which convolved across the width and height of the input volume extending through its depth, computing the dot product between the entries of the input and the filter. This produces a two-dimensional activation map of that filter, and as a result, the network learns filters that trigger when it detects some particular type of feature at some spatial position in the input. The function called rectified linear unit (ReLU) layer will perform elementwise activation function. ReLU is defined in (6),

$$f(x) = \max(0, x) \quad (6)$$

This function is zero for negative values and grows linearly for positive values. This will not affect the volume size. The pooling layer outputs the maximum activation in a region. This down samples the spatial dimensions such as width and height. The output layer is the fully connected layer which is similar to the final layer of the neural network. This layer used commonly used softmax activation to output probability distributions over the number of output classes. Few popular CNN architecture is available in the market; those are LeNet, AlexNet, VggNet, GoogleNet, ResNet. These can be very much helpful in medical imaging.

4 Conclusion

Like every sector, radar industry is also needed to be intelligent, in which the use of AI-ML is incensing day by day. In this article, the authors try to find out the angles in which intelligence can be incorporated in radar. Basically, two directions are highlighted in this paper in which the work is going on. In one way, radar baseband is becoming more adaptive by using adaptive filters, and also, ANN techniques are used for improving pulse compression technique which is the heart of the modern radar. This type of works are increasing the detectibly and decreasing the chance of false alarm rate. Few works are discussed in this direction, which helps us to find a new area in radar domain. In other direction, CNN technique is discussed for improving the radiometric imaging and can be very helpful in medical radar. In this part, AI will help a lot to reduce the repetitive work, and using a huge number of training databases, a preface radio diagnosis is possible in medical field. Basically, this article discusses about the AI techniques, namely ANN and CNN, that can be very useful, especially for medical radar, which will help us a lot for heart rate monitoring, breast cancer detection and many more.

References

1. Caro C, Bloice J (1971) Contactless apnoea detector based on radar. *Lancet* 2:959–961
2. Franks C, Brown B, Johnston D (1976) Contactless respiration monitoring of infants. *Med Biol Eng Compu* 14(3):306–312
3. Lee JY, Lin JC (1985) A microprocessor-based non-invasive arterial pulse wave analyzer. *IEEE Trans Biomed Eng* 32(6):451–455
4. Sharpe SM, Seals J, MacDonald AH, Crowgey SR (1990) Noncontact vital signs monitor. U.S. Patent 4,958,638, 25 Sept 1990
5. Azevedo SG, McEwan TE (1996) Micropower impulse radar. *Sci Technol Rev* 17–29
6. Mogi E, Ohtsuki T (2017) Heartbeat detection with Doppler radar based on spectrogram. In: 2017 IEEE international conference on communications (ICC), Paris, pp 1–6
7. Zhuge X, Saveliyev TG, Yarovoy AG, Ligthart LP (2008) UWB array-based radar imaging using modified Kirchhoff migration. In: Proceedings of the 2008 IEEE international conference on ultra-wideband (ICUWB 2008), vol 3
8. Zhuge X, Yarovoy M (2011) A sparse aperture MIMO-SAR-based UWB imaging system for concealed weapon detection. *IEEE Trans Geosci Remote Sens* 49(1)
9. Allen JL, Diamond BL (1966) Mutual coupling in array antenna. Technical Report EDS-66-443, Lincoln Lab., MIT, 4 Oct 1966
10. Yang YC (2011) UWB antennas and MIMO antenna arrays development for near-field imaging. Dissertation at Delft University of Technology, Oct 2011
11. Obeid D, Sadek S, Zaharia G, El Zein G (2009) A tunable system for contact-less heartbeat detection and a modeling approach. Medical Applications Networking (MAN), IEEE ICC
12. Matuszewski J (2018) Radar signal identification using a neural network and pattern recognition methods. In: 2018 14th international conference on advanced trends in radioelectronics, telecommunications and computer engineering (TCSET), Slavske, pp 79–83. <https://doi.org/10.1109/TCSET.2018.8336160>
13. Williams TC, Bourqui J, Cameron TR, Okoniewski M, Fear EC (2011) Laser surface estimation for microwave breast imaging systems. *IEEE Trans Biomed Eng* 58(5):1193–1199
14. Hagness SC, Taflove A, Bridges JE (1998) Two-dimensional FDTD analysis of a pulsed microwave confocal system for breast cancer detection: fixed-focus antenna-array sensors. *IEEE Trans Biomed Eng* 45(12):1470–1479
15. Hagness SC, Taflove A, Bridges JE (1999) Three-dimensional FDTD analysis of a pulsed microwave confocal system for breast cancer detection: design of an antenna-array element. *IEEE Trans Antennas Propag* 47(5):783–791
16. Bond EJ, Li X, Hagness SC, Van Veen BD (2003) Microwave imaging via space-time beam-forming: For early detection of breast cancer. *IEEE Trans Antennas Propag* 51(8):1690–1705

Ensuring Reliability in Vehicular Collision Avoidance Using Joint RFID and Radar-Based Vehicle Detection



Pallabi Biswas, Mithun Chakraborty, Rabindranath Bera,
and Shubhankar Shome

Abstract RFID tags are very essential for new generation automated vehicles. In this paper, three generations of RFID have been discussed with focus being on third generation that is used for vehicular applications. The main sensor for target detection in autonomous vehicle is automotive radar. Here, RFID-based vehicle detection and radar-based vehicle detection and their applications have been explored.

Keywords RFID · RADAR · Millimeter-wave · IFF · Smart vehicle

1 Introduction

A radio frequency identification (RFID) system works on the principle of a wireless radio link between a tag or transponder which contains details of the device to be identified, and a reader, that has transmitter and receiver [1]. RFID application at ultra-high-frequency (UHF) range is very popular worldwide for tracking of objects upto a range of 10 m. But large readers with big antennas are a drawback for UHF RFID. So, recent researches are concentrating more on the millimeter-wave range that has smaller antennas with highly directional narrow beam to detect targets. The use of radio waves started with the invention of radar around World War II. Radar works on the principle of searching and detecting a target with the help of radio waves and analyzing the received echo signal to obtain parameters of the target. First usage of RFID was the identification friend/foe (IFF) technology with passive RFID which was developed in Britain. This IFF technology is a surveillance system, present at aerodrome that uses millimeter-wave to identify whether any incoming

P. Biswas (✉) · R. Bera

Sikkim Manipal Institute of Technology, Sikkim Manipal University, Majitar, Rangpo, East
Sikkim 737136, India

e-mail: pallabibiswas24@gmail.com

M. Chakraborty

Amity University Jharkhand, Nivaranpur Main Road, Ranchi, Jharkhand, India

S. Shome

St. Mary's Technical Campus, Kolkata, India

aircraft is from an ally country or an enemy. This technology can be incorporated in smart vehicles for detection of target vehicles using radar and RFID. This paper is arranged in following manner, Sect. 2 overviews the working principle of RFID, Sect. 3 explains automotive radar, and Sect. 4 presents the innovative work initiated by the authors.

2 RFID

RFID transponders are mainly used for observation and tracking of objects. A reader is able to scan multiple tags simultaneously. The characteristics of RFID that make it better than barcodes are the non-line-of-sight operation, high-speed operation, ability to read, and write to tags and is provided with an unique ID.

A reader is made up of an antenna emanating EM waves and a RF module. RFID can operate either in near field where antenna operates in low or high-range frequencies or in far field where frequency range is ultra-high frequency (UHF) or microwave frequencies. In case of near-field operation, antenna on the reader produces EM field that causes inductive coupling of tag, and this changing magnetic flux induces current in tag. Subsequently, tag data is modulated to communicate with reader. In case of far-field tag-reader, communication is based on backscattered signal [2]. Tags could be initially in sleep mode and woken up by a UHF carrier signal transmitted by reader. Then, reader could transmit a query signal and obtain backscattered signal from tags and other clutter. After processing of backscattered signals, tags can be detected and localized, and finally, communication between reader and tag is established, as shown in Fig. 1. Field energy decreases proportionally to $1/R^3$ in near field and to $1/R$ in far-field scenarios.

$$\text{Distance limit between near and far field, } R = 2D^2/\lambda \quad (1)$$

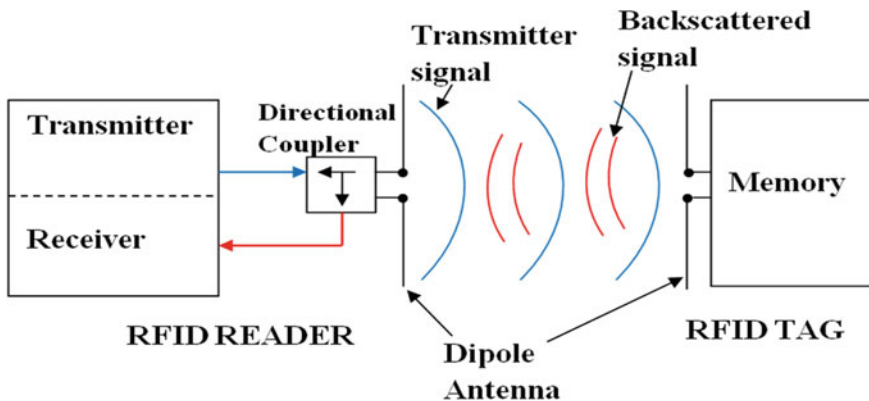


Fig. 1 Basic model of RFID functional block

where D = diameter of antenna, λ = wavelength of radio wave.

Every RFID tag on an object has a unique code called electronic product code (EPC) consisting of EPC standard of 96 bits.

- The first 8 bit header defines the tag version number
- Next comes the EPC manager of 28 bits containing the manufacturer’s identification
- This followed by object class of 24 bits having product identification
- Lastly, the serial number containing the unit ID of 36 bits.

There are three types of tag, namely passive which collects power from reader’s radiated power, semi-passive where battery provides power and active where battery provides power–transmitter present in tag. The power transmitted from reader and received by tag can be demonstrated as,

$$P_{rec} = P_{PA} G_{TX} G_{tag} \left(\frac{\lambda}{4\pi d} \right)^2 \tag{2}$$

where P_{PA} = power of amplifier, G_{TX} = gain of transmitter antenna, G_{tag} = gain of tag, λ = wavelength of carrier signal, and d = distance between reader and tag.

2.1 RFID Generations

The three generations of RFID based on uses and technical constraints have been given in Table 1.

Table 1 RFID use cases

RFID uses	RFID 1st generation	RFID 2nd generation	RFID 3rd generation
Identification	Yes	Yes	Yes
Tracking	No	Yes	Yes
Localization	No	No	Yes
Bandwidth	Low (KHz)	Low (KHz)	Wide (GHz)
RF carrier	Low at 13.56 MHz	UHF carrier at 900 MHz	MMwave carrier at 60 GHz
Antenna beamwidth	Wide toward Omni directional	Narrow	Pencil beam (2°)
Triangularisation	Not applicable	Not applicable	Beamsteering so one reader is sufficient, thus lowering the cost. For UWB RFID, three readers are required

From Table 1, it can be observed that although generation-2 RFID can detect and track the tag position, it does not support localization of tag. Due to low bandwidth in UHF architecture, beamsteering for direction of arrival (DOA) measurements is not accurately measured. RFID of third generation provides ranging accuracy to tag localization by modulation of backscatter signal. But range-based localization requires range measurements from minimum three readers present at each concerned location. Thus, high-directivity millimeter-wave antennas can be integrated into RFID system, enabling the reader to scan surrounding environment and identify, track, and localize tagged objects.

Demonstration of first-generation RFID is the student attendance system used in college [3]. The system consists mainly of a RFID reader, a microcontroller board, and a LCD screen, and every student has her RFID tag each with a unique identification code. When the tag is brought near to the reader, it is identified and name of the student is displayed on screen. Another application is the contactless debit/credit cards like the contactless VISA cards which uses RFID and near-field technology for transactions. The consumer needs to bring the card within range of the terminal equipped with RFID reader and make payment safely.

Application of the second generation of RFID is the automatic toll collection system [4] already introduced in India. In this case, the RFID reader set up at toll booth will read the prepaid RFID tags attached to a vehicle's windshield, and automatically, the required toll amount will be deducted from the owner's linked bank account. This process will also ensure:

- Reduce traffic congestion at toll booths
- Save time and fuel
- Stolen vehicle detection since each vehicle is assigned a unique RFID tag number.

Manufacturers like Alien technologies have designed EPC Class 1 generation-2 RFID tag IC named as HIGGs 3 [5]. The IC provides 800 bit memory, reading sensitivity upto 18.0 dBm, and writing sensitivity upto 13.5 dBm, with enhanced security using a non-digital and non-duplicable 'finger-print' for better security.

The third generation RFID, along with providing localization, is applicable for longer-range communication due to millimeter-wave carrier. So, it can be used as vehicular RFID for identification of vehicles on road leading to safer travel. Millimeter-wave portable RFID reader containing antennas with almost pencil beam can scan the surrounding to identify and localize tags. The tag is identified by backscatter method as done with UHF carrier. The reader transmits a train of N pulses modulated by reader code ' r_n ' ($n = 0, 1, \dots, N$), to every steering direction. After every pulse transmission, reader's antenna is switched from transmitter to receiver to receive backscatter signal. The i th tag modulates the incident signal according to code ($t_n^{(i)}$) and stored data information d_m . For localization, code synchronization is done, where received signal is multiplied with sequence composed by reader code and i th tag's code. Finally, reader transmits another pulse train to obtain the data stored in the tag, and received signal is filtered and time sampled to obtain necessary information. Figure 2 shows the process diagram.

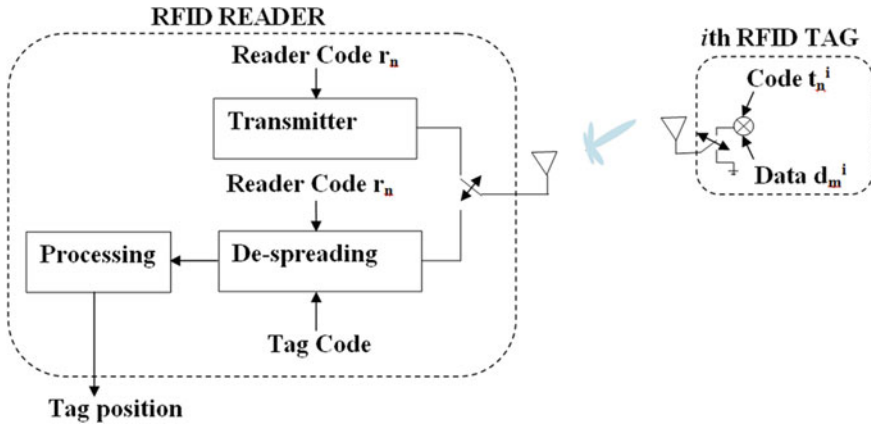


Fig. 2 Millimeter-wave RFID reader tag architecture for localization and communication

Guidi et al., [6] had validated this theory by placing fixed tag in a room and a single movable millimeter-wave reader. It can be compared to a road scenario with tag representing 1 fixed vehicle and shifting positions of second vehicle, i.e., the reader. Since millimeter-wave is used, localization error is minimum and range resolution is maximum. Exploiting this, they have positioned the vehicle very precisely only in x, y directions for performing two-dimensional localization. They had accounted for 36 steering directions for each position of reader, with angle step of 10° that covers the azimuth plane. Their outcome is interesting which shows that signal to noise ratio (SNR) is good if error in estimation of ranging, and steering angle is corrected. So, there is a reduction in false alarm rate. We have similar hardware equipments in our laboratory, so we have initiated related experiment which is stated later.

2.2 Vehicular RFID

Applications of vehicular RFID [7] mainly include management and control of vehicles, managing fleet of vehicles, and vehicular law maintenance.

- Control of vehicles: identification and localization of authorized vehicles
- Managing fleet of vehicles: tracking of different types of vehicles, controlling traffic lights, speed identification, and automatic toll booth operation
- Law maintenance: tracking of stolen vehicles possible because each vehicle has a unique RFID tag, also identification of owners whose road tax payment are due

Vehicular RFID can be used to measure the velocity of a vehicle by calculating the Doppler frequency shift from the backscattered signal.

3 Automotive RADAR

Automotive radars [8] are usually designed for working in 24 and 77 GHz frequency ranges. This spectrum is known as millimeter-wave frequencies as the wavelength lies in millimeter range. The advantages of operating in this band are wider bandwidth, better range resolution, and smaller sensor size suitable to be fitted in cars. Automotive radar is capable of performing functions like: (a) resolution of target (ability to identify separately two closely-spaced targets), (b) range resolution (ability to obtain different range values), (c) velocity of target measurement, and (d) determination of direction of arrival (DOA) of target echo. Along with these extremely important functions, the radar is robust to dirt, fog, and darkness and thus can operate unhindered under all weather conditions. So, for Advanced Driver Assistance System (ADAS) applications, namely Adaptive Cruise Control, park assist, front and rear traffic alert, blind spot detection, etc., in smart vehicles, radar is the primary sensor.

4 Work Initiated by the Authors

The work is based on third generation millimeter-wave RFID technology which is applicable for longer-range target detection, tracking, and localization. So, this RFID can be implemented in smart vehicle architecture for precise road vehicle identification with reduced false alarm rate. The working principle is similar to that of IFF technology. As per the paper discussed before, RFID can be used to identify tagged target vehicles. The reader can be mounted on another vehicle which is enquiring for information. Target detection is achieved by correlation of reader and tag codes. If the correlation value is 1, then the target is assumed to be 'friend' who can be identified and is willing to share its information. But if the correlation value is near to 0, then the target is assumed to be a 'foe' who does not want to be detected. Then, mode of operation will be changed to mm-wave radar, like a 28 GHz radar in our case, to obtain the range profile, velocity, and DOA of the target. The radar will send radio waves to the target, and on analysis of the received echo signal, target state parameters are obtained. Thus, using both RFID and radar modes, the problem of vehicle detection and localization will be solved with negligible false alarm rate leading to lesser collisions and safer driving.

5 Summary/Conclusion

This paper reviews the three generations of RFID, based on uses and technical constraints. The advantages of third generation mm-wave RFID are longer operational range, localization of tags, and beamsteering functions, along with smaller reader. The vehicular RFID can be implemented into vehicles for performing various

tasks like other tagged vehicle identification and for automatic toll booth operation, and so on. The authors have initiated an innovative architecture where RFID and radar modes can be utilized in a switching manner to obtain information on a target vehicle. If the tag on target responds to reader on enquiring vehicle, RFID communication link is established. Otherwise, the enquiring vehicle will be equipped with radar also which can obtain the range, speed, and direction of the target, thus offering safety measures in driving.

References

1. Pawan CT, Shivaraj SH, Manjunath RK (2020) RFID characteristics and its role in 5G communication. In: Proceedings of the fourth international conference on trends in electronics and informatics (ICOEI 2020), pp 473–478
2. Francesco G, Nicolo D, Davide D, Francesco M, Raffaele D (2016) Passive millimeter-wave RFID using backscattered signals. In: IEEE Globecom Workshops. IEEE, pp 1–6
3. Xiaoxu W, Yuesheng W (2018) An office intelligent access control system based on RFID. In: The 30th Chinese control and decision conference (2018 CCDC). IEEE pp 623–626
4. Akshay B, Sadhana P (2017) Advance automatic toll collection & vehicle detection during collision using RFID. In: International conference on Nascent Technologies in the engineering field (ICNTE), pp 1–5
5. HIGGS 3 EPC Class 1 Gen 2 RFID Tag IC Datasheet, Alien Technology LLC, pp 1–3 (2020)
6. Francesco G, Nicolo D, Davide D, Francesco M, Raffaele D (2018) Millimeter-wave beam-steering for passive RFID tag localization. IEEE J Radio Frequency Identification 2(1):9–14
7. Sumathi SM, Nikhitha KM, Manasa R, Jithesh A, Megha DH (2018) Automatic Toll collection system using RFID. Int J Eng Res Technol 6(15):1–7
8. Igal B, Oren L, Shahar V, Joseph T (2019) The rise of radar for autonomous vehicles. Adv Radar Syst Mod Civilian Commercial Appl IEEE Signal Process Mag 36(5):20–31

Signal and Image Processing in Engineering Applications

Dimensional Analysis and Gradation of Rice Grain Using Image Processing



Suman Kumar Bhattacharyya and Sagarika Pal

Abstract In this article, eight Indian rice grain samples have been taken for dimensional measurement and analysis for gradation with respect to their quality. Two categories of rice grains like parboiled and non-parboiled type have been considered here. Various dimensional parameters have been measured after purchasing the rice grain from the market in dry condition as well as after hydrothermal treatment for preparing it as food for consumption. The structural parameters of the rice kernel before and after hydrothermal treatment have been measured and analyzed. Different dimensionless parameters like aspect ratio, shape factor, compactness, roundness, eccentricity, solidity, and bounding box have been derived from the basic dimensional characteristics of the rice grain sample like length, width, projected area, and perimeter. Image processing and machine learning have been applied successfully to analyze the data and to take the decision about the gradation of samples. Accuracy of the gradation observed in the present work is 90.476% which is quite good. The observed gradation for unknown samples have been validated with respect to the market price and customer choice.

Keywords Rice grain dimensions · Hydro thermal treatment · Derived parameters · Gradation · Image processing · Machine learning

1 Introduction

Maximum people in the world depends on the rice grain (*Oryza sativa* L.) for their day today meal. Its food value is also appreciable among the cereals. So, the food market is very much dependent on rice quality.

S. K. Bhattacharyya (✉) · S. Pal
Department of Electrical Engineering, National Institute of Technical Teachers' Training and Research, Kolkata, India
e-mail: sumanbit33ster@gmail.com

S. Pal
e-mail: sagarikapal@nitttrkol.ac.in

Researchers have already covered a long way of food grain quality analysis. Rice grain quality has been measured through feature selection with the hydrothermal treatment in [1]. Active counter and statistical histogram-based models have been used for removing the background in image processing [2]. Modeling and measurement of dimensional changes in the rice kernel have been done during soaking through moisture absorption and cooking through gelatinization condition in [3, 4]. Grading system of rice grains using quality analysis of grain image with pattern processing has been done in [5, 6]. The quality of rice grain through feature selection with vision-based inspection systems have been analyzed in [7]. Appearance and implicit properties of the rice kernel have been correlated with the soaking and cooking time in [8]. Computer vision-based system has been used for sorting rice grains through various physical characteristics in [9, 10]. Potential application of computer vision in quality inspection efficiently estimates the quality of the rice grain which has been shown in [11]. Machine vision technology by selecting feature points in the rice image has been implemented in [12]. In [13], hydrothermal effects for analyzing quality characteristics of milled and cooked rice have been done.

In the present work, different dimensional parameters of rice image [14] before and after hydrothermal treatment have been measured, compared, and analyzed to take the decision about the classification as per grade of sample. Decision tree algorithm [15] using classification and regression tree (CART) method has been applied for gradation of rice samples. The used method for gradation has been successfully applied on unknown samples and validated with respect to the market price.

2 Methodology

In this work, physical parameters of rice samples like length (L), width (W), projected area (A), and perimeter (P) as well as derived parameters like aspect ratio (AR), shape factor (SF), compactness (C), roundness (R), eccentricity (E), solidity (S), and bounding box (B) have been considered for measurement. Customers normally observe the rice grain during purchase and finally judge the quality during consumption as food after hydrothermal treatment. That is why in the present method, above parameters have been measured after purchasing the rice grain from the market in dry condition as well as after preparing it as food for consumption for final quality determination and gradation.

2.1 Rice Samples for the Experimentation

Five parboiled and three non-parboiled Indian rice samples have been taken in this work for initial machine learning. Selected parboiled samples are Sarna, Basmati, Ratna, IG-Basmati, IR 36, and non-parboiled samples are Gobindavog, Atap and

Table 1 Range of market price for the selected rice grains

Rice sample	Sarna	Basmati	Ratna	IG Basmati	IR 36	Atap	Gobindavog	New Atap
Rs./kg	25–32	65–75	35–45	70–80	35–42	30–40	85–95	38–50
Market grade	III	I	II	I	II	III	I	II

New Atap, respectively. The price and gradation of these selected eight rice samples as per market are shown in Table 1.

At a time, 40–45 numbers of grain kernels have been taken for experimentation. Kernels have been organized randomly but not connected with each other. It has been assumed that no cracks are there in these samples. Distilled water has been used for hydrothermal treatment.

2.2 Steps Followed During Hydrothermal Treatment of Rice

Soaking is the first phase of the continuous hydrothermal treatment. In this stage, rice grains of a sample have been taken into a beaker with water for water absorption in normal room temperature (22–25 °C). This phase has been allowed for 30 min time duration. In second phase of hydrothermal treatment, the soaked rice samples obtained after 30 min of water absorption have been heated with excess water. The parboiled samples have been heated for 50 min, and non-parboiled rice samples have been heated for 20 min after soaking until the highest expansion of the rice kernels has been achieved determined by gelatinization of the sample. The gelatinization temperature is different for different samples. In the third phase, after the highest elongation in cooking phase, the rice grains have been separated from hot water and put into a dry plate for subsequent cooling. After completion of the third phase, images have been captured for the samples and processed for measuring dimensional parameters like L, W, A, P in terms of pixels and derived dimensionless parameters like AR, SF, C, R, E, S, B. The detail of these parameters are indicated in Table 2.

2.3 Image Analysis for Parameter Measurement

The image processing techniques, applied for analyzing all the image data obtained in the present observation are mentioned in the following sequence of steps.

Step-1: Image acquisition: A high quality dual digital camera having resolution of (720 × 1520) pixels have been used through proper lighting for capturing all the images. The captured images for a typical sample are shown in Fig. 1a.

Table 2 Various dimensional parameters related with physical attributes of rice grain

Parameter	Used expression	Explanation
Length (L)	L	Major axis length
Width (W)	W	Minor axis length
Projected area (A)	A	Area of the grain region in the binary image
Perimeter (P)	P	Boundary length in binary image
Aspect Ratio (AR)	$AR = \frac{L}{W}$	Ratio of length and width, indicates how long and thin is the kernel
Shape Factor (SF)	$SF = \frac{A}{L \times W}$	Shape factor indicates the exact appearance of the kernel
Compactness (C)	$C = \frac{P^2}{A}$	Compactness means how far the grain is “closed and bounded”
Roundness (R)	$R = \frac{4\pi * A}{P^2}$	Roundness measures how closely it approaches to the perfect circle
Eccentricity (E)	$E = \frac{c}{a} = \frac{\sqrt{a^2 - b^2}}{a}$	Ratio of the distance between foci (2c), and the length of its major axis (2a)
Solidity (S)	$S = \frac{A}{\text{Area of Convex hull}}$	Solidity is area fraction of the projected area as compared to its convex hull. Convex hull is the smallest convex region
Bounding box (B)	$B = L * W$	A bounding box is the rectangle with the smallest possible surface area that bounds the shape

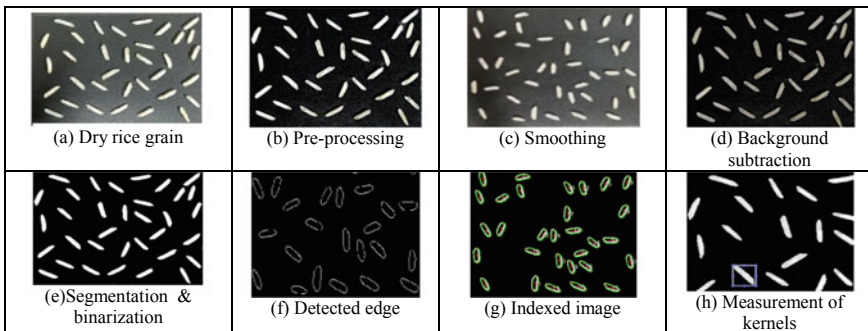


Fig. 1 Sequence of images showing the steps of image processing in basmati rice

Step-2: Pre-processing: Color images have been pre-processed by converting to the grayscale images and then suppressed the unwanted factors with enhancing the necessary image features. This step corresponds to Fig. 1b.

Step-3: Apply smoothing: Images have been smoothed by filtering with Gaussian filter. This process have been used to reduce the noise and contrast to blur the edges

of the images. The following Gaussian function $G(x)$ is used in this work by the formula as follows, $G(x) = \frac{1}{\sigma\sqrt{2\pi}} e^{-\frac{x^2}{2\sigma^2}}$; $\sigma = 2$ for the present application.

Where σ is the mean distribution value, it is assumed that mean distribution value x is centered ($x = 0$). This step corresponds to Fig. 1c.

Step-4: Background subtraction: Background subtraction technique has been applied to extract the foreground of the images for the aim of object recognition by the following operation,

$$P[f(t)] = P[I(t)] - P(B);$$

where t is the time instant, $P[I(t)]$ is the image, and $P(B)$ is the background of the image, and $P[f(t)]$ is the image after background subtraction. This step corresponds to Fig. 1d.

Step-5: Segmentation and Binarization: Image segmentation has been used to locate the objects and boundaries in the images.

Fixed intensity value (T) has been evaluated by using threshold value. Binarization technique has been applied through the choice of intensity between the all background intensity and all foreground intensity. Then, the input image $I1$ is being transformed to an output binary image $I2$ in the following way,

$$I2(i, j) = 1 \text{ for } I1(i, j) \geq T; I2(i, j) = 0 \text{ for } I1(i, j) < T,$$

where T is the threshold value.

$I2(i, j) = 1$ for the object element and $I2(i, j) = 0$ for the background elements. Output of this step corresponds to Fig. 1e.

Step-6: Edge detection: Canny edge detection technique has been used to detect the edges of rice kernels. Horizontal, vertical, and diagonal edges have been recognized in the image by using the following method.

The edge detection operator returns a value for the first derivative in the horizontal direction (G_x) and the vertical direction (G_y) from the edge gradient and direction, $\tan(\theta)$ have been determined using formula, edge gradient (G) = $\sqrt{G_x^2 + G_y^2}$ and angle (θ) = $\tan^{-1} \frac{G_x}{G_y}$. This step corresponds to Fig. 1f.

Step-7: Image Indexing: Image indexing has been used in this work to measure each and every rice kernels presented in the image. This method has been applied with the retrieval of the objects based on spatial relationship and properties. It corresponds to Fig. 1g.

Step-8: Data receiving and analysis: From the indexed images, dimensional parameters like L, W, A, P, and derived parameters like AR, SF, C, R, E, S, and B have been measured. This step corresponds to Fig. 1h.

Step-9: Gradation: In this study, measured dimensional data from rice grains have been classified in three grade category like grade-I (very good), grade-II (good), and grade-III (not so good) as per market and customer choice. This gradation can be

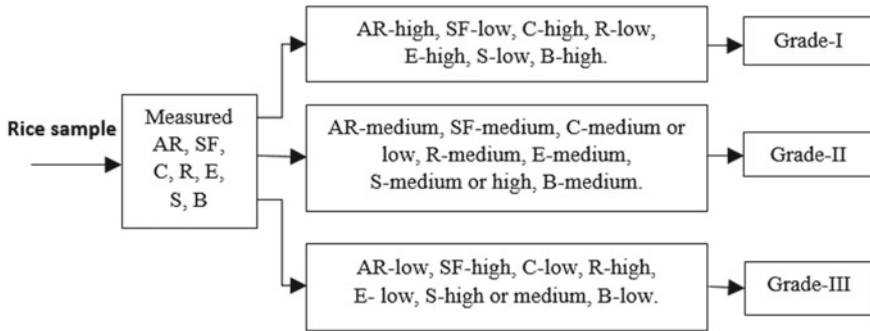


Fig. 2 Gradation in 3-grades (I, II, III) as per the measured trend of the mentioned parameters

assumed using the range of obtained dimensional values in the experiment as shown in Fig. 2.

This experience has been given to the system for grading the rice samples. Decision tree learning model using classification and regression tree (CART) technique has been used in this work to get the result of gradation of the rice grain samples. It uses an index as metric function in classification tree which is sum of the square of probabilities of each class as shown below,

$$\text{Index} = 1 - \sum_{i=1}^n p_i^2$$

where i is the number of classes, p_i is the probability, and the range of index value is $[0, 1]$. The techniques have been used to separate the training examples according to the target classification and to measure how well the task has been achieved through the selected parameters.

3 Experimental Results and Discussions

In the present experiment, the measurement data related with kernel dimensional parameters like L , W , A , and P along with derived parameters AR , SF , C , R , E , S , and B of all the parboiled rice grain samples have been taken in dry condition as well as after cooking through hydrothermal treatment as displayed in Table 3. The same type of measured data for non-parboiled rice grain samples is shown in Table 4. It is to be noted that L , W , A , and P data are indicated in terms of pixel, and other parameters like AR , SF , C , R , E , S , and B are dimensionless quantity. The experimental data as shown in Tables 3 and 4 have been used in the machine learning algorithm for training purpose with respect to gradation of both parboiled and non-parboiled rice

Table 3 Parboiled rice kernel dimensional data in dry and cooked condition

Parameter	Grain condition	Parboiled rice				
		Sarna	Basmati	Ratna	IG-Basmati	IR 36
L	Dry	22.98	38.37	27.96	33.91	26.67
	Cooked	29.15	86.71	48.29	81.901	41.36
W	Dry	20.3	21.3	21.10	21.50	20.7
	Cooked	21.88	29.76	25.06	26.41	23.45
A	Dry	175.82	263.01	203.17	233.38	195.21
	Cooked	210.79	665.01	330.68	568.01	284.35
P	Dry	55.95	83.84	63.45	71.05	61.06
	Cooked	65.46	160.37	100.02	155.65	86.41
AR	Dry	1.132	1.7997	1.3207	1.5728	1.2841
	Cooked	1.332	2.914	1.927	3.101	1.764
SF	Dry	0.3769	0.3215	0.3434	0.3192	0.3524
	Cooked	0.3305	0.2577	0.2732	0.2626	0.2932
C	Dry	1.4176	2.1278	1.5769	1.7222	1.5211
	Cooked	1.618	3.395	3.079	2.091	2.408
R	Dry	0.7054	0.4699	0.6342	0.5807	0.6574
	Cooked	0.6178	0.2945	0.3248	0.4783	0.4152
E	Dry	0.8901	0.9801	0.931	0.971	0.9401
	Cooked	0.8304	0.9936	0.9241	0.9852	0.9381
S	Dry	0.961	0.8901	0.9301	0.8901	0.93
	Cooked	0.9758	0.676	0.9361	0.7782	0.9485
B	Dry	466.49	818.05	591.91	731.1	553.93
	Cooked	637.8	2580.49	1210.15	2162.9801	969.89

kernels. These training data from these two tables have been applied for gradation following the assumption as depicted in Fig. 2.

The market price and gradation are strictly dependent on two observations by the customer, firstly during purchase from shop in dry condition, and secondly after completion of cooking. Following this fact, in the present experimentation, measurement and gradation jobs have been done in both dry and cooked condition, and then, the final gradation has been achieved as indicated in Table 5.

The developed machine learning system for gradation has been applied on three unknown samples during dry and cooked condition, and it is shown in Table 6. The final gradation obtained from the experimental result is in parity with the quality detected by the market price and customer choice.

In the present work, the % accuracy has been calculated to measure the degree of closeness to its actual gradation. In Table 6, sample 1, 2, and 3 have been graded by the system in dry and cooked condition through the measurement of seven derived parameters like AR, SF, C, R, E, S, and B. Here, unknown sample 1, 2, and 3 have

Table 4 Non-parboiled rice kernel dimensional data in dry and cooked condition

Parameter	Grain condition	Non-parboiled rice		
		Atap	Gobindavog	New Atap
L	Dry	22.42	25.5	24.94
	Cooked	34.28	47.45	36.9
W	Dry	21.1	21.2	21.8
	Cooked	23.77	23.7	23.07
A	Dry	179.01	190.01	188.01
	Cooked	300.16	309.01	259.02
P	Dry	57.25	60.15	59.5
	Cooked	94.28	94.99	77.901
AR	Dry	1.0595	1.2037	1.141
	Cooked	1.059	1.203	1.141
SF	Dry	0.3773	0.3493	0.345
	Cooked	0.3773	0.3493	0.345
C	Dry	1.4578	1.5159	1.499
	Cooked	1.4578	1.51586	1.499
R	Dry	0.6859	0.6597	0.667
	Cooked	0.6859	0.65969	0.667
E	Dry	0.92	0.891	0.85
	Cooked	0.8501	0.921	0.89
S	Dry	0.909	0.93	0.941
	Cooked	0.9401	0.909	0.93
B	Dry	474.4072	544.0434	544.9
	Cooked	814.835	1195.66	839.7

been correctly graded 12 times, 14 times, and 12 times, respectively, among the total 14 cases of observation for each sample. For three unknown samples, total observed cases are 42 (i.e., $14 \times 3 = 42$), among which 38 (i.e., $12 + 14 + 12$) number of cases have been correctly recognized, and rest 4 cases are wrongly recognized. So, the calculated values of % accuracy and % error in the present work are shown in Table 7.

4 Conclusions

In the present experiment, Indian methods of food preparation of rice grain, i.e., soaking, cooking, and subsequent cooling, have been followed during measuring the dimensional parameters of cooked grain related to quality aspect.

Table 5 Gradation of rice grains with respect to experimental data

Derived parameter	Grain condition	Gradation of rice samples										
		Parboiled rice					Non-parboiled rice					
		Sarna	Basmati	Ratna	IG-Basmati	IR 36	Atap	Gobinda vog	New Atap			
AR	Dry	III	I	II	I	II	III	I	II	III	I	II
	Cooked	III	I	II	I	II	III	I	II	III	I	II
SF	Dry	III	I	II	I	II	III	I	II	III	I	II
	Cooked	III	I	II	I	II	III	I	II	III	I	II
C	Dry	III	I	II	II	II	III	II	II	III	II	II
	Cooked	III	I	I	II	II	III	II	II	III	II	II
R	Dry	III	I	II	II	II	III	II	II	III	II	II
	Cooked	III	I	I	II	II	III	II	II	III	II	II
E	Dry	III	I	II	I	II	III	I	II	III	I	III
	Cooked	III	I	II	I	II	III	I	II	III	I	III
S	Dry	III	I	II	I	II	III	I	II	III	I	III
	Cooked	III	I	II	I	II	III	I	II	III	I	III
B	Dry	III	I	II	I	II	III	I	II	III	I	I
	Cooked	III	I	II	I	III	II	I	III	II	I	II
Final grade		III	I	II	I	II	III	I	II	III	I	II

Table 6 Gradation of unknown rice samples as per learning process

Derived parameter	Grain condition	Gradation of unknown parboiled rice samples		
		Sample 1 Rs 42–52./kg	Sample 2 Rs. 70–80/kg	Sample 3 Rs 30–40/kg
AR	Dry	II	I	III
	Cooked	II	I	III
SF	Dry	II	I	III
	Cooked	I	I	II
C	Dry	II	I	III
	Cooked	II	I	III
R	Dry	II	I	III
	Cooked	II	I	II
E	Dry	II	I	III
	Cooked	II	I	III
S	Dry	II	I	III
	Cooked	II	I	III
B	Dry	II	I	III
	Cooked	I	I	III
Final grade		II	I	III

Table 7 System performance accuracy

Total number of cases	Correctly graded	Wrongly graded	Accuracy (%)	Error (%)
42	38	4	90.476	9.524

A common practice of the customer is that they initially judge the quality of grain through dimensional observation of dry grain during purchase but they finally validate the quality of the same grain after cooking, i.e., during consumption as food. Following this fact, each and every measured dimensional parameter value has been taken in dry as well as in cooked condition as depicted in Tables 3 and 4.

In the previous research for gradation of rice grains, all different samples have been considered only in dry condition; i.e., after purchase from market, but in the present research, gradation has been done in dry as well as in cooked condition, and then, both the observations have been taken into consideration for final gradation of the rice samples. Here lies the novelty of the present work. Accuracy of the gradation performed by the present work is 90.476% which is quite good. The observed gradation with unknown samples truly validate the quality determined by market scenario and customer choice.

References

1. Bello M, Baeza R, Tolaba M (2004) Quality Characteristics of milled and cooked rice affected by hydrothermal treatment. *J Food Eng* 72:124–133
2. Parveen E, Alam A, Shakir H (2017) Assessment of quality of rice grain using optical and image processing technique. *International Conference on Communication Computing and Digital System (IEEE)*, pp 265–270
3. Yadav B, Jindal V (2007) Modelling changes in milled rice (*Oryza sativa* L.) kernel during soaking by image analysis. *J Food Eng* 80:359–369
4. Yadav B, Jindal V (2007) Dimensional changes in milled rice (*Oryza sativa* L.) kernel during cooking in relation to its physicochemical properties by image analysis. *Sci Direct J Food Eng* 81:710–720
5. Patil V, Malemath V (2015) quality analysis and grading of rice grain images. *Int J Innov Res Comput Commun Eng* 3:5672–5678
6. Ajay G, Suneel M, Kumar K, Prasad P (2013) Quality Evaluation of rice grains using morphological methods. *Int J Soft Comput Eng* 2:35–37
7. Chetima M, Payeur P (2012) Automated tuning of a vision based inspection system for industrial food manufacturing. In: *Proceeding of the IEEE international instrumentation and measurement technology conference (I2MTC'2012)*, pp 210–215
8. Jinorose M, Prachayawarakorn S, Soponronnarit S (2014) A novel image-analysis based approach to evaluate some physicochemical and cooking properties of rice kernels. *J Food Eng* 124:184–190
9. Verma B (2010) Image processing techniques for grading & classification of rice. In: *International conference on computer and communication technology (ICCCT)*, Allhabad, India. IEEE, pp 220–223
10. Zareiforouh H, Komarizadeh M, Alizadeh M (2009) Effect of moisture content on some physical properties of paddy grains. *Res J Appl Sci Eng Technol* 1(3):132–139
11. Zareiforouh H, Minaei S, Alizadeh M, Banakar A (2015) Potential application of computer vision in quality inspection of rice: a review. *Food Eng Rev* 7(3):321–345
12. Neelamegam P, Abirami S, Vishnu PK, Valantina S (2013) Analysis of rice granules using image processing and neural network. In: *Conference on Information and Communication Technologies (IEEE)*, pp 879–884
13. Hamad S, Zafar T, Sidhu J (2018) Parboiled Rice metabolism differs in healthy and diabetic individuals with similar improvement in glycaemic response. *Nutrition*. 47:43–49
14. Gonzalez RC, Woods RE (2018) *Digital image processing*, 4th edn. Pearson, London
15. Mitchell MT (2019) *Machine learning*, Indian edition. McGraw Hill Education, New York

Feature Dimension Reduction for Efficient Classification of Dermoscopic Images with Feature Fusion



Rik Das, Anish Anurag, Govind Kumar Jha, and Mahua Banerjee

Abstract Dermoscopic images carry rich information to identify the malignancy in patients at initial stage. Research initiatives in the domain of content-based image classification can be instrumental in identifying fatal diseases like skin cancer by exploring the dermoscopic image database. This paper has carried out feature dimension reduction for representation of significant content-based image descriptors to the classifiers. The approach has resulted in designing an early fusion based classification model with reduced computational overhead to enhance accuracy of malignancy detection at its inception.

Keywords Skin cancer · Melanoma · Computer aided diagnosis · Principal component analysis · Feature fusion

1 Introduction

Recent advancements in medical imaging have kindled the scope for computer-aided diagnosis (CAD) of life-threatening ailments like cancer. Researchers have made commendable progress in the domain of content-based image classification in identifying benign and malignant categories of the terminal disease [1]. Melanoma is widely known as one of the fatal forms of skin cancer which has claimed innumerable lives. However, timely recognition of the disease has resulted in cure for 99% of the cases within an interval of 5 years of survival. The prime reason of delayed

R. Das (✉) · M. Banerjee
Xavier Institute of Social Service, Ranchi, India
e-mail: rikdas78@gmail.com

M. Banerjee
e-mail: mahuabanerjee2015@gmail.com

A. Anurag · G. K. Jha
Vinoba Bhave University, Hazaribag, India
e-mail: anish.jnu08@gmail.com

G. K. Jha
e-mail: jhagovi@gmail.com

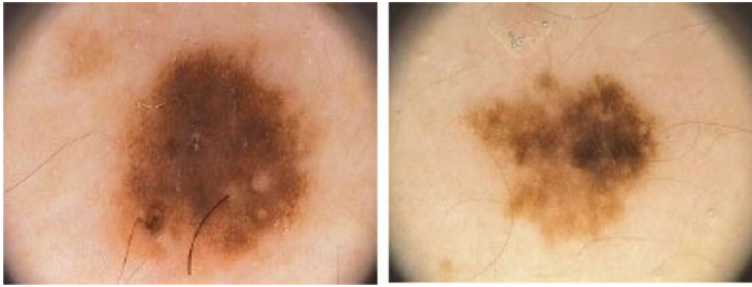


Fig. 1 Illustration of images from PH2 dataset

identification is the extended time for consulting an expert due to their tight schedule of practice [2]. This has stimulated the researchers to design automated system for primary identification of the lethal syndrome by means of content-based image identification. Several attempts are designed to enhance the accuracy of malignancy identification of the disease by designing informative descriptors from the images of the infected portion of the skin. This work has attempted to explore the effect of feature dimension reduction and early feature fusion for identification of malignancy for the melanoma disease. The experiments are conducted with a public dataset named PH2 dataset for which an illustration is shown in Fig. 1 [3].

The results of the experiment have revealed that reduction of feature dimension has resulted in identification of significant feature values influencing classification results. Moreover, reduced feature dimension has lessened the time for classification, which has in turn reduced the runtime of the categorization algorithm.

2 Literature Review

Early skin cancer detection is an emerging field of research in which a comparative study of color constancy, and lesion analysis is carried out [4]. Feature extraction techniques for analysis of dermoscopy images are surveyed to determine the robustness of state-of-the-art techniques [5]. Dermoscopy images are classified using neural networks for melanoma identification [6]. High precision of for melanoma classification is achieved using deep convolutional neural networks [7]. Synergic deep learning techniques are adopted for classification of skin lesion in dermoscopy images [8]. Birthmark mole detection in clinical images are conducted for early melanoma detection [9]. The process has converted the images to monochrome for extraction of significant feature vectors. Feature vectors are extracted from color, shape, and text after performing segmentation of the dermoscopic images [10]. Neural network-based deep ensemble model is evaluated for skin lesion classification in dermoscopic images [11]. Efficient classification of skin lesion is carried

out using attention residual learning [12]. Computer-aided diagnosis of skin cancer has outclassed trained dermatologists with the use of deep neural networks [13].

However, implementation of deep neural networks for melanoma detection is mostly infeasible in real time due to its resource hungry nature. The high processing requirements of deep networks makes it challenging to design light weight devices for instant melanoma detection.

In this work, the authors have addressed this issue and have attempted to carry out melanoma detection with lightweight handcrafted features by means of dimension reduction. The results are promising and have revealed high precision for melanoma detection.

3 Classification Techniques

Feature vector extraction is the foremost step and a precursor for the task of content-based image classification. Dermoscopic images in PH2 dataset are preprocessed prior to feature extraction. The dataset comprises of 200 images on the whole spread across 80 images each for common nevi and atypical nevi and the rest 40 images are of melanoma. The images are segmented using ground truth mask available with the dataset as shown in Fig. 2.

Images are rotated in the range of -180° to 180° for generating 12 diverse forms which for each image as in Fig. 3.

This has augmented the dataset and the total number of images becomes 2400. Each image is further resized to $256 * 256$ dimension.

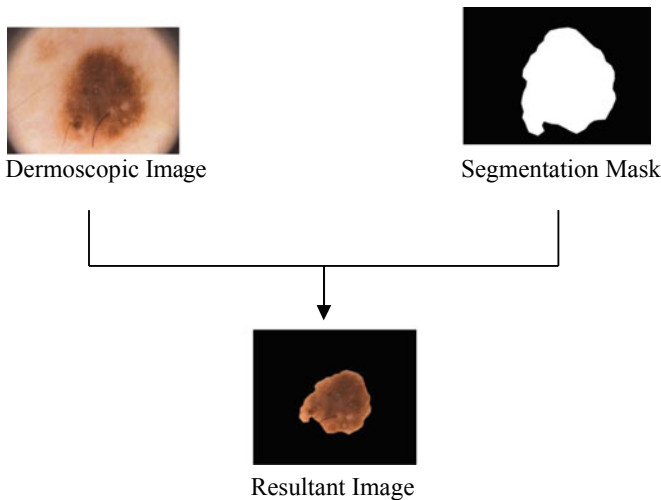


Fig. 2 Image segmentation

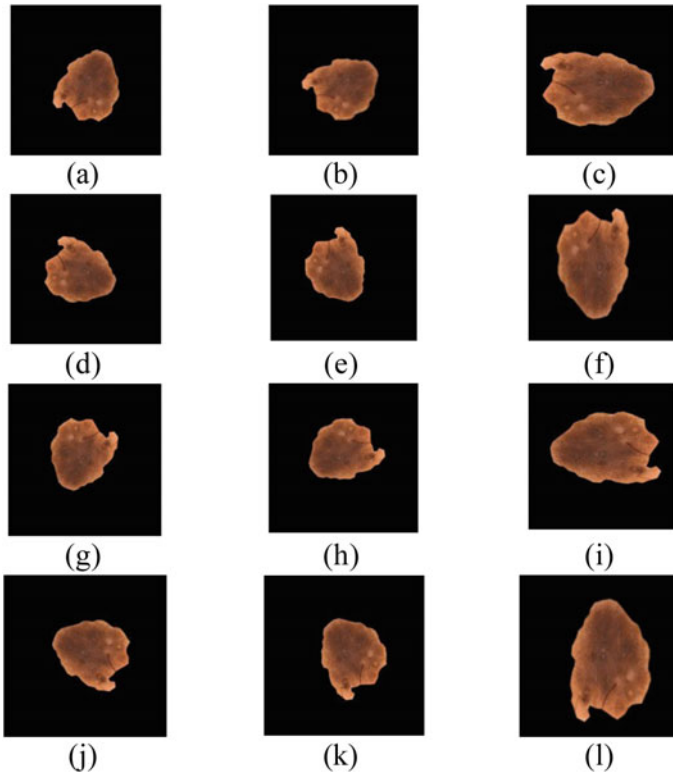


Fig. 3 Image varieties created with angular rotation

Two different feature extraction techniques, namely, histogram of oriented gradients (HOG) and color histogram (CH) are used to extract feature vectors from the dataset.

Henceforth, the feature vectors are reduced in dimension by applying principal component analysis (PCA) [14].

Finally, the two different feature vectors, namely HOG and CH are fused horizontally after their dimensions are reduced.

Classifiers of two different varieties, namely support vector machine (SVM) and logistic model tree (LMT), are applied to evaluate the classification accuracy of the original feature vectors, their reduced dimension varieties, and the fused feature vectors.

4 Classification Techniques

Classification is carried out with tenfold cross-validation for each of the feature extraction techniques. Primarily, the feature vectors with default dimension are evaluated for classification accuracy. Further, PCA is applied for dimension reduction of the feature vectors, and the classification accuracy with reduced dimension of the feature vectors is calculated. Finally, the features with reduced dimension are fused horizontally and are tested for classification accuracies. Time taken to build the classification model in each of the cases is recorded for comparison.

The comparison of accuracies of different feature extraction techniques are shown in Fig. 4.

An integrated comparative result of accuracies, dimensions, and time taken to build classification models is given in Table 1.

The results in Table 1 have revealed highest accuracy for the feature fusion technique in case of both the classifiers. Although, the classification results with single feature (CH) is almost equivalent to feature fusion in case of LMT, but a significant difference is noticed for SVM. This is because the fused features have captured and represented both the color properties and gradient orientation of the images simultaneously to the classifier. Hence, the classifier is able to identify the images with more clarity and consistency across diverse environments compared to any of the

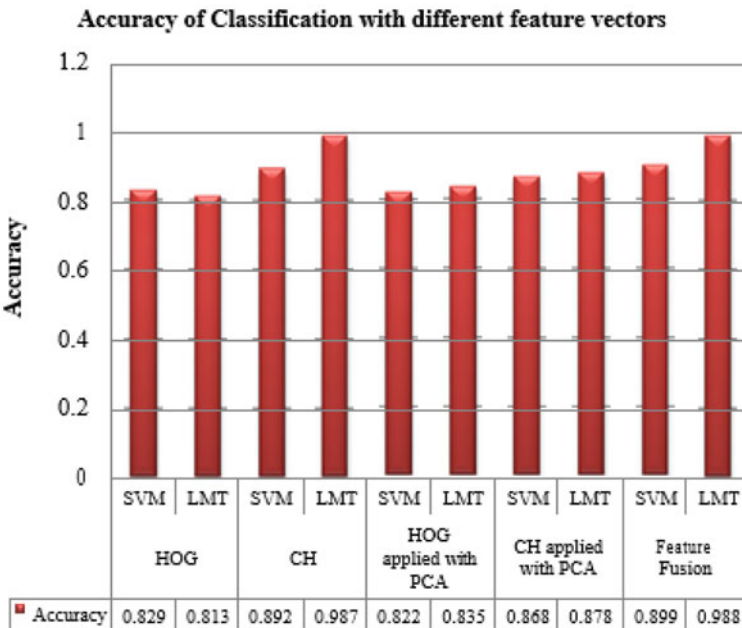


Fig. 4 Comparison of accuracies for different features

Table 1 Comparison of accuracy, dimension of feature vectors, and time taken for building classification model

Features	Classifiers	Accuracy	Dimension	Time (s)
HOG	SVM	0.829	576	13.95
	LMT	0.813		71.64
CH	SVM	0.892	64	0.23
	LMT	0.987		10.23
HOG applied with PCA	SVM	0.822	250	3.36
	LMT	0.835		20.39
CH applied with PCA	SVM	0.868	50	0.21
	LMT	0.878		4.76
Feature fusion	SVM	0.899	300	3.82
	LMT	0.988		47.73

individual feature descriptors which have represented either the color properties or the gradient orientation at a given instance.

Additionally, it is observed that reduction of dimension of the feature vectors with application of PCA has retained significant feature components by eliminating the ones which do not have much influence on classification decision. The time taken for building classification model by the reduced feature vectors is considerably low compared to their original counterparts. Fusion-based features have consumed lesser time in building classification model compared to the original HOG features, but have surpassed the time taken by CH.

Finally, feature dimension in fused feature is much lesser than original HOG features but the accuracy of classification is higher, which indicates toward the efficiency of fusion-based approach.

5 Conclusion

The paper has proposed a design to implement computer-aided diagnosis for classification of melanoma with dermoscopic images. Conventional classification methodologies consider single feature vector as representation of the image data to be classified. However, all the feature values do not have significant weight to influence classification decision. This work has reduced the dimension of features by applying PCA and has reduced the classification time without compromising accuracy. A feature fusion-based approach with reduced features is also shown for enhancing classification accuracy with less computational overhead.

References

1. Hou L, Samaras D, Kurc TM, Gao Y, Davis JE, Saltz JH (2016) Patch-based convolutional neural network for whole slide tissue image classification. In: Proceedings of the IEEE conference on computer vision and pattern recognition, pp 2424–2433
2. Matsunaga K, Hamada A, Minagawa A, Koga H (2017) Image classification of melanoma, nevus and seborrheic keratosis by deep neural network ensemble. arXiv preprint [arXiv:1703.03108](https://arxiv.org/abs/1703.03108)
3. Fernandes SL, Chakraborty B, Gurupur VP, Prabhu G (2016) Early skin cancer detection using computer aided diagnosis techniques. *J Integr Design Process Sci* 20(1):33–43
4. Barata C, Celebi ME, Marques JS (2018) A survey of feature extraction in dermoscopy image analysis of skin cancer. *IEEE J Biomed Health Inform* 23(3):1096–1109
5. Xie F, Fan H, Li Y, Jiang Z, Meng R, Bovik A (2016) Melanoma classification on dermoscopy images using a neural network ensemble model. *IEEE Trans Med Imaging* 36(3):849–858
6. Demyanov S, Chakravorty R, Abedini M, Halpern A, Garnavi R (2016) Classification of dermoscopy patterns using deep convolutional neural networks. In: 2016 IEEE 13th international symposium on biomedical imaging (ISBI). IEEE, pp 364–368
7. Zhang J, Xie Y, Wu Q, Xia Y (2018) Skin lesion classification in dermoscopy images using synergic deep learning. In: International conference on medical image computing and computer-assisted intervention. Springer, Cham
8. Balakrishnan J, David D (2019) Melanoma classification and birthmark mole detection on clinical images. In: 2019 international conference on vision towards emerging trends in communication and networking (ViTECoN). IEEE, pp 1–5
9. Suganya R (2016) An automated computer aided diagnosis of skin lesions detection and classification for dermoscopy images. In: 2016 international conference on recent trends in information technology (ICRTIT). IEEE, pp 1–5
10. Xie Y, Zhang J, Xia Y (2018) A multi-level deep ensemble model for skin lesion classification in dermoscopy images. arXiv preprint [arXiv:1807.08488](https://arxiv.org/abs/1807.08488).
11. Zhang J, Xie Y, Xia Y, Shen C (2019) Attention residual learning for skin lesion classification. *IEEE Trans Med Imaging* 38(9):2092–2103
12. Brinker TJ, Hekler A, Enk AH, Klode J, Hauschild A, Berking C, Utikal JS (2019) Deep learning outperformed 136 of 157 dermatologists in a head-to-head dermoscopic melanoma image classification task. *Eur J Cancer* 113:47–54
13. Satheesha TY, Satyanarayana D, Prasad MG, Dhruve KD (2017) Melanoma is Skin Deep: A 3D reconstruction technique for computerized dermoscopic skin lesion classification. *IEEE J Transl Eng Health Med* 5:1–17
14. Zhang T, Yang B (2016) Big data dimension reduction using PCA. In: 2016 IEEE international conference on smart cloud (SmartCloud). IEEE, pp 152–157

Feature Edge-Detail Preservation of Random-Valued Impulse Noise in Images



Patitapaban Rath, Rajesh Siddavatam, and Pradeep Kumar Mallick

Abstract In this paper, we put forth a progressive, decision-based, two-phase image denoising algorithm for eliminating random-valued impulse noise from images. The manner in which this algorithm deals with noise is a completely pristine method when compared to the other existing image denoising algorithms. In the primary phase, the noise is dealt at a coarse level; in other words, the noisy pixels that are easily differentiable from the neighborhood are eliminated. In the secondary phase, fine-level image denoising is performed. In other words, the left-over fine scale noise in the detected corrupted pixels of the first phase, which cannot be straightforwardly differentiated from the surrounding pixels, is eliminated. In both the phases, separate mechanisms were followed to eliminate noise in the interior regions and edge regions. Hence, the algorithm is edge-detail preserving. Images with very high noise levels, in other words, with 70% noisy pixels were restored successfully. Speaking in terms of quantitative significant measures, the restored images in most cases were better than those of the other existing filters.

Keywords Image denoising · Random-valued impulse noise · Mean structural similarity index (SSIM) · Localized pixel intensity variation (LPIV) filter

P. Rath (✉) · P. K. Mallick
School of Computer Engineering, KIIT University, Bhubaneswar, India
e-mail: pabanrath@gmail.com

P. K. Mallick
e-mail: pradeep.mallickfcs@kiit.ac.in

R. Siddavatam
VVIT, Guntur, India
e-mail: srajesh@ieee.org

1 Introduction

Impulse noise is broadly classified into salt-and-pepper noise and random-valued impulse noise. In images corrupted by salt-and-pepper noise, the noisy pixels can take only the maximum and the minimum values in the dynamic range, while in the images corrupted by random-valued noise (RV noise), they can occupy any value in between the minimum and maximum values in the same dynamic range.

Hence, practically speaking, handling RV noise would be quite tedious. The sources of impulse noise have been explained in [1].

Among the various existing denoising methods, the median filter is used extensively because of its effective noise subduing potential and computational effectiveness. Its denoising power and computational efficiency are elaborated in [3, 4], respectively.

However, the main drawback of a standard median filter is that it is effective only for low-noise densities [5] and the vital original information of the image is lost because it is not a decision-based filter. The other drawback of the median filter was that it was not decision based; in other words, it cannot preserve original information.

In order to ameliorate denoising, many other impulse detector filters were proposed. The weighted median filter [6] and adaptive median-based filters [7] were partially decision based. The adaptive median-based filter using second-generation wavelets [8], multi-state median filter [9], the homogeneous information-based filters [10, 11], the adaptive center-weighted median filter [12], the peak-and-valley filters [13, 14], the signal-dependent filter [15], the iterative method proposed by Luo [16] and other algorithms like [17–21] are decision-based algorithms. Among the two-phase algorithms, the three-state median (TSM) [22], the adaptive center-weighted median (ACWM) [12], the Luo filter [23], the genetic programming (GP) filter [24] are worth stating. The effective detection technique to replace RV noise in images with high noise levels is an open challenge. A partial differential equation-based technique [25] is an interesting method proposed in recent times, which uses a new defined set of controlling functions for impulse noise removal.

As already said, dealing with RV noise is relatively tedious in contrast to salt-and-pepper impulse noise [26].

We hereby propose the localized pixel intensity variation (LPIV) filter which has been proved successfully by Kireeti Bodduna and Rajesh Siddavatam et al. in [27], [28, 29]. The credibility of cardinal splines for interpolation in impulse noise-related problems was again tested by Rajesh Siddavatam et al. in [29].

Our work introduces a two-phase mechanism for random-valued noise removal. In the first stage, the noisy pixels were dealt with at a coarse level. Noise at a very fine level still persists in those detected pixels after the first phase. So in the second phase, for those pixels which were detected as noisy in the first phase, the second part of the proposed algorithm is applied. The fact that edge pixels and interior pixels were separately dealt with in both the phases of the algorithm is the prime reason for edge-detail preservation in the restored images. We make use of dyadic wavelets of canny to determine whether a particular pixel belongs to the interior region or the edge region.

The outline of this paper is as follows: The proposed algorithm and the significant measures are discussed in Sect. 2. The results along with conclusions have been discussed in Sect. 3.

2 Proposed Algorithm

The noise detection job is performed by the LPIV filter [29]. It designates each and every pixel in the window as a noisy pixel or a noise-free counterpart. Once a pixel is detected as noisy, it is replaced by interpolating the noise-free pixels in the neighborhood with cardinal splines. By neighborhood, we mean the particular window in the image where the algorithm is currently active.

2.1 Coarse Level Image Denoising—I

This is the first phase of the algorithm where the noise is removed in local neighborhoods where the noisy pixels can be identified with certainty. “The underlying idea of the localized pixel intensity variation (LPIV) filter is that the gray-scale pixel intensities in a local neighborhood vary insignificantly. Thus, for every central pixel in a window, we find the noise-free pixels in that window. Subsequently, using these noise-free pixels, we calculate a local threshold. Depending on this threshold, we decide the fate of the central pixel whether it is corrupted by noise or not. If corrupted, we replace it by interpolating the noise-independent pixels.

If the center pixel belongs to the interior region of the image, a threshold of $T1 + \square$ is used, where \square is the flexibility parameter for interior regions and is constant for a particular image, but different for various images. Rajesh Siddavatam et al. computational results showed that when it is varied between 20 and 60 dB we obtain better restored images. To be more precise, a particular value of \square in this range gives best interpolation results as elaborated in [29].

In the second case, if the center pixel belongs to the edge region of the image, a threshold of $T1 + \square$ is used, where \square is the flexibility parameter for edge regions [29].

The novelty here lies in the fact that the threshold selected is a function of the window. In other words, the threshold is calculated locally but not globally like in some of the erstwhile proposed filters. This paves way for better detection and hence better restored images.

2.2 LPIV 1 for Interior Regions

INPUT: Coarse scale denoised image $\sum (i, j)$. This algorithm is simulated for only those interior pixels which were detected as noisy in the first phase. Again, we define the 3×3 window $\Omega = \{(s, t) | -1 \leq s, t \leq 1\}$ centered at (O, O) . Here, the center element is the noisy interior pixel detected in phase 1.

Step A:

$$\forall D(i, j) \in \sum (i, j) \in \sum_1$$

(For the detected interior region noisy pixels in phase 1).

$$Z(1) = \Omega(0,1)$$

$$Z(2) = \Omega(0, -1)$$

$$Z(3) = \Omega(-1, 0)$$

$$Z(4) = \Omega(1, 0)$$

$$b \leftarrow (-\beta\alpha^3 + 2\beta\alpha^2 - \beta\alpha)$$

$$b \leftarrow [(2 - \beta)^0\alpha^3 + (\beta - 3)\alpha^2 + 1]$$

$$b \leftarrow [(\beta - 2)^1\alpha^3 + (3 - 2\beta)\alpha^2 + \beta\alpha]$$

$$b \leftarrow (\beta\alpha^3 + 2\beta\alpha^2)$$

$$pt. = b_0 * Z(3) + b_1 * Z(2) + b_2 * Z(3) + b_3 * Z(4)$$

$$\Omega(0,0) = pt.$$

OUTPUT: Interior region fine scale denoised image $\sum (i, j)$.

2.3 LPIV 2 for Edge Regions

INPUT: Interior region fine-level denoised image $\sum (i, j)$. This algorithm is simulated for only those edge pixels which were detected as noisy in the first phase. Again, we define the 3×3 window $\Omega = \{(s, t) | -1 \leq s, t \leq 1\}$ centered at $(0, 0)$. Here the center element is the noisy edge pixel detected in phase 1.

Step B:

$$\forall D(i, j) \in \sum (i, j) \in \sum_2$$

- $Z(1) = \Omega(0,1)$
- $Z(2) = \Omega(0, -1)$
- $Z(3) = \Omega(-1, 0)$
- $Z(4) = \Omega(1, 0)$
- $b \leftarrow (-\beta\alpha^3 + 2\beta\alpha^2 - \beta\alpha)$
- $b \leftarrow [(2 - \beta)^0\alpha^3 + (\beta - 3)\alpha^2 + 1]$
- $b \leftarrow [(\beta - 2)^1\alpha^3 + (3 - 2\beta)\alpha^2 + \beta\alpha]$
- $b \leftarrow (\beta\alpha^3 + 2\beta\alpha^2)$
- $pt. = b_0 * Z(1) + b_1 * Z(2) + b_2 * Z(3) + b_3 * Z(4)$
- $\Omega(0,0) = pt$
- OUTPUT: Edge region fine scale denoised image $\sum (i, j)$. The image $\sum (i, j)$ is the final restored image (Table 1; Fig. 1).

3 Results and Conclusions

Figures 2, 3, 4 and 5 show the final restored images from various noise levels of Lena, Bridge, Peppers and Airplane. Tables 2, 3 and 4 give the comparative analysis with other existing algorithms. The PSNR values are quite impressive keeping in mind the corresponding amount of noise 60% in the original images.

Summarizing the results from the above figures, it can be clearly seen that when the noise density increases, the PSNR and MSSIM values decrease. As the noise density increases, the amount of original information that is available to us decreases. The standard test images were procured from the University of Southern California image database. All the images were 8-bit images with dynamic ranges from 0 to 255. Peak signal-to-noise ratio (PSNR) and structural similarity index measure (SSIM) [32] have been used as quantitative yardsticks to measure the restored images.

Table 1 Parametric values used in the initial iteration of both LPIV 1 and LPIV 2 for various images

Image	α	B	γ (dB)	δ (dB)
Lena	0.5	-1.8	25.0	32.5
Bridge	0.4	-2.3	45.0	60.0
Peppers	0.5	-1.8	25.0	32.5
Airplane	0.4	-2.5	32.5	47.5
Bridge	0.5	-2.1	25.0	62.5

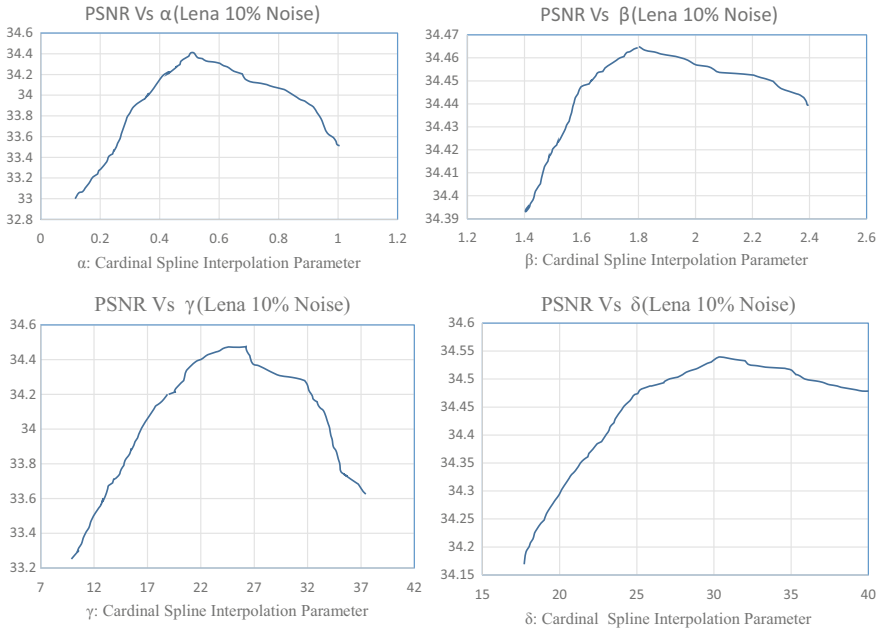


Fig. 1 Parameter optimization for Lena image to obtain optimal PSNR by varying α, β

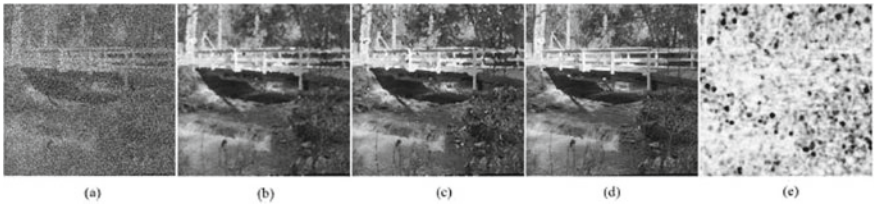


Fig. 2 **a** Noisy image Lena: 60%, **b** LPIV1 (25.96 dB), **c** LPIV2 (25.90 dB), **d** original image, **e** SSIM Map (MSSIM = 0.8906)



Fig. 3 **a** Noisy Bridge: 60%, **b** LPIV1 (21.4 dB), **c** LPIV2 (22.57 dB), **d** original image, **e** SSIM map (MSSIM = 0.7886)



Fig. 4 a Noisy Peppers: 60%, b LPIV1 (24.99 dB), c LPIV2 (22.14 dB), d original image, e SSIM map (MSSIM = 0.8448)

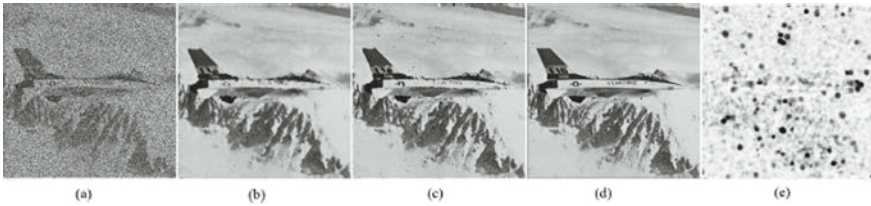


Fig. 5 a Noisy Airplane: 60%, b LPIV1 (23.76 dB), c LPIV2 (24.7 dB), d original image, e SSIM map (MSSIM = 0.8719)

The proposed localized pixel intensity variation (LPIV) filter has two-way mechanism of denoising random-valued impulse noise, and it has been found that the obtained restored images are either superior to those produced by other theoretical models in most cases or almost similar to the results of other works in a very few cases. When compared with other algorithm results (Tables 2, 3, 4 and 5), in a total of 30 cases, in 20 cases LPIV (either LPIV1 or LPIV2) gave best results and in 7 cases, PDE (NSDD + NTVD) gave better results while in only 3 cases GP gave best results. Another advantage of using this method is that it does not involve any time-consuming theoretical equations. Hence, the computational efficiency is impressive. Finally, our proposed methodology also suffices for color images (by extending the LPIV to three dimensions). Future work can be done in applying this filter to 3D mesh models and point cloud graphic models.

References

1. Gonzalez RC, Woods RE (2002) Digital image processing. Prentice-Hall, Englewood Cliffs
2. Pratt WK (1975) Median filtering. Technical report, Image processing Institute, University of Southern California, Los Angeles, Sept 1975
3. Bovik A (2000) Handbook of image and video processing. Academic, New York
4. Huang TS, Yang GJ, Tang GY (1979) Fast two-dimensional median filtering algorithm. *IEEE Trans Acoustics Speech Signal Process ASSP-1*(1):13–18
5. Srinivasan KS, Ebenezer D (2007) A new fast and efficient decision based algorithm for removal of high-density impulse noises. *IEEE Signal Process Lett* 14(3):189–192
6. Brownrigg D (1984) The weighted median filter. *Commun Assoc Comput* 807–818
7. Hwang H, Haddad RA (1995) Adaptive median filters: new algorithms and results. *IEEE Trans Image Process* 4(4):499–502
8. Syamala Jaya Sree P, Kumar P, Siddavatam R, Verma R (2013) Salt-and-pepper noise removal by adaptive median-based lifting filter using second-generation wavelets. *Signal Image Video Process* 7(1):111–118
9. Chen T, Wu HR (2001) Space variant median filters for the restoration of impulse noise corrupted images. *IEEE Trans Circuit Syst II Analog Digit Signal Process* 48(8):784–789
10. Eng H-L, Ma K-K (2001) Noise adaptive soft-switching median filter. *IEEE Trans Image Process* 10(2):242–251
11. Pok G, Liu J-C, Nair AS (2003) Selective removal of impulse noise based on homogeneity level information. *IEEE Trans Image Process* 12(1):85–92
12. Chen T, Wu HR (2001) Adaptive impulse detection using center-weighted median filters. *IEEE Signal Process Lett* 8(1):1–3
13. Windyga PS (2001) Fast impulsive noise removal. *IEEE Trans Image Process* 10(1):173–179
14. Alajlan N, Kamel M, Jernigan E (2004) Detail preserving impulsive noise removal. *Signal Process Image Commun* 19:993–1003
15. Abreu E, Lightstone M, Mitra SK, Arakawa K (1996) A new efficient approach for the removal of impulse noise from highly corrupted images. *IEEE Trans Image Process* 5(6):1012–1025
16. Luo W (2005) A new efficient impulse detection algorithm for the removal of impulse noise. *IEICE Trans Fundam E88-A*(10):2579–2586
17. Syamala Jaya Sree P, Raj P, Kumar P, Siddavatam R, Ghrera SP (2013) A fast novel algorithm for salt and pepper image noise cancellation using cardinal B-splines. *Signal Image Video Process* 7(6):1145–1157
18. Aizenberg I, Butakoff C, Paliy D (2005) Impulsive noise removal using threshold Boolean filtering based on the impulse detecting functions. *IEEE Signal Process Lett* 12(1):63–66
19. Besdok E, Yksel ME (2005) Impulsive noise suppression from images with Jarque-Bera test based median filter. *Int J Electron Commun* 59:105–110
20. Crnojevic V, Senk V, Trpovski Z (2004) Advanced impulse detection based on pixel-wise MAD. *IEEE Signal Process Lett* 11(7):589–592
21. Russo F (2004) Impulse noise cancellation in image data using a two-output nonlinear filter. *Measurement* 36:205–213
22. Chen T, Ma K-K, Chen L-H (1999) Tri-state median-based filters in image denoising. *IEEE Trans Image Process* 8(12):1834–1838
23. Luo W (2007) An efficient algorithm for the removal of impulse noise from corrupted images. *Int J Electron Commun* 61(8):551–555
24. Petrovic N, Crnojevic V (2008) Universal impulse noise filter based on genetic programming. *IEEE Trans Image Process* 17(7):1109–1120
25. Jian Wu, Tang C (2011) PDE-based random-valued impulse noise removal based on new class of controlling functions. *IEEE Trans Image Process* 20(9):2428–2438
26. Ghanekar U, Singh AK, Pandey R (2010) A contrast enhancement based filter for removal of random valued impulse noise. *IEEE Signal Process Lett* 17(1):47–50

27. Bodduna K, Siddavatam R (2012) A novel algorithm for detection and removal of random valued impulse noise using cardinal splines. In: 2012 Annual IEEE proceedings of India conference (INDICON), Dec 2012, pp 1003–1008
28. Bodduna K (2013) A novel algorithm for random-valued-impulse noise detection and removal using Chebyshev polynomial interpolation. In: Proceedings of second IEEE international conference on image information processing (ICIIP), Dec 2013, pp 410–415
29. Jayasree S, Bodduna K, Pattnaik PK, Siddavatam R (2014) An expeditious cum efficient algorithm for salt-and-pepper noise removal and edge-detail preservation using cardinal spline interpolation. *J Vis Commun Image R* 25:1349–1365
30. Unser M (1999) Splines: a perfect fit for signal and image processing. *IEEE Signal Process Mag* 16(6):24–38
31. Unser M, Aldroubi A, Eden M (1991) Fast B-spline transforms for continuous image representation and interpolation. *IEEE Trans Pattern Anal Mach Intell* 13(3):277–285
32. Wang Z, Bovik AC, Sheikh HR, Simoncelli EP (2004) Image quality assessment from error visibility to structural similarity. *IEEE Trans Image Process* 13(4):600–612

Sparse Auto-encoder Improvised Texture-Based Statistical Feature Estimation for the Detection of Defects in Woven Fabric



Sourav Tola, Sugata Sarkar, Jayanta K. Chandra, and Gautam Sarkar

Abstract Machine-intelligence-based detection of woven fabric enhances the quality of fabric. However, the main challenge to the researchers in this domain is the heuristic components superimposed on the regular grating structure of fabric. Several statistical and spectral approaches have been tried to solve this issue. In this paper, an exhaustive set of feature vector derived from distance and orientation-dependent Haralick parameter is obtained. A sparse auto-encoder having suitable sparsity is then used to map the derived feature vector into a low-dimensional manifold, while reducing the over-fitting as well. Finally, the support vector machine is used to classify the given fabric portion into defective or healthy classes. The method is tested on three types of woven fabric, containing a wide variety of fabric defects. Performance of the developed system is measured through several performance matrices, and finally, a defect detection success rate of 95% is obtained.

Keywords Fabric defect detection · Gray-level co-occurrence matrix · Haralick parameter · Sparse auto-encoder · Support vector machine

1 Introduction

The fabric defect can be simply defined as a change in or on the fabric construction with respect to a defined pattern. It has been estimated [1] that the price of fabrics is reduced by 45–65% due to the presence of defects. In the textile industry, the product (end) is inspected for the defects by human or machines [2, 3]. As the perception of fabric defect varies from individual to individual and often, one individual may have different sensitivity from time to time; hence, it becomes a difficult job to detect defects by human beings. Moreover with the modern weaving machines, the production speeds and consequently productivity are faster than ever, which is

S. Tola (✉) · S. Sarkar · J. K. Chandra
Ramkrishna Mahato Government Engineering College, Purulia, India
e-mail: souravbec@gmail.com

G. Sarkar
Jadavpur University, Kolkata, India

far beyond the human perception. The experiments show that the human error rate begins to rise rapidly as information output approaches about 8 bits/s [4]. Also, the relatively hostile working environment near the weaving machines is not suitable for human inspection [5]. Hence, the machine vision system has become an essential for automatic detection of fabric defect. However, fabric inspection still presents a considerable challenge, on account of the variable nature of the weave [6, 7].

One of the fundamental features of the gray scale image of woven fabric sample is texture. The concept of fabric inspection and hence determination of its severity consists of grading the materials based on their overall texture characteristics such as material isotropy, homogeneity, and coarseness [8]. Even though for human eyes, it is very easy to distinguish different textures, yet it is really difficult to put it in the mathematical form. Attempts have been made to define texture for its quantitative representation [9]. It has been found experimentally that the textures which are visually distinguishable, like fabric defect on fabric structure, statistical approaches like gray-level co-occurrence matrix (GLCM) performs better than the spectral approaches like Fourier transform, wavelet, etc., [10] in regard to the extraction of feature. It has also been reported that the GLCM is an effective texture descriptor [11].

In case of a machine-intelligence-based automatic defect detection system, there are two primary steps. In the first step, extraction of relevant feature is required, and in the next step, a classifier is required for the classification of the fabric sub image into defective or healthy classes. Moreover, it is also required to eliminate the redundant features out of the exhaustive set of features to enhance the classification accuracy [12] and to reduce the computational and structural complexity of the classifier.

In this paper from a fabric sub image, feature vector is generated in the form of Haralick parameters [13] by using the GLCM, calculated over different distance and orientations of sub image pixels. Redundancy of relevant features is reduced by sparse auto-encoder, by adjusting its sparsity, that makes a trade-off in between reduction of feature and over-fitting [14]. Finally, the support vector machine (SVM) is used for classification purpose, which attempts to maximize predictive accuracy while automatically avoiding over-fit of the data, by the transformation of hypothesis space to a high-dimensional feature space, defined by a weight vector and bias term by using the statistical learning theory [15].

2 Feature Extraction and Classification of Fabric Sub Image

Since the defect on a fabric sample is defined as deviation of local fabric texture with respect to the global grating structure of fabric, hence for the fabric defect detection the fabric sample is required to be divided into fabric sub images in such a way, so that the defect becomes global or dominant in the sub images containing defect, and at the same time, these contain the primitive fabric grating structure for healthy portion

[16]. Now from each sub image, GLCM based texture feature vector is derived for classification of fabric sub image into defective and healthy classes.

2.1 Determination of Haralick Parameter for Defective and Healthy Portion of Fabric Image

The GLCM, representing the distribution and relationship of pixels [17] in a fabric sub image, either belonging to healthy or defective fabric portion measures texture characteristics by the probability of occurrence of pixel intensity pairs, at different orientations and distances. Let the GLCM of p th gray scale fabric sub image belonging to q th class is represented as, $CM_p^q|_{r,\theta} = [cm_p^q|_{ijr\theta}]$, where $cm_p^q|_{ijr\theta}$ is the (i, j) th entry of $CM_p^q|_{r,\theta}$, and $1 \leq p \leq P, 1 \leq q \leq 2, P$ is the number of fabric sub images in each type of fabric, which can either contain defective or healthy fabric portions out of the Q fabric classes. $cm_p^q|_{ijr\theta}$ is obtained by counting the number of occasion a pixel with value i is adjacent to the pixel with value j having a distance and orientation of r & θ , respectively, in between i and j . Considering N_G as gray level of a fabric sub image, from the elements of $CM_p^q|_{r,\theta}$, the following statistical parameters, i.e., features for the fabric sub image, known as Haralick parameter are evaluated as,

$$H_{1p}^q|_{r,\theta} = \sum_i \sum_j m_p^q|_{ijr\theta}^2 \tag{1a}$$

$$H_{2p}^q|_{r,\theta} = - \sum_i \sum_j cm_p^q|_{ijr\theta} \cdot \log(cm_p^q|_{ijr\theta}) \tag{1b}$$

$$H_{3p}^q|_{r,\theta} = \sum_{n=1}^{N_G-1} n^2 \cdot C_{x-y}^q(n) \tag{1c}$$

$$H_{4p}^q|_{r,\theta} = \frac{\sum_i \sum_j ((i \cdot j)cm_p^q|_{ijr\theta}) - \mu_{x_p}^q \cdot \mu_{y_p}^q}{\sigma_{x_p}^q \cdot \sigma_{y_p}^q} \tag{1d}$$

$$H_{5p}^q|_{r,\theta} = \sum_i \sum_j (i - \mu_p^q)^2 \tag{1e}$$

$$H_{6p}^q|_{r,\theta} = \sum_i \sum_j \frac{1}{1 + (i - j)^2} cm_p^q|_{ijr\theta} \tag{1f}$$

where $C_{x_p}^q(i) = \sum_{i=1}^{N_G} cm_p^q|_{ijr\theta}$, $C_y^q(j) = \sum_{j=1}^{N_G} cm_p^q|_{ijr\theta}$ and $C_{x-y}^q(k) = \sum_{i,j:|i-j|=k} cm_p^q|_{ijr\theta}$, $\forall |i - j| = 0, \dots, N_G - 1$ and $\mu_{x_p}^q, \mu_{y_p}^q, \sigma_{x_p}^q, \sigma_{y_p}^q, \mu_{y_p}^q$ are mean and variances of $C_{x_p}^q, C_{y_p}^q$ and mean of $CM_p^q|_{r,\theta}$, respectively. Equation 1a–1f denote energy, entropy, contrast, correlation, variance, and local homogeneity of the

fabric sub image, respectively, which actually denotes textural uniformity, disorder or complexity of the woven fabric, the spatial frequency of the woven fabric, linear dependence of gray-level values in the texture, spread of data in the texture with respect to its mean, and homogeneity of the woven fabric, respectively. Value of r depends on the grating structure of the fabric sub image. In case a single period of grating, structure of the fabric sub image occupies larger space, i.e., if the coarseness of fabric sub image is more, the value of r should be increased for accommodation of the fabric structure. Since the objective is to work with the exhaustive set of feature of a fabric sub image, hence r is varied beyond a certain critical value (r_C), depending on the coarseness of the fabric sub image and for each value of r , θ is varied at an angle of 0° , 45° , 90° , 135° , and 180° . Corresponding to each set of r and θ Haralick parameters are calculated, the collection of which gives a texture-based feature vector $V_p^q \in \mathfrak{R}^{(1 \times N)}$ of p th gray scale fabric sub image belonging to q th class. The size of fabric sub image and r are so chosen that $V_p^q \in \mathfrak{R}^{(1 \times N)}$ becomes independent of coarseness of fabric, i.e., same for all fabric type, which in turn makes the algorithm de-sensitive to the size of fabric sub image [18].

2.2 Elimination of Redundant Features by Using Sparse Auto-Encoder

As the objective is to create a trade-off between the reduction of the computational cost of the system and over-fitting, hence requirement becomes to represent the feature vector ($V \in \mathfrak{R}^{(P \cdot Q \times N)} = [V_p^q]$) in a low-dimensional hyper-space while reducing its over-fitting. To do so, the sparse auto-encoder is used. The activation from a hidden neuron of the sparse auto-encoder is given by,

$$h_p^q|_k = f \left(\sum_{i=1}^N a_{i,k}^t \cdot V_p^q|_{i,k} \right) \in \mathfrak{R}^{(1 \times 1)} \quad (2)$$

where $V_p^q|_{i,k}$ and $a_{i,k}$ are the input from i th input neuron to the k th hidden neuron and the corresponding weight value at t th iteration and $f(\cdot)$ is the activation function of the k th hidden neuron. Then, concatenating all the activations of all the hidden neurons, the vector $h_p^q \in \mathfrak{R}^{(1 \times M)}$ is obtained, such that $M < N$. Finally, considering all fabric sub images, the fabric feature matrix $h = [h_p^q] \in \mathfrak{R}^{(P \cdot Q \times M)}$ is obtained, which then becomes the input of the support vector machine (SVM) classifier. The decoder part of the sparse auto-encoder is only to estimate the closeness of the encoder input (V) and decoder output (\hat{V}), i.e., to calculate the data loss, $DL = (V \sim \hat{V})$. The sparse auto-encoder also introduces the regularization factor $h_p^q|_k = \hat{h}_p^q|_k$, where very low value of $\hat{h}_p^q|_k$ implements the concept of sparsity, which in turn reduces the over-fitting [19].

2.3 Classification of Fabric Sub Image by Support Vector Machine

Being the problem a two class classification problem, SVM classifier is used [20]. The classifier is trained in a supervised way with $h = [h_p^q] \in \mathfrak{R}^{(P \cdot Q \times M)}$ as the input and the binary target values, representing defective or healthy portions as the output. The time complexity of SVM denoted as $O(n^3)$ [21] largely decreases as M becomes less than N . But again M cannot be reduced arbitrarily as in that case the problem of over-fitting becomes dominant. The SVM classifier ($g(W, b)$) attempts to execute the following linear equation,

$$\text{minimize}(l(W, \alpha, b)) = \left\{ \frac{1}{2} \|W\|^2 + \sum_{sv} \alpha_i [d_i(W^T \cdot h_p^q + b)] - 1 \right\} \quad (3)$$

where $W \in \mathfrak{R}^{(1 \times M)}$ is the weight matrix, $b \in \mathfrak{R}^{(1 \times 1)}$ is the bias term, $d_i \in \mathfrak{R}^{(1 \times 1)}$ is the target value corresponding to i th training sample, α_i is the i th Lagrangian multiplier, and sv are the support vectors, i.e., the closest data points to the linear hyper plane of either class. The above equation tries to maximize the separation between support vectors, subject to the constraint ($d_i(W^T \cdot h_p^q + b) \geq 0$), i.e., the misclassification is a minimum.

However, for nonlinearly separable cases, applying the Cover's theorem, the nonlinearly separable problem in a low-dimensional space is casted nonlinearly in a higher-dimensional space to make it linearly separable by using the following kernel trick.

$$K(h_p^q|_{\text{derived}}, h_p^q) = \Phi^T(h_p^q|_{\text{derived}}) \cdot \Phi(h_p^q) \quad (4)$$

where $h_p^q|_{\text{derived}} \in \mathfrak{R}^{(1 \times T)}$ is the input variable obtained from $h_p^q \in \mathfrak{R}^{(1 \times M)}$ and $\Phi(\cdot)$ is the set of nonlinear transformations that transforms h_p^q to $h_p^q|_{\text{derived}}$, such that $T > M$. Figure 1 is showing the sparse auto-encoder model with SVM classifier.

3 Experimental Results

The proposed method was tested on 160 fabric images containing different types of fabric defects taking place on three different types of fabric from TILDA database [22]. The selected fabric types vary from each other in terms of their coarseness. Images in TILDA database are 8 bit gray and of size (768 × 512) pixels. The concerned fabric types are shown in Fig. 2.

During training, 150-dimensional feature vector was developed for five different inter-pixel distances beyond the critical value and five different angle of orientation of the pixels. 450 such feature vectors from 450 fabric sub images of concerned fabric

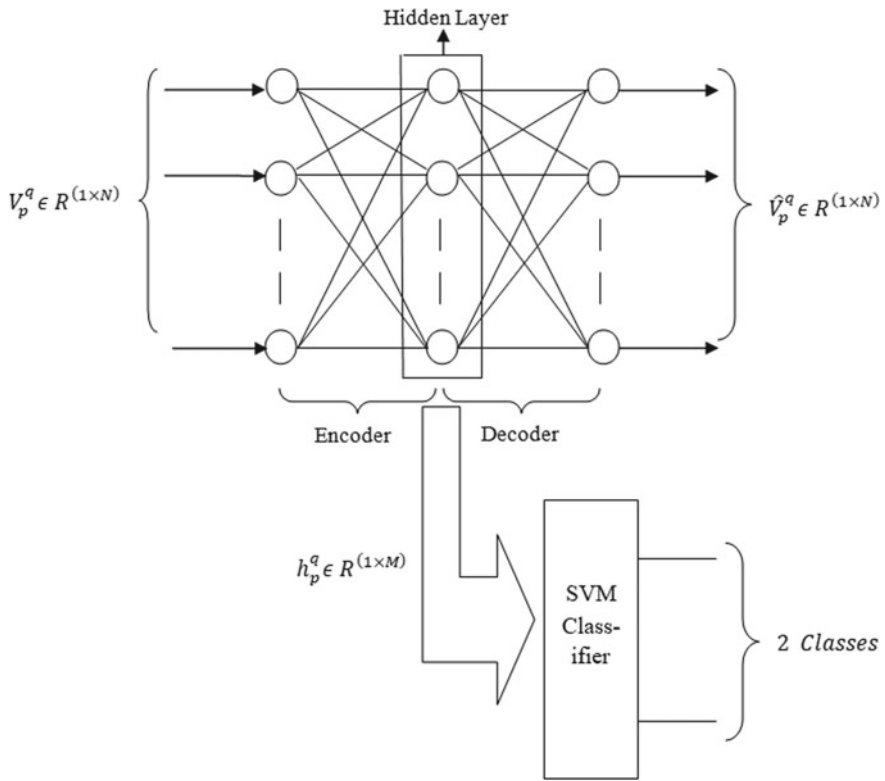


Fig. 1 Sparse auto-encoder model with SVM classifier

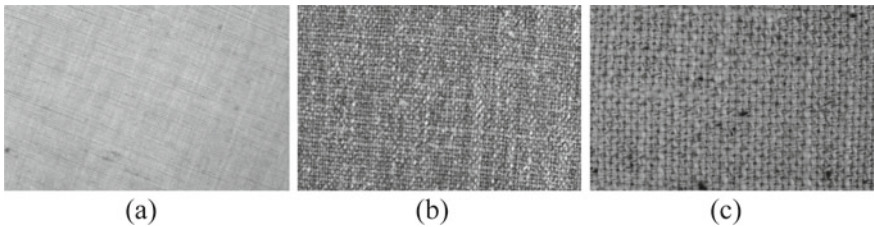


Fig. 2 Types of fabric sub images

types containing concerned types of defects were used for the training purpose. A sparsity factor of 0.05 was chosen, which was found to eliminate problem of over-fitting, while it reduced the feature space from 150 to 70 dimensions. These 70 dimensional feature vectors were used for training the SVM. Table 1 contains the test result.

Table 1 Test results

Types	No. of samples tested	No. of samples detected	TP = DD/AD (in %) (x)	FP = DD/ADF (in %) (y)	FN = DDF/AD (in %) (a)	TN = DDF/ADF (in %) (b)	DSR (in %) = (x + b)/2
Oil mark	44	44	94.1%	4.2%	5.9%	95.8%	95%
Snarls	12	11					
Small holes	9	9					
Slub/ fly	15	13					
Thick yarn	10	9					
Knots	3	3					
Broken pick	23	21					
Short pick	20	18					
Healthy	24	23					

DD Detected defective, AD actually defective, ADF actually defect free, DDF detected defect free, DSR detection success rate

Table 2 Comparative study of the proposed technique with a few other techniques

Author	Obtained DSR (in %)
Deotale et al. [23]	PCA: 50.8 ICA: 64.1 VQ: 74.9 GLCM + Gabor + RDF: 84.5

Comparison of the proposed technique with other techniques applied for same database is given in Table 2.

Figure 3 shows a few of the test results.

4 Conclusion

In this paper, attempt was made to generate the exhaustive set of feature vector from the fabric sub images required for the detection of defect on woven fabric. Moreover, it was also a target to rely on the texture-based statistical method, as intuitively it can be inferred that the textures of the defective and healthy fabric sub images would vary significantly. For this reason, distance- and orientation-based Haralick parameter was determined. For the reduction of the computational cost, a low-dimensional representation of the feature vector was required without increment

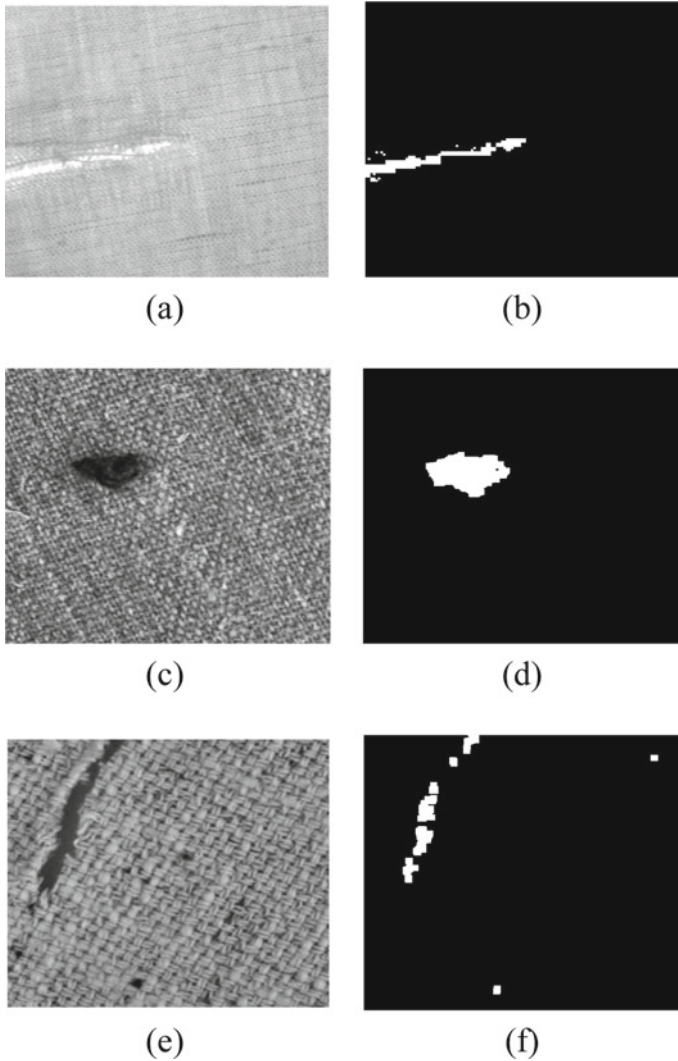


Fig. 3 Test result. First column: fabric images containing defects, Second column: detected fabric defect by the proposed method, after binarization through proper thresholding

in over-fitting of data. For this purpose, a sparse auto-encoder with suitable sparsity was used. Being the problem a binary one, finally the support vector machine was used for classification purpose. Performance of the developed system was measured through several performance matrices which showed the success of the same.

References

1. Catalog of types of fabric defects in grey goods. (1996). International Technical Service 3rd Edition, Schillieren, Switzerland
2. Dastoor PH, Radhakrishnaiah P, Srinivasan K, Jayaraman S (1994) SDAS: a knowledge-based framework for analyzing defects in apparel manufacturing. *J Text Inst* 85(4):542–560
3. Ngan HY, Pang GK (2009) Regularity analysis for patterned texture inspection. *IEEE Trans Autom Sci Eng* 6(1):131–144
4. Conci A, Proença CB (2000) A computer vision approach for textile inspection. *Text Res J* 70(4):347–350
5. Brzakovic D, Vujovic N (1996) Designing a defect classification system: a case study. *Pattern Recogn* 29(8):1401–1419
6. Conci A, Proença, CB (2002) A system for real-time fabric inspection and industrial decision. In: *Proceedings of the 14th international conference on software engineering and knowledge engineering*, pp 707–714
7. Castilho HP, Gonçalves PJS, Pinto JRC, Serafim AL (2007) Intelligent real-time fabric defect detection. In: *International conference image analysis and recognition*. Springer, Berlin, pp 1297–1307
8. Cho CS, Chung BM, Park MJ (2005) Development of real-time vision-based fabric inspection system. *IEEE Trans Industr Electron* 52(4):1073–1079
9. Soille P (2013) *Morphological image analysis: principles and applications*. Springer Science & Business Media
10. Maillard P (2003) Comparing texture analysis methods through classification. *Photogrammetric Eng Remote Sens* 69(4):357–367
11. Nurhaida I, Manurung R, Arymurthy AM (2012) Performance comparison analysis features extraction methods for batik recognition. In: *2012 international conference on advanced computer science and information systems (ICACSIS)*. IEEE, pp 207–212
12. Chandra JK, Majumdar M, Sarkar S (2016) Feature extraction and classification of woven fabric using optimized Haralick parameters: a rough set based approach. In: *2016 2nd international conference on control, instrumentation, energy & communication (CIEC)*. IEEE, pp 541–545
13. Haralick RM, Shanmugam K, Dinstein IH (1973) Textural features for image classification. *IEEE Trans Syst Man Cybern* 6:610–621
14. Deng L, Fan C, Zeng Z (2017) A sparse autoencoder-based deep neural network for protein solvent accessibility and contact number prediction. *BMC Bioinform* 18(16):569
15. Garrett D, Peterson DA, Anderson CW, Thaut MH (2003) Comparison of linear, nonlinear, and feature selection methods for EEG signal classification. *IEEE Trans Neural Syst Rehabil Eng* 11(2):141–144
16. Tola S, Chandra JK, Sarkar G (2020) Improved detection of woven fabric defect by optimized and adoptive cylindrical band-reject filtering. *J Textile Inst*. <https://doi.org/10.1080/00405000.2020.1813409>
17. Kovalev V, Volmer S (1998) Color co-occurrence descriptors for querying-by-example. In: *Proceedings 1998 multimedia modeling (MMM'98)* (Cat. No. 98EX200). IEEE, pp 32–38
18. Humeau-Heurtier A (2019) Texture feature extraction methods: a survey. *IEEE Access* 7:8975–9000
19. Rubinstein R, Zibulevsky M, Elad M (2009) Double sparsity: learning sparse dictionaries for sparse signal approximation. *IEEE Trans Signal Process* 58(3):1553–1564
20. Nwankpa C, Ijomah W, Gachagan A, Marshall S (2018) Activation functions: Comparison of trends in practice and research for deep learning. arXiv preprint [arXiv:1811.03378](https://arxiv.org/abs/1811.03378)
21. Abdiansah A, Wardoyo R (2015) Time complexity analysis of support vector machines (SVM) in LibSVM. *Int J Comput Appl* 128(3):28–34
22. TILDA (1996) Textile texture database, texture analysis working group of DFG. <https://lmb.informatik.uni-freiburg.de/resources/datasets/tilda.en.html>. Accessed 09 Feb 2009
23. Deotale NT, Sarode TK (2019) Fabric defect detection adopting combined GLCM, Gabor wavelet features and random decision forest. *3D Res* 10(1):5

Evaluation of ML-Based Sentiment Analysis Techniques with Stochastic Gradient Descent and Logistic Regression



Mausumi Goswami and Pratik Sabata

Abstract In recent times, along with the expansion of technology, the Internet also has flourished exponentially. World is more connected today not only through the technology, but also through sharing sentiments to express views, either be constructive or destructive in front of the world through social media. Twitter, Facebook, Instagram, etc., are being used as social media to reach the world. The study of understanding people's emotions, intentions, attitudes from unstructured data is opinion mining/sentiment analysis. This is an application of NLP or text mining. In this paper, an attempt is made to realize sentiment analysis's multiple dimensions using approaches such as ML and NLP-based techniques like word frequency and TF-IDF. Using ML approach, experiments were conducted, and the performance of the predictions was visualized. Three different datasets are used. A comparison of logistic regression (LR) and stochastic gradient descent (SGD) algorithms are compared using two different document representation. An extensive comparison is carried out using three different types of dataset. Amazon instant video datasets, bank dataset and movie reviews datasets are being used for the same. Analysis of performance is accomplished by using different graphs. The results indicate that logistic regression performs better than stochastic gradient descent for movie review dataset by using word frequency and TF-IDF-based approach.

Keywords Sentiment classification · Opinion mining · Machine learning · Classification · Stochastic gradient descent · TF-IDF · Word frequency

M. Goswami (✉) · P. Sabata
Christ University, Bengaluru, India
e-mail: mausumi.goswami@christuniversity.in

1 Introduction

With the recent advancement in technology, World Wide Web has also increased indefinitely [1]. Nowadays, in various social networking platforms such as Instagram, Twitter, Facebook, etc., people are more expressive on their views on different products or services [1]. Hence, it becomes vital for companies to understand various concerns faced by consumers for a particular service/product. Companies can perform analysis such as sentiment analysis [2–6], to understand the customer views [1]. In this work, a comparative analysis of sentiment analysis is done.

2 Background

Term frequency and word frequency are being used for text document representation. Opinion mining or sentiment analysis [1, 7–25] used text data. Sentiment analysis [1, 7–15] for simplicity can be thought as realizing people's intentions, views, characters from unstructured data. SA can be performed by various methods as mentioned above. These methods are discussed in detail in the following sub-section.

Lexicon-Based Method

Lexicons are the set of words of meaning, recognized and precompiled. In this approach, we use text to extract sentiment [1, 7–20] and then evaluate its polarity [12]. An alias is a knowledge-oriented method. The approach using lexicon can be decomposed: approach utilizing dictionary and approach utilizing corpus [12]. From the literature [12], view-related terms were classified. A detailed study has been made in the literature [12] to find words with the same meaning and words with a different meaning. Then, a collection of words of views is prepared, and then, extra relevant words of views in a broad corpus dependent upon its context are gathered [12]. A trivial collection of terms representing opinions is collected manually to perform a lexicon approach [12]. This collection is therefore gradually built through the quest for its synonyms and antonyms within popularly used tools [12].

Machine Learning-Based Method

ML suggests a way to solve sentiment [1, 7–15] classification [16–25]. The first step is to create and instruct the model with the training dataset. The next step is to predict the sentiment [1, 7–25] of the test dataset from previous knowledge [12]. This method is categorized as follows: supervised, unsupervised and reinforcement learning [13]. In supervised learning, we use data that are labelled for our model. In unsupervised learning, we use data that are not labelled for our model. In reinforcement learning, purpose is to achieve the target in dynamic space and is based on reward-based system [13].

Deep Learning-Based Method: A Subset of ML

This method [26–30] is a man-made intelligence system that mimics the human brain’s workings in data processing and generates patterns that are used for making decisions [14]. DL is a subcategory of AI/ML which are competent in learning from labelled or unlabelled data without supervision [14]. DL emphasizes multi-layered technique to hidden layers that are present in the neural network [21]. Traditional machine learning approaches identify and extract features either manually or by using the methods of selecting features [21]. Nonetheless, features are identified and automatically retrieved in deep learning models, ensuring greater accuracy and performance [21].

Deep Neural Networks (DNN)

A DNN contains atleast two layers. Few of these layers are hidden [21]. To process data in several different ways, deep neural networks use sophisticated mathematical modelling [21]. It is an adjustable model as it contains various layers in the processes. These layers are input, output and hidden [21].

3 Methodology

The steps followed to apply some of the measures to the datasets mentioned concerning real-life examples are explained below.

Algorithm:

Input: n, D

n: number of documents, D: Collection of documents

Intitialization: Intializing parameters based on the model

Procedure:

Step 1: Read D, collection of documents

Step 2: Select important features from D

Step 3: Build Model Feeding the training data to the Logistic Regression Algorithm

Step 4: Logistic Regression model’s performance is checked by giving input as the testing dataset

Step 5: Model’s performance is evaluated & visualized

Step 6: Build model using Stochastic Gradient Descent by using SGD algorithm

Step7: Test the model and compute accuracy

Step 8: Compare accuracies of both the approaches

4 Experiments and Results

In this section, the experiments and results are discussed.

4.1 Datasets Used for SA

We briefly describe the text [31, 32] datasets that have been used for experimentation purposes. Here, we have used three datasets for carrying out the analysis. The first dataset used for sentiment analysis is Amazon instant video datasets [33]. This dataset is a limited portion of products manufactured by Amazon. It contains 37,126 product reviews with information like reviewerID, reviewername, overall(rating), helpfulness, etc [33]. The satisfaction of a customer with the product is calculated based on the rating given by the customers. We use this dataset to predict whether the user is satisfied with the Amazon instant video or not, based on the rating and reviews. This is yet another application of sentiment analysis using which a company can decide their customer's satisfaction with their product. We represent this dataset as DS_AIV. The second dataset is bank dataset [34]. The bank dataset contains 738 records, that contain the interest rate, credit, durations, previous month details, etc [34]. It contains information about the customer's previous transaction that is represented as successful or unsuccessful. Using this information, we wish to know whether the bank marketing strategy was successful or not [34]. This can be an example of a classification problem. We represent this dataset as DS_BANK. The third dataset is movie reviews from Twitter [35]. This dataset contains 50,000 movie reviews. This dataset has a mixture of positive and negative reviews. We can represent this dataset as movie reviews. The details of all datasets that were used for analysis are portrayed in Table 1.

Table 1 Details of all the two datasets are given below

No.	Name of datasets	Dataset dize	Application
1	DS_AIV	37,126	Sentiment analysis using LR
2	DS_BANK	738	Sentiment analysis using LR
3	Movie reviews	50,000	Sentiment analysis using LR and stochatis gradient descent

4.2 Experimental Setup

This experiment is carried on a system with the configuration as specified below. The system should have storage of 1 TB (recommended) with a RAM of 8 GB for the smooth functioning of the programmes. The system should have a processor higher than intel i3 6th generation. For running the programmes, the system should have anaconda 3 installed with python version 3.8. The python programme can be run in Jupyter notebook (that comes with anaconda, with most of the libraries preinstalled); otherwise, it can be run in the platform provided by Google that is Google Collaboratory, but it requires a stable Internet connection to run it.

4.3 Results

The efficiency of classification of sentiments can be measured through four factors, they are determined as follows:

$$\text{Model_Acc} = \frac{(\text{TruePos_DS} + \text{TrueNeg_DS})}{(\text{TruePos_DS} + \text{TrueNeg_DS} + \text{FalsePos_DS} + \text{FalseNeg_DS})} \quad (1)$$

$$\text{Model_PR} = \frac{\text{TruePos_DS}}{(\text{TruePos_DS} + \text{FalsePos_DS})} \quad (2)$$

$$\text{Model_Rec} = \frac{\text{TruePos_DS}}{(\text{TruePos_DS} + \text{FalseNeg_DS})} \quad (3)$$

$$\text{Model_Fscore} = \frac{(2 \times \text{Model_PR} \times \text{Model_Rec})}{(\text{Model_PR} + \text{Model_Rec})} \quad (4)$$

The results are illustrated in the form of tables indexed with 2, 3, 4 and 5. It also shows the confusion matrix that is useful for calculating the performance of the classifier. The details of *dataset, cases, ratio, records, training, testing, accuracy (%)*, etc., are shown as *CC1, CC2, CC3, CC4, CC5, CC6, CC7*, respectively, in Table 2 and 5.

Table S1: Summary 1

Table 2 Performance of DS_AIV

CC1	CC2	CC3	CC4	CC5	CC6	CC7
DS_AID	1	50:50	37126	18563	18563	90.45
DS_AID	2	70:30	37126	25988	11138	90.63
DS_AID	3	80:20	37126	29701	7425	90.14
DS_AID	4	90:10	37126	33413	3713	88.34

Table 3 Confusion Matrix of DS_AIV

Ratio	TP	FN	FP	TN
50:50	641	1616	156	16150
70:30	491	909	134	9604
80:20	406	621	111	6288
90:10	257	374	59	3023

Table 4 Confusion Matrix of DS_BANK

Ratio	TP	FN	FP	TN
50:50	155	29	24	162
70:30	93	18	13	98
80:20	60	10	11	67
90:10	29	3	9	33

Table 5 DS_BANK

CC1	CC2	CC3	CC4	CC5	CC6	CC7
DS_BANK	1	50:50	738	369	369	85.67
DS_BANK	2	70:30	738	517	221	86.03
DS_BANK	3	80:20	738	592	146	85.81
DS_BANK	4	90:10	738	666	72	83.78

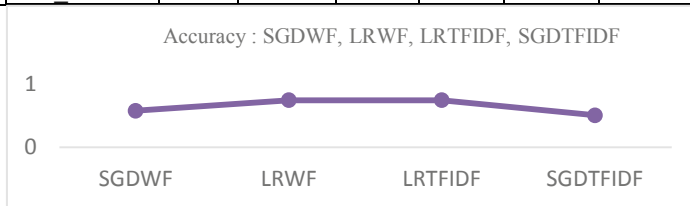


Fig. 1

Table S1: Summary1 shows comparison of stochastic gradient descent and logistic regression. Performance is compared using word frequency-based approach and term frequency—inverse document frequency-based approach. Stochastic gradient descent using word frequency is represented as SGDWF, logistic regression using word frequency is represented as LRWF, logistic regression using tf-idf is LRTF and stochastic gradient descent using word frequency is represented as SGDTF. Performance of LR supercedes performance of SGD as shown in Fig. 1.

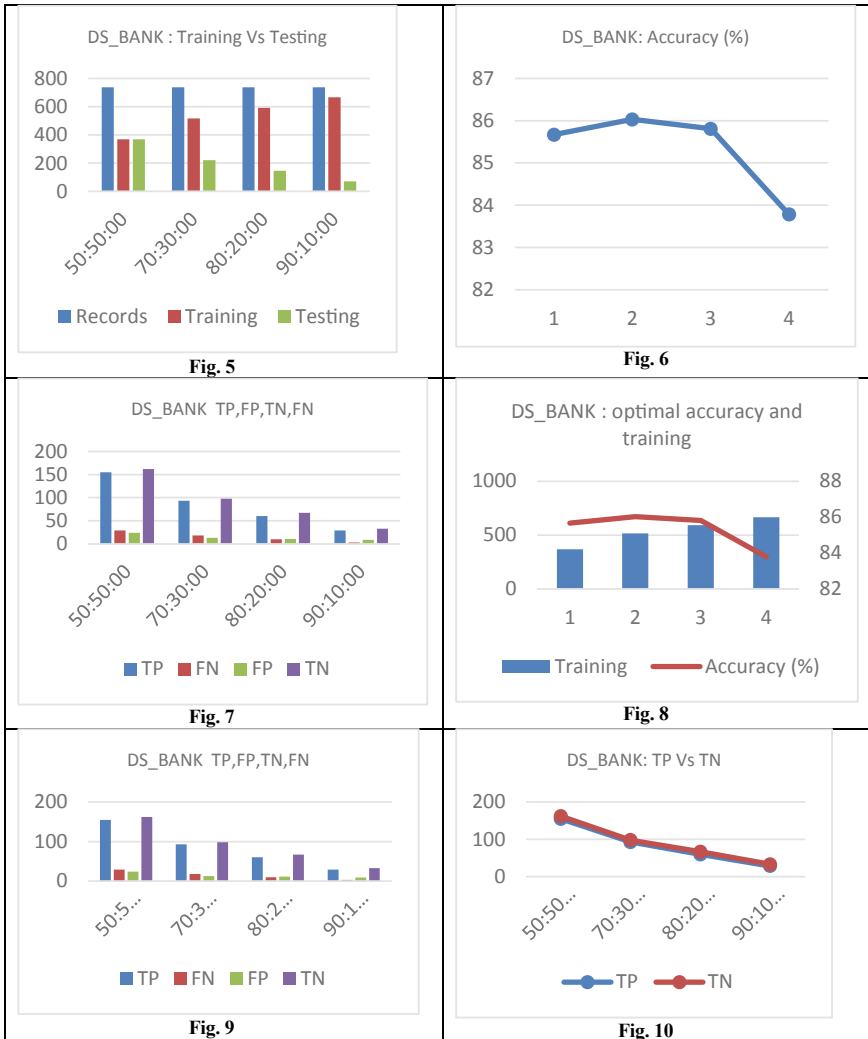
Table S2: Summary 2



In Table S2: Summary 2, the effect of change of training and testing data is demonstrated by using graphs. Also, a bar graph compared the performance of linear stochastic gradient descent (SVM) and logistic regression. Figure 4 demonstrates that logistic regression using bag of words frequency and tf-idf frequency showed better performance than linear SVM.

Table 6 Summary 3 summarizes the results of the experimtns conducted with DS_BANK dataset. It is observed that accuracy is best achieved in case 2 (70:30). In case of DS_AIV.

Table 6: Summary 3



The table contents in Table 6: Summary 3 are arranged in row major order. In first row of Table 6, we have Fig. 5. DS_BANK: training versus testing and Fig. 6 . DS_BANK: accuracy included to demonstrate comparisons visually. In second row, we have Fig. 7. DS_BANK: TP,FP,TN,FN and Fig. 8 . DS_BANK: optimal accuracy

and training are included. Figure 9. DS_BANK: optimal accuracy and testing, Fig. 10. DS_BANK: TP versus TN values are plotted to realize the trends.

5 Discussion and Conclusion

In this paper, we explored what sentiment analysis is and why sentiment analysis is so essential in modern companies or customer retention firms. We have discussed different approaches through which sentiment analysis can be performed. A comparative study has been carried out to understand Machine learning techniques for sentiment analysis in detail. Figures 1, 2, 3a, 3b, 4, 5, 6, 7, 8, 9 and 10 are used to visualize the statistics. Sentiment analysis acts as business intelligence for market research. A comparison of stochastic gradient descent and logistic regression performance is conducted by using word frequency-based approach and term frequency—inverse document frequency-based approach. Stochastic gradient descent using word frequency is represented as SGDWF, logistic regression using word frequency is represented as LRWF, logistic regression using tf-idf is LRWF and stochastic gradient descent using word frequency is represented as SGDWF. Performance of LR supercedes performance of SGD. The best accuracy is obtained in case 2 for two different datasets. Logistic regression performed pretty well, but by using other machine learning models such as SVM with kernel function, Naïve Bayes, etc., may also be applied to inspect if the performance could be increased. In future work, first, we plan to apply the word embedding approach for sentiment analysis as it is simple and has high speed. After this, we plan to use the ANN approach for sentiment analysis, followed by RNN using LSTM. Sentiment analysis using primary datasets collected in real life is also going to be considered in future work.

References

1. Kharde V, Sonawane P (2016) Sentiment analysis of twitter data: a survey of techniques. arXiv preprint [arXiv:1601.06971](https://arxiv.org/abs/1601.06971)
2. Alshari EM, Azman A, Doraisamy S, Mustapha N, Alkeshr M (2017) Improvement of sentiment analysis based on clustering of Word2Vec features. In: 2017 28th international workshop on database and expert systems applications (DEXA). IEEE, pp 123–126
3. Gautam G, Yadav D (2014) Sentiment analysis of Twitter data using machine learning approaches and semantic analysis. In: 2014 seventh international conference on contemporary computing (IC3). IEEE, pp 437–442
4. Maas AL, Daly RE, Pham PT, Huang D, Ng AY, Potts C (2011) Learning word vectors for sentiment analysis. In: Proceedings of the 49th annual meeting of the association for computational linguistics: human language technologies-volume 1. Association for Computational Linguistics, pp 142–150.
5. Maurya AK (2017) Data sharing and resampled LASSO: a word based sentiment analysis for IMDb data. arXiv preprint [arXiv:1705.05715](https://arxiv.org/abs/1705.05715)

6. Mausumi G, Pratik S (2020) A machine learning approach of sentiment analysis using logistic regression. In: International conference on intelligent control and computation for smart energy and mechatronic systems (Iciccsems-2020), Jssate Noida UP, India, 25–26 Sept 2020. Organized By Department Of E&Ce, Cse And Information Technology
7. Chakraborty K, Bhattacharyya S, Bag R (2020) A survey of sentiment analysis from social media data. *IEEE Trans Comput Social Syst*
8. Boiy E, Moens MF (2009) A machine learning approach to sentiment analysis in multilingual Web texts. *Inf Retrieval* 12(5):526–558
9. Amolik A, Jivane N, Bhandari M, Venkatesan M (2016) Twitter sentiment analysis of movie reviews using machine learning techniques. *Int J Eng Technol* 7(6):1–7
10. Hemalatha I, Varma GS, Govardhan A (2013) Sentiment analysis tool using machine learning algorithms. *Int J Emerg Trends Technol Comput Sci (IJETTCS)* 2(2):105–109
11. Jha RK, Khurana S (2013) Sentiment analysis in Twitter.
12. Desai M, Mehta MA (2016) Techniques for sentiment analysis of Twitter data: a comprehensive survey. In: 2016 international conference on computing, communication and automation (ICCCA). IEEE, pp 149–154
13. Neethu MS, Rajasree R (2013) Sentiment analysis in twitter using machine learning techniques. In: 2013 fourth international conference on computing, communications and networking technologies (ICCCNT). IEEE, pp 1–5
14. Ain QT, Ali M, Riaz A, Noureen A, Kamran M, Hayat B, Rehman A (2017) Sentiment analysis using deep learning techniques: a review. *Int J Adv Comput Sci Appl* 8(6):424
15. Kolchyna O, Souza TT, Treleaven P, Ast T (2015) Twitter sentiment analysis: Lexicon method, machine learning method and their combination. arXiv preprint [arXiv:1507.00955](https://arxiv.org/abs/1507.00955)
16. Pang B, Lee L (2004) A sentimental education: Sentiment analysis using subjectivity summarization based on minimum cuts. In: Proceedings of the 42nd annual meeting on Association for Computational Linguistics. Association for Computational Linguistics, p 271
17. Breck E, Cai S, Nielsen E, Salib M, Sculley D (2017) The ml test score: a rubric for ml production readiness and technical debt reduction. In: 2017 IEEE international conference on big data (Big Data). IEEE, pp 1123–1132
18. Singh J, Singh G, Singh R (2017) Optimization of sentiment analysis using machine learning classifiers. *Human-Centric Comput Inform Sci* 7(1):32
19. Tripathy A, Agrawal A, Rath SK (2015) Classification of Sentimental reviews using machine learning techniques. *Procedia Comput Sci* 57:821–829
20. Gupta AA, Vijaykumar S (2020) Mobile price prediction by its features using predictive model of machine learning. *Studies in Indian Place Names* 40(35):906–913
21. Dang NC, Moreno-García MN, De la Prieta F (2020) Sentiment analysis based on deep learning: a comparative study. *Electronics* 9(3):483
22. Lynley M (2010) Online teaching platform Udemy raises \$1 M, still too cool for school. *The New York Times*, 31
23. Müller AC, Guido S (2016) Introduction to machine learning with Python: a guide for data scientists. O'Reilly Media, Inc.
24. Cielén D, Meysman A, Ali M (2016) Introducing data science: big data, machine learning, and more, using Python tools. Manning Publications Co.
25. Wang XW, Nie D, Lu BL (2014) Emotional state classification from EEG data using machine learning approach. *Neurocomputing* 129:94–106
26. Yenter A, Verma A (2017) Deep CNN-LSTM with combined kernels from multiple branches for IMDb review sentiment analysis. In: 2017 IEEE 8th annual ubiquitous computing, electronics and mobile communication conference (UEMCON). IEEE, pp 540–546
27. Hassan A, Mahmood A (2017) Deep learning approach for sentiment analysis of short texts. In: 2017 3rd international conference on control, automation and robotics (ICCAR). IEEE, pp 705–710
28. Le Q, Mikolov T (2014) Distributed representations of sentences and documents. In: International conference on machine learning, pp 1188–1196

29. Rehman AU, Malik AK, Raza B, Ali W (2019) A hybrid CNN-LSTM model for improving accuracy of movie reviews sentiment analysis. *Multimedia Tools Appl* 78(18):26597–26613
30. Hassan A, Mahmood A (2017) Efficient deep learning model for text classification based on recurrent and convolutional layers. In: 2017 16th IEEE international conference on machine learning and applications (ICMLA). IEEE, pp 1108–1113
31. Ramadhan WP, Novianty SA, Setianingsih SC (2017) Sentiment analysis using multinomial logistic regression. In: 2017 international conference on control, electronics, renewable energy and communications (ICCREC). IEEE, pp 46–49
32. Shen D, Wang G, Wang W, Min MR, Su Q, Zhang Y, Li C, Henao R, Carin L (2018). Baseline needs more love: on simple word-embedding-based models and associated pooling mechanisms. arXiv preprint [arXiv:1805.09843](https://arxiv.org/abs/1805.09843)
33. Haque TU, Saber NN, Shah FM (2018) Sentiment analysis on large scale Amazon product reviews. In: 2018 IEEE international conference on innovative research and development (ICIRD). IEEE, pp 1–6
34. Wisaeng K (2013) A comparison of different classification techniques for bank direct marketing. *Int J Soft Comput Eng (IJSCE)* 3(4):116–119
35. Maas AL, Daly RE, Pham PT, Huang D, Ng AY, Potts C (2011) Learning word vectors for sentiment analysis. In: The 49th annual meeting of the association for computational linguistics (ACL 2011)

A Comparative Analysis of Sentiment Analysis Using RNN-LSTM and Logistic Regression



Mausumi Goswami and Prachi Sajwan

Abstract Social media analytics makes a big difference in the success or failure of an organization. The data gathered from social media can be used to get a hit type product by analyzing the data and getting important information about the need of the people. This can be done by implementing sentiment analysis on the available data and then accessing the feelings of the customers about the product or service and knowing if it is actually being liked by them or not. Tracking data of the customers helps the organization in many ways. This study was done to get familiarized with the concept of data analytics and how social media plays an important role in it. Furthermore, Web scraping of Twitter and YouTube data was done following which a standard dataset was selected to do the other analytics. The field of sentiment analysis was used to get the emotions of the people. Logistic regression and RNN-LSTM models were used to perform the same, and then, the results were compared.

Keywords RNN-LSTM · Logistic regression · Descriptive analytics · Predictive analytics · Sentiment analysis

1 Introduction

Social networks data is the raw data that is gathered from the day-to-day social media activities of a person. How long is the person using a channel for, what all channels are being used, what they are being used for, everything is tracked in social media data. It seems each time we visit a site or write a message, it creates a digital foot print. Recently, it has grabbed a lot of interest due to the recent news broadcasted using TV and other media platforms. The raw information includes: shares, mentions, comments, clicks, chats, etc. Data analytics is used to analyze this raw information to come up with a conclusion, to find some trend in the data and get answers. Big companies do data analytics on raw data to get the right customers and the market. Influencers can find out who their followers are using data analytics. A person who

M. Goswami (✉) · P. Sajwan
Christ University, Bengaluru, India
e-mail: mausumi.goswami@christuniversity.in

performs data analytics is called a data analyst. A data analyst can do the following: Use different API services to get the raw data from all the social media channels like Twitter, Facebook, and YouTube. Process the primarily structured data by applying regression, classification, and correlation to get a deep extrospection of the people. Do sentiment analysis on unstructured data, i.e., textual comments, to get the sentiments depicted in them. Utilize tools available for gathering, analyzing, and exploring the raw data for research and other purposes.

This study was done to get familiarized with the concept of data analytics and how social media plays an important role in it. Furthermore, Web scraping of Twitter and YouTube data was done following which a standard dataset was selected to do the other analytics. The field of sentiment analysis was used to get the emotions of the people. Logistic regression and RNN-LSTM models were used to perform the same, and then, the results were compared.

2 Motivation and Background

Sentiment analysis has always been a topic of interest for many people as it can be used in many possible ways. The main reason that this study was started was to see how machine learning and deep learning can be used to depict mental health using social media data. Mental health is the topic of concern at this time and since sentiment analysis can be used to analyze the same, the study became interesting day by day. Mental health is really important, and hence, this study was done in order to help such people. After scrapping some data and performing analysis, the study shifted to a more prominent dataset that is available worldwide.

The study contributes toward encouraging people to perform machine learning on social media data so as to help people in a way no one would have imagined. This study also focuses on comparing machine learning and deep learning in order to help people identify which one would fit their data the best. Logistic regression and recurrent neural network were used to complete this study and make it understandable for everyone. Structured data is quantitative data having predefined data models that can be analyzed easily. Structured data is usually made up of only texts, and hence, it is easy to search for a specific thing in it. This type of data can generally be extracted from relational databases and data warehouses. SQL is used to manage such data which has a high level of organization. It can be easily understood by machine language which is an attractive feature of structured data. Structured data is considered the most conventional type of data storage as the earliest forms of database management systems (DBMS) had the option to store and analyze it. Structured data includes all the information that can be stored in SQL in the form of a table having columns and rows, e.g., relational data. Unstructured data refers to the data that is not organized or has a predefined data model. The data that comes under unstructured can be anything from a text, an image, sound, video, or other formats. Basically, the data that cannot be classified to fit into one model is unstructured data. It is qualitative data that cannot be analyzed by using the traditional methods. The amount

of unstructured data generated today is more than 80% of the total data. Unstructured data if harnessed properly can give a very deep understanding of a human that we can never get from structured data. The storage and processing of such kind of data has become really easy in these years with new tools in the market that can be used for these unstructured data, e.g., word processing, emails, etc.

3 Related Work

To enhance this study, a few studies were reviewed to get a better understanding of the different approaches to sentiment analysis. A trend of using deep learning models to increase the efficiency of sentiment analysis came into notice. One such comparative study was done by Nhan, Maria and Fernando [1] on deep learning models. They basically took eight datasets and identified popular approaches that are being used recently for sentiment analysis. They chose three approaches: CNN, RNN, and DNN and applied them to all the eight datasets to perform sentiment analysis [2–12]. They realized that RNN has a much higher computational time, but it is reliable when word embedding is used. CNN presents a balance between CPU runtime and accuracy while DNN is the simplest model of them all and gives results very quickly, but its accuracy is average. RNN with TF-IDF offers the least accuracy when compared with others while CNN results in the best accuracy. The type of dataset chosen is what makes the main difference. A study was done between SWEM, CNN, and LSTM models on 17 datasets [13] that reported LSTM models which are hard to optimize when compared with CNN or different variations of word embeddings. SWEMs gave either better or comparable performance to CNN and LSTM in most of the datasets. Another study [14] took into consideration the main approaches to sentiments analysis, i.e., Lexicon-based, machine learning-based, and rule-based approach. They studied their pros, cons, efficiency, accuracy, and other factors to get results. They realized that machine learning is the best approach, and hence, they performed many machine learning algorithms like SVM, KNN, and NB on the dataset to further check which model will fit the best in order to improve the efficiency of sentiment analysis [2–12]. Comparative study of classification algorithms [15] that are used in sentiment analysis was done to select the most efficient classification algorithm. Naïve Bayes classifier [16–20], max entropy classifier, boosted trees classifier, and random forest classifier are the classification algorithms used in this research. These algorithms were analyzed on the basis of simplicity, performance, accuracy, memory requirement, and other important factors. At the end, the conclusion was drawn that the selection of the algorithm truly depends on the type of dataset and what kind of classification is required. All the classification algorithms used have their own pros and cons, and hence, all the other important factors should be taken into consideration before selecting a particular classification algorithm.

4 Methodology

In this section, the steps followed during the process are explained. The sentiment analysis using logistic regression is performed as follows:

1. The first step is tokenization of the dataset which is done using CountVectorizer.
2. This is followed by preprocessing of data by removing the stop words, correcting misspelled words, stemming, converting everything to lowercase, and removing punctuations.
3. After that, word grouping is done using the Bag of Words method, and feature weighting is done using IDF and TF-IDF.
4. The equation for implementing IDF and TF-IDF in Scikit-learn is:

$$idf(t, d) = \log\left(\frac{1 + nd}{1 + df(d, t)}\right) + 1 \quad (1)$$

$$tf - idf(t, d) = tf(t, d) * (idf(t, d)) \quad (2)$$

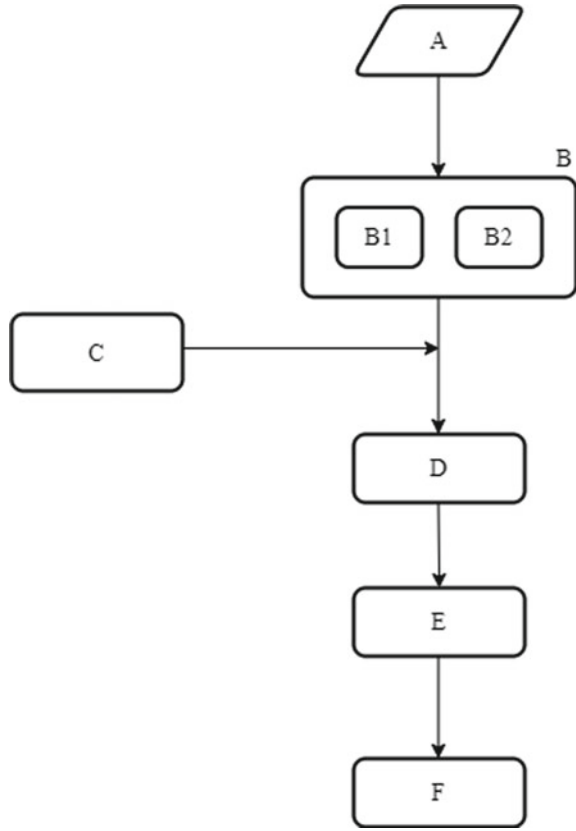
5. After that, text data is transformed into tf-idf vectors, and then, it is classified using logistic regression.
6. At the end, model evaluation is done, and then, classification report is prepared.

Sentiment Analysis Using RNN-LSTM

- The preprocessing of data is done by correcting misspelled words and converting everything to lower case.
- Then, it is passed through an embedding created by us using the dataset, and then, they are converted to lower case. The bigger the vocabulary size, more words from training sets are used, and more the embedding dimension, more the computation power is required.
- The vocabulary size is defined, so that if sequence length is more than that, then post truncation will take place.
- After this, the data is passed through the TensorFlow tokenizer for tokenization, and all the words are mapped to different indices through a reverse word index dictionary.
- Then, it is modeled using an embedding layer, LSTM bidirectional layer, and dense layer.
- At the end, the model for predictions is made, and a confusion matrix is created.

To maintain clarity of the diagrams, few abbreviations are used. Here, a list is shown: A-Input dataset, B-Preprocessing, B1-Correction of misspelled words, B2-Conversion of words to lower case, C- Embedding, D-tokenization using TensorFlow tokenizer, E-Train the model using RNN-LSTM, and F- Evaluate the model. The flow chart of the technique is demonstrated in Fig. 1.

Fig. 1 Flowchart of RNN-LSTM



5 Experiments and Results

In this section, the experiments and results are discussed. The system in which most of the work was done is a hardware from Dell with Windows 10 having an i3 Intel core processor, 4.00 GB RAM, and 1 Tb hard disk space with a 64-bit operating system. For training machine learning models, Jupyter Notebook with Python 3.8 was used, and the deep learning execution work was done on cloud-based Colaboratory (Colab) by Google Research. Colab can be used to run Python code on the browser without actually having a setup on the system. It is used a lot to perform machine learning and deep learning. Colab is based on Jupyter and is free of cost. The package used to perform logistic regression is Scikit-learn, and for RNN-LSTM, Keras and TensorFlow have been used. The work started off by doing Web scraping of the dataset from Twitter and YouTube. Developer accounts for both the social media platforms to use the data collection APIs that were created. For extraction of datasets like Olympics data, cricket data with 50 rows each was done as a start. Performance of basic statistical analysis and text mining on the collected datasets using R and

Fig. 3 Dataset snapshot

	review	sentiment
0	In 1974, the teenager Martha Moxley (Maggie Gr...	1
1	OK... so... I really like Kris Kristofferson a...	0
2	***SPOILER*** Do not read this, if you think a...	0
3	hi for all the people who have seen this wonde...	1
4	I recently bought the DVD, forgetting just how...	0
5	Leave it to Braik to put on a good show. Final...	1
6	Nathan Detroit (Frank Sinatra) is the manager ...	1
7	To understand "Crash Course" in the right cont...	1
8	I've been impressed with Chavez's stance again...	1
9	This movie is directed by Renny Harlin the fin...	1

called error matrix) is used to visualize the performance of an algorithm mostly supervised learning algorithms. The rows of the matrix represent the predicted class instances, while the columns represent the actual class instances or it can be vice versa too. It consists of True Positive (TP), False Positive (FP), True Negative (TN), False Negative (FN). All these values were recorded and accordingly the following graph is constructed as shown in Fig. 4.

Even though the accuracy shown in the graph might be low for RNN-LSTM, it is a deep learning model, and the better it is trained, the better will be the accuracy. The logistic regression model is in its highest accuracy, and no matter how much it is trained, it will hardly increase. Hence, if the deep learning model is trained in a better way like by using GloVe embeddings which has almost all the words in the world or bidirectional encoder representations from transformers (BERT) which is an NLP pretraining technique by Google, then a way better accuracy for a deep learning model when compared to a machine learning model can be achieved. This

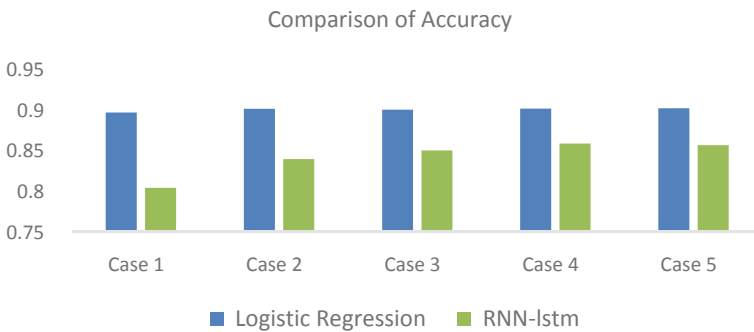


Fig. 4 Comparison of accuracy

basically proves that an algorithm should be selected not only on the basis of the dataset chosen but also on the kind of classification required to be done. This also emphasizes that NLP based document representation techniques have an impact on the accuracy of classification.

6 Discussion and Conclusion

A comparative analysis was performed which started with Web scraping of the datasets, and then, a standard dataset was chosen for a comparative study between sentiment analysis using logistic regression and RNN-LSTM. All the important aspects were explored, and the results are analyzed along with the visual representations. Figure 1 has demonstrated the flow of the methodology, Fig. 2. has demonstrated the word cloud representation, Fig. 3. has shown a snapshot of the dataset, Fig. 4. has compared the accuracy. This comparative analysis has shown that the accuracy of RNN-LSTM approach gets better with each epoch. Total five different cases were considered. Each has shown that with more training, the accuracy was improved. The accuracy of the logistic regression classifier was close to 0.90. For further studies, Web scraping of a large dataset to perform the same has been taken into consideration. Topics like 1. Lightweight deep learning algorithms which is modeling using a normal classifier and then using deep learning for only a part of the modeling to keep the computation low and 2. Transfer learning which is basically storing some knowledge and using it later were also explored and will definitely be included in the future work. Sentiment analysis using word-embedding-based model called SWEM has also been selected as a topic for future work as word embedding has more computational efficiency compared to RNN-LSTM as it has less parameters. RNN suffers from vanishing gradient descent problem; hence, LSTM came for rescue. Now, RNN-LSTM also is not very good with hardware as they are computationally expensive. Attention is proposed very recently and selected as a topic to explore for future work.

References

1. Kharde V, Sonawane P (2016) Sentiment analysis of twitter data: a survey of techniques. arXiv preprint [arXiv:1601.06971](https://arxiv.org/abs/1601.06971).
2. Hemalatha I, Varma GS, Govardhan A (2013) Sentiment analysis tool using machine learning algorithms. *Int J Emerging Trends Technol Comput Sci (IJETTCS)* 2(2):105–109
3. Jha RK, Khurana S (2013) Sentiment analysis in Twitter
4. Desai M, Mehta MA (2016) Techniques for sentiment analysis of Twitter data: a comprehensive survey. In: 2016 international conference on computing, communication and automation (ICCCA). IEEE, pp 149–154
5. Neethu MS, Rajasree R (2013) Sentiment analysis in twitter using machine learning techniques. In: 2013 fourth international conference on computing, communications and networking technologies (ICCCNT). IEEE, pp 1–5

6. Ain QT, Ali M, Riaz A, Noureen A, Kamran M, Hayat B, Rehman A (2017) Sentiment analysis using deep learning techniques: a review. *Int J Adv Comput Sci Appl* 8(6):424
7. Kolchyna O, Souza TT, Treleaven P, Aste T (2015) Twitter sentiment analysis: Lexicon method, machine learning method and their combination. *arXiv preprint arXiv:1507.00955*
8. Pang B, Lee L (2004) A sentimental education: sentiment analysis using subjectivity summarization based on minimum cuts. In: *Proceedings of the 42nd annual meeting on Association for Computational Linguistics*. Association for Computational Linguistics, p 271
9. Breck E, Cai S, Nielsen E, Salib M, Sculley D (2017) The ML test score: a rubric for ml production readiness and technical debt reduction. In: *2017 IEEE international conference on big data (Big Data)*. IEEE, pp 1123–1132
10. Singh J, Singh G, Singh R (2017) Optimization of sentiment analysis using machine learning classifiers. *Human-Centric Comput Inform Sci* 7(1):32
11. Tripathy A, Agrawal A, Rath SK (2015) Classification of sentimental reviews using machine learning techniques. *Procedia Comput Sci* 57:821–829
12. Gupta AA, Vijaykumar S (2020) Mobile price prediction by its features using predictive model of machine learning. *Stud Indian Place Names* 40(35):906–913
13. Chakraborty K, Bhattacharyya S, Bag R (2020) A survey of sentiment analysis from social media data. *IEEE Trans Comput Social Syst*
14. Boiy E, Moens MF (2009) A machine learning approach to sentiment analysis in multilingual web texts. *Inf Retrieval* 12(5):526–558
15. Amolik A, Jivane N, Bhandari M, Venkatesan M (2016) Twitter sentiment analysis of movie reviews using machine learning techniques. *Int J Eng Technol* 7(6):1–7
16. Dang NC, Moreno-García MN, De la Prieta F (2020) Sentiment analysis based on deep learning: a comparative study. *Electronics* 9(3):483
17. Lynley M (2010) Online teaching platform Udemy raises \$1 M, still too cool for school. *The New York Times*, p 31
18. Müller AC, Guido S (2016) *Introduction to machine learning with Python: a guide for data scientists*. O'Reilly Media, Inc.
19. Cielien D, Meysman A, Ali M (2016) *Introducing data science: big data, machine learning, and more, using Python tools*. Manning Publications Co.
20. Wang XW, Nie D, Lu BL (2014) Emotional state classification from EEG data using machine learning approach. *Neurocomputing* 129:94–106
21. Ramadhan WP, Novianty SA, Setianingsih SC (2017) Sentiment analysis using multinomial logistic regression. In: *2017 international conference on control, electronics, renewable energy and communications (ICCREC)*. IEEE, pp 46–49
22. Alshari EM, Azman A, Doraisamy S, Mustapha N, Alkeshr M (2017) Improvement of sentiment analysis based on clustering of Word2Vec features. In: *2017 28th international workshop on database and expert systems applications (DEXA)*. IEEE, pp 123–126
23. Gautam G, Yadav D (2014) Sentiment analysis of twitter data using machine learning approaches and semantic analysis. In: *2014 seventh international conference on contemporary computing (IC3)*, pp 437–442. IEEE
24. Maas AL, Daly RE, Pham PT, Huang D, Ng AY, Potts C (2011) Learning word vectors for sentiment analysis. In: *Proceedings of the 49th annual meeting of the Association for Computational Linguistics: Human Language Technologies*, vol. 1, pp. 142–150. Association for Computational Linguistics
25. Maurya AK (2017) Data sharing and resampled LASSO: a word based sentiment analysis for IMDb data. *arXiv preprint arXiv:1705.05715*
26. Yenter A, Verma A (2017) Deep CNN-LSTM with combined kernels from multiple branches for IMDb review sentiment analysis. In: *2017 IEEE 8th annual ubiquitous computing, electronics and mobile communication conference (UEMCON)*. IEEE, pp 540–546
27. Hassan A, Mahmood A (2017) Deep learning approach for sentiment analysis of short texts. In: *2017 3rd international conference on control, automation and robotics (ICCAR)*. IEEE, pp. 705–710

28. Le Q, Mikolov T (2014) Distributed representations of sentences and documents. In: International conference on machine learning, pp 1188–1196
29. Rehman AU, Malik AK, Raza B, Ali W (2019) A hybrid CNN-LSTM model for improving accuracy of movie reviews sentiment analysis. *Multimedia Tools Appl* 78(18):26597–26613
30. Hassan A, Mahmood A (2017) Efficient deep learning model for text classification based on recurrent and convolutional layers. In: 2017 16th IEEE international conference on machine learning and applications (ICMLA). IEEE, pp 1108–1113
31. Maas AL, Daly RE, Pham PT, Huang D, Ng AY, Potts C (2011) Learning word vectors for sentiment analysis. In: The 49th annual meeting of the Association for Computational Linguistics (ACL 2011)
32. Haque TU, Saber NN, Shah FM (2018) Sentiment analysis on large scale Amazon product reviews. In: 2018 IEEE international conference on innovative research and development (ICIRD). IEEE, pp 1–6
33. Wisaeng K (2013) A comparison of different classification techniques for bank direct marketing. *Int J Soft Comput Eng (IJSCE)* 3(4):116–119
34. Shen D, Wang G, Wang W, Min MR, Su Q, Zhang Y et al (2018) Baseline needs more love: on simple word-embedding-based models and associated pooling mechanisms. arXiv preprint [arXiv:1805.09843](https://arxiv.org/abs/1805.09843)

Android-Based Assistance System for Visually Impaired Person Using Deep Learning and Augmented Reality



Abhigyan Baruah, Aryan Dev, Jasowanta Das, and Santanu Kumar Misra

Abstract With the appearance of technology, the present age has changed significantly. We see a colossal amount of advancement in all fields and spheres of life, starting right from making life more convenient than ever to making the impossible possible. So, we came up with an idea to develop an application which would help blind people recognize objects around them and help them walk around freely avoiding obstacles around them. This proposed support system would help the blind people perceive the surroundings and help them interact with the system about the objects around them. This application is not only for blind people. It has many other applications too. The same concept can be used for autonomous driving, to locate objects in the surroundings and to avoid them and move in a clear path. The proposed system uses the concept of augmented reality and deep learning to detect objects and their distances from the system. Apart from this, the system would help to locate text and differentiate between similar-looking objects like currencies. The android environment is used for the development of the system. The system is validated with rigorous real-time testing.

Keywords Deep learning · Augmented reality · ML kit · Arcore · MobileNet v1 · TensorFlow lite

A. Baruah · A. Dev · J. Das · S. K. Misra (✉)
Computer Science and Engineering Department, Sikkim Manipal Institute of Technology,
Rangpo, Sikkim, India
e-mail: santanu.m@smit.smu.edu.in

A. Baruah
e-mail: abhigyan_201700172@smit.smu.edu.in

A. Dev
e-mail: aryan_201700075@smit.smu.edu.in

J. Das
e-mail: jasowanta_201700110@smit.smu.edu.in

1 Introduction

Significant advancement in deep learning (DL) during the last few years helps us to create complex machine learning (ML) models for detecting objects in images regardless of the required characteristics. This development has empowered engineers to replace existing heuristics-based systems in favor of ML models [1] with enhanced performance. As people are using their mobile phones to a larger extent and expect increasingly advanced performances from their mobile applications, the industry needs to adopt more advanced technologies to meet up to expectations. One such adaptation is using ML algorithms for object detection [2, 3].

Once the objects are detected, the actual distances between the user and objects need to find out that helps the user to react accordingly. Ultrasonic sensors may be an option for it but they cannot be used in places where there are objects in nearby. In this context, application would be a potential solution applying augmented reality (AR) [4]. AR can run on almost all android devices. A basic android device is cheap and is owned by almost every person. Properties of AR such as placing, scaling, and occlusion help us detect the places and also interact with different objects in it. Using different AR algorithms, we can find the distance between the objects [5]. Augmented reality aims in establishing a relationship between virtual worlds to the real world. Consequently, its objective is to provide information written directly in the physical environment [6]. AR can also be applied to computer-assisted communication techniques; it does not matter from AR-film interactions. AR is interactive in real-time and is registered in 3D [7]. AR helps in education [8]. Our proposed system is on healthcare for assistive technology. Surely, it will help in recognizing objects and track them in a 3D space [9, 10].

The proposed system will allow a person to know about the location of an object via audio output. It will help the persons to find surrounding objects without the help of others and devise a path to walk accordingly. It will help them locate text and differentiate between similar-looking objects like currencies. The system works best in a closed room with multiple objects.

The organization of the paper is as follows, and the next section discusses the literature review of related work done in past. Section 3 discusses the applied methods for object recognition. Section 4 explains proposed methodology. Section 5 discusses result, testing, and validation. Section 6 draws the conclusion.

2 Literature Review

A literature survey was conducted on existing technologies and their drawbacks and also reviewed several solutions that can be used to overcome these problems.

Object detection and its implementation on android devices have been proposed by Zhongjie Li and Rao Zhang. They identified the integration of neural networks

with mobile devices. The proper understanding of the workings of neural networks in android devices has been achieved.

Mobile object detection using TensorFlow Lite and transfer learning by Oscar Alsing, Stockholm, Sweden, 2018 [11]. TensorFlow Lite can run on less powerful mobile devices, unlike TensorFlow. The TensorFlow Lite can run on less powerful mobile devices, unlike TensorFlow.

Assistive system for visually impaired using object recognition has been developed by Kumar [12]. The introduction to object recognition and its challenges are described in the proposed model. The proposed model helps in challenges faced while using image recognition.

Real-time object detection and recognition model for blind people has been developed by Mohammad AL-Najjar et al. [13]. Object detection and recognition methodologies for the visually impaired have been discussed. The proposed model helps by supporting a proper understanding of the implementation of different technologies to assist the blind.

Assistive technology for individuals with blindness and vision impairment by Dana A. Draa, MA, CRC, COMS visual impairment services team. The actual findings here are current trends in technology for the blind and visually impaired proprietary versus conventional. It helps to get the answer why do the assistive technologies need for the visually impaired?

In a different study by van Voorst [14], it is quite easily explained why augmented reality has become a general indoor and outdoor navigation solution. As a solution, it proposed that augmented reality can be used as a solution for finding distances at the indoor and outdoor locations to establish the decision for the use of ARCore for handheld devices.

Design and implementation of text-to-speech conversion for visually impaired People have been done by Isewon et al. [15]. The findings of the article are the use of text-to-speech (TTS) synthesizer as an assistive technology for the visually impaired.

3 Methods Applied

3.1 Object Recognition

Object recognition is a significant piece of our vision framework to get by in this world, human, and different animals can play out this assignment immediately and easily, yet this is a difficult issue for a machine because each article in the 3D world can cast the endless number of 2D projections because of relative changes, change in light, and camera perspective. Figure 1 shows the steps for object recognition. Object recognition is a comprehensively considered field, there are many articles accessible on this topic, and all of these are isolated into shallow learning object recognition strategies and deep learning object acknowledgment techniques. In unsupervised learning, the system is prepared with unlabeled information, and it requires some

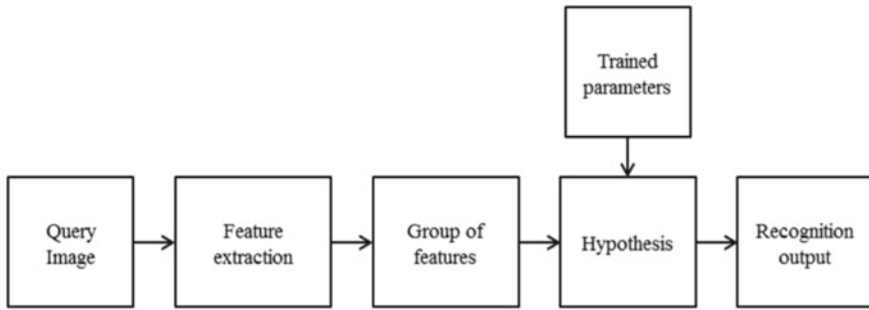


Fig. 1 Object recognition pipeline

investment that too without the utilization of named data [16]. In our undertaking, we have utilized MobileNet V1 which utilized depth-wise convolution followed by point-wise convolution. It is a pre-trained object detection model that was optimized to work with TensorFlow Lite.

3.1.1 Object Recognition Pipeline

The mechanical advancements [17] urge us to build up a framework for the less favored gathering of individuals and the individuals who have debilitations. Many electronic assistive systems that have been developed for them, but only a few of them incorporate computer vision- based machine learning algorithms and the new technology of augmented reality together. Recent developments allow us to incorporate these technologies in our mobile device such as android smartphones which can help us replace existing technologies such as a camera mounted on a glass system, using ultrasonic sensors, helps to reduce the use of wearable technologies.

3.1.2 ML Kit

ML kit [2] is part of the firebase ecosystem and offers a wide range of machine learning features that offer facial recognition, text barcoding, text recognition, image tagging, intelligent response, external language, and identification models. The ML kit also supports special model integrations such as TensorFlow Lite models. All of these APIs are capable of operating offline, which gives us the advantages of a machine learning model without ever having an Internet connection. ML kit makes it easy for us to apply machine learning techniques in our proposed model by bringing Google's machine learning algorithms such as Google cloud vision API, TensorFlow Lite [18], and the android neural network API, together in a single SDK [17]. In our proposed model, we have used specifically used image labeling, landmark recognition, and object detection and tracking to get the idea of where, which object is placed in an environment.

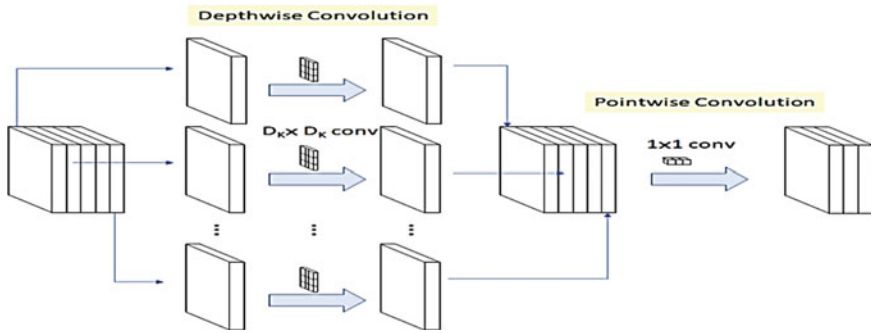


Fig. 2 Depth-wise convolution followed by point wise convolution [3]

3.1.3 Tensor Flow Lite and MobileNetV1

TensorFlow Lite [3] is a set of tools that allows developers to run TensorFlow models on mobile, embedded IoT devices. It works by using on-device machine leaning inferences with low latency and small binary size.

Mobile NetV1 [1] is a pre-trained object detection model that was optimized to work with TensorFlow Lite. We have used a quantized model that offers the smallest model size and fastest performance at the expense of accuracy. Depth-wise separable convolution is used to reduce the size of the model and its complexity, shown in Fig. 2.

Depth-wise convolution is the channel-wise $[DK \times DK]$ spatial convolution. For example, we have six channels in the above figure, then we will have $[6 (DK \times DK)]$ spatial convolution. Point-wise convolution actually is the (1×1) convolution to change the dimension. From that, we have the depth-wise separable convolution cost as:

$$DK.DK.M.DF.DF + M.N.DF.DF \tag{1}$$

where the left side denotes depth-wise convolution cost and the right side denotes point-wise convolution cost. M is the number of input channels, and N is number of output channels, DK denotes kernel size, and DF denotes feature map size. Batch normalization and ReLU are applied in it after each convolution as shown in Fig. 1.3.4.2. When 1.0 MobileNet-224 is used, it outperforms GoogLeNet and VGGNet (Table 1).

Table 1 MobileNet comparison to popular models on the ImageNet dataset [1]

Model	ImageNet accuracy (%)	Million multi-adds	Million parameters
1.0 MobileNet-224	70.6	569	4.2
GoogleNet	69.8	1550	6.8
VCG 16	71.5	15,300	138

4 Proposed Methodology

Similar to Google text-to-speech application, we have proposed our model to give audio feedback to the user about the objects and distance from the object and what objects are in which area. The users can double-tap on the screen which will lead to distance mode and then tap on the screen to find the approximate distance between the object and the user. Voice feedback will be given to the user about how far the objects are from the user.

4.1 Data Flow Diagram

See Figs. 3, 4 and 5.

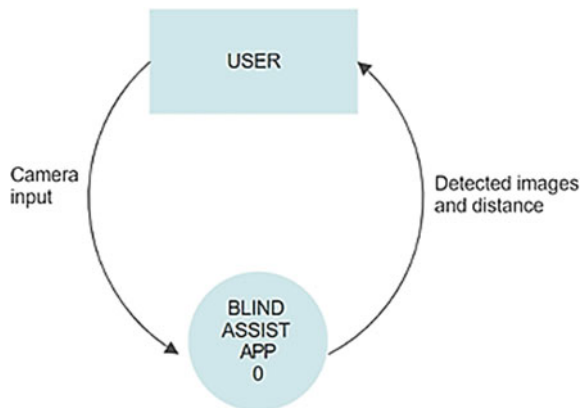
4.2 Identification Mode

The object detection and identification process is carried out in this intent. We have used ML kit to incorporate the TensorFlow Lite model in the application. The algorithm for the process and the flowchart has been explained below (Fig. 6).

4.3 Distance Mode

The straight line distance between the camera and the object is identified by placing an anchor over the object. We have used “ARCore” to calculate the relative distance

Fig. 3 Context level DFD



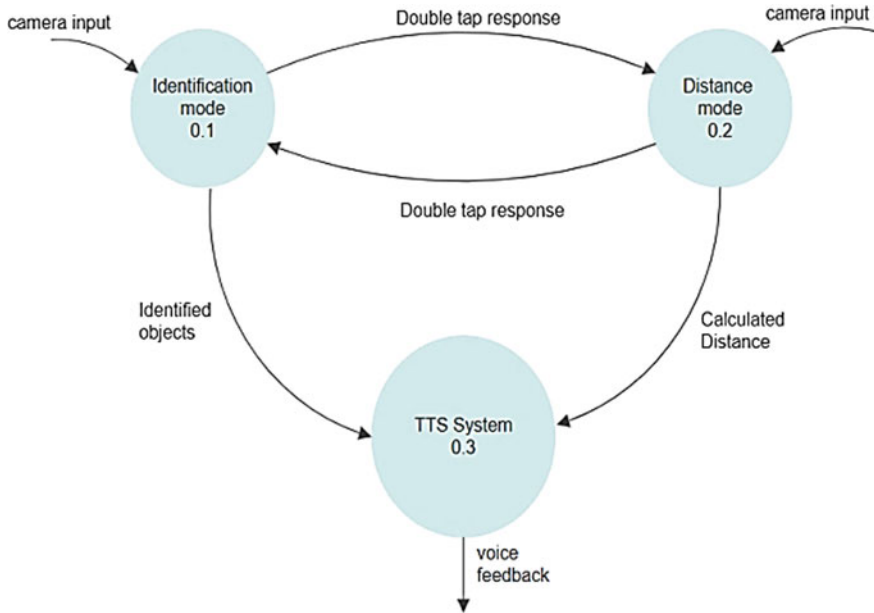


Fig. 4 Level 1 DFD

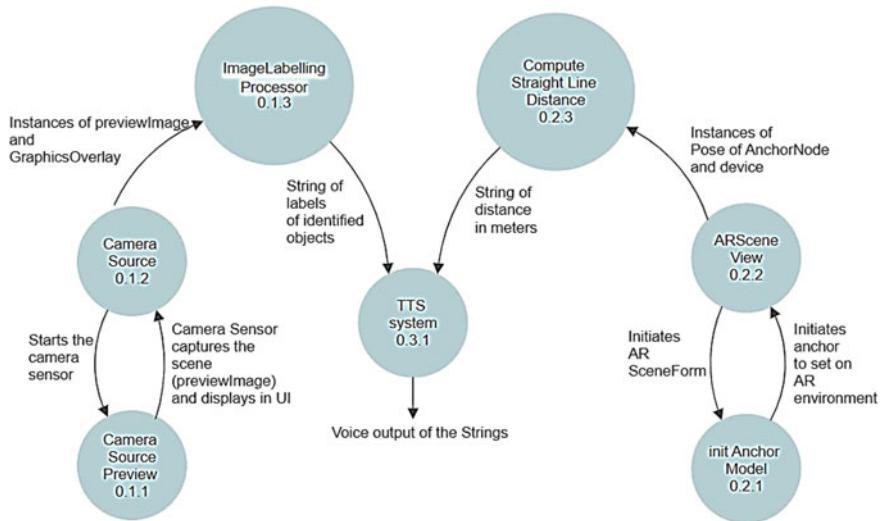


Fig. 5 Level 3 DFD

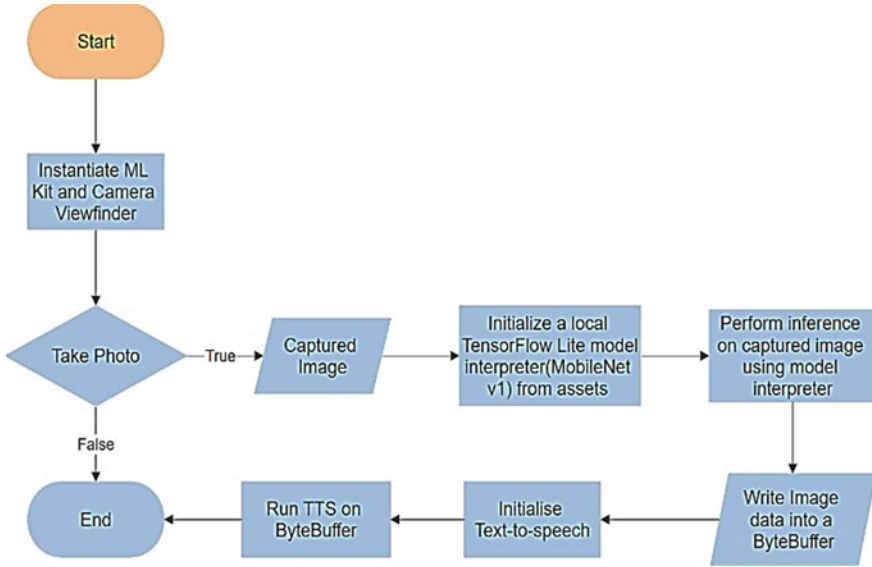


Fig. 6 Flowchart for identification process

to the surface detected by the phone [5]. The phone at first is in identification mode. On double-tapping the screen, it will go to distance mode and start the plane detection automatically using AR fragment. After detecting a plane on a single tap, it will find the distance to that plane and give the output in the form of speech. The flow-chart of distance calculation is shown in Fig. 7. The position of the anchor in the real world can be found out by using the “getPose” function with width, height, and depth. We can calculate the distance using Euclidean distance which says:

$$Distance = \sqrt{(x1 - x2)^2 + (y1 - y2)^2 + (z1 - z2)^2} \quad (2)$$

where $x1$, $y1$ and $z1$ are the “objectPose” and $x2$, $y2$ and $z2$ are the “cameraPose”.

5 Results, Testing and Validation

Results are validated with two different experiments that have been carried out. In the first experiment, the accuracy of our application is tested using our dataset of 1000 objects, and in the second experiment, the algorithm is evaluated for the Euclidean distance. We have identified five different scenarios and then evaluated on it [19–21]. Object category classification accuracy formula given the following equation:

$$Accuracy = \frac{\text{Correctly classified objects}}{\text{Total no. of objects}} \times 100 \quad (3)$$

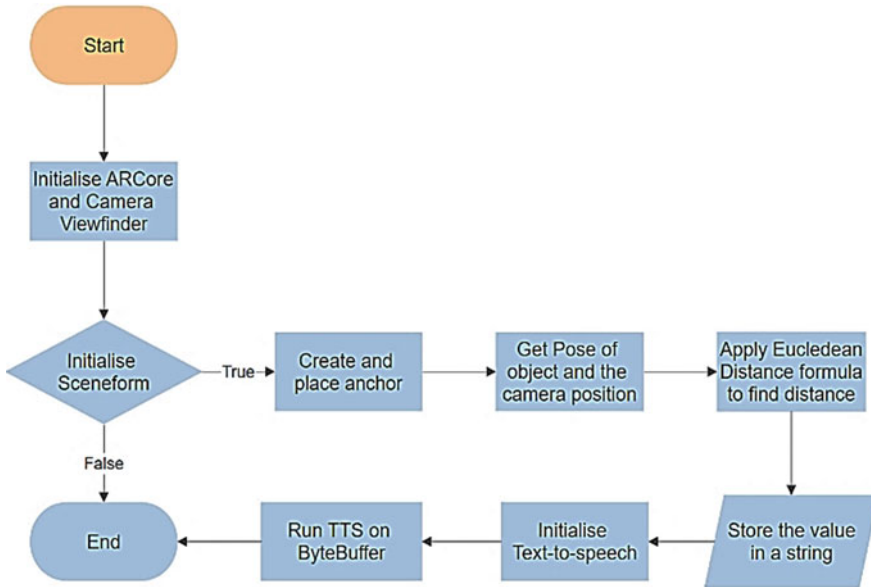


Fig. 7 Flow-chart for distance calculation

Distance calculation accuracy can be given by the equation:

$$DA = 100 - \left| \frac{\text{Actual distance} - \text{Distance in app}}{\text{Actual distance}} \right| \times 100 \tag{4}$$

where DA is the distance accuracy. The screenshot of the test image and the logcat is shared below. The application after many trials, runs as desired.

5.1 Results and Validation

- (a) **Object Classification Accuracy:** Five scenarios in different lighting condition are proposed for test, shown in Fig. 8.
- (b) **Distance Accuracy:** Similarly, the distance accuracy shown in Fig. 9 is calculated. We have used five scenarios in different lighting conditions to the model.

Conclusion for Distance accuracy: Calculating the average of all the tests, we can find the accuracy to be 82.7%. After conducting all the experiments and testing, we can conclude that the application is running as desired, and the results can be

<p>I/OBJECTS DETECTED: You are looking at pot and patio and greenhouse</p>		<p>It identified the objects really well. The pots, patio and greenhouse are clearly described. In this image three out of three classifications are correct.</p>
<p>I/OBJECTS DETECTED: You are looking at sports car and racer and grille</p>		<p>It recognizes the car well along with the grille. The racer in this context can be known. In this image three out of three classifications are correct.</p>
<p>I/OBJECTS DETECTED: You are looking at laptop and web site and space bar</p>		<p>All the objects are correctly classified in this image. Three out of three objects are classified correctly.</p>
<p>I/OBJECTS DETECTED: You are looking at lotion and pot and water jug</p>		<p>It struggles under low light as it can be seen in this case. Lotion is incorrectly classified and even though it looks like a water jug, it is far from it. One out of three objects is classified correctly.</p>
<p>I/OBJECTS DETECTED: You are looking at quilt and dining table and studio couch</p>		<p>Conclusion for image labelling: Correctly classified = 11, Total no of objects classified = 15. Therefore Accuracy = $(12/15) \times 100 = 80\%$</p>

Fig. 8 Object classification accuracy




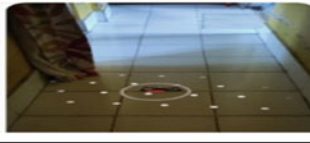

	<p>Distance according to the camera = 1.38 meters Actual distance = 1.1 meters Accuracy = $100 - (1.1 - 1.38 / 1.1) \times 100 = 74.54\%$</p>
	<p>Distance according to the camera = 1.63 meters Actual distance = 1.41 meters Accuracy = $100 - (1.41 - 1.63 / 1.41) \times 100 = 84.39\%$</p>
	<p>Distance according to the camera = 0.39 meters Actual distance = 0.30 meters Accuracy = $100 - (0.30 - 0.39 / 0.30) \times 100 = 70\%$</p>
	<p>Distance according to the camera = 1.21 meters Actual distance = 1.24 meters Accuracy = $100 - (1.24 - 1.21 / 1.24) \times 100 = 96.78\%$</p>
	<p>Distance according to the camera = 0.46 meters Actual distance = 0.41 meters Accuracy = $100 - (0.41 - 0.46 / 0.41) \times 100 = 87.80\%$</p>

Fig. 9 Object distance accuracy

validated with the same. The application has an object recognition accuracy of 80% and a distance accuracy of 82.7% which is quite high for an application.

6 Conclusion

In this paper, we have proposed an assistive system for the visually impaired people in our society, which exploits the new technologies of machine learning incorporated with augmented reality. From literature survey of existing technologies, we have concluded that augmented reality was never used to assist the visually impaired. Our model is one which amalgam AR with other technologies such as machine learning

to achieve 80% accuracy in image classification and 82.7% accuracy in distance measurement. But AR core has some limitation like it does not work well with surfaces with fewer details. It is difficult for the camera to make out the edges. The model size is a bit large 60 MB. Further optimization will reduce the size of the application.

References

1. Review: MobileNetV1—depthwise separable convolution (Light Weight Model), <https://towardsdatascience.com/review-mobilenetv1-depthwise-separable-convolution-light-weight-model-a382df364b69>
2. ML Kit for Firebase, <https://firebase.google.com/docs/ml-kit>
3. Google Inc. Tensorflow Lite, <https://www.tensorflow.org/mobile/tflite/>
4. Google Inc. AR Core, <https://developers.google.com/ar/discover>
5. Yusuke S (2020) Measuring distance with ARCore, 16 Feb 2020
6. Hollerer T, Schmalstieg D (2016) Introduction to augmented reality
7. Azuma RT (1997) A survey of augmented reality
8. Ibanez M-B, Delgado-Kloos C (2018) Augmented reality for STEM learning: a systematic review
9. Silva R, Rodrigues P, Mazala D, Giraldi G (2004) Applying object recognition and tracking to augmented reality for information visualization
10. Deshmukh SS, Joshi CM, Patel RS, Gurav YB (2018) 3D object tracking and manipulation in augmented reality
11. Alsing O (2018) Mobile object detection using tensorflow lite and transfer learning. Independent thesis Advanced level (degree of Master (Two Years)), 20 credits/30 HE credits
12. Kumar R, Meher S (2015) A novel method for visually impaired using object recognition. In: 2015 international conference on communications and signal processing (ICCSP). IEEE
13. AL-Najjar M, Suliman I, Al-Hanani G (2018) Real time object detection and recognition for blind people
14. Voorst V, Jeroen PMA, Koopman PWM (2018) Augmented reality as a general indoor and outdoor navigation solution
15. Isewon I, Oyelade OJ, Oladipupo OO (2012) Design and implementation of text to speech conversion for visually impaired people. *Int J Appl Inform Syst* 7(2):26–30
16. Razavian AS, Azizpour H, Sullivan J, Carlsson S (2014) CNN features off-the shelf: an astounding baseline for recognition. In: CoRRabs/1403.6382 (2014). [arXiv:1403.6382](https://arxiv.org/abs/1403.6382).
17. Batta P, Midha S, Sinha R, Kumar M. All in One Computer Vision Application using ML kit
18. Google Inc. Tensorflow Mobile, https://www.tensorflow.org/mobile/mobile_intro
19. Dimensional Research (2015) Failing to meet mobile app user expectations—a mobile app user survey
20. Augmented Reality in Android Apps using ARCore, <https://medium.com/corebuild-software/augmented-reality-in-android-apps-using-arcore-c6fba0897ce1>
21. Android Studio documentation, <https://developer.android.com/studio/intro>

Data Communication and Information Security

Towards Data Storage, Availability and Scalability with the Aid of Blockchain



Meenakshi Kandpal, Rabindra Kumar Barik, Chinmaya Misra,
and Saneev Kumar Das

Abstract Advent of Internet of things (IoT) and the increase of induced data from IoT's ecosystem has led towards an exponential increase in data storage in the cloud. IoT provides a quick and easy access to the data and hence maintaining the security of data is of paramount importance. In this sensitive scenario, blockchain plays a crucial role in securing and preventing the data from being tempered or forged. Besides, all this demand of scaling up of data in each sector is increasing due to increased amount of data required in market. This paper presents a novel system architecture to visualize a means to store data with scalability as well as availability with the security of blockchain in sync. Furthermore, this paper explains the inevitability of blockchain in solving today's security issues and provides future research directions in this context.

Keywords Cloud · Blockchain · Sharding · Swarming · Data storage · Availability · Scalability

M. Kandpal (✉) · R. K. Barik · C. Misra
School of Compute Engineering, KIIT Deemed To Be University, Bhubaneswar, India
e-mail: meenakshikandpal14@gmail.com

R. K. Barik
e-mail: rabindra.mnnit@gmail.com

C. Misra
e-mail: cmisra@yahoo.com

S. K. Das
College of Engineering and Technology, Bhubaneswar, India
e-mail: saneevdas.061995@gmail.com

1 Introduction

Blockchain gained popularity after the emergence of bitcoin technology in the year 2009 by the person or group of people by the pseudonym Satoshi Nakamoto. Blockchain is the new face of Industry 4.0. Blockchain [1] may be thought of as a ledger which is distributed, transparent, peer to peer, and consensus-based. Convergence of blockchain in diverse applications proves it to be decentralized and changes how we view towards the development. Most of the conventional issues of data failures, i.e. security, privacy, etc., can be eliminated by decentralized way of data storage [2, 3]. Blockchain has redefined security and has brought into play “trustless transactions” that can be securely done without the intervention of trusted third-party. Ethereum is one of the most popular public blockchain-based platforms. Data is cryptographically stored in blockchain and allows easy interaction with the client side. Data storage is a major concern in the era of IoT and many such upcoming technologies. Data in cloud has a security concern, and we need data storage to be done using a blockchain approach in order to secure the highly indispensable data.

A blockchain can have human readable naming system [4] to have ownership, readability, and decentralization. A blockchain is a decentralized P2P architecture where transactions are stored in the form of blocks [5]. These blocks have a world state and a blockchain state. “Blocks” on the blockchain are made up of digital pieces of information. Specifically, they have three parts:

- i. Blocks store information about transactions [6, 7] like the date, time, and dollar amount of your most recent purchase from Amazon. (This Amazon example is for illustrative purchases; Amazon retail does not work on a blockchain principle).
- ii. Blocks store information about who is participating in transactions [6]. A block for your splurge purchase from Amazon would record your name along with Amazon.com, Inc. Instead of using your actual name, your purchase is recorded without any identifying information using a unique “digital signature,” sort of like a username.
- iii. Blocks store information that distinguishes them from other blocks. Much like you and I have names to distinguish us from one another, each block stores a unique code called a “hash” that allows us to tell it apart from every other block [5–7]. Let us say you made your splurge purchase on Amazon, but while it is in transit, you decide you just cannot resist and need a second one. Even though the details of your new transaction would look nearly identical to your earlier purchase, we can still tell the blocks apart because of their unique codes (Fig. 1).

2 Motivation

The prime motivation behind is the securing of data within cloud in a blockchain fashion. The data in cloud with the convergence of blockchain becomes more secure

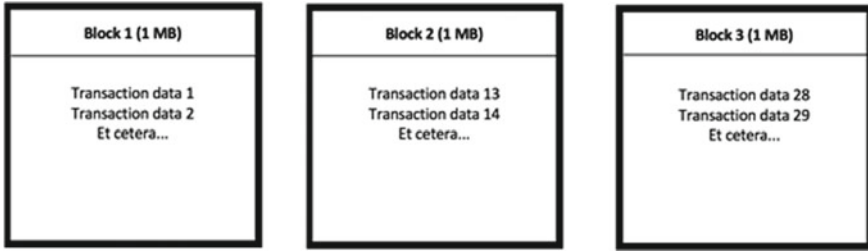


Fig. 1 A structure of a data block in blockchain framework

and reliable. The data must be distributed in such a way that it ensures decentralization along with scalability, availability as well as reliability.

3 Objectives of the Present Work

The main objective of this research is to use blockchain to solve the problem of security of data within the cloud. The proposed model uses two complimentary techniques sharding and swarming to secure cloud data [8, 9]. In sharding, data is split horizontally, and kept together so that it can be easily retrieved by a decentralized and distributed application using a unique partition key. The collective storage of shards is called as swarming. These two techniques help in securing, storing, auditing, scaling and decentralizing of data in cloud.

4 Enabling Techniques

4.1 Sharding

The blockchain and cryptocurrency developers are trying to improve the speed of transactions through several ways, and sharding is one of the ways. Sharding is a solution to scalability, latency and transactions throughput issues [5]. It is a concept that is widely used in databases to make them more efficient and faster. When it is implemented in blockchain, each block will have only the data part and not the entire information. The decentralization is still maintained because nodes that maintain a shard maintain information only on that shard in a shared manner.

4.2 *Swarming*

The collective storage of shards is called as swarming. Swarm [9] provides a platform, an infrastructure for the developers for various things such as leveraging, data streaming, etc. This technique helps in securing, storing, auditing, scaling and decentralizing of data in cloud.

5 **Related Work**

Hepp et al. [10] presented a novel method to safeguard physical assets using craquelure lacquers (PUFs) to ensure privacy of data. Origin-stamp service is used which is open trusted timestamping to acquire integrity. Whenever physical products are linked with blockchain, there will be a requirement of scalability. Moreover, to increase scalability of blockchain, two complimentary techniques swarming and Sharding are used.

Phansalkar [11] mainly focuses on integrating two technologies, i.e. AI and blockchain. Decentralization of blockchain forces AI to do value addition in the field of security, trustiness and efficiency. This paper also discusses about the intrinsic difference between AI and blockchain. Finally, the paper discusses where these both technologies can be used together to get better results such as in financial sector, healthcare sector, government sector, etc. There are various challenges being faced whenever traditional AI becomes distributed or decentralized AI.

Shafagh et al. [3] bring the concept of blockchain secured cloud data. IOT data in cloud needs a high-level security for sharing, auditing, etc. Blockchain provides decentralization, distributed and trustworthiness in IOT-cloud centric data. Author proposed layered architecture for distributed data storage system for IOT consisting of control plane (Blockchain, virtualchain) and data plane (Routing, storage).

Shrestha et al. [12] proposed a model for meta products for decentralized data storage in cloud to ensure privacy and trustworthiness. Traditional model use cloud model (SAAS) for meta products for data storage and processing. Many limitations were found in this type of model like only specific platform can be used by specific product. With the integration of blockchain, a single platform for different users, developers for different requirements has been proposed.

Liang et al. [13] implemented ProvChain an architecture to collect and verify cloud-data provenance. From the features of blockchain technology, the record is with unalterable timestamp, and for each validation of the data, we can generate a blockchain receipt. This architecture helps in auditing, privacy and availability.

Kaaniche et al. [14] combined hierarchical identity-based cryptography mechanism with blockchain technology. This architecture provides a transparent and trusted environment that helps the service providers to have tamper-proof evidence of receiving user's content before processing their personal data. It also ensures a better confidentiality.

Eyal et al. [15] presents a new blockchain protocol known as bitcoin-NG to overcome the problem of scalability that was not there in bitcoin derived blockchain. It provides same trust model as bitcoin with Byzantine fault tolerant blockchain protocol that is robust to extreme churn.

Chauhan et al. [16] discussed the number of transactions increasing every day, and it is the miner who is getting bottle necked. So, the waiting time is increasing. So, developers of bitcoin proposed a new lightning protocol to overcome this situation. Similarly, developers of ethereum proposed the method of sharding to overcome the same (Table 1).

6 Proposed Model

The data of various forms which needs high security is grouped in a data block. The data is further divided into small chunks called shards. Furthermore, the shards [8] are individually encrypted and hashed. Then, the data is ready to be inserted and synced with the blockchain ledger. Then, using a particular algorithm, the data chunks are distributed and grouped into swarms [9]. Each swarm now consists arbitrary data. Now, to secure the data, we cannot use a single cloud service provider to store all the swarms rather each swarm shall be occupied by diverse cloud service providers. Finally, the data is distributed into various clouds and since control is not within a single cloud, decentralization is also preserved (Fig. 2).

7 Concluding Remarks and Future Scope

The proposed system architecture is a novel approach towards data storage, availability and scalability with the aid of blockchain technology. Furthermore, the techniques of sharding and swarming working together provides a future research direction towards the convergence of blockchain technology in storing secure data which may include IoT sensory data, healthcare data and many such. The cloud storage facilities currently available are not fully adequate to provide proper security mechanisms, and thus, the use of blockchain is becoming a mandate in today's era of highly inevitable data. The future research scope towards the swarming algorithms to ensure decentralization as well as distribution of data is gaining popularity, and this paper tries to present a novel approach towards the challenges faced in securing data.

Table 1 Classification of literature survey based on work performed

Author contribution	Data storage	scalability	Availability
Hepp et al. [10]		Proposed a novel method called craquelure lacquers (PUFs) to ensure privacy of data. Open trusted timestamping service called Origin-stamp is being used swarming and sharding	
Chauhan et al. [16]		Proposed a new lightning protocol to overcome the problem of being bottle necked. Developers of ethereum proposed the method of sharding to overcome the same	
Shafagh et al. [3]	Discussed about blockchain-based secured cloud data proposed layered architecture for distributed data storage system for IOT consisting of control plane and data plane		
Shrestha et al. [12]	Proposed a model for meta products for decentralized data storage in cloud blockchain provides a single platform for different users, developers for different requirements has been proposed		
Liang et al. [13]			Implemented ProvChain an architecture to collect and verify cloud-data provenance
Kaaniche et al. [14]			Combined hierarchical identity-based cryptography mechanism with blockchain technology

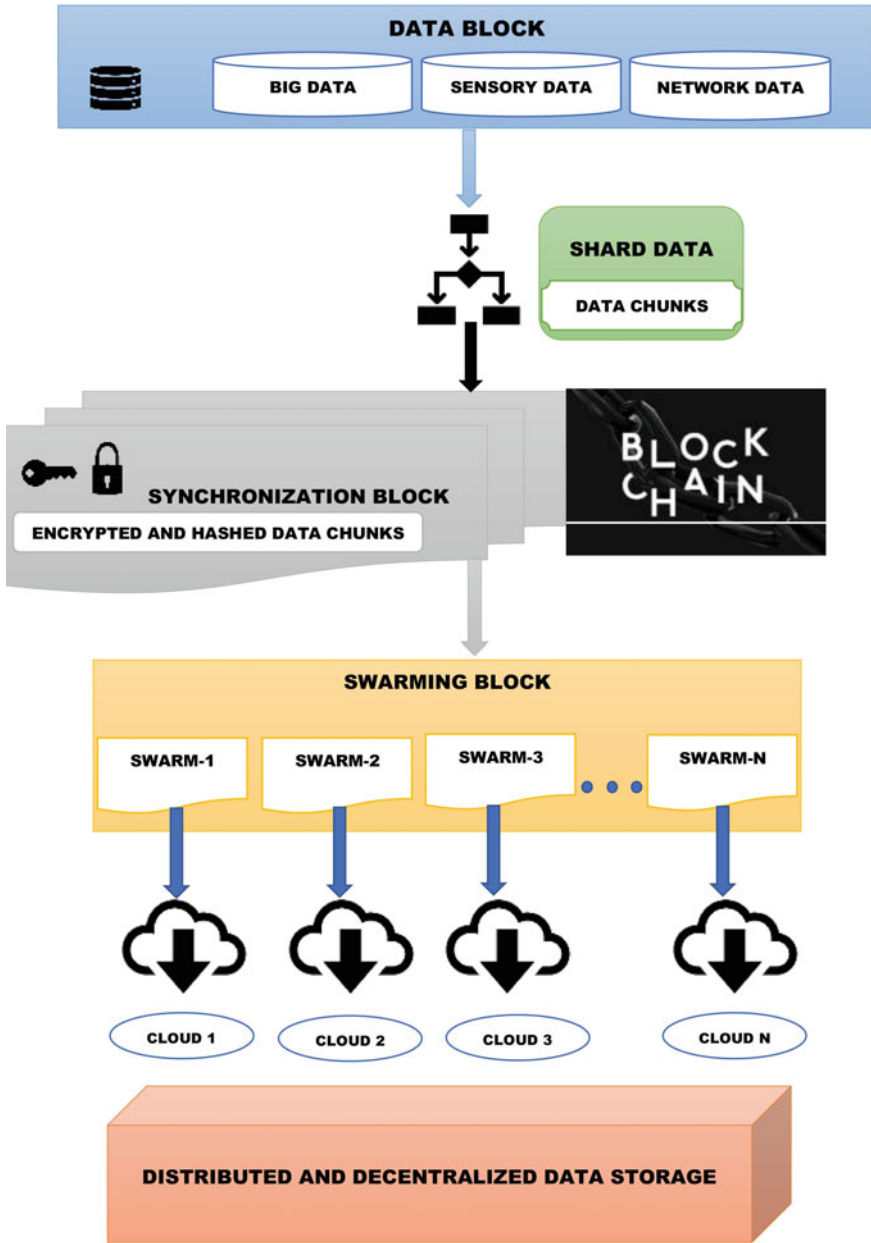


Fig. 2 Proposed system architecture for data storage

References

1. Tschorsch F, Scheuermann B (2016) Bitcoin and beyond: a technical survey on decentralized digital currencies. *IEEE Commun Surv Tutor* 18(3):2084–2123
2. Kuo TT, Kim HE, Ohno L (2017) Blockchain distributed ledger technologies for biomedical and health care applications. *J Am Med Inform Assoc* 24(6):1211–1220
3. Shafagh H, Burkhalter L, Hithnawi A, Duquennoy S (2017) Towards blockchain-based auditable storage and sharing of iot data. In: *Proceedings of the 2017 on cloud computing security workshop*, pp 45–50
4. Ali M, Nelson J, Shea R, Freedman MJ (2016) Blockstack: a global naming and storage system secured by blockchains. In: *2016 annual technical conference*, pp 181–194
5. Ali S, Wang G, White B, Cottrell RL (2018) A blockchain-based decentralized data storage and access framework for ping. In: *2018 17th IEEE international conference on trust, security and privacy in computing and communications/12th IEEE international conference on big data science and engineering (TrustCom/BigDataSE)*. IEEE, pp 1303–1308
6. Antonopoulos AM (2017) *Mastering bitcoin: programming the open blockchain*. O'Reilly Media, Inc.
7. Benet J (2014) Ipf5-content addressed, versioned, p2p file system. arXiv preprint [arXiv:1407.3561](https://arxiv.org/abs/1407.3561)
8. Croman K, Decker C, Eyal I, Gencer AE, Juels A, Kosba A et al (2016) On scaling decentralized blockchains. In: *International conference on financial cryptography and data security*. Springer, Berlin, pp 106–125
9. Rivest RL, Adleman L, Dertouzos ML (1978) On data banks and privacy homomorphisms. *Found Secure Comput* 4(11):169–180
10. Hepp T, Wortner P, Schönhals A, Gipp B (2018) Securing physical assets on the blockchain: Linking a novel object identification concept with distributed ledgers. In: *Proceedings of the 1st workshop on cryptocurrencies and blockchains for distributed systems*, pp 60–65
11. Phansalkar S, Kamat P, Ahirrao S, Pawar A (2019) Decentralizing AI applications with block chain
12. Shrestha AK, Vassileva J (2016) Towards decentralized data storage in general cloud platform for meta-products. In: *Proceedings of the international conference on big data and advanced wireless technologies*, pp 1–7
13. Liang X, Shetty S, Tosh D, Kamhoua C, Kwiat K, Njilla L (2017) Provchain: a blockchain-based data provenance architecture in cloud environment with enhanced privacy and availability. In: *2017 17th IEEE/ACM international symposium on cluster, cloud and grid computing (CCGRID)*. IEEE, pp 468–477
14. Kaaniche N, Laurent M (2017) A blockchain-based data usage auditing architecture with enhanced privacy and availability. In: *2017 IEEE 16th international symposium on network computing and applications (NCA)*. IEEE, pp. 1–5
15. Shafagh H, Burkhalter L, Hithnawi A, Duquennoy S (2017) Towards blockchain-based auditable storage and sharing of IoT data. In: *CCSW'17*, November 3, 2017, Dallas, TX, USA
16. Shrestha AK, Vassileva J (2016) Towards decentralized data storage in general cloud platform for meta-products. In: *BDW'16*, November 10–11, 2016, Blagoevgrad, Bulgaria

Countermeasures of Different Jamming Attacks in Wireless Sensor Networks



Vikash Kumar Agarwal, Amit Kumar Rai, and Nitish Kumar

Abstract Wireless sensor networks, because of its low-cost design and ease of reprogramming, it is easy for the adversary to conduct jamming or radio interference that can easily cause DoS attacks. These attacks can be launched against WSNs. The security attacks on WSNs are increasing drastically, and these degrade the performance in terms of throughput, energy consumption and delay. This article models the jamming attacks behaviour and analyses the WSNs performance. Jamming attack jams the network traffic by blocking the communication channel. The article explores the jamming attack modelling and then presents countermeasures against the jamming attacks. Then, the simulation parameters are presented along with summarizing the severance of various jamming attacks. Finally, we conclude the paper along with the future research scope.

Keywords Jamming attack · Wireless sensor networks · Behavioural modelling · Anti-jamming approach · Denial of service · FHSS · DSSS

1 Introduction

Wireless sensor networks (WSNs) have huge range of applications that includes recording and monitoring of sensitive information. These are used efficiently for security applications such as surveillance systems of secure areas, children, patients, etc., due to temporal disruption of streaming data and high QoS requirements of these applications may lead to disastrous results if there exists security concerns. Jamming is a process of disruption or prevention of signal transmission by directing

V. K. Agarwal (✉) · A. K. Rai · N. Kumar
Department of Computer Science and Engineering, RTC Institute of Technology, Ranchi,
Jharkhand, India
e-mail: vikashhagarwal@yahoo.com

A. K. Rai
e-mail: a.k.raai267@gmail.com

N. Kumar
e-mail: nitish1588@gmail.com

electromagnetic waves towards any communication system [1]. Jamming attack interferes with the radio frequency of the network nodes [2]. Attackers using powerful jamming may disrupt the normal functioning of the WSNs. Thus, countermeasures against jamming attack in WSNs are of utmost importance as WSNs may suffer from several constraints such as limited memory, low computation capability and energy resources.

Jamming attack can be considered as a special type of denial of service (DoS) attacks. Woods and Stankovic in [3] defined DoS attack as “event that eliminates or diminishes the networks performance”.

DoS inhibits flooding network with useless information. The radio frequency signals of jamming attack correspond to useless information. Thus, jamming is a special case of DoS attack.

WSNs are deployed in outdoor and hostile environments such as gardens, marine coasts, large estates, rivers or even battlefields. Such outdoor scenario requires integration of these applications with geographic information system (GIS) applications. These provide visual layout of thousands of sensors on single screen. This GIS is useful for target mobility monitoring in case of machine or human tracking systems. These GIS applications are not used for indoor scenarios and are limited only to outdoor scenarios because of two basic reasons. Firstly, obtaining a GPS location is not possible in indoor environments such as tunnels, building or factories as the signal strength decreases inside buildings. Secondly, deployment of indoor location system is expensive and requires huge processing power.

Jamming is the radio signals emission aimed at disrupting the transceivers operations [1]. Jamming is against any specific target and is intentional whereas radio frequency interference (RFI) is unintentional and is a result of nearby transmitters transmitting very close frequencies.

This article is organized as follows. In Sect. 1, we introduce the jamming attack as a special type of DoS attack. In Sect. 2, we present classification and modelling of jamming attack. Four types of jamming attacks are discussed in this section: constant jamming, deceptive jamming, random jamming and reactive jamming. Section 3 explores various types of countermeasures against jamming attacks: DSSS, FHSS, THSS, CSS and antenna polarization. Simulation parameters and the use of NS-2 to simulate the jamming architecture and countermeasures are presented in Sect. 4. In Sect. 5, we discuss the effect of jamming attack on the WSNs in terms of energy consumption, delay and the throughput. The reason for performance degrading under various jamming attack is also presented in this section. Finally, we conclude our paper in Sect. 6, where we present the side effects of jamming attacks on the WSNs performance, and the future research scope is also discussed.

2 Classification and Modelling of Jamming Attacks

Li et al. [4] proposed a concept of perfect knowledge of strategy of both the network and jammer and the case where these components lack these knowledge. They also

considered energy constraints of the network and the jammer. They also proposed a heuristic jamming technique. Xu et al. [5] proposed enhanced detection protocols for employment of consistency checks. It employs two schemes. The first scheme considered reactive consistency check using signal strength measurements. The second scheme considered consistency check using location information. Jamming attack can be classified into following four types as discussed below.

2.1 Constant Jamming

This jamming technique continuously generates a random data incorporating some interval between this random data generation. This random data transmission is done without checking the channel for its idle state that is without following the rules of MAC protocol [6, 7]. A normal node (n_0) before sending data transmits RTS packets to check the idleness of the channel between destination and source. If the RTS finds the channel to be idle, the destination node (n_5) starts sending CTS packets to normal node (n_0). Suppose a jammer node (n_1), at the same time generates random data and this collides with the CTS arriving from n_5 . The constant jammer is activated after particular interval and generates and transmits data in the network. If another node n_2 sends RTS, it starts sending data after receiving CTS. But the data from node n_1 collides with randomly generated data. This is constant jamming.

2.2 Deceptive Jamming

This jammer continuously sends random data and injects them to the channel. Between successive transmissions, it does not keep any gap and injects all the packets. This continuous stream of data prevents the normal sources to transmit data successfully. The deceptive jammer (n_1) continuously generates malicious data. A normal node (n_0) sends RTS packets and receives CTS before sending data to the destination. These packets may generate collision by colliding with the malicious data on the channel. The continuous generated malicious data from the deceptive jammer increases the network collision and may result in several nodes in receive state being placed in the networks.

2.3 Random Jamming

This is the most intelligent jamming technique in which the jammer considers its own energy and alternates itself between jamming and sleeping after fixed time interval. It is different from other jamming techniques where the jammer continuously transmits data without considering its own energy level. Random jamming may behave as both

deceptive as well as constant jamming. Thus, random jamming detection technique is more difficult as compared to deceptive or constant jamming techniques. In this, the nodes randomly generates data after fixed time interval and also leads to collision after fixed time interval in the same way as a constant jammer. This random jammer tries to save its energy level intelligently by switching itself to the sleep state. The random jammer node switches itself to sleep mode after jamming the network for facilitating energy conservation of the jammer node. After waking up, it may act like a deceptive jammer or constant jammer. It acts as deceptive jammer by increasing collision and jamming the network.

2.4 Reactive Jamming

It is difficult to detect reactive jamming as it is more disastrous, considering network performance. In reactive jamming, the jammer node starts its transmission upon any event detection on the channel. As this is an intelligent jamming technique, it reacts only upon observing any kind of events in the network. The reactive jammer nodes (n1) first analyse the networks state, and if there is no event sensed, it switches itself to quiet state. When normal node (n0) sends RTS, the jammer node upon sensing such activity sends the noise packets to the network. There occurs collision between the noise packets and the CTS packets. The attacker only gets activated only when the jammer sends any event in the channel.

These jamming techniques can be summarized as follows (Table 1).

3 Countermeasures Against Jamming Techniques

A brief description of various techniques and countermeasures in jamming is presented below. In this section, countermeasures dealing with possible radio jamming scenarios are explored.

Table 1 Jamming techniques

Jamming technique	Description
Constant jamming	The MAC protocol is degraded by continuously sending jamming signals to the channel
Deceptive jamming	It involves constant injection of regular packets without any gap to the channel. Thus, the normal node is deceived
Random jamming	It alternates between sleeping and jamming modes. The random jammer performs deceptive or constant jamming for a random time period and then switches to sleep mode
Reactive jammer	It stays quiet until any kind of event on the channel is detected. It spends large amount of energy in channel sensing procedure

3.1 Telecommunications with Spread Spectrum

It is a type of radio transmission technique in which the signals are transmitted over a large spectral width than the original signals bandwidth when transmitted using conventional modulation techniques. This is technique of spreading the communication signals energy over a greater bandwidth. This is done with the help of pseudo random code and reduces the natural interference risks. It also withstands interference and noise at the same time maintains privacy. Security in WSNs is a challenging task because of its energy constrained hardware and open medium. Jamming disrupts the wireless communication by reducing the signal to noise ratio. Spreading of information of narrow band signal over a wide band spectrum decreases the interference effects. All these spread spectral techniques employ a pseudo number for controlling and determining the spread pattern. Spread spectrum withstands high interference, and this is the major advantage of its usage. It provides a robust security approach for variety of WSNs applications [8].

3.2 Direct Sequence Spread Spectrum (DSSS)

This technology is mostly used in LAN wireless transmissions. At the sending station, a data signal is combined with a bit sequence of high data rate. This divides the user data on the basis of spreading ratio. DSSS enables multiple users to share a single channel and shows resistance to jamming attacks. It also shows negligible background noise and timing difference between receivers and transmitters. This technique mixed data signals with pseudo noise code for interference resistance. This results in larger signal bandwidth. DSSS, a modulation technique, described in IEEE 802.11b standards for computer wireless networking, spreads signals over broadband radio frequencies [9].

3.3 Frequency Hopping Spread Spectrum (FHSS)

This technique transmits radio wave signals that use multiple subcarrier channels in a frequency band. This is based on pseudo random sequence which is known both by the receiver and the transmitter. The FHSS is more advantageous than the single frequency usage. The transmitted signal is made more resistant to interference as well as difficult to intercept. The radio attack interference is prevented by this technique. The advantages of FHSS are listed as follows. Firstly, FHSS minimizes jamming and unauthorized interception of radio transmissions. Secondly, it enables co-existence of multiple WSNs in the same area. The major drawback of FHSS is that it requires a wider overall bandwidth than the single carrier frequency [10, 11].

3.4 Time Hopping Spread Spectrum (THSS)

The time hopping signals are divided into frames in THSS. These frames are again subdivided into number of transmission slots. One time slot at a time is modulated in the frames using information modulation. The pseudo noise generator selects the time interval. These code generators are responsible for performing switching using a power switch. These switching leads to some output which needs to be demodulated appropriately. These message bursts are rescheduled and stored to retrieve information. The time axis, in a THSS system, is partitioned into frames, and these frames are again subpartitioned into slots. There may be several slots possible but only one slot is used for one use.

3.5 Chirp Spread Spectrum (CSS)

Sliding of the carrier over some specified range of frequencies in a specified or linear fashion generates a chirp signal. The CSS receiver that employs a filter resembling time dispersed carrier. In this technique, a signal is broadcasted using the entire allocated bandwidth. Chirp uses broad spectrum band making CSS multipath fading resistant and at the same time operating at low power. It does not use any kind of pseudo random elements, unlike DSSS or FHSS. It does not rely on chirp pulses linear nature rather it distinguishes signal from noise in the channel. Doppler effect is very common in several mobile radio applications. CSS overcomes Doppler effect.

3.6 Antenna Polarization

The orientation of radio waves electric field with respect to surface of earth is referred to as antenna polarization. This technique plays an important role in jamming attack prevention. It is useful for LOS communications in WSNs. Right circular polarized antenna is unable to receive left polarized signals, and left circular polarized antenna cannot receive right polarized signals. Thus, for defending jamming attacks in WSNs, the nodes must be capable of changing antenna polarization upon sensing any kind of interference. But this also involves an overhead as the nodes must inform about its peers to facilitate uninterrupted communications. This change in node polarization prevents jamming but requires specialized jamming equipment's capable of rapidly changing its signal polarization during the jamming process [12].

Various countermeasures against jamming attacks are summarized in the (Table 2).

Table 2 Jamming Techniques

Countermeasures	Description
Telecommunications with SS	<ul style="list-style-type: none"> • Reduces the natural interference risks • Withstands interference and noise maintains privacy and secrecy in WSNs
DSSS	<ul style="list-style-type: none"> • Enables multiple users to share a single channel • Shows resistance to jamming attacks • Spreads signals over broadband radio frequencies
FHSS	<ul style="list-style-type: none"> • Based on pseudorandom sequence which is known by both the receiver and the transmitter • Minimizes jamming and unauthorized interception of radio transmissions • Enables co-existence of multiple WSNs in the same area
THSS	<ul style="list-style-type: none"> • Signals are divided into frames which are again divided into transmission slots
CSS	<ul style="list-style-type: none"> • Chirp uses broad spectrum band making CSS multipath fading resistant • Operates at low power • Overcomes Doppler effect
Antenna polarization	<ul style="list-style-type: none"> • Useful for LOS communications in WSNs • Requires specialized jamming equipments capable of rapidly changing its signal polarization during the jamming attack

4 Using the Template

Here, we have used network simulator (NS-2), a discrete event simulator to simulate the jamming architecture and countermeasures. We have used IEEE 802.15.4 MAC radio model for setting the parameters during simulations such as receiving power, sleep power, transmission power and idle power. This MAC layer is required for device communications. This provides the physical channels to access all types of security and transmission mechanisms. In this simulation, there are 50 mobile nodes that move in 750×750 m region for 25 s. Constant bit rate is the simulated traffic where the sources send their data to the sink. We also considered several jamming nodes or malicious nodes. The simulation parameters and settings are summarized in the (Table 3).

The reason for performance degrading under various jamming attack is also presented in this section. Finally, we conclude our paper in Sect. 6, where we present the side effects of jamming attacks on the WSNs performance, and the future research scope is also discussed.

Table 3 Simulation parameters

Parameters	Settings
Interface type	Physical 802.15.4
Radio model	Two ray ground propagation
Link layer	LL
Antenna type	Omni-directional
Queue	Priority queue
Channel type	Wireless
Interface queue length	50
Number of nodes	50
Transmission range	400 m
Area	750 × 750
Routing protocols	AODV
MAC	802.15.4
Initial energy	100 J
Traffic source	CBR
Sources	4
Packet size	512 bytes
Node placement	Randomized

5 Result and Discussion

It is observed that jamming attack degrades the WSNs performance in terms of energy consumption, delay and the throughput.

- *Energy consumption:* Energy consumption is highest for the reactive jamming. The deceptive and constant jamming shows similar increase in energy consumption. Amongst all the jamming techniques, random jamming shows the lowest energy consumption but still more than the no attack condition.
- *Delay:* The delay involved in reactive jamming is highest amongst all jamming techniques while random jamming shows the lowest delay.
- *Throughput:* Throughput of no attack condition is highest, and among all the jamming attacks, the reactive jamming shows the least throughput by far from all other jamming techniques. Constant jamming produces highest throughput followed by deceptive jamming and random jamming techniques.

The reason for performance degrading under various jamming attack is explored below.

- *Constant jamming:* The performance degrading of constant jamming is less than other types of jamming attack. This is because the network is jammed after regular intervals in constant jamming.

- *Deceptive jamming*: As compared to constant jamming, a deceptive jamming shows more performance degrading. This is because of continuous noise generation which increases delay and energy consumption as well as decreases the network throughput due to large number of collisions responsible for jamming the channel.
- *Random jamming*: This jams the WSN randomly using either deceptive jamming or constant jamming. It is not easy to detect as it shows random behaviour.
- *Reactive jamming*: This is the most disastrous type of jamming attack. After any event detection, it introduces noise packets immediately into the network. By introducing severe collision, it corrupts huge number of packets in the WSNs.

6 Conclusion

Considering the low-cost design of WSNs and the ease with which these can be reprogrammed, WSNs are susceptible to radio interference attacks. This paper surveys both defence and attack side of jamming WSNs. The paper models and analyses the side effects of various types of jamming attacks on the WSNs performance. Increasing the safety level and avoiding DoS attacks is of utmost importance in WSNs. The attacker may launch DoS attack by radio channel jamming. Jamming attacks degrades the network performance in terms of energy consumption, throughput and delay. Reactive jamming degrades the network performance to maximum extent, and random jamming shows least degradation in the network. This article provides requirements for efficient jamming defence technique development. The future research will be concentrated on new jamming possibilities in WSN and developing an efficient defence mechanism.

References

1. Adamy DL, Adamy D (2004) In: EW 102: a second course in electronic warfare, Artech House Publishers
2. Shi E, Perrig A (2004) Designing secure sensor networks. *Wireless Commun Magaz* 11(6):38–43
3. Wood AD, Stankovic JA (2002) Denial of service in sensor networks. *Computer* 35(10):54–62
4. Li M et al (2010) Optimal jamming attacks and network defense in wireless sensor networks. *IEEE Trans Mobile Comput*
5. Xu W, Trappe W, Zhang Y, Wood T (2005) The feasibility of launching and detecting jamming attacks in wireless networks. In: *MobiHoc'05*, May 25–27, 2005, Urbana Champaign, Illinois, USA
6. Mpiziopoulos A, Gavalas D, Konstantopoulos C, Pantziou G (2009) A survey on jamming attacks and countermeasures in WSNs. *IEEE Commun Surveys Tutorials* 11(4):42–56
7. Xu W, Ma K, Trappe W, Zhang Y (2006) Jamming sensor networks: attacks and defense strategies. *IEEE Netw* 41–47
8. Pickholtz RL, Schilling DL, Milstein LB (1982) Theory of spread spectrum communications-a tutorial. *IEEE Trans Commun* 20(5):855–884

9. DSSS-wikipedia. <https://en.wikipedia.org/wiki/Direct-sequence-spread-spectrum>
10. FHSS-wikipedia. <https://en.wikipedia.org/wiki/Frequency-hopping-spread-spectrum>
11. Min J (1995) Analysis and design of a frequency-hopped spread-spectrum transceiver for wireless personal communications. University of California
12. Stutzman W, Thiele G (1997) In: Antenna theory and design, Wiley

Detecting Acute Lymphoblastic Leukemia Through Microscopic Blood Images Using CNN



Afrin Alam and Shamama Anwar

Abstract Leukemia refers to cancer, takes place when bone marrow generates excess amount of abnormal blood cells. These abnormal blood cells grow rapidly interrupting the functioning of the other normal cells. Hence, body loses its capability to fight with exterior organism like viruses, bacteria, fungi, and so on, hereby, affecting the immunity of the person. Leukemia, if not treated on time can lead to death. This disease affects adults as well as children. Thus, early detection of the disease would help in proper treatment. The manual diagnosis of this disease is quite laborious, tedious, and time-consuming which involves blood test and biopsy. Thus, to overcome these shortcomings, this paper discusses a computer-aided automated diagnosis system for detection of acute lymphoblastic leukemia (ALL) using deep-learning models. A pretrained AlexNet model is deployed for performing this task. Experiment is done using microscopic blood cell images. This overall framework helps in detecting the malignant cells easily. From the experimental results, it is evident that this proposed method achieves an accuracy of 98% without the use of any image segmentation technique or feature extraction technique. Hence, the work reported in the paper would provide a framework to aid pathologist in diagnosing acute lymphoblastic leukemia accurately and quickly.

Keywords Leukemia · Feature learning · Convolutional neural network · AlexNet

1 Introduction

Blood is one of the major components of the human body. Leukemia is a cancer of blood that mainly happens when bone marrow generates excess abnormal white blood cells [1]. Leukemia are of two types; acute leukemia and chronic leukemia,

A. Alam · S. Anwar (✉)

Department of Computer Science and Engineering, Birla Institute of Technology, Mesra, Ranchi 835215, India

e-mail: shamama@bitmesra.ac.in

A. Alam

e-mail: alamafrin373@gmail.com

based on how fast this disease grows and becomes intense [2]. This acute leukemia is further divided into two sub-classes: acute lymphoblastic leukemia and acute myeloid leukemia (according to French American British standard) [1]. Acute lymphoblastic leukemia is caused due to abnormal growth of lymphoid cell, whereas acute myeloid leukemia is caused by over-growth of myeloid cells. Leukemia can be diagnosed by examining the blood smear under the microscope, immunophenotyping, cytogenetics, etc. But all these process takes lot of time and are tedious, slow, and costly, and due to variation in slide preparation, it can give non-standardized and inaccurate results [1]. Leukemia can also be diagnosed by complete blood count, bone marrow aspiration, and biopsy [3]. But these laboratory tests are also time taking and has variability in their results. It also requires advices of experts, who are experienced in their field [4].

This paper implements a pretrained AlexNet model for identification of blast cells from microscopic blood cell images. The raw (unprocessed) image is fed in this model for performing feature extraction and classification task. The experiment is applied on 368 images of ALL_IDB dataset, achieving accuracy of 98%.

2 Related Work

Since the conception of deep-learning techniques, it has found wide application in different domains of medical sciences. Some of the notable contribution in ALL classification has been listed here. Shafique and Tehsin [3] proposed DCNN for detection of ALL and classifying its sub-types. A pretrained AlexNet model was employed, and experiment was done using ALL_IDB dataset, achieving high accuracy. Mishra et al. [5] proposed a method for ALL. Texture feature was extracted by using discrete orthonormal S transform (DOST). For dimensionality reduction and classification, linear discriminant analysis (LDA) and Adaboost random forest classifier were used.

Mishra et al. [2] in another work designed an automated detection system for the identification of ALL. Segmentation was performed by marker-based segmentation method. Gray level co-occurrence matrix (GLCM) and principle component analysis were used for feature extraction, and random forest-based classifier was used for classification task. Negm et al. [4] also proposed a method for the classification of ALL using k-mean clustering and neural network. Rawat et al. [6] presented a framework for diagnosis of myeloid and lymphoid cell. In this methodology, first the nucleus was segmented from the lymphocyte and various geometrical, chromatic, and texture features were determined. Classification was performed using SVM classifier which was based on genetic algorithm.

Karhikeyan and Poornima [7] suggested a method for identification of leukemia. For image segmentation, fuzzy C means and K means were used where fuzzy C means worked well in comparison to K means. Features such as color and shape were extracted by using the Gabor texture extraction method. These extracted features were then fed into the SVM classifier for the classification task. Li et al. [8] presented a methodology for segmenting WBCs. The method was based on dual threshold

concept. The framework used RGB and HSV color space, image preprocessing followed by threshold-based segmentation, post-processing to remove the unwanted part of the image using mathematical morphology, and median filtering was used. The experiment gave satisfactory result. A fuzzy-based method was proposed in [9]. Gamma, Gaussian, and Cauchy which are fuzzy membership functions were used for analysis. It was concluded that Cauchy gave better segmentation results in identifying leukocyte.

More current work in this domain uses deep-learning techniques for more accurate classification. Sipes and Li [10] proposed a convolutional neural network model for the classification of ALL. Similar work using CNN was also presented in [11]. These deep-learning models did not require any preprocessing or segmentation on the data. The work reported in this paper implements a variation of the AlexNet CNN model for ALL classification.

3 Convolutional Neural Network

Convolutional neural network (also called CNN or ConvNets) is a class of machine learning that has given tremendous success in object recognition and image classification task. CNN performs two major tasks: feature extraction and classification [11]. The layers of CNN architecture are convolution layer, pooling layer, flattening layer, a fully connected network layer, and a dropout layer. The high-level features of any input image are extracted by the convolution layer, and these extracted features are further used by the fully connected layer for performing the classification task. Each layer of CNN is responsible for performing its specific task.

Convolutional layer is responsible for performing convolutional operation. This operation is mainly done to extract the relevant features from the input image, which further behaves as an input to the first layer of convolution layer. ReLU layer is generally used after it. In this layer, operation is applied on each pixel and it suppress all negative values to zero. It brings nonlinearity into the network [10]. Pooling layer is responsible for down sampling operation which results in minimizing the dimension of the feature map. By doing so, it gains the relevant feature from the feature map. After pooling operation is done, flatten layer converts the multi-dimensional representation (array) into a one-dimensional feature vector [11]. Most eminent features get extracted from the input image by the convolutional and pooling layer, which is further used by the fully connected layer for downgrading the input image into different classes to detect the final output categories of the image. Finally, dropout layer places random values of input elements to zero with a fixed probability. This layer also solves the problem of over-fitting [10].

AlexNet is a convolutional neural network designed by Alex Krizhevsky in 2012 [3]. AlexNet consists of eight layers: five convolutional layer and three fully connected layer. ReLU layer which is a nonlinear activation function is applied after every convolutional layer. It is also applied after fully connected layer. The architecture also consists of dropout layer which is applied before first and the second fully

connected layers. By applying dropout layer, it gives us more robust features of input image and also solves the over-fitting problem.

3.1 Implementation

The implemented methodology consists of two phases: feature extraction and classification. The workflow of the methodology is depicted in Fig. 1. The methodology begins with data acquisition. The ALL IDB dataset was used for this study. ALL IDB stands for acute lymphoblastic leukemia image database for image processing and has been obtained through permission from the Department of Information Technology—Università degli Studi di Milano, Italy (<https://homes.di.unimi.it/scotti/all/>). ALL_IDB dataset has two distinct version: ALL_IDB1 and ALL_IDB2. ALL_IDB1 contains 108 images of which 49 are blast cells and 59 are non-blast cells. ALL_IDB2 contains 130 blast cells and 130 non-blast cells. This ALL_IDB2 dataset is a collection of all cropped area of interest of normal cell images and of abnormal cell images of ALL_IDB1. The images are JPG format with 24-bit color depth having resolution of 2592×1944 [12–15]. These images are resized to match the input layer of the pretrained AlexNet as 227×227 .

The aim of the work in this paper is to classify a blood smear image from a suspected leukemia patient. The blood smear image could be of either of the two categories: a blast cell or a non-blast (normal) cell. Since, the pretrained AlexNet was trained to predict the outcome of the ImageNet dataset which comprised of 1000 outcomes, modification was made to use the model on our dataset. The modification was made in the fully connected and output layer, and the model was retrained on the ALL_IDB dataset. Figure 2 depicts the modified AlexNet model used for ALL_IDB classification and Table 1 summarizes the layers used in the CNN model for feature extraction.

Layers 6 and 7 are fully connected layers with 4096 neurons followed by ReLU layer and dropout layer with a probability of 50%. Layer 8 is also a fully connected layer with 2×4096 neurons, where all features are combined. These combined features are fed to a softmax classifier at layer 9, which is the output layer performing the classification task.

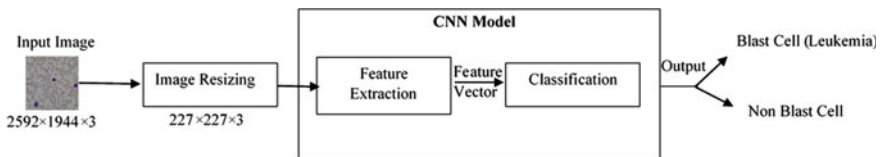


Fig. 1 Workflow of the implemented method

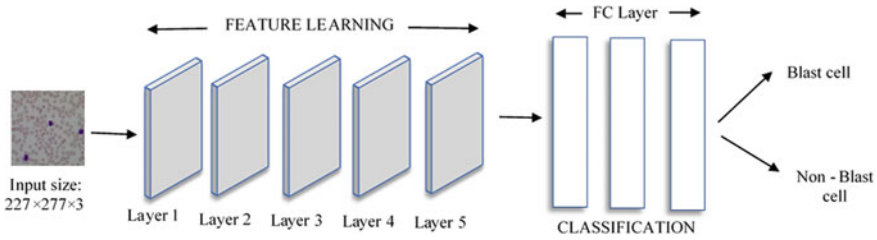


Fig. 2 CNN architecture used for leukemia classification

4 Results and Discussions

The implementation of the above CNN model has been done using the deep network designer tool in MATLAB. The model was trained and validated on 70% of the data and tested on 30% of the data by varying the number of epochs. Total number of training data is 258, whereas testing data is 110. The highest accuracy was achieved on running the model for 20 epochs. Figure 3 shows the accuracy and loss plots achieved during the training and validation phase. It can be observed from the plots that an accuracy of 95.45% has been achieved by training the model for 20 epochs. After successful training of the model, it was tested on the test data reserved for the purpose and a testing accuracy of 98% was reported.

Further, based on the literature survey mentioned in the prior section, it was observed that most of the techniques that used the traditional machine learning approaches had to perform some image processing technique for segmentation. These techniques also required explicit extraction of the features, for the machine learning technique to be able to perform classification. The work implemented in this paper does not require the need of any preprocessing, other than resizing the input image. The raw (unprocessed) image is fed in this model for performing both feature extraction and classification task. Table 2 further summarizes the accuracy obtained by the paper’s methodology and other work presented in the literature.

5 Conclusion

This paper presents an application of the pretrained convolution neural network model, AlexNet. The model was pretrained on the ImageNet database was giving an output of 1000 classes. The model was, hence, modified to classify blood smear images obtained by the ALL_IDB dataset. The model was successfully trained and could predict the outcome of an image as either an infected or uninfected cell. This automated system can help the pathologist in diagnosing leukemia efficiently. A future work might be fruitful by comparing this model with some other architecture of deep learning. Another future direction will be to diagnose other disease by retraining the model with less effort.

Table 1 Feature extraction layers of the implemented CNN model

Layer	Input Type	Activations	Weights
Input	Input image size: $227 \times 227 \times 3$	$227 \times 227 \times 3$	–
Layer 1	<u>Convolution</u> Input image size: $227 \times 227 \times 3$ No. of kernel: 96, Filter size: $11 \times 11 \times 3$ Stride: [4 4], Padding: [0 0 0 0] Activation: ReLU and normalization <u>Max-pooling</u> Size: 3×3 , Stride: [2 2], Padding: [0 0 0 0]	$55 \times 55 \times 96$ $27 \times 27 \times 96$	Weight: $3 \times 3 \times 3 \times 64$ Bias: $1 \times 1 \times 64$
Layer 2	<u>Convolution</u> Input image size: $27 \times 27 \times 256$ No. of kernel: 2×128 , Filter size: $5 \times 5 \times 48$ Stride: [1 1], Padding: [2 2 2 2] Activation: ReLU and normalization <u>Max-pooling</u> Size: 3×3 , Stride: [2 2], Padding: [0 0 0 0]	$27 \times 27 \times 256$ $13 \times 13 \times 256$	Weight: $5 \times 5 \times 48 \times 128$ Bias: $1 \times 1 \times 128 \times 2$
Layer 3	<u>Convolution</u> Input image size: $13 \times 13 \times 256$ No. of kernel: 384, Filter size: $3 \times 3 \times 256$ Stride: [1 1], Padding: [1 1 1 1] Activation: ReLU	$13 \times 13 \times 384$	Weight: $3 \times 3 \times 256 \times 384$ Bias: $1 \times 1 \times 384$
Layer 4	<u>Convolution</u> Input image size: $13 \times 13 \times 384$ No. of kernel: 2×192 , Filter size: $3 \times 3 \times 192$ Stride: [1 1], Padding: [1 1 1 1] Activation: ReLU	$13 \times 13 \times 384$	Weight: $3 \times 3 \times 192 \times 192$ Bias: $1 \times 1 \times 192 \times 2$
Layer 5	<u>Convolution</u> Input image size: $15 \times 15 \times 384$ No. of kernel: 2×128 , Filter size: $3 \times 3 \times 192$ Stride: [1 1], Padding: [1 1 1 1] Activation: ReLU <u>Max-pooling</u> Size: 3×3 , Stride: [2 2], Padding: [0 0 0 0]	$13 \times 13 \times 1256$ $6 \times 6 \times 1256$	Weight: $3 \times 3 \times 192 \times 128$ Bias: $1 \times 1 \times 128 \times 12$

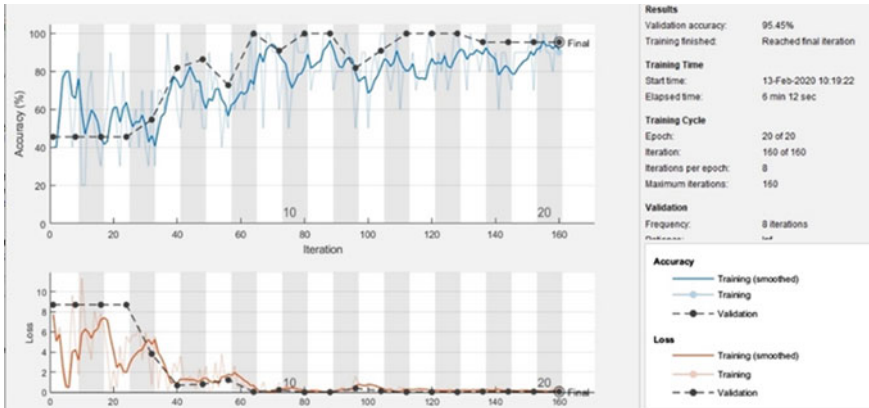


Fig. 3 The training accuracy and loss plot obtained during training the model

Table 2 Comparison of the accuracy obtained through different techniques

Authors	#Images	Technique used	Accuracy achieved (%)
Putzu and Caocci [16]	368	Segmentation, Feature Extraction, SVM	92
Putzu and Ruberto [17]	245	Segmentation, Feature extraction, SVM	92
Singhal and Singh [18]	260	Segmentation, Feature Extraction, SVM	92.3
Rawat et al. [1]	368	Segmentation, Feature extraction, SVM	89.8
Bhattacharjee and Saini [19]	120	Segmentation, Feature Extraction, ANN	95.2
Our work	368	AlexNet	98

References

1. Rawat J, Singh A, Bhadauria HS, Virmani J (2015) Computer aided diagnostic system for detection of leukemia using microscopic images. Proc Comput Sci 70:748–756
2. Mishra S, Majhi B, Sa PK, Sharma L (2017) Gray level co-occurrence matrix and random forest based acute lymphoblastic leukemia detection. Biomed Signal Process Control 33:272–280
3. Shafique S, Tehsin S (2018) Acute lymphoblastic leukemia detection and classification of its subtypes using pretrained deep convolutional neural networks. Technol Cancer Res Treatm 17:1533033818802789
4. Negm AS, Hassan OA, Kandil AH (2018) A decision support system for Acute Leukaemia classification based on digital microscopic images. Alexandria Eng J 57(4):2319–2332
5. Mishra S, Majhi B, Sa PK (2019) Texture feature based classification on microscopic blood smear for acute lymphoblastic leukemia detection. Biomed Signal Process Control 47:303–311
6. Rawat J, Singh A, Bhadauria HS, Virmani J, Devgun JS (2017) Computer assisted classification framework for prediction of acute lymphoblastic and acute myeloblastic leukemia. Biocybernet

- Biomed Eng 37(4):637–654
7. Karthikeyan T, Poornima N (2017) Microscopic image segmentation using fuzzy c means for leukemia diagnosis. *Leukemia* 4(1):3136–3142
 8. Li Y, Zhu R, Mi L, Cao Y, Yao D (2016) Segmentation of white blood cell from acute lymphoblastic leukemia images using dual-threshold method. *Comput Math Methods Med*
 9. Ghosh M, Das D, Chakraborty C, Ray AK (2010) Automated leukocyte recognition using fuzzy divergence. *Micron* 41(7):840–846
 10. Sipes R, Li D (2018) Using convolutional neural networks for automated fine grained image classification of acute lymphoblastic Leukemia. In: 2018 3rd International conference on computational intelligence and applications (ICCIA). IEEE, pp 157–161
 11. Ahmed N, Yigit A, Isik Z, Alpkocak A (2019) Identification of leukemia subtypes from microscopic images using convolutional neural network. *Diagnostics* 9(3):104
 12. Piuri V, Scotti F (2004) Morphological classification of blood leucocytes by microscope images. In: 2004 IEEE international conference on computational intelligence for measurement systems and applications, 2004. CIMSAA. IEEE, pp 103–108
 13. Labati RD, Piuri V, Scotti F (2011) All-IDB: the acute lymphoblastic leukemia image database for image processing. In: 2011 18th IEEE international conference on image processing. IEEE, pp 2045–2048
 14. Scotti F (2006) Robust segmentation and measurements techniques of white cells in blood microscope images. In: IEEE instrumentation and measurement technology conference proceedings. IEEE, pp 43–48
 15. Scotti F (2005) Automatic morphological analysis for acute leukemia identification in peripheral blood microscope images. In: CIMSAA 2005 IEEE international conference on computational intelligence for measurement systems and applications, IEEE, pp 96–101
 16. Putzu L, Caocci G, Di Ruberto C (2014) Leucocyte classification for leukaemia detection using image processing techniques. *Artif Intell Med* 62(3):179–191
 17. Putzu L, Di Ruberto C (2013) White blood cells identification and classification from leukemic blood image. In: International work-conference on bioinformatics and biomedical engineering. Copicentro Editorial, pp 99–106
 18. Singhal V, Singh P (2015) Correlation based feature selection for diagnosis of acute lymphoblastic leukemia. In: Proceedings of the third international symposium on women in computing and informatics. pp 5–9
 19. Bhattacharjee R, Saini LM (2015) Robust technique for the detection of acute lymphoblastic leukemia. In: 2015 IEEE Power, communication and information technology conference (PCITC). IEEE, pp 657–662

Blockchain Marketplace—A Novel Overview for Real-Time Implementation



Anindita Jena

Abstract The renowned security concept called Blockchain is used everywhere nowadays. The Blockchain technology is introduced to the world after the development of bitcoin technology by Satoshi Nakamoto. Recently, many software companies and online marketing companies are trying to adopt this security technology. Except these sectors, other domains are also interested in Blockchain like machine learning, IoT, RFID, etc. In this paper, advancement of Blockchain technology is discussed in the online market sector. The workflow and system architecture of application is explained as well as the results of experimentation are visualized. The procedure to create autonomous Ethereum environment and ether is also explained.

Keywords Blockchain · Ethereum · Smart contract · Ledger technology · Decentralization

1 Introduction

Blockchain was invented by Satoshi Nakamoto in the year 2008 through bitcoin technology. Later, Blockchain is used in several areas for diverse purposes. The definition of Blockchain is described as a decentralized, distributed, digital ledger which is used to keep all the records related to transactions across number of computers with ensured security. Multiple number of blocks are connected sequentially with a chain. First block is known as genesis block. Each block contains block number, block address, records, previous hash, and current hash as shown in Fig. 1. The previous hash of a block is stored at current hash of previous block as shown in Fig. 2. There are N number of blocks that can be connected to a Blockchain network. One block can be added to a Blockchain network after verifying the block. The addition of a block in the network is of three types which are described as follows:

A. Jena (✉)

College of Engineering and Technology, Bhubaneswar 751003, India
e-mail: aninditajena1996@gmail.com

Fig. 1 Generalized structure of blocks

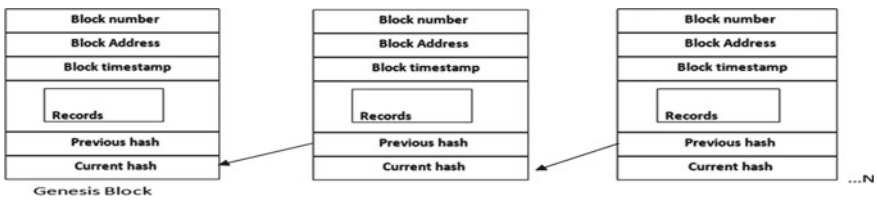
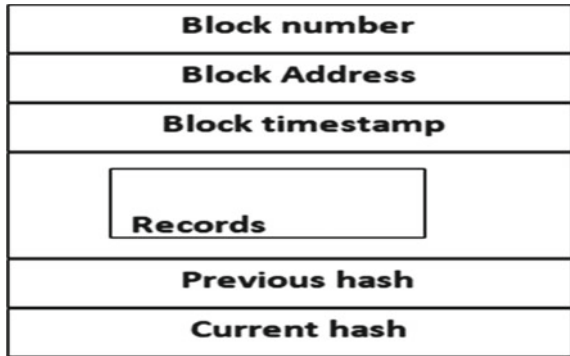


Fig. 2 Detailed generalized structure of blocks

1.1 Public (Permission Less) Blockchain

This type of Blockchain that is accessible by anyone and where users are represented by a random ID is a public Blockchain. Here, the network easily allows the users for participating without the initial check. This Blockchain network is based on proof-of-work (PoW) consensus mechanism. There is another mechanism called proof-of-stake (PoS) which selects the users who own a stake of the network’s tokens [1].

1.2 Private (Permissioned) Blockchain

The private Blockchain grants access only to known users, who have rights to read/write the data. Proof-of-authority (PoA) consensus mechanism is used for the validation of a single block [1].

1.3 Consortium Blockchain

The consortium Blockchain is a multipurpose type which is based on both public (permission less) and private (permissioned) Blockchain. Here, only the verified node or user can validate the new block [1].

2 Enabling Technologies

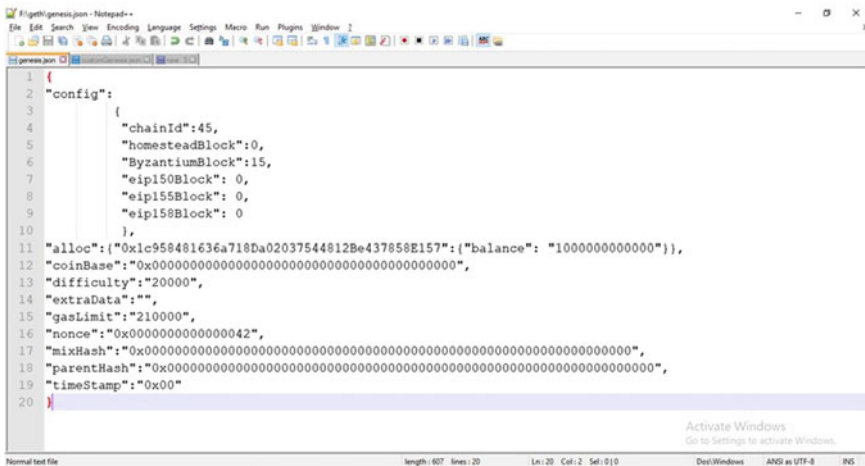
2.1 Ethereum

An Ethereum is a platform which generates few ethers for performing specific computations and for mining of nodes. It is also the only currency which is accepted at the time of payment during a transaction. The concept of Ethereum was proposed by Vitalik Buterin in 2013. Ethereum generates a decentralized virtual machine called Ethereum virtual machine (EVM) which is used for executing scripts in an international network of public nodes.

The procedure behind creation of an Ethereum is as follows:

Step 1: Code is written in json language for creating blocks in the Blockchain. The first Blockchain is called as genesis block. The json format code is shown in Fig. 3.

Step 2: The geth (Goethereum) and Node.js file is installed and enabled both by doing path setup in environment variables.



```
1 {
2   "config":
3     {
4       "chainId":45,
5       "homesteadBlock":10,
6       "ByzantiumBlock":15,
7       "eip150Block": 0,
8       "eip155Block": 0,
9       "eip158Block": 0
10    },
11  "alloc":{"0x1c958481636a718Da02037544812Be437858E157":{"balance": "1000000000000"}},
12  "coinBase": "0x000000000000000000000000000000000000000000000000",
13  "difficulty": "20000",
14  "extraData": "",
15  "gasLimit": "210000",
16  "nonce": "0x00000000000000042",
17  "mixHash": "0x000000000000000000000000000000000000000000000000",
18  "parentHash": "0x000000000000000000000000000000000000000000000000",
19  "timeStamp": "0x00"
20 }
```

Fig. 3 Snapshot of json format code

Step 3: Make a directory file in command prompt by using “geth.” Then, run that json file. After that genesis block is created, and few ethers will be generated (ETH = 50) as shown in Fig. 4.

Step 4: Create a geth console project in command prompt (*geth --networkid=5 -rpc -rpcport 2 console*) with this command line as shown in Fig. 5. After this, a key and an address will be generated.

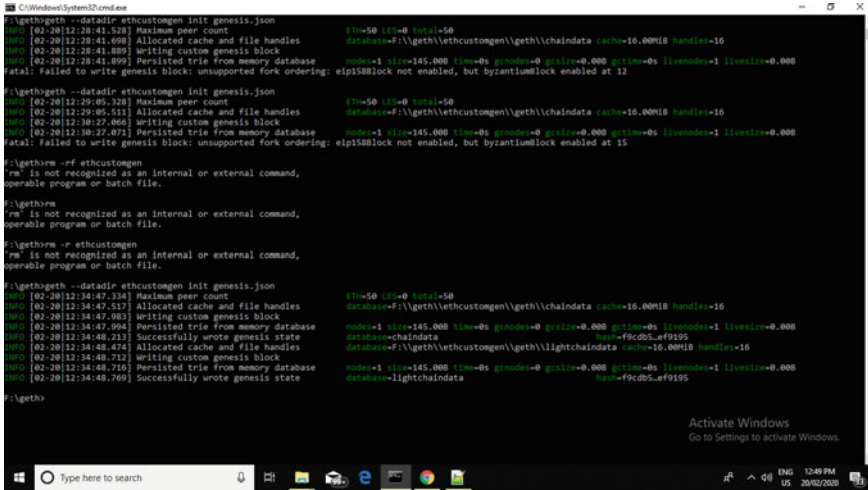


Fig. 4 Snapshot of generated ether after excuting the .json file

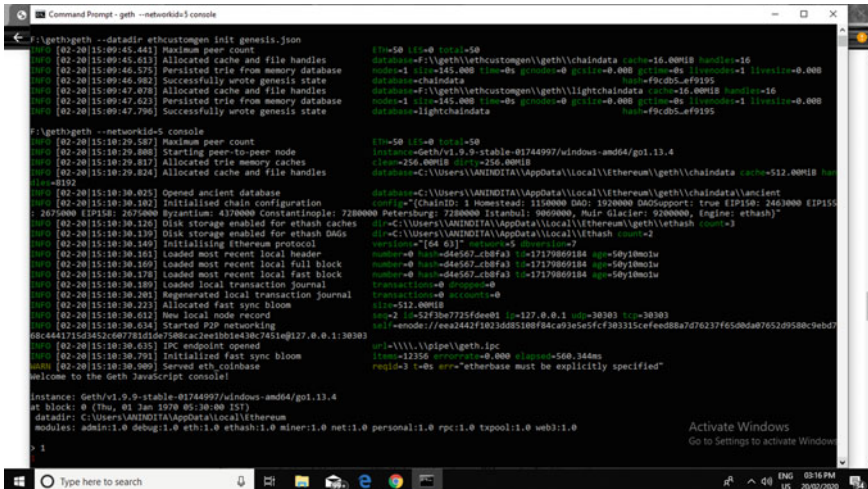
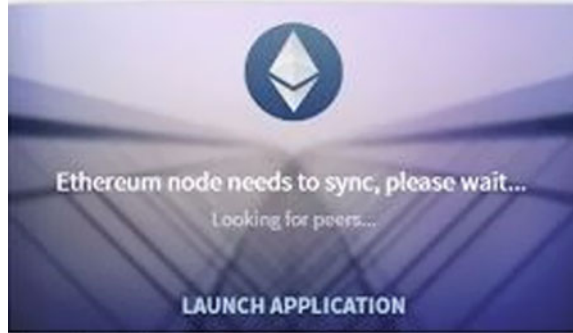


Fig. 5 Snapshot of generated key and address value

Fig. 6 Ethereum mist wallet API for creation of an ethereum account



Step 5: Download an Ethereum Mist Wallet which is an Ethereum platform for creating an account for user that is shown in Fig. 6.

2.2 *Smart Contract*

The concept of smart contract is simply based on simple contracts. In simple contracts, it contains all the agreements and rules which are made between two parties in the presence of a third party. But in smart contract, it does not need a third party, and it is written electronically. It is constructed in the way that no one can violate the smart contract, and it is highly encrypted with the concept of Blockchain.

2.3 *Other Technologies*

While creating a project, it may need JavaScript concept. Here in this paper, JavaScript is used.

3 *Literature Survey*

Balaji et al. contrived a systematic application of Blockchain, which was based on file sharing system. In general, there were two-step processes where a file was needed to be uploaded to the drive first and then downloaded from there itself. Here, sender and receiver had to go through two processes, but after using Blockchain, it would compress the steps into one where sender can transfer directly to the receiver. There are multiple applications available for file sharing. But in this paper, author used some cryptographic algorithms and Blockchain concept to provide security in file sharing system [2].

Knirsch et al. introduced an implementation of Blockchain for satisfying all the legal requirement at the time of transferring energy from shared photovoltaic power plant. In this paper, author described convincing results and some takeaways about which developers should be aware of [3].

Ochôa et al. developed architecture of Blockchain for using it in IoT. In this paper, author used a decentralized application of Blockchain to create an interaction among device, user, and environment. This paper also described some privacy concerns by originating different smart contracts at different levels of Blockchain architecture. The gateway concept was also used in device-user communication, and IPFS service was used for data integrity [4].

Kumar et al. proposed a decentralized application of Blockchain which was based on student management system. In the part of implementation of Blockchain, student records were stored in the form of blocks, and then, it was validated by authorities of universities with the help of smart contracts. Here, in this paper, there were two algorithms used for data encryption, i.e., SHA256 and RSA [5].

Nathan et al. introduced a design of a relational database of Blockchain. The introduced Blockchain relational database was based on decentralized concept which was controlled by multiple administrations. The ordering of block was based on consensus mechanism, and implementation of system was based on PostgreSQL [6].

Albrecht et al. described some factor related to the implementation of Blockchain. This paper presented how the Blockchain technology immensely affected the energy sector. The factors were based on DOI, TOE, and institutional economics. To identify the factors, authors used use cases in their work [1].

Papadodimas et al. provided some theories related to Blockchain used by IoT. In the era of IoT technology, the demand of sensor has increased. The sensors are added to the IoT network, and these networks are growing rapidly. As sensors are generating tremendous amount of data, IoT needs a security concept in it. For that, author explained some concepts about IoT sensor data and Blockchain [7].

Aldred et al. proposed a design of a system based on the guiding principles settled by GDPR in regards to data privacy. Here, Blockchain was used for the removal of data and accessing of data with high security while considering the integrity of Blockchain [8].

Helo and Hao proposed a supply-chain concept with the coordination of Blockchain. There are several challenging features related to supply-chain, and constructing it is a very complicated task. Multiple parties are added in supply-chain, and for that, a shared database is also need for it. If a transaction is recorded once, then it can rarely change in the ledger. In this paper, author collaborated the supply-chain with Blockchain due to above-explained reason, so that parties could easily access invoice, check the status and payment records, etc. [9].

Saxena et al. introduced a permissioned Blockchain infrastructure which was based on energy trading platform. The introduced platform decreased the community peak load by 46% and weekly electricity bill by 6%. The author also added a real-world experiment to validate the energy transfer among DERs within a micro grid [10].

Grigore Rosu explained about a novel language, i.e., vyper which was used for writing the smart contract in Blockchain. In this paper, author provided a brief explanation about vyper language. Currently, vyper is compiled to the Ethereum virtual machine (EVM) Casper, and it is very helpful to save wasteful electricity expenditure [11].

4 Proposed Framework

See Fig. 7.

There are four parts in system architecture which are explained below:

- a. **User:** The person with an address can visit the application browser. The system which is used by a user can be a node. The node is a validated node after satisfying the smart contract. Both publisher and subscriber are user in this application.
- b. **Web-browser:** This is used by publisher and subscriber for transaction or other computational work.
- c. **Frontend:** The frontend part is designed by using HTML and CSS language. It is designed for publisher and subscriber for viewing the Web page.
- d. **Backend:** Blockchain always works on backend part of every system. It is one kind of database which stores all records related to transaction. The Ethereum and smart contract concepts are worked in the backend.

The workflow of marketplace is shown in Fig. 8. Product/object is added by publisher to the network. Publisher is a node of Blockchain. The product/object is purchased by subscriber by paying some Ethereum. The transaction process is validated by smart contract. All the agreement and function are written in smart contract. The smart contract is tested during the process. If it is yes, then transaction is successful; otherwise, it is failed.

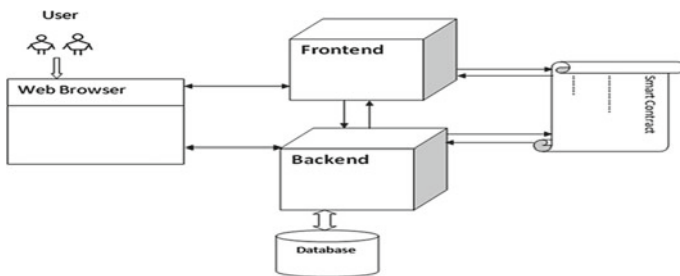


Fig. 7 Implemented system architecture

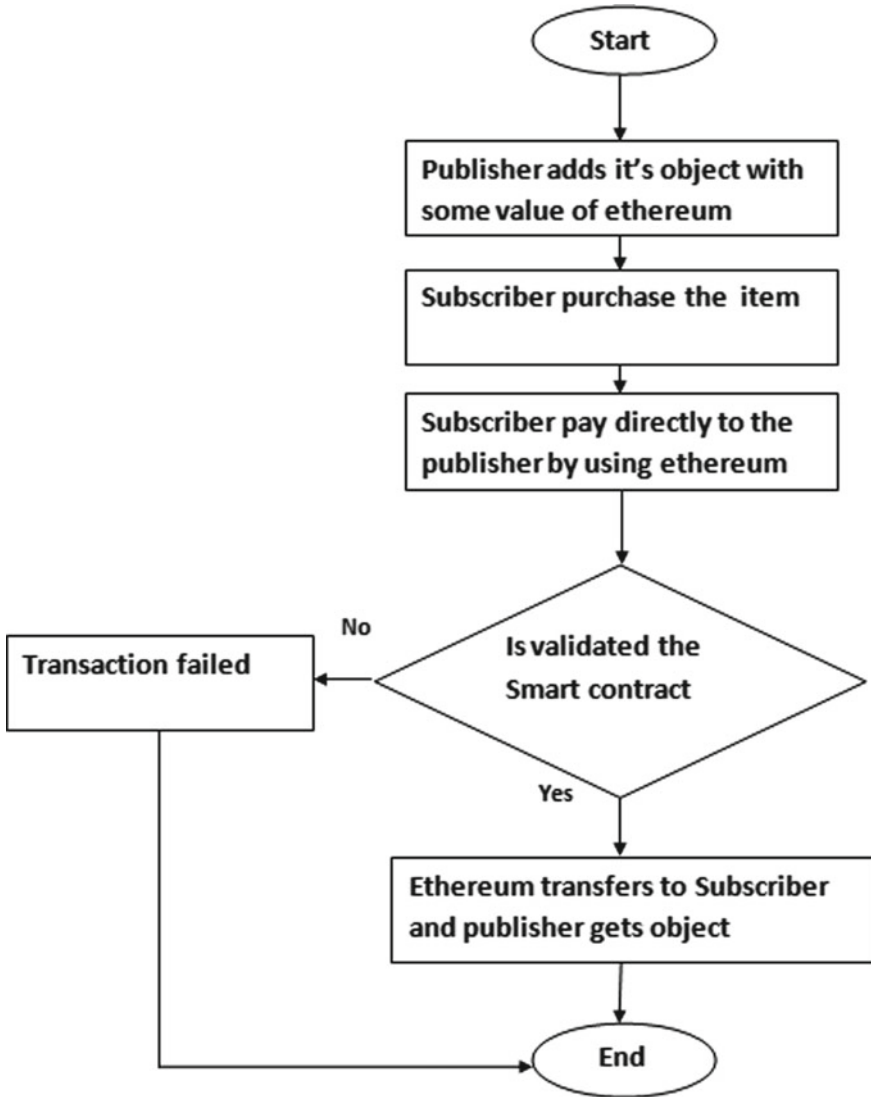


Fig. 8 Workflow diagram for the proposed system implementation

5 Results and Discussions

Ethereum environment can be created by using geth and Node.js tool as explained in Sect. 1.2. Here, all the private keys, ether numbers, and ether addresses are taken from Ganache and added to Metamask [12]. Ganache is an application of Ethereum, where ethers are available for using in projects as shown in Fig. 9. The added configuration of Metamask is shown in Fig. 10. According to system architecture [12], there is a

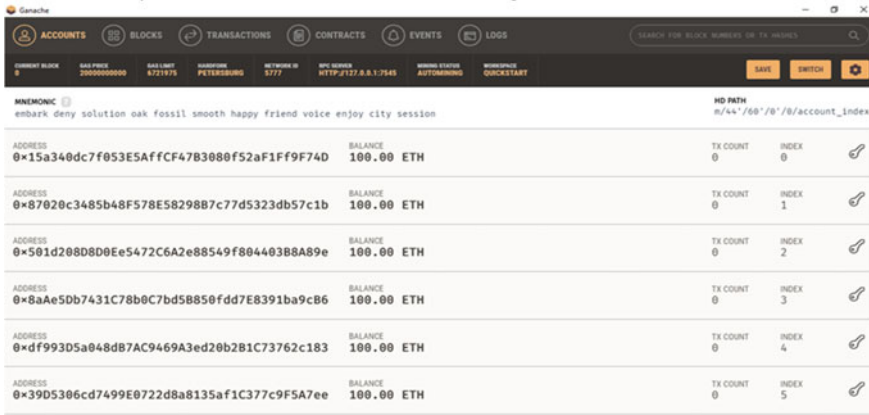


Fig. 9 Visualization of ganache API for available ethers

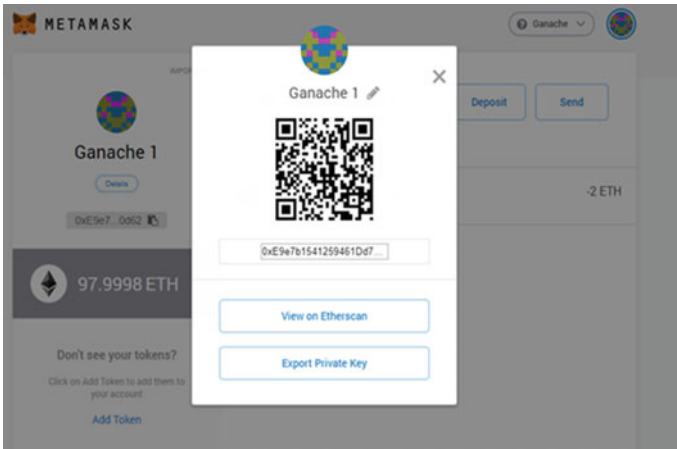


Fig. 10 Generated ether added to metamask application

frontend page which is design by using HTML and CSS which is shown in Fig. 11. While doing the backend setup, you need to create a truffle project environment, where you need to install all packages of Node.js by using command line: npm install -g truffle as shown in Fig. 12. In truffle development environment, genesis block will be created and all details related to block will be shown in your desktop in command prompt as shown in Fig. 13. After deploying the smart contract and passing all the test function in truffle environment successfully, you can enable this Blockchain application. There is a command line “npm run start” which is used in command prompt to start the application. At the time of transaction between publisher (seller) and subscriber (buyer), a Metamasknotification will pop-up due to smart contract. The money transaction is based on ether in this application, and ether

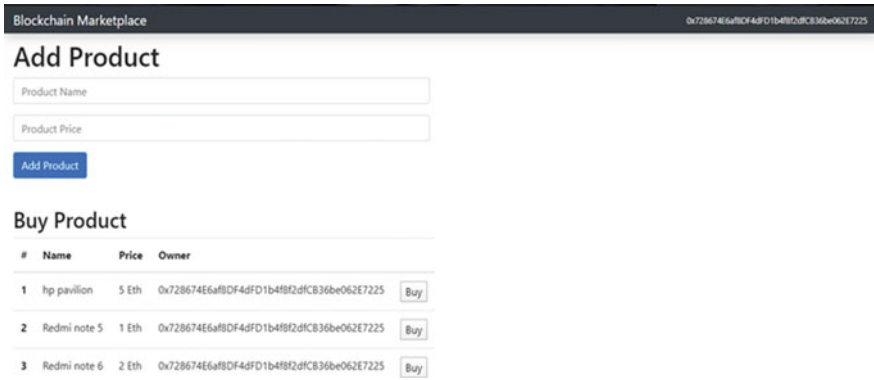


Fig. 11 Frontend for the implemented system of blockchain marketplace

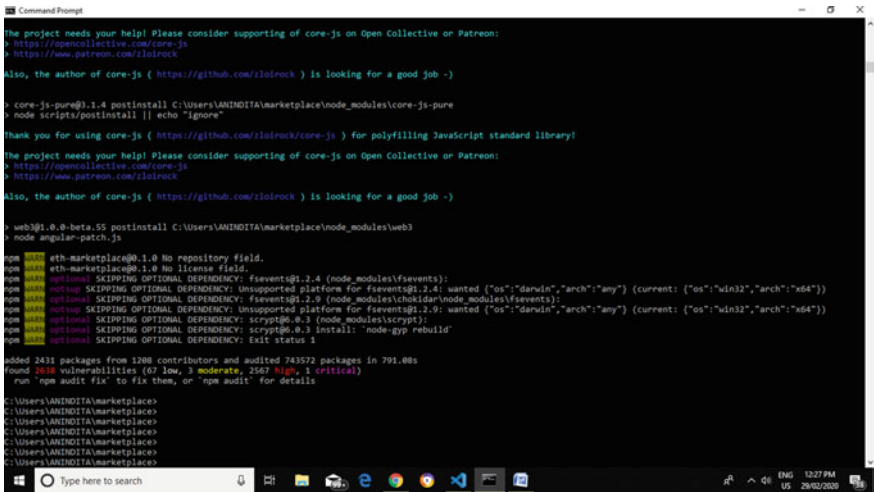


Fig. 12 Procedure for the installing node.js

is automatically generated as settled by the publisher. There must be a gas fee with an ether value as shown in Fig. 14. All the transactions are stored in every node of Blockchain. The records can be mined from any node of Blockchain as shown in Fig. 15.

6 Concluding Remarks

Implementation of Blockchain in webpage application is the prime focus of this paper. So that, the marketplace Web page application is taken here for experiment.

```
Command Prompt
> block number: 1
> block timestamp: 1582966031
> account: 0xe31646093073E3D05ba484D5569FC8a3111f52eb
> balance: 99.99472646
> gas used: 203877
> gas price: 20 gwei
> value sent: 0 ETH
> total cost: 0.00527354 ETH

> Saving migration to chain.
> Saving artifacts
-----
> Total cost: 0.00527354 ETH
-----

1. deploy_contracts.js

Replacing 'Marketplace'
-----
> transaction hash: 0x7721a903891046f895b6dbfd206a4740d35fa2b01d2c3c89bd44c4dad1b1a3
> blocks: 0 Seconds: 0
> contract address: 0xAd01174Df67bfc1E07C8698ad08E5f680da47
> block number: 1
> block timestamp: 1582966038
> account: 0xe31646093073E3D05ba484D5569FC8a3111f52eb
> balance: 99.97573926
> gas used: 907337
> gas price: 20 gwei
> value sent: 0 ETH
> total cost: 0.01814674 ETH

> Saving migration to chain.
> Saving artifacts
-----
> Total cost: 0.01814674 ETH
-----

Summary
-----
> Total deployments: 2
> Final cost: 0.02342028 ETH
```

Fig. 13 Visualization of the content inside the block

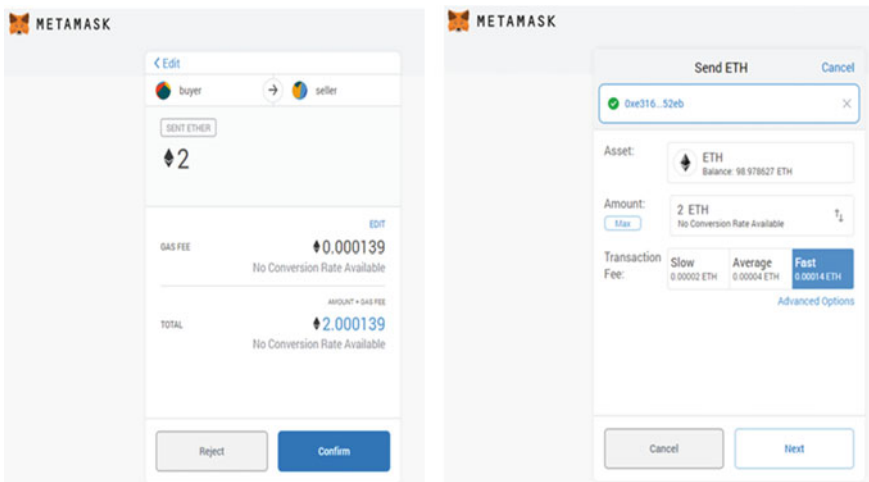


Fig. 14 Transaction occurring in the metamask API

The data can also be mined by every node of Blockchain. This paper also describes how a personal Ethereum environment can be created as well as the code. In future, this paper can be developed by implementing more smart contracts for different units which will be helpful for large marketplace. The efficacy of Blockchain has been shown through the implementation portion where we can realize the difference when no proper and efficient security strategy was involved in marketplace. We focused on the results generated due to the convergence of Blockchain technology

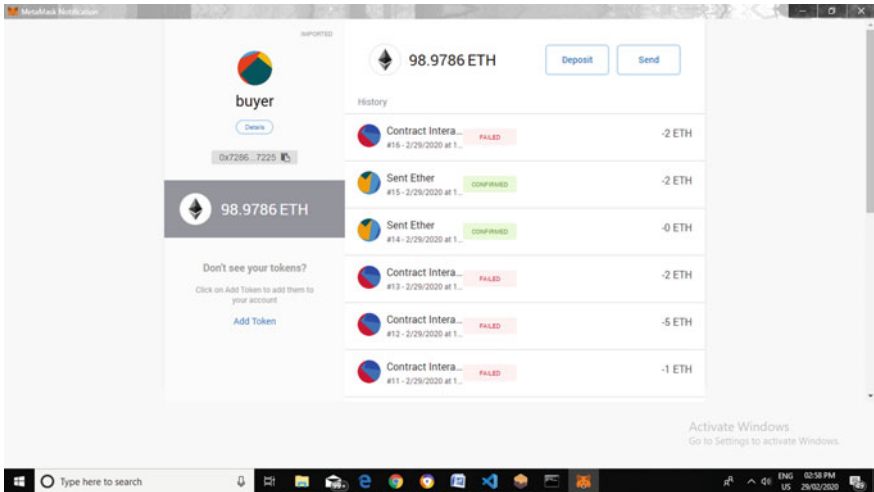


Fig. 15 Process of mining is taking place

in a real-time application. Further research in this direction is extremely necessary in today’s era where security concerns play a key role in diverse sectors. Also, to ensure decentralization in Blockchain, sufficient research with mathematical proofs is necessary.

References

1. Albrecht S et al (2018) Dynamics of blockchain implementation-a case study from the energy sector. In: Proceedings of the 51st hawaii international conference on system sciences
2. Balaji S, Mohan V, Soundarya (2017) Secure and decentralized file transfer application using blockchain
3. Knirsch F, Unterweger A, Engel D (2019) Implementing a blockchain from scratch: why, how, and what we learned. EURASIP J Info Secur 2019(1):2
4. Sestrem Ochôa I et al (2019) PRICHAIN: a Partially Decentralized Implementation of UbiPri middleware using blockchain. Sensors 19.2: 4483
5. Pramod Kumar SMKV, Kiran Kumar K, Sai Krishna R, Aruna Sri PSG (2019) Incorporation of blockchain in student management system. Int J Innov Technol Explor Eng (IJITEE) 2278–3075
6. Nathan S et al (2019) Blockchain meets database: design and implementation of a blockchain relational database. In: Proceedings of the VLDB endowment, vol 12.11, pp 1539–1552
7. Papadodimas G et al (2018) Implementation of smart contracts for blockchain based IoT applications. In: 2018 9th International conference on the network of the future (NOF). IEEE
8. Aldred N et al (2019) Design and implementation of a blockchain-based-consent management system. arXiv preprint [arXiv:1912.09882](https://arxiv.org/abs/1912.09882)
9. Helo P, Hao Y (2019) Blockchains in operations and supply chains: A model and reference implementation. Comput Ind Eng 136:242–251
10. Saxena S et al (2019) Design and field implementation of blockchain based renewable energy trading in residential communities. arXiv preprint [arXiv:1907.12370](https://arxiv.org/abs/1907.12370)

11. Rosu G (2018) Formal design, implementation and verification of blockchain languages (Invited Talk). In: 3rd international conference on formal structures for computation and deduction (FSCD 2018). Schloss Dagstuhl- Leibniz-Zentrum fuer Informatik
12. Nithin M (2018) A blockchain based marketplace build on hyper-ledger. <https://github.com/nithinmurali/Blockchain-Marketplace>
13. Ali G et al (2019) BCON: blockchain based access Control across multiple conflict of interest domains. J Netw Comput. Appl 147:102440
14. Carvalho A (2020) A permissioned blockchain-based implementation of LMSR prediction markets. Decis Support Syst 130:113228
15. Fridgen G, Bernd S, Nils U (2017) Implementation of a blockchain workflow management prototype. ERCIM News 2017.110

Applying Machine Learning Algorithms in Network-Based Intrusion Detection Systems



Nilesh Kumar Sahu and Itu Snigdh

Abstract The growth of computer networks usage with increase in the number of applications running on it has increased the network security concerns. Therefore, the role of Intrusion Detection Systems (IDSs), as special-purpose devices to detect anomalies and attacks in the network, is becoming important. One of the techniques is network intrusion detection systems that provide an array of methods to secure computer systems against network-based attacks. In this paper, we try to present prediction of occurrence of attacks on a network through analyzing different error rates during transfer of data from source to destination. We employ different machine learning models to evaluate the accuracy and prediction of the algorithms.

Keywords Intrusion detection · Machine learning · Anomaly based system · Accuracy · Prediction

1 Introduction

Internet security and breaches have become a prime concern giving rise to research in the field of network security. Network security essentially is an amalgam of policies and practices, adopted to prevent and monitor unauthorized access, misuse, modification, or denial of a computer network and network-accessible resources [1]. Therefore, the role of Intrusion Detection Systems (IDSs), as special-purpose devices to detect anomalies and attacks in the network, is becoming important. The techniques used for intrusion detection systems are anomaly based, misuse based, or signature based [2]. Due to high predictability and accuracy, commercial products adopt misuse-based detection mechanisms [3]. Anomaly based detection is more appropriate for novel attacks when the data patterns is unknown and unpredictable [4]. The literatures show that a lot of research has been done in anomaly detection and

N. K. Sahu (✉) · I. Snigdh
Birla Institute of Technology, Mesra, India
e-mail: mtcs10002.18@bitmesra.ac.in

I. Snigdh
e-mail: itusnigdh@bitmesra.ac.in

have considered various aspects such as learning and detection approaches, training datasets, testing datasets, and evaluation methods. Our task is to build a network intrusion detection system to detect whether there was any anomaly or attacks in the network. There are majorly two problems undertaken in this article, namely:

- Binomial classification: Whether activity is normal or under attack.
- Multinomial classification: Whether Activity is normal or has encountered attacks of the type “DOS” or “PROBE” or “Remote access to Local m/c (R2L)” or “Unauthorized access to Root (U2R).”

Our article focuses on multinomial classification which would not only tells whether the network is normal or not but also would predict the type of abnormality if the network was not normal. For analysis, we consider KDDCUP'99 dataset [5], which is widely used as one of the few publicly available datasets for network-based anomaly detection systems. We have applied machine learning algorithms, namely decision trees, random forest, and XG BOOST to depict the prediction accuracy of the anomaly detection system.

2 Related Work

Among the two methods, namely signature based and anomaly based, the latter presents better prospects. Anomalies or outliers are aberrant observations whose characteristics deviate significantly from the majority of the data or any events that significantly deviate from normal activity are considered to be suspicious [6]. The aim of anomaly detection is to build a normal activity profile for a system. Anomalous activities that are not intrusive are flagged as intrusive, though they are false positives. Actual intrusive activities that go undetected are called false negatives [7]. The anomaly based technique uses statistical methods, cognition models, kernel, and user intention-based data mining models as well as machine learning-based models to name a few in the exhaustive list. There are several literatures on the KDD_99 dataset, which include approaches like fuzzy logic, unsupervised learning models, random forests, and statistical methods [8]. Similarly, fuzzy rough C means (FRCM) integrates the advantages of fuzzy set theory and rough set theory to predict anomalies in the network data [9]. Random forests and data mining algorithm have also been applied in misuse, anomaly, and hybrid network-based IDSs.

3 Proposed Methodology

The dataset description has been followed as expressed in the KDDCUP_99 dataset, wherein the essential features have been summarized in Table 1, and the categories of attacks that we consider in our article have been outlined in Table 2.

Table 2 Attack class

Type	Description	Relevant features
DOS	Depletes the victim’s resources, thereby making it unable to handle legitimate requests, e.g., syn flooding	“Source bytes” and “percentage of packets with errors”
Probing	Gains information about the remote victim, e.g., port scanning	“Duration of connection” and “source bytes”
Unauthorized access to Root (U2R)	Unauthorized access to local super user (root) privileges Uses a normal account to login into a victim system and tries to gain root/administrator privileges by exploiting some vulnerability in the victim, e.g., buffer overflow attacks	“Number of file creations” and “number of shell prompts invoked,”
Remote access to Local (R2L)	Access from a remote machine intrudes into a remote machine and gains local access of the victim machine, e.g., password guessing	“Duration of connection” and “service requested” and host level features —“number of failed login Attempts”

3.1 Steps Followed

Data Transformation

Since machine learning model is mathematical in nature, the model works effectively on numerical data. Hence, we need to transform the nominal data to numerical through one hot encoding method. Separate training set and test set comprising of total 125,974 training data and 21,550 test data were presented to the models. Different machine learning algorithms, namely: Decision Tree, Random Forest, and XGBoost, were used to find the best classification models.

Evaluation criteria

The most important part after applying the classification algorithm was to validate our model for accuracy. The confusion matrix used in this paper to evaluate our model is presented in Table 3.

Formulae used

- (a) Classification rate/accuracy:
- (b) Accuracy = $\frac{TP+TN}{TP+FP+FN+TN}$
- (c) Precision = $\frac{TP}{TP+FP}$
- (d) F_Measure = $\frac{2*Recall*Precision}{Recall+Precision}$
- (e) True Positive Rate : TPR = $\frac{TP}{TP+FN}$
- (f) False Positive Rate : FPR = $\frac{FP}{FP+TN}$

Table 3 Confusion matrix description

Actual Values Predicted values	Event (Positive)	Event did not occur (Negative)
Event (Positive)	True positive	False positive
Event did not occur (Negative)	False negative	True negative

A high value of recall indicates that the class is correctly classified. Precision depicts the degree of correctly predicting the “actual” positive classes out of all the positive classes that have been “correctly” predicted. We use two terminologies as given:

- **High recall and low precision:** This means that most of the positive samples are correctly classified but there are a lot of false positives.
- **Low recall and high precision:** This means that our model missed a lot of positive samples but those we predicted as positive were actually “positive.”

Since it is very difficult to compare two models, having low precision and high recall or vice versa, we use F-score to make them comparable. F-score helps to measure recall and precision at the same time. The true positive rate (TPR) is also called as sensitivity while the false positive rate denoted by TPR is also known as fall out.

4 Results

As we have already discussed about data sampling, two different datasets were considered, and the machine was trained on training data and tested on test dataset. Rather than using the entire dataset, we have considered only the error rates to detect the faults. We try to observe the performance of the considered models when they are subject to a subset of critical parameters in the KDD_99 dataset. We try to analyze whether observing the mentioned parameters are efficient enough to detect network faults, thereby reducing the computational burden on the model developed. The analysis of the models has been done on the basis of the aforementioned parameters as well as the ROC curve. If the area under the curve (AUC) is larger, the model is better. The “steepness” of ROC curves is also very important, since it is ideal to maximize the true positive rate while minimizing the false positive rate.

Figure 1 shows the confusion matrix while Fig. 2 shows the different evaluation criteria. Figure 3 shows the ROC curve, and Fig. 4 shows the accuracy chart for decision tree, random Forest, and XGBoost, respectively.

	0	1	2	3	4
0	5883	130	462	4	2
1	68	9411	232	0	0
2	161	439	1885	33	3
3	0	1751	423	592	19
4	0	5	2	33	12

(a) Decision Tree

	0	1	2	3	4
0	5571	675	234	0	1
1	70	9446	193	2	0
2	121	433	1960	7	0
3	0	2445	116	201	23
4	0	23	0	3	26

(b) Random Forest

	0	1	2	3	4
0	6334	101	46	0	0
1	67	9417	224	3	0
2	168	469	1870	14	0
3	0	2116	309	349	11
4	0	8	0	20	24

(c) XGBoost

Fig. 1 Confusion matrix of decision tree, random forest, and XGBoost

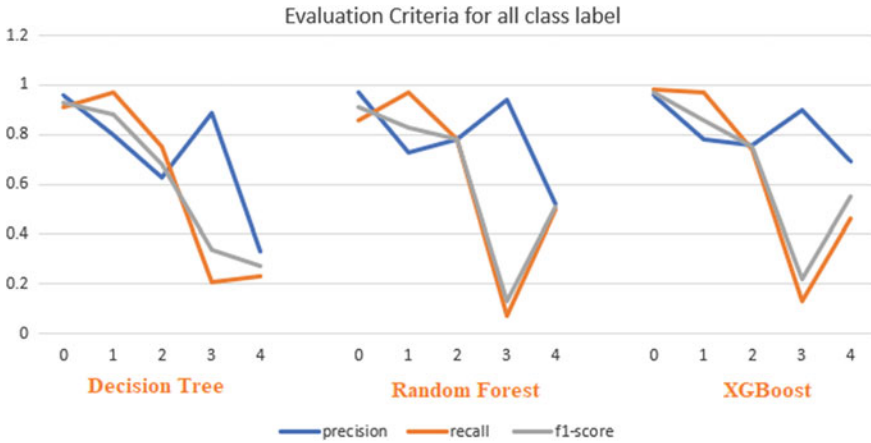
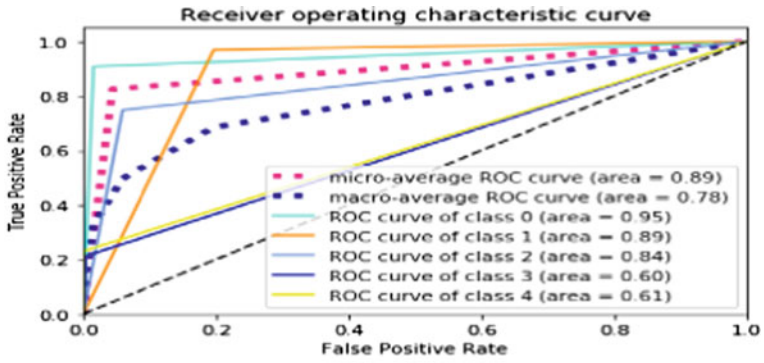


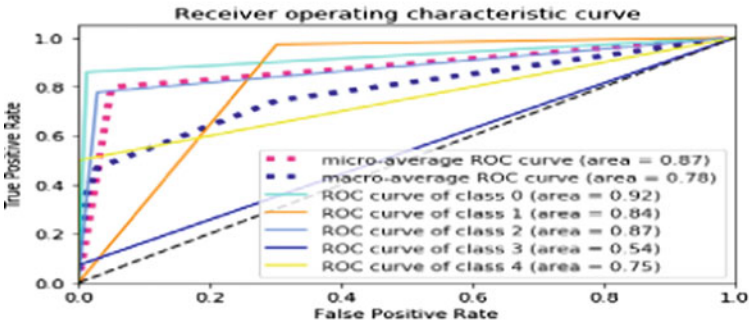
Fig. 2 Evaluation criteria for decision tree, random forest, and XGBoost

5 Conclusion

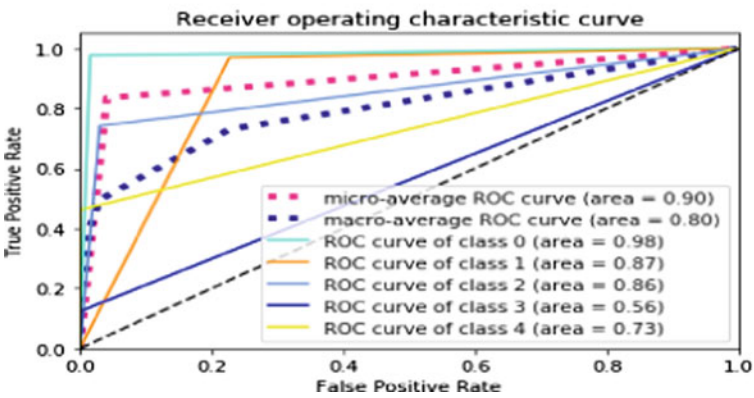
In this paper we obtained that both XGBoost and decision tree achieved the same accuracy rate, i.e., 83%. However, we also show that if we go through F1-score of each class, we can infer that XGBoost outperformed the decision tree in overall



(a) Decision Tree



(b) Random Forest



(c) XGBoost

Fig. 3 a Decision tree, b Random forest, and c XGBoost

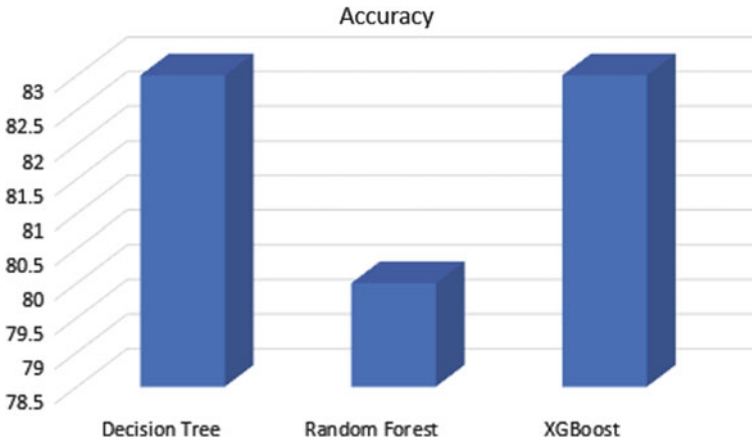


Fig. 4 Accuracy chart

ways. This paper considered all the critical factors in a network which can help us to predict the intrusion and its types. The models developed can be used in real-world networks.

References

1. Bace RG (2000). In: *Intrusion Detection Indianapolis*. In: Macmillan Technical. ISBN 978-1578701858
2. Aydın M, Ali M, Halim Zaim A, GökhanCeylan K (2009) A hybrid intrusion detection system design for computer network security. *Comput Electri Eng* 517–526
3. Sinclair C, Pierce L, Matzner S (1999) An application of machine learning to network intrusion detection. In: *Proceedings 15th annual computer security applications conference (ACSAC'99)*, IEEE, pp 371–377
4. Casas P, Mazel J, Owezarski P (2012) Unsupervised network intrusion detection systems: detecting the unknown without knowledge. *Comput Commun* 35(7):772–783
5. KDDCup (1999) Available-on: <https://kdd.ics.uci.edu/databases/kddcup99/KDDCUP99.html>, 2007
6. Chimphlee W, Abdullah AH, Sap MNM, Srinoy S, Chimphlee S (2006). Anomaly-based intrusion detection using fuzzy rough clustering. In: *2006 international conference on hybrid information technology*, November, vol. 1. IEEE, pp 329-334
7. Mukkamala S, Sung AH, Abraham A (2005) Intrusion detection using an ensemble of intelligent paradigms. *J Netw Comput Appl* 28(2):167–182
8. Jyothsna VVRPV, Prasad VR, Prasad KM (2011) A review of anomaly based intrusion detection systems. *Int J Comput Appl* 28(7):26–35
9. Geramiraz F, Memaripour AS, Abbaspour M (2012) Adaptive anomaly-based intrusion detection system using fuzzy controller. *IJ Netw Secur* 14(6):352–361

Principal Component Analysis in Body Sensor Networks for Secure Data Transmission



Manorama and Itu Snigdh

Abstract With the adoption of Internet of Things, the reconciliation of clinical gadgets and medical treatments' gear has come to pass superior treatments and diagnosis. This would additionally help in remote health monitoring through wearable gadgets and to counsel specialists through associated applications directly. This paper deals with the data collected from various sensors that are connected to a body sensor network and which forward data to destination nodes. With a greater number of sensor data, it is difficult to analyze whether sensor readings are correct or not? Sometimes, this becomes tedious if number of sensors is more. In addition, the data may be corrupt increasing the vulnerability of applications dependent on such data. Hence, the reduction in the dimension of sensors is required for a robust and accurate decision making. This paper presents a principal component analysis for the dimension reduction in sensor networks with the aim to analyze the sensor network data to facilitate secure data transmission.

Keywords Principal component analysis · Body area sensor network · Wearable gadgets · Robust · Security · Clinical gadgets

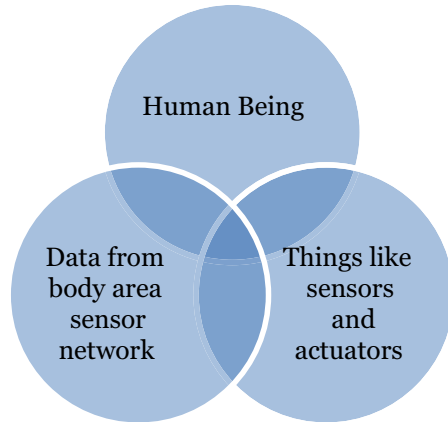
1 Introduction

Internet of Things health care has empowered the cutting-edge advances that are method for the entire business world with remarkable identifiable smart objects interconnected through the Internet. As of late, web foundation is enabled with broadened benefits, for example, network of cutting-edge smart gadgets that improve the situation of Machine-to-Machine (M2M) capacities [1]. Importantly, the Internet of Things speaks about one of the most alluring social insurance applications [2].

Manorama (✉) · I. Snigdh
Department of Computer Science and Engineering, Birla Institute of Technology, Mesra,
Ranchi, India
e-mail: phdcs10071.17@bitmesra.ac.in

I. Snigdh
e-mail: itusnigdh@bitmesra.ac.in

Fig. 1 Components of body area sensor network



Internet of Things and Wireless Body Area Sensor Networks (WBAN) essentially gather and move information utilizing a remote or wired system without needing any human intervention. It could in this manner, oblige numerous applications in clinical fields, for example, elderly care, fitness programs, remote health monitoring, and chronic illnesses.

Figure 1 depicts the major components for such remote monitoring capacities in Wireless Body Area Sensor Networks (WBANs).

Recently, the coronavirus has been declared as a pandemic by the World Health Organization (WHO), raising genuine worries on the wild flare-up. Citizens of various countries such as Singapore, China, USA, UK, Iran, Europe, and India experienced the worst outbreak as it has infected thousands of people. Hence, people who are suffering from these deadly viruses could be remotely monitored by hospital administration with close observation by sensors. Remote clinical sensors could gather different physiological parameters, for example, pulse, heartbeat, oxygen immersion, respiration, and circulatory strain. These sensors are connected to the subject's body and could then be interminably observed in a medical clinic or home.

The data generated by different sensors are enormous in terms of volume, variety, and velocity. For critically analyzing the symptoms, all the data becomes difficult to handle, for which we need to select a few prominent features or components. Principal component analysis is therefore used to reduce the dimension of sensors in order to identify and prioritize the sensor data for relevance in detection of the disease and send it securely on the network.

This paper has been organized into Sect. 2 that describes the security aspects in wireless body area sensor networks, and Sect. 3 illustrates the proposed structure. Section 4 presents the requirements of principal component analysis, with Sect. 5 illustrating the PCA analysis, and Sect. 6 concludes the paper.

2 Security Concerns in Wireless Body Area Sensor Networks (WBANs)

Among the numerous necessities of WBANs, security is the most significant segment. Security parameters that are significant for WBANs are secrecy, realness, accessibility, and honesty [3, 4]. For instance, in the event that we consider a basic use of associated well-being which contains gadgets, for example, an insulin siphon, hacking for wrong organization of the dose could be hazardous [5]. Another issue is that of information protection [6] which as a rule identifies data that should not be openly uncovered. In such cases likewise, the patient's physiological imperative signs are basically observed, particularly if a patient is experiencing an infection, the subtleties of which is not generally proper to uncover. The exposure of such information could make a patient endure mortification. Any breach in the classified information [7] would cause them mental pressure and sometimes cause them to lose their positions. Thus, clinical information should be adequately treated as private. As Internet of Things healthcare technology utilizes handing off data starting with one gadget to the next, it is prone to security ruptures and loss of privacy [8] with respect to the end clients. Other than these potential assaults, certain gadget impediments that influence performance of WBANs are battery life and lightweight computational necessities. Since these works in short range and low data rates, they are very susceptible to attacks and sometimes lack of correct monitoring. The sensors basically collect data under intricate environments, and hence, if not able to show the correct readings, it may create panic among the medical staff unnecessary. This paper presents a simple technique to counter this problem by enabling a check on sensor readings for their authenticity as they work in various ambient. We have implemented a wireless body area network scenario through simulations in NETSIM v11.2 and apply principal component analysis method to reduce the dimensions of multivariate components to a smaller number of components for secure data transmission.

3 Proposed Work

Usually, WBANs comprise of wearable devices that monitor and collect information about ones' physiological condition and activities related to diseases. These wearable health monitoring systems consist of various Micro-Electro-Mechanical Systems (MEMS) sensors and electronic equipment, signal processing units, communication modules (both wireless and wired), and actuators. Also, sensors and electronics require small size, less power consumption and the ability to detect medical signals such as ECG, EEG, PR, and pulse rate. With these sensors, real-time monitoring of a person becomes useful in detection and prediction of diseases, as simple as analyzing posture or as critical as detecting a possible heart attack. For realizing a remote observation facility for patients, WBAN devices that may be used are classified as:

1. Implant node: Nodes placed in human tissue or just below the skin.
2. Body surface node: This is either implanted human body surface or very near (less than 2 cms) the body.
3. External node: Such nodes do not touch human body and are rather placed a few centimeters to or 5 m away from the human body.

The analytical structure depicted in Fig. 2 is simulated in NetSim, and experiments were conducted to evaluate the effectiveness of our PCA-based susceptibility detection. In this simulation, a body area sensor network was established by implanting eleven sensors in a human body. Simulations of 100–500 ms were conducted, and sensory data were collected at the destination node (server). Figure 3 shows the sensors which are connected to a person in remote monitoring phase.

The description of different sensors [9–12] with sensor Ids, which were implanted inside the body and was responsible for collecting the vital information which are illustrated as:

1. **SENSOR ID 1 (SAO₂ SENSOR):** SaO₂ sensor is implanted in tissues of the human cell to find the oxygen label immersion. An SaO₂ sensor estimates oxygen immersion in various tissues.
2. **SENSOR ID 2 (PR SENSOR):** Pressure sensors are implanted inside the human body to measure pressure caused due to inhalation and exhalation in the lungs of the human body.

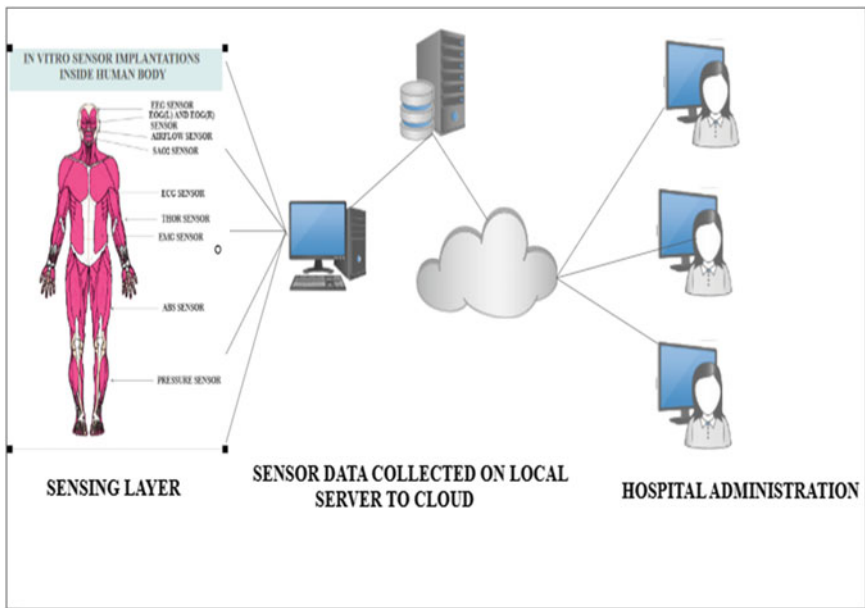


Fig. 2 Sensor data movement in body area sensor network (analytical approach)

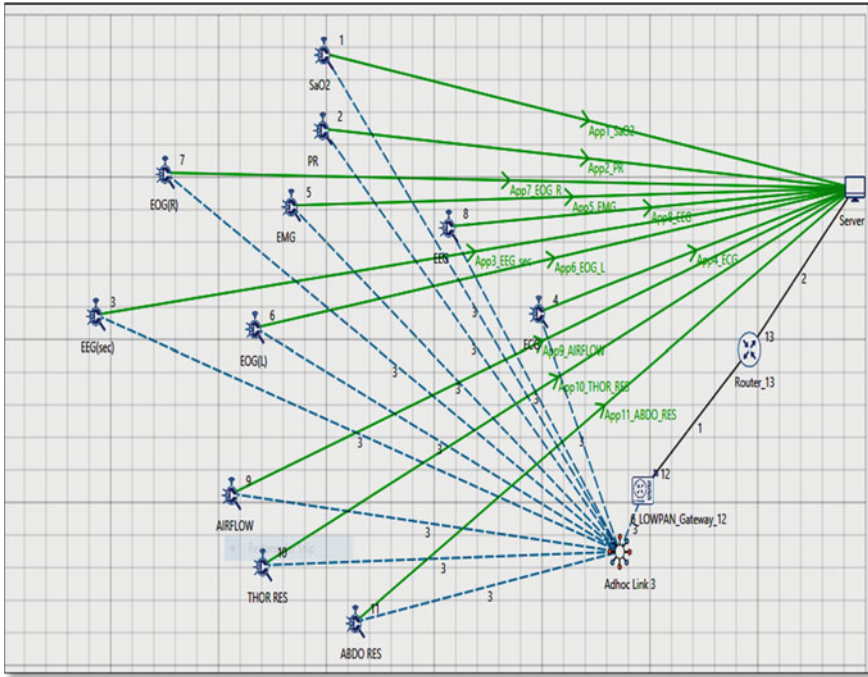


Fig. 3 NetSim simulation of body sensor area network

3. **SENSOR ID 3 (ECG SENSOR):** The Shimmer3 Electrocardiogram (ECG) sensor is implanted to record the pathway of electrical impulses through the heart muscle, and can be recorded on resting and ambulatory subjects, or during exercise to provide information on the heart's response to physical exertion.
4. **SENSOR ID 4 (EMG SENSOR):** Electromyography (EMG) records our muscle movement. In this body sensor network, it is implanted inside of back muscles of the human body.
5. **SENSOR ID 5 and 6 (EEG SENSOR):** Electroencephalography (EEG) is an electrophysiological observing strategy to record electrical activity of the cerebrum.
6. **SENSOR ID 7 and 8 (EOG(R) and EOG(L) SENSOR):** Electrooculography (EOG) is a method for estimating the corneo-retinal standing potential that exists between the front and the rear of the human eye. The subsequent sign is known as the electrooculogram. EOG sensor collects retinal and cornea information of both left and right eyes.
7. **SENSOR ID 9 (AIRFLOW SENSORS):** These sensors use transmitters for measuring air velocity / flow in building automation, pharmaceutical applications or clean rooms.
8. **SENSOR ID 10 and 11 (THOR and ABS Sensor):** ABS sensor detects the livings of a human being by transmitting the rotational information. Thor sensor

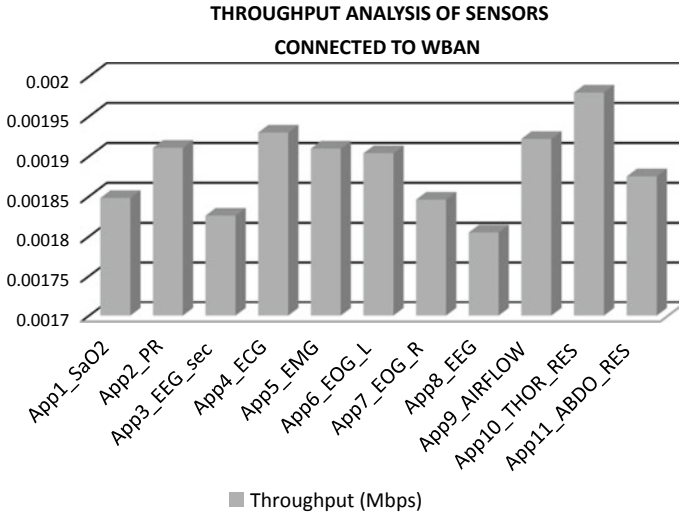


Fig. 4 Throughput analysis of eleven sensors by NetSim simulation

is basically a thermal sensor which measures temperature. It is a passive infrared sensor which detects the presence of a human body by sensing through thermal sensations.

Since there are eleven body sensors are connected together to establish this network, throughput analysis in real time is shown in Fig. 4.

4 Principal Component Analysis

Principal components analysis, or PCA, is basically a data analysis tool capable of reducing the dimensionality (number of variables) of a large number of variables which are interrelated, while holding the basic information (variation) as possible. Principal component analysis is used for calculating an uncorrelated set of variables (components or pc's) [13]. These components are ordered so that the first few retain most of the variation present in all of the original variables.

The basic equation of PCA is, in matrix notation, given by:

$$Y = W'N \tag{1}$$

where “W” may be a matrix of coefficients that has to be determined by PCA with “N” as the number of dimensions.

For the present wireless body sensor network scenario, there are eleven sensors which are responsible for secure data transmission. Hence, these sensors are considered as the features or components for principal component analysis.

4.1 Steps for Calculating PCA

1. The dataset has to be standardized.
2. Create a covariance matrix using the standardized data.
3. Calculate eigenvectors (principal components) and their corresponding eigenvalues by using the resulting matrix.
4. Components are to be sorted in descending order by its eigenvalue.
5. Choose the most variance within the data out of N components which is having better eigenvalue (the largest eigenvalue means the feature explains more variance).
6. The new matrix is created by using the N components.

Usually, sensory information has high spatial and fleeting connections which make PCA a necessity for data reduction in sensor systems. PCA was applied on a lot of perceptions of one variable in every sensor or a lot of sense together, the way that current body area sensor network applications [14, 15] gather multivariate information, for example, temperature sensor, pressure sensor, air flow sensors, Thor sensor, or ABS sensors. These sensors work in very extreme conditions, such as a **Sa_o2** sensor may show erroneous data in high pressure or vice versa. Similarly, in high temperature, ECG or EEG data may be high or low. So, to observe the correctness of the sensor readings, we need to keep a check on these sensor's data. Since we have eleven sensors implanted inside a body area network [16], it is really a tedious task to check each and every sensor reading's all the time. So we have to reduce the dataset of the sensor by principal component analysis for secure and non-erroneous data transmission.

5 PCA Result Analysis

Figure 5 depicts the dimension reduction graph of PCA in wireless body sensor networks. In this graph, we have considered ten features. In this context, features/components respond to individual sensor IDs. This curve corresponds to the variance. The sharpness of the curve is leading to a bend at **fifth (5th)** sensor. This results in concluding that there are five principal components in this body area sensor network, which are **PC1-Sa02 sensor, PC2-pressure sensor, PC3-ECG sensor, PC4-EEG sensor, and PC5-EMG sensor** (PC stands for principal component), out of ten different body sensors. Data sensed/read by these five principal components are to be sensed first in adverse conditions of the network. Sensors

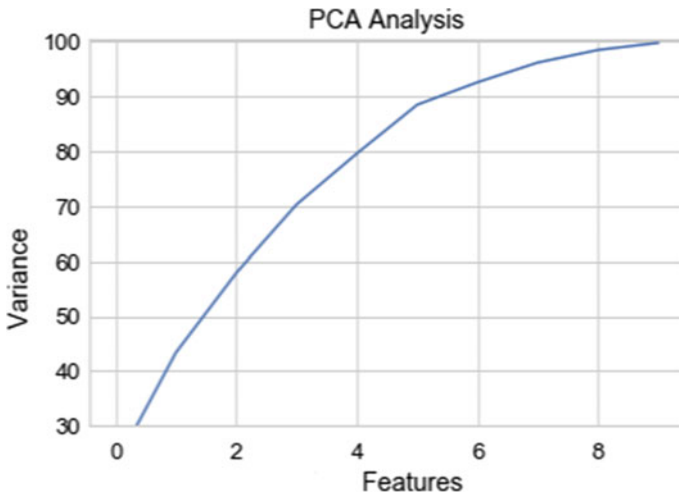


Fig. 5 PCA curve of WBAN with ten features

are also responsible; if any attack or anomaly happens in the body sensor network, then these sensors are to be sensed first and reading must be checked in a low pan gateway as these are principal component. These five principal components are also responsible for secure data transmission to a sink node/low pans gateway.

The time complexity of principal component analysis of the wireless body area sensor networks is equal to $O(n^2)$. This represents that PCA analysis is valid for equal to or less than the total number of components. Hence, this analysis is valid for less than or equal to ten (10) features (as we have ten sensors for analysis) as principal components. Comparative analysis with other feature selection algorithms may be practiced as a future work to this application.

6 Conclusion

Dimension or sensor information decrease can be viewed as a technique for a safe and effective information transmission since it lessens the energy utilization brought. PCA ends up being a vigorous information decreasing technique in multivariate information investigation. At sink/destination nodes, the diminished information is approximated to get the first information with insignificant estimate mistake. Since corona outbreak has become life threatening, hence safe and secure information transmission through body network has become utmost essential in remote monitoring. Therefore, we can conclude that principal component analysis reduces the risk of false/inaccurate data transmission in body sensor network.

References

1. Sethi S, Sahoo RK (2020) Design of WSN in real time application of health monitoring system. Breakthroughs in Research and Practice. IGI Global, Virtual and Mobile Healthcare, pp 643–658
2. Gope P, Hwang T (2015) BSN-Care: a secure IoT-based modern healthcare system using body sensor network. *IEEE Sens J* 16(5):1368–1376
3. Chen M et al (2011) Body area networks: a survey. *Mobile Netw Appl* 16.2: 171–193
4. Halperin D et al (2008) Security and privacy for implantable medical devices. *IEEE Pervasive Comput* 7.1: 30–39
5. He D et al (2015) Robust anonymous authentication protocol for health-care applications using wireless medical sensor networks. *Multimedia Syst* 21.1: 49–60
6. Chen S-L et al (2007) A wireless body sensor network system for healthcare monitoring application. In: 2007 IEEE biomedical circuits and systems conference. IEEE
7. Yuce MR (2010) Implementation of wireless body area networks for healthcare systems. *Sens Actuators A* 162(1):116–129
8. Manorama, Snigdh I (2019) Anonymity in body area sensor networks-an insight. In: 2018 IEEE World symposium on communication engineering (WSCE). IEEE
9. Dinis H, Mendes PM (2017) Recent advances on implantable wireless sensor networks. In: *Wireless sensor networks-insights and innovations 2017* October 4. IntechOpen
10. Majumder S, Tapas M, Deen M (2017) Wearable sensors for remote health monitoring. *Sensors* 17.1: 130
11. Milenković A, Otto C, Jovanov E (2006) Wireless sensor networks for personal health monitoring: Issues and an implementation. *Comput Commun* 29.13–14: 2521–2533
12. Darwish A, Hassanien AE (2011) Wearable and implantable wireless sensor network solutions for healthcare monitoring. *Sensors* 11.6: 5561–5595
13. Das A, Nirmala SR (2017) Wavelet and PCA based ECG compression. *Signal Process* 2:15
14. Hill DJ, Minsker BS (2010) Anomaly detection in streaming environmental sensor data: a data-driven modeling approach. *Environ Model Softw* 25(9):1014–1022
15. Rassam MA, Anazida Z, Maarof MA (2015) Principal component analysis-based data reduction model for wireless sensor networks. *Int J Ad Hoc Ubiquitous Comput* 18.1–2: 85–101
16. Ghadban N et al (2014) Strategies for principal component analysis in wireless sensor networks. In: 2014 IEEE 8th sensor array and multichannel signal processing workshop (SAM). IEEE

Quantum Inspired Multiobjective Optimization in Clustered Homogeneous Wireless Sensor Networks for Improving Network Lifetime and Coverage



Pradeep Kanchan, D. Shetty Pushparaj, and Baraá A. Attea

Abstract The optimization technique in which many objectives are simultaneously optimized is called multiobjective optimization. A wireless sensor network (WSN) consists of many sensors forming a network. These sensor nodes mainly run on battery which deteriorates with time. Our aim is to optimize coverage and lifetime of the network. One of the most effective methods for minimizing energy and increasing lifetime of nodes is clustering. In this paper, we integrate the two objectives of improving network lifetime and increasing coverage. We use quantum bits or qubits in our representation instead of bits. A qubit can be in 0 state, 1 state or a super position of these two states at the same time. This is what makes quantum computing-based algorithms more powerful as we can have more diversity. The proposed algorithm, quantum inspired multiobjective evolutionary algorithm based on decomposition (QMOEAD) is compared with LEACH, SEP, NSGAI and MOEA/D on the basis of coverage and network lifetime. The results show that QMOEAD outperforms the other algorithms mentioned above.

Keywords Quantum computing · Multiobjective optimization · Network lifetime · Coverage · Clustering

P. Kanchan (✉)

Department of Computer Science and Engineering, NMAMIT, Nitte, Nitte, India
e-mail: pradeepnitk2015@yahoo.com

D. S. Pushparaj

Department of Mathematical and Computational Sciences, NITK, Surathkal, India
e-mail: prajshetty@nitk.edu.in

B. A. Attea

Department of Computer Science, University of Baghdad, Baghdad, Iraq
e-mail: bara.a@sc.uobaghdad.edu.iq

1 Introduction

Wireless sensor networks (WSN) are increasingly being employed in diverse fields like military operations, agriculture, traffic control, etc. Since the sensors are deployed in hostile environments, it may not be possible to replace them whenever required. Therefore, energy conservation becomes important.

Clustering is a very effective strategy for energy efficiency in a WSN. In clustering, the cluster head (CH) gathers data from nodes which are forwarded to a base station (BS). Sometimes the network may need to monitor a large area and give information from any part of the monitored area. Then, we can say that the area is being ‘covered’ by the sensors. The nodes which are being covered are called targets. Each node can cover a certain number of targets. Our objective is to cover as many targets as possible. Optimizing the energy consumed in the network leads to optimized lifetime of the network, which is another objective of our work.

Very few works exist which simultaneously consider routing via clusters and target coverage. Multiobjective optimization enables us to consider the two objectives of energy conservation using clustering and target coverage at the same time. One of the well quoted works on multiobjective optimization [1] explains multiobjective problems as those where we have to simultaneously optimize k objective functions. Here, optimization may refer to minimizing all the functions, maximizing all the functions or a combination of minimizing and maximizing all the functions. Multiobjective evolutionary algorithms (MOEAs) are used for dealing with WSN related design problems. Multiobjective optimization (MOO) in case of WSNs may involve optimizing parameters like target coverage, connectivity of the network, lifetime of the network, network energy, etc. [2]. An evolutionary multiobjective crowding algorithm (EMOCA) is discussed in [3]. This manages to strike a balance between dominance and diversity as far as population is concerned. The hybrid MOEA [4] discusses optimizing lifetime and coverage treating them as multiple objectives to be optimized at the same time.

Quantum computing algorithms have been used for optimizing WSN. In [5], a quantum adaptation of artificial bee colony (ABC) algorithm is used for optimizing the energy consumption in WSN. The work by [6] uses quantum ant colony optimization (ACO) and improves target coverage. In [7], quantum particle swarm optimization (PSO) improves energy efficiency in a clustered WSN. In [8], a scheme is developed for optimal coverage using quantum PSO.

As per our knowledge, none of research has explored the possibility of using quantum computing with MOEA/D for solving coverage and lifetime problems in WSNs. Our paper is concerned with developing a quantum inspired MOEAD for energy efficient coverage of targets in a WSN which also improves the network lifetime.

The following are our contributions:

- Representing the WSN using quantum bits/qubits representation.
- Developing a quantum inspired MOEAD for energy conservation and coverage which also improves the network lifetime. We call this algorithm QMOEAD.

- Comparing our algorithm with LEACH, SEP, NSGA II and MOEAD.

The organization of the paper is given below. Section 2 contains a review of the related work. Section 3 explains our algorithm: the quantum inspired MOEAD (QMOEAD). Section 4 contains the experimental results. Section 5 contains the conclusion and future directions for research.

2 Related Work

2.1 Coverage

In [9], a novel scheme is introduced where nodes are divided into disjoint sets in such a way that every set monitors all the targets. At one particular instance of time, only one set is active. The currently active sensors monitor and transmit the data collected while nodes from other sets are said to be in a sleep mode which requires low energy. In [10], a scheme for scheduling is proposed by which a node can be either in an active mode or in sleeping mode. This is done based on information regarding coverage got from the neighbouring nodes. In [11], the protocol makes sure that only some sensors are working while the others are in a non-working or sleeping mode. At random intervals, these sleeping nodes wake up to check if any nodes have failed and need to be replaced. The optimal geographical density control (OGDC) algorithm is proposed in [12] which achieves connectivity and coverage while minimizing the number of nodes.

2.2 Energy Consumption

The widely quoted [13] proposes an algorithm for energy consumption: the low energy adaptive clustering hierarchy (LEACH). Here, a single node becomes a cluster head (CH) with the probability p , and it will broadcast this decision. Those nodes which are not CH determine the cluster they want to belong to based on which CH can be reached with the least energy. In [14], stable election protocol (SEP) is proposed. They introduce a term stability period defined as the time till the death of the first node. There are two types of nodes—the normal ones and the advanced ones (having extra energy). Selection of CH is done in random, based on the energy available in a node. The genetic algorithm (GA) is used in [15] to select CHs while minimizing the network distance. Here, a bit sequence of 0's and 1's is used where each bit represents a node. If the bit is 1, it is a CH; else, it is a normal node. A hierarchical cluster-based routing (HCR) algorithm is proposed in [16]. Here, the nodes are organized into clusters with each cluster being managed by a set of associate nodes, the headset nodes. Each of these associate nodes act as CH at different points using round robin technique. These clusters are in existence for a longer duration. The harmony search

algorithm (HSA) based on music is proposed in [17] for optimization in WSN. This algorithm is successful in optimizing both the distance between clusters and the energy consumption. The energy aware evolutionary routing protocol (EAERP) [18] is based on evolutionary computing. The algorithm yields better results than LEACH, SEP and HCR.

2.3 Energy Conservation and Coverage

The energy aware and coverage preserving hierarchical routing (ECHR) protocol is proposed in [19]. One CH is selected for each round of the algorithm. Other nodes transmit data using multi-hop communication. This algorithm succeeds in both conserving energy as well as maintaining coverage. The techniques discussed in [20] concentrate on those applications in which full network coverage is desired. Their work substantiates that using the sensors with low remaining energy and minimizing usage of sensors in areas which are not densely covered (sparse) will improve the coverage time.

2.4 Multi Objective Optimization (MOO)

The multiobjective optimization (MOO) technique is explained in [1]. In MOO, optimization refers to coming up with a solution consisting of objective functions which can be accepted by a decision maker. It differs from single objective optimization where our aim is to maximize or minimize the objective function. A general multiobjective problem (MOP) can be defined as:

$$\text{Minimize/Maximize } F(x) = (f_1(x), f_2(x), \dots, f_n(x)) \text{ subject to } x \in \Omega \quad (1)$$

where x is the decision variable, $F: \Omega \rightarrow R^n$ denotes objective functions which are n in number, Ω denotes the search space and R^n denotes the objective space. In MOPs, we want to find good enough solution/solutions unlike global optimization where we look for a single solution. Usually, the term Pareto optimum is used to denote such situations. The non-dominated sorting genetic algorithm (NSGA) for multiobjective optimization is proposed in [21]. The non-dominated solutions are those which are superior solutions when compared to all the objectives in search space but inferior to solutions in the space as far as one or more objectives is concerned. The NSGA differs from the usual GA in that before selection, a ranking is done for the population based on the non-domination of an individual. The NSGA has been improved by [22] who proposed the NSGA II algorithm. The multiobjective evolution algorithm based on decomposition (MOEA/D) is proposed in [23]. Here, the MOP is split into smaller problems, and these smaller problems are optimized all at the same time.

The MOEAD in [24] performs optimization of multiple objectives for a WSN—maximizing network lifetime and maximizing coverage. It proved to be better than LEACH, SEP and NSGA II.

2.5 Quantum Inspired Algorithms for WSN

The quantum artificial bee colony (ABC) algorithm [5] optimizes the consumed energy. The comparison of results with LEACH and the standard ABC shows the superiority of the algorithm. Here, the population consists of quantum bits. A particle swarm optimization (PSO) algorithm inspired by quantum computing for energy efficiency in clustered WSNs is proposed in [7]. The algorithm makes sure minimum energy is consumed as compared to LEACH and PSOECHS [25]. The quadrivalent quantum inspired GSA (QQIGSA) is proposed in [26] to be used in precision agriculture. The results show that it is superior to the binary genetic algorithm (BGA) and binary PSO (BPSO).

3 Quantum MultiObjective Evolutionary Algorithm with Decomposition (QMOEAD)

The proposed algorithm, QMOEAD, is developed for cluster-based routing in WSNs. The issues of network lifetime and coverage are treated as the multiple objectives. Our aim is to minimize the energy consumed (which leads to increased lifetime) and increase the area covered / coverage. We use the MOEA/D as in [24]. They are assuming a square field for monitoring. There is a base station (BS) with (x_{BS}, y_{BS}) as its coordinates, a set of m sensor nodes (s_1, s_2, \dots, s_m) with the set $((x_{s1}, y_{s1}, r_{s1}, E_{s1}), \dots, (x_{sm}, y_{sm}, r_{sm}, E_{sm}))$ denoting the locations (x, y) , the radii of coverage r_s and the initial energies E_s of the m nodes.

The set (d_1, \dots, d_l) denotes the l targets with locations $((x_{d1}, y_{d1}), \dots, (x_{dl}, y_{dl}))$.

We can say that we have achieved efficient coverage if every target is covered by a minimum of one sensor, and network lifetime is optimized. We want to optimize coverage area and lifetime of network.

The MOEA/D for the routing protocol is defined as

$$\text{MOEA}/D = (I, \Phi, \Gamma, \psi, l, N, EP, \phi) \tag{2}$$

where I is the individual space. An individual consists of a bit string of size m , which denotes how many nodes are there in the WSN. The bits of each gene can be any of the following: -1 in case of a dead node, 0 in case of inactive node, 1 for a non-CH node and 2 for a CH node.

We can specify the population of N individual solutions $IP = (I_1, \dots, I_N)$ as

$$\forall i \in (1, \dots, N) \text{ and } \forall j \in (1, \dots, m), \tag{3}$$

$$I_{i, j} = \begin{cases} -1 & \text{if } E(s_j = 0) \\ 0 & \text{if } E(s_j > 0) \text{ with } s_j \text{ Inactive} \\ 1 & \text{if } E(s_j > 0) \text{ with } s_j = \text{NonCH} \\ 2 & \text{if } E(s_j > 0) \text{ with } s_j = \text{CH} \end{cases} \tag{4}$$

We are considering only a homogeneous network. During the rounds of the protocol, dynamic number of CHs are formed. Initially, we form a random population. Some assumptions are:

- The probability of an alive node becoming active or inactive is equal
- According to [14], an active advanced node becomes a CH with a probability:

$$p_{adv} / (1 - p_{adv} * (r \bmod 1 / p_{adv}))$$

An active normal node becomes CH with the probability

$$p_{nrm} / (1 - p_{nrm} * (r \bmod 1 / p_{nrm}))$$

Here,

$$p_{adv} = ((P_{opt} * (1 + \alpha)) / (1 + \alpha * \text{Advanced nodes percentage})).$$

$$p_{nrm} = ((P_{opt}) / (1 + \alpha * \text{Advanced nodes percentage})).$$

The optimal election probability used as in LEACH [13] is:

$$P_{opt} = K_{opt} / m.$$

where m = Number of nodes in the network.

K_{opt} = Optimal number of clusters given by

$$K_{opt} = \sqrt{\frac{m}{2\pi}} \frac{2}{0.765}$$

$\Phi: I \rightarrow R^2$ is used to denote that the objective function vector consisting of E , the energy consumed and NC, the number of Uncovered targets, has to be minimized. E consists of the energies used up for transmission, receiving and aggregation of signals [18].

The total energy for activation of sensor is

$$E(I) = \left(\sum_{i=1}^{nc} \sum_{s \in ci} E_{TXs, CHi} + E_{RX} + E_{DA} \right) + \left(\sum_{i=1}^{nc} E_{TXCHi, BS} \right) + \text{Tot } AE \tag{5}$$

Here, nc denotes how many CHs are active.

$s \in c_i$ denotes the active non-CHs which are linked to the i th active CH.

E_{TXn_1, n_2} is the energy required for transmission of data from node n_1 to node n_2 .

E_{RX} is the energy for receiving data.

E_{DA} is the energy for aggregating the data

$$E_{TXn_1, n_2} = \begin{cases} E_{elec}^* l + \varepsilon_{fs}^* l^* d(s_1, s_2)^2 & \text{if } d < d_0 \\ E_{elec}^* l + \varepsilon_{mp}^* l^* d(s_1, s_2)^4 & \text{if } d \geq d_0 \end{cases} \quad (6)$$

$$E_{RX} = E_{elec}^* l \quad (7)$$

The total activation energy, TotAE, for CH and non-CH nodes activated during a particular round is given by

$$\text{Tot } AE = \sum_{i=1}^{nc} AE * a_i + \sum_{s \in c_i} AE * a_s \quad (8)$$

where

$$a_i = \begin{cases} 1 & \text{if sensor}_i \text{ will be activated during current round} \\ 0 & \text{Otherwise} \end{cases} \quad (9)$$

AE is the activation energy of each node.

An objective function, NC , is defined to minimize number of uncovered targets

$$NC(I) = \sum_{i=1}^m \text{Uncovered}(\text{target}_i) \quad (10)$$

Here,

$$\begin{aligned} & \text{Uncovered}(\text{target}_i) \\ &= \begin{cases} 0 & \text{if } \exists s \in \text{sensor active, } d(s, t_i) \leq r_s \\ 1 & \text{Otherwise} \end{cases} \end{aligned} \quad (11)$$

$d(s, t_i)$ denotes the distance between sensor node s and target t_i .

The set Γ consists of the operators used in a GA like crossover, mutation and selection and is defined as below:

$$\Gamma = (c_{\Theta c}, m_{\Theta m}, s_{\Theta s}, I_{c_{\Theta c}}, m_{\Theta m}, s_{\Theta s, I}^N \rightarrow I^N) \quad (12)$$

The crossover and mutation operators can modify the routing solutions.

p_c is a fraction of the pairs of parents of the population chosen for recombination. For every pair of the parents, two points of crossover r_1 and r_2 are selected randomly from the set $(1, \dots, m-1)$. The parents I_1 and I_2 are exchanged at the bit positions between these points. Each new string of bits is also mutated with a probability of p_m . During mutation, 0 is converted into 1 or 2, 1 is converted into 0 or 2, and 2 is converted into 0 or 1. The -1 s are not converted. The generation updation is denoted by:

$$\psi : EP \rightarrow EP'$$

This is the updation of current external population (EP) by removal and/or addition of dominated and/or non-dominated solutions, also applying Γ to the current I^N . The criteria for terminating the MOEA/D is:

$$1 : I^N \rightarrow \{\text{true, false}\}$$

For starting the next round of routing,

$$\Phi : EP \rightarrow I^*$$

Is used. This selects a solution I^* from the EP . The solution which spends minimum energy for performing required coverage is selected. It then decodes it into a clustered solution $\forall i \in \{1, m\}$,

$$s_i = \begin{cases} \text{Dead if } I_i^* = -1 \\ \text{Inactive if } I_i^* = 0 \\ \text{Non CH if } I_i^* = 1 \\ \text{CH if } I_i^* = 2 \end{cases} \quad (13)$$

The above equations explain how MOEA/D is implemented for a WSN represented in the form of bits.

In our work, we create a *quantum population* of bits for representing the WSN state. A qubit may be in '0' state, '1' state or a superposition of these 2 states. Its state can be derived from:

$$|\psi\rangle = \alpha|0\rangle + \beta|1\rangle \quad (14)$$

where α and β represent the probability amplitudes of the corresponding states. $|\alpha|^2$ is the probability of the qubit being in '0' state, and $|\beta|^2$ is the probability of the qubit being in '1' state.

$$|\alpha|^2 + |\beta|^2 = 1 \quad (15)$$

A quantum gate changes the state of the qubit. We have used rotation gate in our work. We can write the Q bit string of m bits as a quantum matrix:

$$\begin{bmatrix} |\alpha_1\rangle & |\alpha_2\rangle & \dots & |\alpha_m\rangle \\ |\beta_1\rangle & |\beta_2\rangle & \dots & |\beta_m\rangle \end{bmatrix} \quad (16)$$

where

$$|\alpha_i|^2 + |\beta_i|^2 = 1, \quad i = 1, 2, 3, \dots, m \quad (17)$$

The rotation gate we have used is

$$U(\Delta\theta_i) = \begin{bmatrix} \cos(\Delta\theta_i) & -\sin(\Delta\theta_i) \\ \sin(\Delta\theta_i) & \cos(\Delta\theta_i) \end{bmatrix} \quad (18)$$

where $\Delta\theta_i, i = 1, 2, 3, \dots, m$ is a rotation angle of each qubit towards either 0 or 1 depending on the sign.

4 Experimental Results

We compare QMOEAD with LEACH, SEP, NSGAI and MOEA/D. We evaluate with respect to number of nodes alive and number of covered targets which we optimize during the rounds of the algorithm. MATLAB R2019a is used for implementing the simulation. We conducted the experiments with 10 WSNs, each containing 100 sensors and 50 targets in an area of $100 \times 100 \text{ m}^2$. We have assumed homogeneous nodes. The details of the radio model used are given below:

E_{elec} , the energy dissipated per bit has the value 20nJ/bit. E_0 , which is initial energy of node has the value 0.1 J. ε_{fs} , the free space energy has the value 10 pJ/bit/m². ε_{mp} , the multipath energy has the value 0.0013 pJ/bit/m⁴. EDA, the energy for data aggregation has the value 5 nJ/bit/report. The sensing radius is 10. The activation energy is $5.0e^{-09}$. The message size, l , is 4000 bits.

The evolutionary components used are listed below:

The value of p_c , the crossover probability, is 0.6. The value of p_m , the mutation probability, is 0.03. The population size, N , is 20. The number of generations, gen_{max} , is 20. EDA, the energy for data aggregation is 5 nJ/bit/report. The neighbourhood size, T , is 4.

Table 1 shows the experimental results of comparison with respect to nodes alive after a number of rounds. The number of nodes alive becomes 0 only after round 375 in case of QMOEAD, whereas in case of the other algorithms, it happens earlier.

Table 2 shows the experimental results of comparison with respect to targets covered after a number of rounds. As can be seen from the table, the number of

Table 1 Comparison of nodes alive after no. of rounds

Rounds	Alive nodes LEACH	Alive nodes SEP	Alive nodes NSGA II	Alive nodes MOEAD	Alive nodes QMOEAD
25	100	100	100	100	100
50	100	100	100	100	100
75	96.6	96.2	99.6	100	100
100	8.8	8.4	97.4	100	100
125	4	6.6	80.3	100	100
150	0	0	75.66	98.78	100
175	0	0	23.56	87.89	100
200	0	0	0.7	34.89	99.76
225	0	0	0	8.78	90.34
250	0	0	0	1.56	68.46
275	0	0	0	0	54.35
300	0	0	0	0	23.86
325	0	0	0	0	1.77
350	0	0	0	0	0.35
375	0	0	0	0	0

Table 2 Comparison of targets covered after no. of rounds

Rounds	Targets covered LEACH	Targets covered SEP	Targets covered NSGA II	Targets covered MOEAD	Targets covered QMOEAD
25	50	50	50	50	50
50	50	50	50	50	50
75	50	50	50	50	50
100	25	27.4	50	50	50
125	10	13	49.5	50	50
150	0	0	40.12	49.8	50
175	0	0	37.78	49.56	50
200	0	0	0.67	38.67	49.9
225	0	0	0	14.44	40.67
250	0	0	0	2.45	35.98
275	0	0	0	0	23.56
300	0	0	0	0	12.87
325	0	0	0	0	2.56
350	0	0	0	0	0
375	0	0	0	0	0

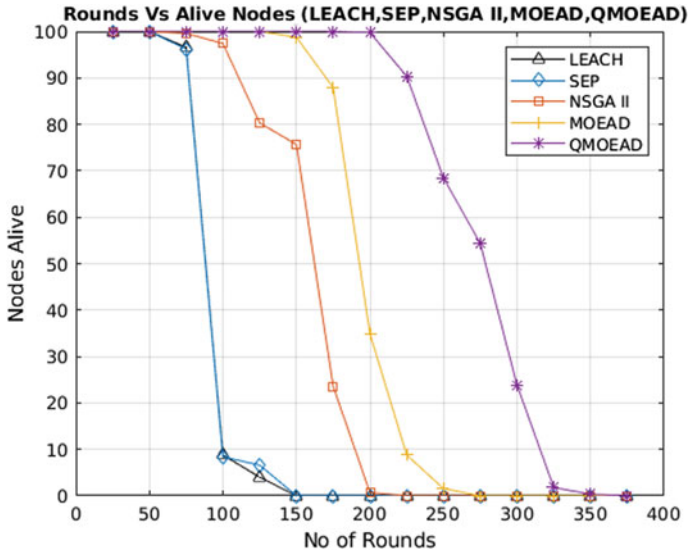


Fig. 1 Alive nodes versus rounds for LEACH, SEP, NSGA II, MOEAD and QMOEAD

targets covered becomes 0 only after round 350 in case of QMOEAD, whereas in case of the other algorithms, it happens earlier.

Figure 1 shows the results where the number of alive nodes after a number of rounds are plotted for LEACH, SEP, NSGA II, MOEAD and QMOEAD. The number of alive nodes becomes zero after larger number of rounds when QMOEAD is used. Figure 2 shows the scenario where the number of targets covered are shown over a number of rounds for LEACH, SEP, NSGA II, MOEAD and QMOEAD. Figure shows that in case of QMOEAD, the number of targets covered reaches zero after larger number of rounds. The inferior performance of LEACH and SEP is because they activate all the alive nodes during the rounds. NSGA II and MOEAD perform better because they activate only a percentage of alive nodes during the rounds. The QMOEAD adds more diversity because of the nature of the qubits.

5 Conclusion and Future Work

The paper proposes QMOEAD algorithm which simultaneously maximizes network lifetime and coverage for homogeneous WSNs by treating them as multiple objectives to be optimized. The algorithm outperforms LEACH, SEP, NSGA II and MOEAD. Future work may involve exploring the QMOEAD algorithm for heterogeneous WSNs.

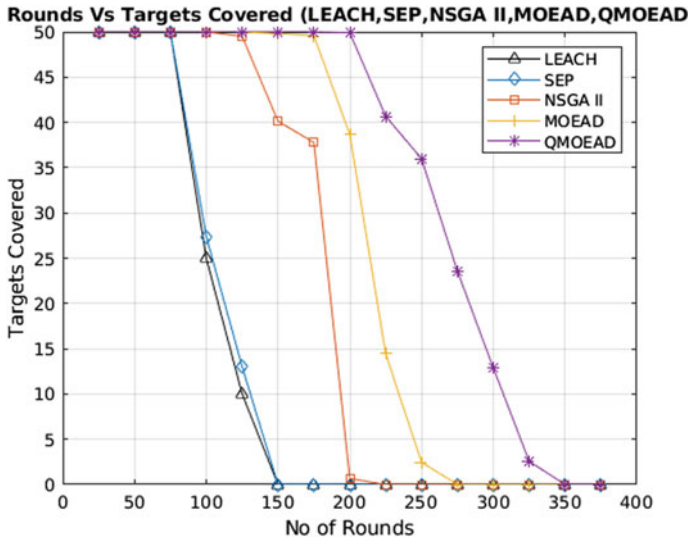


Fig. 2 Targets covered versus rounds for LEACH, SEP, NSGA II, MOEAD and QMOEAD

References

1. Coello CAC, Lamont GB, Van Veldhuizen DA (2007) Evolutionary algorithms for solving multi-objective problems. Springer 5:79–104
2. Marks M (2010) A survey of multi-objective deployment in wireless sensor networks. *J Telecommu Info Technol* 36–41
3. Rajagopalan R, Mohan CK, Mehrotra KG, Varshney PK (2005) An evolutionary multi-objective crowding algorithm (EMOCA): benchmark test function results
4. Martins FV, Carrano EG, Wanner EF, Takahashi RH, Mateus GR (2010) A hybrid multiobjective evolutionary approach for improving the performance of wireless sensor networks. *IEEE Sens J* 11(3):545–554
5. Sandeli M, Meshoul S, Lekhchine R (2018) Optimizing energy in wireless sensor networks using a quantum artificial bee colony. In: *IEEE 3rd international conference on pattern analysis and intelligent systems (PAIS)*, pp 1–5
6. Wang LL, Wang C (2017) A self-organizing wireless sensor networks based on quantum ant Colony evolutionary algorithm. *Int J Online Biomed Eng (iJOE)* 13(7):69–80
7. Kanchan P, Pushparaj SD (2018) A quantum inspired PSO algorithm for energy efficient clustering in wireless sensor networks. *Cogent Eng* 5(1):1522086
8. Huang Y, Qu L, Tang C (2012) Optimal coverage scheme based on QPSO in wireless sensor networks. *J Netw* 7(9):1362
9. Cardei M, Du DZ (2005) Improving wireless sensor network lifetime through power aware organization. *Wireless Netw* 11(3):333–340
10. Tian D, Georganas ND (2002) A coverage-preserving node scheduling scheme for large wireless sensor networks. In: *Proceedings of the 1st ACM international workshop on Wireless sensor networks and applications*, pp 32–41
11. Ye F, Zhong G, Cheng J, Lu S, Zhang L (2003) PEAS: a robust energy conserving protocol for long-lived sensor networks. In: *Proceedings of 23rd IEEE international conference on distributed computing systems*, pp 28–37
12. Zhang H, Hou JC (2005) Maintaining sensing coverage and connectivity in large sensor networks. *Ad Hoc Sensor Wireless Netw* 1(1–2):89–124

13. Heinzelman WB, Chandrakasan AP, Balakrishnan H (2002) An application-specific protocol architecture for wireless microsensor networks. *IEEE Trans Wireless Commun* 1(4):660–670
14. Smaragdakis G, Matta I, Bestavros A (2004) SEP: a stable election protocol for clustered heterogeneous wireless sensor networks. Technical report, Boston University Computer Science Department
15. Jin S, Zhou M, Wu AS (2003) Sensor network optimization using a genetic algorithm. In: *Proceedings of the 7th world multiconference on systemics, cybernetics and informatics*, pp 109–116
16. Hussain S, Matin AW, Islam O (2007) Genetic algorithm for hierarchical wireless sensor networks. *JNW* 2(5):87–97
17. Hoang DC, Yadav P, Kumar R, Panda SK (2010) A robust harmony search algorithm based clustering protocol for wireless sensor networks. In: *Proceedings of IEEE international conference on communications workshops*, pp 1–5
18. Khalil EA, Bara'a AA (2011) Energy-aware evolutionary routing protocol for dynamic clustering of wireless sensor networks. *Swarm Evol Comput* 1(4):195–203
19. Lin TS, Chuang CL, Chen CP, Tseng CL, Yang EC, Yu CS, Jiang JA (2009) An energy-aware and Coverage-preserving Hierarchical Routing protocol for wireless sensor networks. In: *WINSYS*, pp 53–56
20. Soro S, Heinzelman WB (2009) Cluster head election techniques for coverage preservation in wireless sensor networks. *Ad Hoc Netw* 7(5):955–972
21. Srinivas N, Deb K (1994) Multiobjective optimization using nondominated sorting in genetic algorithms. *Evol Comput* 2(3):221–248
22. Deb K, Pratap A, Agarwal S, Meyarivan TAMT (2002) A fast and elitist multiobjective genetic algorithm: NSGA-II. *IEEE Trans Evol Comput* 6(2):182–197
23. Zhang Q, Li H (2007) MOEA/D: A multiobjective evolutionary algorithm based On decomposition. *IEEE Trans Evol Comput* 11(6):712–731
24. Ozdemir S, Bara'a AA, Khalil OA (2013) Multi-objective clustered-based Routing with coverage control in wireless sensor networks. *Soft Comput* 17(9):1573–1584
25. Rao PS, Jana PK, Banka H (2017) A particle swarm optimization based energy efficient cluster head selection algorithm for wireless sensor networks. *Wireless Netw* 23(7):2005–2020
26. Mirhosseini M, Barani F, Nezamabadi-pour H (2017) QQIGSA: A Quadrivalent quantum-inspired GSA and its application in optimal adaptive design of wireless sensor networks. *J Netw Comput Appl* 78:231–241

A Review of Wireless Charging in WSN



Supriya Gupta and Md. Amir Khusru Akhtar

Abstract Wireless energy transfer is the transmission of electrical energy without the use of wires. The use of WET in the management of energy creates a new class of network, i.e., the wireless rechargeable sensor networks. This paper presents a systematic review on wireless charging of sensors nodes in wireless sensor networks and explores the comparison of recognized works. A lot of optimization techniques for designing energy-efficient traveling paths and optimal stopping locations of the WCV has been presented to improve the charging efficiency of WCV. This paper discusses the current work on movement cost of wireless charging vehicles, optimal stopping time of WCV, trajectory design, and conservation of energy. Furthermore, it also enlightens charger placement problems and charge scheduling problems to improve the charging performance of WRSNs. Finally, the research challenges in the field of WRSNs have been proposed.

Keywords Energy-efficient traveling paths · Magnetic resonant coupling · Wireless charging vehicle · Wireless sensor network · Wireless rechargeable sensor network

1 Introduction

Wireless sensor technology is one of the most prominent subjects to be dealt with. Wireless sensor network (WSN) is a complex group of specialized nodes and devices installed in a background that leads to lots of complexities, which has to be taken care by the network planners. WSN is implemented in various sectors such as observations of regions, healthcare sector, emergency alarm in forests, working on the levels of air pollution, natural calamity detection such as landslide, checking for water levels as well as quality, and natural catastrophe prevention. The sensor nodes perceive and

S. Gupta (✉) · Md. A. K. Akhtar
Usha Martin University, Ranchi, India
e-mail: supriyagupta000@gmail.com

Md. A. K. Akhtar
e-mail: amir@umu.ac.in

collect data from the environment and then forward it to the base station for further processing and decisions [1].

In the traditional approach, the wireless sensor is limited by the capacity of the batteries of the sensor nodes. The application and demand for complex processing on sensor end increase energy consumption of sensor nodes. Thus, energy conservation has become the main dimension of WSN in past decade in order to maximize network lifetime. Several solutions have been proposed such as mobile data sink for data gathering and trajectory of the mobile sink to balance and maximize network. These methods enhance network lifetime but battery depletion still causes network failure [2].

By the advent of wireless charging technology, the sensor node can be charged wirelessly. As information is transferred wirelessly, energy can also be transferred wirelessly using electromagnetic fields or magnetic resonant coupling methods. Replenishment of energy of sensor nodes via magnetic resonant coupling is an important development in this area. In this method, source coil transfers energy to the destination coils via electromagnetic fields [3].

The wireless sensor network can remain active for an infinite period if it is charged periodically. A wireless charging vehicle (WCV) can be used for charging the sensors nodes without employing any physical connections. The wireless charging vehicle can be employed in many ways, and the latest advancement is the multi-node charging technology where we are charging more than one node simultaneously [3]. The motivation of this chapter is to understand how to use wireless charging technology as compared to the conventional battery-powered wireless sensor networks. This new network is called wireless rechargeable sensor networks (WRSNs) [2].

The sections of the paper are arranged as follows. Section 2 talks about background of wireless rechargeable sensor network. Section 3 discusses charger placement, charging utilization, and charge scheduling problem. Section 4 presents wireless charging vehicles. Section 5 presents comparison of various techniques and methods for WRSN, and Sect. 6 enlightens the research challenges and future scope of WRSN. Finally, Sect. 7 concludes the paper.

2 Wireless Rechargeable Sensor Network

In the next decade, wireless network relies heavily on sensors to take out practical information from the surroundings. There is an increasing demand for more complex sensor nodes for application in various fields which leads to higher consumption of energy per sensor nodes. Energy conservation of these batteries of the sensor nodes is really important as replacing them would be riskier and infeasible in many applications. There are various ways of maximizing network life, one way is to put the sensor nodes to sleep mode if there is no communication. There is another way of replenishing energy of batteries which is by environmental energy, for example, solar energy and wind energy. This source is unreliable, and if energy is unavailable, then communication between the nodes would lapse [2].

Based on different situations, wireless sensor rechargeable nodes can be divided into two categories: periodical WRSN and event driven WRSN [4]. In periodical WRSN, nodes can be charged in two ways, single node charging method and to increase the efficiency multi-node charging method in which several nodes are charged at the same time [5].

There are several important components of wireless rechargeable sensor network. Charging vehicle is instilled in the system with global positioning system. The vehicles are equipped with cell packs and coils [2]. There are numerous solutions provided for wireless charging vehicles, and wireless charging vehicles can reinstate the power of nodes in different position in the network by moving channels and attain the goals as shown in Fig. 1. It is basically a vehicle-type hardware that helps to charge wireless rechargeable sensor network [6]. When energy level at any node is low, it sends a charging request to moving charging vehicle and MCV services the request. To shorten the charging time and traveling time, there are many theories proposed as the energy consumption of WRSN is not uniform and balanced. Demand-based charging method (DBCS) charges only the emergency nodes which shows improved utilization of energy as compared to nearest-job-next preemption [5].

A base station communicates with the WCV via long-distance communication and with the sensors via short-distance communication [7]. Base station schedules future charging activities and is responsible for network management. The network administrator controls the activities of the mobile charger via base station. If the charging vehicles run down of the power, it returns to the base station for a quick cell renewal [2, 8].

On the other hand, a head node gives the status of the node in the subordinate area, i.e., it aggregates information from each sub-area. A proxy node helps in case of emergency when a node's energy level depletes below the given level, so head nodes act as proxy nodes. It needs to take care off immediately. A node that is not picked as a head node is a normal node, and the role of normal node is to report to

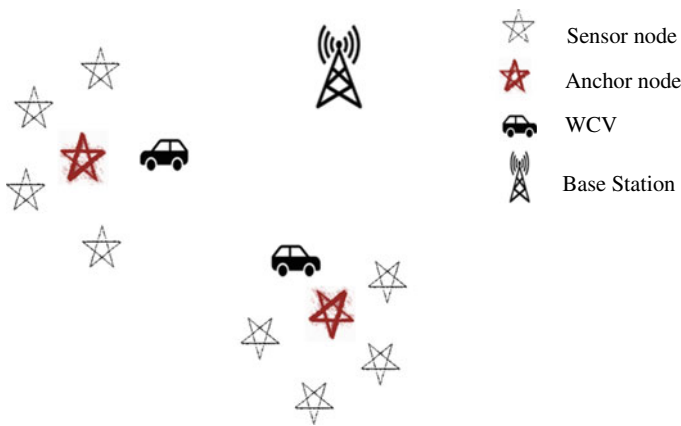


Fig. 1 Wireless charging vehicles (WCV)

head node or send emergency information directly to its proxy node when the power level of a battery depletes below the threshold value [2].

3 Review of Literature

The wireless sensor network can remain active for an infinite period if it is charged periodically. By the advent of wireless charging, a wireless charging vehicle (WCV) can be used for charging the sensors nodes without employing any physical connections. Thus, it improves the network lifetime of wireless sensor network [9]. Several methods and models have been suggested in the writings for the betterment of wireless rechargeable sensor network. This section highlights the current work on charger placement problems and charge scheduling problems.

3.1 *Charger Placement and Charging Utilization Problem*

In wireless charging, chargers are responsible for charging the rechargeable wireless devices wirelessly. A lot of works has been proposed in literature for maximizing the charging utility and diminishing the charging delay. Still charger placement problem is one of the key concerns in wireless rechargeable sensor network [10]. The work on charger placement can be broadly classified in static and mobile. In static charging system, a minimum number of chargers are deployed in the network for charging the devices. In this system, the objective is to minimize the charger count, and the system must ensure sustainable operation. This system has several issues such as human health threat due to radiation [11] and the placement issues. In mobile charging system, several solutions have been proposed such as single mobile charging scheduling algorithm and multiple mobile charging scheduling algorithm. The aim is to increase the charging utility and decrease the number of mobile chargers.

A best charger placement for wireless energy transfer [10] has been proposed. This work focuses on minimization of deployment cost of chargers and maximization of the total charging levels by considering the budget constraint. This work investigated optimal charger placement problems in different scenarios such as omnichargers and directional chargers and proposed four approximation algorithms. Results show that this scheme outperforms other schemes in terms of location constraint, budget, and performance.

In order to overcome the charging problems and power capacity constraints, a novel wireless charging pad deployment in wireless rechargeable sensor networks has been proposed [12]. It uses one wireless charging drone equipped with multiple wireless charging pads for charging the drone in crucial time. This method proposes an effective deployment of wireless charging pad in order to minimize number of pads and creates feasible routing path for the drone to charge the sensor nodes in WRSNs. This work suggests several graph theoretic and geometry methods as well

as it proposes drone scheduling algorithm and shortest manifold hop path algorithm. Results show that this plan outperforms other plan in terms of flight distance, network solidity, and sector size.

Wang et al. proposed a partial charging scheme [13], in which sensor nodes charged partially to minimize node dead time and to maximize network life span. In this method, nodes are charged partially according to the priority of uncharged nodes. The priority of sensors nodes is determined on the basis of their contributions in charging tasks. The most appropriate sensor nodes are selected, and lesser priority nodes are excluded from the priority list. This method outperforms other methods with regard to quicker service time, better survival rate, and lesser waiting queue.

3.2 Charge Scheduling Problem

Wireless recharge scheduling is a NP-complete problem because the defined algorithms are unable to handle large problem instances in practical time [14]. The charge scheduling problem is based on decreasing the charging cost and charging realization time and increasing charging amount and charging stability among the wireless charging channels [15]. Fan et al. [16] presented a view on wireless power transfer-based charging scheduling schemes in wireless rechargeable sensor network. This paper analyzes wireless power transfer (WPT)-based charging schedules in WSNs. This paper classifies and compares various existing charging network schemes with regard to the sensor network parameters.

Zhao et al. proposed a spatial-temporal charging scheduling algorithm in wireless rechargeable sensor network [7]. This work focuses on charge scheduling and charging time allocation for enhancing network life span and charging order. They have presented a mixed integer optimization model for charge scheduling and charging time allotment subject to the maximization of the charging regulation. Simulation results show the effectiveness of the algorithm under periodic and hybrid services.

Wang et al. proposed a sleeping and recharge scheduling algorithm for wireless rechargeable sensor webbing [17]. This work focuses on wireless charging issue on the basis of energy preservation and power replenishment scheduling. This algorithm detects the unnecessary nodes and uses a K-covering redundant node sleeping scheduling algorithm (KRSS) for power reduction. This work proposes distance and energy-oriented charging scheduling algorithm (DECS) by employing many WCVs. Imitation experiments show that the proposed KRSS + DECS algorithm is efficient enough to eliminate unnecessary nodes, better in handling node failures, and enhancing network lifespan.

In order to investigate the issue of charge scheduling and decreasing the number of charging channels, several works have been proposed. Nguyen et al. suggested a mobile charger scheduling algorithm (MCSA) to address the periodic energy replenishment with minimum mobile charger (PERMMC) problem [18]. Considerable simulations show the success of the suggested algorithm.

A three-layer framework in WRSN has been suggested for moving station data aggregation so that sensor nodes remain active for an infinite period. The proposed scheme has three layers such as sensor layer, cluster head layer, and mobile station layer for minimizing traveling time. It uses a centralized clustering pseudo code to arrange sensors into collections and proposes an optimization method for scheduling cooperative charging. This scheme minimizes the total energy consumption and shows its effectiveness in terms of lesser energy consumption in comparison with mobile station in WRSN.

4 Wireless Charging Vehicles

The wireless sensor network can remain active for an infinite period if it is charged periodically. A wireless charging vehicle (WCV) can be used for charging the sensors nodes without employing any physical connections. The wireless charging vehicle can be employed in many ways, and the latest advancement is the multi-node charging technology where we are charging more than one node simultaneously [3]. This section highlights the current work on movement cost of wireless charging channels and optimal stopping time of WCV.

4.1 *Movement Cost of WCVs*

Lots of work have been proposed to minimize the movement cost and recharged profits.

Wang et al. proposed a moving data congregation structure for WRSNs with channel movement costs and capacity limitations [19]. This work employed one data congregation channel and many charging channels. This work organizes sensors into clusters and proposed a mathematical model to obtain the minimum number of WCVs. The authors presented this scheduling issue into a profitable traveling salesman problem on the basis of refilled energy and vehicle movements. This work defined and compared two algorithms: a greedy approach that maximizes the profit and a flexible approach that uses minimum spanning trees. Extensive evaluations and comparisons show its effectiveness in terms of data gathering and latency.

Wang et al. [20] proposed a blended data assembling plan, where data which are critical and important are directly forwarded to the base station and data that are not so time sensitive are assembled by moving collectors, i.e., balancing between routing cost and latency cost. It also focuses on scalability improvement and number of moving vehicles (addressed as SenCars). This paper formulates recharge scheduling into a dual-purpose optimization problem and proposes a two-step estimation algorithm with bounded estimation ratios for each purpose. Their work is on multi-hops wireless charging for WRSNs based on realistic physics models. Charging efficiency of a charging vehicle decays as an inverse cube of distance, and this paper

discusses not only short-range sensor nodes charging, but also long recharge latency and mid-range wireless charging.

Electric vehicles (EV) have gained notable importance due to their high propellant economy and low pollution emanations. This paper investigates impact of wireless charging and mobility of electric vehicle on locational marginal price (LMP). The load of wireless EV is investigated taking into consideration spatial traffic distribution and integrating with economic dispatch. Simulations help to evaluate the proposed network queueing model [21].

Wang and Yang [22] proposed two separate modes: one for data assembling and the other for replenishing power. This is done in view to avoid long delays which happens in the merged approach of data gathering and slow refreshing process. In order to achieve this, it focuses on building a mathematical model in which it harps on the suitable group size to attain a stability and minimum number of recharging vehicles that would be needed to cover all the sensor nodes in the given cluster bound. This combined approach studies the trade-off between data lag and the minimum number of recharging vehicles given other network parameters.

4.2 Optimal Stopping Time of WCVs, Trajectory Design, and Conservation of Energy

Several works have been proposed in the literature to find the best stopping time of WCV to recharge sensors at different locations.

A recurrent charging plan for plotting power structured traveling tracks for multiple WCVs has been proposed in the literature [23]. It organizes network area into clusters, i.e., into subregions so that charging by multiple WCVs is done in a power structured manner. To take the advantage of multi-node charging, this paper aims to find the number of optimal stopping locations based on charging radius of the nearest neighbor approach (CRNN) to plan power structured traveling tracks for WCVs. Extensive simulations show effectiveness in terms of node failure rate, average charging latency, average waiting time, and traveling track distance with extending number of nodes and available WCVs.

A structured plan for trajectory design of moving chargers in wireless sensor networks has been proposed [24]. This paper proposes a power retrieval plan for trajectory design of many WCVs based on the routing burden of the sensor nodes. Extensive simulations on the suggested procedures outshine the existing plans, namely HILBERT and S-CURVES over different performance yardstick such as entire trip distance, average waiting time, average charging latency, entire number of active nodes, and standard deviation of sensor nodes remaining power. ANOVA is conducted along with graphical comparison of confidence interval of the means of all the three plans.

A power structured MCC combined arrangement with extended mobile involvement for next generation webbing has been proposed in literature [25]. This paper

focuses on issues like power misuse experienced by the idle moving assets and suggests a hybrid power-efficient MCC architecture, named Mobilouds, for the purpose of increasing the involvement of the moving gadget in the collaborative MCC implementation eventually to decrease the unacceptable power expending of the idle moving assets with reduced service delays. This Mobilouds can be upgraded or downgraded depending on the requirement, and this helps in conservation of energy. Mobilouds application is a software that runs on the mobile devices to facilitate the usage of the Mobilouds architecture. Performance evaluations show that Mobilouds is successful in achieving best trade-off between process time and power and in lessening the unacceptable power consumptions across all the underlying process components of the MCC process framework.

5 Comparison of Various Techniques and Methods for WRSNs

This section presents a comparison of various techniques and methods for wireless rechargeable sensor networks shown in Table 1. We have shown novel techniques, advantage, and disadvantages of recent research in WRSNs.

6 Research Challenges

Wireless rechargeable sensor network has several research provocations in the area of power management, data collection, reliability, and privacy, etc. [1]. Some of the typical questions of wireless rechargeable sensor network [2] are shown below:

- How to increase the charging utility and decrease the charging delay?
- How to boost the charger placement problem for wireless power transfer?
- How to define a novel charge scheduling problem for decreasing the charging cost and charging completion time and increasing charging amount and charging balance among the wireless charging channels [15]?
- How to find shortest recharge path or Hamiltonian cycle?
- How to decrease the movement cost of wireless charging channels?
- What is the optimal stopping time of WCV to recharge sensors at different locations?
- How to calculate the power utilization rate connecting juncture on the basis of locations and traffic load?
- How to act on sensor node status information especially in emergent status?

In case of emergency situation, the WCV needs to determine manifold crisis at different positions. The challenge is to amplify the entire amount of recharged power in a given timespan on the basis of renewing time and traveling time.

Table 1 Comparison of various techniques and methods for WRSNs

Author/Year of publications	Technique used	Advantages	Limitations
Designing energy-efficient traveling paths for multiple mobile chargers in wireless rechargeable sensor networks [23]	Clustering and multi-node (CR-NN) charging method	Improved node failure rate, norm charging latency, norm stand by time	Run-time requests, i.e., dynamic scenarios of WRSNs not considered
Mobilouds: An energy-efficient MCC collaborative framework with extended mobile participation for next generation networks [25]	Mobilouds, hybrid of MCC architecture and mobile devices	Best barter between energy and time	The possibility of making use of the moving assets and increasing their engagement in the alliance of MCC implementation even when the moving channels face detachments from the process collections
GTCharge: A game theoretical collaborative charging scheme for wireless rechargeable sensor networks [26]	Alliance of charging strategy, namely GTCharge	GTCharge can enhance the energy efficiency	Additional movement value posed by preemptions in taking part in a game
An efficient scheme for trajectory design of mobile chargers in wireless sensor networks [24]	Energy replenishment scheme, route plan of many WCVs based on the routing burden of the SNs	Outperforms in entire trip distance, norm holding back time, average charging latency, complete number of agile nodes, and standard deviation of SNs' remaining power	Dynamic scenarios of WRSNs not considered
Recharging schedules for wireless sensor networks with vehicle movement costs and capacity constraints [27]	Greedy algorithm and adaptive algorithm. for SenCar's recharging	It helps save energy of SNs	SenCars' regime as well as sensors' battery time limit limitations need to be explored
Improve charging capability for wireless rechargeable sensor networks using resonant repeaters [20]	resonant repeaters, multi-hop wireless charging, hybrid data gathering strategy	network scalability	Node topology and density needs to be taken care of

(continued)

Table 1 (continued)

Author/Year of publications	Technique used	Advantages	Limitations
Multi-node wireless energy charging in sensor [3]	Discretization and a novel reformulation–linearization technique (RLT)	Charging extensibility complication in a thick wireless sensor network	During the saturation phenomena, the plan of attaining rechargeable inexhaustible rhythm cannot be tried here

7 Conclusion

This paper highlights the present-day analysis of wireless rechargeable sensor networks. The motivation of the entire chapter is to increase the understanding of the usage of wireless charging technology in conventional battery-powered wireless sensor networks. This paper serves as a foundation to understand the basics of wireless rechargeable sensor networks (WRSNs) and highlights the research challenges in this field. We have discussed several optimization techniques for calculating power structured traveling paths and optimal break-off positions of the WCV to improve the charging organization of WCV. We have shown the current work on movement cost of wireless charging vehicles, optimal stopping time of WCV, trajectory design, and conservation of energy. Moreover, it also enlightens charger placement problems and charge scheduling problems to upgrade the charging execution of WRSNs.

References

1. Prakash S, Saroj V (2019) A review of wireless charging nodes in wireless sensor networks. In: Mishra DK, Yang X-S, Unal A (eds) Data science big data analytics. Springer, Singapore, pp 177–188
2. Yang Y, Wang C (2015) In: Wireless rechargeable sensor networks [Internet]. Springer International Publishing. [cited 2020 Mar 12]. Available from <https://www.springer.com/gp/book/9783319176550>
3. Xie L, Shi Y, Hou YT, Lou W, Sherali HD, Midkiff SF (2015) Multi-node wireless energy charging in sensor networks. *IEEEACM Trans Netw* 23:437–450
4. Guo S, Wang C, Yang Y (2014) Joint mobile data gathering and energy provisioning in wireless rechargeable sensor networks. *IEEE Trans Mob Comput* IEEE 13:2836–2852
5. Dong Y, Wang Y, Li S, Cui M, Wu H (2019) Demand-based charging strategy for wireless rechargeable sensor networks. *ETRI J* 41:326–336
6. Rahman A-B, Saleem N, Ahmad F, Rizwan M (2019) Energy optimization in wireless rechargeable sensor networks. *Int J Sci Res Publ IJSRP* 9:8860
7. Zhao C, Zhang H, Chen F, Chen S, Wu C, Wang T (2020) Spatiotemporal charging scheduling in wireless rechargeable sensor networks. *Comput Commun* 152:155–170
8. Angelopoulos CM, Nikolettseas S, Raptis TP (2014) Wireless energy transfer in sensor networks with adaptive, limited knowledge protocols. *Comput Netw* 70:113–141

9. Zou T, Xu W, Liang W, Peng J, Cai Y, Wang T (2017) Improving charging capacity for wireless sensor networks by deploying one mobile vehicle with multiple removable chargers. *Ad Hoc Netw* 63:79–90
10. Ding X, Wang Y, Sun G, Luo C, Li D, Chen W et al (2020) Optimal charger placement for wireless power transfer. *Comput Netw* 170:107123
11. Guidelines for limiting exposure to time-varying electric, magnetic, and electromagnetic fields (up to 300 GHz) (1998) International Commission on Non-Ionizing Radiation Protection. *Health Physics*. 74:494–522
12. Chen J, Yu CW, Ouyang W (2020) Efficient wireless charging pad deployment in wireless rechargeable sensor networks. *IEEE Access* 8:39056–39077
13. Wang K, Wang L, Obaidat MS, Lin C, Alam M (2020) Extending network lifetime for wireless rechargeable sensor network systems through partial charge. *IEEE Syst J* 1–11
14. Buřcar D (2014) Electric vehicles recharge scheduling with time windows [PhD Thesis]. Master's thesis, Faculty of Informatics, Vienna University of Technology
15. Ki Y, Kim B-I, Ko YM, Jeong H, Koo J (2018) Charging scheduling problem of an M-to-N electric vehicle charger. *Appl Math Model* 64:603–614
16. Fan Z, Jie Z, Yujie Q (2018) A survey on wireless power transfer based charging scheduling schemes in wireless rechargeable sensor networks. In: 2018 IEEE 4th International conference control science systems engineering ICCSSE. pp 194–198
17. Wang K, Wang L, Lin C, Obaidat MS, Alam M (2020) Prolonging lifetime for wireless rechargeable sensor networks through sleeping and charging scheduling. *Int J Commun Syst n/a:e4355*, Wiley Ltd
18. Nguyen TN, Liu B, Chu S, Do D, Nguyen TD (2020) WRSNs: toward an efficient scheduling for mobile chargers. *IEEE Sens J* 1–1
19. Wang C, Li J, Ye F, Yang Y (2016) A mobile data gathering framework for wireless rechargeable sensor networks with vehicle movement costs and capacity constraints. *IEEE Trans Comput* 65:2411–2427
20. Wang C, Li J, Ye F, Yang Y (2015) Improve Charging capability for wireless rechargeable sensor networks using resonant repeaters. In: 2015 IEEE 35th International conference distribution computing systems 2015, pp 133–42
21. Ou C-H, Liang H, Zhuang W (2015) Investigating wireless charging and mobility of electric vehicles on electricity market. *IEEE Trans Ind Electron* 62:3123–3133
22. Wang C, Li J, Yang Y (2015) Low-latency mobile data collection for wireless rechargeable sensor networks. In: 2015 IEEE international conference communications ICC. pp 6524–6529
23. Tomar A, Jana PK (2017) Designing energy efficient traveling paths for multiple mobile chargers in wireless rechargeable sensor networks. In: 2017 Tenth international conference contemporary computing IC3, pp 1–6
24. Tomar A, Nitesh K, Jana PK (2020) An efficient scheme for trajectory design of mobile chargers in wireless sensor networks. *Wirel Netw*
25. Panneerselvam J, Hardy J, Liu L, Yuan B, Antonopoulos N (2016) Mobilouds: an energy efficient MCC collaborative framework with extended mobile participation for next generation networks. *IEEE Access* 4:9129–9144
26. Lin C, Wu Y, Liu Z, Obaidat MS, Yu CW, Wu G (2016) GTCharge: a game theoretical collaborative charging scheme for wireless rechargeable sensor networks. *J Syst Softw* 121:88–104
27. Wang C, Li J, Ye F, Yang Y (2014) Recharging schedules for wireless sensor networks with vehicle movement costs and capacity constraints. In: 2014 Eleventh annual IEEE international conference sensors communications networks SECON. pp 468–76

Vibration Measurement Using Accelerometer Sensor and Fast Fourier Transform



Sarita Kumari

Abstract Vibration monitoring is necessary for any system for its effective performance, product quality, safety and life span. It helps to diagnose the health of system for any predictive maintenance needed. This paper presents the analysis of vibration signal using fast Fourier transform (FFT). Frequency spectrum of vibrating source gives information of the vibration level. The natural frequency of the vibrating source was found to be 17 Hz with total harmonic distortion (THD) of 0.000177%. The analysis was carried out using NI LabVIEW software.

Keywords Vibration · Sensor · Accelerometer · FFT · LabVIEW

1 Introduction

Vibration can be described as the periodic motion in alternately opposite directions about a reference equilibrium position. For proper functioning of a plant or system, it is very important that all machines should work properly. Vibration is one of the key parameters to measure and analyze constantly for good quality product and safety. It also helps in diagnosing the health of the system and predictive maintenance. Routine monitoring of vibration is necessary to avoid any failures. Vibration measurements are considered as a part of performance test for instrument while in use. It gives an indication of how well the instrument or system has been designed and manufactured and can also provide advanced warning of possible operational problems.

There are various factors influencing vibration measurements which include cross-axis sensitivity, capacitance effect, sensor loading, coupling and other external factors such as temperature and magnetic field.

A body is said to vibrate when it oscillates about a reference point. Vibration is caused by mechanical disturbance from some source and is transferred to the system in contact with it. The need of vibration measurement is required due to growth of environmental testing and health of the system. It can be expressed in terms

S. Kumari (✉)

Department of Electronics and Communication Engineering, Amity University Jharkhand, Ranchi 834001, India

e-mail: gs.sarita@gmail.com

of displacement, velocity or acceleration. The analysis, measurement and testing of vibration are usually done for the rotating or reciprocating instruments. All the system or machine performance should withstand a particular level of vibration for effective running of the process. If the system is not able to withstand the vibration of the instrument, then it may collapse or lead to complete failure of the system. It is not possible to make completely perfect system as per design or mathematical model. Vibration detection is applicable in the working of machines, construction of buildings and bridges, structural health monitoring, security reasons, forecasting of natural disasters such as earthquake and tsunami.

Most vibrations are sinusoidal in nature about its mean position. The quantities required to be measured in a vibrating system are displacement (x), velocity (v) and acceleration (a) expressed in Eqs. (1), (2) and (3), respectively. Sinusoidal vibrations are expressed in terms of amplitude and frequency or maximum velocity (v_0) or maximum acceleration (a_0) in Eqs. 4 and 5, respectively.

$$x = x_m \sin \omega t \quad (1)$$

where x_m is amplitude, and ω is angular frequency in terms of rad/s.

$$v = \dot{x} = x_m \omega \cos \omega t \quad (2)$$

$$a = \ddot{x} = -x_m \omega^2 \quad (3)$$

$$v_0 = x_m \omega \quad (4)$$

$$a_0 = -x_m \omega^2 \quad (5)$$

Any sensor which is sensitive to the amplitude (displacement), velocity or acceleration can be used to measure vibration. Seismic transducer is the device to measure the same which can be used in two different modes, i.e., displacement mode and acceleration mode. There are other types of vibration sensors available such as inductive sensor, capacitive sensor, piezoelectric sensor, magnetic sensor, optical fiber sensor and photoelectric sensor. Accelerometer is the most common sensor used for vibration analysis and data collection. Many accelerometers are available based on their working principles such as capacitive accelerometer, piezoelectric accelerometer and hall effect accelerometer.

Mathematical model of vibration in matrix form can be represented as equation of motion as given in Eq. (6). M , C and K represent inertia matrix, damping matrix and stiffness matrix, respectively, where x is position vector and F is input vector.

$$M\ddot{x} + C\dot{x} + Kx = F(t) \quad (6)$$

Various works in the field of vibration are done by many researchers worldwide. Song et al. [1] and team have explained uncertainties of measurement of vibration in terms of acceleration. Usuda and Imai [2] explained a different prospect of vibration activity measurement using IMEKO TC22. Chen et al. [3] designed an optical fiber-based model for vibration detection. It was based on the changes in geometric curvature of the optical fiber with respect to any vibration. Uchimura et al. [4] have described wireless sensing of vibration through IEEE 802.11-based TSF counter. Igor Kurytnik [5] and team have proposed ZigBee sensor network for detection of vibration. Sivakumar [6] has simulated the random vibration analysis of complete aircraft for active and passive gears. It was found that performance and life of aircraft was improved with active gears. A mathematical model of moving vehicle is simulated by Zhou and Qiu [7], and vehicle performance was mostly effected by seat vibration and engine vibration. Zhang et al. [8] have analyzed vibration using finite element method and FFT. Sabato [9] has monitored pedestrian vibration using wireless MEMS accelerometer board. Wada et al. [10] have sensed multipoint vibration using FBG and current modulated laser diode. A new cost-effective vibration sensor is developed based on micro-wire sensor system using FFT [11]. Using SCILAB simulation software, mathematical modeling and analysis of vibration were done for rotating machinery [12]. Maruthi et al. [13] have done the mathematical analysis of unbalanced magnetic pull and detection of mixed air gap eccentricity in induction motor by vibration analysis using MEMS accelerometer. Hu Jingjing [14] and team have studied the equivalent simplified model of multilayer vertical isolation structure under heavy load train vibration. The structure is based on the equivalent principle of the first two order frequency and the total axial force.

2 Experimental Setup

The experiment setup, shown in Fig. 1, consists of a vibrating source, accelerometer sensor, pulse analyzer and a computer to display the output. Sensor module consists of a vibrating device to generate vibration, magnetic dart and an accelerometer as sensor. An accelerometer is attached to the vibrating source to pick up the vibration. Pulse analyzer is used as signal processing unit. Figure 2 shows the block diagram of the complete measurement setup. The pulse analyzer (OR38, OROS 3-Series/NVGate) receives signal from the accelerometer. The detected vibration output is in terms of acceleration (m/s^2) with respect to frequency (Hz) with the interval of 50 Hz. Figure 3 shows the output received from pulse analyzer on the computer.

The output data taken from pulse analyzer are processed using fast Fourier transform in National Instruments (NI) LabVIEW software.

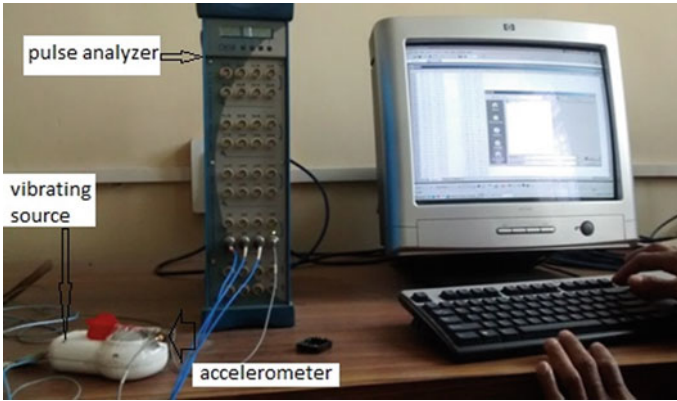


Fig. 1 Vibration measurement setup includes a vibrating source, accelerometer, pulse analyzer and computer



Fig. 2 Block diagram of vibration measurement setup

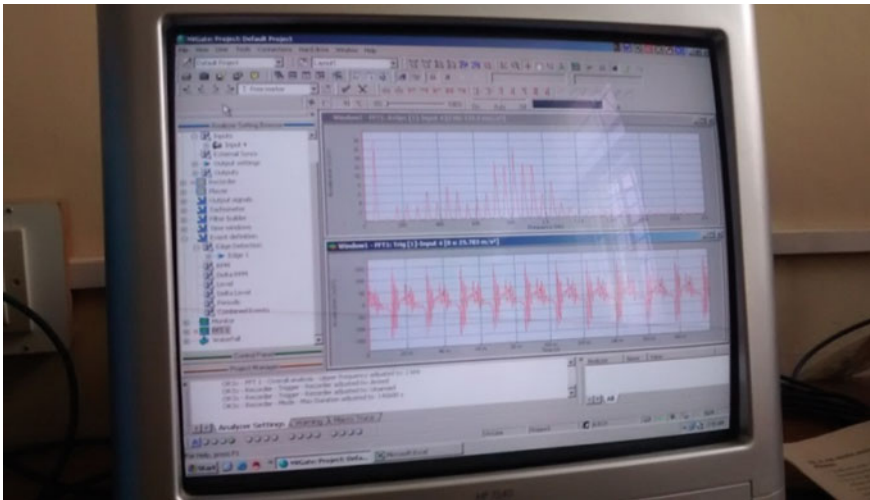


Fig. 3 Pulse analyzer output display in computer

3 Result and Discussion

Figures 4 and 5 show the vibration spectrum analysis waveforms (output) received from pulse analyzer in terms of acceleration (m/s^2) with respect to change in frequency (Hz) from 0 to maximum of 2 and 20 kHz frequency, respectively. The experiment was carried out for different frequency range. An efficient algorithm, i.e., fast Fourier transform (FFT) is used for computation of data. The Fourier transform converts output of vibration amplitude as a function of frequency so that the analyzer can detect the source the vibration. Figure 6 represents frequency (Hz) which is plotted with respect to acceleration (m/s^2) using NI LabVIEW software. The maximum acceleration was observed at 17 Hz frequency.

For the purpose of spectrum analysis, the conventional discrete Fourier transform (DFT) is one of the popular tools [15]. It gives satisfactory result for the vibration under the stationary conditions. The advent of fast Fourier transform (FFT) has made spectra measurement easier and more efficient. Figures 7 and 8 show that the FFT results for the vibration signal are acquired and analyzed using FFT. The data received were received by pulse generator, and figures show the FFT in magnitude and phase, respectively. The frequency spectrum represents the total amplitude at each of these frequencies; it is calculated as the square root of the sum of the squares of the coefficients of the sine and cosine components. The fundamental frequency

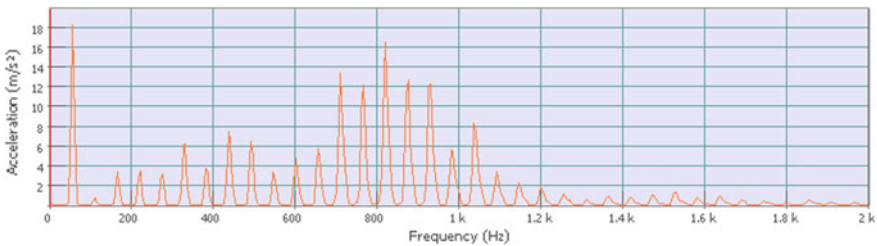


Fig. 4 Vibration spectrum analysis: acceleration (m/s^2) vs frequency (Hz) plot generated by pulse analyzer in the range of 0–2 kHz frequency

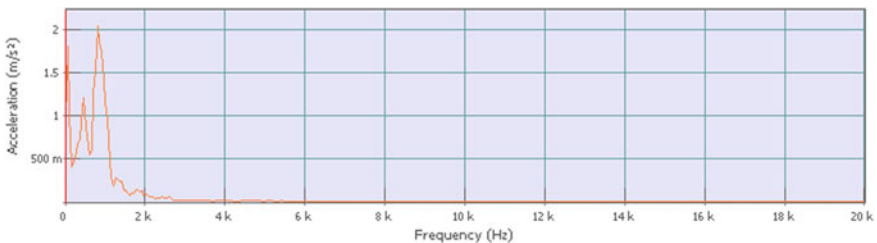


Fig. 5 Vibration spectrum analysis: acceleration (m/s^2) versus frequency (Hz) plot generated by pulse analyzer ranging from 0 to 20 kHz frequency

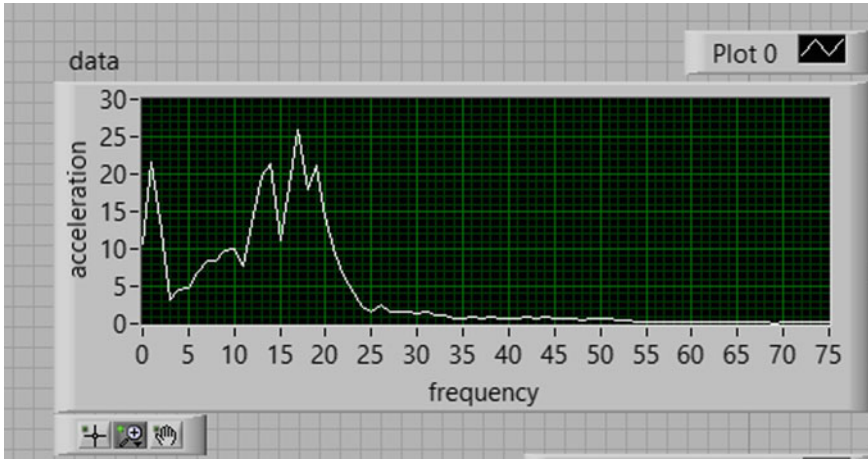


Fig. 6 Vibration spectrum analysis: frequency (Hz) versus acceleration (m/s^2) plot in NI LabVIEW software

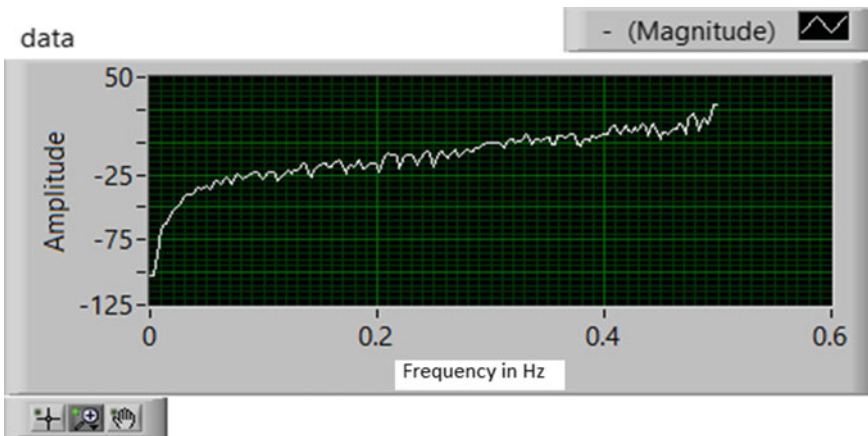


Fig. 7 FFT analysis (amplitude) using NI LabVIEW software

measured is 17 Hz, and the second highest peak appears at 850 Hz. 0.000177% total harmonic distortion (TDH) was calculated.

4 Conclusion

This paper shows the vibration spectrum analysis using fast Fourier transform. The measurement and frequency analyses of the vibration signal are measured from a

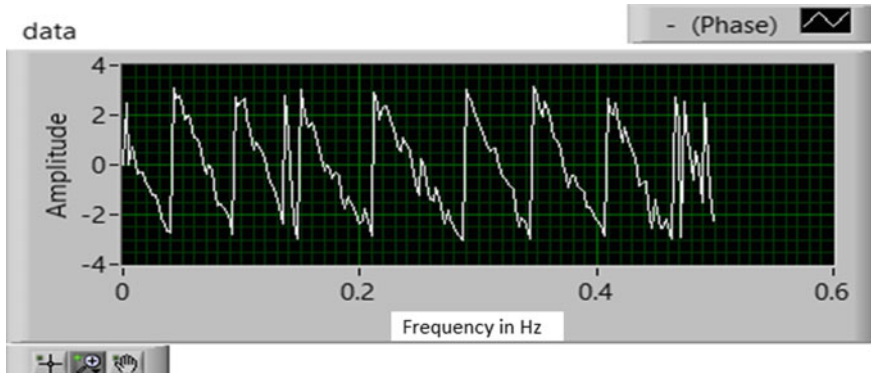


Fig. 8 FFT analysis (phase) using NI LabVIEW software

vibrating source. Vibration was picked by the accelerometer and sent to pulse generator for signal processing. Natural frequency of vibrating source for the setup was calculated as 17 Hz. Second highest peak was observed at 850 Hz with 0.000177% THD.

5 Future Scope

A new optical method for vibration detection can be explored using magneto-optic sensor. This will make the sensor fast and accurate without electrical and environmental interference.

References

1. Song Q, Zhou DH, Niu BL, Zhu CC (2004) Uncertainties in the vibration acceleration measurement. In: Instrumentation and measurement technology conference (IMTC), Como, Italy, 18–20 May 2004
2. Usuda T, Imai H (2007) Activities of new TC22 “vibration measurement. In: SICE Annual conference 2007, September 17–20, 2007, Kagawa University, Japan
3. Chen J, Hu X, Xu L (2008) Research of distributed curvature modal sensors with optical fiber on vibration measurement for thin structures. In: The 3rd international conference on innovative computing information and control, 2008
4. Uchimura Y, Nasu T, Takahashi M (2008) “EEE 802.11 timing synchronization based wireless sensor system for vibration measurement. In: SICE annual conference, August 20–22, 2008
5. Kurytnik I, Borowik B, Karpinski M (2009) Deploying ZigBee sensor network for vibration measurement. In: 10th International conference—the experience of designing and application of CAD systems in microelectronics
6. Sivakumar S, Haran AP (2015) Aircraft random vibration analysis using active landing gears. *J Low Frequency Noise Vibr Active Control* 34(3):307–322

7. Zhou H, Qiu Y (2015) A simple mathematical model of a vehicle with seat and occupant for studying the effect of vehicle dynamic parameters on ride comfort. In: 50th United Kingdom conference on human responses to vibration, held at ISVR, University of Southampton, Southampton, England, 9–10 September 2015
8. Zhang H, Gao R, Zhang J, Wang L (2009) Vibration analysis for switched reluctance motor system based on finite element and FFT. In: Proceedings of IEEE international conference on mechatronics and automation, August 9–12, Changchun, China
9. Sabato A (2015) Pedestrian bridge vibration monitoring using a wireless MEMS accelerometer board. In: Proceedings of IEEE 19th international conference on computer supported cooperative work in design (CSCWD)
10. Wada A, Tanaka S, Takahashi N (2016) Multipoint vibration sensing using fiber bragg gratings and current-modulated laser diodes. *J Lightwave Technol* 34(19)
11. Rota-Rodrigo S, López-Aldaba A, Ana Pérez-Herrera R, Carmen López Bautista M, Esteban O, López-Amo M (2016) Simultaneous measurement of humidity and vibration based on a microwire sensor system using fast fourier transform technique. *J Lightwave Technol* 34(19)
12. Bayya SS, Vedaraj ISR, Sivasubramanian K (2013) Vibration monitoring mathematical modelling and analysis of rotating machinery. *Int J Adv Res Electri Electron Instrum Eng* 2(4)
13. Maruthi GS, Hegde V (2013) Mathematical analysis of unbalanced magnetic pull and detection of mixed air gap eccentricity in induction motor by vibration analysis using MEMS accelerometer. In: IEEE 1st international conference on condition assessment techniques in electrical systems 2013
14. Jingjing H, Jiayun X, Can Z, Haifeng B, Yiqian Y (2016) Research on equivalent simplified model of multi-level vertical isolated structure under Heavy-haul train vibration. In: IEEE International conference on intelligent transportation engineering
15. Lin H-C, Ye Y-C, Huang B-J, Jia-Lun Su (2016) Bearing vibration detection and analysis using enhanced fast fourier transform algorithm. *Adv Mech Eng* 8(10):1–14

Intelligent Fire Outbreak Detection in Wireless Sensor Networks



Dhiraj Chaurasia, Saikat Kumar Shome, and Partha Bhattacharjee

Abstract The outbreak of fire is a serious hazard which is very likely to happen, resulting in loss of lives and property. The traditional fire alarms generally make use of just one sensor and some threshold to trigger the alarm. Smoke is generated in several forms in daily lives, and a single parameter is not reliable to detect an outbreak. This paper mainly focuses on the intelligent use of sensors by deploying learning algorithms and AI techniques to reduce false alarm and increase efficiency. Additionally, the application of such a system has been demonstrated and analyzed in terms of detection rate, prediction score of the model, confusion matrix, logarithmic loss and AUC. The performance results show that the model is able to predict the outbreak with an error rate of less than 0.2%. The complexity of computation has also been worked out.

Keywords Fire detection · Machine learning · Random forest · Wireless sensor network · Intelligent fire alarm

1 Introduction

Fires outbreak can happen anywhere ranging from the bedroom to the office, and the conditions can vary vastly. According to a report published in 2012 by the National Crime Records Bureau, India, fire accounted for 5.9% (23,281) of the deaths reported. Another report of the biggest losses of the Indian Insurance Companies reported in 2007–2008, 45% of the claims were due to fire hazards [1]. The simplest way to

D. Chaurasia

National Institute of Technology Durgapur, M G Avenue, Durgapur 713209, West Bengal, India
e-mail: dc18u10737@btech.nitdgp.ac.in

S. K. Shome (✉) · P. Bhattacharjee

CSIR-Central Mechanical Engineering Research Institute, M G Avenue, Durgapur 713209, West Bengal, India

e-mail: saikatshome@cmeri.res.in

P. Bhattacharjee

e-mail: parthabhat@cmeri.res.in

detect a fire is by using smoke detectors, which is generally sensitive to ionization or obscuration [2]. While one set of sensing parameters may be suitable for a given preset, it may be impractical in another situation. This results in the triggering of false alarms. According to a report of NFPA, in the years 2009–2012, 48% of the fire alarms were false, excluding malicious triggers [3]. About 6,684,500 fire accidents happened in the US, and 4,879,685 of them had fire detection systems installed. However, the evolution of sensors and robust learning algorithms brings about great prospects for making smoke alarms smart and reliable. Let us briefly discuss the contributions made in this domain. Jun et al. proposed a dependable fire detection system with a multifunctional AI framework which includes a set of machine learning algorithms and an adaptive fuzzy algorithm [4]. Bagheri et al. combined a novel k-coverage algorithm and the fire weather index to detect fires [5]. To enhance fault tolerance and put unused sensors in standby, the algorithm uses k (or more) sensor nodes to screen every point. Qin et al. proposed a smoke alarm system that uses an ensemble decision tree algorithm to detect smoke and Zigbee communication protocol to make a wireless network [6]. Umoh et al. used support vector machine to classify and predict fire outbreak [7]. Turns et al. discussed how smoke, dust, temperature, and pressure parameters can be used to determine a fire outbreak [8]. Zhang et al. suggested a deep learning technique for forest fire detection by training a model of fire patch classifier in a deep joined CNN [9].

The works listed above follow two general approaches to make predictions more accurate. The first is to use only one kind of sensor but a complex algorithm to detect a fire outbreak. This approach can be seen in the work presented in [10], where a flame sensor is the only module used but a complex algorithm (fuzzy-wavelet classifier) is deployed. In contrast, the second approach is to use a set of sensor modules, but simple mathematics for detection of fire. An example of this approach can be seen in the work presented in [11], where CO concentration and ION sensors are used but a simple mathematic operation is used to judge fire outbreaks.

In this paper, the two methods have been combined to devise an approach that overcomes the shortcomings of the individual approaches like unreliability on only one kind of sensor and time taken to respond by a complex algorithm-driven system. An appropriate array of sensors was prepared based on the sensor variable importance and sensor feedback correlation. This array was then used on a contextually robust and fast machine learning algorithm-driven IoT system. The details are discussed in the following subheadings.

2 Methodology

The paper is focused on intelligent detection of fire outbreak by making use of machine learning techniques. Machine learning techniques provide our system with the ability to automatically learn and improve from experiences and remove the factor of explicit programming. To train the model, a dataset obtained from an experiment [12], which imitated several fire hazard situations in a manufactured home, was

Table 1 Classification algorithm effect comparison

Classification algorithm	Error rate	Error rate of train sets (five-fold CV)	Error rate of test sets (five-fold CV)
Random forest	0.00917431	0.00733893	0.01560482
KNN	0.01284404	0.01330302	0.01929565
Decision tree	0.01100917	0.01238506	0.02201854
Bagging	0.01100917	0.00940367	0.01835297
SVM	0.10893766	0.12001146	0.12363654

used. These sensor data were feature engineered to obtain an annotated dataset, and a classifier model was trained which would classify the real-time data to predict an outbreak. A detailed discussion on algorithm and design follows in the subsections below.

2.1 Algorithm Proposition

The “No Free Lunch” theorem states that there is no such algorithm that is optimal in all cases [13]. To make the system contextually robust, a classification algorithm that ensures the accuracy of prediction and has fast processing speed for a small volume dataset at the same time is required. To find the best-suited algorithm, several classification algorithm models were trained on the dataset, and a cross-validation test was performed (Table 1). The experiment was conducted on the dataset which is discussed in Sect. 3.1.

A five-fold CV method was used to fit each method. It can be observed that only bagging closes the accuracy of random forest as random forest is in fact a type of bagging algorithm, but it uses a subset of randomly selected features instead of all features like bagging [14]. The margin is close in the experiment because there are only a few features. These results were also in agreement with the results of an experiment [15] that compared random forest and J48 (a decision tree generating algorithm) on a UCI ML repository dataset, where a difference of 26.9% was seen. It can be established from these experiments that the random forest classifier is better suited for this experiment.

2.2 Random Forest Classifier

Random forest is an ensemble learning algorithm that builds a multitude of decision trees from a randomly selected subset of the training set with different features. The key idea is to build a large number of uncorrelated decision trees and sum up the votes from all decision trees to decide the class of the test object. As the time taken

by each tree to spit out the result is now lesser and the forest can be parallelized, the algorithm can classify at a much faster rate. Besides, random forest overcomes the problem of overfitting, is less sensitive to outlier data, and eliminates the need for pruning trees. It also decides the variable importance and accuracy automatically.

Let us assume such a classifier $\{h_j(x, \theta_i, i = 1, \dots, N)\}$, where the label classification is attained by each decision tree $h_j(x, \theta_i)$, and the probability averaging for the test object is x . The prediction class tag c_p outputs 0 or 1, 1 being fire outbreak.

$$c_p = \underbrace{\arg \max}_c \left(\frac{1}{N} \sum_{i=1}^N I \left(\frac{n_{h_j, c}}{n_{h_j}} \right) \right),$$

$$c_p = \underbrace{\arg \max}_c \left(\frac{1}{N} \sum_{i=1}^N I \left(\frac{n_{h_j, c}}{n_{h_j}} \right) \right),$$

where argmax implies the parameter c with the maximum score, N is the total number of decision trees constructed at training time, $I(*)$ is the exponential function, (n_{h_j}, c) is the classification result for the object class c , n_{h_j} denotes the number of leaf nodes of the decision tree h_j , and w_i denotes the weight of the i th tree in the forest [16].

2.3 System Architecture

In the outbreak detection system, an array of temperature, smoke obscuration, CO, CO₂, and O₂ concentration sensors has been used. The array of these sensor modules is connected to a microcontroller unit through the I/O pins. The values obtained from these sensors are fed to a program installed on the microcontroller's processor. The data is then sent in a request parameter as a string through a Wi-Fi module to a data receptor (web interface) that captures and pre-processes the data. The data is then fed to the trained classifier model which makes a real-time prediction triggering the alarm and reports the results to a report database which can be accessed from the User Interface (UI). The UI can be used for visualization or reinforcing the learning algorithm (Fig. 1).

3 Empirical Results and Discussion

To evaluate the proposed approach, the set of data was fed to the trained model, and the obtained results were analyzed as discussed below. Subsection 3.1 discusses the dataset, Sect. 3.2 consists of the performance metrics employed, Sect. 3.3 consists

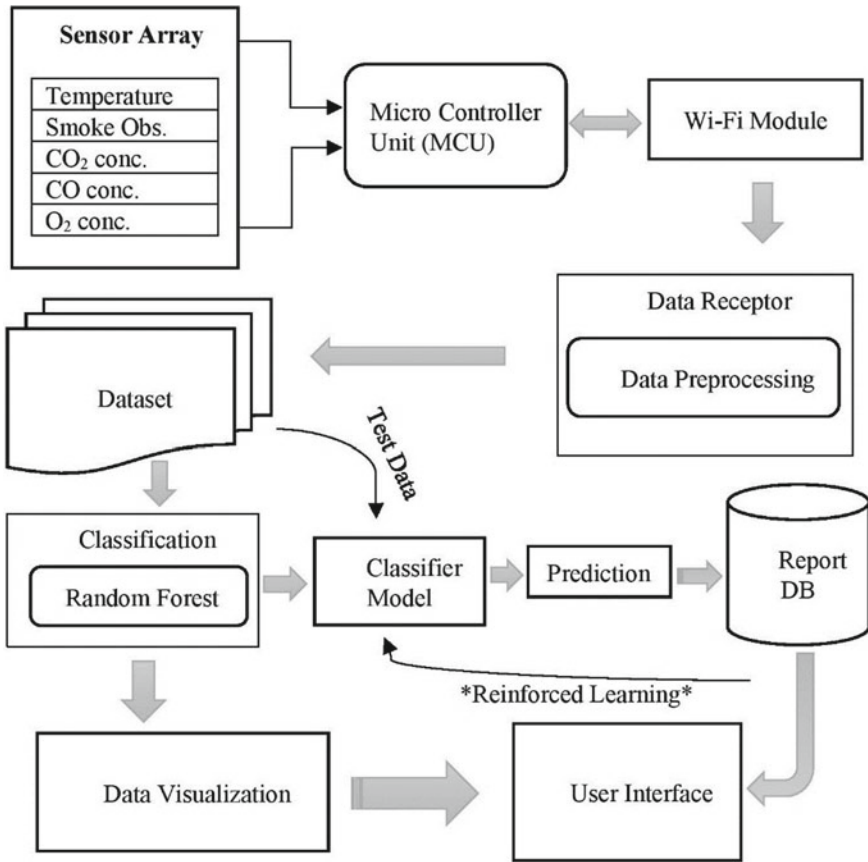


Fig. 1 Conceptual architecture of the outbreak detection system

of the experimental reports, and Sect. 3.4 discusses the computational complexity consideration.

3.1 The Dataset

The dataset used in the research was obtained from the NIST Website <https://www.nist.gov/el/nist-report-test-fr-4016>. Different fire hazard situations like a smoldering chair, flaming mattress, cooking oil fire, etc. were recreated in controlled experimental, and the concentrations of CO, CO₂, and O₂, smoke obscuration, and temperature at multiple locations in the structure were recorded. A total of seven datasets (*sdc01 ... sdc07*) were combined to obtain a total of 5450 entries, 80% of which was used for training the model and 20% for testing the model. The compiled CSV can

be obtained at <https://github.com/dch239/Fire-Outbreak-Detection/blob/master/sdcCompiled.csv>. It may be noted that only five sensor parameters were fed to the model based on the correlation with output and feature importance graph as discussed in the results.

3.2 The Performance Metrics

The evaluation of the model was done based on the model score, logarithmic loss, and the AUC-ROC curve. To further visualize the performance of the model, a confusion matrix was obtained.

Logarithmic loss penalizes false classifications. Log loss nearer to 0 indicates higher accuracy. If N samples are belonging to M classes ($M = 2$ for binary classification), then the logarithmic loss is calculated as below.

$$\text{Logarithmic Loss} = -\frac{1}{N} \sum_{i=1}^N \sum_{j=1}^M y_{ij} * \log(p_{ij})$$

where y_{ij} indicates whether sample i belongs to class j or not, and p_{ij} indicates the probability of sample i belonging to class j .

The Receiver Operator Characteristic (ROC) curve is a metric for the assessment of binary classification models. It is a plot of true positive rate against false positive rate at the threshold values and basically tells the signal from the noise. The area under the curve is a measure of the probability of detection or classification. Given that we have only two classes, positive (1) and negative (0), $\text{AUC} = 1$ implies that the classifier has perfectly classified all the positive and negative test objects (Fig. 2). AUC between 0.5 and 1 implies a good chance of correct classification (Fig. 3). An AUC of 0.5 implies that the classifier cannot distinguish between positive and negative class objects which mean that either the classifier is predicting randomly or static class for all the test objects (Fig. 4).

A confusion matrix is a table of True Positive (TP), False Negative (FN), True Negative (TN), and False Positive (FP). It is often used to visualize the accuracy of a classification model on a set of labeled test data.

3.3 Experimental Results

Let us first analyze the dataset. To visualize the relationship between different sensor parameters, a correlation matrix was obtained which is shown in Fig. 5. The correlation ranges from -1 to 1 which corresponds to maximum negative correlation to maximum positive correlation. As seen in the plot, the correlations range from -0.85 to 0.36 . This implies that the parameters are strongly correlated. It can be

Fig. 2 AUC = 1

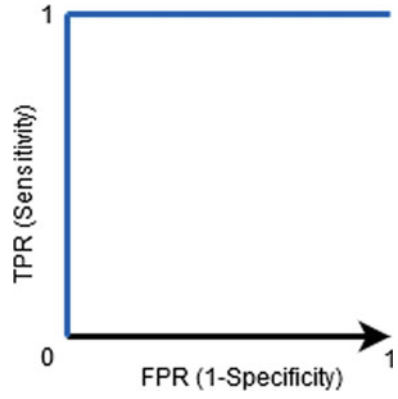


Fig. 3 $0.5 < AUC < 1$

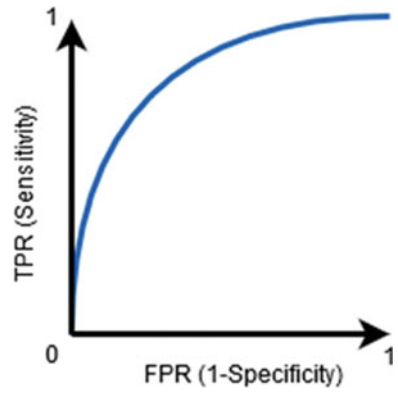


Fig. 4 AUC = 0.5

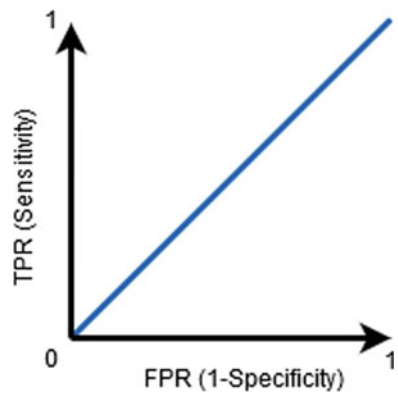
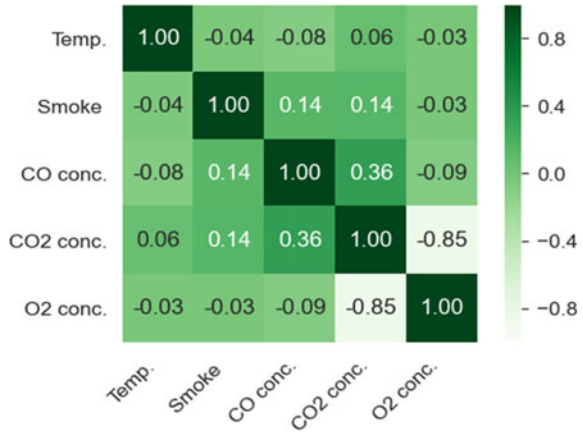


Fig. 5 Correlation matrix of sensor parameters



observed that some parameters are positively correlated (increase in smoke results in an increase of CO and CO₂ concentrations) while some are negatively correlated (increase in CO₂ concentration (possibly due to fire outbreak) results in a rapid decrease of O₂ concentration). Random forest classifier decides the variable importance automatically which can be seen in Fig. 6. The rising pattern of the cumulative importance curve helps us understand that the temperature sensor placed right above the burning object, and smoke sensor shares the greater weight and the rest follows as shown. The dataset had 5450 data records, which were divided to 4360 training data and 1090 test data. The training dataset was fed to the model, and after training, the performance metrics were employed for evaluation. A model score of 0.98990 or 98% and a logarithmic loss of 0.34856 were recorded. This indicates that our model has been able to classify the test dataset with very good accuracy. A log loss close to 0 ensures that the uncertainty of the probability spitted by our model is less, hence better the accuracy. An AUC ROC curve was obtained with an AUC score

Fig. 6 Feature importance

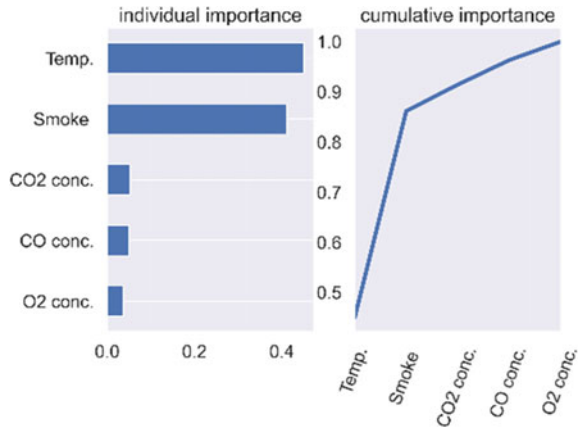


Fig. 7 AUC-ROC curve

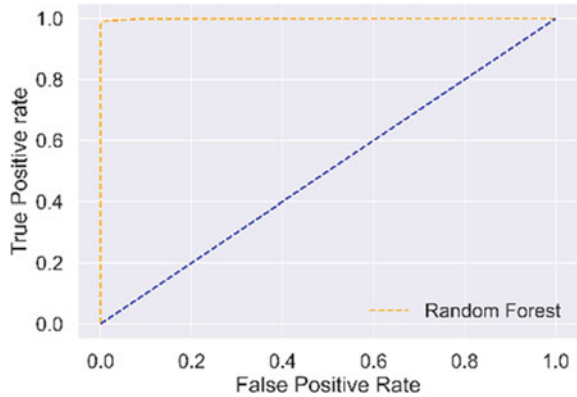
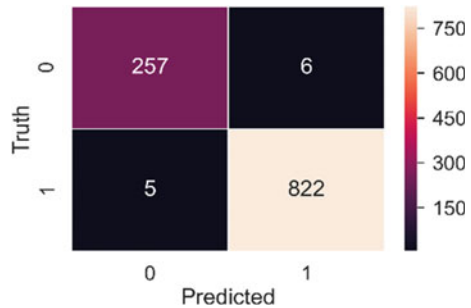


Fig. 8 Confusion matrix



of 0.99892. The curve is shown in Fig. 7. This AUC score near to 1 supports the model score and log loss and further ensures the class prediction accuracy. It is clear from the scores that the model has efficiently classified the test data with a very less error rate which can be seen in the confusion matrix obtained. Figure 8 shows the confusion matrix of the prediction, where TP (Actual: true, Predicted: true) = 822, FN (Actual: false, Predicted: false) = 257, TN (Actual: true, Predicted: false) = 5, and FP (Actual: false, Predicted: true) = 6.

3.4 Computational Complexity Consideration

Random forests work by building a multitude of decision trees. Let us calculate the time complexity for building a complete decision tree that is not pruned. If n is the number of records and v is the number of variables/attributes, we have $O(v * n \log(n))$. Assuming the number of trees to be built in random forest ensemble is n_{tree} and at each node, m_{try} variables are to be sampled, the complexity to build one tree would be $O(m_{try} * n \log(n))$. If a random forest having n_{tree} number of trees is to be built, the time complexity would be $O(n_{tree} * m_{try} * n \log(n))$. Assuming the

depth of the tree is $O(n \log(n))$, which is the worst-case scenario, the above result is obtained. But often, the build process of a tree terminates before this as computational complexity increases. Furthermore, the depth of the trees in our random forest can also be restricted. If the maximum depth of our tree is restricted to “d”, then the complexity calculations can be optimized to $O(n_{\text{tree}} * m_{\text{try}} * d * n)$. Considering the complexity for random selection of variables that needs to be done at each node, an additional $O(v * d * n_{\text{tree}})$ may be factored.

4 Conclusions

In this paper, an implementation of a learning algorithm-based smoke alarm system with system architecture, discussion of the algorithm deployed, and visualization of the results obtained has been presented. The central purpose of the paper was to find a solution for the false alarm of the traditional alarm system which has been addressed. The results indicate that the random forest classifier-based fire outbreak detection has been able to provide a solution to the problems associated with existing fire outbreak detection systems.

References

1. Nair RR (2012) In: Fire safety in India—an overview. Safety and Health Information Bureau, Vashi, Navi Mumbai
2. Majid B, Nirvana M, Paul H (2009) Use of AI techniques for residential fire detection in wireless sensor networks. *IEEE J Quantum Electron* 475:311–321
3. Karter MJ (2013) False alarm activity in the US 2012. National Fire Protection Association Fire Experience Survey, pp 1–8
4. Jun HP, Seunggi L, Seongjin Y, Hanjin K, Won-Tae K (2019) Dependable fire detection system with multifunctional artificial intelligence framework. *Sensors* 19(9): 2025
5. Bagheri M, Hafeeda M (2007) Efficient K-coverage algorithms for wireless sensor networks and their applications to early detection of forest fires, Technical Report, Computing Science 2007, Simon Fraser University
6. Qin W, Jiashuo C, Chuang Z, Ji H, Zhuo L, Shin-Ming C, Jun C, Guanghui P (2018) Intelligent smoke alarm system with wireless sensor network using ZigBee. *Wireless Commun Mobile Comput* 1–11
7. Uduak U, Edward U, Nyoho E (2019) Support vector machine-based fire outbreak detection system. *Int J Soft Comput Artif Intell Appl* 08:1–18
8. Turns SR (1996) *IN: An introduction to combustion*. vol 287. McGraw-Hill, New York, NY, USA
9. Qingjie Z, Jiaolong X, Liang X, Haifeng G (2016) Deep convolutional neural networks for forest fire detection. In: *Proceedings of the 2016 international forum on management, education and information technology application*. Atlantis Press, pp 568–575
10. Thuillard M (2000) Application of fuzzy wavelets and wavelets in soft computing illustrated with the example of fire detectors. *Wavelet Appl*. VII 4056:351–361
11. Daniel TG, Michelle JP, Richard JR, Craig LB (2002) Advanced fire detection using multi-signature alarm algorithms. *Fire Saf J* 37:381–394

12. Richard DP, Jason DA, Richard WB, Paul AR (2005) Home smoke alarm project, manufactured home tests at building and fire research laboratory. National Institute of Standards and Technology. NIST Report of Test FR 4016
13. David HW, William GM (1997) No free lunch theorems for optimization. *IEEE Trans Evol Comput* 1(1):67–82
14. Leo B (1996) Bagging predictors. *Machine Learn* 24(2):123–140
15. Jehad A, Rehanullah K, Nasir A, Imran M (2012) Random forests and decision trees. *Int J Comput Sc (IJCSI)* 9(5) 3:272–278
16. Jin-Shyan L, Yu-Wei S, Chung-Chou S (2007) A comparative study of wireless protocols: bluetooth, UWB ZigBee and Wi-Fi. In: *IECON 2007—33rd annual conference of the IEEE industrial electronics society*. pp 46–51

IoT and Cloud Computing

Lightweight Authenticated Encryption for Cloud-assisted IoT Applications



Zainab S. AlJabri, Jemal H. Abawajy, and Shamsul Huda

Abstract In an increasingly connected cyberspace where cloud-enabled Internet of things (IoT) applications are exploding, ensuring trust and privacy are two major requirements but often neglected. In this paper, we discuss a lightweight authenticated encryption for simultaneously protecting authenticity and privacy of messages in the cloud-enabled IoT platforms.

Keywords Authenticated encryption · Internet of things · Cloud computing · Lightweight

1 Introduction

Cloud-enabled IoT frameworks that integrate an IoT devices such as wearable wristbands and implanted pacemaker with cloud computing have recently become prominent [1, 2]. The IoT devices [3, 4, 5] collect information such as patient daily activities and physiological parameters. As the data normally monitored by IoT devices is very sensitive, privacy preservation of the patient information is a key requirement [6] in cloud-enabled IoT platforms. Moreover, the IoT devices transmit the collected patient information to a third party (i.e., cloud) for further processing. In order for the IoT devices and the cloud to securely communicate, there is a need for trust to be established between the communicating parties. This mandates a strong authentication to ensure that IoT devices and cloud can be trusted to be what they purport to be.

Therefore, measures ensuring privacy and authentication are needed to be established. The focus in research is mainly to develop privacy preserving mechanisms [6] or authentication mechanism [7]. There are very little work that try to

Z. S. AlJabri · J. H. Abawajy (✉) · S. Huda
School of Information Technology, Deakin University, Geelong, VIC 3220, Australia
e-mail: jemal@deakin.edu.au

Z. S. AlJabri
e-mail: zaljabri@deakin.edu.au

S. Huda
e-mail: shamsul.huda@deakin.edu.au

address both privacy and authentication concurrently in platforms that integrate IoT and cloud computing for the purpose of handling sensitive data. This is because achieving both privacy and authentication simultaneously for cloud-enabled IoT platforms is extremely challenging. Part of the problem emanates from the inherently limited computing power of the IoT devices. This resource constraint basically rules out the standard resource hungry cryptographic solutions that are developed for general purpose devices. In this paper, how the authenticity and privacy of messages exchanged between the IoT devices and cloud could be simultaneously achieved using a lightweight authenticated encryption (AE) is discussed. We also discuss various challenges associated with AE as related to IoT devices.

The rest of the paper is organized as follows. Section 2 will give a brief description of IoT platform architecture. In Sect. 3, authenticated encryption algorithm is discussed. The conclusion is given in Sect. 4.

2 Internet of Thing Framework

2.1 IoT System Architecture

A typical IoT deployment consists of four major components as shown in Fig. 1. At the sensing layer, IoT devices such as wearable are used to collect or sense data based on the application. The data collected by the IoT devices and then transferred to the network layer. A vital role of this layer is to connect the things altogether and exchange sensed data for further analysis. The service layer mainly consists of

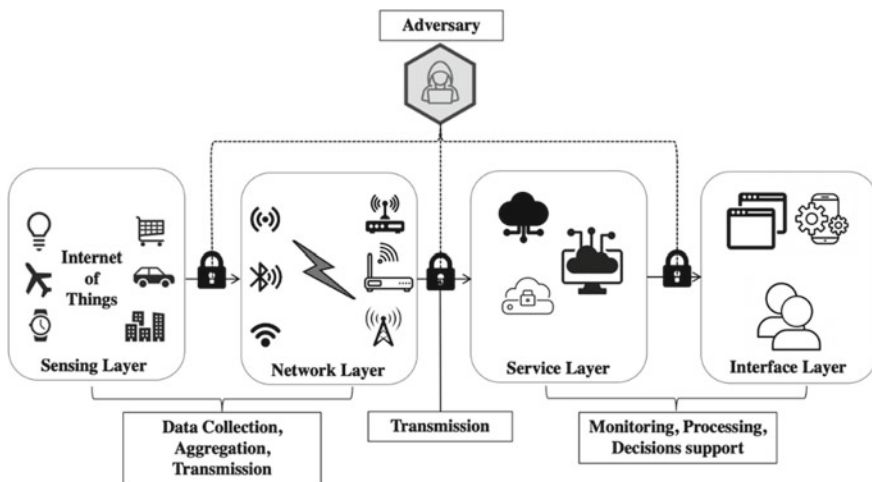


Fig. 1 Typical IoT system architecture

the middleware devices to provide a collaborative IoT services related to identification, authorization, aggregation, decision support and reactions. These technologies cooperate with services and IoT applications to provide a cost-effective products. For instance, a cloud-based service used to maintain, analyze and process data collected on a smart city, such that limited resources things connected together. At the same time, it supports the insertion of processed information, collaborates and provides results to users' application layer. The interface layer potential overcomes the various technology vendors interconnection, where searching service is integrated. This layer facilitates the identification and matching of application requirements. The user views the results and decisions using application (i.e., smart phones, PCs).

2.2 Authenticated Encryption

The security of the IoT-enabled systems is necessary to ensure the reliability and availability of the system protection [8]. The standard encryption algorithm can be used to address the confidentiality of the messages. Within cloud-assisted IoT applications, this is of limited significance unless it is complemented with message authentication. Authenticated encryption (AE) offers confidentiality and integrity of the messages exchanged between genuine senders and receivers of the messages. Figure 2 shows the engine interfaces of authenticated encryption. AE is typically integrated within the system model as shown in Fig. 1 between sensing layer and network layers, various connections within network layer, network and service layers and service and interface layers.

The various categories of AE schemes can be categorized as a one or two-pass approach. One-pass AE scheme performs one run to compute the encryption and tag using one key for both or two separate keys for each. The two-pass AE scheme processes the message twice. The IoT devices do not have the compute and storage power required by the conventional AE schemes, which make the standard AE schemes of less practical significance in the cloud-assisted IoT platform. In the next section, we discuss a lightweight AE scheme suitable for cloud-assisted IoT platform.

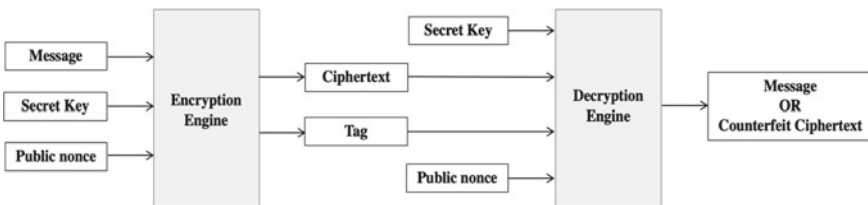


Fig. 2 Authenticated encryption and decryption engine interfaces

3 Lightweight Authenticated Encryption Schemes

Designing lightweight authenticated algorithm (LAE) suitable for resource-constrained IoT devices such as wearable wristbands, implanted pacemaker and smart meters is an active area of research. LAE allows IoT devices to send a signed message to the cloud while the cloud will simultaneously recover and verify the message received from the IoT device. Existing LAE schemes such as the Hummingbird-2 (HB-2) [9] and ElmD [12] have been designed based on well-established symmetric key cryptographic primitives. Hummingbird-2 [9] is an LAE with low area and low power that makes it suitable for resource-constrained IoT devices. Although HB-2 with a key size of 128 bits and a 64 bit initialization vector is immune to many known attacks, it is shown that the initial key can be recovered [11]. ElmD [12] is another LAE that suffers from forgery and key recovery attacks [13]. Although Constrained Application Protocol [10] is a popular lightweight IoT protocol, it is susceptible to many well-known attacks [14]. LAE requires less computation, footprint, power and energy relative to the conventional AE algorithms. LAE requires negotiated secret key a priori, which is common in the existing protocols, and no extra overhead is incurred. Moreover, LAE offers desirable security level and can be readily incorporated within existing protocols and IoT devices.

4 Conclusion

LAE promises to offer message authentication and privacy at the same time, which is especially appropriate for resource-constrained IoT devices. LAE is lightweight by design which consumes less computation compared to existing algorithms in current communication protocol, which tolerate a small footprint, low power consumption and energy. Additionally, it provides the desirable security level and can be easily integrated within existing protocol algorithms and restricted embedded devices.

References

1. Ghanavati S, Abawajy JH, Izadi D, Alelaiwi AA (2017) Cloud-assisted IoT-based health status monitoring framework. *Cluster Comput* 20(2):1843–1853
2. Abawajy JH, Hassan MM (2017) Federated internet of things and cloud computing pervasive patient health monitoring system. *IEEE Commun Mag* 55(1):48–53
3. Izadi D, Abawajy J, Ghanavati S (2014) An alternative node deployment scheme for WSNs. *IEEE Sens J* 15(2):667–675
4. Mahdin H, Abawajy J (2011) An approach for removing redundant data from RFID data streams. *Sensors* 11(10):9863–9877
5. Ray BR, Abawajy J, Chowdhury M (2014) Scalable RFID security framework and protocol supporting internet of things. *Comput Netw* 67:89–103
6. Luo E, Liu Q, Abawajy JH, Wang G (2017) Privacy-preserving multi-hop profile-matching protocol for proximity mobile social networks. *Future Gener Comput Syst* 68:222–233

7. Fernando H, Abawajy J (2012) A hybrid mutual authentication protocol for RFID. In: Lecture notes of the institute for computer sciences, Social-informatics and telecommunications engineering, vol 73 LNICST, pp 310–311
8. Abawajy J, Huda S, Sharmeen S, Hassan MM, Almogren A (2018) Identifying cyber threats to mobile-IoT applications in edge computing paradigm. *Future Gener Comput Syst* 89:525–538
9. Engels D, Saarinen M-JO, Schweitzer P, Smith EM (2012) The Hummingbird-2 lightweight authenticated encryption algorithm. In: Juels A, Paar C (eds) *RFIDSec 2011*, LNCS 7055, pp 19–31
10. Arvind S, Narayanan VA (2019) An overview of security in CoAP: attack and analysis. In: 2019 5th international conference on advanced computing and communication systems
11. Zhang K, Ding L, Guan J (2012) Cryptanalysis of hummingbird-2. *IACR Cryptology ePrint Archive*, vol 2012, pp 207
12. Bossuet L, Datta N, Mancillas-López C, Nandi M (2016) ELMd: a pipelineable authenticated encryption and its hardware implementation. *IEEE Trans Comput* 65(11):3318–3331
13. Bay A, Ersoy O, Karakoç F (2016) Universal forgery and key recovery attacks on ELMd authenticated encryption algorithm. In: International conference on the theory and application of cryptology and information security, pp. 354–368
14. Randhawa RH, Hameed A, Mian AN (2019) Energy efficient cross-layer approach for object security of CoAP for IoT devices. *Ad Hoc Netw* 92:101761

Botnet Dynamics and Measures for India



Md. Amir Khusru Akhtar, Mohit Kumar, and Ashwani Kumar

Abstract The observations of Indian Computer Emergency Response Team (CERT) shows that botnet infected systems in India was 25,915 in 2007 which increased to about 6.5 million in 2012. The infected system grew very rapidly and reached over 60 per cent in first half of 2013. Since then, there have been many outbreaks, with the greatest being the current 2019 outbreak. This paper presents the use of calculus to model botnet epidemics. Our model is based on an $S \rightarrow I \rightarrow R$ (susceptible, infected, recovered) scheme. The aim of this research is to model the transmission dynamics of botnet to predict the outbreak of malicious code. This research is very significant to the current situation in India for understanding the rate of transmission of epidemic. We have compared the data collected from the SIR model with the observed data of the infectious nodes. The simulation uses the fourth-order Runge-Kutta algorithm and implemented in Python 3. The results of the present analysis are supportive in controlling the infection and serves as a foundation for planning, design, and defense of a computer network.

Keywords Botnet · Epidemics · Malware · Ddos · SIR model

1 Introduction

Bots are used commonly on the internet for malicious activities such as information stealing and act as a launching pad for distributed attacks [1]. The malware's gets installed on user computer without their knowledge and issue the control

Md. A. K. Akhtar (✉)
Usha Martin University, Ranchi, India
e-mail: amir@umu.ac.in

M. Kumar
Cambridge Institute of Technology, Ranchi, India
e-mail: mohitsmailbox13@gmail.com

A. Kumar
Vardhaman College of Engineering, Hyderabad, India
e-mail: ashwani.kumarcse@gmail.com

of the machine to a remote attacker. These machines are generally known as zombie machines. The attacker uses several techniques such as Web/Mail Download, malware installation from fake sources, scan exploit, etc. The malicious contents like trojans, bots, etc. are installed by exploiting known vulnerabilities in end user system.

Over 4.2 million devices were infected in India by botnet malware for various kinds of cybercrimes [2]. The observations of Indian Computer Emergency Response Team (CERT) shows that botnet infected systems in India was 25,915 in 2007 which increased to about 6.5 million in 2012. Botnet infected systems grew rapidly and touched over 60 per cent in first half of 2013. Since then, there have been many outbreaks, with the greatest being the current 2018 outbreak. A lot of malicious activities such as hacking of sites, snooping, frauds, phishing attack, DDoS, etc. are undeviating attacks on the safety and security which affects the institutional integrity and places these institutions or government bodies at stake. Several cyber forensics tools have been used to know the modus operandi of the attacks. This paper presents the use of calculus to model botnet epidemics. After the launch of the Cyber Swachhta Kendra in India, there has been a 51% decline in malware infections. This center monitors the flow of internet and sends notifications to internet service providers, to alert the current situation. This work is developed to understand the propagation of malicious code in a network and play a key role in risk measurement and in policy making in India.

This paper presents the use of calculus to model botnet epidemics. Our model is based on an $S \rightarrow I \rightarrow R$ (susceptible, infected, recovered) scheme [3–5]. The aim of this research is to model the transmission dynamics of Bontnet to predict the outbreak of malicious code. This research is very significant to the current situation in India for understanding the rate of transmission of epidemic. We have compared the data collected from the SIR model with the observed data of the infectious node. The simulation uses the fourth-order Runge-Kutta algorithm and implemented in Python 3. The proposed epidemic model serves as a foundation for planning, design, and defense.

The rest of the paper is organized as follows. The related work is presented in Sect. 2. Section 3 describes the proposed mathematical model. Numerical simulation is shown in Sect. 4. Finally, Sect. 5 concludes the paper.

2 Related Work

The most related research to our presented work is discussed in [6–8] to study the effects of the epidemic. In order to understand the transmission of information in networks, several frameworks have been proposed in the literature [9].

Farooq and Zhu [6] proposed an analytical model to study the D2D propagation of malicious software in IoT networks. It uses leveraging tools from dynamic population processes and point process theory to capture malicious software infiltration and coordination process. The mean-field equilibrium in the population is used to avoid

botnet formation. The proposed model is valuable for planning, design, and defense of wireless IoT networks.

Kumari et al. [7] proposed media coverage factor in the firewall security to detect and minimize the virus propagation. The idea of optimal control theory is presented for monitoring the virus propagation. It performs a sensitivity analysis to determine the virus dispersion in networks. The proposed firewall security eliminates the malicious node propagation in a network by dropping the infection level.

Mishra et al. [8] proposed a two-fold epidemic model. This model is primarily based on Mirai botnet made of internet of things devices with three main DDoS attacks in 2016. The model examines the equilibrium points to discover the environments for local and global stability. Numerical simulations show the effectiveness of the developed model.

However, traditional epidemiological models [10] are not sufficient to analyze the botnet dynamics in a particular geographical region due to the behavior and operation style of the region.

3 Proposed Epidemic Model

This section presents the dynamics of Botnet for India. The following assumptions have been made to model the problem [5]. The attack is transmitted by execution of malicious code

- (a) Malicious code is any type of code in any part of software or any script that cause damage, security breaches or undesired effects to a system.
- (b) The latent period for the attack is negligible; hence the node gets infected instantaneously upon execution of malicious code.
- (c) Each and every susceptible individual are equally susceptible and infected individuals are equally infectious. The population size is fixed where no births or migration occurs.

We have assumed that the population is fixed and having N individuals. This model finds the amount of susceptible, infected, and recovered people in a population.

Since the population size fixed, the population is either susceptible to the attack or infected with the attack. Let the independent variable be time, t , and also let:

$S(t)$ = number of nodes that are susceptible to malware at time t

$I(t)$ = number of nodes infected with malware at time t

β = the rate of infection of nodes

γ = rate of recovery of nodes

The categories of nodes and the transmission between the categories can be summarized in the in Fig. 1.

The SIR model uses two parameters which can be used standardize it, β and γ with $\beta, \gamma > 0$, the model uses three differential equations [3–5].

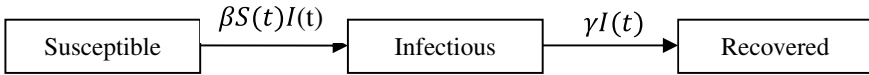


Fig. 1 Nodes Compartments

$$\frac{dS}{dt} = -\beta S(t)I(t) \tag{1}$$

$$\frac{dI}{dt} = \beta S(t)I(t) - \gamma I(t) \tag{2}$$

$$\frac{dR}{dt} = \gamma I(t) \tag{3}$$

where $\frac{dS}{dt}$ means the rate of change of the number of nodes susceptible to the malware over time, $\frac{dI}{dt}$ means the rate of change of the number of nodes infected and $\frac{dR}{dt}$ means the rate of change of the number of nodes recovered over time. These variables change with respect to time (t) and t is time in days with $t = 0$ at the start of observation. The total population size is always N , and since all nodes are either susceptible or infected or recovered

Thus,

$$N = S(t) + I(t) + R(t) \tag{4}$$

In order to know the initial state of the population assume that at time $t = 0$, S_0 is susceptible population and a very small number, I_0 is infective, So,

$$S(0) = S_0 = N - I_0; I(0) = I_0; R(0) = 0$$

The rate of Infection of nodes (β) and rate of recovery of nodes (γ), is calculated using duration of disease (D) and rate of mortality (M).

The infection rate of nodes (β)

$$\beta = \frac{M}{S} \tag{5}$$

and rate of recovery of nodes (γ)

$$\gamma = \frac{1}{D} \tag{6}$$

4 Numerical Simulation and Discussion

The observations of Indian Computer Emergency Response Team (CERT) shows that botnet infected systems in India was 25,915 in 2007 which increased to about 6.5 million in 2012. The number of botnet infected system grew rapidly and reached over 60 per cent in first half of 2013. From the observation the parameters can be assigned with the following values.

Let us assume total population/nodes of India, $N = 1000$, the number of nodes infected, $I = 60$. Where R is initially 40 and it is slightly less than infected because an infected node can be recovered by cleaning or simply restarting.

$$\begin{aligned} N &= 1000 \\ I &= 60 \\ R &= 40 \end{aligned}$$

Therefore, $S = N - I + R = 1000 - 60 + 40 = 980$.

The rate at which the infections spread can be established by dividing 1 by the duration of the infection. The duration of the attack ranges from 1 to 10 days, therefore we could roughly estimate the duration of the disease at the midpoint, i.e. 5 days.

$$\begin{aligned} D &= 5 \\ \gamma &= \frac{1}{D} = \frac{1}{5} = 0.2 \end{aligned}$$

Using the observed data, the percentage of infected nodes reached over 60 per cent

$$\beta(\text{the rate of infection}) = \frac{M}{S} = \frac{0.6}{1000} = 6.0 \times 10^{-4}$$

The simulation uses the fourth-order Runge-Kutta algorithm and implemented in Python 3. Figure 2. shows the plot of the time series of how many nodes were infectious in 2 months. Initially, the number of individuals infected increases sharply and after a longer period of time, the numbers finally decreases. This happens because the number of people recovered increases and infected individuals decrease. The tip of the graph depicts the maximum number of individuals constantly to be infected and after this peak point the numbers decreases. This graph shows that the total number of nodes remains constant throughout the analysis period because $N = S(t) + I(t) + R(t)$.

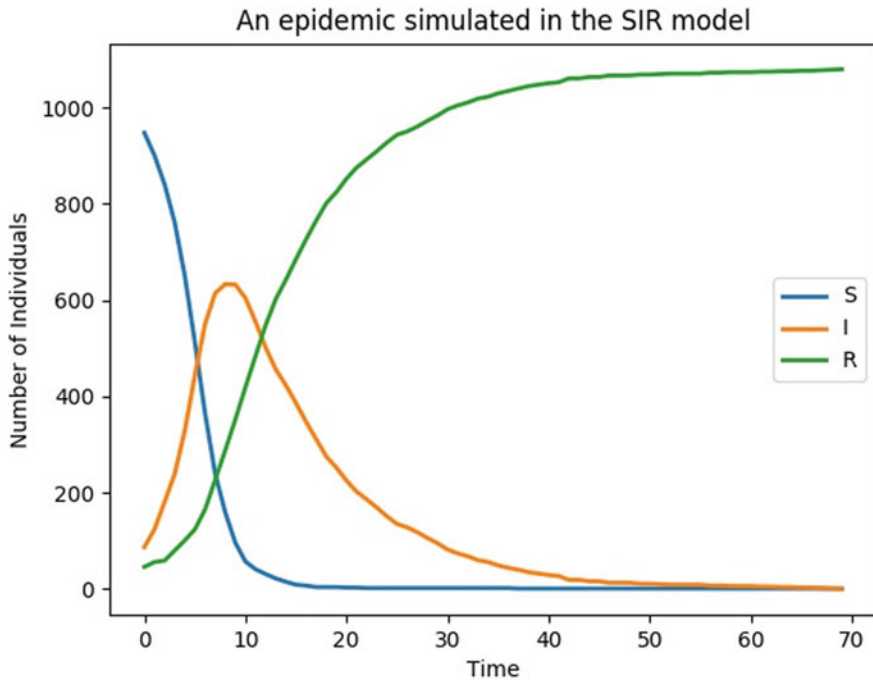


Fig. 2 SIR Model for Botnet outbreak in India, May–June 2013

4.1 Using the SIR Model for Botnet Outbreak in India

The below list shows the data collected from the SIR model for the infected nodes.

Infected List from SIR Model: [87, 124, 181, 239, 329, 444, 550, 614, 633, 632, 604, 555, 501, 456, 423, 386, 347, 311, 275, 252, 225, 202, 186, 169, 151, 135, 128, 118, 106, 95, 82, 74, 68, 60, 56, 49, 44, 40, 35, 32, 29, 27, 19, 19, 16, 16, 13, 13, 13, 11, 11, 10, 9, 9, 9, 9, 7, 7, 6, 6, 6, 5, 5, 4, 4, 3, 3, 2, 1, 0].

The observed data of the infectious is shown below.

Infected List from observation: [60, 70, 80, 90, 100, 110, 120, 130, 140, 150, 160, 170, 180, 190, 200, 210, 220, 230, 240, 250, 260, 270, 280, 290, 300, 310, 320, 330, 340, 350, 360, 362, 364, 360, 340, 330, 320, 310, 300, 290, 280, 270, 260, 250, 240, 230, 220, 200, 190, 180, 170, 160, 150, 140, 130, 120, 110, 110, 100, 100].

The number of infected nodes over time is shown in Fig. 3. The tip of the graph depicts the maximum number of nodes constantly to be infected by the bots

The comparison graph of the model and observed data for the infected nodes is shown in Fig. 4. The observed data does not keep up a better correspondence from the model data and can be improved by changing the gamma and beta values.

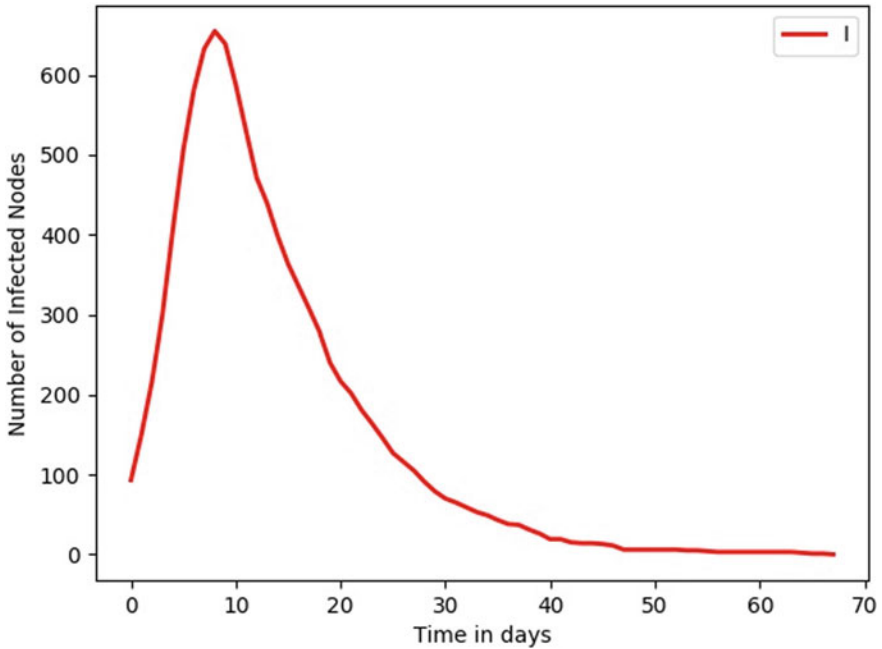


Fig. 3 Infected nodes, May–June 2013

4.2 Measures

The following are important for planning, design, and defence of a computer network

- The results of the present analysis are supportive in controlling the infection and serves as a foundation for planning, design, and defence of a computer network.
- This model is very fast and results can be used in immediate evaluation and prediction of malicious code.
- This model is very understandable and can be used to distinguish between the number of individuals susceptible, infected and recovered.
- The model is generally used to understand the effects of the epidemic.

5 Conclusion

The SIR model is very useful in the study of botnet dynamics. We have presented the $S \rightarrow I \rightarrow R$ (susceptible, infected, recovered) scheme to model the transmission dynamics of botnet. The SIR model provides an essential framework for the analysis of the epidemic spread. The simulation uses the fourth-order Runge-Kutta algorithm for solving the three ordinary differential equations. It is very quick model and the result can be used in immediate evaluation and prediction. This model can be used to

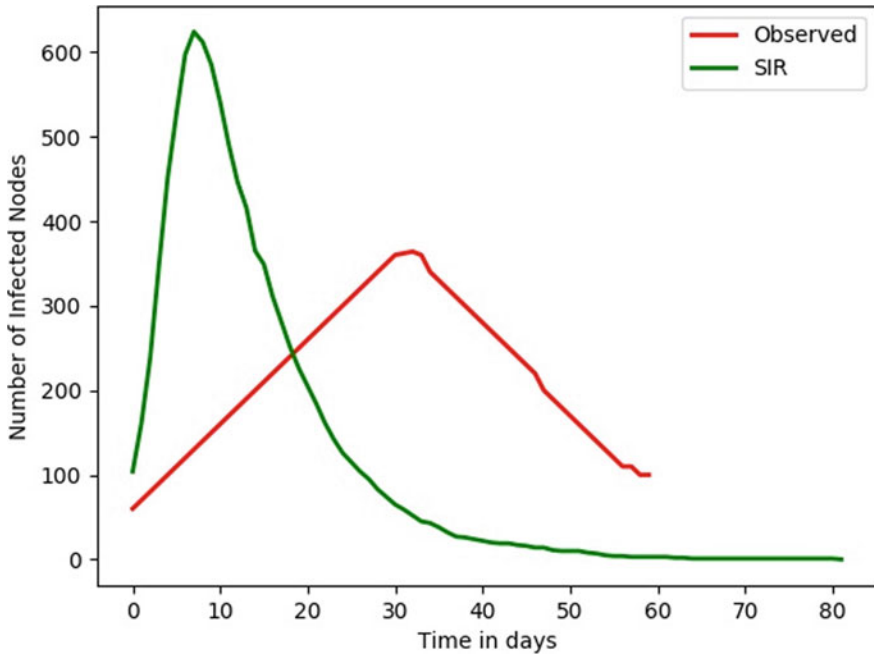


Fig. 4 Comparison of model versus observed data, May–June 2013

distinguish between the number of individuals susceptible, infected and recovered. Numerical simulations are used to validate our obtained analytical results. The result of the present analysis serves as a foundation for planning, design, and defense of a computer network.

References

1. Indian—computer emergency response team. <https://www.cert-in.org/in/>
2. Over 42 lakh Indian computers infected with malware. <https://www.businesstoday.in/technology/news/over-42-lakh-indian-computers-infected-with-malware/story/204432.html>, last accessed 2019/10/21
3. Brauer F, Castillo-Chavez PC (2001) *Mathematical models in population biology and epidemiology*. Springer-Verlag, New York
4. kermack1927.pdf. <http://www.math.utah.edu/~bkohler/Journalclub/kermack1927.pdf>
5. Brauer F, *Mathematical models in population biology and epidemiology* Springer. <https://www.springer.com/gp/book/9781441931825>, last accessed 2019/10/21
6. Farooq MJ, Zhu Q (2019) Modeling, analysis, and mitigation of dynamic botnet formation in wireless IoT networks. *IEEE Trans Inf Forensics Secur* 14:2412–2426. <https://doi.org/10.1109/TIFS.2019.2898817>
7. Kumari S, Singh P, Upadhyay RK (2019) Virus dynamics of a distributed attack on a targeted network: effect of firewall and optimal control. *Commun Nonlinear Sci Numer Simulat* 73:74–91. <https://doi.org/10.1016/j.cnsns.2019.02.006>

8. Mishra BK, Keshri AK, Mallick DK, Mishra BK (2019) Mathematical model on distributed denial of service attack through Internet of things in a network. *Nonlinear Eng* 8(1):486. <https://doi.org/10.1515/nleng-2017-0094>
9. Farooq MJ, Zhu Q (2018) On the secure and reconfigurable multi-layer network design for critical information dissemination in the Internet of Battlefield Things (IoBT). *IEEE Trans Wireless Commun* 17:2618–2632. <https://doi.org/10.1109/TWC.2018.2799860>
10. Lloyd AL, May RM (2001) How viruses spread among computers and people. *Science* 292:1316–1317. <https://doi.org/10.1126/science.1061076>

Google Controlled Car



Sagnik Ghosh and Prasun Chowdhury

Abstract The present day scenario is actively moving ahead towards smarter things. Smart things signify of connected devices, objects and more. Its feasibility is achievable by using IoT (Internet of Things) technology. Driver-less vehicles has been a very hot topic in the market. This paper focuses on using IoT technology towards developing driverless cars using Google Assistant. The car is operated via a MCU which functions according to commands given by Google Assistant. Exploring the current situations of pollution and congestions that take place this car can be of utmost help to mankind thus-making the society smarter.

Keywords Driver-less cars · Internet of things · Google assistant · Smart things

1 Introduction

The Google Controlled car aims at providing hassle free transport. It is one more step towards developing smart societies or communities using IoT (Internet of Things) [1], [2] technology wherein everything is controlled automatically. Google Controlled Car is an automatic driverless robot car [3, 4] that operates based on commands we give to Google Assistant. Furthermore the Google controlled car (henceforth termed as bot) is very efficient because it provides us with the information of the obstacle present in front, back, left or right of it. Moreover, the data of the bot's movement is uploaded into Google Maps for tracking its position and movement. It is hosted on Google Maps for proper visualization and observability. The bot's movement can be followed and corresponding traffic be avoided easily. In this way it saves time, energy, money and overall human labour. Also if applied properly it

S. Ghosh · P. Chowdhury (✉)

Department of Electronics and Communication Engineering, St. Thomas' College of Engineering & Technology, Kolkata, India

e-mail: prasun.jucal@gmail.com

S. Ghosh

e-mail: sgsagnikghosh@gmail.com

can be an additional aid to reduce or minimize pollution. It will also be very cost effective since it requires minimal resources for its application. The authors of the paper [5] Esra et al. develop a voice controlled car is made based on Bluetooth and an android application. The system fails for remote monitoring of the car because of the limited range of Bluetooth. Our paper focuses on using IoT technology towards developing driverless cars using Google Assistant. It can be operated from anywhere in the world provided there is an Internet connection. The car would be battery operated so fuel cost will be saved. Hence it can be used as a measure to resolve crisis like traffic congestion, pollution and be a boon towards a smart society. It is a very emerging concept. It encompasses information communication, environmental protection, energy conservation and safety. This car can be said as a convergence of connected vehicles and IoT technology.

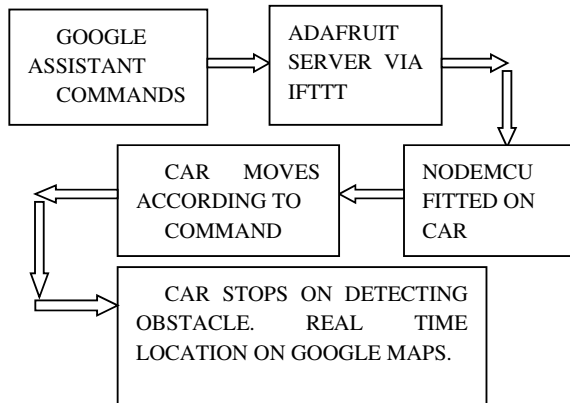
2 Work Description

The entire operation of this car is based on the principles of IoT (Internet of Things) [1], Google Assistant, Google Maps and a microcontroller board, namely NODEMCU [6]. This microcontroller board is programmed using the Arduino IDE through USB cable. To begin with, on giving a voice command to Google Assistant the car moves according to the command. The command we give to Google Assistant is sent to the, IFTTT [7] (if this then that) portal, used here. In IFTTT [7] applets are made according to the desired directions we want the car to move. There can be quite a number of applets depending on how we want our car to move. When a certain applet is triggered the corresponding data is sent to the server, Adafruit.io. [8] On basis of this data, whether a certain field in the channel is high or low the microcontroller starts its action. The microcontroller, Node MCU [4] used here is fitted with a ESP8266-01 chip, popularly known as (WiFi) chip, establishes connection between the server and the microcontroller board. The board communicates with the cloud from which the data is fetched as to which pin(s) in the microcontroller board should be working. A motor driver IC then drives the motors attached to the car according to the data obtained.

After the command execution is over Google Assistant replies back as we ask it to. Next to observe smooth movement an Ultrasonic sensor is fitted to the device to detect obstacle in front of the car. As soon as it senses obstacle it stops. The distance between the obstacle and car is pre specified in the coding section. The location of the car is seen from Google Maps. As the car moves its current latitude and longitude is sent and after three such iterations the average of the latitude and longitudes is set to be the current location. It is then retrieved into Google Maps for better viewing. Based on this many important things and events can be determined. Figure 1 shows the block diagram of the entire working.

In order to operate the entire thing we need to properly configure the server first. For this initially we need to setup WiFi client class in order to connect with the MQTT [9] (*Message Queuing Telemetry Transport*) server. This follows setting up

Fig. 1 Block diagram of the system



the MQTT [9] client class by passing in the WiFi client and MQTT [9] server and login details. Adafruit server [8] now establishes connection with Node MCU [6] board. We can publish data or subscribe from (obtain data) the server freely after MQTT [9] connects properly. Next MQTT [9] subscription is done so that feeds (channels) can subscribe to changes, i.e., update channels according to voice commands given from Google Assistant. Nothing would be possible if there’s no connection with MQTT [9] server. The following things were used to implement this:

2.1 Internet of Things

Internet of things [1, 2] has evolved from the convergence of technologies like real-time analytics, machine learning, commodity sensors, and embedded systems. Various implementations of embedded systems, wireless sensor networks, control systems, automation, and others contribute to the formation of Internet of things. In Internet of Things, all the things in that communicate with the internet continuously can be put into three categories:

1. Things that gather information and then send it.
2. Things that obtain information and then act on it.
3. Things that do either.

All three of these have enormous benefits feed on each other. The Internet of Things is able to include transparently and seamlessly a substantial number of different and heterogeneous systems. It additionally provides an open access to selected subsets of information or data for development of enormous number of digital services. Likewise over here we have used IoT to take voice inputs from Google Assistant (actuator) [3] and then publish it to server upon which the car moves with the help of the microcontroller Node MCU [6]. This helps to encompass the Google Controlled Car.

2.2 MQTT (Message Queuing Telemetry Transport)

MQTT [9] stands for Message Queuing Telemetry Transport. It is a publish/subscribe, extremely simple and lightweight messaging protocol, designed for constrained devices and low-bandwidth, high-latency or unreliable networks. In this paper, we setup WiFi client to establish connection with MQTT, following which we are able to connect with the Adafruit [8] server for exchanging data. This helps us to control the operation of the car.

2.3 Adafruit

Adafruit.io [8] is a *cloud service*—that provides us with the easiest way to interact, log and stream with our data and also manages it. It is a free server platform which can display data on real time online, control motor, read sensor data. It also can connect projects to web services like Twitter, RSS feeds, weather services. Adafruit.io can handle and visualize multiple feeds of data at the same time. The Communication API is relies on MQTT client with Adafruit servers. The data obtained from IFTTT [7] via Google Assistant is published here. According to his data the microcontroller board functions thereby moving the car.

2.4 IFTTT

If This Then That, better known as IFTTT [7] is a web-based service to create series or sequences of simple conditional statements, called applets. An applet is triggered when changes occur within other web services like Gmail, Instagram, PinInterest. Likewise in this paper, when a command is given via Google Assistant an action is triggered, i.e., sending data to adafruit.io server. The “this” consists of the commands given to Google Assistant and the “That” part consists of sending data to Adafruit.io server.

3 Results and Discussions

The employment of IoT and cloud servers provides a huge amount of confidence on the perfect running of the car. We have conducted a series of tests for observing the performance of the vehicle. The purpose is to check the longest runtime of the car without interruption alongside proper functioning of the car according to the commands given over Google Assistant. Figure 2 Shows the commands that are given using Google Assistant.

Fig. 2 Voice commands to Google assistant



Figure 3 shows the applets that are setup on basis of Google Assistant commands. Figure 4 Shows the Adafruit server with feeds for exchanging data from IFTTT and sending it to Node MCU.

Fig. 3 IFTTT applets setup accordingly

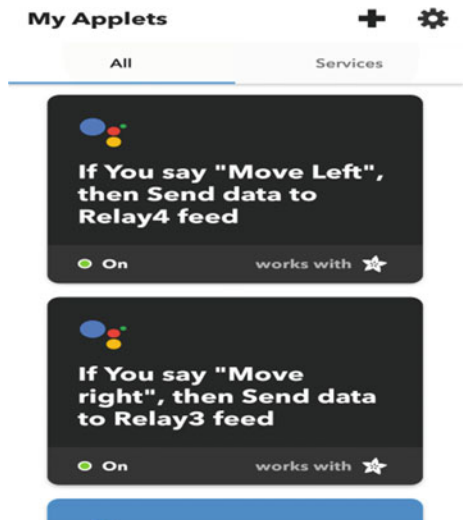
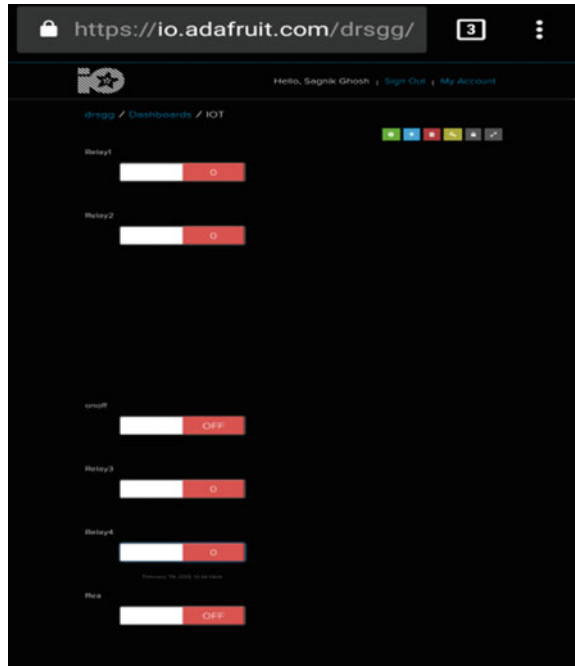


Fig. 4 Adafruit.io server with feeds for exchanging data



The simplest situation occurs when there is absolutely no obstacle in front of it. Figure 5 shows the movement of the vehicle. Response in that case always remains high. However the other complex cases provide us with satisfactory results. At most the worst case arises when there is no WiFi connectivity or when the data link is obstructed by some obstacles. The results signify that these concepts can readily be

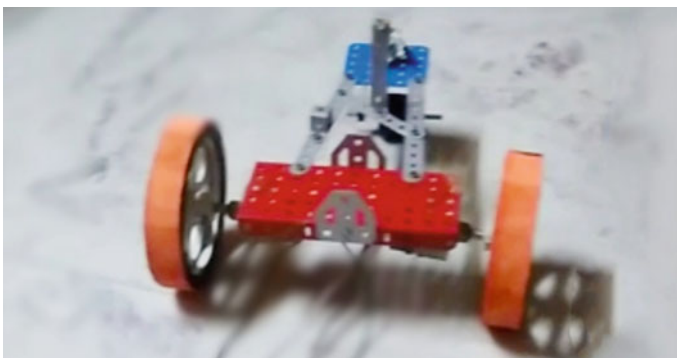


Fig. 5 Movement of the Google controlled car

applied to real world platform in order to experimentally verify its ability to become an everyday part of our lives.

Internet of Things signifies connected things in a network. This is achieved in this project. Moreover the car can steer away from an accident due to presence of Ultrasonic Sensor. It can easily bypass the shortcoming of suffering from loss of data thereby improving its performance. Since the car is automatic and driver-less it helps in traffic assistance. The things required here to control it requires user friendly websites or applications. Overall it can provide us with a new revolution towards cars with intelligent transportation system, for no collision, smart high efficiency transportation system with low traffic congestion and better improved fuel and energy consumption.

4 Conclusion

Vehicles are on their way to becoming the most sophisticated mobile devices in the world of IoT. Driver-less cars hold significant potential in making transportation safer, more convenient, and efficient.

Nowadays people are switching towards becoming smarter in every sector of their lives. We are making automatic cars that will be controlled by Google Assistant. Performance remains high because these cars are non-polluting since they do not require fuel. It will also be one more step ahead towards smart cities. The impact of launching these cars will be affirmative because ultimately human beings will be benefited highly. Moreover technological advancement will take place and smart cities and environment can be created where everything is automatic.

References

1. Marosi AC, Lovas R, Kisari Á, Simonyi E (2018) A novel IoT platform for the era of connected cars. In: 2018 IEEE international conference on future IoT technologies (Future IoT), pp 1–11
2. Devi YU, Rukmini MSS (2016) IoT in connected vehicles: challenges and issues—a review. In: 2016 international conference on signal processing, communication, power and embedded system (SCOPEs), Paralakhemundi, pp 1864–1867
3. Sun J, Zhang Y, Fan J (2011) SmartAgents: a scalable infrastructure for smart car. In: 2011 12th international conference on parallel and distributed computing, applications and technologies, Gwangju, pp 99–103
4. Ydenberg A, Heir N, Gill B (2018) Security, SDN, and VANET technology of driver-less cars. In: 2018 IEEE 8th annual computing and communication workshop and conference (CCWC), Las Vegas, NV, pp 313–316
5. Yılmaz E, Ozyer S (2019) Remote and autonomous controlled robotic car based on arduino with real time obstacle detection and avoidance. *Univ J Eng Sci* 7(1):1–7
6. https://cdn-shop.adafruit.com/product-files/2471/0A-ESP8266_Datasheet_EN_v4.3.pdf
7. <https://ifttt.com/>
8. <https://www.adafruit.com/>
9. <http://mqtt.org/>

Security of IoT with Blockchain: Basic Study



Anindita Jena

Abstract Internet of things has emerged to be a ubiquitous technology which has been proved to be a boon for the field of computer science. Many of the domains of computer science can be enhanced by the novel technology of IoT. With the advent of IoT, the need for unique identity to each IoT device came to the scene. Since IoT is comparatively a new domain in computer science and also involves the technology of embedded systems, there comes the necessity to focus on a secure architecture for IoT. This paper will focus on the enhancement of security in IoT by merging the technology of blockchain with it. IoT currently has a centralized architecture and has the security issues but blockchain is a decentralized and distributed platform and implementing blockchain in IoT thus resolves many security threats and vulnerabilities. Furthermore, the issues of data distortion can also be resolved since blockchain includes cryptographic algorithms at the backend. IoT with integrated blockchain can be competent of decentralization, autonomy and trustworthiness. The coordination between millions of IoT devices which in future is also going to increase rapidly can be tracked with high security of blockchain. This paper explores efficiency of blockchain in IoT application. Along with this paper discusses some case studies which is based on blockchain based IoT. There are some steps are described which will give a theoretical idea about how to build a blockchain in an IoT system.

Keywords Blockchain · IoT security · Disadvantages of blockchain based IoT · Architecture of IoT-Blockchain · Access management of IoT-Blockchain · Cloud computing-IoT-Blockchain

1 Introduction

The term “Internet of things” is a very prominent technology among the all established technology. The usage of this renowned technology has increased now a day. IoT is used in different sectors and also used by many people all over the world.

A. Jena (✉)

College of Engineering and Technology, Bhubaneswar, India 751003

e-mail: aninditajena1996@gmail.com

But the security part of this field is comparatively not advanced. So, Blockchain is very famous for best security system in every field's aspect. For that, it is also used for Internet of Things (IoT). Another reason of using Blockchain with IoT is to make IoT a decentralized system. The whole IoT system is centralized. Centralized means giving someone full authority of a system like operating, managing, security, authenticity. But After using Blockchain, Authority is given to each node connected to the chain.

A Blockchain is a kind of database which stores all processed data in chronological order. This data/information is published as a public ledger that can't be modified and every user or node in the network maintains the same ledger. Every block of Blockchain is chained together with hashes and store same and equal amount of data/information.

Generally in an IoT network, all transactional details are public to corresponding network. At the same time blockchain is of three types (a) public/permissionless blockchain, (b) private/permissioned blockchain and last one is (c) consortium blockchain. The public blockchain will be very much compatible with IoT, which will create a P2P transparent network for user. To maintain the consistency, the consensus mechanism is used. But in public blockchain based IoT, there is a possibility of Sybil attack. For this, proof of work (pow) mechanism is used. For some currency transaction private blockchain is used. The consortium blockchain is not fully private or public. It is the combination of both. Muneeb Ul Hassan et al. have described this concept in his paper [1].

Madhusudan Singh et al. have explained several areas which require security in an IoT system. So, blockchain can be used in this area for the purpose of protection. Under the security issued, blockchain has divided into 2 parts. One is functional security and another part is platform security. Under the functional security, there are security issues, legal issues, threat issues. Blockchain can be implemented on any of them. Then under the platform security, the security is needed for device, network and cloud. To solve legal issues the smart contract concept can be used. For data security, the ethereum concept will be helpful. For cloud security, ethereum is useful.

Ali dorri et al. has described a blockchain implemented smart home where there is a concept called clustering, which is used in cloud computing for cloud storage. So author makes a cluster by gathering number of house and the number of house is equal to number of blocks in blockchain. Then all the transaction will be secure in the blockchain and all data will be retrieved and stored in cloud computing like usually done in IoT. The author has defined an overlay network where there are a number of clusters. The authors have implemented this concept practically and found out some interesting output [2].

It has proved that blockchain can be implemented in a practical manner on IoT. But in every system, the speed is a prior need. Zhou et al. have done some experimental calculation and proved that system can increase the working speed by reducing the block interval in a blockchain.

The blockchain always works on the backend of a system. The blockchain is software in contrary the IoT starts with hardware devices. To run the blockchain

software, IoT needs some high power devices, because low power devices do not have enough horse power to run blockchain application. For that Kazim et al. have done some research to enable the low power device capable for blockchain. The infamous Lora concept has used for this [3].

The industry 4.0 plays a major role in an IoT era. So implementing blockchain in industrial IoT is a challenging task. But Junqin huang et al. had done some mathematical calculations to make it possible. In industrial IoT (IIoT) there are several types of sensors, actuators and devices. In the other hand it is well known that blockchain is very power intensive. So here authors have credit-based consensus algorithm for IIoT. Along with (POW) proof of work mechanism is used for other IoT devices [4].

2 Related Work

Samaniego et al. explained about lightweight devices in his papers. The embedded system, IoT is composed of lightweight devices which is faced so many challenges like lack of storage space with security performance. Due to this reason Blockchain is used in IoT. Lightweight devices used IoT needs a lightweight Blockchain. Here in this paper authors have proposed various methods to overcome the above limitations by using Fog computing and cloud computing [5]. Buccafurri et al. also proposed some methods related to lightweight devices and implementation of public ledger which is suitable for lightweight devices [6].

Fremantle et al. discussed about the gaps which is not explained by any of the middleware. This paper has told some points related to gaps in regards to the requirements in security of IoT [7]. So, the Blockchain can be used as solution to these security issues in an IoT.

Dorri et al. proposed a Blockchain based IoT architecture where it handles security and privacy threats in an IoT along with performance quality. This Blockchain deployed IoT architecture is based on smart home [8]. Kshetri et al. has answered the above question which is “may be” as it used in many industries [9]. Khan et al. has explained about security issues in this paper. IoT system is very insecure due to the absence of secure and strong hardware and software design. The authors have divide all the security issues in 3 parts that are high- level, intermediate-level, low-level IoT layers [10].

Lee et al. has explained a new firmware which is suitable for embedded device present in an IoT as well as strengths and weakness of proposed system [11]. Zhang has explained a business model related to IoT where it stands with DACs and discusses all the details like entity commodity and transaction process of IoT E-business. So, here in this paper Blockchain is based IoT E-Business model [12]. Samaniego et al. proposed an idea which is related to permission based Blockchain for supplying IoT services on edge host. It has used smart contract in Blockchain technology [13].

Boohyung et al. focused on embedded devices that are used extremely in Internet of Things surrounding. IoT devices are worked with each other without interruption of users though the processes, which must be accurate against attacks. For that reason

this paper focused on update issue of secure firmware. The secure firmware update issue is a central security challenge for the extremely used embedded devices which are used in IoT environment. A new update scheme for firmware was using blockchain technology for security. The IoT embedded device demands its format to inform the nodes of blockchain network and gets an answer for determine whether the firmware is updated or not. This proposed scheme promises the firmware of embedded device is a newest updated firmware and the firmware is secured [11].

Zhang et al. proposed a business model for Internet of Things. The decentralized concept is introduced to IoT e-business model. In this paper the stages of e-business model are divided again according to the IoT e-business model i.e. pre-transaction preparation stage and next one is negotiation stage then contract signing stage and contract fulfillment stage. As blockchain is a decentralized technique and IoT is a centralized technique, blockchain is used in IoT e-business model for making it decentralized model. In order to achieve this, author used a peer-to-peer transaction mode with blockchain. Again for achieving the business with paid data and smart property there is a method which is designed with basis of encrypted coins and smart contract. The theories of ebusiness model of IoT are verified by paid data and smart property. The smart property is developed by smart devices/equipment which has NFC module, which helps to work on apps. NFC module has some capabilities which is aware of ownership exchange and is copied information whose target is to achieve the control of smart property. Again paid data, an API, a uniform data format, classifying mechanism are designed. The paid data helps the people to find required data, and then they can also pay to the provider [12].

Kshetri et al. gave a brief description and technical idea about blockchain role in supply chain i.e. linked to IoT devices. The main focus of this paper was highlight of the security benefits of supply chain which is linked to IoT devices. Again it also explains about blockchain which helps to prevent IoT security violation. Deploying blockchain in supply chain should be mandatory for economic benefits and security. Blockchain ecosystem enriches public-private partnerships [14].

Shi-cho-cha et al. proposed a blueprint of a blockchain that linked with gateway. Its security and flexibility preserves the privacy leakage. The gateway successfully protects the user's private data from being hacked. There is a mechanism called digital signature is anticipated for authentication and security [15].

Gupta et al. focused on the use of blockchain to ensure security of IOT network and sensing some malicious behavior. In this paper author proposed an architecture of blockchain protocol that is in the middle of the application and transport layers. It makes a use of token rewards which is similar to bitcoin but used it as units of voting power [16].

He et al. had put forwarded pricing policies for blockchain based transactions. This blockchain based distributed p2p transactions is based on some mechanism which have some application that applies a bitcoin to motivate users for intervention. In this mechanism, there is a benefit for a user that the users with a positive transfer get recognized. As users in the blockchain p2p systems might display self regarding actions on plot with one another. For that author suggested a mechanism to integrate

a pricing and validation method for incentive purpose with the help of evaluation study and game theoretical analysis [17].

Jesus presented the stalker and a variant of selfish miner that prevents a node to produce its block on the main chain of blockchain. There is dissimilarity between the selfish mining and the stalker. The selfish mining increases price where the stalker denies for a specific target not worrying about the profit. Some processes i.e. adopt, wait and publish heuristics is used by this attack because overlay and match were making node which increases the relative revenue [18] (Table 1).

3 Comparison Between IoT and Blockchain Based IoT

Case study 1

Lei Hang and Do-Hyeun Kim has presented some experimental results which are based on the sensing data of IoT Blockchain. The presented paper uses a real-life case for experiment i.e. smart space in order to prove the practical implementation of IoT-Blockchain. In a simple Blockchain technology deployment, there will be a web-client, Blockchain network where all data related to the process stored in network and user interface, etc. But in an IoT-Blockchain project, above all will present along with all IoT devices of IoT network. In an IoT Blockchain process, data will be collected through sensors and stored in Blockchain network through an IoT server and that IoT server is also connected to web client for user. So, that user can view all the process and can operate through user interface. Authors have described all about experimental hardware devices for an IoT and software devices for both IoT and Blockchain along with programming environment. The usage of smart contract has also shown in the paper with screenshot. The execution time and performance time difference also shown with different number of devices. The above proposed experiment is only useful for friendly interface projects, low number transaction and zero number of currency exchanges [19] (Fig. 1).

Case study 2

Donhee Han et al. have given some theoretical models for IoT Blockchain which is based on smart door lock system. In a simple smart door system, data/information are collected and stored via using sensors. But sensors are very weak which is very easy to hack. So once if these sensors are hacked, then the smart door which is the way to enter to our house can easily open and lock. So, it is very necessary to secure it. So, the authors have proposed some model by using Blockchain. In the proposed model, all the data which is collected by sensors are transferred to Blockchain network through IoT server. In Blockchain network each user can be block or one user can have many blocks by using multiple electronic devices like smart watches, phones, tab, etc. Blockchain based smart door system can be used for both open and lock system [20] (Fig. 2).

Table 1 Literature Review of Blockchain based IoT

Sl. No.	Heading of the paper	Authors	Finding	Description	Ref. No.
1.	Blockchain as a Service for IoT	Samaniego et al.	Lightweight technology	– Lightweight Blockchain for lightweight devices used IoT by using Fog computing and cloud computing	[5]
2.	Overcoming Limits of Blockchain for IoT Applications	Buccafurri et al.	Lightweight technology	– Implementation of public ledger which is suitable for lightweight devices of IoT	[6]
3.	Survey of secure middleware for the Internet of Things	Fremantle et al.	IoT middleware security	– Requirements in security of IoT	[7]
4.	In internet of things: challenges and solutions	Dorri et al.	Smart-home security with blockchain	– Blockchain based IoT architecture where it handles security and privacy threats in an IoT along with performance quality	[8]
5.	Can blockchain strengthen the internet of things?	Kshetri et al.	Can Blockchain Strengthen the Internet of Things?	– May be	[9]
6.	IoT security: Review, blockchain solutions, and open challenges	Khan et al.	IoT security issues with levels	– Security issues in IoT by dividing it into 3 layers	[10]
7.	Blockchain-based secure firmware update for embedded devices in an Internet of Things environment	Lee et al.	Blockchain-based secure firmware	– A firmware which is suitable for embedded device present in an IoT as well as strengths and weakness of proposed system	[11]
8.	The IoT electric business model: Using blockchain technology for the internet of things	Zhang	E-business model	A business model related to IoT where it stands with DACs and discusses all the details like entity commodity and transaction process of IoT E-business	[12]

(continued)

Table 1 (continued)

Sl. No.	Heading of the paper	Authors	Finding	Description	Ref. No.
9.	Using blockchain to push software-defined IoT components onto edge hosts	Samaniego et al.	Edge host	– To permission based Blockchain for supplying IoT services on edge host	[13]
10.	Blockchain-based secure firmware update for embedded devices in an Internet of Things environment	Boohyung et al.	Secure firmware	– Embedded devices that are used extremely in Internet of Things surrounding – The IoT embedded device demands its format to inform the nodes of blockchain network and gets an answer for determine whether the firmware is updated or not	[11]
11.	The IoT electric business model: Using blockchain technology for the internet of things	Zhang et al.	E-business model	– Used in IoT e-business model for making it decentralized model – The theories of e-business model of IoT are verified by paid data and smart property	[12]
12.	Blockchain’s roles in strengthening cybersecurity and protecting privacy	Kshetri et al.	Blockchain in supply chain	– The security benefits of supply chain which is linked to IoT devices – Blockchain which helps to prevent IoT security violation	[14]
13.	A blockchain connected gateway for BLE-based devices in the internet of things	Shi-cho-cha et al.	Blockchain linked with gateway	– Security and flexibility preserves the privacy leakage – Digital signature is anticipated for authentication and security	[15]

(continued)

Table 1 (continued)

Sl. No.	Heading of the paper	Authors	Finding	Description	Ref. No.
14.	The applicability of blockchain in the Internet of Things	Gupta et al.	Security of IOT network	–An architecture of blockchain protocol that is in the middle of the application and transport layers	[16]
15.	A blockchain based truthful incentive mechanism for distributed P2P applications	He et al.	Pricing policies	– Blockchain based distributed p2p transactions is based on some mechanism which have some application that applies a bitcoin to motivate users for intervention	[17]
16.	A survey of how to use blockchain to secure internet of things and the stalker attack	Jesus	Selfish miner	– The selfish mining increases price where the stalker denies for a specific target not worrying about the profit	[18]

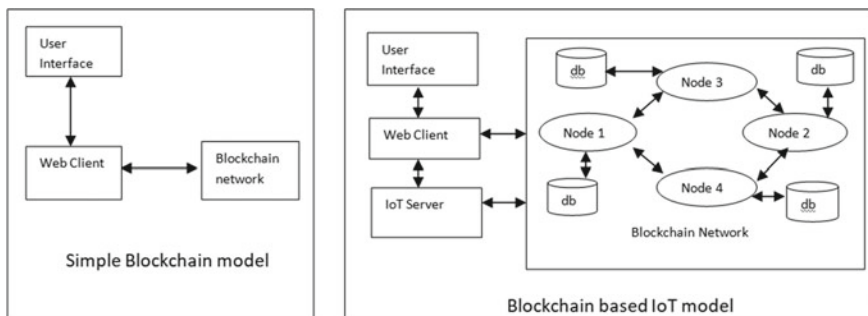


Fig. 1 Difference between simple Blockchain and IoT-Blockchain

Case study 3

Seyoung huh et al. have proved “proof of concept” by using Blockchain concept IoT devices. The proposed work has used smart phones as user interface and Raspberry pis for 3 devices i.e. meter, light bulb, air conditioner. Then the Blockchain concept is merged with above entities as an ethereum. Now this ethereum is worked under smart contract. Since ethereum is using smart contract, three smart contracts has to written Authors have written those three smart contracts and manage the IoT

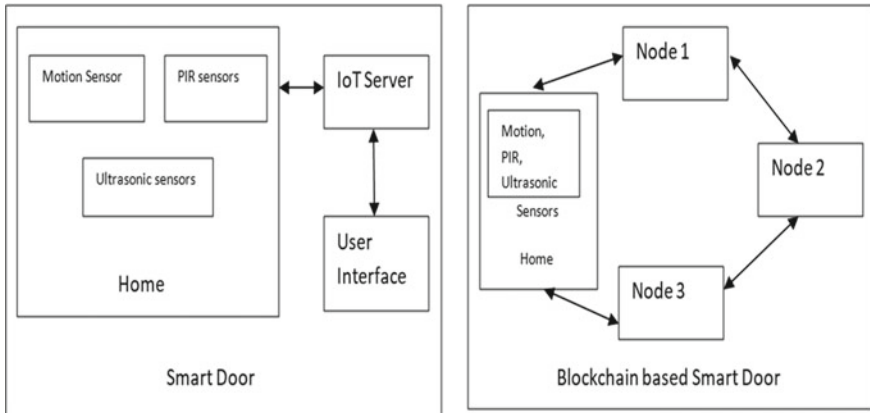


Fig. 2 Difference between Smart door and Blockchain based smart door

devices. This technology has various advantages but it can be advantageous when limited number of IoT based devices is used. But now IoT has gained huge attraction whose integration help in advancement of technology, that led to IoT use modern devices and large number of devices. Due to this reason managing IoT devices by using Blockchain is quite difficult [21].

4 Blockchain Based IoT

4.1 Access Management

The first area to implement blockchain concept in IoT field can be on access controlled management. Some of attribute needs authority power in any system. Permissioned blockchain or private blockchain are the best to implement and it can use proof of concept mechanism in network. Some authors have finished their research on it. Sheng Ding et al. had given an architecture for attribute based access control system for IoT using blockchain [22]. Oscar Novo had given a scalable access management system for IoT using blockchain.

4.2 Blockchain Based IoT Cloud Framework

Another field to implement blockchain on IoT is cloud. In an IoT system data are collected through sensors and passing through the gateway, all the data are saved in cloud. Further the data are retrieved as per the requirement. So here ethereum concept can be used here. Nachiket Tapas et al. have done this possible by making

an use of smart contract over ethereum [23]. Now the problems come with the data integrity. So that bin lia et al. [24] have introduced framework for data integrity in a blockchain based IoT system.

4.3 AI Enabled Blockchain for IoT

Mehrdad et al. had proposed a 2 step consensus protocol which will strengthen than consensus mechanism of blockchain. So this 2 step consensus protocol has used an outlier algorithm which will detect some anomaly activities in its first step. Then in second step it has used practical byzantine fault tolerance (PBFT) as consensus protocol for ledger updation. Here consensus mechanism is a blockchain concept. PBFT & outlier algorithm is machine learning or AI concept. Here author used this concept and measure the performance and the output they have got are very favorable [25].

4.4 Use of Smart Contracts in IoT Application

Smart contracts are the best blockchain concept to implement in IoT. This can be used as public blockchain or private blockchain. You can use ethereum for making blockchain nodes/blocks. Then for accessing or storing data the smart contract concept can be used. Georgios et al. have given some example of smart contracts which can be implemented on IoT [26]. In the other hand chun-feng liao et al. have shown, where to use smart contract and also presented a comparison between fully centralized, pseudo distributed IoT, distributed things and fully distributed IoT which is based on smart contract [27].

4.5 Real Time Implementation on a Smart City

Wu et al. have implemented blockchain on a smart city. Smart city must have smart griding system, smart home, smart road, smart irrigation system, Smart building and smart car. So in presented blockchain system, smart grid is a block; smart homes are a block likewise. All-together they are making a blockchain. The authors have made it possible through by using different software or hardware sensors. For example:- they have used SND controllers for collecting data and used a web interface to display it. They have also used raspberry pi along with different sensor and different protocols. In the end consensus mechanism is used for a successful output [28].

5 Steps for Creating a Blockchain Based IoT System

There are some steps, which can be followed to develop a blockchain based IoT (Fig. 3).

- Step 1: First find out all the area which needs security in an IoT system, for example:- data accessin, cloud, legal issues part, etc.
- Step 2: Then select a concept of blockchain which will be effective on that area and can give proper security. For example: - Ethereum, smart contracts, hyper ledger, etc.
- Step 3: After that, select a mechanism if there is any need of it for some performance calculations. For example: - consensus, proof of work (POW), proof of concept (POC), etc.
- Step 4: Then install hardware for integrating IoT devices with blockchain. If you merge smart contracts with sensors it will transform a simple sensor into a DAGs (Decentralized autonomous corporation).

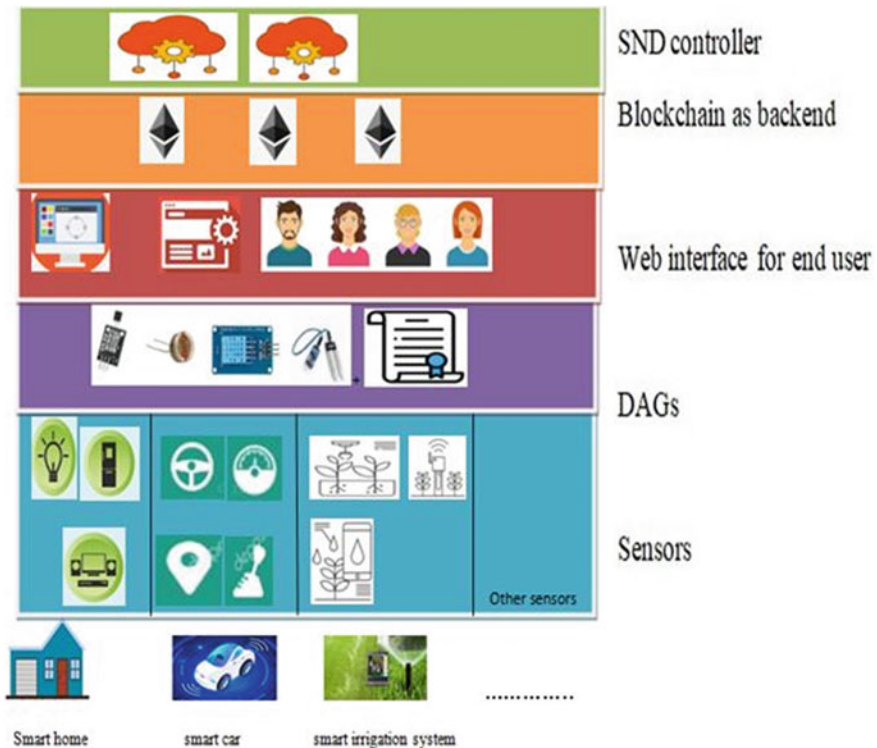


Fig. 3 Layered architecture for implementing blockchain based IoT

Step 5: Then install software for enabling the concepts of blockchain. For example:
- download ethereum mist for ethereum, develop smart contract using solidity etc.

Step 6: Make a front end web interface for end-user.

In the introduced layered architecture of blockchain based IoT, the specific sensors will be deployed. Then smart contracts will be merged with sensors for developing smart contracts. Then design a fronted page, which will work as interface between sensors and end user. Then all data will store in blockchain and controlled by SND controller. So in normal IoT, the data which are stored in cloud now it can store in blockchain as a database. It is the major advantage of blockchain that it can be used as database.

6 Deploying Blockchain in IoT (Disadvantages)

Advantages of Blockchain are well known and everybody is well informed about its benefits. But there are also some disadvantages or it can be considered as obstacle in IoT Blockchain. At first, Blockchain is a database which needs a management system as IoT generates huge amount of data. Some IoT devices are unable to store the Blockchain public ledger and to perform the Blockchain mining. In the other hand, all the IoT devices cannot use Blockchain functionality in its system. Some of the devices of an IoT system can deploy the Blockchain technology successfully in practical but some other devices cannot. So we need to design an architecture which shows the selected deployed devices of an IoT or some process needs to discover to overcome the limitations. Because the modern IoT systems are integrated with many embedded technology like edge computing and cloud computing [29].

7 Conclusion

In this paper, the relation between IoT and Blockchain is described in aspect of different area. This paper also shows the benefits of merging IoT with Blockchain system as well as disadvantages. This model shows the workflow of IoT-Blockchain architecture which is based on smart home, smart room or smart office. In future work, the IoT-Blockchain model architecture will focused on two categories i.e. Blockchain enabled devices and Blockchain forbidden devices of an IoT.

References

1. Hassan MUI, Rehmani MH, Chen J (2019) Privacy preservation in blockchain based IoT systems: integration issues, prospects, challenges, and future research directions. *Future generation computer systems* 97: 512–529
2. Dorri A, Kanhere SS, Jurdak R (2017) Towards an optimized blockchain for IoT. In: 2017 IEEE/ACM Second International Conference on Internet-of-Things Design and Implementation (IoTDI). IEEE, 2017
3. Özyilmaz KR, Yurdakul A (2017) Work-in-progress: integrating low-power IoT devices to a blockchain-based infrastructure. In: 2017 International Conference on Embedded Software (EMSOFT). IEEE, 2017
4. Huang J et al (2019) Towards secure industrial IoT: blockchain system with credit-based consensus mechanism. *IEEE Trans Ind Inform* 15.6: 3680–3689
5. Samaniego M, Deters R (2016) Blockchain as a Service for IoT. In: 2016 IEEE International Conference on Internet of Things (iThings) and IEEE Green Computing and Communications (GreenCom) and IEEE Cyber, Physical and Social Computing (CPSCom) and IEEE Smart Data (SmartData), IEEE, 2016
6. Buccafurri F et al (2017) Overcoming limits of blockchain for IoT applications. *Proceedings of the 12th International Conference on Availability, Reliability and Security*. ACM, 2017
7. Fremantle P, Scott P (2017) A survey of secure middleware for the Internet of Things. *PeerJ Comput Sci* 3:e114
8. Dorri A, Kanhere SS, Jurdak R. (2016) Blockchain in internet of things: challenges and solutions. arXiv preprint [arXiv:1608.05187](https://arxiv.org/abs/1608.05187)
9. Kshetri N (2017) Can blockchain strengthen the internet of things? *IT Professional* 19(4):68–72
10. Khan MA, Salah K (2018) IoT security: review, blockchain solutions, and open challenges. *Future Generation Computer Systems* 82: 395–411
11. Lee B, Lee JH (2017) Blockchain-based secure firmware update for embedded devices in an Internet of Things environment. *J Supercomput* 73(3):1152–1167
12. Zhang Y, Wen J (2017) The IoT electric business model: using blockchain technology for the internet of things. *Peer-to-Peer Network App* 10(4):983–994
13. Samaniego M, Deters R (2016) Using blockchain to push software-defined IoT components onto edge hosts. In: *Proceedings of the International Conference on Big Data and Advanced Wireless Technologies*
14. Kshetri N (2017) Blockchain's roles in strengthening cybersecurity and protecting privacy. *Telecommun policy* 41(10):1027–1038
15. Cha SC et al (2018) A blockchain connected gateway for BLE-based devices in the internet of things. *IEEE Access* 6: 24639–24649
16. Gupta Y et al (2018) The applicability of blockchain in the Internet of Things. In: 2018 10th International Conference on Communication Systems & Networks (COMSNETS). IEEE, 2018
17. He Y et al (2018) A blockchain based truthful incentive mechanism for distributed P2P applications. *IEEE Access* 6: 27324–27335
18. Jesus EF et al (2018) A survey of how to use blockchain to secure Internet of Things and the stalker attack. In: *Security and Communication Networks 2018*
19. Hang L, Kim DH (2019) Design and implementation of an integrated IoT blockchain platform for sensing data integrity. *Sensors* 19(10):2228
20. Han D, Kim H, Jang J (2017) Blockchain based smart door lock system. In: 2017 International conference on information and communication technology convergence (ICTC). IEEE, 2017
21. Huh S, Cho S, Kim S (2017) Managing IoT devices using blockchain platform. In: 2017 19th international conference on advanced communication technology (ICACT). IEEE, 2017
22. Ding S et al (2019) A novel attribute-based access control scheme using blockchain for IoT. *IEEE Access* 7: 38431–38441
23. Tapas N, Merlino G, Long F (2018) Blockchain-based IoT-cloud authorization and delegation. In: 2018 IEEE International Conference on Smart Computing (SMARTCOMP). IEEE, 2018

24. Liu B et al (2018) Blockchain based data integrity service framework for IoT data. In: 2017 IEEE International Conference on Web Services (ICWS). IEEE, 2017
25. Salimitari M, Joneidi M, Chatterjee M (2019) Ai-enabled blockchain: an outlier-aware consensus protocol for blockchain-based iot networks. In: 2019 IEEE Global Communications Conference (GLOBECOM). IEEE, 2019
26. Papadodimas G et al (2018) Implementation of smart contracts for blockchain based IoT applications. In: 2018 9th International Conference on the Network of the Future (NOF). IEEE, 2018
27. Liao CF et al (2017) On design issues and architectural styles for blockchain-driven IoT services. In: 2017 IEEE international conference on consumer electronics-Taiwan (ICCE-TW). IEEE, 2017
28. Wu J et al (2020) Application-aware consensus management for software-defined intelligent blockchain in IoT. *IEEE Network* 34.1: 69–75
29. Xiong Z et al (2020) The best of both Worlds: a general architecture for data management in blockchain enabled Internet-of-Things. *IEEE Network* 34.1: 166–173

IoT-Based Smart Irrigation and Related Environment Parameters Monitoring: An Empirical Review



Parijata Majumdar, Sanjoy Mitra, and Munesh Chandra Trivedi

Abstract Agriculture is the backbone of economy. The agrarian economy mainly depends on two parameters viz—weather monitoring and irrigation monitoring. Real-time weather monitoring is an important tool to visualize climate conditions prevailing in a field to solve production of crop and its yield associated problems by better understanding of surrounding weather. The main aim is to view weather conditions of any agricultural field and on-demand access of the current data of any near and remote locations of an agricultural field. Also, with discontinuous monsoon, farmers have to use other unsupervised alternate means of freshwater for the crops leading to scarcity of water. Therefore, farmers are facing challenges to make best irrigation schedules. The ever-augmenting technologies like Internet of Things (IoT) paved the way for smart weather stations and smart irrigation management with the help of wireless sensors to sense data for adapting changes of crop design, remote field site, and irrigation patterns taking into account all sort of environment constraints. IoT is capable to sense data, monitor, accurately predict climate conditions and is capable to limit water wastage, thus improving overall crop yield. This paper offers a detailed review of the broader aspect of IoT-based smart agriculture system depending on weather and irrigation.

Keywords Smart · IoT · Agriculture · Weather · Irrigation

P. Majumdar · M. C. Trivedi
Department of Computer Science and Engineering, National Institute of Technology, Agartala
Barjala West Tripura, 799046, India
e-mail: er.parijata@gmail.com

M. C. Trivedi
e-mail: drmunesh.nita@gmail.com

S. Mitra (✉)
Department of Computer Science and Engineering, Tripura Institute of Technology, Agartala
Narsingarh West Tripura, 799009, India
e-mail: mail.smitra@gmail.com

1 Introduction

Agricultural monitoring is receiving a steady growth among the emerging concept of Internet of Things (IoT) and its application areas, as it contributes major share in the world economy. Monitoring agriculture primarily depends on two key factors like weather and monsoon to save water for irrigation purpose. Weather stations help us to understand the influence of climate change on the crop yield and to determine which seeds to plant in the right type of weather. But problems like distant location from the place during surveillance make the data subjected to variation and is unstable. Centralized IoT architecture enables data acquisition through cost-effective sensors embedded into small sized microcontrollers, where data is exchanged using suitable communication protocols from nearby or distant areas in real time unlike existing weather stations. This will equip farmers with accurate climate data for better crop management to cope up with drought season and to regulate the water supply minimizing water scarcity and improving crop yield. Similarly, irrigation can be monitored by analyzing soil moisture level and weather updates. IoT can solve real-time problems to carry out irrigation mechanisms like determining soil conditions, soil moisture content, environmental factors, fertilizer usage, crop rotation and harvesting, etc., which is unaddressed by conventional agricultural techniques. Figure 1 shows different approaches of IoT combined to acquire real-time precision data of weather and irrigation.

2 Literature Review of IoT-Based Weather and Irrigation Monitoring

The review work is mainly done to acquire knowledge of IoT-based approaches and to analyze sensor data with the pros and cons of the methodologies for building smart agriculture monitoring. The proposed system to be designed based on the knowledge gathered from review work can assist farmers for improving crop yield by precision sensor generated data and minimize crop loss. Table 1 explains different weather stations proposed by different authors with their claimed advantages and shortcomings.

Table 2 gives the brief review of the different smart irrigation systems proposed by different authors with their claimed advantages and shortcomings.

After extensive literature review, it is seen from Fig. 2 that in most of the papers, micro-controller is used to develop weather and irrigation monitoring system. Cloud computing based-weather and irrigation monitoring system has not been much explored. Cloud computing can be used to enhance sensor data connectivity by adding dedicated data storage from locations far and near in the cloud to increase system confidence and safeguard against network failures. Therefore, a cloud computing-based framework can be designed for precision and smart agriculture monitoring. Cloud computing-based IoT technology offers high flexibility, ease of use, and device

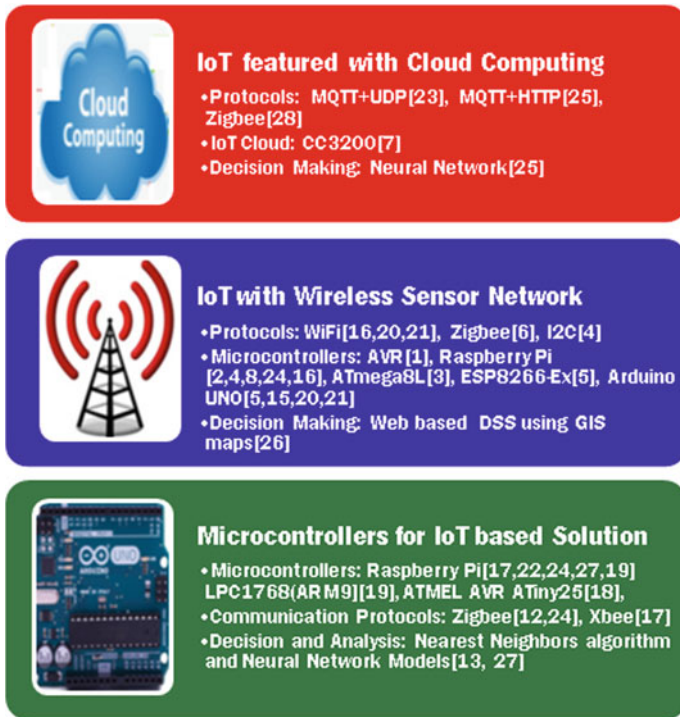


Fig. 1 IoT-based approaches for smart weather and irrigation monitoring

autonomy for appropriate decision-making by local farmers based on sensed data (Fig. 3).

After thorough analysis of the literature reviewed from Fig. 4, in most of the papers, temperature and humidity are the most widely used sensor generated variables. Whereas, altitude, air pollutants, and pressure variables are not so much monitored sensor generated variables. More the number of variables sensed, more is precision in prediction of irrigation schedules and weather variables monitoring for intelligent agriculture monitoring.

3 Other Recent Contributions

Sensor-based inexpensive weather station where weather variables are measured with limited memory usage is developed that requires additional storage [11]. A sensor-based inexpensive weather station developed using renewable energy but requires extra energy storage for backing up data [12]. A sensor-based weather stations that allows detection of weather variations is already developed earlier.

Table 1 Review of different IoT-based smart weather stations

Weather stations	Environment parameters	Claimed advantages	Shortcomings
Microcontroller based [1]	Temperature, humidity	Easy consistent monitoring	Power use and sensor accuracy
Microcontroller based [2]	Temperature, light, humidity, wind speed, soil moisture	Cost-effective monitoring	More Parameters for precision in monitoring
Microcontroller based [3]	Temperature, wind, humidity, rain, UV radiation	Economic monitoring	Increase user-weather interaction
Microcontroller based [4]	Temperature, wind direction, pressure, humidity	Inexpensive monitoring	Poor net connectivity in rural areas
Microcontroller based [5]	Temperature, light intensity, rainfall humidity, pressure	Low-cost monitoring	Power consumption and sensor accuracy
Microcontroller based [6]	Temperature, wind speed, pressure, humidity	Low-cost monitoring	Long-time weather data surveillance using multiple sensors
Cloud computing based [7]	Temperature, humidity	Real-time device independent monitoring	Power consumption and sensor accuracy
Microcontroller based [8]	Temperature, altitude, humidity, pressure	Real-time adaptable monitoring	More sensors with low power consumption
Cloud computing based [9]	Temperature, wind speed, wind direction	Inexpensive real-time monitoring	Power consumption and sensor accuracy
Wireless sensor based [10]	Temperature, humidity, pressure, wind speed, rainfall	Automated real-time monitoring	Need of statistical parameter analysis

But multiple sensors are needed to increase real-time efficiency [13]. An inexpensive microcontroller-based weather station is developed in [14] but no analysis of precision of sensor data. A microcontroller-based weather station is presented in [15] to access weather variables anytime and anywhere but critical feedback of analysis is needed. A microcontroller-based weather station for reliable access of weather parameters is presented in [16]. A wireless sensor-based flexible weather station is shown in [17]. A wireless sensor-based weather station to generate sensor-based data for assisting farmers to cultivate crops is developed in [18]. A micro-controller-based weather station developed to save energy but problems of network transmission failure is there [19]. A reliable and inexpensive microcontroller-based weather station consuming low power is introduced in [20]. A wireless sensor-based weather station to improve environmental conditions is presented in [21]. A cloud computing-based weather station is developed to take

Table 2 Review of different IoT-based smart irrigation systems

Irrigation system	Environment parameters	Claimed advantages	Shortcoming
Microcontroller based [24]	Gases, soil moisture light intensity	Inexpensive monitoring	Reducing water use with more sensors
Cloud computing based [25]	Planted crop details, water level	Inexpensive remote data monitoring	Power consumption and sensor accuracy
Wireless sensor based [26]	Temperature, rainfall, humidity, pressure	Restructuring land using GIS maps	Need of constant data acquisition
Wireless sensor based [27]	Temperature,air moisture	Fully automated economic monitoring	Power consumption, sensor data accuracy,security
Cloud computing based [28]	Soil moisture, air temperature, humidity and water	Judicious use of water with low power and cost	Power consumption and sensor accuracy
Microcontroller based [29]	Temperature, soil moisture, humidity, air pollutants	Smart and self-adaptive monitoring	Power consumption and sensor accuracy

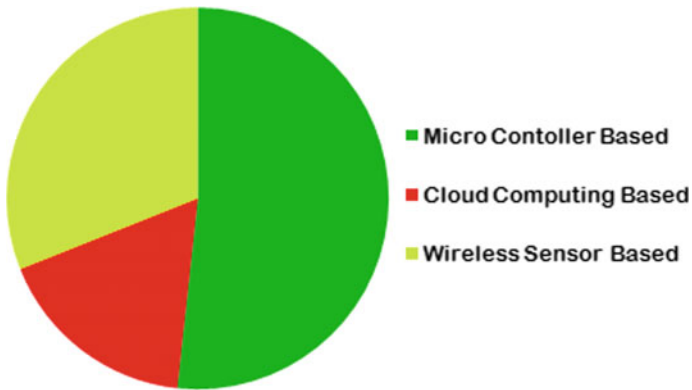


Fig. 2 Type of contribution for IoT-based smart weather and irrigation monitoring system

remote actions to adjust weather parameters [22]. An inexpensive, easily accessible microcontroller-based weather station is presented in [23].

4 Future Research Direction

The results obtained from keen analysis have clarified the need for an automated mechanism which could be made more robust by accurate interpretation of sensor data. Data correlation using statistical measures for analysis of sensor data is also needed while reducing power consumption of multiple sensors. The sensors

Fig. 3 Cloud computing framework designed for smart agriculture using weather and irrigation monitoring

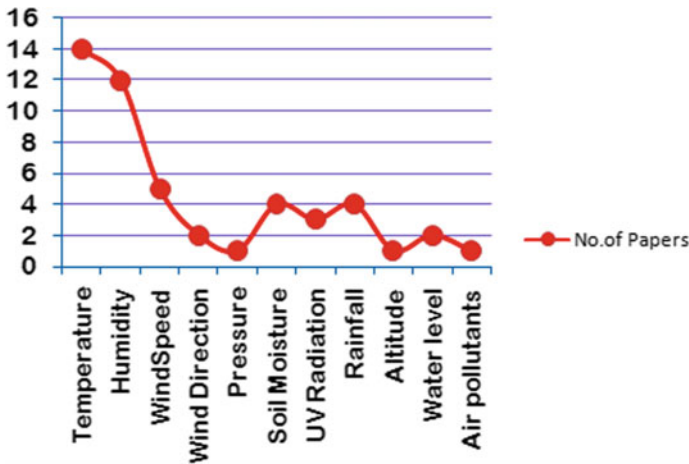
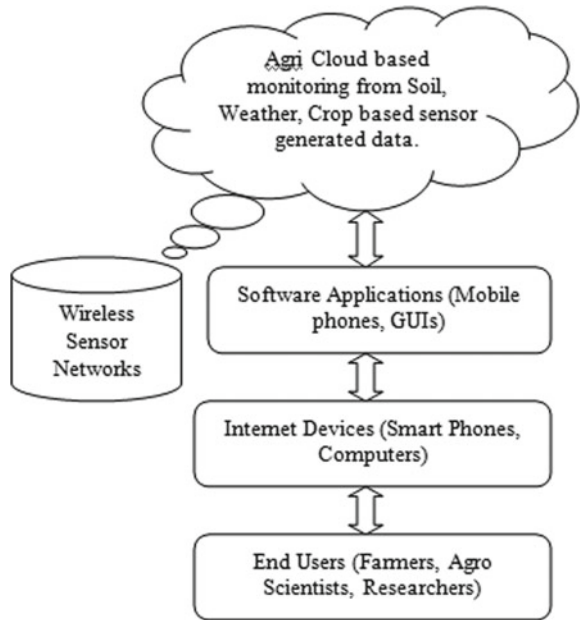


Fig. 4 Most common parameters sensed for smart weather and irrigation monitoring system using IoT

have to be calibrated for acquisition of more nonlinear weather parameters like harmful gases, pollutants, altitude, water level, etc., to figure its effect on crop yield while deciding irrigation schedules. Cloud computing platform has to be utilized for cost reduction, increased scalability with increase or decrease in number of sensed weather variables with effective memory utilization.

5 Conclusion

The survey on the robust techniques for irrigation and weather monitoring can help us in creating a real-time automated system based on real-time weather data acquisition from sensors to regulate water supply in field and to combat crop loss by precision in prediction of environmental constraints. The survey helps us to understand the correlated parameters for developing an efficient cost-effective, accurate, portable decision-making system for those farmers who are having very limited income, where climate data is easily accessible from anywhere and anytime irrespective of far or near location using IoT techniques. It would also facilitate farmers to create an irrigation plan to conserve water while increasing crop yield.

References

1. Halder S, Sivakumar G (2017) Embedded based remote monitoring station for live streaming of temperature and humidity. In: International conference electrical, electronics, communication, computer and optimization, pp. 284–328
2. Tenzin S, Sriyang S (2017) Low cost weather station for climate-smart agriculture. In: International conference on knowledge and smart technology, pp. 1–10
3. Solano G, Lama F (2017) Weather station for educational purposes based on Atmega8L. In: IEEE international, electrical engineering computing, pp. 1–10
4. Brito RC, Favarim F (2017) Development of low cost weather station using free hardware and software. In: Latin American Robotics Symposium (LARS) and Brazilian symposium on robotics, pp. 1–10
5. Kodali RK, Sahu A (2016) An IOT based weather information prototype using WeMos. In: 2nd International conference on Contemporary Computing and Informatics, pp. 612–616
6. Saini H, Thakur A (2016) Arduino based automatic wireless weather station with remote graphical application and alerts. In: International conference on signal processing and integrated networks, pp. 605–609
7. Palle D, Kommu A, Kanchi RR (2016) Design and development of CC3200-based cloud IOT for measuring humidity and temperature. In: International conference on electrical, electronics, and optimization techniques, pp. 3116–3120
8. Savic T, Radonjic M (2015) One approach to weather station design based on Raspberry Pi platform. In: 23rd telecommunication forum Telfor, pp. 623–626
9. Shaout A, Li Y, Zhou M, Awad S (2014) Low cost embedded weather station with intelligent system. In: International computer engineering conference, pp. 100–106
10. Mittal Y, Mittal A (2015) Correlation among environmental parameters using an online smart weather station system. In: IEEE India conference, pp. 1–6
11. Munandar A, Fakhurroja H (2017) Design of real-time weather monitoring system based on mobile application using automatic weather station. In: 2nd international conference on automation, cognitive science, optics, micro electro-mechanical system and information technology, pp. 44–47
12. Ghosh A, Srivastava B (2013) Solar powered weather station and rain detector. In: Texas instruments India educators conference, pp. 131–134
13. Catelain M, Ciani L (2016) Measurement and characterization of air temperature sensors for weather stations. In: IEEE international instrumentation and measurement technology conference proceedings, pp. 1–7
14. Goudal KC, Preetham VR (2014) Microcontroller based real time weather monitoring device with GSM. Int J Sci. Eng Technol Res, 1960–1963

15. Katyal A, Yadav R (2016) Wireless Arduino based weather station. *Int J Adv Res Comput Commun Eng*, 274–276
16. Vivek Babu K, Anideep K (2017) Weather forecasting using Raspberry Pi with (IoT). *ARPN J Eng Appl Sci*, 5129–5134
17. Devarakonda Uma K, Kumar R (2016) Design of weather monitoring system using Raspberry Pi and Arduino. *Int J Adv Technol Innov Res*, 4633–4638
18. Kishorebabu V, Sravanthi R (2020) Real time monitoring of environment parameters using IoT. *Wireless Personal Commun*, 1–24
19. Sung WT, Hsiao SJ, Shih JA (2019) Construction of indoor thermal comfort environmental monitoring system based on the IoT Architecture. *J SensS*
20. Das A (2018) Design of an IoT based real time environment monitoring system using legacy sensors. In: *MATEC Web of Conferences*. EDP Sciences
21. Sonawane S, et.al. (2018, November) IoT based smart environmental monitoring using wireless sensor networks and raspberry Pi. *Int J Res Appl Sci & Eng Technol (IJRASET)*
22. Sahay MR, et al. (2019) Environmental monitoring system using IoT and cloud service at real-time
23. Jaladi AR et al (2017) Environmental monitoring using wireless sensor networks (WSN) based on IoT. *Int Res J Eng Technol* 4.1, 1371–1378
24. Dhineesh T, et al. (2019) Analysis of IoT based wireless sensors for environmental monitoring in agriculture
25. Nawandar NK, Satpute VR (2019) IoT based low cost and intelligent module for smart irrigation system. *Comput Electron in Agri* 162, 979–990
26. Fourati MA, Chebbi W (2014) Development of a web-based weather station for irrigation scheduling. In: *International colloquium in information science and technology*, pp. 37–42
27. Shekhar Y (2017) Intelligent IoT based irrigation system. *Int J Appl Eng Res*, 7306–7320
28. Saraf SB, Gawali DH (2017) IoT based smart irrigation monitoring and controlling system. 2nd RTEICT
29. Choudhury S (2019) Smart irrigation: IoT-based irrigation monitoring system. In: *Proceedings of international ethical hacking conference*. Springer, Singapore

Smart Water Management in Irrigation System Using IoT



Aparajita Das, Yasharth Gupta, Neeraj Vijay Wedhane,
and Md. Ruhul Islam

Abstract India is a wide country, where people mainly do agriculture for their living. This is the most important earning source for most of the Indian families residing here. Agriculture in India contributes to about 13% of total exports, 6% of total industrial investment, and 16.5% of total GDP. The main resource to continue agriculture in the country requires water resources. Irrigation can help in this area but there will be wastage of water in some way or the other. Many of the farmers usually supervise on a widely spread area for farming activities which becomes very difficult to manage and keep track of every corner. Sometimes, there are cases of uneven water sprinklers. This leads in bad production which results in financial losses of farmers (Pandit in IoT based Smart irrigation system using soil moisture sensor and ESP8266 NodeMCU, July 15, 2019, [1]). Automation of the activities required to carry out irrigation will reduce the need of human supervision or intervention, which will lead to transforming the system from static and manual to dynamic and intelligent which will, in the end, result in higher production (Hariharan in Int J Emerg Technol Innov Eng 5(3), 2019, [2]). The modern irrigation systems like the drip irrigation system and the sprinkler irrigation system need to be combined with the Internet of Things (IoT) for better productivity in agriculture activities and efficient water usage. This task aims at monitoring parameters for soil like, soil moisture, humidity, and temperature while also regulating and monitoring the water level of the water tank. Smart irrigation system will improve crop fields while also saving water. Smart irrigation system can be used to control greenhouse. The system uses wireless sensor

A. Das · Y. Gupta · N. V. Wedhane · Md. R. Islam (✉)
Department of Computer Science and Engineering, Sikkim Manipal University, Majitar, Sikkim,
India
e-mail: ruhulislam786@gmail.com

A. Das
e-mail: aparajitad60@gmail.com

Y. Gupta
e-mail: yashgupta1719@gmail.com

N. V. Wedhane
e-mail: neerajlp7@gmail.com

network to detect and control the different parameters dynamically in real time for efficiently managing and maintaining the whole system.

Keywords Internet of Things · Automation · Automated irrigation · Arduino · Agriculture

1 Introduction

Agriculture plays an important role in the economy of India. India is seventh largest agricultural exporter worldwide, exporting agricultural products to more than 120 countries. Internet of Things (IoT) is a series of components (nodes) which are interrelated and share/transfer data with each other with or without human interaction. When we apply the concepts of internet of Things with agriculture, there are any things which get affected by it like cost, manpower, etc. Using Internet of Things in agriculture, we can boost up the productivity. The whole new IoT ecosystem includes the sensors which detect the real-time temperature, rainfall, humidity, and so on accurately. These sensors monitor all the conditions around the crop and the weather surrounding them. If anything is found inappropriate, the message is sent immediately to the operator. By this, the farmers are well informed about their farms, and hence, the productivity is increased. The sensor lets the farmer get the information about the amount of moisture that will make the soil fertile and yields the best results in terms of crops and harvesting. To interchange valuable controllers in current obtained systems, the Arduino UNO is utilized in this model because it is a reasonable microcontroller. The Arduino UNO is programmed to analyze some signals from sensors like wet, temperature, and rain. A pump is employed to pump the water into the irrigation system. The employment of simply obtainable part reduces the producing and maintenance prices. This makes the planned system to be a cheap, acceptable, and an occasional maintenance resolution for applications, particularly in rural areas and for little-scale agriculturists. This analysis work increased to assist the small-scale cultivators can increase the yield of the crops increasing the government's economy.

Our contributions are summarized as follows:

- (a) To the best of our knowledge, the presented project has been upgraded from the many other research papers that are referred, by integrating and enhancing all the components in a single project.
- (b) We have also added a real-time cloud database to the project which will process and display the required data to the user in real time.
- (c) In addition to integrating all the components and adding a cloud database, we have also used ultrasonic sensor connected with the water reservoir for the completeness of smart water management and smart irrigation system.

The organization of the paper is as follows:

The problem definition has been briefly described in Sect. 2 which is followed by our proposed solution along with the design of the system for the problem in Sect. 3. Section 4 includes the block diagram of the system, the flow charts of the working of the system along with the circuit diagram of our model, showing all the components used in the system. Results obtained is given in a tabular format in the Sect. 6 with the conclusions stated in Sect. 7.

2 Problem Definition

In India, continuing agriculture for their livelihood is a necessity. Also, it is one of the main sources of livelihood. The unending need for consumption of water is increasing day by day, which will ultimately lead to problems of water scarcity.

The conventional irrigation system uses methods like overhead sprinklers. Here, the entire soil surfaces are left to be saturated, and the surface often stays wet long after the irrigation process is completed. The new methods such as drip irrigation system is a method of doing irrigation which slowly applies small amount of water to the part of a plant root level zone. Usually, in drip irrigation system, water is supplied to the plants frequently; water here is supplied often to the plants, to maintain soil conditions and prevent the moisture stress content in the plant with proper water resource the drip irrigation system saves water because only the root part of the plant receives water. Little water is lost in situations, where proper amount of water is applied.

Drip irrigation is used very often because it increases crop yields while decreasing both water requirements and labor. Compared to surface irrigation or sprinkler irrigation, drip irrigation requires about half of the water required by the latter. Lower is the operating pressures and flow rates, it results in lower energy costs required. In this case, water can be controlled in high degree. During irrigation, the plants can be supplied with more accurate amounts of water. Disease in plants and insect attacks reduces because the plant foliage stays dry. In this process, the whole operating cost is usually reduced [3].

Problems in traditional systems: In traditional systems, irrigation by farmers are done manually. As the water is released directly in the soil, the plants planted go through a high stress from variation in the soil level moisture; therefore, the appearances of plant are reduced. This is because there is no automation. The absence of automatic controlling of the system can result in improper water control. The major reasons for these limitations are the exponential growth of population at a very faster rate. Today, the wastage of water has led to serious scarcity of water, a global water crisis where managing scarcity of water has become a serious job. The economically poor countries face this problem having shortage of water resources. So, this being the problem in the traditional irrigation systems.

Limitations of existing system:

1. Physical work of farmer to control drip irrigation.
2. Wastage of water and time.
3. Wastage of money.
4. Water in irrigation system, malarial mosquito breeds.

3 Proposed Solution Strategy

The era defining IoT technologies can be used to solve the problems mentioned above. IoT provides an easy to implement and efficient solution to the problem at minimum cost. The various components included in our model are ultrasonic sensor, Humidity sensor, centralized Arduino controller, relay module, and a water pump. The humidity sensor that is placed in the soil which is connected to the Arduino controller. The Arduino will have the program coded in its IDE that will analyze the moisture content received from the humidity sensor and this Arduino which is also connected to a water pump will trigger the pump ON if the moisture content is less than what is required in the soil. The pump will turn OFF when the moisture content has become sufficient. Now, to have a proper water management and to prevent unnecessary wastage of water, an ultrasonic sensor is connected to the Arduino as well. The ultrasonic sensor will be placed over the water container. This ultrasonic sensor will measure the height (the distance of the surface of water from it) of the water level and send this value to the Arduino. The Arduino has a program coded that analyzes this distance of water level by comparing it with a predefined water level height that must be maintained in the water container, and if it is more than that value, only then it triggers ON the water pump; otherwise, a message will be displayed notifying the user about the insufficient water level.

The user can monitor this whole process. The moisture content and water level readings will be sent to the user. The cloud stores these values and sends the values to the user's device. This makes this development easy to be monitored from anywhere and hence makes it useful.

The components incorporated in this model are:

1. Ultrasonic sensor
2. Humidity sensor
3. Arduino microcontroller
4. Relay module
5. Water pump
6. Cloud data storage

The figure given below shows the design layout, and how the signal and data are received and sent from the microcontroller to the various sensors. The diagram shows how the system works and which components interact with each other. The information received by the Arduino from the humidity sensors triggers the water

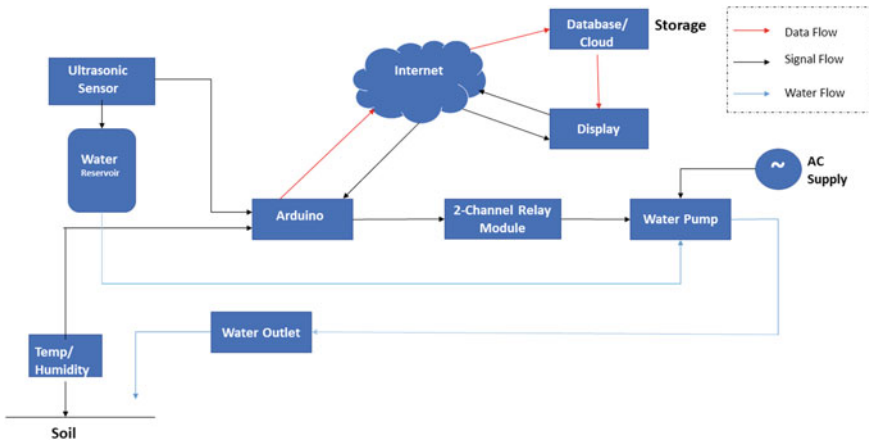


Fig. 1 Design layout of the system

pump considering that there is sufficient water level present in the water reservoir to prevent wastage of water (Fig. 1).

4 Design Strategy for the Solution

The above flowcharts (Figs. 2, 3, and 4) depict the series of actions that will be taken based on the different readings received from the sensors. The conditional statement

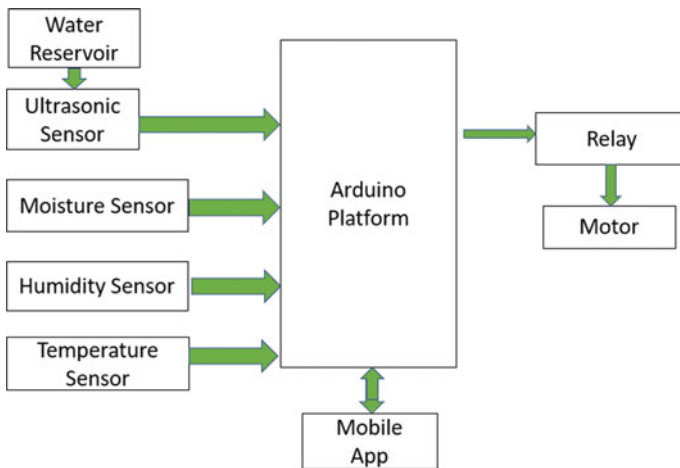


Fig. 2 Block diagram of proposed system

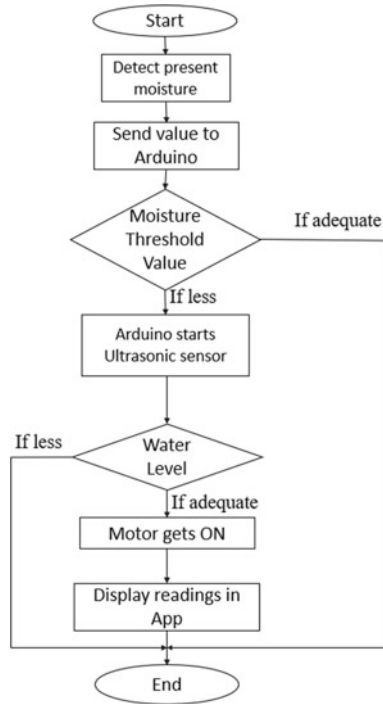


Fig. 3 Flowchart for moisture detection

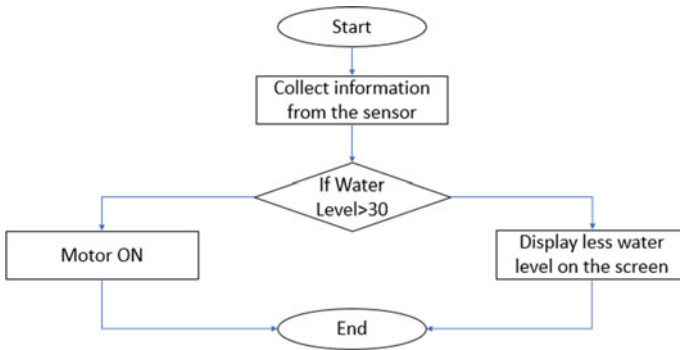


Fig. 4 Flowchart of water level detection

of the program written in IDE will check for the conditions, and based on the output from the sensors will analyze and perform the appropriate action (Fig. 5).

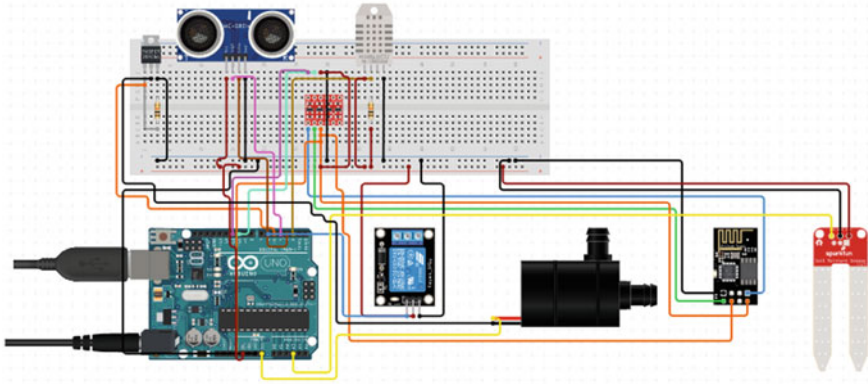


Fig. 5 Circuit diagram of the model

App Interface:

Given is the interface of display (Fig. 6), which shows the reading.

1. Humidity status value is displayed from stored firebase.
2. Temperature status value is displayed from stored firebase.

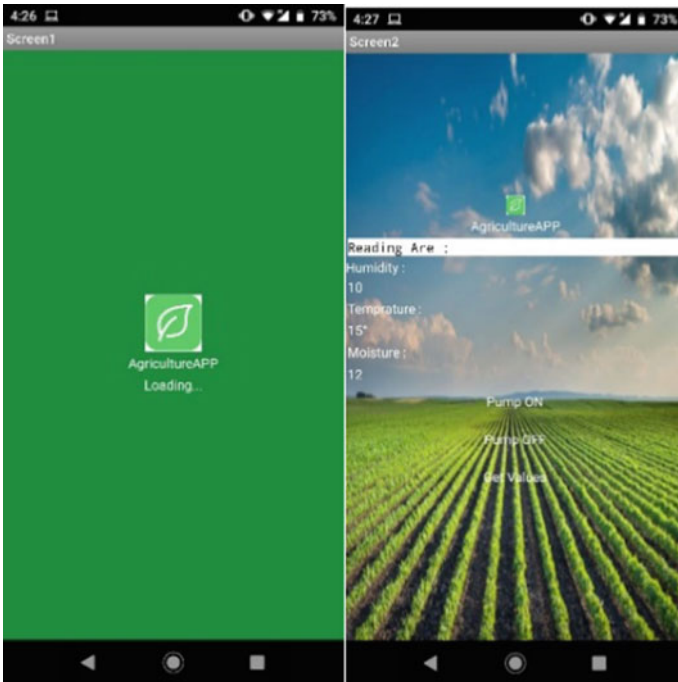
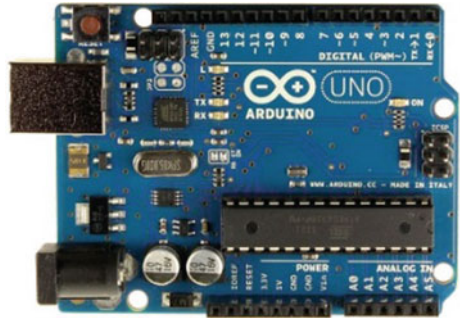


Fig. 6 App interface

Fig. 7 Arduino UNO R3

3. Moisture status value is displayed from stored firebase.
4. On and Off button for the water pump.

5 Working Principle

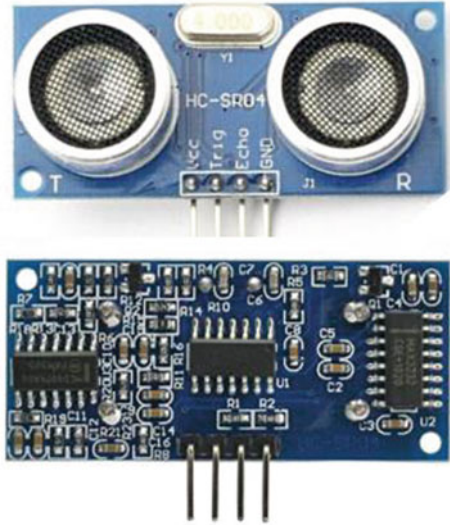
5.1 *Arduino UNO R3*

An Arduino is a microcontroller that is used for processing and operating or communicating between multiple devices such as sensors or other modules that can be used for making different kinds of jobs. The Arduino can be programmed using simplified version of C++ and C, and hence, this makes it easy to use without any need for learning new language. One of the features of Arduino is that it is open source, and there are various communities for it that makes it very easy for anyone who is stuck with a problem to ask other people in community for help. The Arduino is the central system for coordination for the task we are doing and is monitoring and controlling all the movements and the activities going on, in the system (Fig. 7) [4].

5.2 *Ultrasonic Sensor*

The ultrasonic sensor is an acoustic sensor that can be used to measure the distance. It has a transmitter and a receiver. The transmitter sends ultrasonic sound waves and starts a timer, and then, the receiver part in the sensor receives the waves that bounces back after collision with an object and stops the timer. We then use the distance formula in the program to calculate the distance using the timer value received from the sensor (Fig. 8) [5].

Fig. 8 Ultrasonic sensor (HC-SR04)



5.3 Humidity and Moisture Sensor

Temperature and moisture of soil are the two important aspects in agricultural area. This sensor is made for applications that require specific monitoring on moisture and temperature circumstances. The classic temperature goal is 0.4 °C, while the classic moisture goal is 3% RH (Fig. 9) [6].

Fig. 9 DHT-11

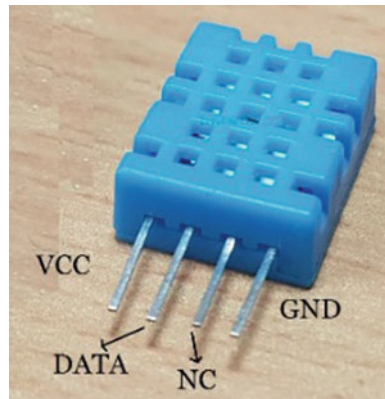
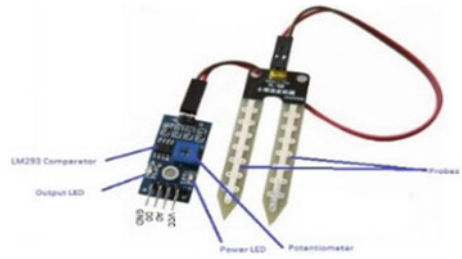


Fig. 10 Soil sensor (FC-28)



5.4 Soil Sensor

It is a device that measures the moisture content in the soil. How it works is that it has two probes. The electric current is supplied by the nodes in this to the soil, and then, the resistance offered by the soil is measured. So, naturally, when there is more water content, the soil will allow more current to flow through it, and when it is less, the current flow will also be less. This is used to detect the presence of water content in the soil (Fig. 10).

5.5 Relay Switch

It is an electrical switch that can be turned ON/OFF allowing to let the current flow through or not. It maintains the other devices connected to the Arduino with the low voltage of Arduino that is to be 5v. This protects the Arduino from damage. Here, for this model, we are using two channel relay module to control an AC water pump with an Arduino (Fig. 11) [7].

Fig. 11 Relay switch 5 V-2



Fig. 12 Wi-Fi module



5.6 WI-FI Module

This is a module that is used in the Arduino to connect the Arduino with a Wi-Fi Internet connection, and the various access points nearby are displayed and can be connected to. The Arduino connects with Internet in our model using this module so that we can send the data to the cloud storage. This module can also act as an access point and create a WI-FI hotspot to provide Internet to other devices (Fig. 12) [8].

6 Implementation and Result

See Table 1.

Table 1 Implementation test case with their results

Sl. No.	Test case	Response
1	Testing the Arduino by in-built blinking LED	LED blinking Arduino working message
2	Testing ultrasonic sensor working	The serial monitor in the Arduino IDE shows the readings of the distance of the water surface from the sensor received
3	Testing moisture sensor	The other serial monitor for the program of retrieving the moisture content detected by the sensor which is connected to the Arduino is displayed on this serial monitor at regular intervals
4	Testing water pump	The flow or movement of water from the water reservoir to the soil
5	Testing Wi-Fi module	The connection of Arduino with the Internet, the readings sent to the cloud storage to be accessed by any device from anywhere via Internet

7 Conclusion

This discussed design has result in cutting down wastage of water supplied to the irrigation system methods such as drip irrigation. IoT provides an easy to implement and efficient solution to a problem at a minimum cost. This whole system not only saves precious water resources but also enhances the system by using the sensor values to produce correct results, for the whole irrigation system to work productively. This model will make farmers life easy, as there will be no need to supervise the system often. This work can be done from a distance, comfortably sitting at home. This will lead to a dynamic lifestyle for farmers, compared to the traditional static lifestyle.

The model will work, also as the foundation model for the future upcoming new technologies which may be construct on or over it. The model has a great deal of scope for IoT applications in agriculture industry setups as well as all the other industries requiring water resources. More upcoming advanced technologies like IoT, AI, and cloud computing can be built over and applied in the system to make more amount of operations in the system dynamic or automated and authorize remote monitoring and control of the same discussed system [9, 10].

References

1. Pandit A (2019) IoT based Smart irrigation system using soil moisture sensor and ESP8266 NodeMCU, July 15, 2019
2. Hariharan U (2019, March) Smart irrigation mechanism for soil management using BBC Micro: bit in Internet of Things. *Int J Emerg Technol Innov Eng* 5(3). ISSN: 2394-6598
3. Naik P, Kumbi A, Katti K, Telkar N (2018) Automation of irrigation system using IoT. *Int J Eng Manuf Sci* 8(1):77–88. ISSN: 2249-3115 © Research India Publications
4. Priyadharsnee K, Rathi S (2017, May) An IoT based Smart irrigation system. *Int J Sci Eng Res* 8(5): 44. ISSN: 2229-5518
5. <http://arduinolearning.com/code/hc-sr04-ultrasonic-sensor-example.php>
6. Parameswaran G, Sivaprasath K (2016) Arduino based Smart Drip Irrigation System using Internet of Things 6(5), <https://doi.org/10.4010/2016.1348>. ISSN: 2321-3361 © 2016 IJESC
7. Durga SN, Ramakrishna M (2018, June) Smart irrigation system based on soil moisture using IoT. *Int Res J Eng Technol (IRJET)* 5(6), e-ISSN: 2395-0056, p-ISSN: 2395-0072
8. Ismail N et al (2019) Smart irrigation system based on Internet of Things (IoT). *J Phys: Conf Ser* 1339 012012
9. Nath A, Konwar HN, Kumar K, Islam MR (2020) (Chapter 14) Technology enabled smart efficiency parking system (TESEPS), Springer Science and Business Media LLC
10. Kathuria S, Kumar R, Bhatia T (2018, June) e-Krishi: an IoT based smart irrigation system, *International J Electr, Electron Data Commun* 6(6), p-ISSN: 2320-2084, e-ISSN: 2321-2950

A Study on Cloud Employment Tracking System



Manisha Gupta, Poulami Paul, and Abhishek Roy

Abstract As a developing nation India have to strive hard for delivery of multi-faceted public services to the doorstep of populace. This task becomes more challenging due to direct and indirect effect of global economic meltdown and job loss as aftermath of global pandemic of Corona virus (COVID19) which have forced us to maintain social distancing and isolation. Moreover the global lock down of affected countries have stalled their economic and business transactions which have adversely affected their financial backbone thereby leading towards mass unemployment of Citizen (i.e. Worker). In this situation, Information and Communication Technology (ICT) based applications may be used to develop an efficient electronic mechanism to support worker find new employment thereby maintaining the rules of social isolation. With this objective to assist unemployed Citizen to find their suitable employment and also support economy rolling in this lockdown situation, authors have proposed a smart card based Cloud Employment Tracking System (CETS), which will bridge the gap between employers and their prospective employees thereby maintaining the rules of social isolation.

Keywords Cloud computing · Employment tracking · Smart card

1 Introduction

As a developing nation India have to strive hard for delivery of multifaceted public services to the doorstep of populace. This task becomes more challenging due to direct and indirect effect of global economic meltdown as aftermath of COVID19 pandemic.

M. Gupta · P. Paul · A. Roy (✉)

Department of Computer Science & Engineering, Adamas University, Kolkata, India

e-mail: dr.aroy@yahoo.com

URL: <http://adamasuniversity.ac.in>

M. Gupta

e-mail: manisha98gupta@gmail.com

P. Paul

e-mail: ppaulcse@gmail.com

© The Author(s), under exclusive license to Springer Nature Singapore Pte Ltd. 2021
M. Chakraborty et al. (eds.), *Trends in Wireless Communication and Information Security*,
Lecture Notes in Electrical Engineering 740,
https://doi.org/10.1007/978-981-33-6393-9_36

353

This deadly virus transmits from person to person through their droplets and affects the entire society in an exponential manner thereby leading to large amount of human casualties within a very short span of time. As we are yet to find the vaccine of this deadly virus, the only solution left to us is to break the chain of virus transmission to arrest the rate of infection within the society. As a result people are forced to maintain social isolation to break the transmission chain of Corona virus (i.e. COVID19). This approach of social isolation have directly affected Citizen from availing various services which are delivered through conventional ways. Evenmore, the condition is more critical for the base of our societal pyramid who have bare minimum means to maintain their livelihood. It may be noted that, India have witnessed death of large number of migrant workers who left their home town long back in search of employment and was forced to return by walking thousands of kilometers after losing their job, shelter and food due to the nation wide lockdown. Death due to road and rail accidents of these helpless migrant workers have become an unfortunate daily affairs nowadays. Focusing on the gravity of this situation, authors have proposed a Citizen centric smart card based Cloud Employment Tracking System (CETS) which will help Citizen to find suitable professional openings and help economy rolling in this crisis situation thereby maintaining the rules of social isolation to remain safe from the infection of Corona virus.

Section 2 states the origin of our research work. Section 3 describes our proposed Cloud Employment Tracking System (CETS). Section 4 draws the conclusion and also explores future scope of work.

2 Origin of Work

This research work have originated from the idea of an Integrated Electronic Service Delivery System (IESDS). As a result a Citizen centric smart card based Electronic Governance and Cloud Governance [1–4] models were already proposed to deliver multivariate electronic services [4–6] like Electronic Voting, Electronic Banking, Electronic Education, etc to the doorstep of populace, so that, as an ultimate end user they can avail all services through virtual medium (i.e. Internet) irrespective of their geospatial location. The primary components those models are described below:

1. Citizen denotes SERVICE SEEKER who transmits SERVICE REQUEST.
2. Government [1–3] denotes STATE ADMINISTRATOR who validates identity of Citizen and keep track of all electronic transactions under its jurisdiction.
3. Service Provider, denotes any THIRD PARTY SERVICE PROVIDER who generates SERVICE RESPONSE for Citizen.
4. Internet denotes virtual communication medium which is used for transmission of SERVICE REQUEST and SERVICE RESPONSE through STATE ADMINISTRATOR.

In this current scenario of job loss and economic slow down, to assist Citizen (i.e. Workers) to search new employment [7–10], attend online interview, avail various economic support schemes of Government and Non Government Organizations, we have proposed a Cloud Employment Tracking System (CETS), which is discussed through Sects. 3 and 4 respectively.

3 Proposed Cloud Based Employment Tracking System

The Block Diagram and Conceptual Diagram of proposed Cloud Employment Tracking System (CETS) are explained in Sects. 3.1 and 3.2 respectively.

3.1 Block Diagram

Figure 1 shows the block diagram of proposed Cloud Employment Tracking System (CETS) using Multipurpose Electronic Card (MEC), which is discussed below:

1. Citizen initiate transaction using Multipurpose Electronic Card (MEC).
2. Citizen transmit SERVICE REQUEST to Government through public cloud.
3. Government receives the SERVICE REQUEST and verifies the identity of Citizen.
 - (a) In case of invalid user (i.e. Citizen), Government aborts the transaction.
 - (b) In case of valid user (i.e. Citizen), Governments allows the transaction to proceed further.
4. Government transmit SERVICE REQUEST to proposed Cloud Employment Tracking System (CETS) through Public Cloud.
5. Cloud Employment Tracking System (CETS) receives SERVICE REQUEST and verifies the identity of Citizen.
 - (a) In case of invalid user (i.e. Citizen), Cloud Employment Tracking System aborts the transaction.
 - (b) In case of valid user (i.e. Citizen), Cloud Employment Tracking System allows the transaction to proceed further.
6. CLoud Employment Tracking System (CETS) assess the SERVICE REQUEST of Citizen and interacts with private companies (through READ and WRITE operations) to generate the SERVICE RESPONSE.
7. Finally, Citizen receives the SERVICE RESPONSE from proposed Cloud Employment Tracking System (CETS) through Public Cloud to complete the electronic transaction successfully.

The detailed explanation of proposed Cloud Employment Tracking System (CETS) is explained further in Sect. 3.2 through its conceptual diagram.

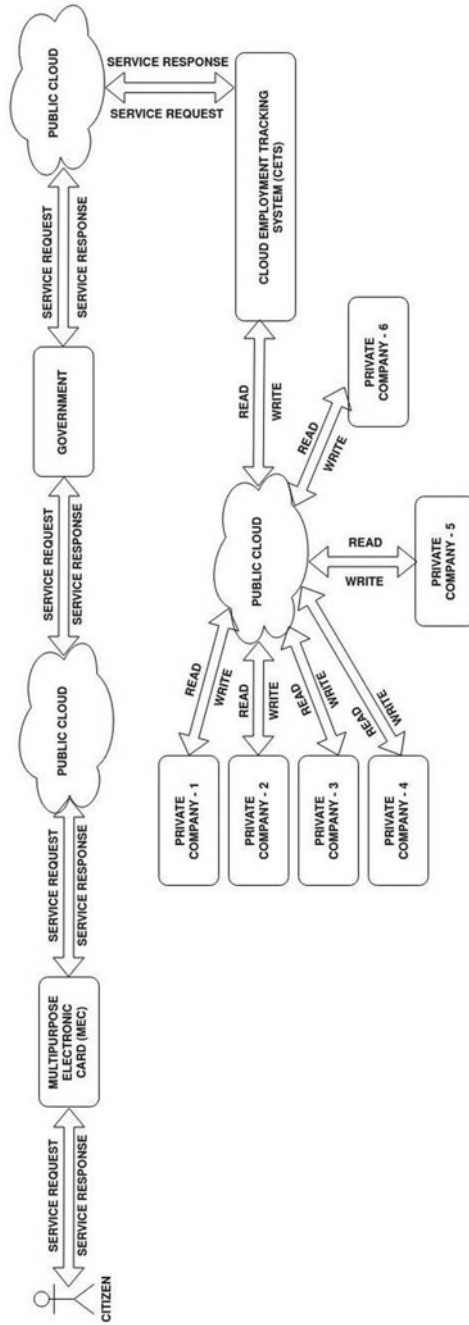


Fig. 1 Block diagram of cloud employment tracking system (CETS)

3.2 Conceptual Diagram

Figure 2 shows the conceptual diagram of proposed Cloud Employment Tracking System (CETS) which is described during Citizen to Cloud Employment Tracking System (CETS) to Citizen (C2E2C) type of transaction. Since the role of Government have been already stated in Sect. 2, here in Sect. 3 we will focus on Cloud Employment Tracking System (CETS) only.

1. Primary Participants:

- (a) Citizen.
- (b) Cloud Employment Tracking System (CETS).
- (c) Mode of Communication: Public Cloud.

PHASE-I: This phase mainly denotes the communication between Citizen and Cloud Employment Tracking System (CETS).

2. Citizen side:

- (a) Citizen initiates electronic transaction and sends SERVICE REQUEST to Cloud Employment Tracking System (CETS) through Public Kiosk (i.e. Public Cloud) using Multipurpose Electronic Card (MEC), which is shown through Path-1 of Fig. 2. In case the Citizen is interested to search a new job, then it should provide all educational qualifications, desired job type, previous professional experiences (if any), expected salary, preferred location etc along with the SERVICE REQUEST.

3. CETS side:

- (a) CETS Interface receives SERVICE REQUEST of Citizen through the Firewall installed within its system.
- (b) CETS verifies the identity of Citizen.
 - i In case of invalid user, SERVICE REQUEST is aborted and Citizen is notified using System Timeout through Path-2 of Fig. 2.
 - ii In case of valid user, SERVICE REQUEST is permitted to proceed further.
- (c) As shown in Fig. 2 SERVICE REQUEST from valid Citizen are send towards multiple SERVICE REQUEST SERVER through Router to maintain its proper sequence of arrival.
- (d) Scheduler receives all SERVICE REQUEST from SERVICE REQUEST SERVERS and sends it to Private Cloud through Path-1 of Fig. 2 thereby maintaining its proper sequence of arrival.
- (e) Private Cloud uses the SERVICE REQUEST obtained from Scheduler for Data Mining to extract a precise decision based on all the information provided by Citizen along with its SERVICE REQUEST.

Data Mining Phase:

- i Data Collector receives all information from Private Cloud and store it in Central Database of Cloud Employment Tracking System (CETS).

- ii Central Database store the information of Citizen as per its educational qualification and professional experience (if any) into its respective logical compartments in a well structured manner.
 - iii Data Miner fetches the structured information from the Central Database and send it to Decision Maker.
 - iv The main task of Decision Maker is to generate a Precise SERVICE REQUEST in a well structure manner, which will be used for searching of job for the Citizen.
- (f) Precise SERVICE REQUEST generated by Decision Maker will be send to Scheduler through Private Cloud of the proposed system.
- (g) Scheduler will send all Precise SERVICE REQUEST to Transaction Master for matching with the job openings available to Transaction Master.

PHASE-II: This phase mainly denotes the communication between Cloud Employment Tracking System (CETS) and other private companies or agencies to create a Job Pool.

4. Job Pool is a specific component of our Cloud Employment Tracking System (CETS) which interacts with multiple private companies, staff out sourcing agencies and job protals to generate a centralised job pool.
5. Centralised job pool is provided to Transaction Master of the proposed system to help employers search their prospective employee and help economy rolling in this lock down situation.

PHASE-III: This is the final phase of operation which generates SERVICE RESPONSE for the Citizen.

6. Transaction Master matches with Precise SERVICE REQUEST (obtained from Scheduler) with the job openings available at Job Pool and find out the probable job openings for the Citizen based on the information provided through SERVICE REQUEST.
7. Transaction Master generates a Final SERVICE RESPONSE for the Citizen containing the probable list of job openings and send it to Citizen through Public Kiosk (i.e. Public Cloud).
8. **Citizen side:** Citizen avails the Final SERVICE RESPONSE using its Multipurpose Electronic Card (MEC).

Our proposed Cloud Employment Tracking System (CETS) will help Citizen to search job using cloud platform thereby maintaining the rules of social isolation to break the transmission chain of Corona virus (COVID19) within the society. Moreover, it will also help society in broader sense by rolling the economy in this global lockdown situation. Section 4 concludes the discussion of this paper.

4 Conclusion

The objective our paper was to propose a Cloud Employment Tracking System (CETS) which will help Citizen to search job as per the educational and professional credentials. This system was proposed viewing the global lockdown due to pandemic COVID19 where several professionals are losing their job which have badly affected the base level of our societal pyramid. In India lockdown of economy have forced the migrant workers to return back to their home town by walking thousands of kilometers after losing their job, shelter and food. The condition is so critical that death of these helpless migrant workers by road and rail accidents have become an unfortunate daily affairs in India nowadays.

The proposed Cloud Employment Tracking System (CETS) can be further improved using Blockchain technology to keep track of all the SERVICE REQUEST and SERVICE RESPONSE in a secure manner. Hybrid cryptosystem may be used to ensure the Privacy, Integrity, Authentication and Non-Repudiation (PINA) of electronic transaction. Even, the Central Database Server may be enhanced to store information of all type of professionals and workers in a structured manner, which may be considered as future scope of this research work.

References

1. Ghosh A, Das T, Majumder S, Roy A (2020) Authentication of user in connected governance model. In: Batra U, Roy NR, Panda B (eds) Data science and analytics. Springer, Singapore, pp 110–122. ISBN 978-981-15-5830-6. doi: https://doi.org/10.1007/978-981-15-5830-6_10
2. Roy A (2020) Object-oriented modeling of multifaceted service delivery system using connected governance. In: Jena A, Das H, Mohapatra D (eds) Automated software testing. ICDCIT 2019. Services and business process reengineering. Springer, Singapore, pp 1–25. https://doi.org/10.1007/978-981-15-2455-4_1
3. Roy A (2019) Smart delivery of multifaceted services through connected governance. In: 3rd international conference on computing methodologies and communication (ICCMC). IEEE, India, pp 476–482. <https://doi.org/10.1109/ICCMC.2019.8819851>
4. Khatun R, Bandopadhyay T, Roy A (2017) Data modeling for E-voting system using smart card based E-governance system. Int J Inform Eng Electron Bus (IJIEEB) 9(2):45–52. <https://doi.org/10.5815/ijieeb.2017.02.06>
5. Biswas S, Roy A (2019) An intrusion detection system based secured electronic service delivery model. In: 2019 3rd international conference on electronics, communication and aerospace technology (ICECA), Coimbatore, India, pp 1316–1321. <https://doi.org/10.1109/ICECA.2019.8822016>
6. Biswas A, Roy A (2019) A study on dynamic ID based user authentication system using smart card: Asian J Convergence Technol (AJCT) 5(2) ISSN 2350-1146. Retrieved on 08 Mar 2020 <http://www.asianssr.org/index.php/ajct/article/view/871>
7. Wang X, Li G, Sun X (2019) Design of employment tracking system for public administration graduates. In: 2019 9th international conference on management and computer science (ICMCS 2019), China, pp 148–150. <https://doi.org/10.25236/icmcs.2019.030>
8. Oyong I, Abid A, Afif H, Utami E (2017) Concept and data model of AK/I card digitization as employment information distribution media. In: 2017 5th international conference on cyber and IT service management (CITSM), Indonesia (IEEE), pp 1–6. <https://doi.org/10.1109/CITSM.2017.8089276>

9. Roy A, Shah V, Zalzal AMS (2015) A feasibility study for the development of an employment system for underserved communities. In: 2015 IEEE Canada international humanitarian technology conference (IHTC2015), Canada (IEEE), pp 1–4. <https://doi.org/10.1109/IHTC.2015.7238036>
10. Muderedzwa M, Nyakwende E (2010) A framework for improving the effectiveness of IT in employment screening. In: 2010 IEEE student conference on research and development (SCOReD), Malaysia (IEEE), pp 133–138. <https://doi.org/10.1109/SCORED.2010.5703988>

A Study on Medclaim Processing in Connected Healthcare System



Subhasish Mohapatra and Abhishek Roy

Abstract Advancement of Information and Communication Technology (ICT) have explored new dimensions of digital service delivery system between the distant users, who are virtually connected to each other through open channel like Internet. Internet serves as a budget friendly and faster communication channel between **SERVICE SEEKER** and **SERVICE PROVIDER** for delivery of **SERVICE REQUEST** and **SERVICE RESPONSE** respectively. As a result, it helps to bring down the operational cost of service delivery system within the affordability of populace. However, this easy accessibility of Internet also makes it susceptible to infringement attempts of adversaries, which widens exponentially with multiparty engagements during any electronic transaction. If these security lapses can be identified and sanitized properly, electronic communication medium can serve as an efficient service delivery system for multivariate sectors like public healthcare, medical research, finance, public transport, agro-based sectors, etc. This concept of Citizen centric electronic service delivery system becomes highly relevant in global pandemic situation like Corona virus (COVID-19), where people are compelled to maintain social distancing (by staying at home) to break the chain of virus transmission within the society. Furthermore, to integrate all these Citizen centric electronic services, a single window based Integrated Electronic Service Delivery System (IESDS) may be proposed to proceed towards unbiased and corruption free healthy society. In this paper authors have proposed a Cloud based Healthcare Integrated Development Environment (HIDE) using Multipurpose Electronic Card (MEC) through a connected system for accessing online Healthcare facilities and its subsequent Medclaim Processing. Authors have used Block Diagram, Conceptual Diagram and Class Diagram to elaborate the proposed Cloud based Healthcare Integrated Development Environment (HIDE).

Keywords Cloud healthcare · Medclaim processing · Class diagram

S. Mohapatra · A. Roy (✉)
Department of Computer Science & Engineering, Adamas University, Kolkata, India
e-mail: dr.aroy@yahoo.com

S. Mohapatra
e-mail: mohapatra.subhasish@gmail.com

© The Author(s), under exclusive license to Springer Nature Singapore Pte Ltd. 2021
M. Chakraborty et al. (eds.), *Trends in Wireless Communication and Information Security*,
Lecture Notes in Electrical Engineering 740,
https://doi.org/10.1007/978-981-33-6393-9_37

363

1 Introduction

Our urban lifestyle have encouraged us to explore faster means of message communication to perform proper utilization of our valuable time. As a result Information and Communication Technology (ICT) based message communication between virtually connected users have gained popularity among masses. Though Internet facilitates its user to communicate instantly through cost effective manner, it have its highs and lows also. As an open communication channel Internet is susceptible to infringement attempts of adversaries. If we can prevent the unauthorized access of adversary over the electronic message communication, it can be utilized for prompt deliver of essential public services like healthcare facilities and its subsequent expenses, medical research, finance, public transport, agro-based sectors (i.e. public ration distribution system) etc. Specifically, this approach of Citizen centric electronic service delivery system becomes more relevant in present global pandemic situation of Corona virus (COVID-19), where people are compelled to maintain social distancing and isolation (by staying at home) to break the chain of virus transmission within the community or society. In this critical situation of global pandemic and economic disaster, a concrete step should be taken to deliver Citizen centric essential services to the doorstep of populace through an integrated environment and single window interface. If we can really transmit **SERVICE REQUEST** and **SERVICE RESPONSE** securely between **SERVICE SEEKER** and **SERVICE PROVIDER** through cloud connectivity, at least we can try to break the chain of community transmission (i.e. infection) of deadly disease like Corona virus (COVID-19) and save the mankind. Furthermore, to ensure identification and subsequent neutralization of adversaries during these sensitive electronic communication, involvement of Government will help to build trust between **SERVICE SEEKER** and **SERVICE PROVIDER**. However, critics may raise concern about privacy issues of Citizen due to involvement of Government during these transactions. Due to security of our nation which is a regular victim of cross border terrorism, we can not afford unbounded liberty of Citizen mainly to keep our society secure from any type of disaster like biological disaster, economic disaster, environmental disaster, etc. To achieve this objective in this paper authors have proposed a Healthcare Integrated Development Environment (HIDE) using Multipurpose Electronic Card (MEC), which will help to deliver healthcare facilities to populace and settle down its subsequent expenses through Mediclaim Processing in a compact manner.

1.1 Paper Organization

Section 2 briefly states the origin of our research work i.e. Cloud Governance model where Government act as primary coordinator for delivery of electronic services like healthcare facilities and other electronic services to Citizen. Section 3 explains our proposed Cloud based Healthcare Integrated Development Environment (HIDE)

and payment of medical expenses through Medicaid Processing. Section 4 further elaborates the static structure of our proposed model using Class Diagram, so that we can perform detailed Object Oriented Modelling (OOM) in next paper. Section 5 draws conclusion of our present work and also explore its future scope.

2 Origin of Work

The Citizen centric Cloud Governance [1–6] model is the origin of our present research work. The primary components of our Cloud Governance model are: **Citizen** (i.e. **Service Seeker**), **Government** (i.e. **State**) and **Service Provider** (i.e. Third party service providers like healthcare [1, 7–9], Medicaid and insurance, public transport, public education, etc). To avail multivariate electronic services through Cloud [10–16], Citizen uses a smart card based interface namely Multipurpose Electronic Card (MEC). In this paper we have extended this Cloud Governance model to Cloud based Healthcare Integrated Development Environment (HIDE), so that Citizen can avail healthcare facilities and pay their medical expenses through Medicaid Processing.

3 Proposed Cloud Healthcare System

To provide Healthcare [1] facilities to Citizen through virtual medium, we have proposed Healthcare Integrated Development Environment (HIDE) whose Block Diagram and Conceptual Diagram are explained in Sects. 3.1 and 3.2 respectively.

3.1 Block Diagram

Figure 1 shows the block diagram of our proposed Healthcare Integrated Development Environment (HIDE), which is discussed below:

1. Primary entities:

- (a) **Patient**—It denotes the person who wants to avail medical facilities through online mode of communication.
- (b) **Government**—Government coordinate with following entities under its jurisdiction.
 - i. **HIDE**.
 - i Scheduler.
 - I. ENT. II. Cardiology. III. Orthopedic. IV. Pediatric.
 - ii Transaction Master.
 - ii. **Bank**—Though it is a Third Party Service Provider, it have a vital role to play for payment of medical expenses of a Patient.

- iii. Insurance Company (i.e. **Mediclaim company**)—Though it is also a Third Party Service Provider, it have a vital role to play for payment of medical expenses of a Patient.
2. Mode of communication among the participants:
Mainly Public Kiosk (i.e. Public Cloud) will be used for message communication and Private Cloud will be used only during message communication within the proposed Healthcare system.
3. Mode of operation: Step wise explanation of our proposed Healthcare Integrated Development Environment (HIDE) during Patient to Government to Healthcare System to Patient (P2G2H2P) type of transaction is described below.

Patient side:

1. Patient initiate electronic transaction using Multipurpose Electronic Card (MEC), which acts as a Citizen centric single window interface to avail multivariate electronic services through cloud platform.
2. Patient transmit following information to Government through Public Kiosk (i.e. Public Cloud):
 - (a) Its unqiue parameters like Multipurpose Electronic Card (MEC) Number, Userid, Password, etc to validate its identity.
 - (b) It also send **SERVICE REQUEST** to avail desired medical facility.

Government side:

1. Government receives unique parameters of Patient(i.e. Citizen) and verifies its identity.
Scenario 1 (Verification Success): In this case Government permits the electronic transaction and it proceeds towards Step-2.
Scenario 2 (Verification Failure): In this case Government aborts the electronic transaction and Patient is notified through System Timeout.
2. Government transmit **SERVICE REQUEST** to Healthcare Service Provider through Public Kiosk (i.e. Public Cloud).

Healthcare service provider side:

1. Healthcare Integrated Development Environment (HIDE) receives **SERVICE REQUEST** of Patient through Public Kiosk and verifies the identity of Patient.
Scenario 3 (Verification Success): In this case **SERVICE REQUEST** of Patient (i.e. Citizen) proceeds towards Step-2.
Scenario 4 (Verification Failure): In this case **SERVICE REQUEST** of Patient (i.e. Citizen) is aborted and notified through System Timeout.
2. Scheduler maintains a proper sequence of multiple **SERVICE REQUEST** of Patients using First In First Out (FIFO) algorithm and transmit it further to respective medical unit like ENT, Cardiology, Orthopedic, Pediatric, etc to deliver desired medical service to Patient. To provide enhanced services to Patient additional medical units may be engaged within the proposed healthcare system.

3. Healthcare Integrated Development Environment (HIDE) also sends a **SERVICE REQUEST LOG** to Transaction Master, which matches it with **SERVICE RESPONSE** generated from respective medical units. As shown in Fig. 1, Transaction Master have to coordinate with Third Party Service Provider like Insurance (i.e. Medicaid) company and Bank for payment of medical expenses of Patient.
4. Insurance (i.e. Medicaid) company and Bank communicate with Transaction Master of Healthcare Integrated Development Environment (HIDE) through Public Kiosk (i.e. Public Cloud) through **READ** and **WRITE** operations for payment of medical expenses of a Patient.
5. Transaction Master finally delivers the complete **SERVICE RESPONSE** and Test Report to Patient through Public Kiosk (i.e. Public Cloud).

Patient side:

1. Patient avails desired medical facility i.e. **SERVICE RESPONSE** using Multipurpose Electronic Card (MEC) through Public Kiosk (i.e. Public Cloud).

3.2 Conceptual Diagram

Figure 2 shows the conceptual diagram of our proposed Healthcare Integrated Development Environment (HIDE), which is explained during Patient to Health care system (P2H) type of electronic transaction. Since we have already discussed the role of Government in Sect. 3.1 while explaining Fig. 1, in Sect. 3.2 we will only focus on our proposed Cloud Healthcare system, which is shown through Fig. 2.

1. Patient initiate electronic transaction using Multipurpose Electronic Card (MEC).
2. Patient transmit its unique parameters like Multipurpose Electronic Card (MEC) number, User id, Password, Phone number, etc and **SERVICE REQUEST** to Cloud Healthcare system through Public Kiosk (i.e. Public Cloud).
3. Cloud Healthcare Interface receives unique parameters and **SERVICE REQUEST** of Patient through Public Kiosk (i.e. Public Cloud). During this phase of operation, it also sends the **SERVICE REQUEST LOG** to Transaction Master, so that it can be finally matched with the services actually availed by Patient.
4. Cloud Healthcare system verifies the identity of Patient.
 - Scenario 1 (Verification Success): In this case **SERVICE REQUEST** is allowed to proceed further through Step-5.
 - Scenario 2 (Verification Failure): In this case **SERVICE REQUEST** is aborted and Patient is informed through System Timeout.
5. Router handles the large number of **SERVICE REQUEST** and channelizes it through Cloud Healthcare Server1 and Cloud Healthcare Server2. To keep our conceptual diagram simple we have shown only two server in Fig. 2, which may be increased depending on the load of **SERVICE REQUEST**. As a future scope of research, during this phase of operation the concept of Distributed Database Management System and Block Chain may be used to gain trust of end user.

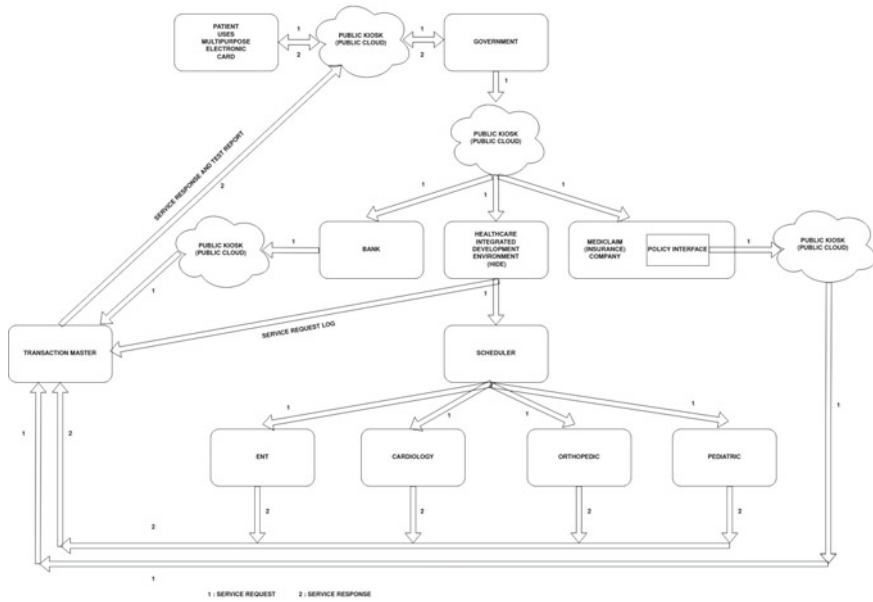


Fig. 1 Block diagram of healthcare integrated development environment

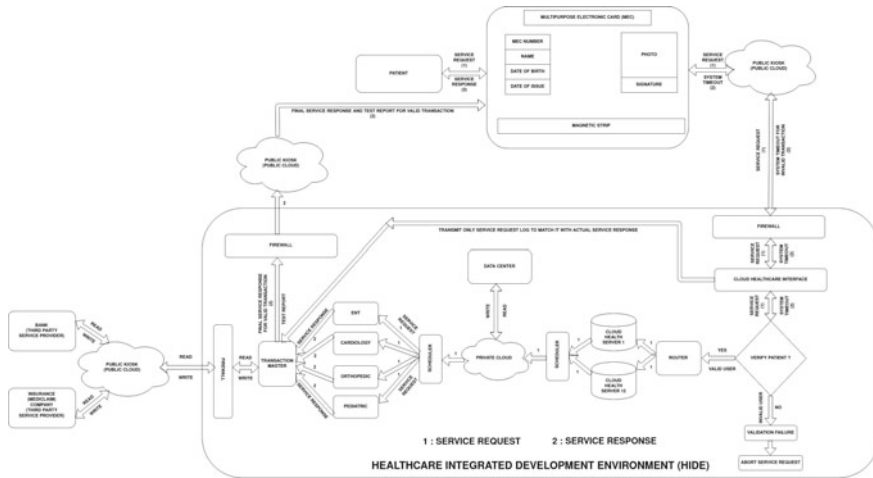


Fig. 2 Conceptual diagram of healthcare integrated development environment

6. Scheduler receives **SERVICE REQUEST** from Cloud Health Server1 and Cloud Health Server2 and creates a proper list based on First In First Out basis and send it towards Private Cloud to perform necessary **READ** and **WRITE** operation over the Data Center attached to it.
7. Scheduler on the other side of Private Cloud receives the **SERVICE REQUEST** in sequential manner and transmit it to respective medical unit (as desired by the Patient) for final execution of **SERVICE REQUEST**. These medical units like ENT, Cardiology, Orthopedic, Pediatric, etc generates **SERVICE RESPONSE** which are recorded and matched at Transaction Master. As Patient have to pay for the medical facilities, Transaction Master also interacts with Third Party Service Providers like Medicaid Company and Bank through Public Kiosk (i.e. Public Cloud). The Third Party Service Providers responds to Transaction Master through **READ** and **WRITE** operations for payment of medical expenses.
8. After payment of all medical facilities availed by Patient, **FINAL SERVICE RESPONSE** and Test Report are send to Patient Public Kiosk (i.e. Public Cloud).
9. At the last phase of operation, Patient receives those **FINAL SERVICE RESPONSE** which includes Medical Bill Payment Receipt, Test Report, etc using its Multipurpose Electronic Card (MEC).

3.3 Primary Components

The Primary Components of proposed Healthcare Integrated Development Environment (HIDE) shown through Figs. 1 and 2 are explained below:

1. Public Kiosk: It performs electronic communication within our proposed Healthcare system.
2. Patient: It denotes the **SERVICE SEEKER**.
3. Healthcare Integrated Development Environment (HIDE): It denotes the proposed cloud healthcare system.
4. Scheduler: It helps to maintain a proper queue of **SERVICE REQUEST**.
5. Transaction Master: It denotes the overall Service Controller of our proposed system which performs the following operations:
 - (a) Maintains a log of **SERVICE REQUEST**, so that it can be finally matched with the list of medical services actually availed by Patient.
 - (b) It interacts with Medicaid company (precisely, with its Policy Interface component) and Bank through Public Kiosk (i.e. Public Cloud) for payment of medical expenses of Patient.
6. The following medical units actually generates **SERVICE RESPONSE** corresponding to its **SERVICE REQUEST** of Patient.
 - a. ENT. b. Cardiology. c. Orthopedic. d. Pediatric.
7. Bank: It denotes Third Party Service Provider for payment of medical expenses of Patient. It receives total Policy Claim Statement and Medical Bill of Patient from

Mediclaime company and makes payment after performing proper verification of its Client (i.e. Patient).

8. Insurance (i.e. Mediclaime) Company: It is Third Party Service Provider which coordinates with Bank for payment of medical expenses of Patient. Mediclaime company generates the Policy Claim Statement (for which a Patient is entitled to get the total health coverage) and its actual Medical Bill and send to Bank through Public Kiosk (i.e. Public Cloud). Transaction Master coordinates the entire operation and generates **FINAL SERVICE RESPONSE** and Test Report to Patient after successful payment of all medical expenses.

In Sect. 4 we have further explained the static structure of our proposed model using Class Diagram.

4 Static Structure of Proposed Model

Class Diagram of primary components of our proposed model like Public Kiosk, Patient, HIDE, Mediclaime company, Policy Interface are shown through Figs. 3, 4, 5, 6 and 7 respectively. The attribute names of these classes are self explanatory in nature.

Figure 3 shows the following essential components of PUBLIC_KIOSK class: KIOSK_ID, OTP, KIOSK_ADDRESS, FLAG, SERVICE_REQUEST, SERVICE_RESPONSE, BIOMETRIC.

Figure 4 shows the following essential components of PATIENT class: MECNO, USERNAME, PASSWORD, DOB, AGE, ADDRESS, PHONE, SERVICE_REQUEST, SERVICE_RESPONSE, BIOMETRIC.

Figure 5 shows the following essential components of CLOUD_HIDE class: SERVERIP, SERVERDNS, VIRTUAL_MACHINE, SERVICE_REQUEST, SERVICE_RESPONSE.

Figure 6 shows the following essential components of MEDICLAIM_COMPANY class:

CLAIM_CITIZEN_MEC_NO, STATUS_POLICY, AMOUNT.

Figure 7 shows the following essential components of POLICY_INTERFACE class: CLAIM_CITIZEN_MEC_NO, COVERAGE, STATUS_POLICY.

Our proposed model will provide healthcare facilities to Citizen using these classes stated in this paper. However, the detailed Object Oriented Modelling (OOM) of this Cloud based Healthcare Integrated Development Environment (HIDE) may be considered as future scope of this work.

Fig. 3 Class diagram of public Kiosk

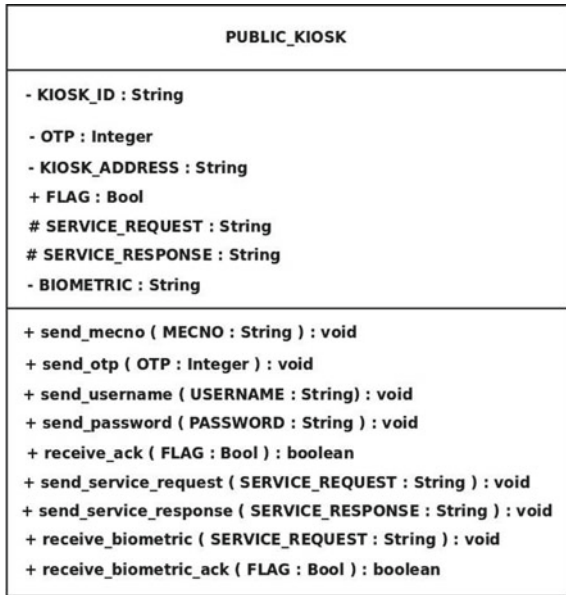
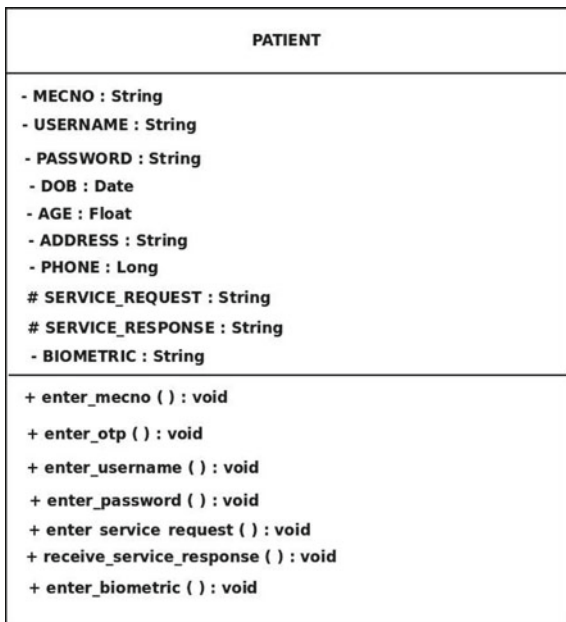


Fig. 4 Class diagram of patient



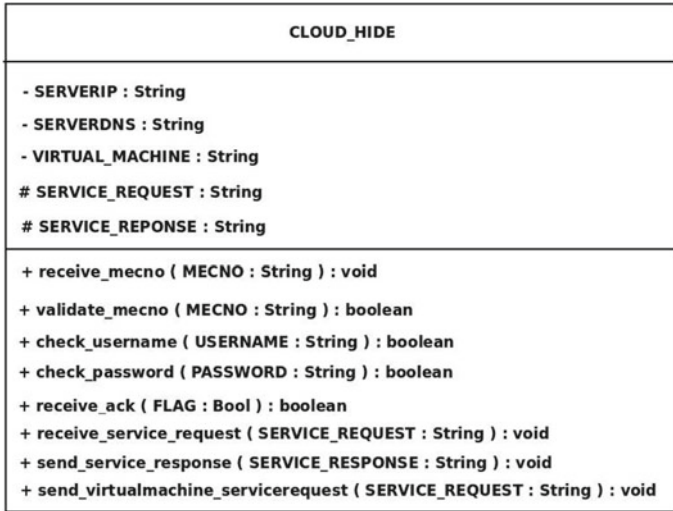


Fig. 5 Class diagram of proposed cloud healthcare system

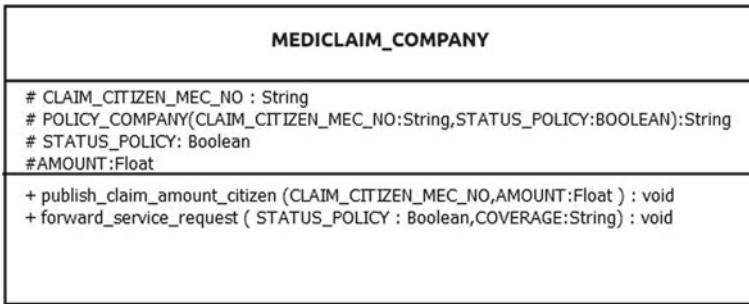


Fig. 6 Class diagram of mediclaim company

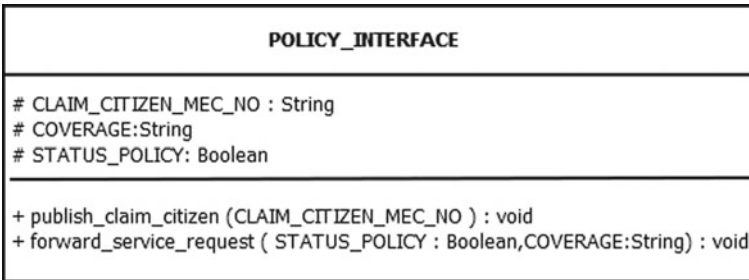


Fig. 7 Class diagram for policy interface of mediclaim company

5 Conclusion

In this paper we have proposed a Cloud based Healthcare Integrated Development Environment (HIDE), which will deliver healthcare facilities to its users (i.e. Patients) through a Citizen centric single window interface namely Multipurpose Electronic Card (MEC). Application of this single window interface will help Patient (i.e. Citizen) to avail healthcare facilities in a more integrated manner. In this paper we have shown Block Diagram, Conceptual Diagram and Class Diagram of our proposed model and have focused mainly on **SERVICE REQUEST** and **SERVICE RESPONSE** and its corresponding **MEDICLAIM PROCESSING** for payment of medical expenses of Patient with engagement of multiple third party players like Mediclaim company and Bank. The number of medical units (i.e. ENT, Cardiology, Orthopedic and Pediatric) shown in this paper will be enhanced in our future work. Furthermore, the concept of distributed database management and Block Chains may be applied within our proposed healthcare system to establish its data security and integrity so as to gain trust of its end user (i.e. Patient).

References

1. Mohapatra S, Paul K, Roy A (2021) Object-oriented modeling of cloud healthcare system through connected environment. In: Mandal, JK, Mukhopadhyay S, Roy A (eds) Applications of internet of things (2021), Proceedings of ICCCIOT 2020. Springer, Singapore, pp 151–164. https://doi.org/10.1007/978-981-15-6198-6_14. ISBN: 978-981-15-6198-6
2. Roy A (2020) Object-oriented modeling of multifaceted service delivery system using connected governance. In: Jena A, Das H, Mohapatra D (eds) Automated software testing. ICDCIT 2019. Services and business process reengineering. Springer, Singapore, pp 1–25. <https://doi.org/10.1007/978-981-15-2455-4-1>
3. Roy A (2019) Smart delivery of multifaceted services through connected governance. In: 3rd international conference on computing methodologies and communication (ICCMC). IEEE, India, pp 476–482. <https://doi.org/10.1109/ICCMC.2019.8819851>
4. Biswas S, Roy A (2019) An intrusion detection system based secured electronic service delivery model. In: 2019 3rd international conference on electronics, communication and aerospace technology (ICECA), Coimbatore, India, pp 1316–1321. <https://doi.org/10.1109/ICECA.2019.8822016>
5. Biswas A, Roy A (2019) A study on dynamic ID based user authentication system using smart card: Asian J Convergence Technology (AJCT) 5(2) ISSN 2350–1146. Retrieved on 08 Mar 2020 <http://www.asianssr.org/index.php/ajct/article/view/871>
6. Khatun R, Bandopadhyay T, Roy A (2017) Data modeling for E-voting system using smart card based E-governance system. Int J Inform Eng Electron Bus (IJIEEB) 9(2):45–52. <https://doi.org/10.5815/ijieeb.2017.02.06>
7. Hossain MS, Muhammad G, Alamri A (2019) Smart healthcare monitoring: a voice pathology detection paradigm for smart cities. Multimedia Syst 25(5):565–575. <https://doi.org/10.1007/s00530-017-0561-x>
8. Abdullah A, Md ZA, Anirban B, Shinsaku K, Mohammad SR (2019) Privacy-friendly platform for healthcare data in cloud based on blockchain environment. Future Generat Comput Syst 95:511–521. <https://doi.org/10.1016/j.future.2018.12.044>
9. Abomhara M, Lazrag MB (2016) UML/OCL-based modeling of work-based access control policies for collaborative healthcare systems. In: 2016 IEEE 18th international conference on

- e-health networking, applications and services (Healthcom). IEEE, Germany, pp 1–6. <https://doi.org/10.1109/HealthCom.2016.7749461>
10. Yassine A, Singh S, Hossain MS, Muhammad G (2019) IoT big data analytics for smart homes with fog and cloud computing. *Future Generat Comput Syst* 91:563–573. <https://doi.org/10.1016/j.future.2018.08.040>
 11. Meri A, Hasan MK, Danaee M, Jaber M, Safei N, Dauwed M, Abd SK, Mohammed A (2019) Modelling the utilization of cloud health information systems in the Iraqi public healthcare sector. *Telemat Inform* 36:132–146. <https://doi.org/10.1016/j.tele.2018.12.001>
 12. Chen M, Ma Y, Li Y, Wu D, Zhang Y, Youn CH (2017) Wearable 2.0: enabling human-cloud integration in next generation healthcare systems. *IEEE Commun Magaz* 55(1):54–61
 13. Mohit P, Amin R, Karati A, Biswas GP, Khan MK (2017) A standard mutual authentication protocol for cloud computing based health care system. *J Med Syst* 41(4). <https://doi.org/10.1007/s10916-017-0699-2>
 14. Tyagi S, Agarwal A, Maheshwari P (2016) A conceptual framework for IoT-based healthcare system using cloud computing. In: 2016 6th international conference-cloud system and big data engineering (Confluence). IEEE, India, pp 503–507. <https://doi.org/10.1109/CONFLUENCE.2016.7508172>
 15. Yang JJ, Li JQ, Niu Y (2015) A hybrid solution for privacy preserving medical data sharing in the cloud environment. *Future Generat Comput Syst* 43–44:74–86. <https://doi.org/10.1016/j.future.2014.06.004>
 16. Deng M, Petkovic M, Nalin M, Baroni I (2011) A home healthcare system in the cloud—addressing security and privacy challenges. In: 2011 IEEE 4th international conference on cloud computing. IEEE, USA, pp 549–556. <https://doi.org/10.1109/CLOUD.2011.108>

Designing and Implementing Cloud Security Using Multi-layer DNA Cryptography in Python



Md. Irfan Alam and Satya Narayan Singh

Abstract Cloud computing is the latest technology. Provides various on-demand services and online for network services, platform services, data storage, etc. Many organizations are not thrilled with using cloud services due to data security concerns, as the data resides on the cloud service provider's servers. To address this problem, various researchers around the world have applied various approaches to strengthen the security of data stored in cloud computing. The latest development in the field of cryptography is DNA encryption. It arose after the disclosure of the computational ability of deoxyribonucleic acid (DNA). DNA encryption uses DNA as a computational tool along with various molecular techniques to manipulate it. Due to the large storage capacity of DNA, this field is becoming very promising. This paper used a layered DNA encryption method for the data encryption and decryption process. Using the four DNA bases (A, C, G, T), we generate dynamic DNA tables to replace the message characters with a dynamic DNA sequence. The implementation of the proposed approach is performed in Python and the experimental results are verified. The resulting encrypted text contains information that will provide greater security against intruder attacks.

Keywords Cloud computing · Cloud security · DNA computing · DNA sequencing · Encryption · Decryption · Cryptography techniques

Md. Irfan Alam (✉)
Jharkhand Rai University, Ranchi, Jharkhand, India
e-mail: irfan.alam1@gmail.com

S. N. Singh
Department of IT, Xavier Institute of Social Service, Ranchi, Jharkhand, India
e-mail: snsinghxiss@rediffmail.com

1 Introduction

Cloud computing is the field of computing in which an organization or individual stores data such as text, images, or video on remotely hosted servers, rather than keeping it all on their local storage machine or computer. The concept of cloud computing has existed since the late 1970s in the form of distributed computing, but was popularized by Amazon.com in 2006. Today, cloud technology is one of the most widely used computing technologies.

1.1 Motivation

Cloud storage service offers tremendous benefits to customers. Despite these benefits, the concern over security and privacy associated with cloud model seems to be the biggest hurdle in adopting cloud by many individuals and organizations. First problem is, since the data resides on third party's premises, data owners lose control over their outsourced data. Second problem is data owners need to take high risk in trusting cloud service provider on all circumstances. Finally, the multi-tenancy nature of cloud brings in several malicious internal and external attacks. Lack of data security in cloud environment poses major challenges to data owners. The motivation of this research work is to seek cloud data security concerns and proposes secure and efficient protocols for multilevel security in cloud environment to preserve confidentiality, authorized access to stored data, authenticity, and integrity of data from the perspective of data owners.

1.2 Contributions of the Paper

The main contribution of this paper is to design and implement multi-layer DNA cryptography security system for the data outsourced to cloud data storage that preserves data confidentiality, authenticity, and integrity from the perspective of data owners. The main objective of this research work is to provide model for data protection. This model is designed in such a way to resist vulnerabilities and threats that jeopardize the data being transferred through an open communication medium. This could be possible with the strong cryptographic schemes with strong key generation mechanism.

1.3 Fundamental Concepts of Clouds

According to NIST, there are five core concepts in the cloud [1, 2] such as cloud functionality, service models, hosting, deployment models, and roles which are elaborated broadly as follows:

1.3.1 Cloud Features

The cloud contains five main features as follows:

- (i) **Services on demand:** No human interaction with the resource provider is required for the provision of IT services such as storage, server time.
- (ii) **Access to the ubiquitous network:** IT services are available on the network and can be accessed with the aid of standard methods using heterogeneous consumer platforms (e.g., mobile phones, laptops).
- (iii) **Location independent resource pool (multi-tenant):** Resources are collected to serve multiple customers with the help of the multi-tenant paradigm where resources are dynamically allocated and reallocated on demand. Customers have no idea where the services are.
- (iv) **Quick elasticity:** Resources are supplied quickly with good enough elasticity and similarly released to scale.
- (v) **Measured services:** The use of resources is controlled by providing a measurement capability. Customers pay the bill based on the measured usage of the resources provided for a specific session.

1.3.2 Service Models

Cloud service models can be grouped into three classifications as follows:

- i. **SAAS:** Software-as-a-Service is a product conveyance model in which applications are facilitated by a supplier or specialist co-op and made accessible to clients over an organization, and as a rule, the Internet. SaaS is additionally regularly connected with a pay-more only as costs arise membership authorizing model.
- ii. **PAAS:** Platform-as-a-Service (PaaS) is a lot of improvement devices and programming facilitated on the supplier's workers. It is a layer on head of IaaS in the stack and edited compositions everything down to the working framework. This offers an incorporated arrangement of advancement condition that a designer can use to manufacture their own applications without understanding what is happening under the administration.

- iii. IAAS: Model that incorporates its arrangement administrations, for example, stockpiling, network limit, preparing components to permit clients to run their applications [3].

1.3.3 Deployment Model

Cloud can be conveyed in four models:

- i. Private cloud: These are executed distinctly inside an endeavor or association. Venture or outsider claims it. Private mists are worked inside an endeavor firewalls and on location worker run them. They offer types of assistance, for example, virtualization, multi-occupancy, consistent arrangement, security, and access control [4].
- ii. Public cloud: Public cloud portrays distributed computing in the customary standard sense, whereby assets are powerfully provisioned on a fine-grained, self-administration premise over the Internet, by means of Web applications/Web administrations, from an off-Webpage outsider supplier who shares assets and bills on a fine-grained utility figuring premise. It is ordinarily founded on a compensation for each utilization model, like a prepaid power metering framework which is adaptable enough to cook for spikes popular for cloud advancement [5]. Public mists are less secure than the other cloud models since it puts an extra weight of guaranteeing all applications and information got to on the public cloud.
- iii. Hybrid cloud: It is a collection of private, public, and network mists. Public and private mists both are worked by cross-breed cloud at the same time. Half breed cloud is a private cloud connected to at least one outside cloud administrations, midway oversaw, provisioned as a solitary unit, and delineated by a safe organization [6].
- iv. Community cloud: A mutual foundation is characterized in this sort of cloud and a few associations uphold it.

1.4 Cryptography

Cryptography is the study of techniques or methodology to encode the plain text into ciphered text and vice versa. Cryptography consists of basically two complementary sub-techniques:

- (1) Encryption
- (2) Decryption.

Encryption is the technique to convert a plain text (understandable form) into ciphered/encrypted text (not understandable form). This process is known as ciphering or encrypting. Decryption is the technique to convert the ciphered/encrypted text (not understandable form) to plain text (understandable

form). This process is also known as deciphering or decrypting. Implementing cryptography makes the medium of communication secure and thus channel becomes a more reliable medium to send some secret data.

Cryptography can be broadly divided into two categories:

- (i) Symmetric cryptography
- (ii) Asymmetric cryptography [5].

Symmetric cryptography consists of same secret key at side, sender and receiver. This means that in symmetric cryptography, the Encryption Key and Decryption Key are same. Asymmetric cryptography uses two types of secret keys:

- i. Private key
- ii. Public key.

Cryptography is time taking and requires intensively complex processing but yet maintaining the security as maximum as possible. To make DNA-based cryptography, a more reliable but yet a fast medium to implement security we will use the symmetric cryptography technique. To increase security further, we will use various existing cloud-based system security techniques. There are various cryptography implementing techniques but the core thing among all is that the degree of uncertainty and randomness in the process of generation of secret key. Higher the degree of uncertainty and randomness, the more secure and stable medium we have but eventually increasing the processing requirement.

1.5 DNA Structure

DNA stands for deoxyribonucleic acid. DNA is molecule that is made up of two components. First, it has four types of bases that are Thymine (T), Guanine (G), Cytosine (C), and Adenine (A). Second, DNA contains sugar phosphate which makes its backbone as shown in Fig. 1. DNA bases are also known as nucleotides. DNA consists of two biopolymer strands and forms a double helix structure that is described in Fig. Between strands, lie base pairs that are bonded together with strong hydrogen bonding. This pair exists only in certain manner such that “Adenine (A) can only make Hydrogen Bond (double bond) with Thymine (T)” and “Cytosine (C) can only make Hydrogen Bond (triple bond) with Guanine (G)”. The sequence of these base pair defines the rules for formation of cell, eventually whole body of an organism. DNA is found in every cell of every living being. Basically, it is found in every nucleus of the cell and also in mitochondria. It is a biological storage device that stores all the genetic information and instructions which helps in formation of cells. DNA molecule has two chemical polarities that are 5' and 3' at top and bottom as described in Fig. 1. These two polarities enable DNA to bind together and transform itself into a double strand helix structure from single strand structure. DNA molecule

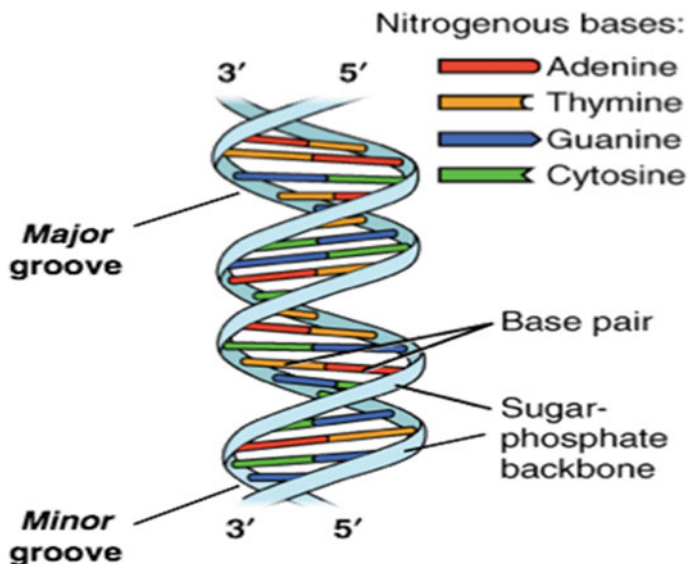


Fig. 1 DNA double helix (<https://openstax.org/books/concepts-biology/pages/9-1-the-structure-of-dna>)

is responsible for transmitting messages among the cells. DNA uses proteins to interact with its environment. DNA uses messenger ribonucleic acid (mRNA) to send information. There are two processes that are involved in transmitting a message: (i) Transcription (ii) Translation. In transcription, DNA passes the information to the mRNA. In translation, mRNA uses the information to interact with proteins and passes on the desired message. DNA has the phenomenal biological property where it replicates without losing the original DNA.

1.5.1 DNA Computing and DNA Cryptography

DNA computing is the field of computing bringing together the computer science, Biological Science and Molecular Science to understand and solve some primary NP problem [6, 7]. Earlier, it was introduced by Leonard Max Adleman but now it has evolved as one of the most fascinating platform to develop something new by teachings of Mother Nature. DNA computing is the best example of biomolecular computing. Biomolecular computers are those computers where all the computing components are made up of molecular compounds, i.e., all Input/Output and Software/Hardware are all in form of a molecular compound. DNA computing involves various steps such as melting, annealing, merging, amplification, and selection. DNA actually behaves like a Turing machine that is why it can be used as a data storage

device. Adleman has showed that DNA computing can be used as an effective tool to solve the NP problems like Hamiltonian graph problem or travelling salesman problem (TSP) [9]. He showed that DNA computing can be used to solve complex combinatorial problems like TSP and finite state problem. Here, the basic idea is that all the operations are performed over DNA (more precisely using DNA Bases or Nucleotide) not in DNA. DNA computing can be classified as intermolecular DNA computing, intramolecular DNA computing and supramolecular DNA computing. DNA Computers form a self-replicating system. DNA cryptography uses DNA nucleotides only to generate a set of symmetric cryptographic key. For, DNA cryptography, many techniques has already been established in many researches [8, 9] but here, I aimed to develop a technique to make the existing cloud-based data storage security systems more accurate and giving the encrypting and decrypting capability directly to the authorized client on its own machine. In this technique, first, we have to define three types of information. First of all, we need certain standard library named as DNA reference sequence that includes the 4-bit base sequence uniquely defined for all 256 ASCII characters in random order as shown in Table 1. This DNA reference sequence encodes the plain text message into DNA bases sequence text. Second table will replace the existing genome DNA base sequence to other DNA base sequence. Third component we need is the base-binary library that store the information about the equivalent conversion of DNA base sequence message to a long binary string, i.e., Table 3. This base-binary library is also not standardized as it can be defined by the user itself (Table 2).

2 Proposed Algorithm

Aim of this proposed algorithm is to provided client end cryptography using DNA computing which when.

integrated with existing cloud system storage server security methods can increase reliability and secrecy of the data. Important feature of this algorithm is that the data getting stored or data under transmission if even get.

hacked or intruded, that data will be of no use for the middle man even to that data administrator of the cloud storage facility.

Table 1 DNA reference sequence

TTTT	NUL	TTTC	Space	TTTG	@	TTTA	`	TTCT	Ç	TTCC	á
TTCG	L	TTCA	Ó	AAAG	■	AAAA	nbsp				
TTGT	SOH	TTGC	!	TTGG	A	TTGA	a	TTAT	ü	TTAC	í
TTAG	⊥	TTAA	β	TCTT	STX	TCTC	"	TCTG	B	TCTA	b
TCCT	é	TCCC	ó	TCCG	⊥	TCCA	Ô	TCGT	ETX	TCCG	#
TCCG	C	TCGA	c	TCAT	â	TCAC	ú	TCAG	⊥	TCAA	Ò
TGTT	EOT	TGTC	\$	TGTG	D	TGTA	DEL	TGTT	ä	TGCC	ñ
TGCG	—	TGCA	ö	TGGT	ENQ	TGGC	%	TGGG	E	TGGA	e
TGAT	à	TGAC	Ñ	TGAG	†	TGAA	Õ	TATT	ACK	TATC	&
TATG	F	TATA	f	TACT	â	TACC	ª	TACG	ã	TACA	μ
TAGT	BEL	TAGC	'	TAGG	G	TAGA	g	TAAT	ç	TAAC	°
TAAG	Ã	TAAA	þ	CTTT	BS	CTTC	(CTTG	H	CTTA	h
CTCT	ê	CTCC	ì	CTCG	⊥	CTCA	þ	CTGT	TAB	CTGC)
CTGG	I	CTGA	i	CTAT	ë	CTAC	®	CTAG	⊥	CTAA	Ú
CCTT	LF	CCTC	*	CCTG	J	CCTA	j	CCCT	è	CCCC	¬
CCCG	⊥	CCCA	Û	CCGT	VT	CCGC	+	CCGG	K	CCGA	k
CCAT	ı	CCAC	½	CCAG	⊥	CCAA	Ù	CGTT	FF	CGTC	,
CGTG	L	CGTA	l	CGCT	î	CGCC	¼	CGCG	⊥	CGCA	ý
CGGT	CR	CGGC	-	CGGG	M	CGGA	m	CGAT	i	CGAC	i
CGAG	=	CGAA	Ý	CATT	SO	CATC	.	CATG	N	CATA	n
CACT	Ä	CACC	«	CACG	⊥	CACA	—	CAGT	SI	CAGC	/
CAGG	O	CAGA	o	CAAT	Å	CAAC	»	CAAG	α	CAAA	'
GTTT	DLE	GTTC	0	GTTG	P	GTTA	p	GTCT	É	GTCC	⊥
GTCG	ð	GTCA		GTGT	DC1	GTGC	l	GTGG	Q	GTGA	q
GTAT	æ	GTAC	⊥	GTAG	Ð	GTAA	±	GCTT	DC2	GCTC	2
GCTG	R	GCTA	r	GCCT	Æ	GCCC	⊥	GCCG	Ê	GCCA	—
GCGT	DC3	GCGC	3	GCGG	S	GCGA	s	GCAT	ô	GCAC	
GCAG	Ë	GCAA	¾	GGTT	DC4	GGTC	4	GGTG	T	GGTA	t
GGCT	ö	GGCC	⊥	GGCG	È	GGCA	¶	GGGT	NAK	GGGC	5
GGGG	U	GGGA	u	GGAT	ò	GGAC	Á	GGAG	ı	GGAA	§
GATT	SYN	GATC	6	GATG	V	GATA	v	GACT	û	GACC	Å
GACG	Í	GACA	÷	GAGT	ETB	GAGC	7	GAGG	W	GAGA	w
GAAT	ù	GAAC	À	GAAG	Î	GAAA	,	ATTT	CAN	ATTC	8
ATTG	X	ATTA	x	ATCT	ÿ	ATCC	©	ATCG	Ï	ATCA	°
ATGT	EM	ATGC	9	ATGG	Y	ATGA	y	ATAT	Ï	ATAC	⊥
ATAG	⊥	ATAA	~	ACTT	SUB	ACTC	:	ACTG	Z	ACTA	z
ACCT	Û	ACCC		ACCG	Γ	ACCA	.	ACGT	ESC	ACGC	;
ACGG	[ACGA	{	ACAT	ø	ACAC	⊥	ACAG	■	ACAA	'
AGTT	FS	AGTC	<	AGTG	\	AGTA		AGCT	£	AGCC	⊥
AGCG	■	AGCA	³	AGGT	GS	AGGC	=	AGGG]	AGGA	}
AGAT	Ø	AGAC	¢	AGAG	‡	AGAA	²	AATT	RS	AATC	>
AATG	^	AATA	~	AACT	×	AACC	¥	AACG	İ	AACA	■
AAGT	US	AAGC	?	AAGG	_	AAGA	DEL	AAAT	f	AAAC	⊥

Table 2 DNA base to other DNA base sequence

DNA code	Corresponding DNA
A	T
T	G
G	C
C	A

Table 3 DNA base to binary library

DNA code	Binary value
A	00
T	01
G	10
C	11

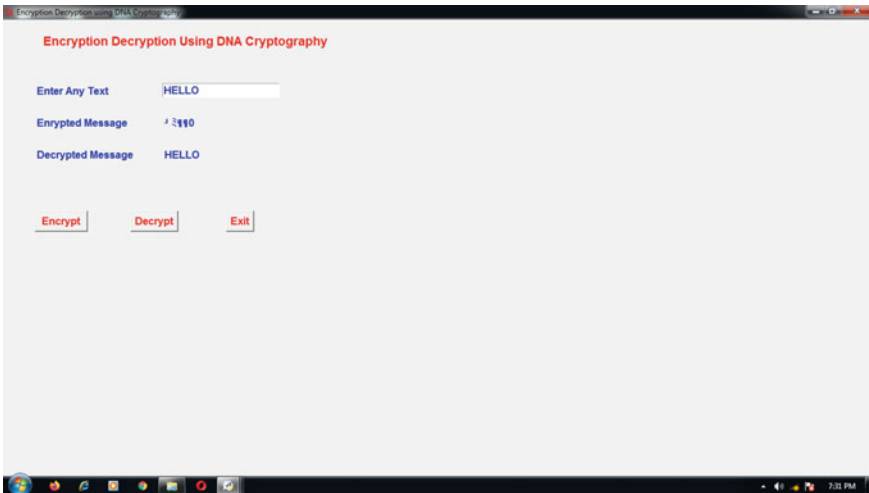
A. ENCRYPTION:

- Step1: Let Message be: M = "A"
- Step 2: M can be encode as follows Using Table 1 as follows:
M1 = "TTGG".
- Step 3: Message M1 can be encoded using Table 2 as follows:
M2 = "GGCC".
- Step 4: Using Base-Binary Library Message M2 can be encoded as follows using Table 3:
M3 = 10101111.
- Step 5: A Random number is generated, this random number is XORED with the message M3
Let the random number generated=5
M4=10101111 XOR 00000101=10101010
- Step 6: Converting Binary String M4 into equivalent Decimal Value.
M5 = 170.
- Step 7: Convert message M5 to its equivalent ASCII character
M6=ASCII character of (M5)
Send this data, M6 to the Cloud Server.
- Step 8: Generate the decryption key as:
[Corresponding DNA Base Value for A][Base-Binary for A][Corresponding DNA Base Value for C][Base-Binary for C][Corresponding DNA Base Value for G][Base-Binary for G][Corresponding DNA Base Value for T][Base-Binary for T][Random Number]
Example: Decryption Key: - "T00A11C10G0100000101".

B. DECRYPTION:

- Step1: Download the file from the Cloud Server i.e. M6
- Step 2: Retrieve the decryption key i.e. Decryption Key: - "T00A11C10G01".
- Step 3: Convert the ASCII character of message to equivalent decimal number, thus we get message M5. M5=170
- Step 4: Convert the decimal of message M5 to its binary equivalent .message M4 obtained M4=10101010
- Step 5: XORED the message M4 with random number, message M3 obtained M3=10101111
- Step 6: Convert the binary to its equivalent DNA base M2=GGCC
- Step 7: Convert the message M2 to its corresponding DNA base M1=TTGG
- Step 8: Convert the message M1 to its equivalent character M=A

3 Implementation of Above Algorithm in Python



4 End and Future Work

In this paper, a DNA-based multi-layer encryption technique is proposed for storing data in the cloud mainly in the public cloud and for SaaS users where security is a major concern. The technique will provide improved security as it includes the

computational complexity by using biocomputing techniques in addition to cryptography. User can check the integrity of the data without relying on the third party. The proposed DNA cryptography is a novel encryption technique for secure storage of data in the cloud environment, using DNA cryptography for cloud has great scope considering the importance of cloud storage in the industries and day-to-day life. Everywhere data is bombarding in the form of video, image, and other digital forms. So, a platform for storage is very important and DNA encryption is a trending new concept which will dominate the security world in the future. The proposed DNA cryptographic method utilizing dynamic character-DNA succession table, DNA base to its equivalent DNA base table and DNA base-binary table to builds the degree of information security. The above algorithm is implemented in Python. Many cryptanalyst has just said that the future of cryptography lies in the multidisciplinary studies of different aspects of science and Mathematics.

References

1. Global Netoptex Incorporated. Demystifying the cloud. Significant chances, pivotal choices. p 414. Available: <https://www.gni.com>. 13 Dec 2009
2. Brodtkin J (2008, June) Gartner: seven distributed computing security hazards. Infoworld, Available: <https://www.infoworld.com/d/security-focal/gartner-seven-loudcomputingsecurity-chances> 853? Page=0, 1 13 Mar 2009
3. Kuyoro SO, Ibikunle F, Awodele O (2011) Distributed computing security issues and challenges. Global J Comput Networks (IJCN) 3(5)
4. Mell P, Grance T (2011) The NIST definition of cloud computing. IT Laboratory NIST, Gaithersburg, MD, Tech. Rep. 800-145, pp 1–3
5. Pallavi N, Singh A, Dwivedi SP (2016) A DNA based secure data hiding technique for cloud computing. Int J Current Eng Technol 6(4)
6. Adleman L (1994) Sub-atomic calculation of arrangements of combinatorial issues. Science 266:1021–1024
7. Nimje AR (2012) Cryptography in cloud-security using DNA (genetic) techniques. Int J Eng Res Appl (IJERA) 2(5):1358–1359 ISSN: 2248-9622. www.ijera.com
8. Jain A, Rajpal N, Adaptive key length based encryption algorithm utilizing DNA approach. In: International conference on machine intelligence research and advancement
9. Rahman NHU, Balamurugan C, Mariappan R, A novel DNA computing based encryption and decryption algorithm. In: International conference on information and communication technologies

Intelligent Electronic Devices

Nanometer-Scale Photodetectors for High Performance and Unique Functionality



Hiroshi Inokawa, Hiroaki Satoh, Amit Banerjee, Anitharaj Nagarajan, Revathi Manivannan, Alka Singh, Tomoki Nishimura, and Koki Isogai

Abstract As opposed to the case with MOSFETs widely used in the very-large-scale integrated circuit, miniaturization of the photodetectors to the nanometer scale does not always lead the performance improvement mainly due to the reduced thickness and area for the light absorption. However, it is still possible to circumvent the drawback by introducing the optical antenna and to improve the performance by miniaturization. Moreover, the nanometer-scale photodetectors exhibits unique functionalities such as incident angle detection and biosensing. In this report, some examples found in the photodiode with SP antenna, MOSFET single-photon detector, SET-based ultrahigh-frequency rectifier, and terahertz bolometer are introduced.

Keywords Silicon on insulator (SOI) · Surface plasmon (SP) antenna · Single-photon detector · Single-electron transistor (SET) · Bolometer

1 Introduction

In the case of metal-oxide semiconductor field-effect transistors (MOSFETs) widely used in the very-large-scale integrated circuit (VLSI), miniaturization of the transistor guided by the scaling law [1] leads to multiple merits such as higher transistor density (lower cost per transistor), higher operation speed, and lower power consumption per transistor, which have rationalized the evolution of the VLSI technology and industry

H. Inokawa (✉) · H. Satoh
Research Institute of Electronics, Shizuoka University, Shizuoka, Japan
e-mail: inokawa.hiroshi@shizuoka.ac.jp

A. Banerjee
Department of Electrical and Computer Engineering, National University of Singapore, Singapore, Singapore

A. Nagarajan · R. Manivannan · A. Singh
Graduate School of Science and Technology, Shizuoka University, Shizuoka, Japan

T. Nishimura · K. Isogai
Graduate School of Integrated Science and Technology, Shizuoka University, Shizuoka, Japan

for more than 40 years based on the miniaturization, and now, the transistor size has reached nanometer range.

In the case of photodetectors, the miniaturization also leads to the performance improvement in some aspects. The photon detectors, such as pn-junction photodiode (PD), can operate faster due to the reduced capacitance or reduced carrier transit time, and show smaller dark current due to the small volume or surface area including generation centers. The thermal detectors, such as bolometer, can realize higher responsivity due to the reduced thermal conductance, faster response due to the reduced heat capacitance, and smaller power consumption if the bias current is required. The electronic receivers, which utilize transistor or diode to detect (demodulate) the signal from the antenna, can get the direct benefit from the miniaturization as the MOSFET does.

However, the miniaturized photodetectors suffer seriously from the reduced quantum efficiency (QE) due to the small thickness for light absorption, and the small light receiving area (cf. light cannot be focus on the area smaller than the wavelength). This drawback can be solved by the use of optical antenna that can concentrate the light energy into a small area or volume. The antenna not only increases the absorption efficiency, but also adds interesting features such as wavelength selectivity, direction detection, and biosensing via refractive index measurement.

In this report, such new opportunities and challenges in miniaturized photodetectors are discussed by showing silicon on insulator (SOI) PD with surface plasmon (SP) antenna, SOI MOSFET single-photon detector, ultrahigh-frequency single-electron transistor (SET) rectifier, and nanowire terahertz (THz) bolometer as examples.

2 SOI PD with SP Antenna

The SOI enables fabrication of silicon devices in a thin silicon (Si) layer on top of the insulator (SiO_2) and realizes high-performance VLSIs by improving electrostatics related to parasitic capacitances, short-channel effect, sharpness of turn-off characteristics, etc. However, thin Si is almost transparent (e.g., the light with a wavelength of 700 nm attenuates in 100-nm-thick Si only by 2%), and was not considered to be useful for photodetectors.

In order to address this issue, the SP antenna consisting of a gold (Au) line-and-space (L/S) grating is placed above the lateral pn-junction PD, which resonantly enhances the absorption at a specific wavelength set by the grating period p (e.g., absorption efficiency for $p = 300$ nm reaches 60% at the wavelength of 700 nm) [2].

This PD with SP antenna has wavelength and polarization selectivities and is useful in hyperspectral imaging, polarized imaging, polarization-based optical communications, etc. Since the L/S grating serves as an optical coupler between incoming light and laterally propagating light in the SOI slab waveguide, the phase matching condition between the diffracted light and the waveguiding modes depends sensitively on the light incident angle. The spatial pattern of QE in the polar coordinate of azimuth and elevation angles is precisely analyzed, and the PD is found to

surpass the conventional angle-sensitive pixel (ASP) in terms of angular resolution and QE [3, 4]. This will bring new opportunities in monocular three-dimensional (3D) imaging, lensless imaging, etc.

Since the phase matching condition is modulated by the refractive index (RI) of the medium around the SP antenna, the PD can also be used as a RI-based biosensor, in which the coupling between the analyte and the receptor at the sensor surface is detected as the change in the effective RI. We could successfully demonstrate that the detection limit was as small as 2.4×10^{-5} RI unit [5], which was comparable to that of conventional surface plasmon resonance (SPR) sensor. Note that the largest advantage of the proposed biosensor is that a large number of sensors can be integrated in a single chip, and thereby, the throughput of the analysis can be greatly enhanced.

3 SOI MOSFET Single-Photon Detector

As the size of the MOSFET is shrunk to tens of nanometers, the charge sensitivity becomes so high that a single charge (i.e., individual electron or hole) can be detected. When holes are generated in the body of n-channel SOI MOSFET by the incident photons, holes are stored below the negatively biased top gate, and the presence of the holes are detected as the discrete change of the electron current in the bottom channel induced by the positively biased bottom gate (substrate) [6]. This type of single-photon detector features low dark count ($\sim 0.01 \text{ s}^{-1}$) even at room temperature, low-voltage ($\sim 1 \text{ V}$) operation, and photon number resolution, which cannot be realized by the conventional single-photon detectors such as photomultiplier tube (PMT) and avalanche photodiode (APD).

The drawback of this nanometer-scale photodetector is the small QE due the small volume of Si for light absorption, which can be partially resolved by the use of the SP antenna [7]. Another issue is the complex output signal waveforms with rising and falling edges that correspond to hole generation by the photon incidence and spontaneous hole recombination, respectively, and current levels corresponding to number of stored holes include the memory of the previous hole generation and are not the same as the latest hole generation. In order to analyze the waveforms and find out the timing and number of generated holes in the latest photon incidence event, dedicated signal processing algorithm is developed and implemented to field programmable gate array (FPGA) to process the signal in real time [8]. The proper operation of the signal processor is successfully verified by the photon number statistics in a given observation time at various light intensities, which accurately follows the Poisson distribution.

4 Ultrahigh-Frequency SET Rectifier

The electronic receiver can get the direct benefit from the miniaturization of transistors and diodes for increasing the operation frequency. However, the maximum frequency of the conventional transistors is still around 1 THz or less, and further development is required to explore the photonic area. The ultimate miniaturization of transistor can be pursued by the SET, which consists of nanometer-scale island separated from the source and drain electrodes by tunneling barriers. The source, drain, and gate capacitances can be made in the order of attofarad (10^{-18} F), and the intrinsic cutoff frequency f_c set by the CR time constant well exceeds 1 THz. Moreover, we found experimentally that the rectification behavior can be observed when a RF signal is applied to the drain continued at frequency beyond the conventional f_c [9]. This could successfully verified by the simulation based on the time-dependent master equation [10]. It was found that although the charging state of the SET island cannot follow the rapid change of the RF signal above the f_c , the asymmetry in the tunneling probability with respect to the drain voltage still remains, and the rectification continues. This finding leads to the high-sensitivity SET-based photodetector for frequencies far beyond 1 THz.

5 Nanowire THz Bolometer

The bolometer is a kind of thermal detector, in which the temperature rise caused by the absorption of the incident light is detected by the thermometer. In the infrared (IR) region, absorber-type bolometers are widely used, but, for longer wavelength in the THz region, antenna-coupled bolometer is more viable, in which the light is received by the antenna, and the current from the antenna heats up the thermometer. Once the antenna is made separately, the performance of the heater-thermometer part can be improved by the miniaturization. By using the 100-nm-wide titanium (Ti) wire delineated by electron-beam lithography as a thermometer (temperature-dependent resistor), we could attain the responsivity R_v as high as 787 V/W, and the noise-equivalent power (NEP) as low as 185 pW/Hz^{1/2} [11]. A MOSFET can also be used as a thermometer, in which the temperature-dependent change of the threshold voltage is amplified by itself, and the MOSFET-based bolometer realizes the R_v of 1.64 kV/W and NEP of 170 pW/Hz^{1/2} although the degree of miniaturization is less, *i.e.*, the device was fabricated by the 600-nm technology [12]. Since the electrical resistance is correlated to the thermal resistance, the performance can further be improved by proper miniaturization of heater, which results in increased thermal resistance and larger temperature rise. This will pose a challenge in the design of high-impedance antenna that matches the high-resistance heater (load resistor) [13].

6 Summary and Conclusion

In this report, the impact of miniaturization on the photodetectors is discussed, and the opportunities found in different types of photodetectors, i.e., photon detectors, thermal detectors, and electronic receivers, are introduced. It is shown that the optical antenna is the key to solve the issue of the reduced QE and the light receiving area, to make the best use of the advantages attained by the miniaturization, and to realize new functionalities such as the incident angle detection and biosensing via RI measurement. Although the SP antenna is successful for the thin and large-area SOI photodiodes, further development of the antenna is anticipated for the SOI MOSFET single-photon detector and the THz bolometer to concentrate the incident light power into a small volume.

Acknowledgements This work was supported by Japan–India Science Cooperative Program between JSPS and DST (Grant No. JPJSBP120207708), JSPS KAKENHI (Grant No. 18K04261), the Cooperative Research Project of the Research Center for Biomedical Engineering with RIE, Shizuoka University, and the Cooperative Research Project Program of RIEC, Tohoku University. The authors are indebted to the Solid State Division of Hamamatsu Photonics K.K. for providing the SOI photodiodes and MOSFETs.

References

1. Dennard RH, Gaensslen FH, Yu H, Rideout VL, Bassous E, LeBlanc AR (1974) Design of ion-implanted MOSFET's with very small physical dimensions. *IEEE J Solid-State Circuits* 9(5):256–268
2. Satoh H, Ono A, Inokawa H (2013) Enhanced visible light sensitivity by gold line-and-space grating gate electrode in thin silicon-on-insulator p-n junction photodiode. *IEEE Trans Electron Devices* 60(2):812–818
3. Nagarajan A, Hara S, Satoh H, Panchanathan AP, Inokawa H (2020) Angular selectivity of SOI photodiode with surface plasmon antenna. *IEICE Electron Express* 17(13):20200187
4. Nagarajan A, Hara S, Satoh H, Panchanathan AP, Inokawa H (2020) Angle-sensitive detector based on silicon-on-insulator photodiode stacked with surface plasmon antenna. *Sensors* 20(19):5543
5. Satoh H, Isogai K, Inokawa H (2019) Optical response of SOI photodiode with gold line-and-space grating to biomolecular interactions. In: *Progress in electromagnetics research symposium (PIERS) abstracts*, p. 260 (Xiamen, China, Dec 17–20)
6. Du W, Inokawa H, Satoh H, Ono A (2011) SOI metal-oxide-semiconductor field-effect transistor photon detector based on single-hole counting. *Opt Lett* 36(15):2800–2802
7. Sharma Y, Satoh H, Inokawa H (2018) Application of bow-tie surface plasmon antenna to silicon on insulator nanowire photodiode for enhanced light absorption. *IEICE Electron Express* 15(11):20180328
8. Manivannan R, Satoh H, Inokawa H (2020) Photon-number statistics observed by SOI MOSFET single-photon detector with real-time signal processing. In: *IEEE silicon nanoelectronics workshop (SNW-20)* pp. 65–66 (Honolulu, HI, USA (Virtual), June 13–14)
9. Takahashi Y, Takenaka H, Uchida T, Arita M, Fujiwara A, Inokawa H (2013) High-speed operation of Si single-electron transistor. *ECS Trans* 58(9):73–80

10. Inokawa H, Nishimura T, Singh A, Satoh H, Takahashi Y (2018) Ultrahigh-frequency characteristics of single-electron transistor. In: IEEE international conference on electron devices and solid-state circuits (EDSSC'18) T1A01 (Marriott Hotel Golden Bay, Shenzhen, P.R. China, June 6–8)
11. Banerjee A, Satoh H, Elamaram D, Sharma Y, Hiromoto N, Inokawa H (2019) Performance improvement of on-chip integrable terahertz microbolometer arrays using nanoscale meander titanium thermistor. *J Appl Phys* 125(21):214502
12. Elamaram D, Suzuki Y, Satoh H, Banerjee A, Hiromoto N, Inokawa H (2020) Performance comparison of SOI-based temperature sensors for room-temperature terahertz antenna-coupled bolometers: MOSFET, PN junction diode and resistor. *Micromachines* 11(8):718
13. Inokawa H, Banerjee A, Elamaram D, Satoh H, Hiromoto N (2019) Impact of downscaling on terahertz antenna-coupled bolometers. In: 16th international conference on quality in research (QiR), paper ID: 75 (Padang, Indonesia, Jul. 22–24)

Design and Development of Terahertz Medical Screening Devices



M. P. Karthikeyan, Debabrata Samanta, Amit Banerjee, Arjya Roy,
and Hiroshi Inokawa

Abstract This paper highlights the prospect of design and development of a terahertz medical screening system, giving an overview of existing devices, systems, for THz spectroscopy and imaging of biological samples (e.g., cell, tissue imaging or screening). Considering the non-ionizing nature of THz waves along with its reasonable soft-tissue sensitivity, terahertz instrumentation has opened up possibilities for medical screening devices. Some THz imaging systems presently use raster scanning for calculation of image region of interest. Here, a particular system is proposed as a medical screening device and factors like signal-to-noise ratio, image resolution, image contrast, etc., have been described and correlated with relevant clinical results for exploring possible prospects in medical applications of terahertz waves.

Keywords Medical imaging · Thz spectroscopy · Medical screening devices

M. P. Karthikeyan

Department of Computer Science, PPG College of Arts and Science, Coimbatore, India

D. Samanta (✉)

Department of Computer Science, CHRIST (Deemed to be University), Bengaluru, India

e-mail: debabrata.samanta.369@gmail.com

A. Banerjee (✉)

Physics Department, Bidhan Chandra College, Asansol, India

e-mail: amitbanerjee.nus@gmail.com

A. Roy

Department of Biotechnology, Vellore Institute of Technology, Vellore, Tamil Nadu, India

H. Inokawa

Research Institute of Electronics, Shizuoka University, Hamamatsu, Japan

1 Introduction

Terahertz (THz) waves between microwaves and infrared frequency range in the electromagnetic spectrum roughly spread from 0.1 THz (wavelength $\lambda \sim 3000 \mu\text{m}$) to 10 THz (wavelength $\lambda \sim 30 \mu\text{m}$). We experience THz and microwave radiation from different galaxies, stars, and even every living organisms; however, they remain undetected due to the lack of efficient detection systems. One cannot go beyond 0.3 THz using electronic sources due to the inherent restriction in the fast electron oscillation time [1]. Also generation or detection of radiation below 10 THz using semiconductor materials is not possible considering the conventional band gaps of such materials are of the order of a few eV, whereas an order of magnitude higher than the energy-related to THz hole is only a few meV [2].

Figure 1 shows the THz frequency region in the electromagnetic spectrum. In the THz regime, energy level ($1 \text{ THz} \cong 4.1 \text{ meV}$) is much smaller than the quantized thermal unit of radiation kBT , which is the thermal energy at room temperature ($1 \text{ kBT} \cong 25 \text{ meV}$ at $T = 300 \text{ K}$), which makes it difficult to detect. THz field has been experiencing unprecedented growth in the last decade due to the invention of few interesting THz generators and THz detectors, which could be used in imaging applications also. In the 1990s and early 2000s, researchers were mainly interested in studying efficient ways to generate and detect THz radiation with sufficient energy, which includes the use of new types of photoconductive (PC) antennas, electro-optic materials, multi-ferroic materials, and intense fem to second lasers down to 15 fs and some essential spectroscopic study of polar liquids and thin films [3]. Recently, researchers keen on the application ranging from THz devices (e.g., THz polarizers and wave-plates, THz shielding, THz conductivity manipulation), THz giant-magneto resistance, materials and spintronics, ultrafast data storage, computer performing operations at the rates of teraflops, THz communication systems, gas sensing electronic devices on the picoseconds time scale to THz astronomy, THz applications in security, imaging, and healthcare, etc. Several research groups are also involved in studying exotic fundamental studies in the field of superconductor carrier dynamics, ultrafast demagnetization mechanisms, magnon propagation in anti-ferromagnets, phonon modes in

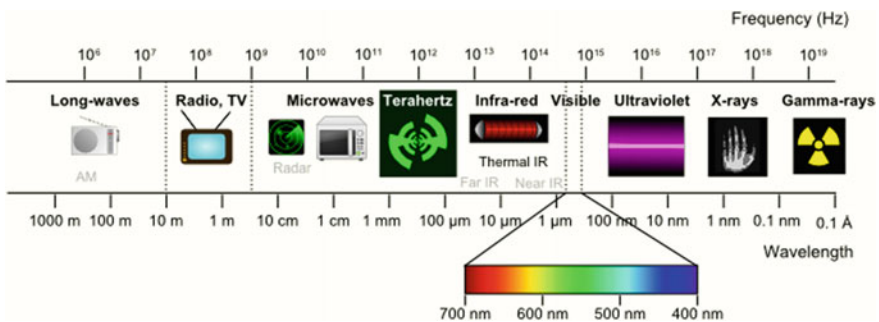
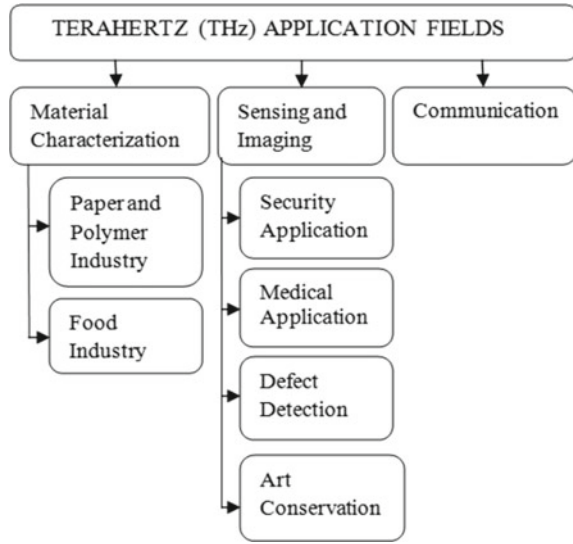


Fig. 1 THz frequency region in electromagnetic spectrum

Fig. 2 Potential THz application areas



nanostructures, understanding water dynamics, carrier relaxation mechanism in two-dimensional (2D) systems (like graphene, molybdenum sulfide, boron nitrate), etc. Figure 2 shows the application of the THz radiation to various fields.

Present report mainly focuses on the medical image processing of THz, and remainder of the paper is organized as follows: THz medical dataset prediction and its related work; discussion on the proposed strategy; proposed system and existing systems experimental results, the idea to extend and utilize on our on-chip integrable terahertz detector arrays for development of screening and diagnostic medical devices, and the concluding remarks and future scope of the work [4].

2 Terahertz in Biomedical Applications

Terahertz components such as antennas, frequency selective surface (FSS), and metamaterials are necessary to manipulate the incident THz signal for various applications that include sensing, filtration, THz detection, etc. Apart from traditional THz spectrum applications such as imaging and security, this band is widely accepted for future wireless communication. The necessity in high-speed and high data rate communication from the users would push the electromagnetic spectrum from the microwave region to the THz band. Current scientific research ranging from cancer detection, THz spectroscopy application in the biomedical field due to occurrence of collective and vibration modes of DNA molecules is proteins in this range. Considering THz radiations which are non-invasive and non-ionizing, it could be a good substitute for X-rays and for studying live cells. As mentioned earlier, the reflection of EM radiation affects the heterogeneous spontaneous system. THz even an added advantage

for medical imaging applications comparatively other infrared, ultrasonic's waves, etc. [5].

3 Terahertz Non-invasive Medical Systems and Devices

The following are the reasons for the movement toward THz band used to non-invasive medical systems and devices:

- Microwave region is almost completely occupied for various applications and offers low bandwidth.
- Diffraction in the THz signal is low compared to microwave and millimeter waves
- It provides a better line of sight (LOS) communication link.
- Even at THz, the metals can be assumed to a perfect conductor which is not the case with infrared frequency.
- The THz band provides secured communication particularly through the use of the spread spectrum technique.

Though the THz band offers many advantages, it has the main issue of high atmospheric attenuation. But, with advancements, researchers are focusing on developing highly directional and high gain antennas, which could compensate for atmospheric losses. Many techniques such as array configuration, photonic, and electromagnetic band gap structure antenna, multilayered substrate, and planar Yagi-Uda antenna have been developed and reported for improvement of the directivity characteristics [6].

4 Literature Review

A brief introduction to the terahertz radiation, characteristics, and applications in different fields with short survey of literature relating to the present work is also available with details of laser micromachining used for creating precise and tiny features on a variety of materials in making terahertz components such as metamaterials, frequency selective surface, and antenna [7]. However, it is important to cite, the THz field has evolved as a consequence of the invention of maser and laser in the year 1960s, which leads to the invention of various THz gas lasers (CO₂ pumped methanol laser at 2.5 THz, A. I. M. [7]). The photoconductive dipole antenna was used to generate far-infrared radiation in the year 1970 by D. H. Auston at Bell laboratories [8]. The first nonlinear THz generation and detection technique was initiated by the development of ultrafast laser amplifiers followed by the development of photoconductive switches, which is closely connected to the invention of Ti: sapphire laser in the year 1991 (Moulton 1986; Kafka et al. 1992). Faries et al. [8] demonstrated difference frequency generation (DFG) between the two ruby lasers, and then, the frequency range of 0.05–0.5 THz was achieved by DFG from a single laser pulse in

lithium niobate (LiNbO_3) [9]. THz generation and detection are being done with the help of photoconduction and optical rectification mechanism. Materials of a large variety have been used for these processes such as lithium niobate (LiNbO_3), gallium arsenide (GaAs), zinc telluride (ZnTe), and other organic crystals [10]. During the initial period in the development of THz radiation, it has found application in many fields [9]. The development of THz-TDS leads to the characterization of materials and extraction of the properties (refractive index, dielectric, conductivity, etc.), spectroscopy due to rotational and vibrational resonance of the molecules at the THz frequency range.

5 Medical Screening and Detection

Various advanced technologies have improved the application of microelectronic devices for medical applications, with further use of communication and information technology [10], however, requiring sophisticated instrumentations like photolithography and vacuum deposition technology at ultraclean rooms. Here, we studied a system with electro-optic crystals used to generate terahertz pulses through optical rectifications (OR) by using sub-picosecond laser pulses on medical sensors. The electric field of the terahertz pulses of electro-optic sampling is captured as an image [11]. The first molecule added to a completed layer will be held by only one bond, and this requires even higher energy. This process, which is known as 'surface nucleation', involves longer delay [12]. This necessitates the simultaneous arrival of a number of molecules on the surface, forming a sustainable nucleus. In this mechanism, the crystal grows by the spreading of layers of constant thickness across the face, and the thickness of the layers must be very small compared to the distance between the advancing fronts. This argument does not depend on the assumptions about the detailed mechanism in a certain medical image like Kung, brain, etc., by which units are added to the crystal [13]. Hence, Volmer suggested that the face-adsorbed molecules would be able to diffuse/migrate freely to a considerable distance before re-evaporating and thus overwhelmingly facilitate the rate of growth of crystal by the repeatable step mechanism. The above theory of sustained growth by the addition of repeatable steps, even when assisted by surface diffusion, cannot account for the observed rate of spreading of layers and less so for the rate of surface nucleation [14]. Have calculated the concentration of kinks in a step and rate of diffusion of molecules? Their theory requires a super saturation of at least 25–50% for an observable growth rate. The two-dimensional nucleation theories, though on a strong footing, could not account for these experimental observations, and this disparity was yet to be resolved (Fig. 3).

The proposed crystalline spectroscopy (THz signal)-based approach achieved the following objectives.

- Fruitful attempts have been made to synthesize the currently available materials by appropriate route and purified cancer image captured by recrystallization process.

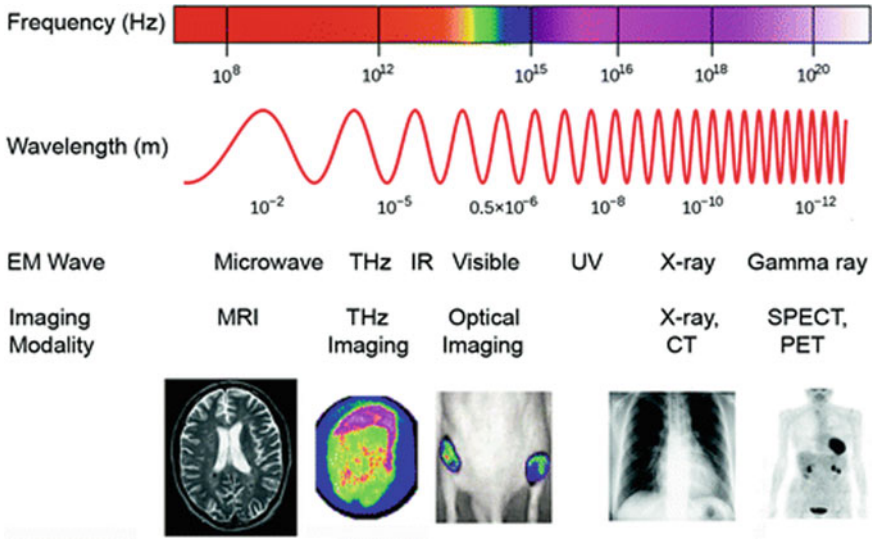


Fig. 3 Time domain spectroscopy terahertz medical imaging

- Systematic approach has been made to grow large size and high quality using polar protic and aprotic solvents single crystals by solution technique.
- The single-crystal properties such as morphology, crystalline phase, and optical transparency have been investigated (Fig. 4).

The main aim of designing proposed THz based image processing approaches is to minimize the execution time and maximizes the scalability. In this system, the

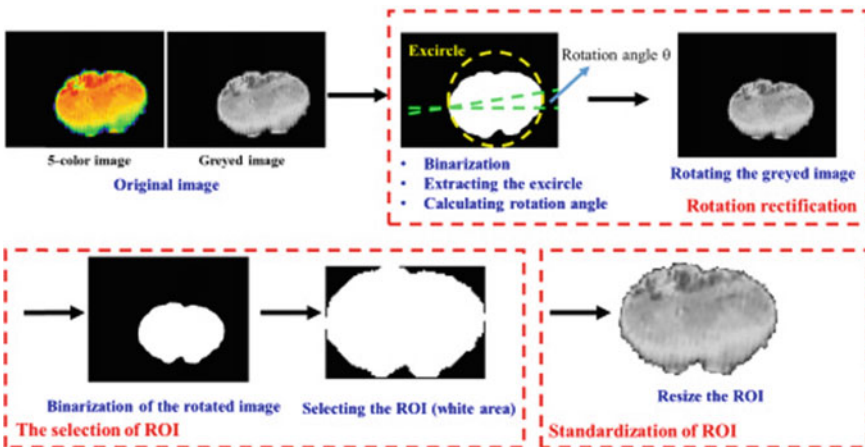


Fig. 4 Spectroscopy THz imaging architecture design

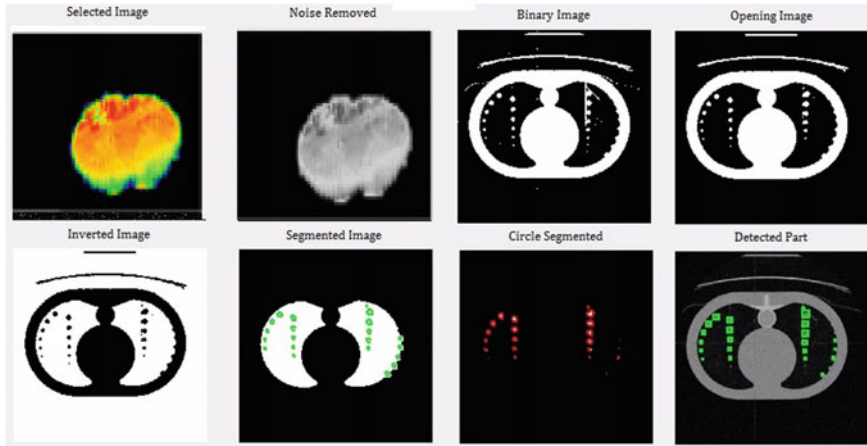


Fig. 5 Terahertz medical image classification

methods are focusing on automatic detection and classifying cancer as benign or malignant using final THz based input images. Here, the whole system of input is classified into the following steps: (a) preprocessing, (b) post-processing, and (c) feature extraction (Fig. 5).

First, before the preprocessing, the input image has been capturing and performing some action for further processing. Here, the MATLAB function captured the input image, which is the resizing and preprocessing step; the noise has been removed through the median filter, which is called adaptive noise removal filtering. Normally, the Wiener filter is used to smoothing the image based on the variance, and it works better when the noise is Gaussian white noise. It is always better than linear filtering based on noise removal.

In the segmentation step, the image can be a threshold. After segmentation, the morphological operations are performed by using erosion and dilation. The main purpose of this morphological operation is removing the unwanted portion from an image and separating the needful parts from an entire image. In feature extraction, the features can be extracted and calculated for classifying the brain THz image. In the classification step, the clustering can be used to classify the benign or malignant by using some extracted features from a previous step. Here, the features are trained and tested, which is used to correct the classification of a brain THz image.

The proposed system has been used very effective thresholding, segmentation techniques, and powerful feature extraction techniques. Compared to other existing systems, the proposed system gives better results in classifying begin and maligned classification.

The proposed system gives an accuracy of 93.35%. The same approach for MRI, CD, and X-ray images produced only comparatively less amount. Pictorial representation of Table 1 and Fig. 6 shows that overall image data classification accuracy of the proposed clustering method is 4.2% better result for existing image datasets that

Table 1 Cancer image dataset accuracy comparison

Image	Accuracy (%)
THz image	93.5
MRI image	89.3
CD image	87.5
X-ray image	83.33



Fig. 6 Cancer image dataset accuracy comparison

only achieves 89.3%, and other methods are 87.5% of the CD image 83.3% of X-ray image method.

Terahertz Medical Screening Devices by Uncooled Terahertz Detector Arrays

Current work is expected to extend and utilize on our recent reports [15–21] regarding the high performance on-chip integrable uncooled terahertz microbolometer arrays, with possibility of development of medical devices for screening and diagnostic application. These devices are fabricated and compatible with state-of-the-art and medium-scale semiconductor device processes and hence are commercially viable for large-scale implementation. Following up our previous reports [22–25] on the scope of medical device and systems applications, here, we have explored the development of thermal screening devices.

6 Conclusion

This paper is devoted to understanding the electro-optic properties of different types of nanostructures in the THz frequency range and using those nanostructures efficiently in manipulating THz radiation in application purposes. From the results, we could observe that the results obtained for the symbolic approach are better than the

conventional approach. Since a great part of this research involves growing crystals from low-temperature solutions, a brief introduction to general theories of crystal growth is given, with special emphasis on solution growth. This technique can play a very important role in detecting cancer and through this technique to reduce the percentage of cancer in humans.

The main aim of designing proposed crystalline spectroscopy (THz signal and image processing) approaches is to minimizing the execution time at a high scalability for automatic detection and classification. This work would extend on our previous reports regarding on-chip integrable terahertz detector arrays for possible development of medical devices for screening and diagnostic application.

References

1. Sim YC, Ahn K, Park JY, Park C, Son J (2013) Temperature-dependent terahertz imaging of excised oral malignant melanoma. *IEEE J Biomed Health Inform* 17(4):779–784. <https://doi.org/10.1109/JBHI.2013.2252357>
2. Reid CB, Reese G, Gibson AP, Wallace VP (2013) Terahertz time-domain spectroscopy of human blood. *IEEE Trans Terahertz Sci Technol* 3(4):363–367
3. Peter BS, Yngevesson S, Siqueira P, Kelly P, Khan A, Glick S, Karellas A (2013) Development and testing of a single frequency terahertz imaging system for breast cancer detection. *IEEE Trans Terahertz Sci Technol* 3(4):374–386
4. Zhou Q et al (2019) Electromagnetic responses and coupling effect in asymmetric terahertz metamaterials. In: 2019 44th international conference on infrared, millimeter, and terahertz waves (IRMMW-THz), Paris, France, 2019, pp 1–2. <https://doi.org/10.1109/IRMMW-THz.2019.8874255>
5. Li H, Li Z, Wan W, Zhou K, Cao JC (2019) Compact real-time terahertz spectroscopy based on quantum cascade lasers. In: 2019 44th international conference on infrared, millimeter, and terahertz waves (IRMMW-THz), Paris, France, 2019, pp 1–2, <https://doi.org/10.1109/IRMMW-THz.2019.8874275>
6. Zhu Z, Zhou J, Zhou L, Zheng Y, Wang J (2019) A polarization insensitive metasurface for terahertz biosensing applications. In: 2019 44th international conference on infrared, millimeter, and terahertz waves (IRMMW-THz), Paris, France, 2019, pp 1–2, <https://doi.org/10.1109/IRMMW-THz.2019.8874289>
7. Hassanin AIM, Shaaban ASE, Abd El-Samie FE (2019) Medical applications of image reconstruction using electromagnetic field in terahertz frequency range. In: 2019 international symposium on networks, computers and communications (ISNCC), Istanbul, Turkey, 2019, pp 1–4. <https://doi.org/10.1109/ISNCC.2019.8909157>
8. Son J (2015) Challenges and opportunities in terahertz biomedical imaging. In: 2015 40th international conference on infrared, millimeter, and terahertz waves (IRMMW-THz), Hong Kong, 2015, pp 1–1. <https://doi.org/10.1109/IRMMW-THz.2015.7327837>
9. Hung Y, Yang S (2019) Terahertz deep learning computed tomography. In: 2019 44th international conference on infrared, millimeter, and terahertz waves (IRMMW-THz), Paris, France, 2019, pp 1–2. <https://doi.org/10.1109/IRMMW-THz.2019.8873944>
10. Vohra N, Bailey K, El-Shenawee M (2020) Terahertz experimental measurements of human breast tissue. In: 2020 94th ARFTG microwave measurement symposium (ARFTG), San Antonio, TX, USA, 2020, pp 1-4. <https://doi.org/10.1109/ARFTG47584.2020.9071691>
11. Xu R, Gao S, Izquierdo BS, Gu C, Reynaert P, Standaert A, Gibbons GJ, Bösch W, Gadringer ME, Li D (2020) A review of broadband low-cost and high-gain low-terahertz antennas for wireless communications applications. *IEEE Access* 8:57615–57629

12. Park JY, Choi HJ, Cheon H, Cho SW, Lee S, Son J-H (2017) Terahertz imaging of metastatic lymph nodes using spectroscopic integration technique. *Biomed Opt Express* 8:1122
13. Vilagosh Z, Lajevardipour A, Wood AW (2020) Computational absorption and reflection studies of normal human skin at 0.45 THz. *Biomed Opt Express* 11:417
14. Musina GR, Gavdush AA, Chernomyrdin NV, Dolganova IN, Ulitko VE, Cherkasova OP, Kurlov VN, Komandin GA, Zhivotovskii IV, Tuchin VV, Zaytsev KI (2020) Optical Properties of Hyperosmotic Agents for Immersion Clearing of Tissues in Terahertz Spectroscopy. *Opt Spectrosc* 128:1026
15. Tiwari A, Satoh H, Aoki M, Takeda M, Hiromoto N, Inokawa H (2014) *Sens Actuators A: Phys* 222:160
16. Banerjee A, Satoh H, Tiwari A, Apriono C, Rahardjo ET, Hiromoto N, Inokawa H (2017) *Jpn J Appl Phys* 56:04CC07
17. Banerjee A, Satoh H, Sharma Y, Hiromoto N, Inokawa H (2018) *Sens Actuators A: Phys* 273:49
18. Banerjee A, Satoh H, Elamaram D, Sharma Y, Hiromoto N, Inokawa H (2018) *Jpn J Appl Phys* 57:04FC09
19. Biswas A, Sinha S, Acharyya A, Banerjee A, Pal S, Satoh H, Inokawa H (2018) 0 THz GaN IMPATT source: effect of parasitic series resistance. *J Infrared, Millimeter, Terahertz Waves* 39(10):954–974
20. Banerjee A, Satoh H, Elamaram D, Sharma Y, Hiromoto N, Inokawa H (2019) *J Appl Phys* 125:214502
21. Elamaram D, Suzuki Y, Satoh H, Banerjee A, Hiromoto N, Inokawa H (2020) *Micromachines* 11(8):718
22. Banerjee A, Chakraborty C, Kumar A, Biswas D (2020) Emerging trends in IoT and big data analytics for biomedical and health care technologies. In: *Handbook of data science approaches for biomedical engineering*, pp 121–152
23. Banerjee A, Vajandar S, Basu T (2020) Prospects in medical applications of terahertz waves, terahertz biomedical and healthcare technologies materials to devices, pp 145–165
24. Basu T, Banerjee A, Vajandar S (2016) 2D materials as THz generators, detectors, and modulators: potential candidates for biomedical applications terahertz biomedical and healthcare technologies, pp 75–87
25. Banerjee A, Chakraborty C, Rathi M (2020) Medical imaging, artificial intelligence, internet of things, wearable devices in terahertz healthcare technologies, terahertz biomedical and healthcare technologies materials to devices, pp 225–239

Design and Characterization of a Multilayer Reversible “Carry Look-Ahead Adder” by Using QCA Spin Technique



Rupsa Roy, Swarup Sarkar, and Sourav Dhar

Abstract In present nano-technical world, the quantum cellular automata (QCA) is a novel widely used technology where electrons are used in the quantum cells for information storing and transmitting. The analytical and numerical designs of different type of combinational and sequential components with the help of QCA spin technology are now under process. The current research paper presents the design and characterization of low power reversible carry look-ahead adder (CLA) at high bit-rate by using “Quantum dot Cellular Automata (QCA) Spin Technique”. The proposed circuit is a multilayer, portable, cost-effective, energy efficient, and optimized fault tolerance which is designed by three input ‘TSG’ reversible gate with three input ‘MV’ (Majority voter). QCA-Designer is used for logic and circuit level design of proposed devices and QCAPro is used for its power calculation. Along with this, the complex CMOS design of proposed circuit is performed by Xilinx and validated through FPGA Spartan 3E kit. The outcome and comparative table established the superior performance of reversible CLA designed by QCA compared to CMOS design.

Keywords Carry look-ahead adder · Multilayer · Reversible · Quantum cellular automata spin technology · MajorityVoter · Qcapro

R. Roy (✉) · S. Sarkar · S. Dhar
Department of ECE, Sikkim Manipal Institute of Technology, Sikkim Manipal University,
Gangtok, Sikkim, India
e-mail: onerupsa@gmail.com

S. Sarkar
e-mail: swarup.s@smit.smu.edu.in

S. Dhar
e-mail: sourav.d@smit.smu.edu.in

1 Introduction

According to Gordon Moore's interpretation, the number of components on a chip is increased two times after every two years and the processing speed of integrated circuits is also doubled for every three years. This prediction of used components' growth in a single chip is followed by CMOS or "Complementary Metal Oxide Semiconductor" technology to select the number of transistors in a die. But, the complexity of used transistors, processing delay, and amount of dissipated power create difficulties of smooth processing of circuits, at the time of component-density-increment in a chip. But, the optimization of these above parameters in a circuit becomes a major challenge in today's nano-electronic platform. "Quantum Dot Cellular Automata Spin Technique", an effective replacement of CMOS at present, is the selected advance technology of this work done. Multilayer 3D structure, which is not possible in CMOS platform till now due to the overlapping-complications of CMOS transistors, can be designed in this selected technical platform easily and also reversible gates can be used in this technology to compensate the temperature effects of multi-layer circuitry. Adder is an important component of arithmetic and logic unit which is a core unit of any processor in this modern digital era.

Presently, adder can be designed by using various types of advanced circuitry [1] to reduce the propagation delay of multi-bit adder circuit. Ripple carry adder, carry save adder, carry select adder, carry look-ahead adder are the different types of advance adder formation in this current technical era. Carry look-ahead adder can be used to achieve a developed adder circuit with fast computing nature, less operating delay, and less required power [2]. In normal ripple carry adder, at first, the carry and sum output generate and then the carry-propagation takes place to the next full adder as a carry input which increases the propagation time of carry output. This logic can be reduced by using a faster "Carry-Look-Ahead Logic", where two new terms carry-generate and carry-propagate are introduced. Carry generate or ' g_i ' is an 'AND' operation of two inputs and carry propagate or ' P ' is the 'XOR' operation of the same inputs. If ' C_i ' is the carry input of first full adder and ' C_{i+1} ' is the carry in of next adder, then $C_{i+1} = g_i + (P \cdot C_i)$ and sum output ' S_i ' is equal to the 'XOR' operation of ' P ' and ' C_i ' [3]. The Conditions of a "Carry-Look-Ahead Logic" are presented in this paper in Table 1.

'QCA' or "Quantum Dot Cellular Automata" with spin technique is the selected technology in this work to form a power-effective, fault-free, high frequency and portable "Carry Look-Ahead Logic" design. 'QCA' is proper alternative of CMOS or complementary metal oxide semiconductor technique. In "QCA Spin Technique" spintronic electrons are used in quantum cells for information storing and transmitting purpose with very low internal current flow in quantum cells. It is a low-power technology due to the above reason where '100 W' power is dissipated for every cm^2 area with 'THz' frequency range [4] more than the CMOS technique. This technology can access two times higher bit-rate than other conventional transistor level technologies due to the presence of qubit in "QCA Spin Technique". A quantum-bit or qubit, which are two types: '+1' and '-1' [5] depends on the rotational

Table 1 Truth table of “carry-Look-Ahead Logic”

Input 1	Input 2	Carry input (' C_i ')	Carry input of next adder(C_{i+1})	Conditions
0	0	0	0	No carry generate
0	0	1	0	
0	1	0	0	
0	1	1	1	No Carry Propagate
1	0	0	0	
1	0	1	1	
1	1	0	1	Carry generate
1	1	1	1	

direction of trapped electrons in a quantum-cell’s potential well, has two bits unlike the conventional digital components. This selected technical platform can design properly multilayer three-dimensional component-structure [6].

Figure 1 represents a multilayer three-dimensional quantum-wire (is used for information flow in ‘QCA’ from source to destination by placing quantum cells one after another) crossing. The advantages of this above structure type are reflected through power, delay, and unit-area occupation optimization. But sometimes the

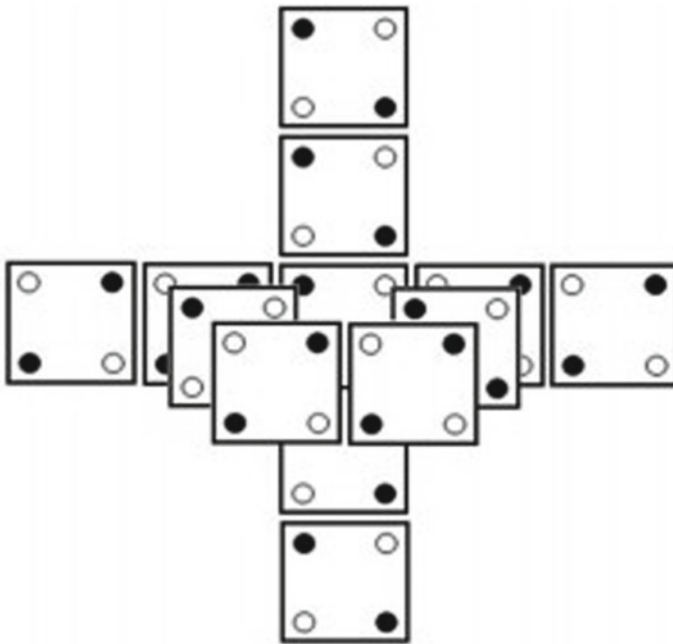


Fig. 1 Multilayer three dimensional structure in “QCA Spin Technology”

required cell numbers are increased in upward direction by using this above formation. Device is affected by extra temperature generation due to this above reason. This problem can be compensated by using adiabatic logic [7], which is possible by using reversible gate. In conventional gate, output is a function of input. But, in reversible computing, inputs are also the function of outputs [8]. Energy dissipation for every single bit can be reduced by using this selected gate type, because a different type of clock-scheme is used here. In this clock scheme, information are copied before erase [9]. This phenomenon can explore the advantages of adiabatic logic to reduce the energy dissipation of proposed device and the temperature effect is also can be reduced in multilayer 3D formation to achieve a low power fault-free outcome.

2 Circuit Design and Logic Level Design of Proposed Component

This portion of this paper represents parametric comparison between CMOS technique and “QCA Spin Technique” after simulating the proposed adder design in two different platforms which are mentioned above. This paper presents a logic level design of basic “Carry-Look-Ahead Logic”, where used inputs are A, B, and C_{in} and outputs are S for sum out and C_{out} for carry out. The logic-gate design of used three input “AND Gate” and three input “XOR Gate” are also given in this portion. A circuit level design of a reversible proposed device by using a “QCA- Designer” software also given.

Figure 2 represents a logic level design of proposed “Carry-Look-Ahead Logic”, where three input buffer, two output buffer, one carry block, and a sum-block are used.

Figure 3a, b shows the logic level design of carry-out and sum-out which are placed inside the carry block and sum block of Fig. 2, respectively. The used transistors can be calculated from these above features which are presented in Figs. 2 and 3a, b. These logical representation requires ‘128’ total number of transistors two design a logic level technology schematic of proposed adder design. But this design can be formed by using ‘92’ quantum cells when the different components of proposed device are placed in different layers (multilayer 3D structure). Multilayer design can reduce the unit-area and delay of the design but, the extra heat generation creates temperature-problem in the proposed design. This problem can be reduced by using reversible gate which is discussed here in previous portion. A reversible modified three input ‘TSG’ gate [10] is utilized in this work to form sum output and carry-propagate output (P) with a garbage value. The temperature increment can be reduced by energy-dissipation reduction which can be possible by using adiabatic logic with reversibility of proposed design.

Different layers of proposed circuitry are presented in Fig. 4 in this paper. The first layer presents the proposed reversible gate which follows the above Table 2 and the secondlayer works as a communication-line between first and third layer. The

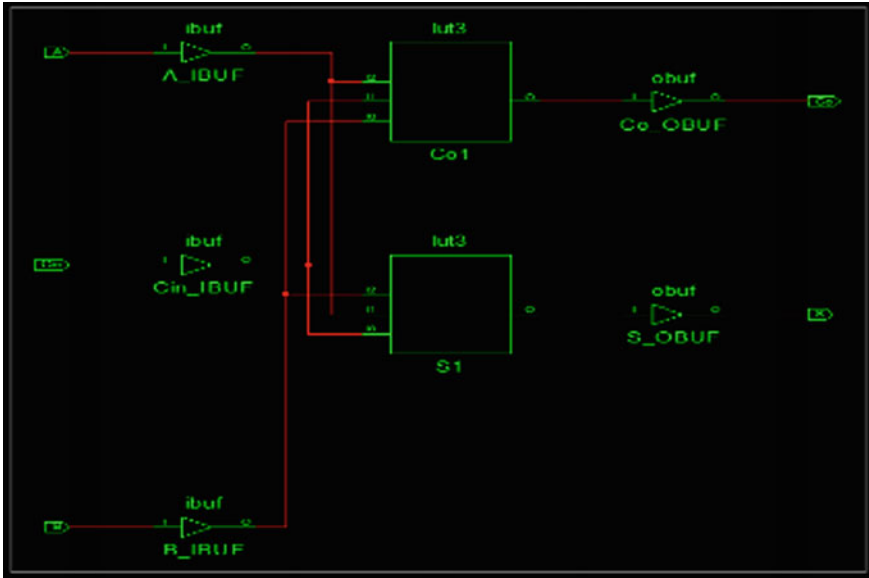


Fig. 2 Logic level design of proposed “Carry-Look-Ahead Logic”

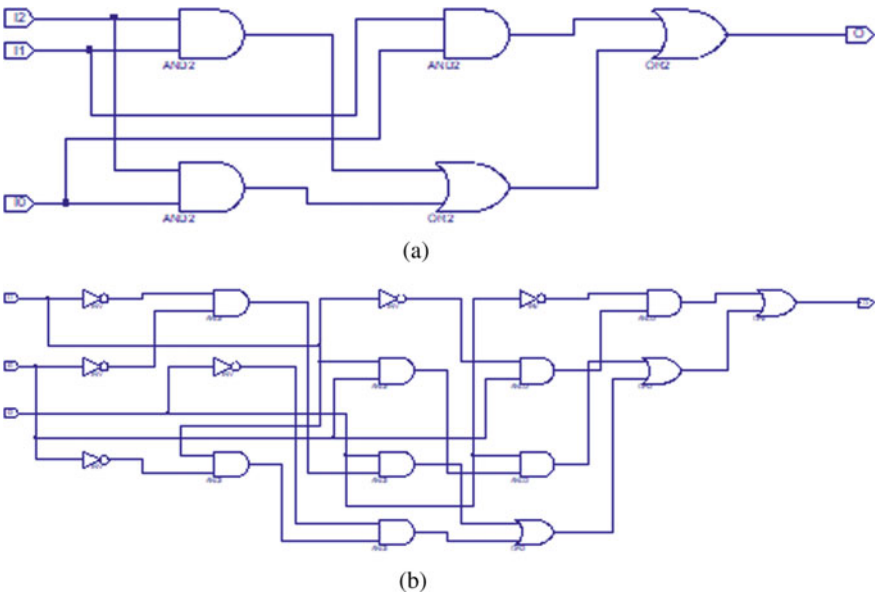


Fig. 3 a Logic level design in carry block and b logic level design in sum block

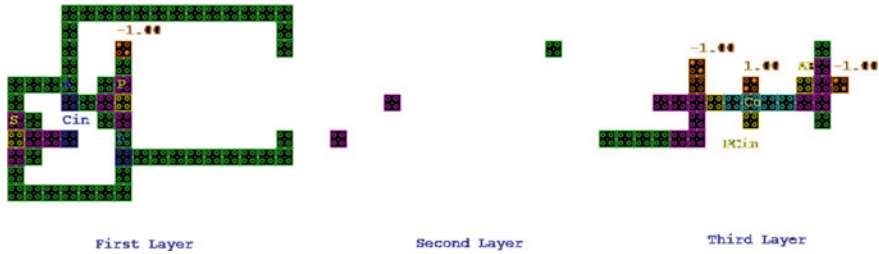


Fig. 4 First, second and third layer of proposed reversible multilayer 3D “Carry-Look-Ahead Logic”

Table 2 Truth table of reversible modified three input ‘TSG’ gate

Input			Output		
A	B	C	A	A XOR B XOR C	A XOR B
0	0	0	0	0	0
0	0	1	0	1	0
0	1	0	0	1	1
0	1	1	0	0	1
1	0	0	1	1	1
1	0	1	1	0	1
1	1	0	1	0	0
1	1	1	1	1	0

third layer, where three “3-input majority-voter (‘mv’) gate” are required, is used to represent the ‘AND’ operation of carry-propagate and carry-in, carry-generate and the carry-out function of proposed circuit design. The garbage value of selected reversible gate (direct outcome of input A) acts as an input of presented ‘mv’ gates in this design.

3 Simulated Results

This part of the paper reflects the outcomes after logic level design and circuit level design of the proposed logic of adder by using “Xilinx” and “QCA-Designer” software, respectively. This portion is also used to represent the “FPGA” implementation of proposed circuitry for validity checking, where “Spartan 3E” kit is used.

Figure 5a shows the simulated waveform of proposed “Carry-Look-Ahead Logic” after the logic level design simulation by using the Verilog code of proposed adder structure, where the ultimate outcomes carry-out and sum-out are presented as a function of input ‘A’, ‘B’, and carry-in or ‘Cin’. The simulated outcome of the

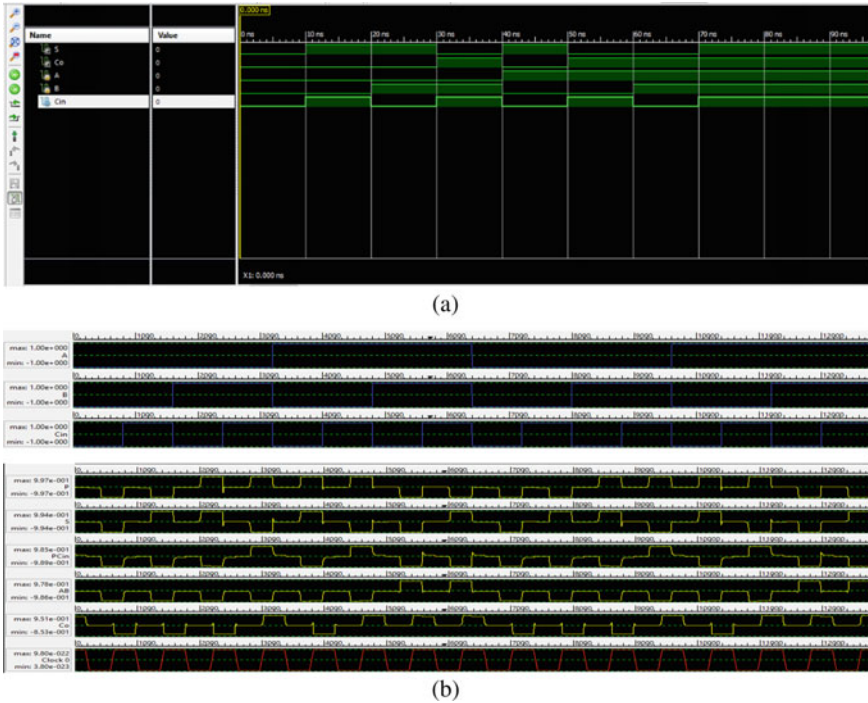


Fig. 5 a Time-scaling outcome of proposed “Carry-Look-Ahead Logic” after simulating in “Xilinx” b Simulated first, second and third layer of proposed reversible multilayer 3D “Carry-Look-Ahead Logic” by using “QCA-Designer” software

proposed circuit level design of reversible multilayer 3D “Carry- Look-Ahead Logic” is reflected in Fig. 5b. In the 2nd figure, carry-propagate output, carry-generate output, ‘AND’ operation of carry-propagate and carry-in and the ultimate adder outputs sum and carry-out are represented in output ‘P’ (‘XOR’ of ‘A’, ‘B’), ‘AB’ (‘AND’ of ‘A’ and ‘B’), ‘PCin’ (‘AND’ of ‘p’ and ‘Cin’), ‘S’ (‘XOR’ of ‘A’, ‘B’ and ‘Cin’), and ‘Co’ (‘AND’ of ‘A’, ‘B’ and ‘Cin’), respectively. The comparison table of the parameters (area, power and delay) of two simulated designs is also given in Table 3, which proves the advantages of “QCA Spin Technique” over CMOS technique to reduce the area, power and delay of the proposed device.

The Verilog code of design is presented in this portion in Fig. 6a after the configure of target device is launched successfully and Fig. 6b also shows the successful implementation of used code in “FPGA”Spartan 3E board which helps to check the proper validity of the proposed design.

Table 3 Comparison table between CMOS technique and “QCA Spin Technique” by using “Xilinx” and “QCA-Designer”

“Carry-look-Ahead Logic” Design	Logic level design by using “Xilinx” software			Circuit level design by using “QCA-Designer” software			
	Area (used transistors)	Delay	Power-Dissipation	Area	Delay	Calculated power-Dissipation	Cell-Complexity
	128	5.8 ns	42 mW	0.08 μm^2	0.4 ns	80 nW	92

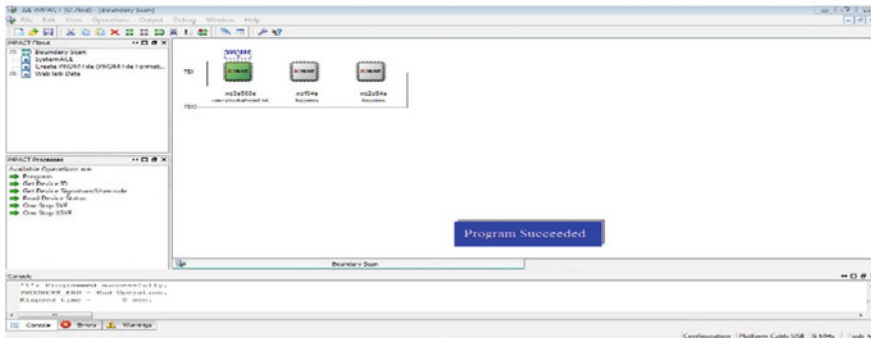
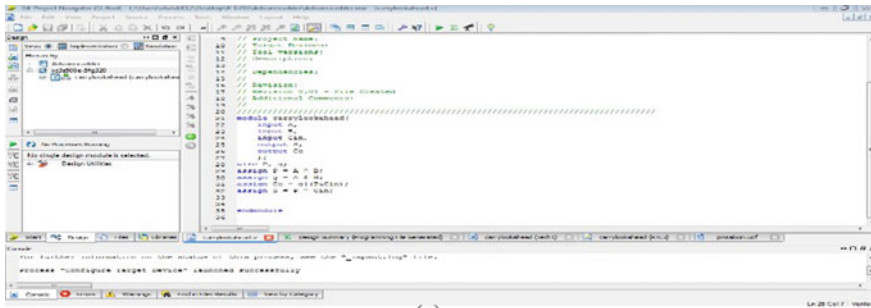


Fig. 6 **a** Used Verilog code of proposed design **b** Program of proposed design is successfully implemented in “FPGA” kit for validity checking

4 Conclusion

This paper presents a multilayer 3D circuit design of a reversible “Carry-Look-Ahead Logic” using low-power, high-frequency, nano-size-based “QCA Spin Technique” and also reflects a parametric comparison between this above technique and CMOS technique by simulating a logic level design of proposed component in “Xilinx” by using Verilog code. The comparison proves the advantages of “QCA Spin Technique”

over transistor-level CMOS technique to optimize the area occupation (28%), calculated dissipated power ('mW' range to 'nW' range), and delay (more than 90%). In this proposed work, the presented fault free and low cost (2.56 according to paper [8]). The design is also validated successfully by "FPGA"partan 3E hardware kit. In the future, this proposed advanced adder design can be converted from single bit to multi-bit by using reversible gate and QCA spin technique. In the future, fabrication of the proposed design will be an important requirement after proper design rule check and proper validation (by implementing the design-code in "FPGA Board") of proposed efficient portable advanced multi-bit "Carry-Look-Ahead Adder" structure.

References

1. Miao J, Li S (2017) A novel implementation 4-bit carry look-ahead adder. *IEEE Xplore*, pp 1–2
2. Sarkar M, Sengupta R et al (2017) Carry look ahead adder design using CMOS output wired logic based majority gate. *Optronix, IEEE Xplore*, pp 1–5
3. Erniyazov S, Jeon J-C (2019) Carry save adder and carry look ahead adder using inverter chain based coplanar QCA full adder for low energy dissipation. *Microelectron Eng* 211:37–43
4. Laajimi R (2018) Nanoarchitecture of quantum-dot cellular automata (QCA) using small area for digital circuits. In: *Advanced electronics circuits—principles, architectures and applications on emerging technologies*, pp 67–84
5. Oskouei SM, Ghaffari A (2019) Design a new reversible ALU by QCA for reducing occupation area. *J Supercomput* 75:5118–5144
6. Babaie S, Sadoghifar A, Bahar AN (2019) Design of an efficient multilayer arithmetic logic unit in quantum-dot cellular automata (QCA). *IEEE Trans Circuits Syst II* 66(6):963–967
7. Pidaparathi SS, Lent CS (2018) Exponentially adiabatic switching in quantum-dot cellular automata. *J Low Power Electron Appl* 8(30):1–15
8. Ahmad F, Ahmed S, Kakkar V, Mohiuddin Bhatt G, Bahar AN, Wani S (2018) Modular design of ultra-efficient reversible full adder-subtractor in QCA with power dissipation analysis. *Int J Theor Phys* 57:2863–2880
9. Sarvaghad-Moghaddam M, Orouji AA (2018) New symmetric and planar design of reversible full-adder/subtractor in quantum-dot cellular automata. *Euro Phys J*, pp 1–13
10. Gaur HM et al (2018) In-depth comparative analysis of reversible gates for designing logic circuits. *Proc Comput Sci* 125:810–817

Author Index

A

Abawajy, Jemal H., 295
Abonmei, Athon, 19
Acharjee, Juin, 27
Agarwal, Vikash Kumar, 197
Akhtar, Md. Amir Khusru, 261, 301
Alam, Afrin, 207
AlJabri, Zainab S., 295
Amutha, N., 43
Anurag, Anish, 121
Anwar, Shamama, 207
Attea, Baraá A., 247

B

Banerjee, Amit, 69, 389, 395
Banerjee, Mahua, 121
Banerjee, Saswata, 27
Barik, Rabindra Kumar, 189
Baruah, Abhigyan, 175
Bera, Rabindranath, 81, 89, 99
Bhattacharjee, Partha, 281
Bhattacharyya, Suman Kumar, 109
Bidyath, Khaidem, 19
Biswas, Pallabi, 99

C

Chakraborty, Mithun, 69, 81, 89, 99
Chandra, Jayanta K., 143
Chauhan, Anamika, 9
Chaurasia, Dhiraj, 281
Chowdhury, Prasun, 311

D

Dara, Biswajit, 81, 89

Das, Aparajita, 341
Das, Jasowanta, 175
Das, Rik, 121
Das, Saneev Kumar, 189
Dev, Aryan, 175
Dhar, Sourav, 405

G

Ghosh, Sagnik, 311
Goswami, Mausumi, 153, 165
Gupta, Manisha, 353
Gupta, Supriya, 261
Gupta, Yasharth, 341

H

Huda, Shamsul, 295

I

Inokawa, Hiroshi, 389, 395
Irfan Alam, Md., 375
Islam, Md. Ruhul, 341
Isogai, Koki, 389

J

Jena, Anindita, 215, 319
Jha, Govind Kumar, 121

K

Kanchan, Pradeep, 247
Kandar, D., 69
Kandpal, Meenakshi, 189

© The Editor(s) (if applicable) and The Author(s), under exclusive license
to Springer Nature Singapore Pte Ltd. 2021

M. Chakraborty et al. (eds.), *Trends in Wireless Communication and Information Security*,
Lecture Notes in Electrical Engineering 740,
<https://doi.org/10.1007/978-981-33-6393-9>

Karthikeyan, M. P., 395
 Kumar, Ashwani, 301
 Kumar, Asok, 61
 Kumari, Sarita, 53, 273
 Kumar, Mohit, 301
 Kumar, Nitish, 197
 Kumutha, N., 43

M

Maji, Bansibadan, 61, 69, 89
 Majumdar, Arun K., 3
 Majumdar, Parijata, 333
 Mallick, Pradeep Kumar, 129
 Mandal, Kaushik, 27
 Manivannan, Revathi, 389
 Manorama, 237
 Misra, Chinmaya, 189
 Misra, Santanu Kumar, 175
 Mitra, Sanjoy, 333
 Mohapatra, Subhasish, 363

N

Nagarajan, Anitharaj, 389
 Nishimura, Tomoki, 389

P

Pal, Ayan, 27
 Pal, Sagarika, 109
 Panja, Arunabho, 27
 Paul, Poulami, 353
 Puneet, 9
 Pushparaj, D. Shetty, 247

R

Rai, Amit Kumar, 197
 Rath, Patitapaban, 129
 Roy, Abhishek, 353, 363
 Roy, Arjya, 395
 Roy, Rupsa, 405

S

Sabata, Pratik, 153
 Sahoo, Pritam Keshari, 37
 Sahu, Nilesk Kumar, 229
 Sajwan, Prachi, 165
 Samadder, Amibrata, 27
 Samanta, Debabrata, 395
 Sarkar, Gautam, 143
 Sarkar, Mrinmoy, 61
 Sarkar, Sugata, 143
 Sarkar, Swarup, 405
 Satoh, Hiroaki, 389
 Shome, Saikat Kumar, 281
 Shome, Subhankar, 89, 99
 Siddavatam, Rajesh, 129
 Singh, Alka, 389
 Singh, Satya Narayan, 375
 Snigdha, Itu, 229, 237
 Sur, Samrendra Nath, 81

T

Tola, Sourav, 143
 Tongbram, Simon, 19
 Trivedi, Munesh Chandra, 333

W

Wedhane, Neeraj Vijay, 341